Environmental responses to abrupt climatic change during the Last Glacial-Interglacial Transition (ca 16-8 Cal. ka BP): delineating climatic drivers and landscape responses during millennial- and centennial-scale climatic variability

Ashley Mark Abrook

Centre for Quaternary Research,
Department of Geography,
Royal Holloway, University of London

Thesis submitted for the degree of Doctor of Philosophy,
Royal Holloway, University of London
September 2018

Declaration of authorship

I, Ashley Mark Abrook, hereby declare that the work presented in this thesis is entirely my own. Where I have consulted the work of others this is clearly stated.

Signed:

Date:

Abstract

The Last Glacial-Interglacial Transition (LGIT; 16-8 Cal. ka BP) is one of the most recent periods in geologic history where the climate system underwent major reorganisation, linked to variability in oceanic and atmospheric circulation. In northern Europe, the LGIT is a well-characterised period of abrupt climatic change where millennial-scale oscillations in climate led to large-scale reorganisation of ecosystems. Imprinted upon these longer-term episodes are a series of centennial-scale climatic events which are less well understood. These short-lived events appear spatially and temporally complex and frequently have either not been identified or are shown to have limited impact. Furthermore, many sequences have not been studied for proxies that provide evidence of drivers and responses, or they are not resolved in sufficient detail. Consequently, responses and phase relationships between driver and response variables are unknown.

Given this context, a systematic study across Britain was performed. Sequences were identified that held potential for analyses which span a latitudinal and climatic gradient in Britain with sites selected from, Orkney; the Grampian Highlands, Scotland; the Vale of Pickering, north-east England and within the Brecon Beacons, south Wales. From these sequences, high-resolution climatic reconstructions ($\delta^{18}O$ and $\delta^{13}C$; chironomid-inferred temperatures, compound specific δD biomarker analyses) were performed alongside high-resolution environmental reconstructions (pollen; micro-macro-charcoal). Where possible all analyses were performed from the same stratigraphic core sequence.

The results of this thesis indicate that abrupt centennial climatic events can be identified in Britain across different climatic parameters, which within centennial timescales, are broadly synchronous with changes in Greenland. For each of the climatic events observed, palynological/vegetation responses are clear. However, both the style and amplitude of response are spatially heterogeneous; reflecting the latitudinal position, amplitude of climatic forcing and antecedent conditions. Whilst the timing of these changes are comparable across Europe, the amplitudes of change are variable; revealing continent wide climatic and vegetation gradients. Phase relationships between drivers and response variables are complex with different climatic parameters oscillating at different times but with response variables always lagging the onset of climatic change.

Publications arising from this study

Blockley, S.P.E., Candy, I., Matthews, I.P., Langdon, P., Langdon, C., Palmer, A.P., Lincoln, P., **Abrook, A**., Taylor, B., Conneller, C., Bayliss, A., MacLeod, A., Deeprose, L., Darvill, C., Kearney, R., Beavan, N., Staff, R., Bamforth, M., Taylor, M., and Milner, N. (2018). 'The resilience of postglacial hunter-gatherers to abrupt climate change.' *Nature ecology and evolution*, 2, pp. 810-818.

Blockley, S.P.E., Matthews, I.P., Palmer, A.P., Candy, I., Kearney, R., Langdon, P., Langdon, C., **Abrook, A**., Lincoln, P., Farry, A., Darvill, C., and Deeprose, L. (2018). 'Climate Research.' In: Milner, N., Conneller, C., and Taylor, B. (Eds.). Star Carr Volume 2: Studies in Technology, Subsistence and Environment, York: White Rose University Press, pp. 113-121.

Candy, I., **Abrook, A**., Elliot, F., Lincoln, P., Matthews, I.P., and Palmer, A.P. (2016). 'Oxygen isotopic evidence for high-magnitude, abrupt climatic events during the Lateglacial Interstadial in north-west Europe: analysis of a lacustrine sequence from the site of Tirinie, Scottish Highlands.' *Journal of Quaternary Science*, 31(6), pp. 607-621.

Monkey killing monkey killing monkey over pieces of the ground,
silly monkeys give them thumbs they make a club;
and beat their brother down.
How they survive so misguided is a mystery[1]

[1] Keenan, M.J., Jones, A., Carey, D., and Chancellor, J. (2006). 'Right in Two.' *TOOL: 10,000 Days*, Volcano Entertainment

Acknowledgements

There are many people who I would like to express my thanks and gratitude to throughout the course of this thesis. The support I have received has been immeasurable.

First and foremost, I would like to thank my supervisors Dr Ian Matthews and Dr Alice Milner who I owe a debt of gratitude for the guidance and encouragement I have received over the last four years. I would also like to thank Prof. Ian Candy and Dr Adrian Palmer who have been on hand to discuss many aspects of this research at any point without fail. Additional thanks must go to the following staff members who have made my time at Royal Holloway thoroughly enjoyable: Prof. J. Lowe, Prof. S. Blockley, Dr Claire Mayers, Dr Marta Perez, Dr R. Housley, Dr M. Dolton, Dr. V. Thorndycraft, Dr C. Gallant, Ms Katy Flowers, Mr I. Valcarel, Mrs. J. Thornton and Mr R. Aung.

In particular, I would like to thank colleagues at the Deutsches GeoForschungs Zentrum (GFZ) Dr Dirk Sachse, Dr Oli Rach and Mr David Maas who taught me the mysteries of organic geochemistry and provided hours of support in an unfamiliar environment. A special thanks goes to David who acted as my translator, shared one of his guitars, gave me a bicycle and through our shared love of 'heavy' music provided many a loud laboratory day.

I would also like to thank the following people Prof. Oliver Heiri, Dr Stefan Engels, Dr Francesco Muschitiello, Dr Frank Mayle, Prof. Pete Langdon and Dr Nelleke van Asch for openly sharing published and unpublished data for use within this thesis.

I would also like to express my thanks to the past and present PhD students and post-docs whom I have shared many experiences with. I would especially like to thank Dr Rhys Timms for Thursday beers; Dr Paul Lincoln for that one trip to Yorkshire; Dr Jacob Bendle for 'Big John'; Dr Jenni Sherriff for Late-Glacial critique; Adam Badger for human geography insight, Benjamin Newman for the world cup and the gossip column; and Rachel Devine for beef enchiladas. Additionally, I would like to thank: Richard Clark-Wilson, Julian Martin, Xuanyu Chen, Amy Walsh, Dave Arnold, Alice Carter-Champion, Angharad Jones, Richard Clark-Wilson, Chris Francis, Josh Pike, Eric Andrieux, Nathalie Diaz and members of the GVML who have made this final year bearable.

To Sinéad, who has always been there for me, and throughout this final year has provided so much support and encouragement, and to my parents Martin and Caroline, and to my sister Samantha, thank you for everything over the last four years.

Contents

List of Figures

Chapter 4. Methodology

Chapter 5. Results from Quoyloo Meadow

Chapter 6. Results from Tirinie

List of Tables

Chapter 8. Results from Llangorse

Chapter 9. Synthesis of climatic variability during the Last Glacial-Interglacial transition (LGIT)

Chapter 10. Synthesis of vegetation responses to abrupt climatic events during the Last Glacial-Interglacial Transition (LGIT)

Table I. Main palaeoecological, palaeoclimatological and geochronological proxies used within this thesis. Shown are the five sites where the proxies have originated from and the researcher who completed the analyses. The date shows when these analyses were completed. Bulk sedimentological analyses are not shown here but are detailed within Chapter 4.

Site	Main Proxy	Researcher (date completed)
Quoyloo Meadow	Pollen	This study (2016)
	Charcoal	This study (2017)
	Stable Isotopes	Lawrence Abel and Rhys Timms (2016)
	Compound-specific isotopic biomarkers	David Maas (2016)
	Chironomid-Inferred Temperatures	Agnieska Mroczkowska and Rhys Timms (2017)
	Tephra	Rhys Timms (2016)
Tirinie	Pollen	This study (2015)
	Charcoal	This study (2017)
	Stable Isotopes	Christopher Francis, Ian Candy and this study (2015-2017)
	Compound-specific isotopic biomarkers	This study (2018)
	Chironomid-Inferred Temperatures	Christopher Francis and Lucy Turner (2016-17)
	Tephra	Paul Lincoln (2014)
Palaeolake Flixton (Core B)	Pollen	This study (2016)
	Charcoal	This study (2017)
	Stable Isotopes	Ian Candy (2017)
	Chironomid-Inferred Temperatures	Pete Langdon and Cathy Langdon (2015-2017)
	Tephra	Ian Matthews (2016)
Palaeolake Flixton (Core C)	Pollen	This study (2017)
	Stable Isotopes	Christopher Darvil and Ian Candy (2011-2017)
	Chironomid Inferred Temperatures	Pete Langdon and Cathy Langdon (2015-2017)
	Tephra	Christopher Darvil (2011)
Llangorse	Pollen	This study (2017)
	Charcoal	This study (2017)
	Stable Isotopes	Ian Candy and Adrian Palmer (2017-2018)
	Tephra	Ian Matthews and Alison MacLeod (2017)

Chapter 1. Introduction to the study

The Quaternary period, the most recent geological subdivision in Earth's history, containing the Pleistocene (2.58 Ma-11.7 Ka) and the Holocene (11.7 Ka-present) epochs, is the period within which the frequency and magnitude of large-scale warm and cold events are manifest. These cold periods, termed glacials, exhibit increased frequencies of and an intensification of ice-sheet growth, whilst the warm periods, termed interglacials, experienced a waning of ice with temperatures as warm if not warmer than the present day. The periodicity of these cycles (ca 100 ka) are controlled by orbital theory, called Milankovitch cycles (e.g. Hays et al., 1976; Martinson et al., 1987; Imbrie et al, 1992; 1993), with changes in Earth's orbit (eccentricity; 100 ka cycle) and the configuration of Earth's axes (obliquity; 41 ka; and precession; 21 ka cycles) influencing radiation budgets and providing a means for initiation and termination of ice growth. However, imprinted on these cycles are phases of high-frequency climatic change, which can be grouped into millennial-, centennial- and decadal-scales, which are, by association, referred to as 'sub-Milankovitch' variability (e.g. Johnsen et al., 2001).

These variations are frequently identified in highly-resolved archives, in ice-core (e.g. Dansgaard et al., 1993; Johnsen et al., 2001; Rasmussen et al., 2014) and marine records (e.g. Bond et al., 1993), and are governed by intra-planetary variability, namely the interplay between ocean dynamics, atmospheric circulation and glacial configuration (e.g. Clark et al., 2001). Of paramount importance are these shorter-term variations, which produce large swings in temperature from relative interglacial warmth to the severe temperatures of glacial phases. Providing quantified estimates of the magnitude and timing of these 'events' (e.g. Lowe et al., 2008) is crucial for not only a better understanding of internal climatic variability; but also to prepare against future climate change scenarios (IPCC, 2007) within which these short term variations are not fully appreciated. The climatic expression and environmental impact of these events are fundamental to parameterise not only changing environmental patterns but also the potential impacts these shifts may have on societies.

1.1 The Last Glacial-Interglacial Transition

One of the most intensely studied periods in Earth's recent history is the Last Glacial-Interglacial Transition (LGIT; 16.0-8.0 Cal. ka BP). This is one such period following the last glaciation and continental ice retreat, where millennial-scale climatic reorganisations, between stadials (phases of climatic deterioration) and interstadials (periods of climatic favourability) are clear and well defined (Björck et al., 1998). The best evidence of this is presented from Greenland, within the GICC05 NGRIP isotopic record (e.g. Rasmussen et al., 2006; 2007; 2014; Figure 1.1). Interspersed within this well-understood LGIT

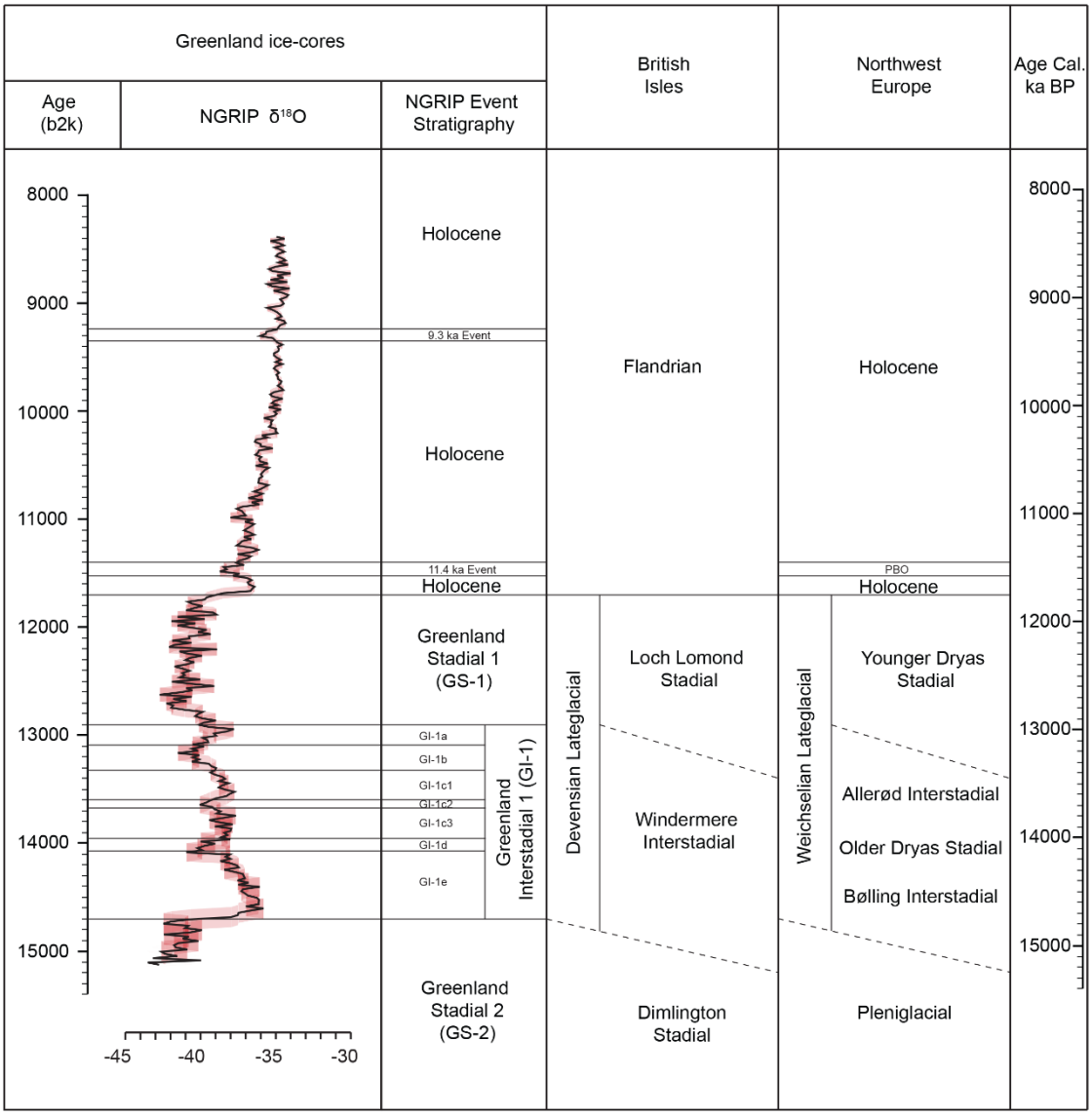

Figure 1.1 $\delta^{18}O$ record from NGRIP plotted on the GICC05 timescale. Shown is the NGRIP event stratigraphy, with the centennial climatic events GI-1e-a, the 11.4 ka and the 9.3 ka events highlighted. Also shown are the bio- and climatostratigraphic phases from the British Isles and Northwest Europe, highlighting the different nomenclatures of different time-periods used interchangeably across Europe. Adapted from Lowe and Walker (2014).

framework (e.g. Björck et al., 1998; Lowe et al., 2008), are phases of high-magnitude, abrupt centennial-decadal scale climatic oscillations, that, within NGRIP have been demarked and sub-divided based on their climatic structure (e.g. Björck et al., 1998; Lowe et al., 2008). Within Greenland Interstadial 1 (14.6-12.9 ka BP; GI-1), a series of cold events termed GI-1d, GI-1Cii and GI-1b can be observed, with similar features in the Holocene (11.7-8.0 ka BP), the 11.4 ka BP event for example. However, the terrestrial manifestation of these centennial-scale 'sub-Milankovitch' events are spatially complex and are far less well understood. Principally, not only do few quantified climatic records exist, they often have limited chronologies. Therefore, the (a)synchroneity of climate between the regional NGRIP stratotype (Lowe et al., 2008) and European

records for these climatic events is largely unknown. This has led to differing views of both the climatic regime, forcing factors and landscape responses across this period (e.g. Firestone et al., 2007; van Asch et al., 2012a; Muschitiello et al., 2015; Bromley et al., 2018; Schenk et al., 2018).

In this regard, the geographic position of Britain is key. The proximity of the Isles to the North Atlantic, where oceanic perturbations are believed to have caused the abrupt climatic events observed in the ice-cores (Broecker et al., 1989; Clark et al., 2001; Thornally et al., 2010), dictates sensitivities perhaps not observed elsewhere in Europe. Britain is therefore an ideal natural laboratory to examine the patterns of and responses to abrupt climatic events.

1.2 The Last Glacial-Interglacial Transition in Britain

Following the retreat of Devensian (Weichselian) ice in Britain (ca 19-14 ka BP; Clark et al., 2012a), many hundreds of lacustrine basins were formed. These basins gradually infilled with sediments that contain evidence of climatic modes and environmental conditions during the LGIT. Sedimentological associations during this time-period can frequently be divided into four lithostratigraphic units: 1) minerogenic silts/clays at the base of the sequence representing the cold climate of the Dimlington Stadial (GS-2, Pleniglacial); 2) an organic unit composed of lake-mud/gyttja or calcium carbonate representing warm climates of the Windermere Interstadial (GI-1; Bølling-Allerød); 3) a secondary minerogenic silt/clay unit reflecting climatic deterioration and landscape instability during the Loch Lomond Stadial (GS-1; Younger Dryas); and 4) lake-mud/gyttja or calcium carbonate associated with warm climates during the early Holocene. In particularly sensitive sequences the organic units are interrupted by phases of mineral sediment accumulations, which are a product of climatic variability akin to the centennial-scale events depicted above.

These broad sedimentological units are supported by proxy evidence. In Britain, climatic warmth is suggested during the Windermere Interstadial through chironomid-inferred summer temperature reconstructions (C-ITs) or enriched isotopic values (e.g. Marshall et al., 2002; Brooks et al., 2012). The analysis of pollen reveals vegetation development from a pioneering phase, dominated by open herbaceous vegetation, through to the development of woody vegetation following plant migration under favourable conditions, including *Juniperus* and open *Betula* woodland (Birks and Matthewes, 1978). The transition into the Loch Lomond Stadial sees a depression of temperatures and in Scotland the expansion of ice (e.g. Brooks and Birks, 2000a; Golledge, 2010; Marshall et al., 2002). In association with this decrease, vegetation assemblages shift to those

dominated by Arctic tundra assemblages frequently with *Artemisia*, *Rumex* and Poaceae (Walker, 1975). The change in landscape conditions shows heightened landscape instability and an increase in catchment erosion under unfavourable climates. The transition into the Holocene is revealed by a further phase of climatic warmth and the establishment of suitable landscape conditions to facilitate the expansion and successive replacement of grassland, *Juniperus* scrubland, *Betula* woodland and *Betula*/*Corylus* woodland.

1.3 Research rationale

Despite the generally accepted picture of millennial-scale climatic variability, and despite the many hundred vegetation reconstructions covering this period (e.g. Walker and Lowe, 2017) evidence of vegetation change in response to centennial-scale climatic variability is not fully understood. Therefore, it can still be argued, that neither climatic proxies or pollen have received sufficient study to understand spatial and temporal variations across short latitudinal distances (Brooks et al., 2016). At certain sequences, tentative correlations to one or more climatic events during the LGIT are proposed (Bartley, 1962; Watts, 1970; Pennington et al., 1972; Day, 1996; Tipping, 1991a; Walker et al., 2012; Figure 1.2), however, they do not reveal vegetation revertences (Section 2.6) associated with the full suite of climatic events identified (Rasmussen et al., 2014; Figure 1.1). In part the lack of evidence relates to palynological investigations being undertaken at a time prior to the understanding of climatic complexity, afforded by the Greenland ice-cores (e.g. Pennington et al., 1972; Lowe and Walker, 1986; Tipping, 1991b) but also due to researcher goals at the time of study. The level of temporal resolution sought for many of these studies are therefore not sufficient to detect palynologically inferred vegetation responses to abrupt climatic change. Further, it may be that: 1) the magnitudes of the climatic oscillations are not substantive to generate a response in vegetation; 2) that vegetation is insensitive to change; and 3) where certain vegetation responses have been identified, difficulties remain in relating vegetation change to climate (e.g. Tipping, 1991a).

In relation to these above propositions, the magnitudes of climatic change during the Windermere Interstadial are large. In certain localities these oscillations exhibit changes in summer temperatures which are similar in magnitude to the change associated with the Loch Lomond Stadial (e.g. Brooks and Birks, 2000a; Lang et al., 2010; Brooks et al., 2012). The Loch Lomond Stadial exhibits a clear and obvious vegetation response (e.g. Lowe and Walker, 1977). Secondly, it is unlikely that vegetation is insensitive to change across these short-timescales. For example, evidence suggests that vegetation

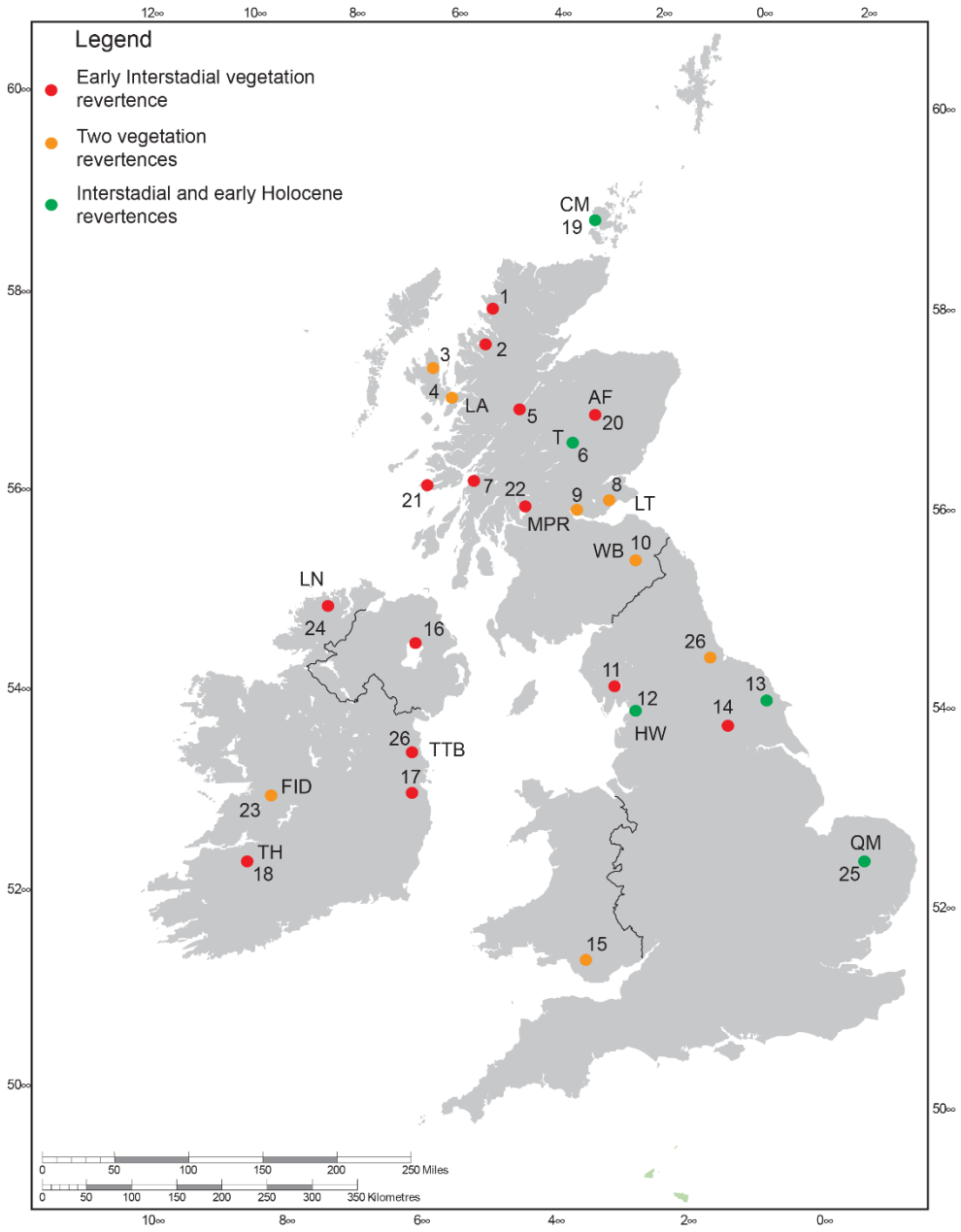

Figure 1.2 Location of sites in the British Isles that have been analysed throughout the LGIT that reveal palynological revertences. The red dots represent sites displaying an early Windermere Interstadial revertence; the orange dots represent sites that record two episodes of revertence; and the green dots show changes across the Interstadial and early Holocene. Lettering represents sequences that exhibit climatic reconstructions, either through chironomid-summer temperature reconstructions or stable isotopic reconstructions at the same site as the vegetation reconstruction. These sequences are: CM) Crudale Meadow (Whittington et al., 2015); AF) Abernethy Forest (Birks and Matthewes, 1978; Brooks et al., 2012); LA) Loch Ashik (Walker and Lowe, 1990; Brooks et al., 2012); T) Tirinie (Lowe and Waker, 1977; Candy et al., 2016); LT) Lundin Tower (Whittington et al., 1996); MPR) Muir Park Reservoir (Vasari; 1977; Brooks et al., 2016); WB) Whitrig Bog (Mayle et al., 1997; Brooks and Birks, 2000a); LN) Loch Nadourcan (Watts, 1977; Watson et al., 2010); HW) Hawes Water (Marshall et al., 2002; Jones et al., 2002); TTB) Thomastown Bog (Turner et al., 2015); FID) Fiddaun (van Asch et al., 2012a); TH) Tory Hill (O'Connell et al., 1999); QM) Quidenham Mere (Jeffers et al., 2011). Crucially however, many of the proxies extracted from these sequences were not analysed contemporaneously and from the same stratigraphic sequence. Of these only CM, T, WB and FID state that the same core sequence was used. See references in text and appendices for site details and numbering.

responses to the abrupt centennial-scale event at 8.2 ka BP can be identified (Tinner and Lotter, 2001). Equally, the recent publication of a study detailing climatic and vegetation change during the Holocene confirms that abrupt climatic change, that approximates the magnitude of the 8.2 ka BP event, can generate vegetation responses (Blockley et al., 2018). Finally, and perhaps most crucially, very few studies reveal evidence for both driver and response variables (e.g. van Asch et al., 2012a; Whittington et al., 2015), hence the difficulty in climatic attribution of environmental change. Where these studies exist, often they were not analysed for these variables contemporaneously with analyses completed decades apart. Abernethy Forest, for example, was analysed palynologically in the 1970's (Birks and Matthewes, 1978) whilst climatic reconstructions were only undertaken in the 2000's (Brooks et al., 2012). This produces uncertainty and homotaxial error with insecure correlation and therefore a lack of understanding between the temporal differences between the two variables. However, recent work has utilised this approach and formed much better conclusions through linking the climatic and environmental variables in a multi-proxy approach with analyses performed from the same sequence (e.g. van Asch et al., 2012a; Whittington et al., 2015).

Despite recent advances, multi-proxy driver and response studies are scarce and clear gaps in understanding exist. Principally these gaps include: 1) the spatial expression and variable magnitudes of climatic events in Britain; 2) whether these deteriorations can be identified across multiple different climatic parameters; 3) how vegetation responds to these events across Britain; and 4) whether variable magnitudes of vegetation responses exist between different sites. Owing to this lack of understanding, and the knowledge of climatic complexity during the LGIT further study is warranted.

1.4 Study site locations

To better constrain phases of vegetation change in response to abrupt climatic events, four sites were chosen (Figure 1.3) that span a latitudinal and climatic gradient across Britain. Quoyloo Meaodow, Orkney; Tirinie, Grampian Highlands, central Scotland; Palaeolake Flixton, Vale of Pickering, north-east England; and Llangorse, Brecon Beacons, south Wales (Figure 1.3). Further an additional sequence has been analysed from Palaeolake Flixton, taking the total sequence number to five. Covering the breadth of the country, these sequences will enable an understanding of the spatial complexities of climatic evolution and variability of vegetation response. Whilst these sequences are not new to science, barring the lower units of Llangorse, they have been selected as within original studies (e.g. Lowe and Walker, 1977; Walker et al., 1993b; Bunting, 1994; Day, 1996) the sequences were shown to hold potential for future research. This stems from either the type of sediment they contain (lacustrine marl for stable isotopic analyses)

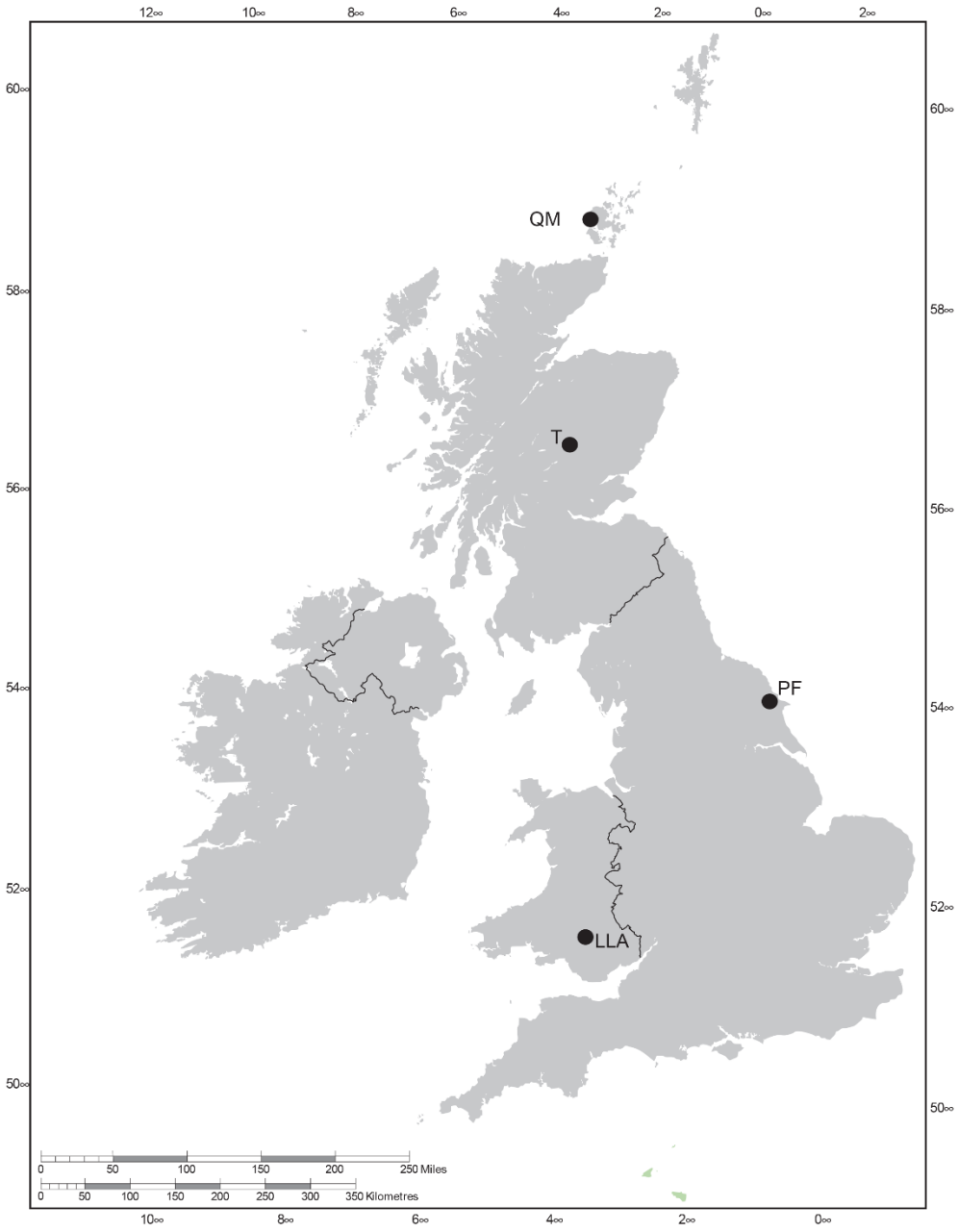

Figure 1.3 Sequences analysed as part of this research along a latitudinal and climatic transect in Britain: QM) Quoyloo Meadow, Mainland, Orkney Islands; T) Tirinie, Grampian Highlands, central Scotland; PF) Palaeolake Flixton, Vale of Pickering, north-east England; LLA) Llangorse, Brecon Beacons, south Wales.

or the suggestion of sensitivities in the palynological record which was not built upon (e.g. Lowe and Walker, 1977). These sequences therefore contain the potential to develop a better understanding of climate and vegetation change during the LGIT.

1.5 Thesis aims and objectives

The aim of this thesis is to better understand the environmental and vegetation response to abrupt climatic events during the Last Glacial-Interglacial Transition across the British Isles. Whilst the primary aim is focussed on understanding vegetation dynamics in

response to centennial-scale climatic variability across Britain, the construction of a climatic framework allows for secondary aims including:

1) Greater understanding of the climatic structure of the LGIT across Britain and site/region specific variability in the expression of abrupt climatic events.
2) The reconstruction of different climatic parameters during the LGIT. This allows for knowledge to be developed related to how different elements of the climate system evolve during this period.
3) The formulation of a series of highly-resolved sequences across Britain and Europe to begin the construction of an ecological lattice, where additional sequence can be compared to.

To achieve these aims several objectives need to be accomplished:

1) Perform high-resolution palynological sampling to reconstruct detailed vegetation histories from each of the sequences. The high-resolution sampling will better enable the detection of vegetation responses to abrupt climatic events.
2) To undertake statistical treatment of the palynological data to better constrain episodes of vegetation change. This will reveal the onset and magnitudes of environmental variability.
3) To perform macro- and micro-charcoal analyses matching the sampling intensity of the pollen reconstruction. This will enable the assessment of whether fire drives landscape change or whether it is only important as a response to changing climatic conditions.
4) Where required, perform additional high-resolution palaeoclimatic ($\delta^{18}O$ and $\delta^{13}C$; chironomid-inferred temperature; compound specific δD lipid biomarker) reconstructions to characterise and parameterise climatic variability during the LGIT.
5) To chronologically constrain each sequence either using tephrochronology and/or radiocarbon analyses to place identified variability in time.
6) Where possible perform all analyses from the same stratigraphic sequence to reduce homotaxial error and to establish lead/lag relationships. The placement against age will also allow for the quantification of lags between driver and response variables on calendar timescales.

1.6 Thesis structure

This thesis is divided into eleven chapters, excluding contents, references and appendices. Chapter 2 provides an overview of the structure of climatic change during

the LGIT, the mechanisms behind such change and evidence for the development and responses of vegetation. Chapter 3 presents the study sites selected across Britain within this project, provides background to each of the study regions and highlights where previous work has been undertaken. Chapter 4 introduces the principal methods employed within this thesis. Chapters 5-8 reveal the lithostratigraphic, palynostratigraphic and climatostratigraphic results for each site within this thesis. These chapters also seek to reconstruct the climatic and environmental history of the surrounds of each of the sequences during the LGIT. Chapter 9 synthesises the climatic data across each site and provides evidence for the timing, duration and magnitudes of climatic change in Britain. The climatic data within this chapter is then compared to other climatic data from Europe and the British Isles. Chapter 10 follows the same approach as Chapter 9 but synthesises the environmental data from each site and provides evidence of vegetation change in Britain during the LGIT. Chapter 11 summarises the major findings of this research and presents directions for future study.

Chapter 2. Climatic and environmental variability across Europe during the Last Glacial-Interglacial Transition (LGIT; 16-8 ka BP)

Between the end of the last glacial (Devensian in Britain; Weichselian in Europe) and the present interglacial, the Holocene, was a period characterised by high-amplitude climatic variability (e.g. Björk et al., 1998). This includes the period associated with the Last Glacial-Interglacial Transition (LGIT; 16.0-8.0 Cal. ka BP; Lowe and NASP Members, 1995; Rasmussen et al., 2014) one of the most recent periods of climatic variability in Earth's history (Dansgaard et al., 1993). The LGIT has been sub-divided, on the basis of climatostratigraphy, with millennial to decadal climatic oscillations (Rasmussen et al., 2014) encompassing temperature variability between near glacial and interglacial conditions (Lowe et al., 2008). The LGIT is one of the most intensively studied time-periods in the Quaternary owing to: 1) the abundance of preserved sedimentological evidence which permits study at high temporal resolution (Walker et al., 2001); 2) observations that the climate and environmental system underwent large scale restructuring with clear ocean-atmosphere-terrestrial linkages and; 3) the high chronological precision achievable across multiple sedimentary archives.

Previous climatostratigraphic research suggested that millennial-scale climatic transitions are time-parallel across much of the northern hemisphere (e.g. Hughen et al., 1996). This broad synchroneity suggests common forcing mechanisms during the LGIT. However, the publication of highly-resolved, chronologically constrained sequences across wide geographic areas suggests that climatic evolution was time-transgressive at centennial-scales. For example, in the onset of the Younger Dryas (Rach et al., 2014; Muschitiello and Wohlfarth, 2015), and lagged responses to the positions of the polar front within the Younger Dryas (Brauer et al., 2008; Bakke et al., 2009; Lane et al., 2013). However, it is presently unknown how centennial-scale climatic changes are manifest across Europe. As common forcing mechanisms are thought to drive both millennial-scale and centennial-scale oscillations, climatic records reveal a complex interplay of a variety of oceanic-atmospheric-terrestrial components and are spatially heterogeneous in their impacts across Europe. This chapter seeks to review the climatic structure of the LGIT across Europe and in Britain and assess the mechanisms behind these climatic changes. Finally, this chapter presents environmental responses to observed to climatic change, across Europe during the LGIT.

2.1 Traditional European climatostratigraphies of the LGIT

Traditionally the sub-division of the LGIT was a result of the correlation of climatic periods to palynological biozones in Scandinavia (Mangerud et al., 1974; e.g. Figure 2.1)

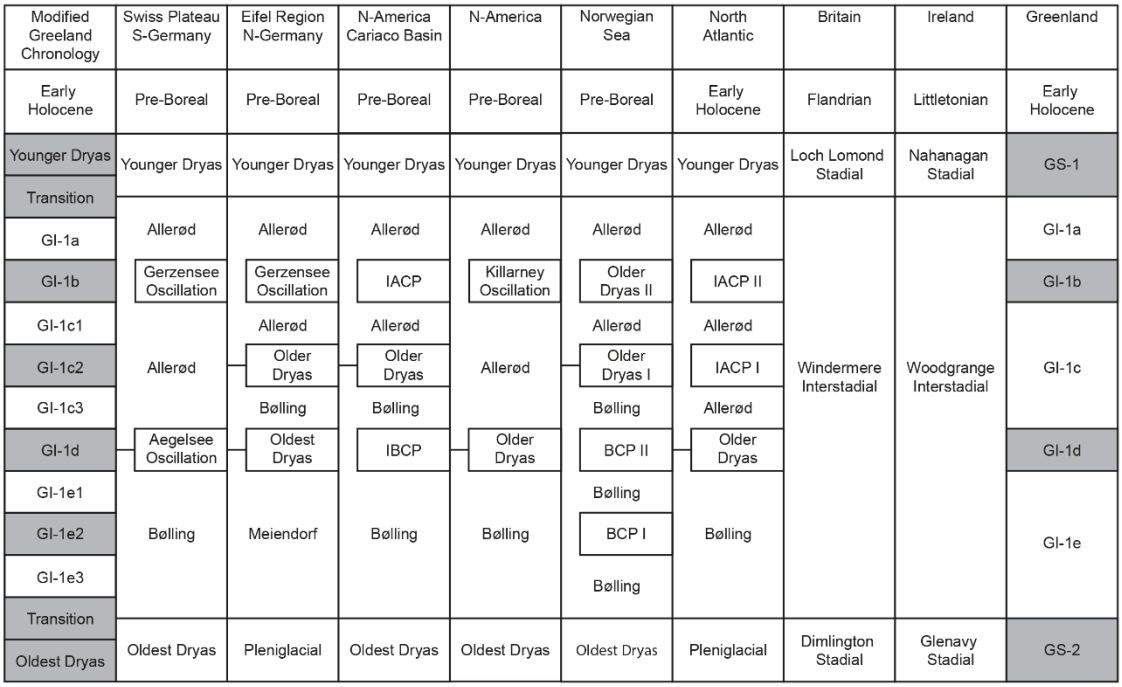

Figure 2.1 Overview of the different terminologies for different climatostratigraphic phases across the North Atlantic. This schematic highlights the assumption of synchroneity as the figure highlights that these events are thought to be broadly synchronous. Modifed from van Raden et al. (2013).

From this model the LGIT was split from the cold Pleniglacial/Oldest Dryas (>14.7 Cal. ka BP) into two warm interstadials, termed the Bølling and the Allerød which are separated by the cold Older Dryas and Younger Dryas Stadials (Figure 2.1). The period following the Younger Dryas, the current interglacial, is termed the Holocene. Through radiocarbon dating, these broad bio-zones became the basis of chronozones (Mangerud et al., 1974), and have been adopted as the chronostratigraphic model for Europe. However, subsequent studies have demonstrated that the Scandinavian scheme cannot be applied to regions beyond Scandinavia as it largely ignores climatic/vegetation complexity outside of this region.

Furthermore, in Britain, the LGIT is traditionally split into four phases, again based on lithostratigraphic and biostratigraphic associations. The first is aligned with the Pleniglacial/Oldest Dryas of Scandinavia, termed the Dimlington Stadial (Rose, 1985), this is surpassed by the warm Windermere Interstadial (Pennington, 1977), the cold Loch Lomond Stadial (Grey and Lowe, 1977), and into the current warm period the early Holocene (Figure 2.1). Like Scandinavia these stratigraphic zones have become chronozones. In both examples, the use of lithostratigraphic and/or pollen-based biostratigraphic boundaries to define different phases of Europe's history is problematic. Principally vegetation is a response variable to changing climatic parameters and will always lag the onset of climatic change (e.g. Pennington, 1986). Changes in vegetation

or lithostratigraphy are then not suitable as a defined position from which to infer changes in climatic regime. Equally, vegetation-based responses are time-transgressive across Europe (e.g. Muschitiello and Wohlfarth, 2015), reflecting spatial variability in vegetation change, however the use of a chronostratigraphic boundary implies synchronous vegetation or climatic shifts across Europe. The basis of both models is defined from bulk radiocarbon dates, which are problematic owing to a mixed carbon source, incorporating both older and younger materials, producing erroneous calibrated ages (Walker et al., 2001). Thus, the precision is often not sufficient to constrain climatic/vegetation parameters at the centennial- or decadal-scale. However, despite being ill-advised (e.g. Björk et al., 1998; Lowe et al., 2008) the nomenclature from the Scandinavian model is still routinely used. Not only do terrestrial sequences need to be locally defined but also independently constrained in time using terrestrial plant macrofossils and tephrochronology (Lowe et al., 2008).

2.2 The INTIMATE proposal- NGRIP as a European stratotype

Owing to problems of assumed synchroneity and issues with imprecise radiocarbon dating during the LGIT (Lowe and Walker, 2000; Walker et al., 2001) the INTIMATE group (INTegration of Ice, MArine, and TErrestrial records) have suggested the North Grip (NGRIP) ice-core isotopic stratigraphy, using a multi-core, multi-parameter timescale, the Greenland Ice-Core Chronology 2005 (GICC05), as a regional stratotype for climatic change during the LGIT (Lowe et al., 2008; Figure 2.2). The suggestion to use NGRIP as the regional stratotype is in part due to the precise nature of the annually resolved time-series, which at the onset of the LGIT has a maximum counting error of 186 years (Table 2.1) (Rasmussen et al., 2006; 2014), but also due to the nature of isotopic data and climatic reconstructions therein (e.g. Dansgaard et al., 1993; Johnsen et al., 2001; Rasmussen et al., 2006; Steffensen et al., 2008). Isotopic records are shown to be sensitive to climatic change from a variety of archives (Candy et al., 2011) as the isotopic ratio reflects the ratio of a chemical element with different atomic weights in precipitation (Dansgaard et al., 1964; Rozanski et al., 1993). Ice-core isotopic reconstructions are centred upon two separate parameters, $\delta^{18}O$, which in glacial ice, reflects the temperature of precipitation at formation (Johnsen et al., 1992; Dansgaard et al., 1993), and thus can be used as a palaeothermometer, and δD and δD-excess which can be used to infer temperature and changing moisture source regions (Jouzel et al., 1987; Masson-Delmotte et al., 2005; Steffensen et al., 2008). Thus, owing to both factors the record reveals a precise climatic template from which European records can be compared with (Lowe et al., 2008).

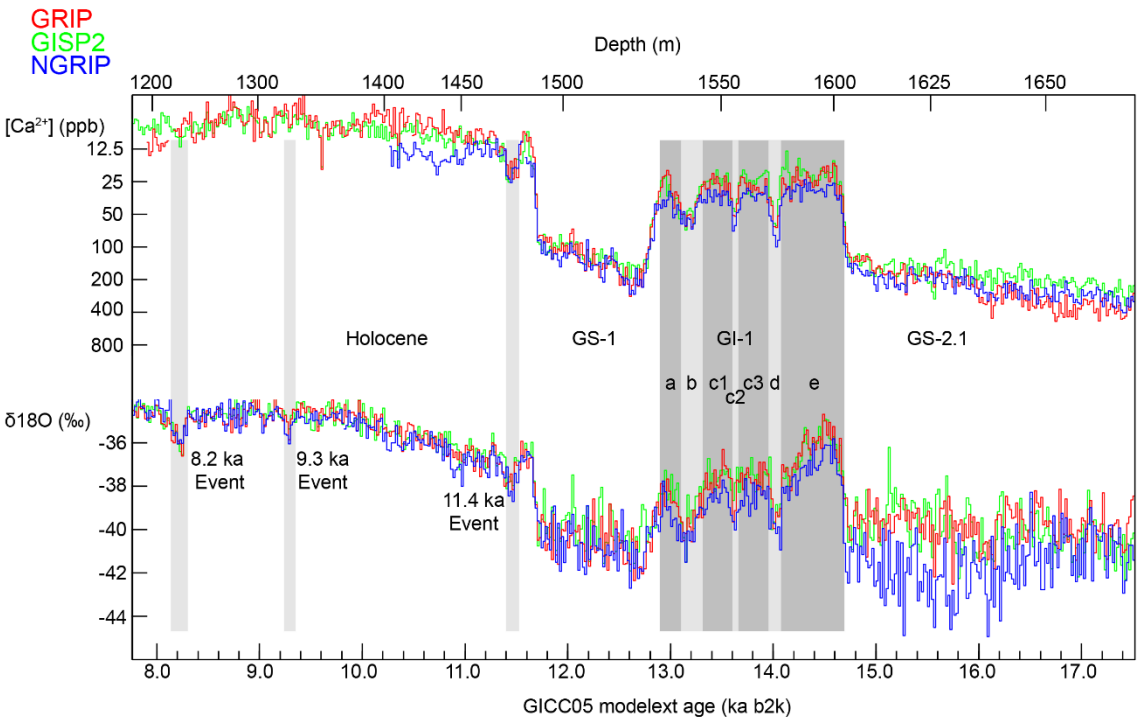

Figure 2.2 20-year average values for $\delta^{18}O$ and Ca^{2+} from the GRIP (red), GISP2 (green) and NGRIP (blue) between ca 17.2-8.0 ka years b2k. Shown are the millennial-scale climatic trends GS-2.1, GI-1, GS-1 and the Holocene; also highlighted are the high-magnitude centennial-scale climatic oscillations that characterise the LGIT and form the GICC05 'event' stratigraphy. Adapted from Rasmussen et al. (2014).

This record forms an event stratigraphy for the region, through the numbering of stadials and interstadials (Björk et al., 1998; Lowe et al., 2008; Figure 2.1). In this format, cold stadial periods are termed Greenland Stadials (GS) with the warm interstadials termed Greenland Interstadials (GI). Therefore, the late Pleniglacial of Scandinavia is termed, GS-2.1a (17.48-14.69 ka b2k). This is then succeeded by GI-1 (14.69-12.89 ka b2k) a comparative of the Bølling/Allerød. The next phase of millennial-scale cooling in association with the Younger Dryas, termed GS-1 (12.89-11.7 ka b2k) and the final period, the early Holocene (11.7-8 ka b2k) (Figure 2.2). Despite this general stratigraphy, GI-1 and the early Holocene have further sub-divisions based on oscillations in the climatic signature which are centennial or decadal in duration. The warm phases are termed: GI-1e, GI-1ciii, GI-1ci and GI-1a whilst the cooler phases, which in some instances reveal similar magnitudes of cooling as stadial climatic transitions, are termed GI-1d (14.07-13.95 ka b2k), GI-1cii (13.66-13.6 ka b2k) and GI-1b (13.31-13.09 ka b2k) (Figure 2.2). During the Holocene a climatic oscillation between 11.5-11.4 ka b2k is termed the 11.4 ka event which is comparable to the Pre-Boreal Oscillation (PBO) in Europe (Björk et al., 1997; Rasmussen et al., 2007). Other early Holocene climatic oscillations may be present in Greenland. However, they are commonly only identified in single ice-core records and may relate to temperature change, but also contain accumulation rate changes (Rasmussen et al., 2007; Blockley et al., 2018) and have

Table 2.1 Onset and duration of abrupt events within the GICC05 timescale. The depth of the event as recorded in NGRIP is highlighted with the maximum counting error for these depths. sequence. Modified from Lowe and Walker (2014).

Event	NGRIP Depth (m)	Age (a b2k) and definition uncertainty	Maximum counting error (years)
End of 9.3 ka BP event	1322.88	9240 +30/ -10	68
Start of 9.3 ka BP event	1331.65	9350 +10/ -20	70
End of 11.4 ka BP event	1476.16	11,400	96
Start of 11.4 ka BP event	1482.32	11,520	97
Start of Holocene	1492.45	11,703 +/- 4	99
Start of GS-1	1526.52	12,896 +/- 4	138
Start of GI-1a	1534.5	13,099	143
Start of GI-1b	1542.1	13,311	149
Start of GI-1c1	1554.75	13,600	156
Start of GI-1c2	1557.08	13,660	158
Start of GI-1c3	1570.5	13,954	165
Start of GI-1d	1574.8	14,075	169
Start of GI-1e	1604.64	14,692 +/- 4	186
Start of GS-2.1a	1669.09	17,480	330

not been defined formally. Nonetheless these include climatic deviations from the trend at 11.1 ka, 10.3 ka and 9.95 ka b2k (Rasmussen et al., 2007). Therefore, the regional stratotype has been argued to contain a template for climatic change across Europe. While a highly-resolved record containing mechanistically understood climatic proxies, the ice-cores represent a single locale in the northern hemisphere and to fully explore both drivers and response to abrupt climatic change it is also necessary to understand climatic evolution from different regions, enabling an understanding of climate phasing and the duration of climatic events. This will be considered below.

2.3 The climatic structure of the LGIT in Europe

Following the establishment of the stratotype it is necessary to look at records from across Europe to reveal the climatic structure of the LGIT. Whilst the focus will be centred

upon the British Isles, it will also reference the climatic structure of Europe. This structure will form the basis to reference the palaeobotanical structure in Britain and Europe.

2.3.1 GI-1/Bølling-Allerød/Windermere Interstadial

The transition from GS-2.1 into GI-1 is shown within the NGRIP record by a change to depleted δ*D* and enriched $\delta^{18}O$ relating to an approximate 10°C increase in air temperature, and northerly shift in source waters following the melting of sea-ice and reorganisation of atmospheric circulation (Steffensen et al., 2008). The circulation change occurs rapidly over three years (Steffensen et al., 2008). Climatic warmth continues throughout GI-1 until GS-1, however peak warmth is associated with GI-1e (Rasmussen et al., 2006; 2014) with air temperatures then following a declining trend.

In Europe and the British Isles, the principal method for obtaining quantifiable temperature estimates is through the use of chironomid-inferred summer temperature reconstructions (C-IT) (Figure 2.3) (e.g. Brooks and Birks, 2000a; Heiri et al., 2007; Brooks et al., 2012; 2016; Brooks and Langdon, 2014) and Coleopteran Mutual Climatic Ranges (MCR) (e.g. Bishop and Coope, 1977; Atkinson et al., 1987; Lemdahl, 1991; Elias and Matthews, 2014). Both palaeoecological proxies provide a means from which summer temperature estimates can be gained. Winter temperature estimates can also be gained from Coleopteran records although the errors are often large. Evidence from the latter suggests that across Europe from the preceding cold stage into the Interstadial, temperatures rose by 5-10°C (Coope and Lemdahl, 1995; Coope et al., 1998). In Britain, the climatic optimum is revealed during the early stages of the Windermere Interstadial (Walker et al., 1993a; 2003), presumably correlated with GI-1e in Greenland. This is also the case with C-IT records, where peak summer temperatures are observed at the onset of the Interstadial (Figure 2.3) (Brooks and Birks, 2000a; Bedford et al., 2004; Lang et al., 2010; Brooks et al., 2012). This is in contrast to C-IT records across Europe which suggest that the Allerød period is warmer, comparable to GI-1ciii/GI-1ci (Figure 2.3), than the onset of the Interstadial (e.g. Brooks and Birks, 2000b; Heiri et al., 2007; Larocque-Tobler, 2010; Wohlfarth et al., 2017). This discrepancy with peak warmth across Europe points to spatial and temporal heterogeneity in climatic development. From the above records, the observation of a climatic gradient across Europe is also noted, with generally warmer summer temperatures in central and eastern Europe and cooler summer temperatures in association with sequences close to the ocean or at higher latitudes or altitudes. Not only does this demonstrate regional climatic gradients but also the time-transgressive nature of climatic evolution (Brooks and Langdon, 2014).

In contrast to these palaeoecological reconstructions, sedimentological evidence, using stable isotopes, reveal a different picture (Figure 2.4). As the controls on isotopic data are complex (Chapter 4) stable isotopic analyses need careful consideration to unpick the climatic signal. However, as the overarching influence is the isotopic composition of meteoric water, which is affected by Rayleigh Fractionation (Dansgaard, 1964; Rozanski et al., 1993; Leng and Marshall, 2004) reflecting the rates of vapour condensation with temperature, a temperature component is implied, specifically mean annual temperatures through seasonal averaging. Like NGRIP, stable isotopic records from Britain and Europe, reveal rapid climatic amelioration between the Pleniglacial/Dimlington Stadial and the Bølling/Windermere Interstadials (e.g. Marshall et al., 2002; van Asch et al., 2012a; Figure 2.3). In contrast to the palaeoecological methods, isotopic reconstructions reveal peak annual warmth throughout the Interstadial, with continental sequences showing a GI-1e correlation (e.g. von Graffenstein et al., 1999; Lotter et al., 2012; van Raden et al., 2013; Larsen and Nygaard, 2014). Whilst sequences closer to the moisture source suggest peak annual warmth in association with GI-1c or the Allerød (e.g. Marshall et al., 2002; van Asch et al., 2012a). Owing to the relative paucity of isotopic reconstructions it is presently unknown whether continental and maritime differences are true manifestations of climatic signatures.

Throughout the Interstadial, across Europe, high-magnitude climatic oscillations akin to the GI-1d, GI-1cii and GI-1b climatic oscillations in Greenland are observed. These oscillations appear in both palaeoecological and sedimentological proxies, with summer temperature declines between 0.5-4.9°C (Figure 2.3) (Brooks and Birks, 2000a; Bedford et al., 2004; Heiri et al., 2007; Brooks et al., 2012; Wohlfarth et al., 2017) towards the onset of the Interstadial. This is associated with the GI-1d climatic oscillation in NGRIP (14.07-13.95 ka b2k), the Older Dryas in the Scandinavian model, and is usually the most commonly identified centennial-scale oscillation across Europe. At certain continental sequences, Gerzensee (Lotter et al., 2012), the temperature increases by ca 1.5°C. In Britain, this oscillation is the strongest across multiple proxy sources. This is contrasted with the latter Interstadial climatic oscillation which is in association with GI-1b in the Greenland (13.31-13.09 ka b2k) or the Inter-Allerød Cold Period (IACP).

Across Britain and Europe this oscillation exhibits a summer temperature decline of 1.0-3.0°C (Figure 2.3) (Brooks and Birks, 2000a; Bedford et al., 2004; Heiri et al., 2007; van Asch et al., 2012a; Wohlfarth et al., 2017). In Britain, this summer temperature oscillation demonstrates a reduced magnitude compared to the former climatic oscillation; however, the climatic oscillation appears stronger than the former in Europe (Figure 2.3; 2.4) (e.g. von Graffenstein et al., 1999; Heiri and Millet, 2005; Heiri et al., 2007; Wohlfarth et al.,

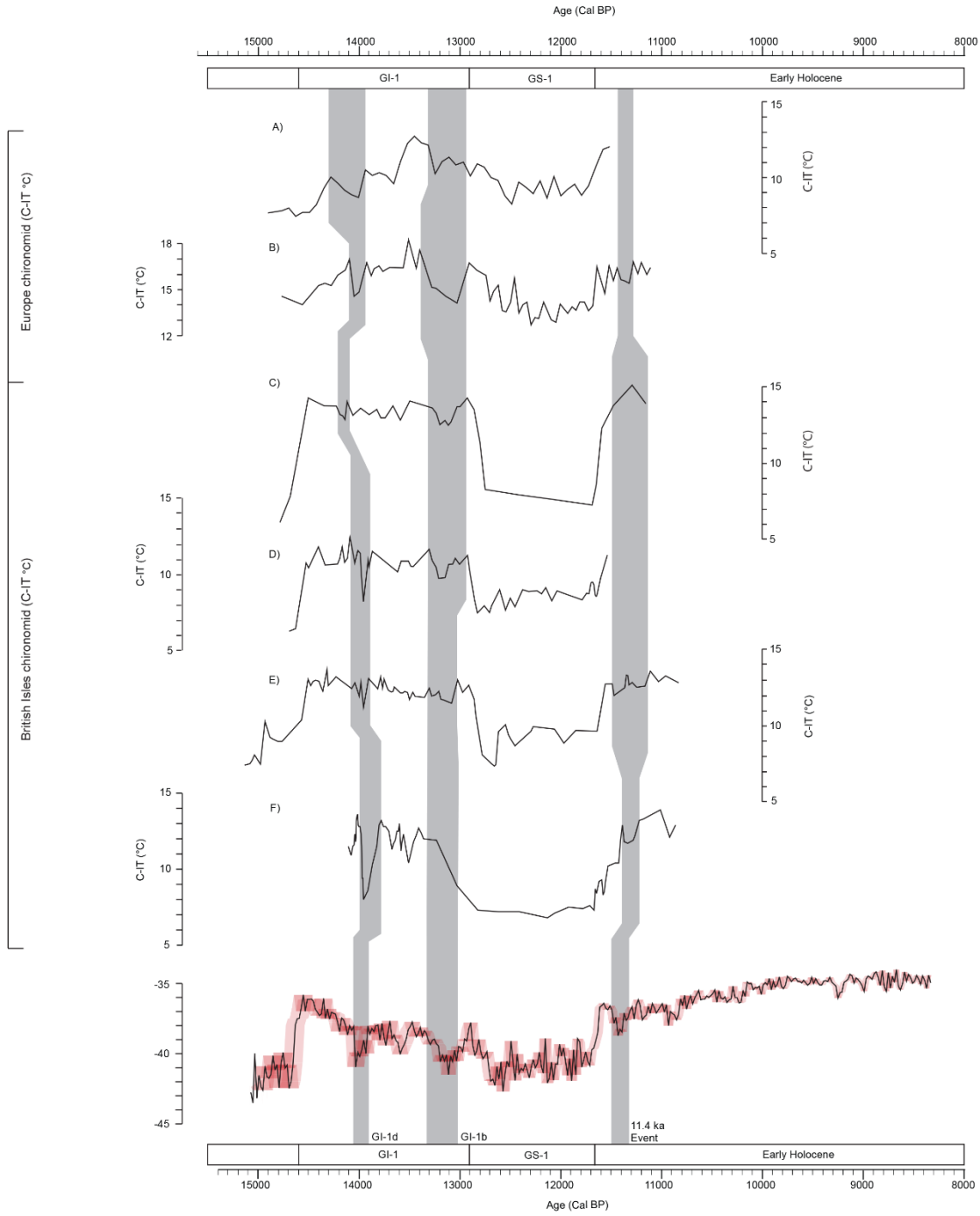

Figure 2.3 A compilation of selected chironomid inferred summer temperature reconstructions from Britain and Europe during the LGIT. C-ITs from A) Hässeldala Port (Watson, 2008); B) Hijkermeer (Heiri et al.,2007); C) Fiddaun (van Asch et al., 2012a); D) Whitrig Bog (Brooks and Birks, 2000a); E) Hawes Water (Bedford et al., 2004); and F) Abernethy Forest (Brooks et al., 2012). Also shown is the NGRIP isotopic stratigraphy, with the abrupt climatic oscillations (GI-1d, GI-1b and 11.4 ka events) shaded with a grey bar. Of these sequences only Hässeldala Port and Abernethy Forest are chronologically constrained. The age model from Abernethy Forest has less precision after the GI-1d event. The remaining sequences have been aligned for illustrative purposes only.

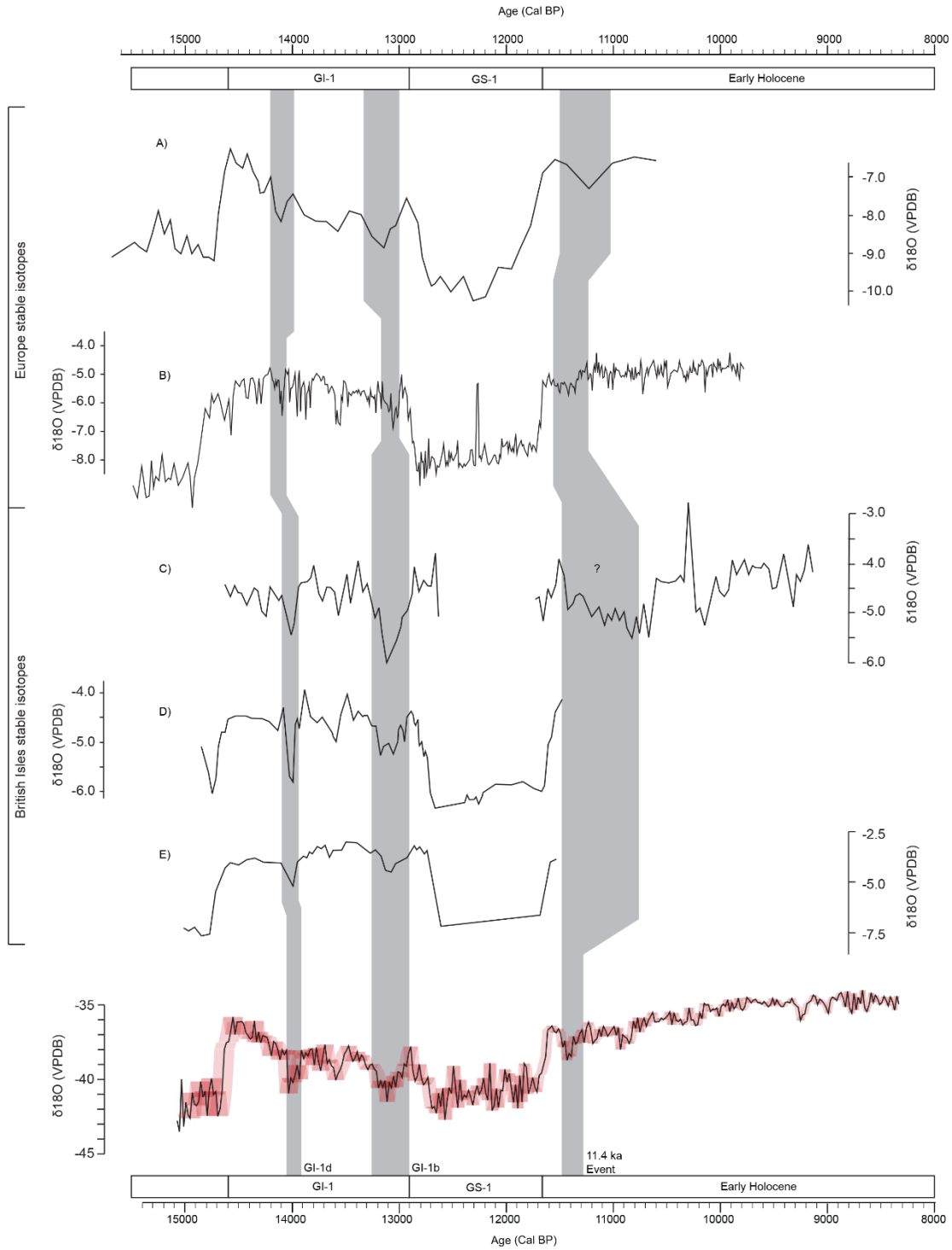

Figure 2.4 A compilation of selected $\delta^{18}O$ reconstructions from Britain and Europe during the LGIT. $\delta^{18}O$ from A) Gerzensee (Lotter et al., 1992); B) Ammersee (von Graffenstein et al., 1999); C) Crudale Meadow (Whittington et al., 2015); D) Hawes Water (Marshall et al., 2002); and E) Fiddaun (van Ash et al., 2012a). Also shown is the NGRIP isotopic stratigraphy, with the abrupt climatic oscillations (GI-1d, GI-1b and 11.4 ka events) shaded with a grey bar. None of these sequences demonstrate a robust chronology, with Ammersee 'wiggled' to the ice core records. As the chronologies are insufficient, the placing of these sequences together is for illustrative purposes only. All analyses are performed on authigenic carbonates barring Ammersee, where $\delta^{18}O$ observations were conducted on ostracod tests meaning this record and the other records are not directly comparable.

2017). During the GI-1/Bølling-Allerød/Windermere Interstadials the expression of abrupt climatic events is therefore complex and spatially heterogeneous (Brooks and Langdon, 2014; Moreno et al., 2014) with sequences recording variable magnitudes of climatic change.

Unfortunately, these rapid climatic oscillations often suffer from a lack of independent chronology, thus it is impossible to understand the spatial complexities of these climatic deteriorations; including phasing and synchroneity. In Britain, the GI-1d-type oscillation is often pinned between the Borrobol Tephra (14,098±47 Cal. BP; Turney et al., 1997; Bronk Ramsey et al., 2015) and the Penifiler Tephra (13,939±66 Cal. BP; Matthews et al., 2011; Bronk Ramsey et al., 2015). Thus, the isochronous deposition of tephra affords greater certainty in the timing of the climatic event. However, the latter Interstadial climatic oscillation often goes unconstrained because there is no pinning tephra in Britain or associated radiocarbon dates (although the Laacher See Tephra (LST) (12,944±40 Cal. ka BP; Bronk Ramsey et al., 2015) does pin the GI-1b oscillation across Germany and central Europe). Thus, the events are often 'wiggled' to the GICC05 timescale and assumed synchronous (e.g. Whittington et al., 2015). This is problematic and a greater emphasis needs to be placed on generating robust chronologies during the LGIT, to better understand complex climatic associations and evolution across a wide area.

2.3.2 GS-1/Younger Dryas/Loch Lomond Stadial

The transition from GI-1 into GS-1, in Greenland, is defined by an abrupt shift in δD (+ 2-3 ‰) occurring within one year (Steffensen et al., 2008), reflecting a rapid change in atmospheric circulation. In contrast, the cooling associated with $\delta^{18}O$ depletion occurred over ca 213 years, reflecting the progressive thermal decline into GS-1 despite rapid atmospheric reorganisation (Steffensen et al., 2008).

The transition into GS-1/Younger Dryas/Loch Lomond Stadials is well represented in palaeotemperature proxies. From across Britain and Europe summer and winter temperatures are markedly depressed (Coope and Lemdahl, 1995). Greatest summer temperature declines and coldest absolute temperatures (between 4.5 and 6.0°C) are seen in the polar latitudes of Norway (e.g. Brooks and Birks, 2000b; Birks et al., 2014) with central Europe showing reduced temperature declines and higher reconstructed temperatures (8.0-15°C) (e.g. Heiri and Millet, 2005; Heiri et al., 2007; Samartin et al., 2012a; van Asch et al., 2012b; Wohlfarth et al., 2017). In contrast, Britain sits between these extremes, with summer temperature declines of between 3 and 6°C (Figure 2.3), of which the strongest temperature declines are observed in the northern latitudes of Britain (e.g. Brooks and Birks, 2000a; Brooks et al., 2012; van Asch et al., 2012a).

Throughout this phase winter temperatures are suggested to be much more severe (Atkinson et al., 1987; Renssen and Isarin, 1998). Whilst this is generally accepted a recent study, modelling temperatures derived from plant macrofossil indicator species, suggests that warm summers, harsh winters and short growing seasons characterised the Stadial (Schenk et al., 2018). However, in this paper, the upper thermal range limits of the warmest plant taxa were calculated from Finland. This may produce greater skew in the data and temperatures should be based on a wide geographic area and, incorporate cold adapted taxa. Equally, mostly aquatic taxa were used in Schenk et al. (2018) and these would be affected by additional parameters other than temperature, e.g. water depth, nutrient status, level of disturbance. Therefore, the indicator approach, as used in this study, may not define summer conditions during the Stadial. Additionally, many of the sequences used had poor chronological control, with the placement of the warmest sample based on biostratigraphy. Nonetheless, whilst issues may be present in Schenk et al. (2018) climatic warmth is suggested during GS-1, which contrasts with C-IT data and warrants further testing.

Where highly-resolved annual records exist, the spatial and temporal complexity of GS-1/Younger Dryas/ Loch Lomond Stadial climates can be better understood (e.g. Brauer et al., 2008). The onset of the Stadial, has previously been shown to be time-transgressive across Europe between 12.7-13.16 Cal. ka BP (Muschitiello and Wohlfarth, 2015). Equally, varved sequences covering the LGIT, like those of Meerfelder Maar (e.g. Brauer et al., 1999; Rach et al., 2014) show that hydrological change across Europe, obtained through compound specific biomarker δ*D* sources, lag behind the onset of GS-1 in Greenland by ca 170 years (Figure 2.5) (Rach et al., 2014). This 170-year difference relates to a continent-wide delay in aridification characterising the stadial following the displacement of westerly storm tracks with the build-up of sea-ice in the North Atlantic (Figure 2.5) (Rach et al., 2014).

Whilst the onset of the Stadial is shown to be time-transgressive, recent studies have also revealed mid-Stadial climatic complexity (e.g. Bakke et al., 2009; Lane et al., 2013). Following the southward migration of the polar front during the Stadial (Isarin et al., 1998) a reduction in varve thickness and greater X-ray fluorescence (XRF) Ti counts occur prior to the deposition of the Vedde Ash at Meerfelder Maar (12,240±40 varve years (Brauer et al., 1999; Lane et al., 2013; Figure 2.6). This has been suggested to relate to greater spring snow-melt in western Germany (Lane et al., 2013). This XRF-Ti signal is also observed at Kråkenes (Bakke et al., 2009) although it occurs 20 years after the deposition of the Vedde Ash in Norway (Figure 2.6) (Bakke et al., 2009; Lane et al., 2013). This mid-YD shift reflects the northward migration of the polar front in Europe,

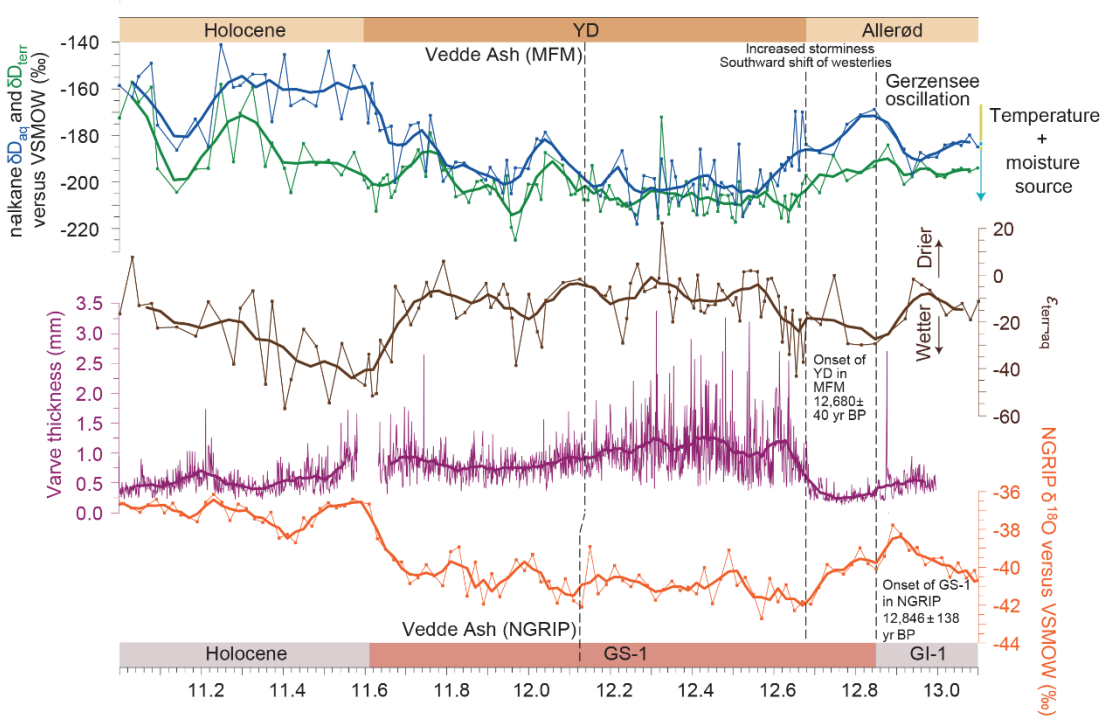

Figure 2.5 Evidence of the time-transgressive nature of climatic change at the onset of the Younger Dryas between Greenland and Meerfelder Maar, Germany. The principal data sources are δ*D* reconstructions from both aquatic (blue) and terrestrial (green) biomarker sources with a mathematical function (brown line) highlighting changes in aridity. The change in NGRIP $\delta^{18}O$ occurs 170 years prior to the onset of aridification in west Germany reflecting the time taken for shifts in sea-ice and westerly winds. Purple shows changes in varve thickness throughout the record. The position of the Vedde Ash is also highlighted. Modified from Rach et al. (2014).

taking approximately 120 years to shift from a lower to a higher latitudinal position (Figure 2.6). The climatic expression of this event, in northern Europe, thus shows a transition from a cold and stable early Younger Dryas to a warmer unstable second half of the Younger Dryas (Bakke et al., 2009). The diachronous observations reveal the asynchroneity of climatic change (Lane et al., 2013), which may also relate to late glacier advance during the Loch Lomond Stadial in Scotland (e.g. MacLeod et al., 2011). It is presently unknown whether this mid-Younger Dryas climatic variability is observed in Britain. Nonetheless, lagged climatic parameters, highlight time-transgressive climatic change across Europe and the need for robust chronologies (Lowe et al., 2008). It is presently unknown whether this observation holds true for the less studied centennial-scale climatic events, including the abrupt events during GI-1/Bølling-Allerød/Windermere Interstadial and the early Holocene.

2.3.3 Early Holocene

The Pleistocene-Holocene boundary is placed at 11.7 ka b2k based on the GICC05 timescale (Walker et al., 2009; Rasmussen et al., 2014). The transition from cold climates of GS-1 into the current interglacial is shown by depletion in δ*D* and enrichment in $\delta^{18}O$

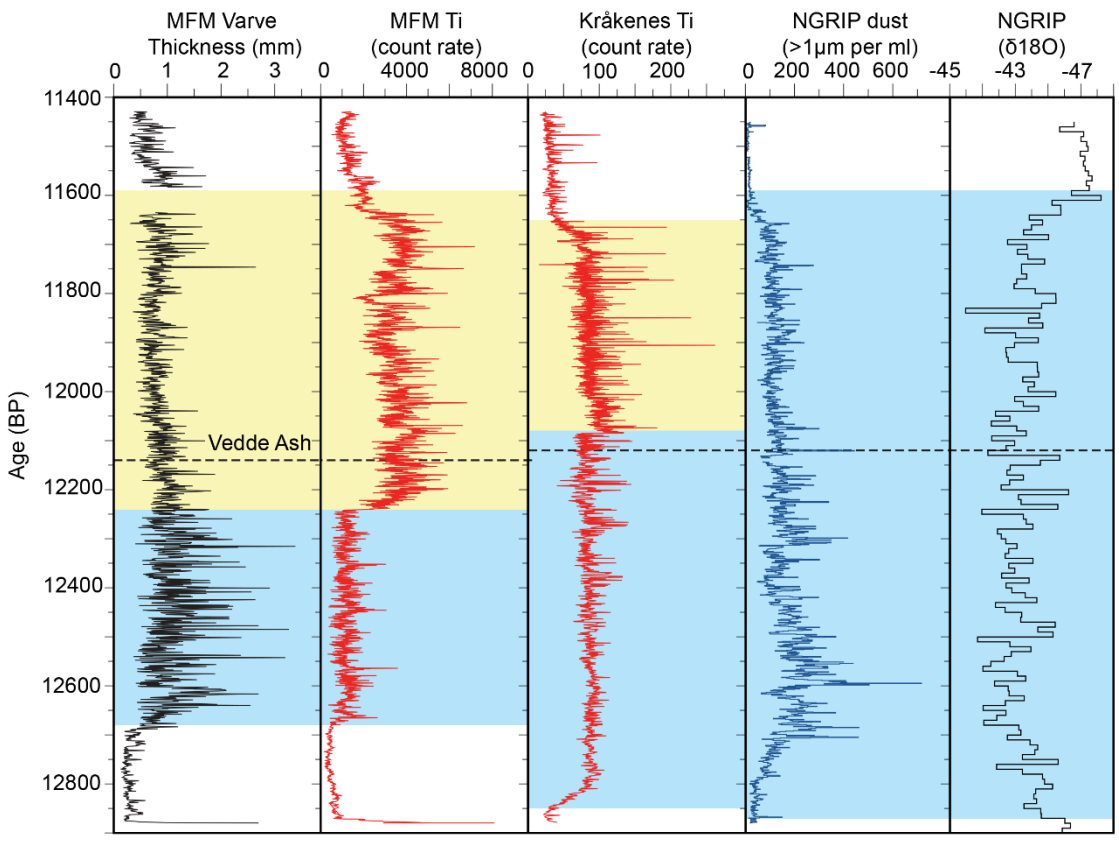

Figure 2.6 Evidence of the time-transgressive nature of climatic change during the mid-Younger Dryas period. The change in varve thickness and Ti at Meerfelder Maar precedes that at Kråkenes by approximately 120 years based on the position of the Vedde Ash. This relates to AMOC strengthening and the northward migration of the polar front from Germany earlier than Norway. Adapted from Lane et al. (2013).

within NGRIP. The former once again occurred rapidly, within three years, with the warming trend associated with $\delta^{18}O$ occurring within 60 years (Steffensen et al., 2008).

Climatic proxy records from across Britain and Europe reveal this amelioration by a 3-9°C increase in summer temperature proxies (Figure 2.3) (e.g. Brooks and Birks, 2000a; Brooks et al., 2012). Unfortunately, across many sequences, mean annual temperature ($\delta^{18}O$) reconstructions are not possible during the Stadial owing to unsuitable core material (e.g. Candy et al., 2016). However, where isotopic reconstructions are possible the isotopic stratigraphy shows rapid amelioration, with isotopic enrichment between 2 and 4 ‰ (Figure 2.4) (Lotter et al., 1992; Marshall et al., 2002). The remainder of the Holocene is then relatively stable across Europe. Equally at Meerfelder Maar, enrichment in leaf wax δD reveals climatic warming but also the return of locally moist conditions (Figure 2.5) through the decline of sea-ice and subsequent migration of westerly storm tracks (Rach et al., 2014). This transition in northern Europe has also been shown to lag Greenland by 100-150 years (Lohne et al., 2014).

Although the Holocene has been described as relatively stable, abrupt, centennial-scale climatic events can be observed. The 11.4 ka BP event, formally identified in Greenland, exhibits isotopic depletion of approximately 2 ‰ (Rasmussen et al., 2007; 2014). Another may relate to the 11.1 ka event, which is not formally defined in Greenland (Rasmussen et al., 2007) but has been identified in terrestrial sequences (Blockley et al., 2018). Unfortunately, many sequences with quantified temperature constructions do not extend into the early Holocene, nevertheless, in Britain some sequences do reveal minor cooling of ca 0.5-1°C (e.g. Lang et al., 2010; Brooks et al., 2012; Whittington et al., 2015; Brooks et al., 2016) although these remain chronologically unconstrained.

At 10.3 ka BP one additional climatic deterioration is identified. This deterioration is aligned with the deposition of the Saksunarvatn Ash; 10,200±70 Cal. BP; Lohne et al., 2014). At 10.3 ka BP a phase of greater ice-rafting is observed across the northern North Atlantic (Bond et al., 1997; Dahl et al., 2002) with glacier advances (Dahl et al., 2002) and lacustrine changes also observed (Björk et al., 2001). The evidence suggests a phase of cold temperatures centred upon 10.3 ka BP, which relates to a glacial Erdalen Event (Dahl et al., 2002). Nevertheless, quantified temperature estimates through this period are lacking allied to a lack of terrestrial evidence for this proposed event (e.g. Björk et al., 2001). During the earliest Holocene, there is a lack of chronologically constrained palaeoclimatic data, therefore the expression of Holocene climatic variability is largely unknown. A key goal for researchers should be to generate Holocene palaeoclimatic data to understand climatic evolution during the current interglacial. The remainder of the Holocene is outside of the scope of this review and will not be considered further.

2.4 Mechanisms of climatic change

The purpose of this section is to provide an overview of the different forcing mechanisms affecting climatic change during the late-Quaternary. Many different drivers affect the Quaternary climatic structure, some of which are relevant on wide glacial-interglacial timescales (e.g. Imbrie et al., 1992) whilst others may affect climate on a more regional or hemispheric scale (e.g. Shackleton, 2000). Through these mechanisms it is noted that climatic change relates to a complex feedback system linking the ocean-atmospheric-terrestrial realms (Broecker and Denton, 1989). The different drivers of change presented within this section include: orbital forcing, oceanic forcing and solar variability. A complete review of climatic forcing is beyond the scope of this thesis; however, a focus will be placed on forcing during the LGIT.

2.4.1 Orbital forcing

Numerous authors have wrestled with the theories underpinning glacial-interglacial cycles (Martinson et al., 1987; Imbrie et al, 1992; 1993; Ruddiman, 2006). However, Milankovitch suggested that external forcing, in varying orbital parameters, drive changes in the total amount of radiation received at a specific point on the surface of the Earth. Hays et al. (1976) demonstrated summer insolation, driven by linear changes in the configuration of Earth's axis (obliquity and precession) operating on 41 ka and 21 ka cycles respectively, were critical to the initiation and termination of glacial phases. Despite the approximate 100 ka periodicity of glacial phases (Figure 2.7), the shape of Earth's orbit (eccentricity), operating on a 100 ka cycle, is not thought to exhibit dominant control on glacial cyclicity. This has been suggested to relate to the impact of eccentricity on total insolation (Ruddiman, 2006). For example, at 65°N, where the greatest landmass exists, total radiation receipt is driven by precession and obliquity (Berger, 1978; Berger and Loutre, 1991). The termination of the last glacial cycle is also controlled by orbital variation, however, the series of climatic changes during the LGIT cannot be attributed to orbital forcing as the pacing of insolation changes outweigh the pacing of millennial- and centennial-scale climatic change during this period. Nonetheless, the termination of the last glacial phase, which saw the waning of northern hemisphere ice sheets, coincides with a period of rising insolation at 65°N (Figure 2.7) (Denton et al., 2010). This increase in insolation led to the initiation of complex feedback mechanisms; including oceanic freshwater flux and ocean circulation perturbations, which further impact: sea-ice abundance, cold anomalies, ocean ventilation and greenhouse gas changes (Cheng et al, 2009). These changes are not solely a northern hemisphere phenomenon, with changes occurring on inter-hemispheric scales through the action of the 'Bipolar Seesaw' (Broecker, 1998). The 'bipolar seesaw' is a potential mechanism driving climatic change following the termination of the last glacial period; with northern and southern hemisphere climatic change anti-phased (Blunier et al., 1998). The influence of oceanic forcing in this instance appears key.

2.4.2 Oceanic forcing

As observed in Section 2.3 overprinted on the longer term glacial-interglacial cycles are periods of abrupt climatic change akin to the millennial to centennial-scale climatic oscillations (Stocker, 1999). Abrupt here is defined as a shift in the climate system that occurs at a faster rate than the processes controlling the change in the system (Alley and Ágústsdóttir, 2005). Abrupt change is characteristic of $\delta^{18}O$ records from ice-cores (e.g. Johnsen et al., 2001) with a clear 'saw-toothed' pattern between warm interstadial phases interspersed with cold stadial episodes. These events, termed Dansgaard/Oeschger (D/O) events stretch from the LGIT to the last interglacial (Bond et

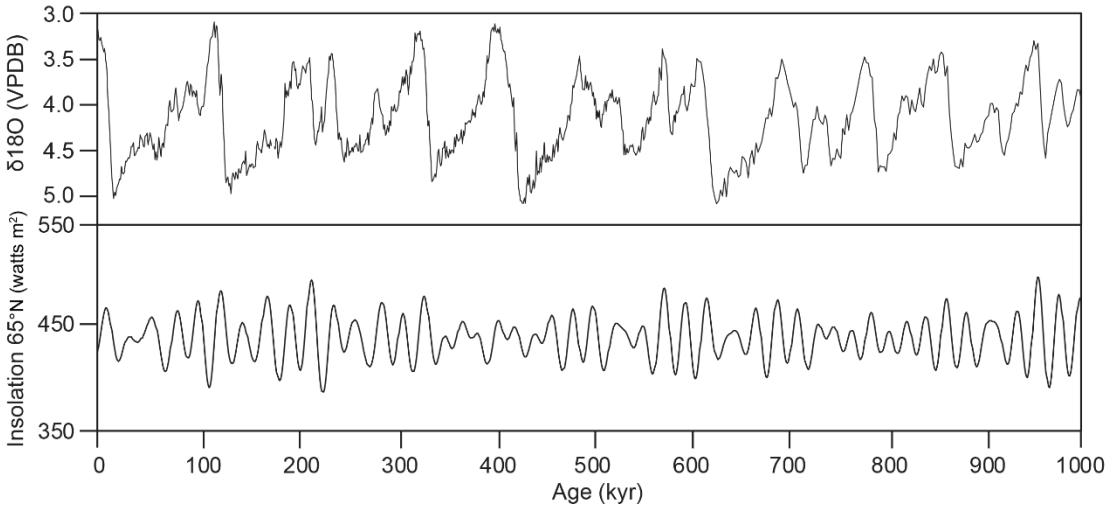

Figure 2.7 The LR04 benthic oxygen isotopic recorded, stacked covering the last 1 ma (Lisiecki and Raymo, 2005) showing the approximately 100 ka pacing of ice age cycles with depleted values revealing Interglacials and enriched values revealing glacial phases. The lower box contains insolation values covering the same time-period at 65°N (Berger and Loutre, 1991). A link between peak insolation and the termination of glacial phases is clear.

al., 1993; 1999). Thus, the LGIT is the last D/O event recorded; all of which are said to be driven by variations in ocean circulation (e.g. Clark et al., 2001) specifically the strength of Atlantic Meridional Overturning Circulation (AMOC) and the effect this has on heat transfer to the northern latitudes (Figure 2.8).

Heat transfer to the North Atlantic is dominated by the salty surface flow of the Gulf Stream driven by prevailing westerly wind direction and strength (Lowe and Walker, 2014). As this salty water cools, upon reaching the northerly high latitudes, it undergoes buoyancy loss, a loss of heat to the atmosphere and sinks (North Atlantic Deep Water (NADW) formation) following greater salinity concentrations (Figure 2.8). The returning limb returns to the lower latitudes as basal flow (Buckley and Marshall, 2016). These two flows, surface and basal, are termed the Atlantic Meridional Overturning Circulation (AMOC). AMOC is inter-hemispheric with deep-water formation observed in the Southern Ocean, termed Antarctic Bottom Water (ABW). The role of AMOC is pivotal in oceanic and subsequent atmospheric heat transfer (Figure 2.8) to the north from the equator which results in a warmer northern hemisphere than southern hemisphere (Buckley and Marshall, 2016). It has been argued that disruption or weakening of this conveyor reduces latent heat transfer and results in climatic shifts akin to those observed during the LGIT (Clark et al., 2001). This is underlined by the three operational modes of AMOC (Clark et al., 2002). Mode one relates to a strong AMOC and NADW formation in the Nordic Seas (interstadial/interglacial mode); mode 2 relates to weakened AMOC and NADW formation in the sub-polar Atlantic (stadial mode) whilst Heinrich mode relates to

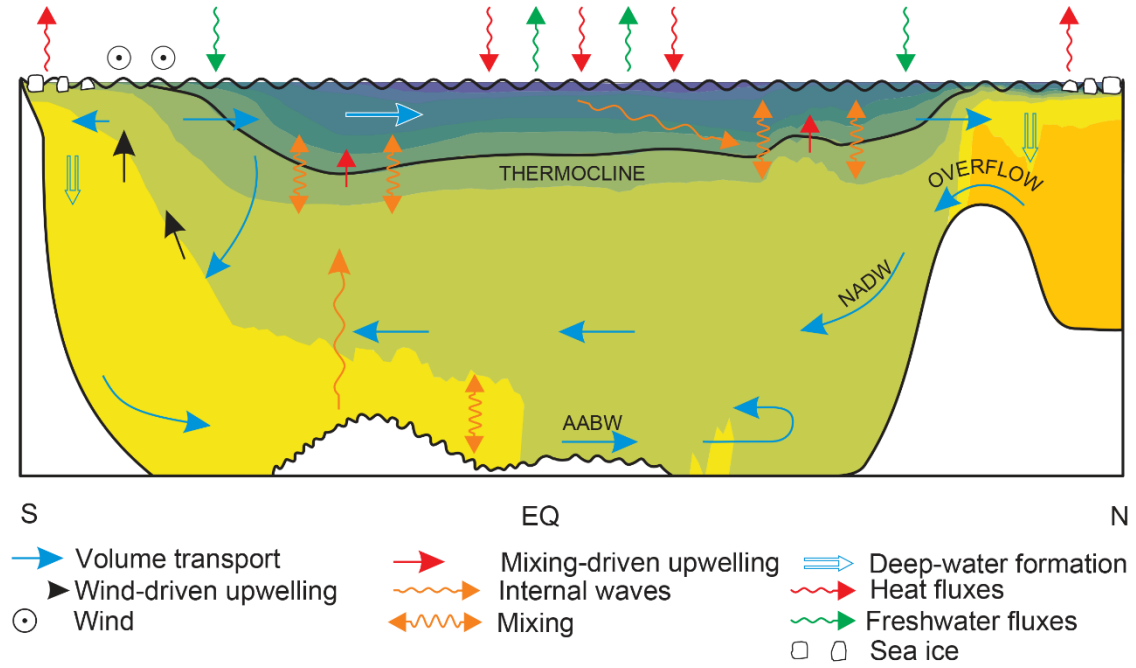

Figure 2.8 A schematic of Atlantic Meridional Overturning Circulation (AMOC) showing surface flow towards the north heat exchange with the atmosphere and North Atlantic and Antarctic Deep/Bottom Water (NADW; AABW) formation. Shading give the approximate thermal stratification of the Atlantic. From Kuhlbrodt et al. (2007).

the cessation of NADW formation with the North Atlantic filled with Antarctic waters (glacial mode) (Figure 2.9) (Rahmstorf, 2002).

During interstadial mode, AMOC operates as above and transports warmth to northern Europe, however, during the latter two modes the cessation of northward heat transport bring cool/cold oceans thus climatic conditions to Europe (Figure 2.9). Variability between AMOC modes that characterise the LGIT, is suggested to relate to freshwater perturbations (Clark et al., 2001; Broecker, 2006; Thornally et al., 2010). However, the source of this freshwater input is disputed; some favour freshwater influence from the Laurentide Ice Sheet (Broecker et al., 1989; Licciardi et al., 1999; Clark et al., 2001), whilst others favour freshwater flux from Baltic sources (Muschitiello et al., 2015), the northern Arctic (Tarasov and Peltier, 2005) or the Southern Ocean (Deschamps et al., 2012; Golledge et al., 2014). Modelling studies of the effect of freshwater perturbations suggest that NADW formation is curtailed through dilution of salty waters and forcing AMOC into the Stadial or Heinrich mode, which reduces meridional heat transport leaving cool waters in the northern high latitudes (Clark et al., 2001). Therefore, through the dissolution of cool waters climatic conditions become cooler in Europe. A possible scenario is postulated below for the LGIT.

During the last deglaciation, following an increase in insolation at 65°N following the Last

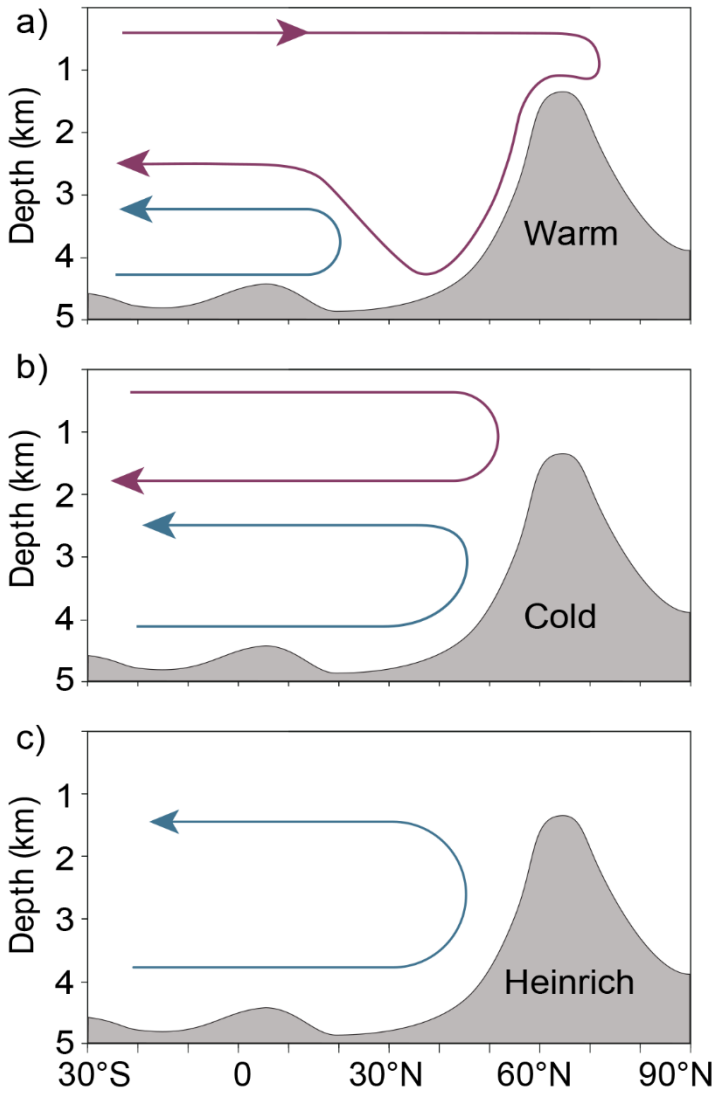

Figure 2.9 A schematic of the three discussed modes of AMOC. a) Interglacial mode with strong deep-water formation; b) Stadial mode of AMOC with cooler conditions and a greater influence of lower deep ocean flow; and c) Heinrich mode with no deepwater formation and subsequent cooling. These modes are suggested during different climatic phases during the LGIT following freshwater perturbation. Adapted from Rahmstorf (2002).

Glacial Maximum at 21 ka BP (Mix et al., 2001) it is suggested that ice-sheet melting caused a freshwater flux disrupting NADW formation and a shutdown in AMOC. Feedbacks through the release of CO_2 from ice-sheets caused further warming still and kept AMOC in Stadial mode. At 14.65 Cal. ka BP, the northern hemisphere abruptly warmed. This may relate to continued warming of the southern oceans causing freshwater flux terminating ABW formation (Deschamps et al., 2012; Golledge et al., 2014) in this instance termed Meltwater Pulse 1a (MWP-1a) highlighting the effects of the Bipolar Seesaw (Broecker, 1998) or relates to a pre-conditioning of the northern seas, for NADW formation, through continued ice rafting in the north during Heinrich Stadial 1 (17.5-15 ka BP) (Bond et al., 1999; Stanford et al., 2011). Both scenarios are

therefore plausible for the abrupt restart of AMOC and heat transport at 14.65 Cal. ka BP.

Once AMOC was established in interglacial/interstadial mode, short freshwater Perturbations, which force AMOC into a different mode, define GS-1/Younger Dryas/Loch Lomond Stadial cooling and centennial-scale oscillations, GI-1d, GI-1cii, GI-1b during the LGIT (Broecker et al., 1985; Broecker, 1989; Clark et al., 2001; Tarasov and Peltier, 2005; Thornally et al., 2010; Muschitiello et al., 2015). However, positive feedbacks associated with the suppression of AMOC act to intensify phases of cold climate across Europe. For each of the climatic deterioration episodes observed in Europe, summer temperature declines and phases of isotopic depletion probably coincided with enhanced sea-ice production (Isarin et al., 1998; Brauer et al., 2008). This sea-ice then caused greater atmospheric effects following the southerly displacement of the polar front (Bakke et al., 2009) with seasonal changes in Europe suggested to relate to an amplification of westerly winds bringing cold and dry climatic conditions. During the mid-YD, strengthening of AMOC is suggested to break up sea-ice bringing the polar front northwards once more (Bakke et al., 2009; Lane et al., 2013). These effects are clearly recordable in highly-resolved studies (Brauer et al., 2008; Bakke et al., 2009; Lane et al., 2013). Variability in AMOC clearly affects European climate on a variety of scales with positive feedback mechanisms amplifying negative climatic excursions. It is postulated that AMOC variability is the key mechanism in controlling centennial climate oscillations during the LGIT.

2.4.3 Solar variability

One final mechanism that may explain the abrupt climatic shifts identified in northern Europe is solar variability. Variability in Total Solar Irradiance (TSI) result from cyclic variations in magnetic activity from the sun (Engels and van Geel, 2012). Variations in solar activity relate to an 11-, 22-, 88-, 200-year and greater length cycles (Chambers and Blackford, 2001). The measurement of solar variability is straightforward with historical records, however further back in time solar variability is measured through Beryllium-10 (^{10}Be) in ice-core or tree ring records. When solar activity is high, cosmic ray strength is lower and ^{10}Be production and flux is lower. During low solar activity however, cosmic ray strength is higher and ^{10}Be production and flux is higher (Steinhilber et al., 2009; 2012). The effects of solar variability are well documented for the late Holocene, where sun-spot and grand solar minima cause a depression of European temperatures through the weakening of the polar vortex with a cold ozone layer forming a negative North Atlantic Oscillation (NAO) (Mauquoy et al., 2002; Martin-Puertas et al., 2012). However, the effects of solar variability during the LGIT are unknown, but

potentially important in the knowledge that minor solar variability can affect European climate (Engels and van Geel, 2012). Following the elucidation of ^{10}Be in ice-core records, Adolphi et al. (2014) suggest that solar variability may have impacted European climate at the termination of the last glacial through a negative-NAO phase. Pressure anomalies, possible through the Laurentide ice-sheet are proposed for 'wave-breaking' events which drive a southerly migration of the westerly wind system (Adolphi et al., 2014), bringing cool temperatures to Europe but moisture to Greenland. If this is accepted, it is possible that solar variability and consequent NAO-likes change may influence the dominant climatic regime on centennial to decadal-scales and be an overprinting force on oceanic and orbital forcing during the LGIT.

2.5 The vegetation structure of the LGIT in Europe

Following the delineation of climatic variability across Europe, vegetation change during the LGIT can be considered. Vegetation changes are defined by two contrasting hypotheses; the disequilibrium and the dynamic equilibrium hypotheses (Prentice et al., 1991). The former is dominated by autogenic drivers, including; migrationary lags, differential seed dispersal, population dynamics and plant-plant interactions, whereas, the latter proposes that allogenic climatic forcing is the dominant control of vegetation (Seddon et al., 2015). Several authors have aligned themselves to these theories, for example the equilibrium (e.g. Godwin,1975) or the disequilibrium hypotheses (e.g. Davis, 1983; Huntley, 1991), however, it is probable that these two hypotheses are not mutually exclusive and as Huntley (1991) postulates, all taxa respond individualistically to climate, producing ecological complexity. Moreover, Williams et al. (2011) suggest that observed vegetation changes could be a direct result of allogenic forcing mediated through specific vegetative traits, including plant-plant interactions (Jeffers et al., 2011). Despite this theoretical framework, little work has been undertaken to assess the influence of climate on vegetation during the LGIT. Whilst it has been suggested that high-magnitude climatic change can impact system-wide vegetation (Birks and Ammann, 2000) few studies have demonstrated evidence of climatic driver and vegetation response, specifically related to centennial-scale climatic deteriorations. This section highlights known vegetation change during the LGIT across Britain and Europe and presents some of the key challenges that are addressed in this thesis.

2.5.1 GS-2.1/Pleniglacial/Dimlington Stadial

Where competent basins exist, sediments older than ca 14.6 ka BP are associated with degraded thermophilous pollen types (e.g. *Pinus*, *Quercus*) (Ammann and Lotter, 1989; Lotter et al., 1992; Litt and Stebich, 1999). Strong evidence of cold climate indicates that the degraded thermophilous pollen are a product of sedimentological reworking and the

influx of far travelled components (*Pinus*) and therefore, do not reflect local growth within the catchment. This phase is often not observed in Britain due to the lack of sedimentation during the Dimlington Stadial and the lack of vegetation within the landscape (e.g. Hunt and Birks, 1982; Mayle et al., 1997). Thus, whilst many British palaeobasins did not accumulate sediments prior to the Interstadial; Europe was characterised by sparse vegetation coverage (Litt and Stebich, 1999).

2.5.2 GI-1/Bølling-Allerød/Windermere Interstadial

During the GI-1/Bølling-Allerød/Windermere Interstadials, climatic amelioration is reflected by the colonisation of lacustrine systems by aquatic plant taxa (Pennington, 1986). Across Britain and Europe, similar terrestrial taxa colonise catchments at the onset of the Interstadial. These taxa, pioneering and often heliophilic, for example *Artemisia*, Poaceae, Cyperaceae, *Rumex*, *Salix* and Saxifragaceae, colonise bare rock or deglaciated substrates, and thrive in low nutrient conditions (Figure 2.10; 2.11). These taxa form part of a tundra, low alpine, and steppic vegetation community across Europe (e.g. Pennington et al., 1972; Birks, 1973; Watts, 1977; Lowe and Walker, 1977; Bennett, 1983; Litt and Stebich, 1999; Hoek and Bohncke, 2002). As established in Section 2.4 the climate was warm across Europe during the earliest phases of the Interstadial, however pioneering low-lying herbaceous vegetation is not thermophilic and an anti-phase relationship between climate and vegetation is thought to exist at the onset of the LGIT. Thus, at this time, the dominant vegetation control appears to be edaphic conditions and habitat suitability with climate exerting an indirect influence.

Following initial colonisation, vegetation reconstructions diverge across Europe reflecting variable migration rates, temperature variability and local edaphic conditions (Walker et al., 1994; Hoek and Bohncke, 2002). Across central Europe the pioneering phase is replaced by initially *Betula*, in prostrate form, then by open *Betula* woodland, and open *Betula* and *Pinus* woodland (Figure 2.10) (Lotter et al., 1992; Hoek, 1997; Litt and Stebich, 1999; Hoek and Bohcnke, 2002; Rey et al., 2017). This is directly contrasted to sequences across Britain and Ireland. Commonly, the pioneering phase in Britain is replaced by either *Empetrum nigrum* dominated heathland or *Juniperus* scrubland (Figure 2.11) (Watts, 1977; Lowe and Lowe, 1989; Walker and Lowe, 1990; Day, 1996; van Asch et al., 2012a). Previously the establishment of *Juniperus* scrub was suggested to indicate the onset of the interstadial in Britain (e.g. Walker et al., 1993a), however, it is established that climatic warmth (Section 2.4) encompasses a phase of pioneering vegetation; suggesting that the establishment of *Juniperus* is delayed from the onset of the WI. Further, the exact timing of *Juniperus* and *Empetrum* development is poorly understood but appears variable in sites around Scotland, with sequences on the Isle of

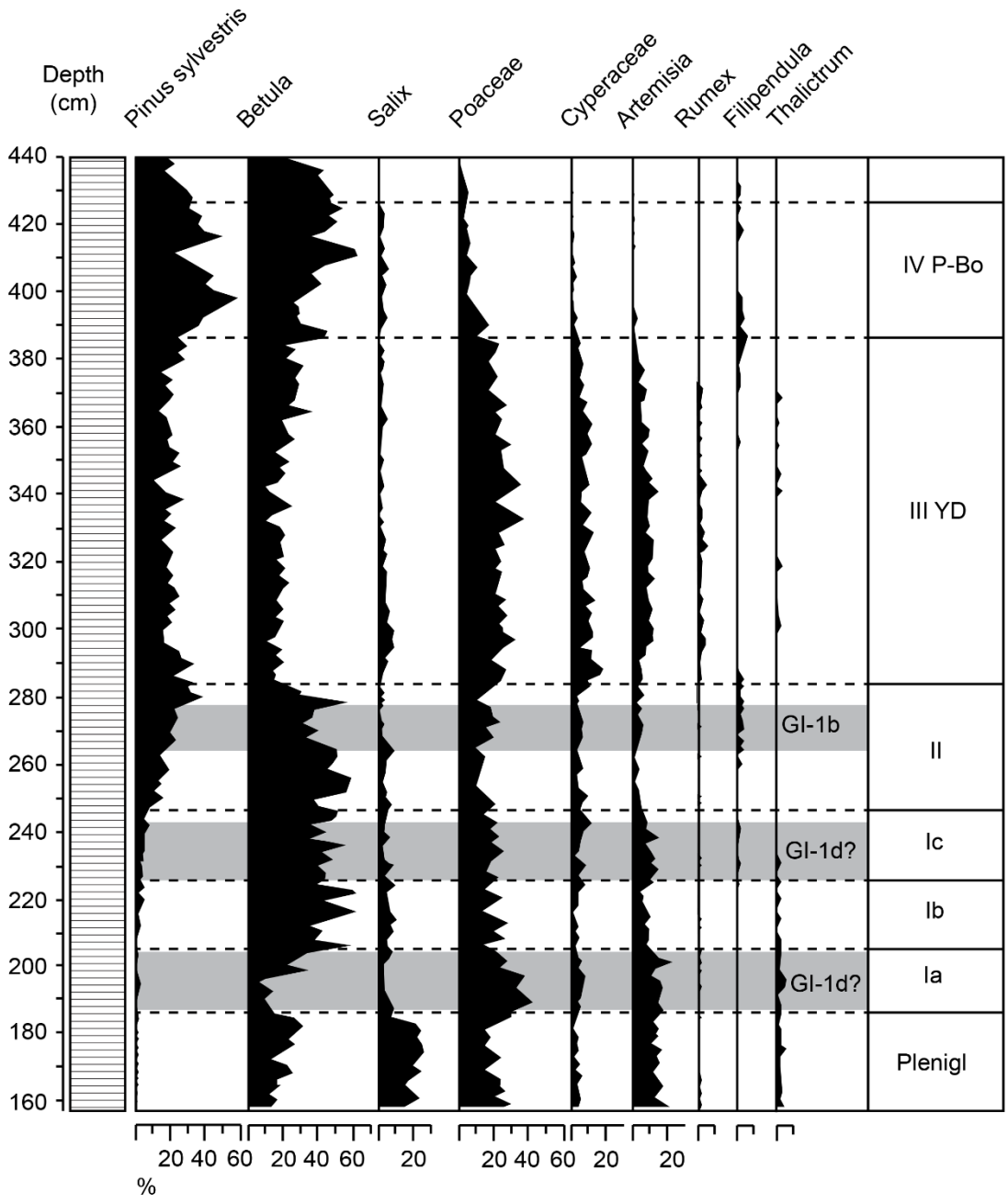

Figure 2.10 Selected terrestrial pollen percentage diagram from Meerfelder Maar, Germany. This diagram highlights the shifts in assemblage from the Pleniglacial phase in Europe, the Interstadial, Stadial and into the early Holocene (shown on the right of the diagram. Also highlighted are the areas where vegetation changes are noted in relation to abrupt climatic oscillations. Adapted from Litt and Stebich (1999).

Mull displaying a concurrent *Juniperus*/*Empetrum* rise (Lowe and Walker, 1986), although on the Isle of Skye *Juniperus* precedes the rise in *Empetrum* (Walker and Lowe, 1990). As *Juniperus* thrives on well drained mature soils (Lowe and Walker, 1986) edaphic conditions may be key for the proliferation of *Juniperus* scrub. Nonetheless commonly occurring taxa alongside *Juniperus* include *Salix*, *Filipedula,* Poaceae and *Betula cf. nana*, reflecting an increase in taxon diversity during the Interstadial.

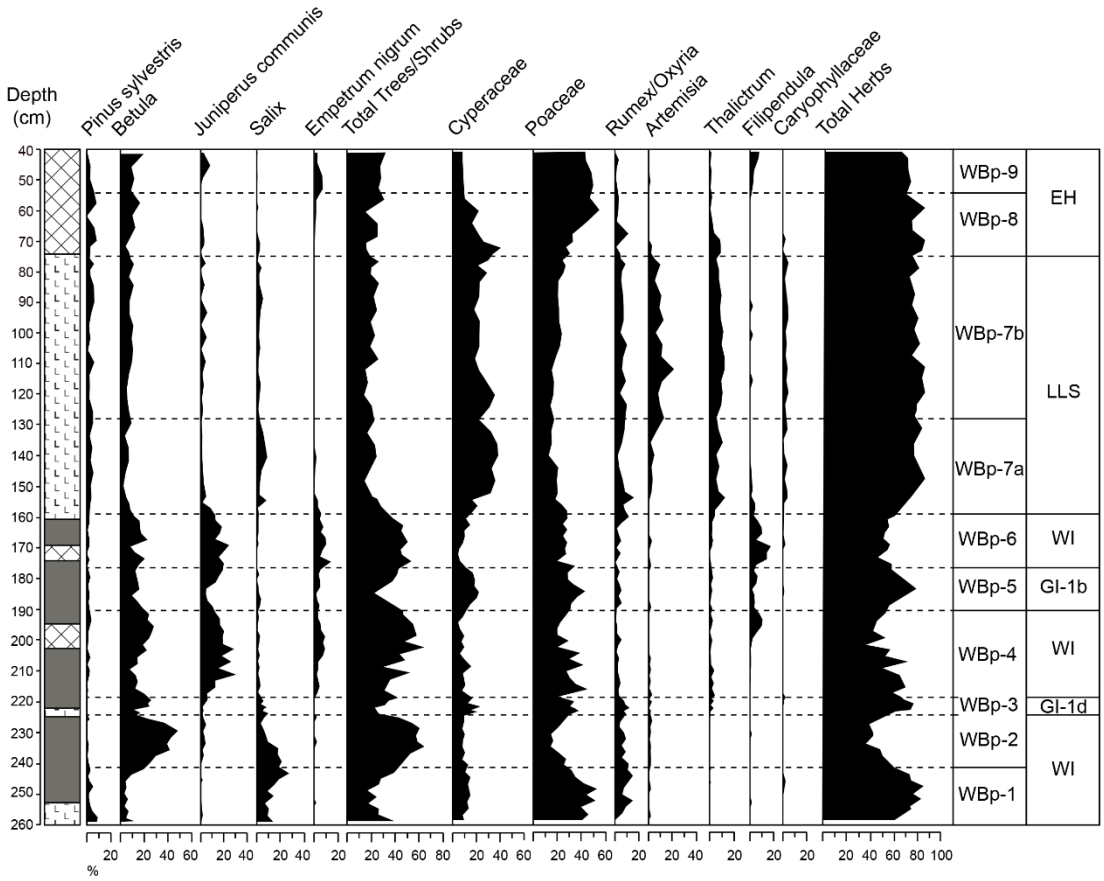

Figure 2.11 Selected pollen percentage diagram from Whitrig Bog, south-east Scotland, representing commonly occurring taxa. This diagram highlights the shifts in assemblage from the onset of the Windermere Interstadial, through the Loch Lomond Stadial into the early Holocene alongside local pollen assemblage zones. Clearly visible are changes in association with abrupt climatic events from Greenland. In this instance trees and shrubs are replaced by Poaceae, *Artemisia* and *Rumex*. Adapted from Mayle et al. (1997).

Succeeding the heath and scrubland phase the common taxon expanding across Britain is *Betula*. In England, this expansion is formally attributed to tree *Betula*, likely *B. pubescens* with the development of open *Betula* woodland supporting regionally specific herb taxa (Day, 1996). The development of *Betula* woodland indicates warm climates favourable to *Betula* migration and expansion. However, Pennington (1986) postulates that soil maturity is likely important to explain the observed 500 to 1500-year lag between the onset of climatic amelioration and the establishment of *Betula* in northern Britain. These lags are not as prevalent in the east of England (e.g. Birks, 1989) owing to the European land connection and direction of *Betula* migration following its refugial position in Europe (Willis et al., 2000). In his review of the vegetation of northern Europe, Walker et al. (1994) indicated that *Betula* woodland did not extend into Scotland. However, this is contentious as certain sites including Loch Etteridge and Abernethy Forest (Walker, 1975; Birks and Matthewes, 1978) show elevated percentages of *Betula* perhaps indicative of small copses where local conditions were favourable for growth. Thus, further studies are required that detail whether *Betula* grew in Scotland during the

Windermere Interstadial. Regardless, this contentious issue is contrasted with Ireland and Orkney where *Betula* woodland is not established (e.g. Bunting, 1994; van Asch et al., 2012a). The lack of *Betula* woodland during the Interstadial is surprising given expected soil development and predominantly warm conditions (Section 2.4). However, grazing pressures from herbivores have been suggested for the lack of tree presence in Ireland (Bradshaw and Mitchell, 1999). On mainland Orkney, *Betula* is not established due to barriers to colonisation including competition and harsh environmental conditions (e.g. Bunting, 1994; 1996). Nonetheless, vegetation development at the millennial-scale shows that vegetation across Britain is predominantly out of phase with peak climatic conditions (early Interstadial/mid-Interstadial).

The general vegetation structure of European sequences is well documented, however, as the climatic record reveals centennial-scale oscillations (Section 2.4) it is prudent to assess whether vegetation responds to these oscillations. As aforementioned the relationship between climate and vegetation is often unknown owing to the lack of paired climate/vegetation reconstructions from the same sequence. However, although scarce, revertences can be observed in pollen data superimposed on general vegetation development. Vegetation revertence is defined here by Table 2.2. Although pollen is a proxy for vegetation, based on the work of Watts (1970), Tipping (1991a) and Edwards and Whittington (2010), who inferred periods of climatic change based on phases of palynological change, the criteria from Table 2.2 are being used here to infer phases of landscape or vegetation change. Thus, where a change in pollen is noted it is assumed to relate to a change in vegetation types in the surrounds of sequences.

During the earliest phases of the Interstadial, comparable to the GI-1d (14.07-13.95 ka b2k) climatic oscillation, the Aegelsee or Older Dryas period in Europe is characterised by regionally variable vegetation change splitting the Bølling/Allerød Interstadials. In Switzerland, the Aegelsee oscillation is manifest by an increase in non-arboreal pollen (NAP), specifically *Artemisia,* coincident with a loss of *Betula* pollen (Lotter et al., 1992; Ammann et al., 1994), suggesting outward migration and southerly treeline movement (Wick and Tinner, 1997). In Germany, a similar scenario is observed (Litt and Stebich, 1999; Figure 2.10), however in the southern latitudes of Germany this regressive phase does not occur (de Klerk, 2008). Elsewhere in Europe, this is again characterised by increased NAP but with *Juniperus*, *Salix* and *Helianthemum* (Hoek and Bohncke, 2002; Heiri et al., 2007; Mortensen et al., 2011). In contrast, in Britain this period is not formally defined (Tipping, 1991a), however, a regressive phase can be identified early within the Interstadial, coinciding with a phase of clastic sedimentation (Figure 2.11) (e.g. Mayle et al., 1997; Candy et al., 2016). Depending on latitudinal position and variability in taxon

Table 1.2 Criteria for identifying a palynologically inferred revertence during the LGIT. Originally defined by Watts (1970) updated by Whittington and Edwards (2010).

Criteria for defining vegetation revertences during the LGIT
1) Pollen flora counted and identified to a good modern standard; clearly distinct from the flora identified in underlying and overlying sediments.
2) Clear evidence of a climatic reversion.
3) Revertence clearly identified in a number of pollen spectra; including number of spectra.
4) Relative changes in sedimentology, plant macrofossils or other stratigraphic indicators.
5) Evidence for a short-lived climatic deterioration; changes in quantified palaeoclimatic reconstructions.

migration, this phase shows a decline *Betula* pollen, perhaps *B. nana*, with an increase in open herbaceous pollen and disturbance indicators, including *Artemisia*, *Rumex*, Poaceae, Cyperaceae and *Helianthemum* (Figure 2.11) (e.g. Bartely. 1976; Walker, 1982; Walker and Lowe, 1990; Day, 1996; Mayle et al., 1997; Jones et al., 2002). Across Europe then variable palynological evidence exists for a period of centennial-scale vegetation change, with an increase in disturbance indicators and those associated with a tundra community which reflects the climatic deterioration between ca 14.02-13.9 Cal. ka BP.

A second phase of regression can be identified within the Allerød period in Europe, associated with the GI-1b climatic oscillation (Section 2.4), termed, in Europe, the Inter-Allerød cold period (IACP) or the Gerzensee oscillation (Lotter et al., 1992). During this oscillation, in Switzerland, the pollen signal shows a loss of *Betula* pollen with an increase in *Pinus* (Wick, 2000) with no associated increase in NAP (Lotter et al., 1992). In Denmark a similar pattern is observed (Mortensen et al., 2011), on the contrary, at Meerfelder Maar in Germany, an increase in Poaceae is observed and presumed to reflect the expression of the Gerzensee oscillation in this location (Figure 2.10) (Litt and Stebich, 1999). Greater confidence in assigning this oscillation to the Gerzensee oscillation through the identification of the Laacher See Tephra (LST) (12,944±40 Cal. ka BP; Bronk Ramsey et al., 2015) provenanced from the Eifel Volcanic Field (van den Bogaard, 1995) sitting above this revertence, supporting the assumption of GI-1b comparability. Vegetation change must be older than this isochron and is older than the associated climatic deterioration due to lagged responses of vegetation to climatic

change, more so, if the climatic evolution is time-transgressive across Europe (e.g. Lane et al., 2013).

In Britain, this revertence may be observed in certain records, however in contrast to the early Windermere Interstadial revertence, the style of vegetation response is dissimilar. Principally, *Artemisia* is not recorded amongst the pollen taxa (e.g. Mayle et al., 1997; Figure 2.11). However, reductions in *Betula* are noted across England and Wales, which points to an opening of *Betula* woodland, with replacement taxa largely consisting of Poaceae (e.g. Bartley, 1962; Walker, 1982; Day, 1996; Figure 2.11) Contrastingly, sequences in Scotland appear to reveal a greater presence of *Rumex* during this revertence (Pennington et al., 1972; Walker and Lowe, 1990) highlighting a potential vegetation gradient across Britain for the GI-1b-type climatic event. Despite the suggestion of a late WI vegetation revertence in Britain showing a different environmental response, vegetation communities are commonly associated with a latitudinally variable open-grassland or steppe-type assemblage (Figure 2.11). This variability may relate to the different magnitudes of climatic change, or entirely localised effects, however owing to the lack of paired reconstructions, this is unknown. As a result vegetation reconstructions are often incorrectly compared to the nearest climatic source and the local climatic effects are largely ignored (e.g. Walker et al., 2012). Further, despite the number of pollen analytical investigations in Britain during the LGIT, few reveal vegetation changes in response to interstadial climatic events. Therefore, regional complexities of vegetation change at the centennial-scale is derived from a low number of high-resolution reconstructions. To better characterise vegetational changes across Britain a greater number of high-resolution reconstructions are required from across a wide spatial area.

2.5.3 GS-1/Younger Dryas/Loch Lomond Stadial

Following the decrease in temperature that typified the Stadial (between 12.9-11.7 ka BP GICC05 ice-core years), the vegetation dynamic experiences a marked change. Further the type of vegetation community established across Europe depends on latitudinal and longitudinal position, and dominant climatic regime. For example, across the Swiss Alps and Germany, the vegetation retains an element of the tree taxa that persisted towards the latter stages of the Interstadial, including *Pinus* (Figure 2.10) (Lotter et al., 1992; Litt and Stebich, 1999; Ammann et al., 2000; Litt et al., 2001). In the central latitudes of Europe including the lowlands of the Netherlands, Belgium and Denmark, *Pinus* is still recorded but less so than in southerly locations, but *Betula*, both prostrate and tree are also recorded (Hoek and Bohncke, 2002; Heiri et al., 2007; Mortensen et al., 2011). Whilst variability in arboreal pollen is noted, all sequences show

an increase in non-arboreal pollen (NAP) principally in heliophilic taxa associated with disturbed ground and arid climates, including *Artemisia*, Poaceae and *Salix* (Hoek, 2001). These low-lying herbaceous taxa occur in greater quantities in northern latitudes.

Across Britain, all thermophilic taxa decline and are replaced by open ground herbaceous vegetation (Figure 2.11) (Poaceae, Cyperacaee, Caryophyllaceae) and by taxa characteristic of disturbed/unstable ground, upon which periglacial processes operate (*Artemisia*, *Rumex*, Saxifragaceae, *Selaginella*). These assemblages constitute to an Arctic/alpine or herbaceous tundra community (Walker et al., 1994). Whilst greater percentages of herbaceous vegetation are observed for the higher latitude and higher altitude sequences in Scotland (Lowe and Walker, 1977; Birks and Matthewes, 1978) it is also noted that greater percentages of *Artemisia* are observed during the latter phases of the Stadial in Scotland (e.g. Pennington et al., 1972; Lowe and Walker, 1977; Tipping, 1991b; Walker and Lowe, 1990) this trend may highlight a greater aridification across Scotland during this phase as *Artemisia* is a xeric herb (Walker, 1975). In support of this, modelling studies suggest that the latter half of the Loch Lomond Stadial is more arid than the former at higher latitudes (Isarin et al., 1998; Bakke et al., 1998). In contrast, lower latitude sequences from England and Wales reveal greater *Artemisia* earlier in the Stadial (e.g. Bartley et al., 1976; Hunt and Birks, 1982; Walker, 1982) suggesting a hinge point between the English lowlands and Scottish Highlands. In comparison, sequences from England and Wales also demonstrate higher percentages of *Betula* pollen throughout the Stadial (Walker, 1982; Day, 1996). This may relate to the localised presence of tree birch in these lower latitude sequences, with warmer conditions in sheltered localities (Mayle et al., 1999), however it is also likely that greater *Betula* is a product of either reworking or the continued presence of *Betula nana* on the landscape (Walker, 1982).

In contrast to the vegetation development during the Interstadial, the vegetation dynamic during the Stadial clearly responds to the climatic deterioration in a predictable and directional manner. Therefore, vegetation response to this millennial-scale climatic deterioration seemingly conforms to the dynamic equilibrium hypothesis, with greater abundances of Arctic/alpine communities present where the strongest climatic deteriorations and lowest absolute temperatures are felt. Whilst secondary vegetation controls likely modulate vegetative presence, including but not limited to edaphic conditions, exposure and disturbance (Walker et al., 1994) the dominant control on vegetation during this event is climate.

2.5.4 Early Holocene

Across Europe, the vegetational succession sequence for the early Holocene is well documented. Rapid climatic amelioration (Section 2.4) causes a transition from an open herbaceous tundra community to a diverse species-rich grassland, often like the earliest Interstadial with increases in aquatic plant taxa including *Myriophyllum*, *Potamogeton* and *Nuphar lutea* (Walker et al., 1994). In Europe, where tree taxa were present during the preceding stadial, concentrations of *Betula* and *Pinus* rise with concomitant losses in NAP highlighting increased landscape stability (Figure 2.10) (Litt and Stebich, 1999). Subsequently, Europe is characterised by open then closed *Betula* woodland with *Pinus* also becoming an established component of the boreal forest (Hoek, 2001; Hoek and Bohncke, 2002). Later during the Holocene this is then surpassed by *Populus tremula* (Hoek and Bohncke, 2002) and *Corylus* (Walker et al., 1994).

Vegetation development in Britain is somewhat different, largely a product of the traditionally defined thermophilous taxa becoming established following climatic amelioration during the earliest Holocene. In Britain, following the establishment of a species-rich grassland at the onset of the Holocene, *Juniperus communis* expands. In Scotland this is associated with *Empetrum nigrum*, akin to early phases of the Interstadial (Walker and Lowe, 1990) or on mainland Orkney, *Empetrum* colonises landscapes without *Juniperus* (Whittington et al., 2015) highlighting that *Juniperus* did not migrate to the Orkney archipelago. Following *Juniperus*, tree *Betula* spreads across Britain in a radial manner from Stadial limits in Europe (Birks, 1989), suggesting landscape stability. This is then overtaken by a *Betula*-*Corylus* woodland then *Corylus* woodland, with *Corylus* proliferating in the canopy considering its shade intolerant ecology (Walker, 1975; Boyd and Dickson, 1986). This succession in Britain is identified in all Holocene pollen diagrams reflecting warming climates, but the succession of taxa also relates to soil status, plant competition and migration rates (Birks, 1989). Thus, regionally specific assemblages may be identified which are a product of the equilibrium hypothesis, but considerable control is exerted by climate, therefore the disequilibrium hypothesis.

Akin to the abrupt vegetation changes within the Interstadial, a series of revertences are also observed during the early Holocene. Evidence of climatic instability during the early Holocene was largely identified through a palaeobotanical means (e.g. Björck et al., 1997) with the Pre-Boreal Oscillation (PBO), originally defined between 11.35-11.1 Cal. ka BP in Norway (Björck et al., 1996; Björck et al., 1997). However, the terrestrial manifestation or vegetation changes associated with the PBO are difficult to trace, regionally specific and notoriously difficult to constrain chronologically (Björck et al., 1997). In part this is due to two radiocarbon plateaux at 10.0-9.9 ^{14}C ka BP and 9.6-6.5

^{14}C ka BP (Björck et al., 1997). Nevertheless, where sequences have been attributed to the PBO, short episodes of *Betula* decline are noted with increases in *Empetrum*, *Rumex* and *Hippophae* (Björck et al., 1997). Recently however, there has been a suggestion that the PBO cannot be solely attributed to one simple climatic deterioration, and multiple Pre-Boreal Oscillation(s) exist (e.g Bos et al., 2007; Fiłoc et al., 2018) all of which are dominated by a decline in *Betula* and increase in open grassland taxa (Fiłoc et al., 2018). Inconsistency in timing is exemplified with evidence from Germany, suggesting that the expression of climatic deteriorations in west-central Germany occurred 300 years after the climatic episode within the ice-cores (Bos et al., 2001). This may be a real PBO type oscillation or related to other coolings at 10.7, 10.5 and 10.3 Cal. ka BP (Paus, 2010).

In contrast with Europe, evidence for the PBO in Britain is scarce. However, studies from Traeth Mawr, Llangorse and Lanillid in Wales (Walker, 1982, Walker and Harkness, 1990; Walker et al., 1993b), on the Isle of Skye (Walker and Lowe, 1991) and Inverlair and Loch Etteridge in Scotland (Kelly et al., 2017) suggest a brief regressive phase, with small inversions in *Betula* and *Juniperus* pollen and coincident increases in grassland taxa. At the latter two sequences the revertence occurs prior to the deposition of Askja-S Tephra (10,824±97 Cal. ka BP; Kearney et al., 2018) suggesting that this revertence likely reflects one or more of the Pre-Boreal Oscillations. However, the landscape expression of climatic deteriorations in the early Holocene is still poorly understood, which may in part be due to the incomplete nature of LGIT palaeoecological investigations and low stratigraphic resolutions employed. To better define landscape responses to early Holocene oscillations further investigation is warranted.

2.5.5 Drivers of vegetation change

Despite evidence of vegetation change at the millennial- and centennial-scales, what drives changes in vegetation is contentious as few studies suitably demonstrate evidence of driver and response variables from the same sequence (e.g. van Asch et al., 2012a; van Asch and Hoek, 2012). Vegetation presence is limited by its physiological limits to environmental factors, termed fundamental niche, however, taxa near the limit of their distributional and ecological range, realised niche, will be prone to greater changes following a climatic or environmental perturbation (Birks and Birks, 2014). In this respect it may be that temperature, precipitation and site-specific conditions control the abundance of a particular plant type in any given location (Birks and Birks, 2014). Two recent reviews attempt to delineate the main driving forcing behind change. In Ireland, van Asch and Hoek (2012) correlated *Betula* and *Juniperus* abundances, during the Lateglacial Interstadial, with summer temperature variability, suggesting that regressive vegetation phases align with dominant shifts in summer temperature. In

contrast, in a synthesis across northern Europe, Birks and Birks (2014) suggest, at least at the millennial-scale, that summer temperature is a poor predictor of vegetation development. They base their argument on a lack of vegetation development between a relatively dry northern Norway and moist western/southern Norway, where vegetation became more developed. Again, based on chironomids, Birks and Birks (2014) suggest that local conditions and moisture availability was the ultimate control and not summer temperature as summer temperatures remained constant between the two regions but vegetation development differed. Based on these two studies it is likely that regional differences in driving factors exist. However, these two studies used one reconstructed climatic parameter. Therefore, the impact of moisture variability, annual temperature variability and summer temperature variability is largely unknown and warrants further study. Whilst it may be that at both the millennial- and centennial-scales multiple parameters work in concert and drive these vegetation changes, at present this is untested.

2.6 Chapter Summary

This chapter has: 1) presented the current state of knowledge of the climatic structure of the LGIT across Europe; 2) presented the current understanding of the forcing mechanisms behind the millennial- and centennial-scale abrupt events that are observed; and 3) presented the vegetation structure of Europe and Britain. Crucially however, this chapter has also highlighted the current knowledge gaps within climatological and environmental research during the LGIT. Some of the key gaps include; the lack of understanding on the magnitudes of climatic change across the terrestrial realm and also the timing of these changes. Further, this chapter highlights the lack of understanding of how vegetation responds to these abrupt events, as the current understanding is limited to few highly resolved studies. Thus, investigation into these events and their responses is warranted. This thesis seeks to provide new information into this framework to help understand if, how and when vegetation responds to abrupt climatic events.

Chapter 3. Study site rationale and locations

The aims of this chapter are three-fold: 1) to demonstrate the rationale behind selecting each site within this research; 2) to introduce each region in terms of its geology and glacial history; and 3) to introduce each site studied as part of this research and acknowledge any previous work undertaken at each site in question. The geology and glacial history of different regions have been included here to demonstrate additional factors that could affect plant distributions and to provide details of the formation of each site. Whilst several factors are biotic, dispersal biology and migration, population dynamics, and herbivory; abiotic factors including topography, edaphic conditions, climate, and geology also exert influence. For this thesis, the investigation is primarily focussed on how climate affects vegetation. However, in some respect geology also offers a control through the incorporation of base geological components into soils or substrates (Kruckeberg, 2004). Thus, the underlying geology will be considered for both the region and sites studied within this research.

3.1 Study site rationale

There are many vegetation studies from the British Isles spanning the period from the Last Glacial Maximum (LGM) to the present day. A considerable number of these studies either focus on or incorporate the Last Glacial-Interglacial Transition (LGIT) (Chapter 2); the last major period of climatic complexity across northern Europe. However, only a select number of studies aim to reconstruct vegetation histories for the LGIT at high-resolution. The comparable lack of high-resolution investigations likely stems from the contrasting research *foci* and the lack of understanding of climatic complexity within the LGIT at the time of study. Following the publication of high-resolution palaeoclimatic data from ice-core (e.g. Rasmussen et al., 2006; 2007; 2014) and terrestrial records (e.g. Brooks and Birks et al., 2000a; Marshall et al., 2002; Lang et al., 2010; Brooks et al., 2012; 2016) both millennial and centennial-scale climatic variability have been shown to exist during the LGIT (Chapter 2). However, the paucity of high-resolution vegetation reconstructions prevents any assessment of how vegetation responds to abrupt climatic change. Therefore, there are intra-site disparities, where little is known about the response of vegetation to abrupt climatic change within individual sites; and inter-site disparities, where little is known about the responses across the British Isles.

The decision to focus on the British Isles as opposed to other sites in Europe, was largely a function of the number of recent palaeoclimatic datasets revealing both similarities and differences in the climatostratigraphy between Britain and Europe (Chapter 2) but also the proximity of Britain to the North Atlantic, where oceanic perturbations cause climatic variability (Chapter 2).

Across the British Isles, a series of sites would need to be studied to test disparities of vegetation change. Therefore, different site selection criteria were established. Principally, sites from key locations were selected based on: 1) observed climatic and latitudinal gradients in Britain during the LGIT; 2) the occurrence of pre-existing palaeoclimatic data; or the generation of palaeoclimatic data alongside this research; 3) the demonstration that each site can be attributed to the LGIT, either through existing chronological control or chronologies developed throughout this research and; 4) the presence of expanded sedimentary sequences or sites that demonstrate key lithological changes in association with abrupt climatic events.

The most important criterion was to analyse sites across climatic and latitudinal gradients. Selecting sites from across these gradients would, theoretically, produce discrepancies between shifts in vegetation assemblages. At the northern edge of the transect for example, it might be expected that climatic oscillations would be greater in magnitude than farther south; due to the greater expression of fluctuations in ocean circulation at higher latitudes (Bakke et al., 2009). This may result in greater shifts in vegetation assemblages where certain taxa were close to ecological boundaries. Furthermore, it was considered that vegetation would be more developed at the southern edge of the transect, resulting in a different style of vegetation response.

Secondly, the availability of pre-existing palaeoclimatic data from each site was essential. Whilst some palaeoclimatic data has been generated alongside the vegetation reconstructions, it was not physically possible to generate the wealth of data within this thesis. Furthermore, as a key theme is to demonstrate how vegetation responds to climatic events; this research would not be possible without a climatostratigraphic context. This context enables an understanding as to whether climate is the overriding control on vegetation types present (e.g. Tipping, 1991a). For the same reasons existing chronological control was vital to both place a site within the LGIT and provide evidence of the timing of events in each record.

Finally, sites needed to demonstrate the presence of an expanded sedimentary sequence. Shorter sequences with low sedimentation rates will be affected by the resolutions of certain techniques. For example, individual cubic centimetres for pollen analyses in short sequences may, hypothetically, represent 100 years per sample. If the climatic event is 100 years in duration, then the event will be expressed as a mixed assemblage in the pollen record or show no change between successive samples. If, however, the sequence is expanded, with increased sedimentation rates, then the event

may be spread over many samples; demonstrating the increased likelihood of detecting shifts in vegetation assemblages. Equally, if it can be demonstrated that events have a lithostratigraphic impact, resulting from changes in landscape stability, the probability of detecting individual events increase.

Based on these criteria, four sites were selected across Britain (Figure 1.3). The most northerly of which lies on the Orkney archipelago; one in the Grampian Highlands of Scotland; two within the Vale of Pickering, in north-east England and; one on the Brecon Beacons in south Wales. These sites not only provide the framework for this research but also form the basis of a network of sites that additional highly resolved studies can fall into.

3.2 Northern Scotland: Orkney

The Orcadian Islands are located approximately 14 kilometres from the north coast of Caithness, Scotland and 125 kilometres from the Shetland Islands. In total, the archipelago consists of approximately 70 islands, with the largest being Mainland; and the remainder of the islands residing around the perimeter of Mainland. The relief of the Orkney islands is low, many of the central islands are below 75 metres a.s.l, with areas of elevated topography rarely exceeding 150 m.

Recent examination of two basins in mainland Orkney have demonstrated the existence of carbonate sediments (e.g. Moar, 1969; Bunting, 1994; Whittington et al., 2015) highlighting the applicability of Orkney for high-resolution palaeoclimatic reconstruction. Furthermore, pollen-based vegetation reconstructions demonstrate that the basins formed following the Devensian glaciation and contain lithological and palynological sequences attributable to the LGIT (Bunting 1994). These observations make Orkney an ideal northerly origin point for a transect of sites across the British Isles. Equally, the Shetland Isles could have formed this northern origin point, however, investigations across Shetland (e.g. Bennet et al., 1992; Hulme and Shirriffs, 1994; Whittington et al., 2003) have demonstrated that most sediment sequences do not cover the duration of the LGIT, do not contain carbonate sedimentary infills and do not reveal vegetation variability; likely reflecting the extreme oceanic placement of Shetland buffering any terrestrial vegetation response (Whittington et al., 2003). Therefore, Orkney provided the best option for the most northerly point of the transect.

3.2.1 Geology of Orkney

The underlying basement rocks of Orkney are granitic formations which link to the Moinian Supergroup in northern Scotland (Mykura, 1976). Overlaying this granitic

complex are the dominant rock types found on Orkney, the Devonian-aged Old Red Sandstones. The oldest of these, which are restricted to the vicinity of Yesnaby, are the Lower Old Red Sandstones, termed the Yesnaby Sandstone Group. This group exists as two different formations, the Harra Ebb Formation and the Qui Ayre Formation. The most extensive rock types on Orkney are the Middle Old Red Sandstones and they cover a significant proportion of Mainland (Figure 3.1). This mid-Devonian aged group can be further split into the Stromness Flags (Figure 3.1), both upper and lower groups, the Rousay Flags and the Eday Beds. The two flags contain thinly or rhythmically bedded siltstones, shales, and fine-grained sandstones (Mykura, 1976). It was noted that the two flags appear to contain identical lithologies, however, they have been split on the observations of fewer faunal remains in the Rousay Flags compared to the Stromness Flags (Mykura, 1976). The Eday Beds are largely restricted to the Isle of Eday and alternate between massive sandstones and marl. The final sandstone group seen on Orkney, the Upper Old Red Sandstones, are the Hoy Sandstones which are the major components of the Isle of Hoy.

3.2.2 Glacial history of Orkney

Defining the glaciation of Orkney is of critical importance in delineating ice occupation on the archipelago but also of northern Scotland and within the North Sea basin. Early glaciological investigations undertaken by Geickie (1877) and Peach and Horne (1880) identified a series of glacial sediments, principally confined to coastal sections and low ground. From these observations, Peach and Horne (1880) derived a single phase of glaciation over Orkney, with glacially striated bedrock indicating ice-flow in a westerly direction. Due to the presence of lithologies of central Scottish provenance sourced from the Moray Firth, it was concluded that ice radiated from central Scotland, streamed out of the Moray, up the North Sea and subsequently across Orkney (Peach and Horne, 1880; Mykura, 1976). Whilst this is generally accepted, recent investigations into till deposits appear to demonstrate a more complicated glacial history. The identification of the superimposed Digger, Scara Taing and Quendal till formations, with sharp erosive contacts, demonstrate three separate phases of ice-flow across Orkney (Rae, 1976; Hall et al., 2016a). One of these till members, the Scara Taing, contains Scandinavian erratics (e.g. Rae, 1976) which may suggest a Scandinavian ice influence. This has been refuted based on the abundance of Scottish lithologies in the till matrix and likely represents reworking of Scandinavian erratics from either earlier glaciations or a reworking of clasts of Scandinavian origin from the North Sea basin (e.g. Davies et al., 2011). Nevertheless, despite increased complexity, it is largely accepted that the glacial features on Orkney were formed by phases of glaciation, following the deflection of the British and Irish Ice Sheet (BIIS) by the Fennoscandian Ice Sheet (FIS), during the late Devensian.

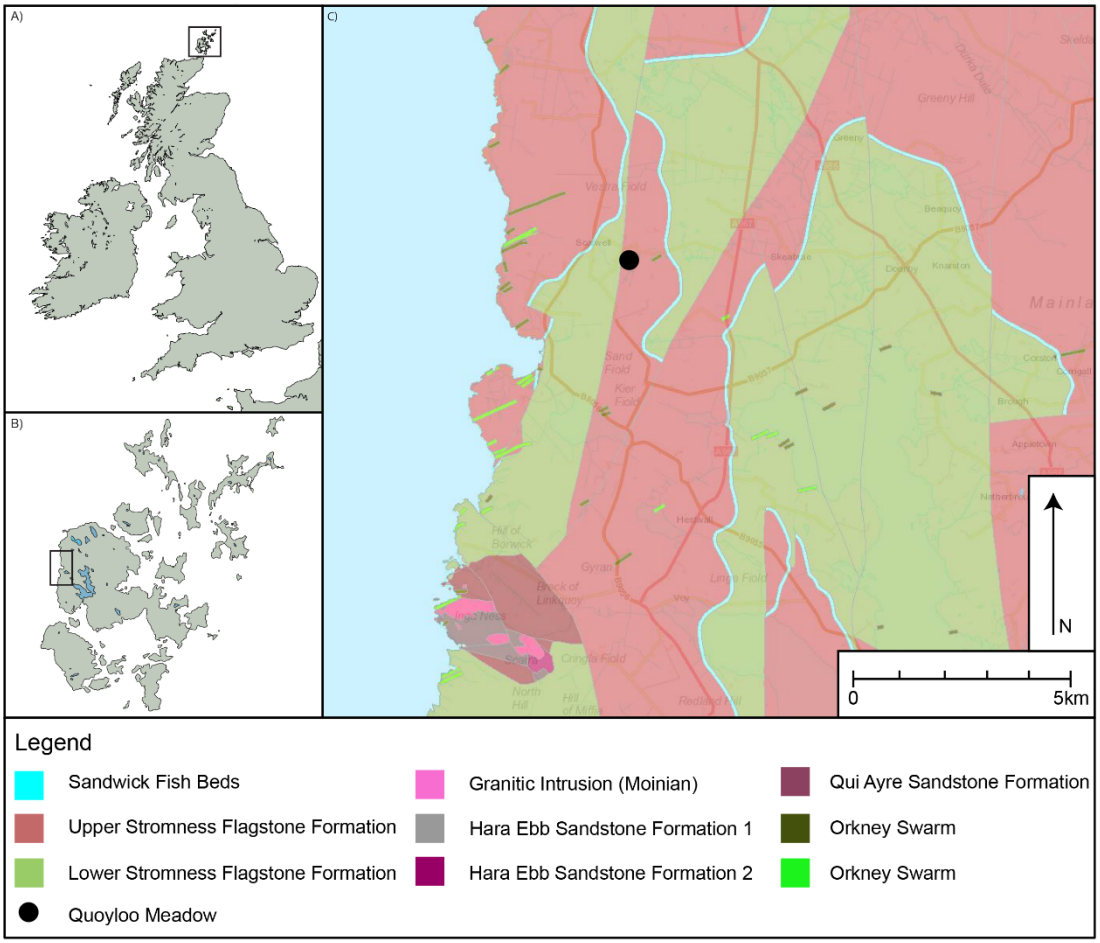

Figure 3.1 Geological map of west Mainland Orkney. Insets reveal A) The location of Orkney within Britain; B) a general map of Orkney; and C) a geological map of west Mainland Orkney showing the major basement lithologies and the location of Quoyloo Meadow (Contains British Geological Survey materials © UKRI 2018).

Despite elucidating how the features formed, the absolute timing of events has been a point of contention. Some suggest that Orkney remained ice free during the LGM; arguing that ice traversed the archipelago during an earlier Devensian stage (e.g. Rae, 1976; Sutherland, 1991; Bowen et al., 2002). Whilst others propose that ice was present on Orkney during the LGM (Hall and Whittington, 1989). This debate has origins in the relative timing of ice occupancy and the confluence of the BIIS and the FIS in the North Sea basin during the Devensian. However, it is now commonly accepted that ice was present in the North Sea during the LGM (Bradwell et al., 2008; Ballantyne, 2010; Sejrup et al., 2015; Sejrup et al., 2016). This has implications for the timing of ice on Orkney, and cosmogenic exposure dating of boulders and glacially eroded bedrock suggest that the archipelago was ice free between 17 and 15 Ka BP (Phillips et al., 2008; Hughes et al., 2016). This implies that that the topographic lows that were formed following ice retreat began accumulating sediments during the Dimlington/Windermere periods. It is further noted that there is limited evidence for Loch Lomond Stadial glaciation on Orkney. Much of Orkney appeared ice-free during the Stadial episode, however, on the island of

Hoy, owing to areas of increased altitude, evidence for small local corrie glaciers has been observed (Sutherland, 1993; Ballantyne et al., 2007).

3.2.3 Quoyloo Meadow- site description

Of the two basins presented in Moar (1969) and Bunting (1994) the Crudale Meadow sequence, containing carbonate sediments covering the Windermere Interstadial and early Holocene, looked to be most attractive to reinvestigate. However, owing to recent high-resolution pollen and stable isotope reconstructions at that site (e.g. Whittington et al., 2015) a second Orcadian site of Quoyloo Meadow was selected.

Quoyloo Meadow is located on western Mainland, approximately 2.5 kilometres north east of the Skara Brae archaeological site. Quoyloo Meadow (59.066417, -3.309333; HY250206) occupies a topographic depression within the Upper Stromness Flagstone. To the north east of the site the geology shifts to the Lower Stromness Flagstone. At its maximum extent the basin is 0.6 km x 0.3 km, occupies an area of 0.1 km^2, and lies at an altitude of 33 m a.s.l. (Timms et al., 2017; Figure 3.2). The catchment of the site is estimated to approximately 1.6 km^2 however it was likely to have been much larger in the past. In its present configuration a drainage network extends across the basin (Figure 3.2). This modification was a result of the need for increased agricultural lands, and further, has channelised the natural inflows and outflows of the basin (Timms, 2016). The site currently has one inflow, a natural spring focused from the hills to the west; and one outflow at the northern fringes of the basin (Figure 3.2). It is unknown whether the site contained a greater number of inflows and outflows in the past. The physical expression of the basin, in its present configuration, is an active valley mire, but during the LGIT, the site was occupied by a shallow open water body (Timms, 2016; Bunting 1994).

3.2.4 Quoyloo Meadow- previous investigations

The earliest investigation at Quoyloo Meadow was undertaken by Bunting (1994). Bunting (1994) reported a 260 cm core sequence with the lowest 160 cm containing a tripartite sequence spanning the LGIT. The basal lithostratigraphic unit is split in two with the lower unit representing the Windermere Interstadial (WI) and the overlying unit attributed to the Loch Lomond Stadial (LLS). Despite this division, both units display clastic material, with the Interstadial unit described as a silty organic clay, transitioning into clay (Bunting, 1994; 1996). Overlaying these clastic sediments are organic marls. Based on this framework a palynological investigation demonstrated that the basal clay sediment contained no pollen; hinting at an unvegetated landscape surrounding the basin during the early WI. With increased organic sedimentation however, the catchment stabilised (QM-P1a) and the vegetation was dominated by a low lying dwarf shrub

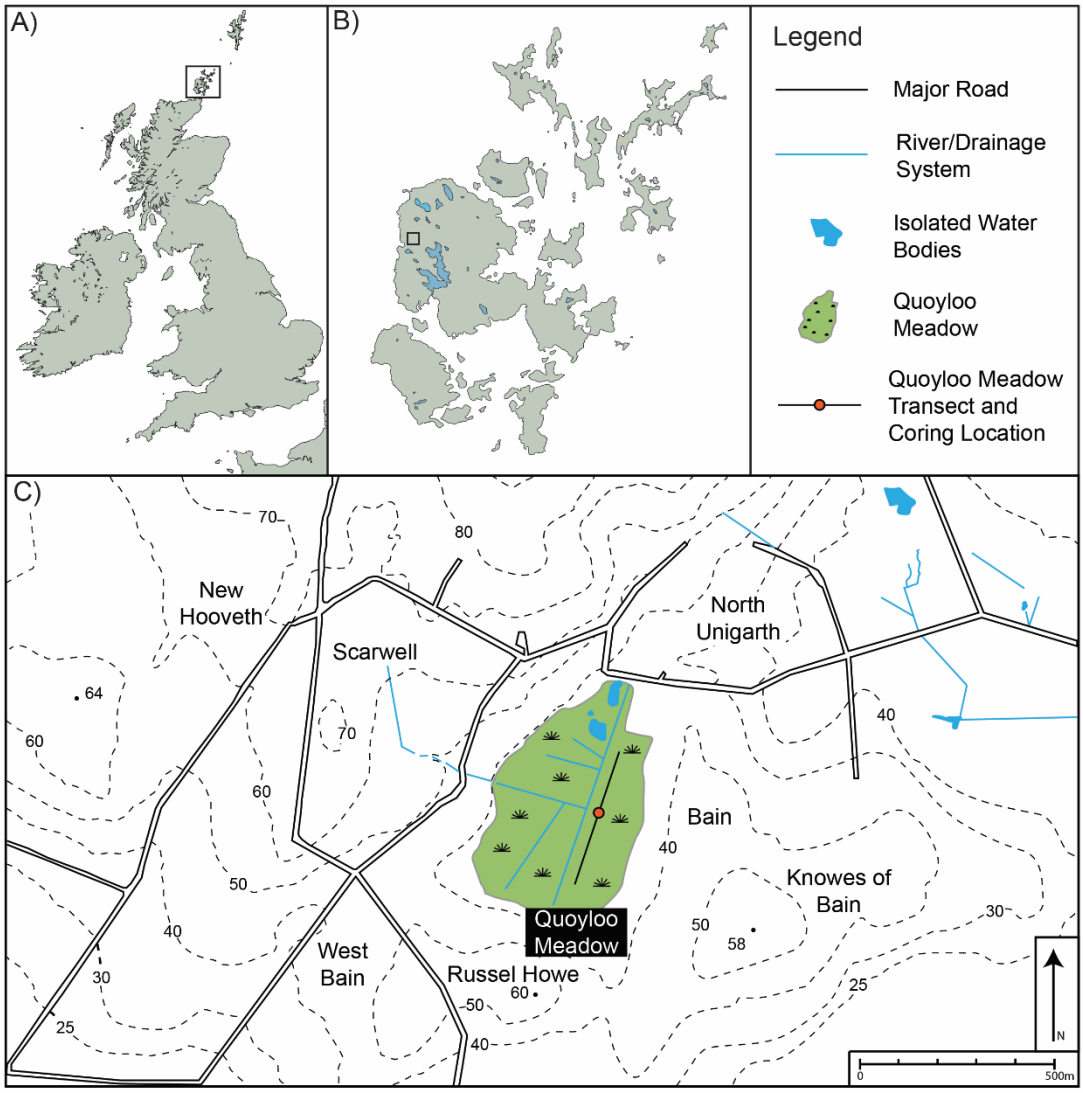

Figure 3.2 Topographic map of the Quoyloo Meadow basin. A) reveals the position of Orkney is Scotland; B) shows the position of Quoyloo Meadow in relation to Mainland Orkney; and C) is the topographic map of the site. Shown are 10 m contours, the Quoyloo Meadow bog, the transect at the sequence and the location of the coring site.

heathland (*Emptrum nigrum*) and an open grassland (Poaceae, Cyperaceae; Figure 3.3). The second pollen sub- zone, QM-P1b, exhibits a decrease in heathland taxa coupled with an increase in herbaceous taxa, notably *Artemisia* and *Rumex*. Coupled with a return to minerogenic sedimentation, these taxa suggest of a phase of landscape instability and a period of climatic deterioration. Within QM-P2, the vegetation is predominantly composed of heathland taxa with increased proportions of *Betula*, demonstrating ameliorating climates. The remainder of the LGIT sequence, QM-P2b: QM-P3a, shows further catchment stabilisation with the dominance of tall coryloid shrubs.

In a later study, O'Conner and Bunting (2009) present plant macro-fossil and molluscan evidence from the same core sequence as was reported in Bunting (1994). The focus of

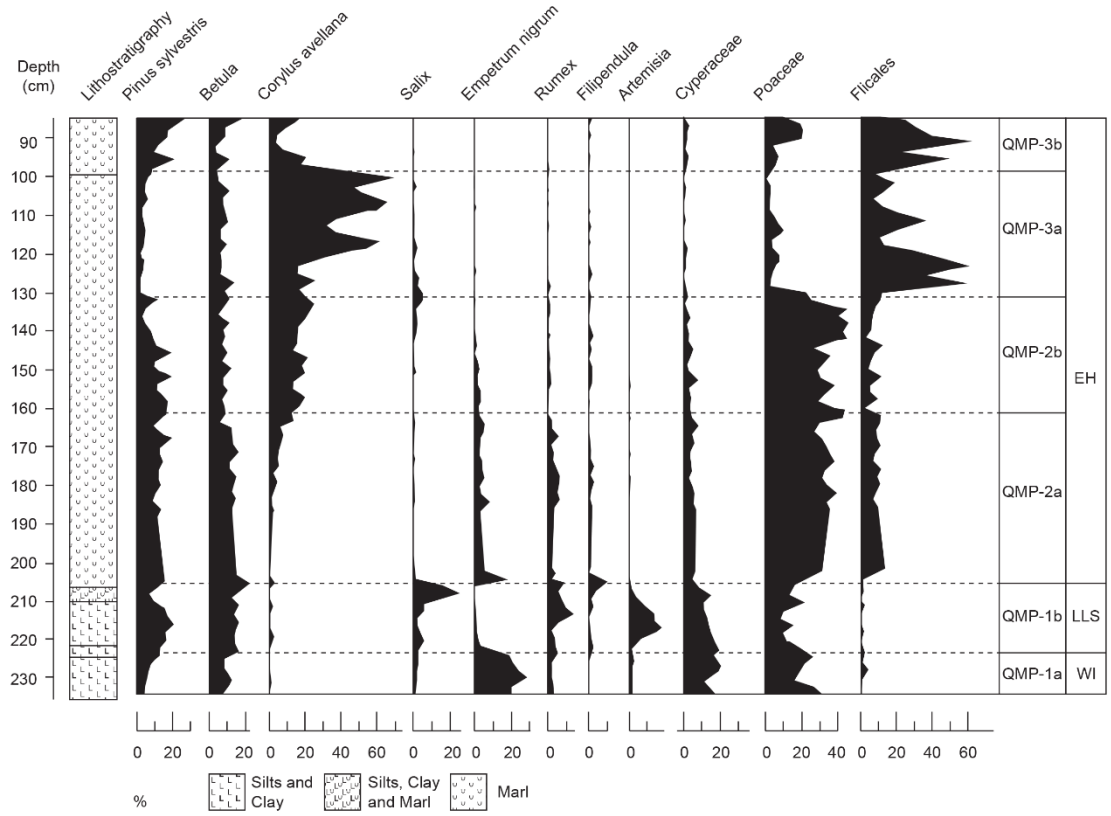

Figure 3.3 The previous lithostratigraphic and palynological investigation of the Quoyloo Meadow site. Shown here is a truncated version of the record, revealing the approximate vegetation assemblages during the LGIT. Highlighted are the principal taxa, exhibiting slight variability throughout the LGIT. Adapted from Bunting (1994).

which was to better understand wetland development at Quoyloo Meadow. The WI and LLS sections of the core are devoid of molluscan taxa and are equally sparse in plant macro-fossils. However, *Chara* oospores can be observed in the deepest clays; with disappearance perhaps demonstrating increased turbidity or a lake level changes during the later WI and LLS periods (O'Connor and Bunting, 2009). Their subsequent recovery indicated a return to favourable conditions in the wetland environment. The presence of oospores and *Lymnaea peregra* within early Holocene marl sediments suggest a shallow and clear freshwater habitat throughout (O'Connor and Bunting, 2009). In Bunting (1994; 1996) a visible tephra horizon was reported. This tephra layer was subsequently geochemically characterised as the Saksunarvatn Ash.

A recent study (Timms et al., 2017) revisited the Quoyloo Meadow site to develop a tephrostratigraphy for the region. It was deemed that the Orkney Isles offer a unique opportunity to identify and correlate many tephra horizons because of its northerly latitudinal position in Britain; and its placement with respect to Icelandic source volcanoes. The recovered sequence presented in Timms et al. (2017) closely resembles that of Bunting (1994) albeit with a shorter stratigraphy (242 cm and 260 cm

respectively). Nevertheless, multiple tephra were identified throughout the sequence; two in interstadial sediments, one in stadial sediments and the remainder within the early Holocene marl. The two tephra layers identified within Interstadial sediments, QM1-218; QM1-213, are chemically indistinguishable to tephras of 'Borrobol-type' (e.g. Turney et al., 1997). Of the tephra known to exist in the British Isles that contain this chemistry, it might be considered that they correlate with the Borrobol and Penifiler Tephra, however, based on their stratigraphic position within the sequence, arguably late Interstadial (Rhys Timms, pers. comm. 2017) later than has been reported elsewhere (e.g. Pyne-O'Donnell et al., 2008) correlations were not made. Subsequently, within the silts and clays, QM1-198 contained distinctive 'Katla-type' chemistry with observations of brown basaltic glass. This tephra was therefore correlated to the Vedde Ash (12,023±43 Cal. ka BP; Bronk Ramsey et al., 2015). Within the early Holocene marls the following tephras were identified, QM1-192 tentatively correlated with the Hässeldalen (11,387±135 Cal. ka BP; Ott et al., 2016), QM1-188 correlated with the Askja caldera derived Askja-S (10,824±49 Cal. ka BP; Kearney et al., 2018), QM1-187 correlated with the Ashik (10,400±300 Cal ka BP; Timms et al., 2017), QM1-160 the visible layer correlated to the Saksunarvatn Ash (10,210±35 Cal. ka BP; Lohne et al., 2014), QM1-154 correlated to the Fossen (10,200±100 Cal. ka BP; Lind and Wastegård et al., 2011), and QM1-133 correlated to the An Druim (9648±79 Cal ka BP; Timms et al., 2017). The quantity of tephras identified across the Quoyloo sequence demonstrated that the site could be robustly chronologically constrained without radiocarbon assays. Owing to this framework, the same sequence as presented in Timms et al. (2017) was selected for high-resolution palaeoenvironmental study.

3.3 Central Scotland: Grampian Highlands

The Grampians in Scotland are the areas of highland that stretch across most of central Scotland. They are bounded to the east by the North Sea, to the west by the Irish Sea, to the north by the Great Glen Fault, and to the south by the Highland Boundary Fault. The altitudinal range of the highlands is variable with lowlands surrounding the coastal areas near the Inner Hebrides and Aberdeenshire but rising to the highest point in the British Isles, Ben Nevis 1345 m a.s.l. near Fort William.

The Grampian Highlands have been extensively studied in the past and a detailed knowledge exists of the key palaeoenvironmental changes that took place following the late Devensian glaciation (e.g. Pennington et al.,1972; Walker, 1975; Lowe and Walker, 1977; Vasari, 1977; Birks and Matthewes, 1978; Tipping, 1989; Brooks et al., 2012; Brooks et al., 2016; Kelly et al., 2017). Many of these investigations were completed to constrain the extent of the LLS ice cap (e.g. Golledge, 2010). As a result, many of the

sequences are not resolved in sufficient detail to examine the effects of abrupt climatic change. As many sites of LGIT age have been identified, including sites at higher elevations, the Grampian Highlands of Scotland are an obvious choice for further study.

3.3.1 Geology of the Grampians

The geology of the Grampian Highlands is a complex mix of igneous and metamorphic rock types. These rocks are primarily derived from eroded areas of the Caledonian mountain belt (Stephenson and Gould, 1995). The predominant rock type across the Grampian Highlands however, are the metamorphosed sedimentary rocks of the Dalradian Supergroup. These rock types, likely forming during the late pre-Cambrian, overlay the Central Highland Migmatite Complex and appear stratigraphically as the Grampian, Appin, Argyll and Southern Highland Groups (Stephenson and Gould, 1995). The Grampian group is composed predominantly of psammites which make up a considerable component of the basal lithology of the central and south-west Highlands. The Appin Group consists of pelite, quartzite and limestone. Geologies attributed to this group are confined to a narrow band surrounding the Grampian Group. The most extensive member, the Argyll Group (Figure 3.4), outcrops at various points across the Grampians, it makes up an area of approximately 5700 km^2 and can be traced from the south-west Highlands to the east coast of Scotland, north of Aberdeen. Major components of this group include sandstone, quartzite, siltstone, mudstone, and limestone (Stephenson and Gould, 1995; Figure 3.4). The final Dalradian Group member is the Southern Highland Group. This group outcrops in the Southern Highlands and the east-central Highlands and is composed of metagreywacke sandstones and siltstones (Stephenson and Gould, 1995). Sedimentary rock formation is restricted in the Grampians, however, along the northern edge of the Great Glen Fault; the coastline of Moray and Nairnshire; the Highland Boundary Fault; and basins within the Highlands sedimentary rock makes up part of the basement complex. The dominant rock type links with Orkney and they are predominantly, the Devonian-aged, Old Red Sandstone. Across the Central Highlands there are a series of acid and basic igneous intrusions and dyke swarms, which outcrop to form the Caledonian Igneous Suite (Stephenson and Gould, 1995).

3.3.2 Glacial history of the Grampians

Two competing hypotheses exist for ice cover in Scotland during the late Devensian: 1) that ice extent was restricted (e.g. Sutherland, 1984; Bowen et al., 1986); and 2) that an extensive ice sheet existed covering most of Scotland and Ireland with ice streaming down the Irish Sea basin (e.g. Clark et al., 2004; 2012; Ó Cofaigh and Evans, 2001; Sejrup et al., 2005; Ballantyne et al., 2008; Bradwell et al., 2008). Geomorphological and

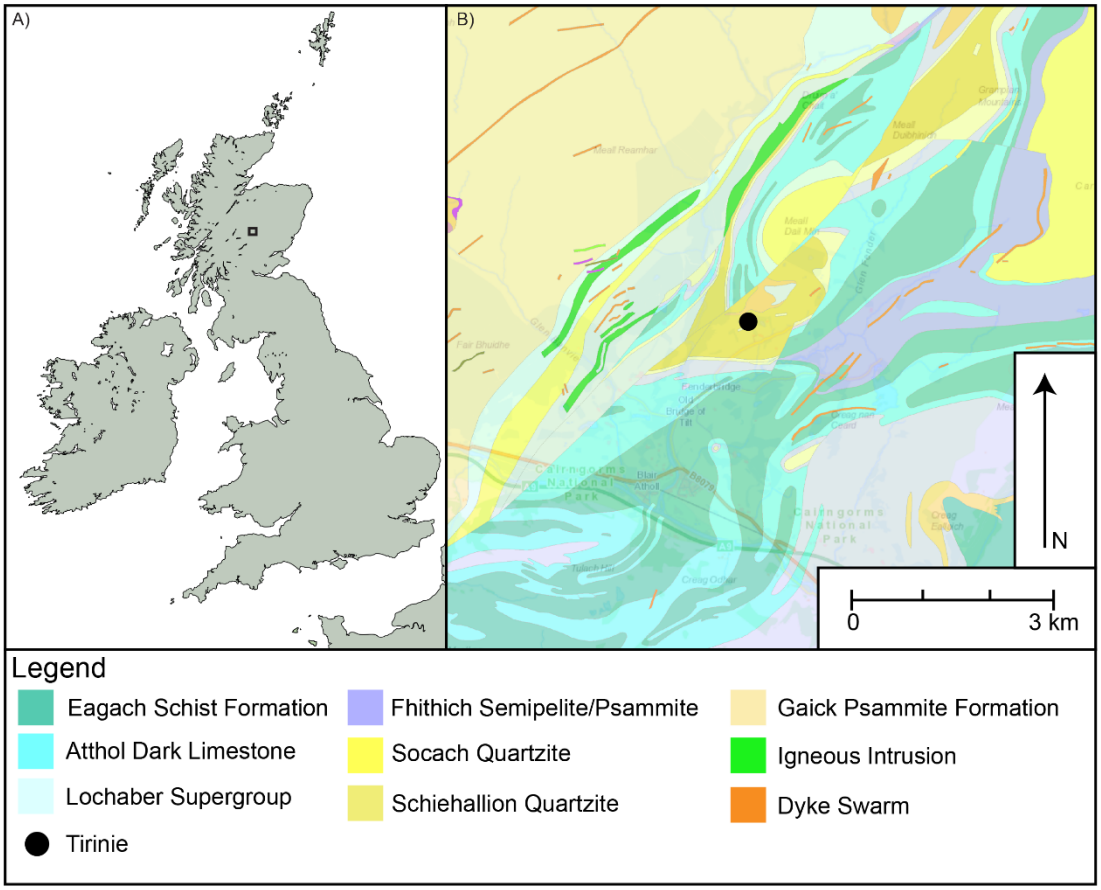

Figure 3.4 A) Location of the central Grampian Highlands in Scotland and B) a detailed geological map of the area surrounding the study site (Contains British Geological Survey materials © UKRI 2018).

sedimentological evidence from both onshore and offshore localities appear to favour this second view.

Despite eventual consensus on the extent of glaciation, the sequence of events during deglaciation is poorly constrained (Hall et al., 2016b). Initial phases of deglaciation saw ice retreat north from England, rapid Irish Ice Stream retreat, a decoupling of the BIIS and the Irish Ice Sheet (IIS) and down-wasting of the remaining ice masses (Clark et al., 2012). In central Scotland, the Scottish Ice Sheet (SIS) subsequently retreated up through the main valley networks, including the Strath Spey in the Grampian Highlands towards major ice-accumulation centres (Hubbard et al., 2009; Hall et al., 2016b). As ice retreated various episodes of localised ice splitting would have occurred, including the splitting of Western Highland ice with Cairngorm ice (Clark et al., 2012). Coincident with glacial melting and retreat, glaciofluvial landforms, i.e. kame and kettle topography, would have been deposited across Scotland; due to the calving of ice from the glacier's snout and meltwater depositing sediments at the glacier margins.

Despite this generalised pattern of deglaciation, it is apparent that ice was active in retreat and underwent a series of stillstands and readvances. Prior to interstadial conditions in Scotland, a readvance has been identified in the Strath Spey region of the Cairngorms, with the identification of trimlines, moraines and glaciotectonised lacustrine sediments under till, dated through cosmogenic exposure dating to ca 15.1 ka BP (Hall et al., 2016b). This coincides with the advance at Wester Ross in northern Scotland and advances on the Isle of Skye, 14.7 and 15.2 ka BP respectively (Ballantyne and Stone, 2012; Small et al., 2016); collectively termed the Wester Ross Readvance. Following readvance, retreat continued to local ice-accumulation centres by the onset of the Windermere Interstadial. Using a Greenland stratigraphy, this implies that the readvances occurred during the final stages of GS-2.1. Evidence suggests that retreat was rapid due to the identification of the Borrobol tephra at Abernethy Forest (Matthews et al., 2011) modelled to 14,098±47 Cal. ka BP (Bronk Ramsey et al., 2015) and a bulk radiocarbon date from Loch Etteridge (Walker, 1975) recalibrated to 16,989-14,398 Cal. ka BP. Whilst the Etteridge date appears old, likely incorporating older carbon due to the bulk nature of the date, both sites are within the Strath Spey and would have been overridden by re-advancing ice. But by the onset of the Interstadial both sites demonstrate glacial retreat and organic sedimentation.

A subsequent phase of glaciation in Scotland, that has received the most attention, is the Loch Lomond Readvance (LLR). Extensive geomophological mapping and modelling of the Scottish Highlands has delimited the extent of the Stadial readvance in different regions. This has formed a suite of ice limits within the Western Highlands (e.g. Sissons 1978; Sissons 1979a, b; Bennet and Boulton, 1993; Finlayson, 2006; Benn and Evans, 2008) the Northwest Highlands (e.g. Benn and Lukas, 2006; Bradwell, 2006; Finlayson and Bradwell, 2007) the Hebridean Islands (e.g. Ballantyne, 1989) and the Central Highlands including the Gaick Plateau, Cairngorms and south-west Grampians (e.g. Sissons, 1979c; 1980; Sissons and Sutherland, 1976). During the LLS, summer temperatures decline by up to 4-6°C (Brooks et al., 2012). This widespread drop in temperature and changing precipitation patterns reinitiated ice growth within the Western and peripheral highlands. It is currently unclear how long Stadial ice remained in the different areas with some supporting, through different methods of chronological control, e.g. varve accumulation and cosmogenic exposure dating, late stadial advances, therefore late deglaciation within the Stadial or early Holocene (e.g. Palmer et al., 2010; Small and Fabel, 2016). Others however, favour early deglaciation by the mid-Stadial (Bromley et al., 2014). It is noteworthy, that these studies have a focus on Rannoch Moor, a supposed area of ice accumulation and it is currently difficult to reconcile all

dating evidence. Nevertheless, the ice presence in upland areas during at least part of the Stadial is not disputed.

Finally, through incorporating different lines of evidence for LLR ice limits, biostratigraphy was also incorporated. The theory held that if a site sat 'inside' the limits of glacial ice then it would contain Holocene sediments and vegetation assemblages only, for example within Rannoch Moor (e.g. Walker and Lowe, 1977). This is a result of the lateral force of glacier movement removing previous deposits. If, however, a site lay outside the limits of Stadial ice, they would be unaffected by the movement of the glacier and hold a classically tripartite sedimentary sequence with vegetation assemblages attributable to the LGIT (e.g. Lowe and Walker, 1977). This theory of 'inside' versus 'outside' sites, not only had the effect of delineating glacial histories, but also led to the identification of key late Quaternary LGIT sites that must have been formed following the wastage and stagnation of late Devensian ice.

3.3.3 Tirinie- site location

The Tirinie palaeobasin is located in Glen Fender, Scotland at the south-west fringes of The Cairngorms National Park in the south-east Grampian Highlands. More precisely the site lies approximately 13 km to the north-west of Pitlochry (56.787500, -3.815319; NN886681; Figure 3.5). Tirinie sits in a topographic low within the Schiehallon Quartzite Formation; part of the Islay Subgroup, a component of the Argyll Group (Figure 3.4). The neighbouring hills and surrounding slopes are predominantly of the Blair Atholl Dark Limestone and Dark Schist Formation, of the Blair Athol subgroup within the Appin Group. Additional basement lithologies surrounding Tirinie include Cnoc An Fhithich Banded Semipelite and Drumchastle Pale Limestone Formations; and the granitic Meall Gruaim Pluton. The basin has a maximum extent of 0.05 x 0.12 km, occupies an area of 3886 m^2, and lies at an altitude of 323 m a.s.l. (Candy et al., 2016; Figure 3.5). In its present formation the basin in an active floating bog. The site currently has a series of inflows, with the major inflow being a natural spring to the north-east with secondary streams draining the Meall Gruaim hillslope directly to the north (Figure 3.5). The only outflow from the site is on its western edge where a stream drains to the south-west. The catchment of the site is significantly larger than the size of the basin and is approximated to an area of ca 454,500 m^2 (Candy et al., 2016). Whilst Tirinie is now a mire, during the LGIT a water body existed (Lowe and Walker, 1977), and was likely to have been larger following deglaciation.

3.3.4 Tirinie- previous investigations

The Tirinie basin was first studied by Lowe and Walker (1977). Lowe and Walker (1977)

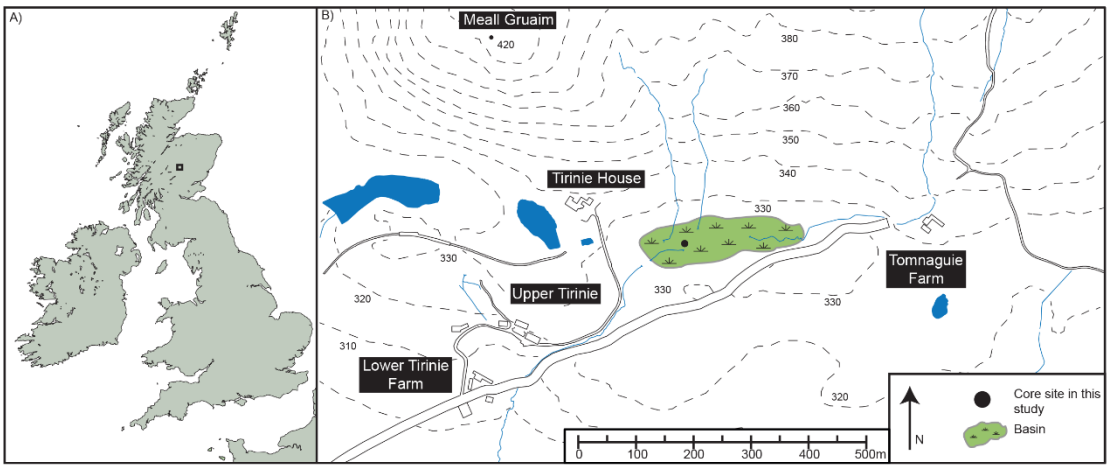

Figure 3.5 Topographic map of the Tirinie basin. A) reveals the position of Tirinie in central Scotland; B) shows a topographic map of the site. Shown are 10 m contours, the Tirinie mire and the coring location within this study.

recovered a 420 cm sediment sequence that contained a classically tripartite sedimentological structure. In their profile, minerogenic silts and clays were overlain by lacustrine marl which was further overlain by silts and clays with a secondary marl phase. The classically tripartite nature of the sediments, coupled with palynological assemblages, confirmed placement of the sequence within the LGIT. During the earliest phase of sediment accumulation, the vegetation surrounding the basin, T1, was dominated by Poaceae, *Rumex* and *Artemisia* (Figure 3.6). This is suggestive of open ground with active erosion in the landscape. The increase in *Empetrum nigrum* and *Juniperus* during T2, shows the colonisation of the ground surrounding the Tirinie basin by a low-lying Juniper scrub heath. Further landscape stability is suggested by high percentages of *Betula* during T3 and T4 (Figure 3.6). It is unknown whether this relates to *Betula pendula*/*pubescens* or *Betula nana.* The observation of increased percentages of herbaceous, open ground taxa, including *Rumex*, *Artemisia*, *Selaginella*, *Saxifraga* and moderate percentages of Poaceae and Cyperceae in T5 and T6, coupled with a sedimentological shift to silts and clays; suggests of a phase of climatic deterioration (Figure 3.6). Lowe and Walker (1977) attribute this stage to the LLS. The secondary marl unit, which sedimentologically demonstrates that climate had ameliorated; was dominated initially by open ground taxa, and subsequently follows a traditional Scottish successional sequence where *Empetrum* heath and *Juniperus* scrub was successively replaced by open *Betula* woodland and *Corylus* (Figure 3.6).

Whilst there is some evidence of cyclicity in the pollen record presented by Lowe and Walker (1977; Figure 3.6); notably in the *Rumex* spectrum during the Interstadial. There is no mention of any sedimentological variability. In a recent paper, Candy et al. (2016) explored sedimentological variability through a high-resolution multi-proxy investigation

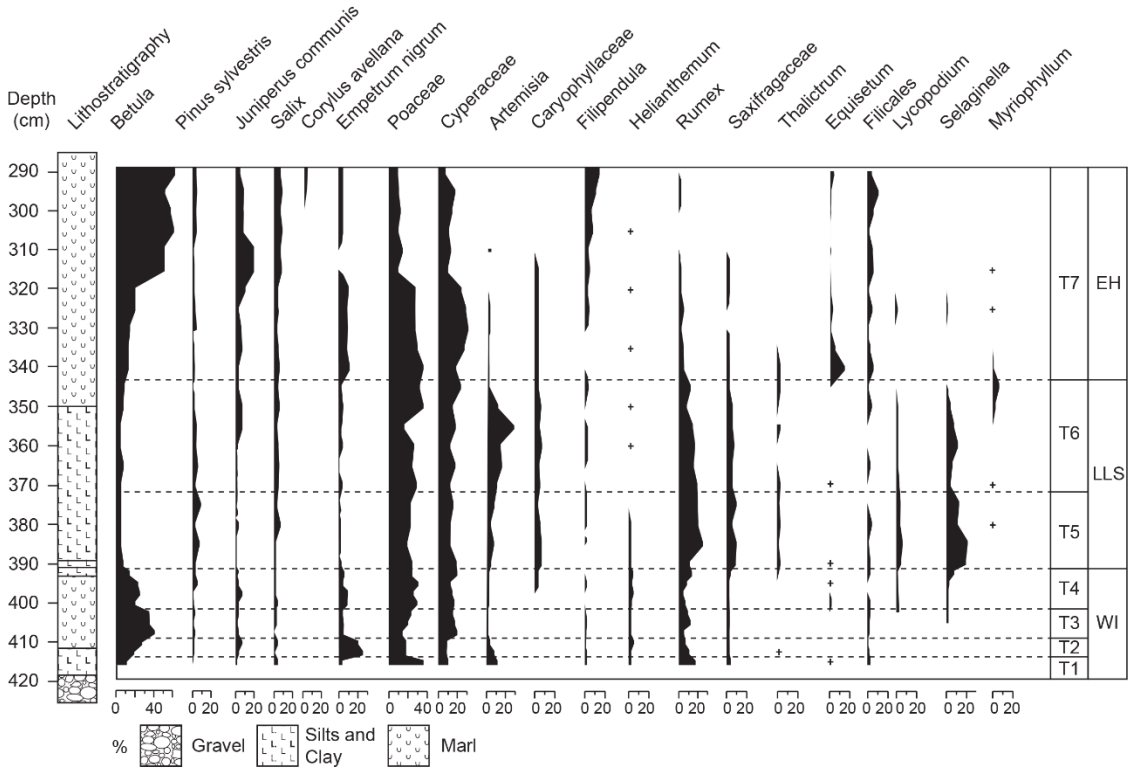

Figure 3.6 The previous lithostratigraphic and palynological investigation from the Tirinie site. Shown here is the full record, revealing the different vegetation assemblages during the LGIT. Shown here are principal taxa only and in percentage format, revealing variability throughout the LGIT. Adapted from Lowe and Walker (1977).

incorporating isotopic and palynological reconstructions within a tephrostratigraphic framework. The geochemical fingerprinting of the Penifiler Tephra (13,939±66 Cal. ka BP; Bronk Ramsey et al., 2015) and the Vedde Ash (12,023±43 Cal. ka BP; Bronk Ramsey et al., 2015) confirm the assumptions of Lowe and Walker (1977) that the lowest marls are of WI age overlain by the LLS. Furthermore, oxygen isotopic investigations, inferred to reflect predominantly a temperature signal (Candy et al., 2016) reveal a level of complexity comparable to the Greenland ice-core records. It was demonstrated that during the Interstadial there are two major, TIR-Od and TIR-Ob, and one minor, TIR-Oc, depletion episodes. These are likely to reflect cold climatic deteriorations, and were tentatively correlated to GI-1d, GI-1Cii, and GI-1b on the basis of stratigraphy; and the Penifiler Tephra being placed on the rising limb of the first depletion event (Candy et al., 2016). Allied with this was the demonstration that for the two major events in the climatic record, vegetation appears to respond. For each of these events, there is a clear replacement of woody taxa with taxa that thrive on broken and disturbed ground, notably *Artemisia* and *Rumex*. The authors note that the magnitudes of isotopic depletion, which are greater than any other record for this chronozone in the British Isles (Candy et al., 2016) and are accompanied by rapid vegetative reorganisation, is due to the latitude and altitude of the site. This study demonstrated that vegetation can be highly responsive to

abrupt climatic events and formed a pilot study for this research. Therefore, the sequence presented in Candy et al. (2016) is the same sequence studied as part of this thesis.

3.4 Vale of Pickering, north-east England

The Vale of Pickering, in northern Yorkshire, is bounded to the north and south by the high ground of the North York Moors, ca 450 m a.s.l, and the Yorkshire Wolds, ca 240 m a.s.l. The Vale is constrained on its eastern edge by the North Sea and its western edge by the Howardian and Hambleton Hills. At its greatest extent, the Vale is 12 km wide near Pickering; narrowing to 4 km wide near Seamer. Further, its lateral range is approximately 50 km between the Yorkshire coast line and Helmsley to the west. The valley floor is relatively flat being approximately 25 m a.s.l. rising to 70 m a.s.l. at the Coxwold-Gilling Gap on the western edge of the Vale.

The palaeoenvironmental history of Yorkshire and surrounding environs has been relatively well documented (e.g. Bartley, 1962; 1976; Walker et al., 1993a; Mellars and Dark, 1998; Lincoln, 2017). These studies clearly demonstrate the applicability of this region to contain sediments attributable to the LGIT. Further, whilst extensive studies within the Vale of Pickering exist, including at the early Mesolithic human occupation site of Star Carr, in light of new sedimentary core sequences obtained (e.g. Candy et al., 2015; Palmer et al., 2015) and ongoing palaeoclimatic work, this area presents a unique opportunity to extend the transect to this locale.

3.4.1 Geology of the Vale of Pickering

In contrast to areas of Scotland, the underlying geology of the Vale of Pickering is considerably younger. Much of the basal lithology in the Vale is the Kimmeridge Clay and Ampthill Clay Formations of Upper Jurassic age (Kent, 1980). The dominant Kimmeridge Clay Formation is primarily composed of soft, shelly and calcareous mudstones and has origins near the Hambleton Hills in the west of the Vale running east to the coast at Filey (Cope, 1974; Figure 3.7). Within this area there are outcrops of the Speeton Clay Formation (Figure 3.7), which appears localised from West Heslerton to west of Muston. The Speeton Clays within this area are composed of clay and have been attributed to the lower Cretaceous (Kent, 1980). North of the Vale of Pickering within the North York Moors the geological setting becomes more complex. Rising from under the Kimmeridge Clay Formation are the older members of the Corallian group. This group sits on the southern edge of the North York Moors, forming the Tabular and Hambleton Hills (Kent, 1980). The group is composed of the Lower Calcareous Grit, the Coralline Oolite and the Upper Calcareous Grit. The lithologies that form these groups are defined as fine-grained calcareous sandstones (Kent, 1980). The Corallian group is also

identified south of the Vale and form most of the Hawardian Hills (Cope, 1974). To the east of the Howardian Hills encompassing much of the Yorkshire Wolds is an extensive area of chalk. Different chalk members include the Ferriby, Welton, Burnham and Flamborough Chalk Formations (Kent, 1980) which contain very fine grained, pure, white Limestone.

3.4.2 Glacial history of the Vale of Pickering

The late Devensian glacial history of the north east England is complex, however, during the LGM, most of Vale of Pickering (VoP) remained ice free. The LGM limit is suggested to reside north of the North York Moors (e.g. Kendall, 1902). Nevertheless, depositional features within the Vale predominantly reflect the interplay between the North Sea Ice Lobe (NSIL) and the Vale of York Ice Lobe (VYIL), both of which, during the LGM, advanced past the Vale and into East Yorkshire and Lincolnshire (e.g. Bateman et al., 2008; Bateman et al., 2015; Evans and Thompson, 2010; Evans et al., 2017). Of critical importance for the VoP are the different phases of ice lobe advance and retreat which dam drainage routes around the Vale. This culminates in the development of a series of glacial lakes; Glacial Lake Humber to the south of the VYIL and Glacial Lake Pickering to the west of the NSIL.

During southerly ice advance, an offshoot of the NSIL entered the eastern Vale of Pickering (eVoP). Observations of a package of sediment in the eVoP, termed the Hutton Buscel Sands and Gravels and a kame terrace termed the Wykeham moraine, is the debated maximum extent of the NSIL into the Vale during the LGM (Evans et al., 2005; Evans et al., 2017). Although a secondary position is proposed at Thornton-le-dale through observations of glacial till. Regardless of its position, ice in the Vale coupled with ice from the Vale of York, which deposited the Ampleforth moraine in the Coxwald-Gilling Gap on the western edge of the Vale, formed Glacial Lake Pickering. The highest lake levels attained by Glacial Lake Pickering, ca 70 m a.s.l. are inferred to reflect blocked drainage pathways by the VYIL through the Coxwold-Gilling Gap and Kirkham Priory Gorge, at 68 and 65 m a.s.l. respectively (Eddey et al., 2017). Subsequent ice retreat of the NSIL formed the Flamborough Moraine on the eastern coast of the Vale. Coeval with the retreat of the NSIL, the VYIL retreated north (Bateman et al., 2015). The retreat of ice from both locations is suggested to have allowed the lake levels to fall, via spillway drainage, to ca 45 m. This elevation is close to the maximum lake levels of Glacial Lake Humber, suggesting inter-lake connectivity at this time (Fairburn and Bateman, 2016).

Based on optically stimulated luminescence dates from the Sherbern Sands, deposited on the north escarpment of the Wolds following easterly ice migration out of the Vale, an

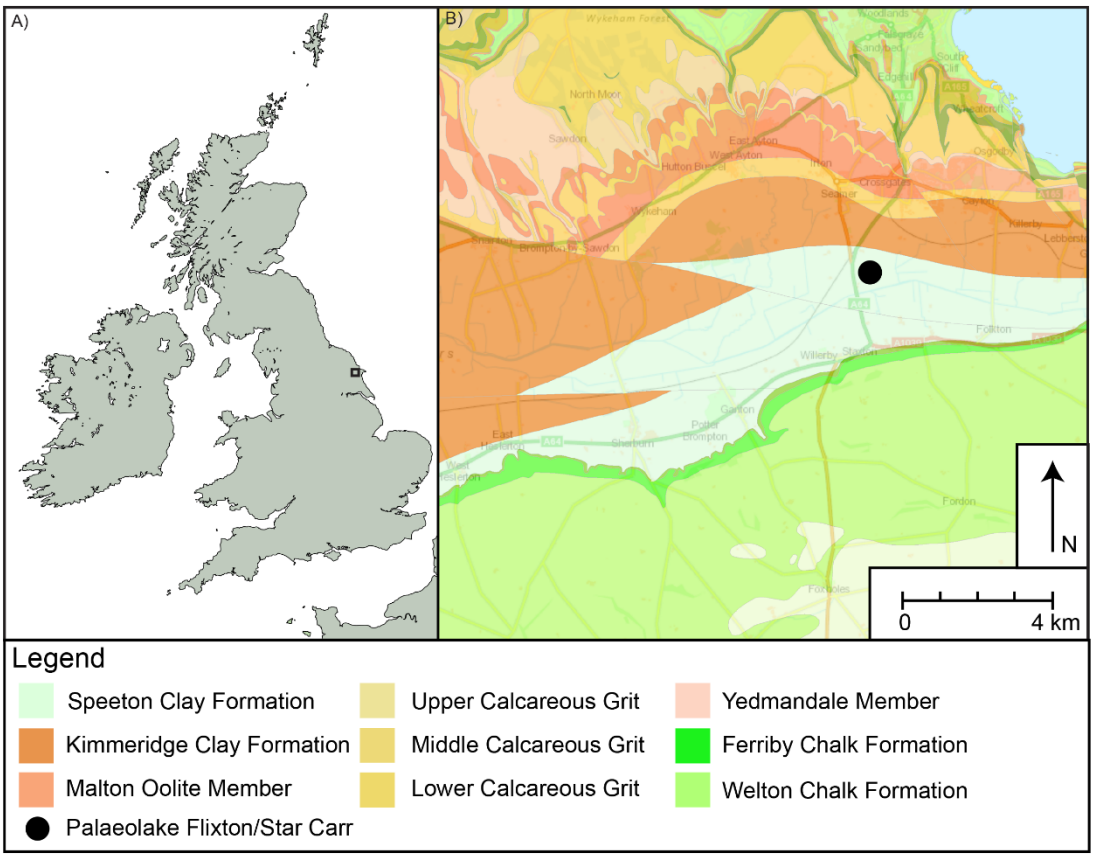

Figure 3.7 A) Location of the VoP in north-east England; and B) a detailed geological map of the basement complex of the eVoP. Highlighted is the approximate position of Palaeolake Flixton (Contains British Geological Survey materials © UKRI 2018).

initial lake level fall is suggested to have occurred between 17-18 ka BP (Evans et al., 2017). Subsequently, ice continued to retreat away from the Vale, and lake levels fell to 30 m a.s.l. either by cutting and draining through the Kirkham Priory Gorge or through the Flamborough moraine (Eddey and Lincoln, 2017). Evidence of the 30 m lake is ascribed to a fan delta existing at the Newtondale spillway, draining the North York Moors, at an elevation of 30 m a.s.l. (Eddey et al., 2017). Ice retreat and the fall in lake level likely occurred between 17 and 15 ka BP. The exact number of lake levels of Glacial Lake Pickering is debated. The recent elucidation of complexity within Glacial Lake Humber (e.g. Fairburn and Bateman, 2016) and a series of different terrace levels in Kirkham Gorge (e.g. Eddey and Lincoln, 2017) suggest Glacial Lake Pickering exhibits a complex lake level history which, at the time of writing, is not fully understood.

Nevertheless, following deglaciation and climatic amelioration during the WI, Glacial Lake Pickering underwent further lake level reduction and substantial spatial contraction. This final lake stage within the eVoP, termed Palaeolake Flixton, existed throughout the LGIT and its lake levels were principally controlled by the fluctuations of the water table (Candy et al., 2015; Palmer et al., 2015).

3.4.3 Palaeolake Flixton (Star Carr)- site location

Star Carr resides in the Vale of Pickering, Northern Yorkshire and is approximately 7.5 km west south west of Scarborough (54.215919, -0.42034507; TA031811). The site sits on the former western shorelines of Palaeolake Flixton, with the latter located within the eastern Vale of Pickering between Staxton and West Flotmanby. The palaeolake had an extent of approximately 4.0 x 2.5 km, occupied an area of approximately 14.0 km^2 (Figure 3.8), and lay at an altitude of between 23 and 27 m a.s.l. The basin itself sits amongst the Speeton Clay and the Kimmeridge Clay Formations (Figure 3.7). Since the 20th century the land occupying the former palaeolake has been used for both pastoral and arable farming; and the observations of drainage networks, peat cuttings, and field ploughing have affected the hydrology of the site (Milner et al., 2011a; Dark, 2017). As a result, the current land surface is dominated by ploughed fields as opposed to a natural mire as perhaps would be expected. During the residence of Palaeolake Flixton, the site would have been fed by a series of streams from the higher ground of the North York Moors and Yorkshire Wolds; and drained by the Hertford palaeoriver, linking with the River Derwent in the west of the Vale. Two sequences have been studied as part of this research.

3.4.4 Palaeolake Flixton (Star Carr)- previous investigations

Palaeolake Flixton and Star Carr are perhaps most famously known for their archaeology (e.g. Clark, 1954; Mellars and Dark, 1998; Conneller, 2004; Milner et al., 2011b). The association of Star Carr finds including reworked bone, barbed antler points, antler head-dresses, worked timber platforms (e.g. Clark, 1954) and more recently, evidence of a post-built structure (e.g. Milner et al., 2011b) increased evidence of material culture (e.g. Taylor et al., 2017) and evidence of shale pendant artistry (e.g. Milner et al., 2016) with robust chronologies, are suggestive of phases of early Mesolithic occupation during the Holocene (Conneller, 2007). It is noted however that the nearby archaeological sites of Flixton Island and the Seamer Carrs may push occupation back into the Interstadial (Conneller, 2007). Within this archaeological context there are a series of palaeoecological investigations at Star Carr (e.g. Walker and Godwin, 1954; Cloutman, 1988, Cloutman and Smith, 1988; Dark, 1998a, b, c; Albert et al., 2016; Dark, 2017). The latter two investigations principally focus on the deterioration of the landscape around the site. Whilst peat desiccation has occurred which has affected the pollen held within, the authors note that the pollen deterioration is a result of the sequences residing on the landward side of the palaeolake, with areas of lacustrine sedimentation unlikely to be affected.

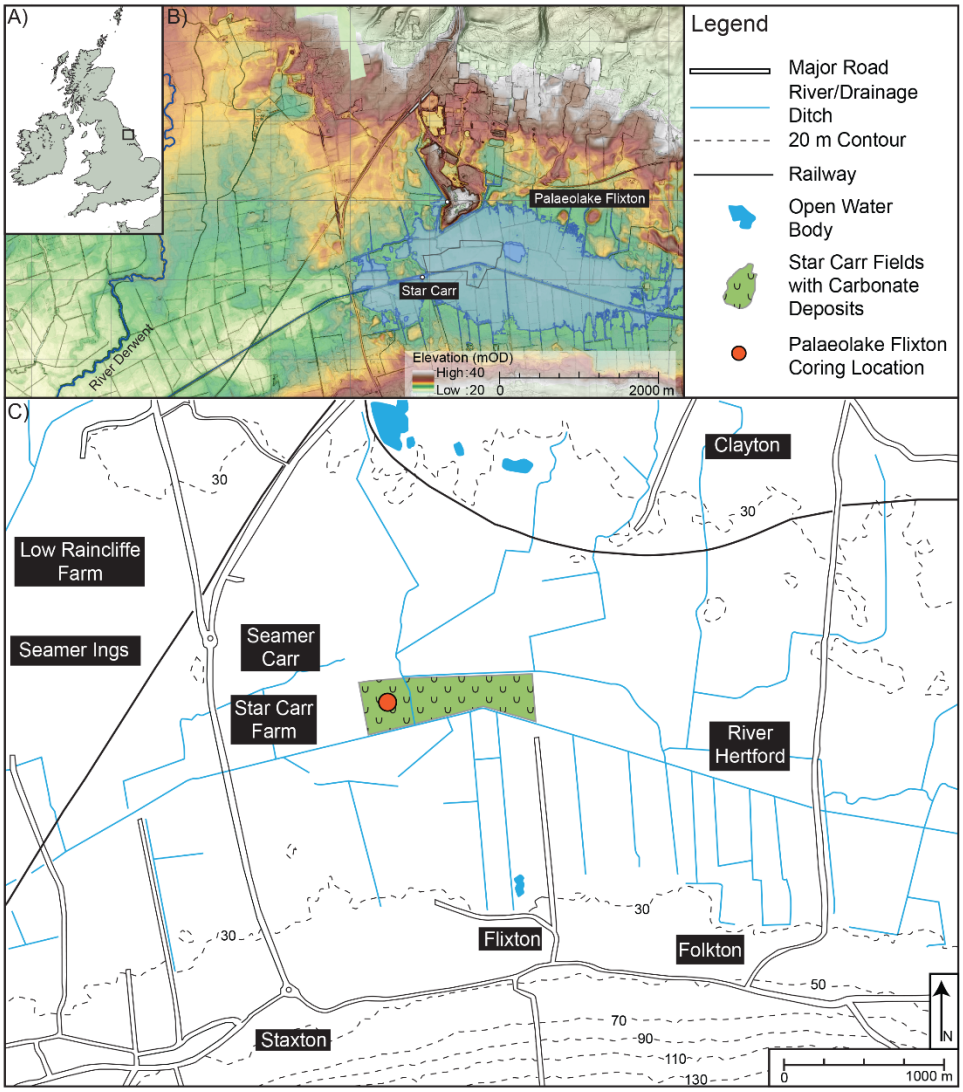

Figure 3.8 Topographic map of the eastern Vale of Pickering. A) reveals the position of the Vale in England; B) shows a hillshade model of the eastern Vale of Pickering, with the position of Palaeolake Flixton (adapted from Lincoln, 2017); and C) a topographic map of the study site. Shown are 20 m contours, the Star Carr fields and the coring location within this study.

In contrast, the aim of the earlier palaeoecological investigations was two-fold: 1) to provide evidence of the vegetation history surrounding Star Carr and 2) to demonstrate the interaction between early Mesolithic occupants at Star Carr and the landscape. The earliest investigation (e.g. Walker and Godwin, 1954) focussed on reconstructing vegetation at Star Carr, albeit at low resolutions, and found no evidence of human modification of the landscape (Dark, 1998d). Through a series of systematic surveys, subsequent work by Cloutman (1988) provided much of the understanding of the underlying bathymetry and stratigraphy of the western edge of Palaeolake Flixton. From these surveys Cloutman and Smith (1988) undertook higher resolution pollen analysis from four sequences in the hope that these vegetation studies would refine the earlier work of Walker and Godwin (1954) to better understand human-landscape interactions.

However, as Dark (1998d) states, the resolution was still too coarse to detect these changes.

As a result, in 1998, the most highly resolved multi-proxy investigations at Star Carr were published (e.g. Dark, 1998a, b, c). This work focussed on high-resolution pollen and charcoal reconstructions with the generation of a robust chronology. Like previous work, Dark (1998a, b, c) focussed the investigation on shorter shoreline deposits and a longer lake centre core sequence (Figure 3.9) in the hope to discriminate between ecological events and potential landscape modification. The shorter sequences, detailing a localised vegetation history, provided unequivocal evidence that Mesolithic populations were actively modifying vegetation. Further, the sequences analysed were recovered adjacent to significant archaeological excavations (e.g. Dark, 1998a; on the southern perimeter of the Clark, (1954) excavations and Monoliths 1, 2, 3; 30m east from Clark, (1954)). From these investigations Dark (1998a) concluded that periodic burning of reedswamp vegetation and changes in vegetation assemblage alongside phases of platform building, demonstrated active human-environment interactions. The dates of these events place them firmly within the early Holocene. It was therefore determined that palaeoecological investigations from archaeologically rich sediments (e.g. worked timbers and artefacts) can be used to elucidate unanswered human occupation theories.

The longer sedimentary sequence from lake centre sediments (e.g. Dark, 1998c) demonstrated the changes in vegetation from a regional viewpoint and provided evidence of vegetation change throughout the LGIT. From this 677 cm lake centre sequence, seven local pollen assemblage zones were identified (e.g. Dark, 1998c; Figure 3.9). Based on biostratigraphic principles, pollen zones S-1:S-3b are attributed to the WI, S-3c to the LLS and the remaining zones to the early Holocene. During the Interstadial the vegetation was dominated initially by open grassland herbaceous taxa including Poaceae, Cyperaceae, *Artemisia* and *Rumex* before becoming increasingly woody (Figure 3.9). The first expression of woody taxa was *Betula*, which may reflect *Betula nana*, then *Juniperus* existing as a widespread *Juniperus* scrub and a subsequent period of *Betula pubescens* open woodland (Dark, 1998c; Figure 3.9). The LLS shows moderate percentages of Poaceae and Cyperaceae with increasing percentages of disturbed ground indicators including *Artemisia*, *Rumex* and *Thalictrum* suggesting the landscape was dominated by an open grassland community. A successional sequence of *Salix*, *Juniperus*, *Betula* woodland and finally *Corylus* dominated in the early Holocene. Despite these observations, during the Interstadial and perhaps during the early Holocene, vegetation oscillated between two states. Initially, during S-2, woody taxa were replaced by *Juniperus*, and later, within S-3b and S-4, *Betula* was replaced by

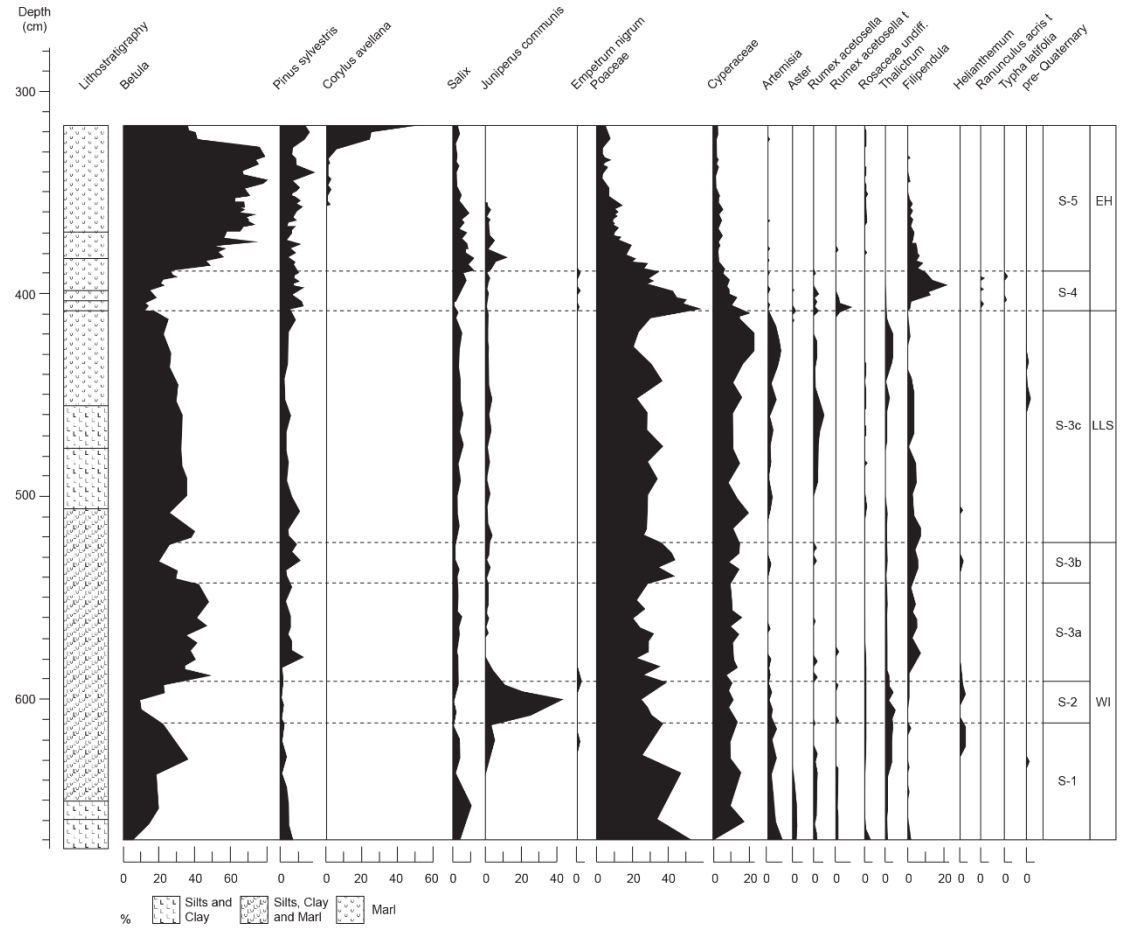

Figure 3.9 The previous lithostratigraphic and palynological investigation from the lake centre Palaeolake Flixton sequence. Shown here is a truncated record, revealing the different vegetation assemblages during the LGIT. Within this figure are principal taxa only and shown in percentages, revealing variability throughout the LGIT. Adapted from Day (1998d).

Poaceae (Figure 3.9). These changes in the vegetation record potentially reflect a vegetative response to climatic oscillations observed from elsewhere in the British Isles (Dark, 1998c). However, without additional climatic and chronological data this cannot be fully quantified, as it might be unlikely that *Juniperus* expansion would be the result of a climatic deterioration due to its association with warm conditions and suitable soils.

Finally, recent surveying of the bathymetry of Palaeolake Flixton surrounding Star Carr has revealed an increasingly complex basal topography with a suite of basins separated by areas of higher ground (e.g. Palmer et al., 2015). Analysis of the sedimentological infill (e.g. Candy et al., 2015; 2017; Blockley et al., 2018) has revealed palaeoclimatic oscillations that can are comparable to the GI-1d, 11.4 Ka and 11.1 Ka BP climatic oscillations within the ice-core records (Rasmussen et al., 2006; 2007). The elucidation of these events within the Star Carr records permit further study to understand how vegetation responds to these events in north-east England.

3.5 Brecon Beacons, south Wales

The Brecon Beacons National Park is principally situated towards the south of Powys county, south Wales and extends from the Black Mountains in the east to the Carmarthen Fans in the west (Carr et al., 2007). The Beacons have a relatively high relief, lower elevations are to the west, rising to areas of higher ground, including the highest point, Pen-y-Fan 886 m a.s.l. towards the middle of the park.

Many areas of south Wales are poorly studied compared to Scotland and northern England. Much of the palaeoenvironmental detail from this region stems from Treath Mawr (Walker, 1982), Llangorse (Walker et al., 1993b) and Llanilid to the south of the Beacons (Walker et al., 2003). Therefore, increasing the level of palaeoenvironmental information from this area is important to elucidate palaeoclimatic and palaeoenvironmental differences from the rest of Britain.

3.5.1 Geology of the Brecon Beacons

Like Orkney, the underlying basal lithologies to the north of the Brecon Beacons can be divided amongst the Old Red Sandstone Group. The oldest rock types noted within the region are observed between Hereford, north-east of the Beacons and stretch to the town of Brecon. This Raglan Mudstone Formation forms part of the early Devonian-aged, Lower Old Red Sandstone Group and is predominantly composed of red-brown micaceous mudstones and fine sandstones (George, 1970; Howells, 2007; Figure 3.10). Overlaying this to the south, but still confined to the north of the Beacons National Park, is the St Maughans Formation; forming a further component of the Lower Old Red Sandstone Group (Howells, 2007; Figure 3.10). Stretching from the Black Mountains in Monmouthshire and tapering to the west of the park are the two highest Lower Old Red Sandstone group members; the Senni and Brownstone Formations. The Senni Formation is noted for its green colouration, whereas, the Brownstone contains red-brown sandstones (George, 1970; Figure 3.10). To the south of the Brecon Beacons thin outcrops of late Devonian Upper Red Sandstone Members are observed. In ascending order these are composed of the Plateau Beds Formation, which is overlain by the correlated Grey Grit Formation and to the east the Quartz Conglomerate Group (Howells, 2007). The remainder of the basal lithology of the region around the south of the Brecon Beacons can be placed into the Carboniferous Period. Highly faulted members of the Pembroke Limestone and Marros Groups, formerly Millstone Grit can be traced through Merthyr Tydfil to Carmarthen Bay. Finally, and perhaps most characteristic of this area of South Wales are the Lower and Middle Coal Measures that are predominantly composed of pyritic and micaceous shales (George, 1970).

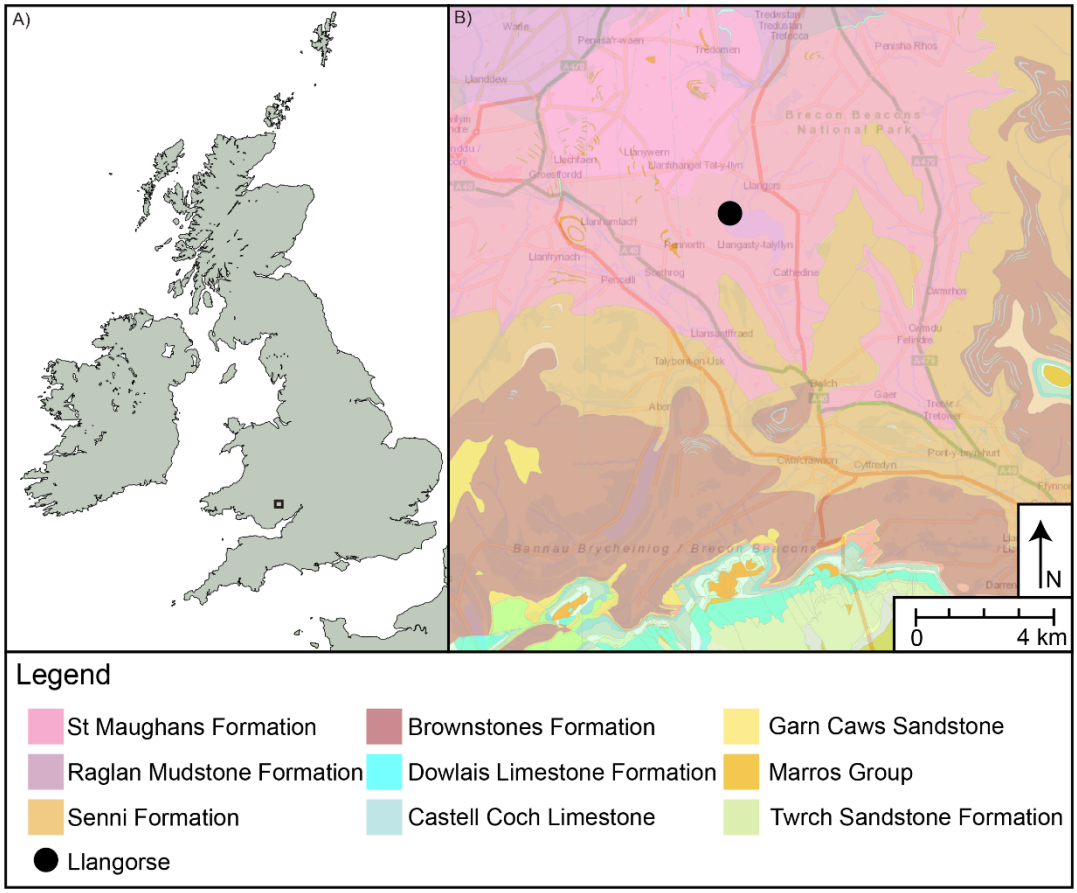

Figure 3.10 A) Location of the Brecon Beacons in south Wales; and B) a detailed geological map of the basement complex of the eastern Brecon Beacons. Highlighted is the position of Llangorse (Contains British Geological Survey materials © UKRI 2018).

3.5.2 Glacial history of the Brecon Beacons

The Brecon Beacons lie close to the reconstructed late Devensian ice sheet limit for this region (e.g. Charlesworth, 1929; Bowen, 1973; Bowen et al., 2002; Clark et al., 2012a). The Beacons are therefore important in determining not only the character of glaciation through the region but also interactions with Irish Sea ice (e.g. Ó Cofaigh and Evans, 2001) and deglaciation histories. Principally, the extent of the last glaciation has been demarked based on the position of the South Wales End Moraine on the Gower Peninsula (Charlesworth, 1929). Although positions of the margin changed through the identification of subsequent geomorphological evidence (Evans et al., 2005) it is widely accepted that the BIIS at its maximum extent overtopped the Brecon Beacons. This is largely from the observation of erratics with a north Wales and Lake District provenance (e.g. Ellis-Gruffydd, 1977). It is further suggested that ice reached the southernmost limit in Wales by 23.2 ka BP (Phillips et al., 1994). During retreat of the ice in south Wales, the Welsh Ice Sheet (WIS) decoupled from the BIIS (Clark et al., 2012) before eventually receding.

Detailed work within the Brecon Beacons suggest a complex history of ice advance and retreat however. The model proposed by Janssen and Glasser (2008) suggests, based on glacial lineations, that initially ice sourced locally within the Brecon Beacons radiated out of the highlands before the LGM. A subsequent phase where locally sourced Brecon ice coalesced with ice from the WIS, flowing in a southerly direction, is then proposed during the LGM. Retreat phases for the Beacons are poorly constrained, however, one of the more studied areas, the Llynfi basin to the north of the national park, contains two models of ice retreat (e.g. Lewis, 1970; Humpage, 2007). Lewis (1970) proposed that lobes of the WIS retreated to the north of the Brecon Beacons, through the Wye Valley, with four stages of ice retreat forming a series of moraine ridges. This model has recently been challenged by Humpage (2007) who suggests that based on material sourced from the Usk Valley and the formation of dead-ice topography in the Llynfi basin, early retreat of the WIS, through the Wye Valley, may have allowed the easterly advance of local ice lobes within the Usk Valley (Humpage, 2007). Furthermore, a glacial lake in this region has been identified, termed Glacial Lake Llangorse (e.g. Walker et al, 1993b; Palmer et al., 2008). Lewis' (1970) model suggests that Glacial Lake Llangorse was created during the second retreat phase with drainage damned by the moraine ridge, whereas Humpage (2007) argues that the ice lobes themselves may have blocked drainage of the Llynfi River. Nonetheless, whilst both models are still debated, both allow for the formation of Glacial Lake Llangorse.

Evidence of LLS glaciation in the Brecon Beacons has been contentious as it represents the most southerly point in the British Isles where ice built up following the LGM (e.g. Lewis, 1970; Ellis-Gryffydd, 1977; Shakesby and Matthews, 1993; Carr, 2001). Despite a distinct lack of geomorphological evidence, the identification of a suite of short depositional ridges, many with locally striated clasts have demonstrated evidence of LLS cirque glaciation (Bickerdike et al., 2018). Further evidence of restricted stadial glaciation is provided by biostratigraphic studies. Sites that lie outside the limit of cirque glaciation contain vegetation associations with the WI and the LLS, for example Traith Mawr (e.g. Walker, 1982) and Waen Ddu Bog (e.g. Coleman and Parker, 2007), whereas sites that have been overridden by stadial glaciation contain records attributable to the Holocene only, for example Craig-y-Fro (Walker, 2007a) and Craig Cerrig-gleisiad (Walker, 2007b). Whilst the deglacial history is contentious, areas outside the limits of the local LLR within the Brecon Beacons have the potential to contain records attributable to the LGIT.

3.5.3 Llangorse- site location

Llangorse Lake (Llyn Syfaddan) is the largest body of open water in south Wales; located in the north-east Brecon Beacons, within the Llnyfi basin, approximately 1.5 km south

west of Llangorse village and approximately 8 km east-south-east of Brecon (Figure 3.11). The lake itself (51.930930, -3.2625103; SO132265) sits in a topographic low within the St Maughans Formation which is composed of interbedded sandstones, siltstones and mudstones (Howell, 2007). To the south-east and south-west of the lake the geology shifts to the Senni Formation. Presently the lake is an irregular shape and at its maximum extent the basin is 1.6 x 1 km, occupies and area of 1.12 km^2, and lies at an altitude of 155 m a.s.l. (Figure 3.11). The lake is also relatively shallow and only at two areas within the lake do water depths exceed 8 m (Jones et al., 1985). Principally, the lake is fed, at its southern edge by the Afon Llynfi River, a tributary of the River Wye, with its headwaters near the River Usk (Chambers, 2007). However, the lake is also likely fed by a series of small streams from the Mynydd Llangorse hillslope to the east, which rises to 500 m a.s.l, and the elevated ground to the west (Figure 3.11). Llangorse lake is drained by the Afon Llynfi to the north. Despite its current setting, during the LGIT and immediately following deglaciation the lake would have been considerably larger. This created a glaciolacustrine system where Llangorse Lake at is maximum extent was 6 km x 3 km and up to 60 m deep (Palmer et al., 2007; 2008). Observations of lacustrine marl sediments to the north-east of the basin (e.g. Walker et al., 1993b) further confirm the existence of a much larger lake in the past.

3.5.4 Llangorse- previous investigations

Initial analyses at Llangorse applied modern chemical and biological methods to derive different limnological parameters of the lake from recent history (e.g. Jones et al., 1985; 1991; Bennion and Appleby, 1999; Benson-Evans et al., 1999) Further, through preliminary pollen analytical work, Jones et al. (1985) postulated a human modification of the landscape surrounding the lake during the mid-Holocene. Later palaeoecological research sought to provide further evidence of human influence, but also detail the baseline environmental conditions before human impact (e.g. Chambers, 1985; Chambers, 1999). These investigations indicated that the environment surrounding Llangorse was dominated by closed canopy woodland thriving on stable soils during the mid-Holocene (e.g. Chambers, 1985; Chambers, 1999). Only following sediment retrieval from the Llangorse crannog site (e.g. Campbell and Lane, 1989; Walker et al., 1993b) was further palaeoenvironmental research undertaken.

From the crannog sequence, 273 cm in length, it was demonstrated that lake marl makes up a considerable portion of the basin infill (Walker et al., 1993b). Beneath the marl, laminated sediments, thought to be annual laminae, were identified (Walker et al., 1993b; Chambers, 1999). In a detailed multi-proxy investigation which focussed principally on the lacustrine marl; Walker et al. (1993b) established the environmental history of

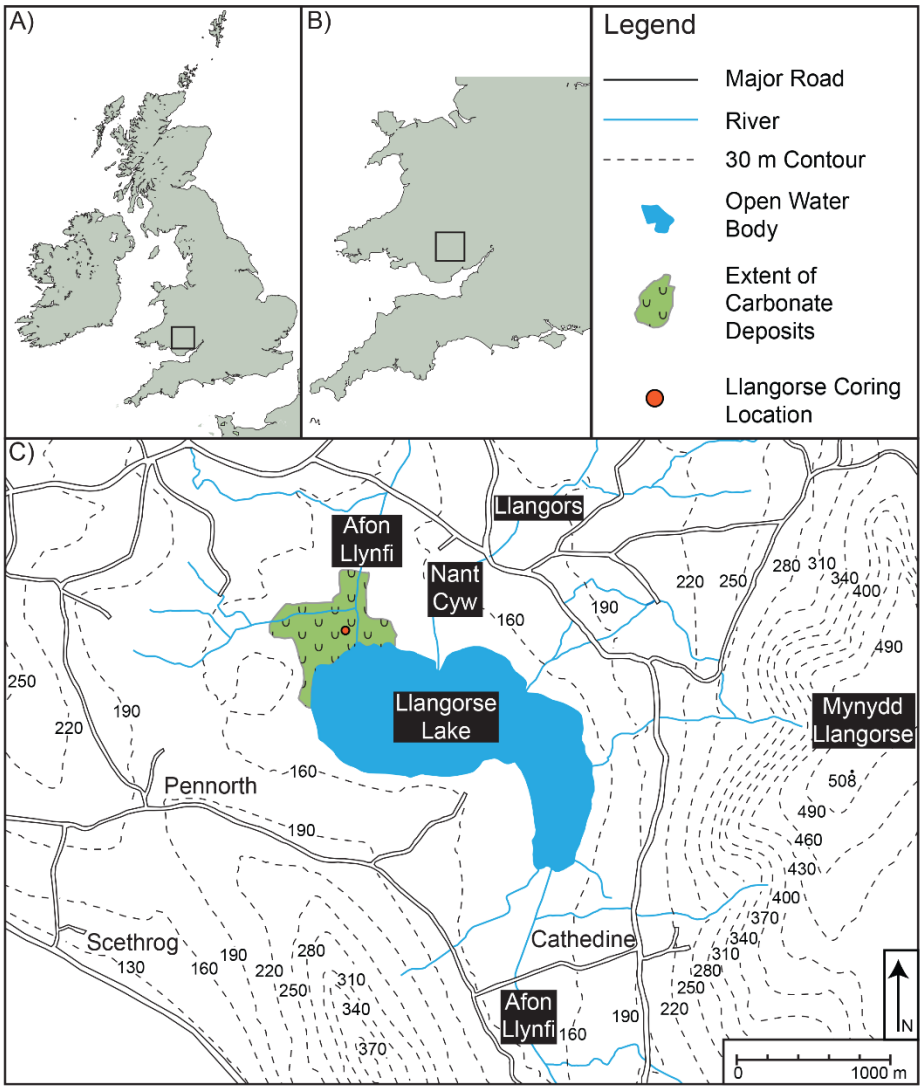

Figure 3.11 Topographic map of Llangorse and surrounds. A) reveals the position of Brecon Beacons in south Wales; B) shows a closer image within south-west England and Wales; and C) shows a topographic map of the study site. Shown are 30 m contours, Llangorse Lake and the calcareous deposits as mapped by Walker et al. (1993b).

Llangorse from the LLS-Holocene transition and during the early Holocene. The basal pollen zone, L-1, is dominated by Poaceae, *Artemisia* and *Rumex*, which reflects the general open nature of the landscape following climatic amelioration from the underlying Stadial episode (Figure 3.12). Pollen zones L2-L4 demonstrate phases of increasingly woody taxa within the landscape, including a low lying expansive *Juniperus* scrub during, an initially open developing into a closed *Betula* woodland, and a closed boreal forest with *Betula*, *Pinus* and *Salix* with minimal non-arboreal taxa (Walker et al., 1993b; Figure 3.12). During zone L-3, there is evidence of a return to open/disturbed ground conditions, albeit confined to two samples (Figure 3.12). This was taken to reflect a potential climatic event (Walker et al., 1993b). The remainder of the sequence, L-5 and L-6, demonstrates first the establishment of a *Corylus* woodland and subsequently a *Corylus* woodland with a broad leaf tree component (Walker et al., 1993b).

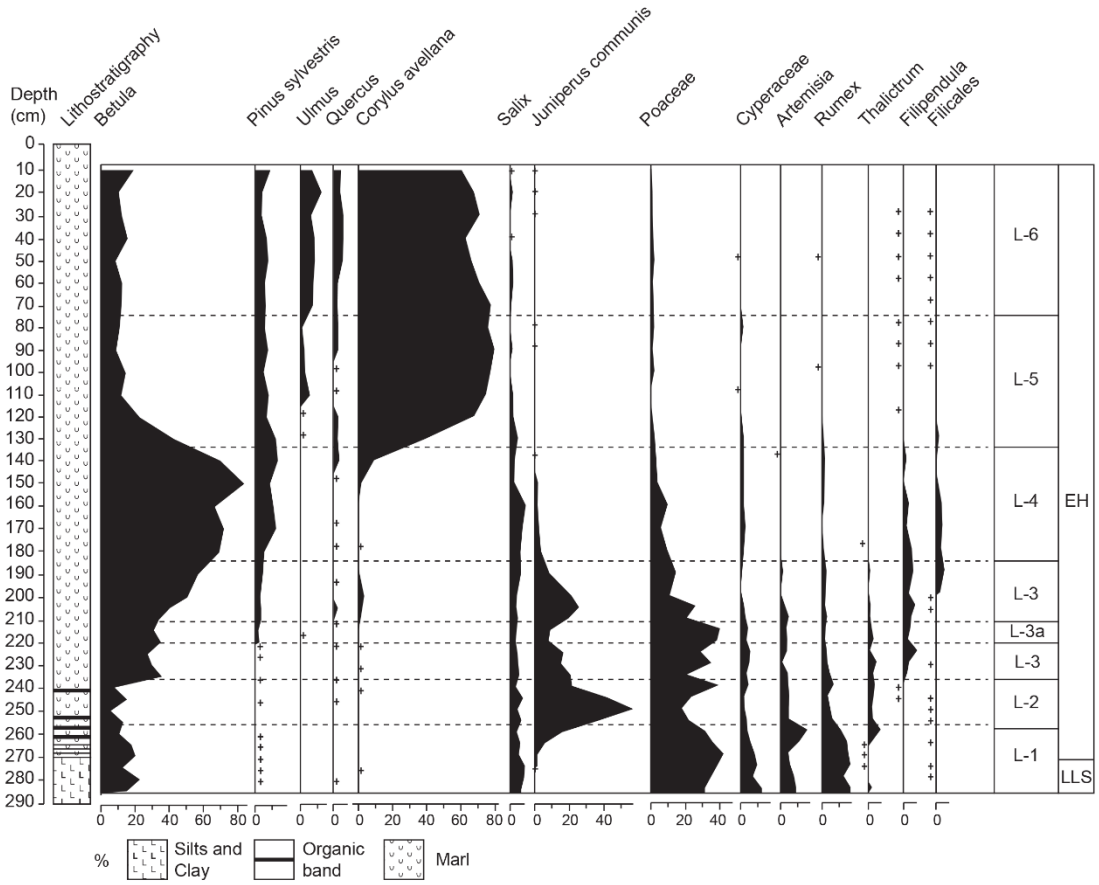

Figure 3.12 The previous lithostratigraphic and palynological investigation into Holocene sediments from the Llangorse crannog. Shown here is a truncated record, revealing the different vegetation assemblages during the Holocene only, no sediments were attributable to the LGIT at the crannog sequence. Within this figure are principal taxa only which are shown as percentages. Adapted from Walker et al. (1993b).

Additional research from Llangorse has focussed on the annually laminated sediments beneath the carbonate sediments at the crannog site (e.g. Palmer et al., 2007; 2008). Using micromorphological techniques Palmer et al. (2008) identified four microfacies groups with lamination sets that are typical of glaciolacustrine varves whereby the coarser layers are deposited during the summer as glaciers melt; and the clay layer deposited during the winter, in still water environments following lake freezing (Palmer et al., 2008). This implies that Llangorse existed as a proglacial lake following deglaciation. Further, varve thickness data generated by Palmer et al. (2007; 2008) implies that ice retreat from the Llangorse area was relatively slow 5.2 ma^{-1} (metres annually). The characterisation of annually laminated sediments can therefore reveal critical information regarding the nature of deglaciation in this area. Furthermore, it was reported in Palmer et al. (2007) that no evidence exists for sediments pertaining to the WI or LLS and the crannog sequence contains a hiatus in sedimentation. Since this publication, in 2014 marl sediments were retrieved from the north-east of Llangorse (e.g.

Walker et al., 1993b) which appeared to demonstrate a tripartite sequence. Further work from these sequences is therefore warranted.

3.6 Chapter summary

The aims of this chapter were threefold: 1) to provide a rationale for transect placement and site selection within the British Isles; 2) to provide contextual information including bedrock geology and late Devensian glacial histories of each region being studied; and 3) to provide detailed site location information and the history of research undertaken at each site. Four sites were chosen from different climatic and latitudinal regions of Britain to understand to elucidate vegetation dynamics during the LGIT. Each site was chosen based the availability of pre-existing climatic data, the demonstration that each site can be attributed to the LGIT and that each site has an expanded sedimentary sequence or contains variations in lithostratigraphy. The selected sites are all good candidates in understanding how vegetation responds to abrupt climatic events. Furthermore, the wide spatial area of this transect, from Orkney to south Wales offer the potential for the creation of a bounded network for which to include additional highly resolved sites.

Chapter 4. Methodology

This chapter provides details on the field methods, laboratory protocols and data analytical approaches within this research. A generalised overview of the field methods will be presented in this chapter with any site-specific approaches detailed in individual results chapters. Importance is given to the pollen processing and extraction methodologies as this was the prime focus of the research. Throughout the thesis it became apparent that one extraction methodology may not yield pollen in adequate quantities. At certain sites therefore, two approaches to pollen extraction have been applied. Where data is presented but analyses have not been undertaken by the author of this thesis (chironomid/tephra analysis) methods are not presented.

4.1 Field methods

4.1.1 Depth sounding and bathymetric surveys

To determine the most appropriate sediment sequences from each of the four sites selected (Chapter 3) a series of systematic surveys were set up to constrain the size of the basin(s). Stratigraphically expanded sediment sequences were then selected across each of the four sites. Point depth measurements across each site were carried out using hand operated augering equipment, 'Russian' coring devices and 1.0 m extension rods. Individual results sections detail the survey approach used at each site.

4.1.2 Sediment extraction

Sediment sequences were extracted using variable length and variable diameter 'Russian' corers (Jowsey, 1966). As the sites contained predominantly organic sediments, hand operated 'Russian' corers were preferred over mechanical corers, to preserve sedimentological structures. Two boreholes were created at each site for the extraction of overlapping cores. This overlap is vital as the 5 cm nose-cone on the 'Russian' corer disturbs sediment 5 cm beneath the previous sample. Across all sites, where particularly important sections were noted in the field, core duplicates were obtained from additional boreholes. From key sections and for certain methodologies, for example radiocarbon dating, larger diameter corers were used to extract larger volumes of material.

4.2 Sedimentological methods

4.2.1 Sediment description

Before sub-sampling for bulk sedimentological or palaeoenvironmental analyses, sedimentary core sequences were cleaned perpendicular to the main axis of the core using a scalpel. The cleaned surfaces from each core section were described in the laboratory using the Troels-Smith (1955) sediment classification scheme. This

classification scheme determined the physical properties of the sediments including stratification and elasticity; but also detailed the composition of the sediments, contacts between sedimentological units and Munsell colours. This standardised approach for determining sedimentological descriptions allowed for the creation of sediment logs for the pictorial delineation of different sediment units within and between core sequences.

4.2.2 Sediment imaging

Each of the cleaned core sequences was digitally imaged using a Cannon DSLR camera mounted to a camera stand. To ensure images were of the highest quality, light mounts were used to illuminate the core profile and the position of the camera was kept constant. Individual photographs of the core sections were 'stitched' together using Adobe Photoshop CC to produce composite images of core sequences. These composite images work in tandem with the sedimentological descriptions and logs to provide evidence of lithological changes within the sediment sequences.

4.2.3 Loss on Ignition (LOI)

Loss on ignition is usually employed as a first approximation of the organic constituents of sediments. LOI predominantly involves the oxidation of organic matter to carbon dioxide in a furnace at 500-550°C (e.g. Dean, 1974; Boyle, 2001; Heiri et al., 2001). Heating at these temperatures can remove additional materials including structurally bound water, volatile salts and inorganic carbon (Heiri et al., 2001). The method for determining LOI for this study (Table 4.1), followed Bengsston and Enell (1986), whereby ca 1 cm^3 of sediment was dried at 105°C overnight, weighed, placed in a furnace at 550°C for four hours and reweighed. To calculate the percentage of organic matter the following equation was used:

$$\% \, LOI = \left(\frac{AW}{DW}\right) * 100$$

Where, AW reflects ashed weight at 550°C; and DW reflects dry weight of the sediment.

4.2.4 Total Organic Carbon (TOC)

The standard method for obtaining organic matter concentrations in lacustrine sediments is through LOI analysis (e.g. Lowe, 2001). However, organic matter contains approximately 50 % organic carbon so LOI percentages reflect roughly twice this amount (Meyers and Lallier-Vergès, 1999), and sedimentary LOI values are influenced by losses of inorganic carbon, potentially elevating the percentage of organic matter observed. A more precise way to quantify organic matter in carbonate sediments is to use Total Organic Carbon (TOC), which provides with greater certainty an estimate of organic

Table 4.1 LOI sample details for different sites within this study. LOI was not analysed at Tirinie, Llangorse or Palaeolake Flixton as TOC was considered more robust.

Site	Sequence	Depth (cm)	Resolution	Analyst
Quoyloo Meadow	QM; Composite	242.5-120.5	1 cm	Timms (2016)
Palaeolake Flixton	Star Carr B 2017	473.5-289.5	8-12 cm	This study (not presented)
		289.5-245.5	4 cm	
Palaeolake Flixton	Star Carr C 2017	669.5-597.5	24 cm	This study (not presented)
		597.5-301.5	8-16 cm	

matter concentrations. TOC was measured using the Walkley and Black (1934) titration method and applied to a selection of carbonate sequences at Tirinie, Palaeolake Flixton and Llangorse (Table 4.2). It was not measured for the Quoyloo Meadow. To express the percentages of TOC the following equation was used:

$$\%\,TOC = \frac{[(10 - (Vt * Mf)) * 0.3 * 1.33}{W}$$

Where Vt is the volume of ferrous ammonium sulphate solution for titration; Mf volume of ferrous ammonium sulphate solution for blank titration; and W is sample weight.

4.2.5 Calcimetry

Calcimetry is used to denote the carbonate content within sediments. As the sequences worked on as part of this study predominantly contain carbonate rich sediments, estimates of the carbonate content of these sediments may be important in revealing subtle lithostratigraphic changes and potential shifts in vegetation profiles. Two methods for determining carbonate content have been used within this research: a secondary ashing phase post-LOI measurements, whereby sediments are exposed to temperatures of 925°C for four hours (Heiri et al., 2001), and the gasometric method outlined by Gale and Hoare (1991). The second, more precise method, involves measuring the carbon dioxide eluted from dried sediments with the addition of Hydrochloric acid (HCl) in a Bascomb calcimeter. Water displacement from the increase in gas pressure is then directly related to the amount of carbonate within the sample. Where possible, this secondary method was applied, however, where time constraints prevailed the former

Table 4.2 TOC sample details for different sites within this study. No TOC data is present from Quoyloo Meadow.

Site	Sequence	Depth (cm)	Resolution	Researcher
Tirinie	TIR 2012;	354.5-265.5	1 cm	Elliot (2012)
	Composite	294.5-194.5	1 cm	Francis (2012)
Palaeolake Flixton	Star Carr C 2010;	732.5-282.5	4 cm	Darvill (2011)
Llangorse	LLaN 14;	663.5-594.5	1-8 cm	Palmer (2016)
	Composite	594.5-487.5	1-2 cm	
		487.5-344.5	2-24 cm	
		344.4-220.5	1 cm	

method was adopted (Table 4.3). To express carbonate content from the LOI method the following equation was used:

$$\%\ CaCO3 = \left(\left(\frac{AW}{DW}\right) * 1.36\right) * 100$$

Where, AW is ashed weight at 925°C; and DW is dry weight of the sediment.

Using the gasometric method, with increased precision, calcium carbonate is estimated by:

$$CaCO3 = \frac{VpC}{MT}$$

Whereby, V is the volume of carbon dioxide evolved during the reaction (cm^3); p is barometric pressure (mm Hg); C is a constant of 0.1605; M is the mass of the sample (g); and T is temperature (°C + 273.15).

4.2.6 Magnetic susceptibility

Magnetic susceptibility is a measurement of the 'magnetisability' of a material (Dearing, 1999) and is used to understand fluctuations in iron bearing mineral components of sedimentary sequences. For this research, magnetic susceptibility measurements have been used in conjunction with the bulk analyses to provide evidence of sedimentary change. All materials were analysed at variable stratigraphic resolutions with all measurements undertaken on a Bartington Instruments MS2C core-scanning sensor and values recorded as magnetic susceptibility x 10^{-5} SI units.

Table 4.3 Calcimetry sample details for different sites within this study.

Site	Sequence	Depth (cm)	Resolution	Researcher
Tirinie	**TIR 2012; Composite**	354.5-262.5	1 cm	Elliot (2012)
		294.5-194.5	1 cm	Francis (2013)
	Core 4 2017	339.5-330.5	1 cm	This study (not presented)
		330.5-240.5	2 cm	
Palaeolake Flixton	**Star Carr B 2012;**	Analyses performed from stable isotopic determinations		
	Star Carr B 2017	473.5-289.5	8-12 cm	This Study (LOI method; not presented)
		289-257	4 cm	
Palaeolake Flixton	**Star Carr C 2010;**	732.5-698.5	1-6 cm	Darvil (2011)
		698.5-640.5	1 cm	
		640.5-600.5	1-4 cm	
		600.5-282.5	4 cm	
	Star Carr C 2017	719.5-630.5	1 cm	This Study
		630.5-509.5	8-24 cm	This study (LOI method)
		509.5-381.5	16 cm	
		381.5-301.5	8cm	
Llangorse	**LlaN 14; Composite**	663.5-640.5	8 cm	Palmer (2016)
		640.5-484.5	1 cm	
		484.5-356.5	8 cm	
		356.5-220.5	1 cm	

4.3 Palaeoenvironmental methods

4.3.1 Pollen analysis

To reconstruct vegetation histories of a region two methods are usually adopted: plant macro-fossil or palynological analyses. Plant macro-fossils, visible plant remains identified within sediments, reveal vegetation present from the local catchment surrounding a lake basin (Birks and Birks, 2000). However, because taphonomic considerations can preclude the use of macro-fossils in reconstructing vegetation histories in lacustrine carbonates, such as, the paucity of remains in sediments; pollen is usually the preferred method.

Palynological assessments have taphonomic considerations of their own. This includes issues in deposition, variable representation and production, and dispersal (Figure 4.1). These considerations are largely a product of the ‘natural’ purpose of pollen;

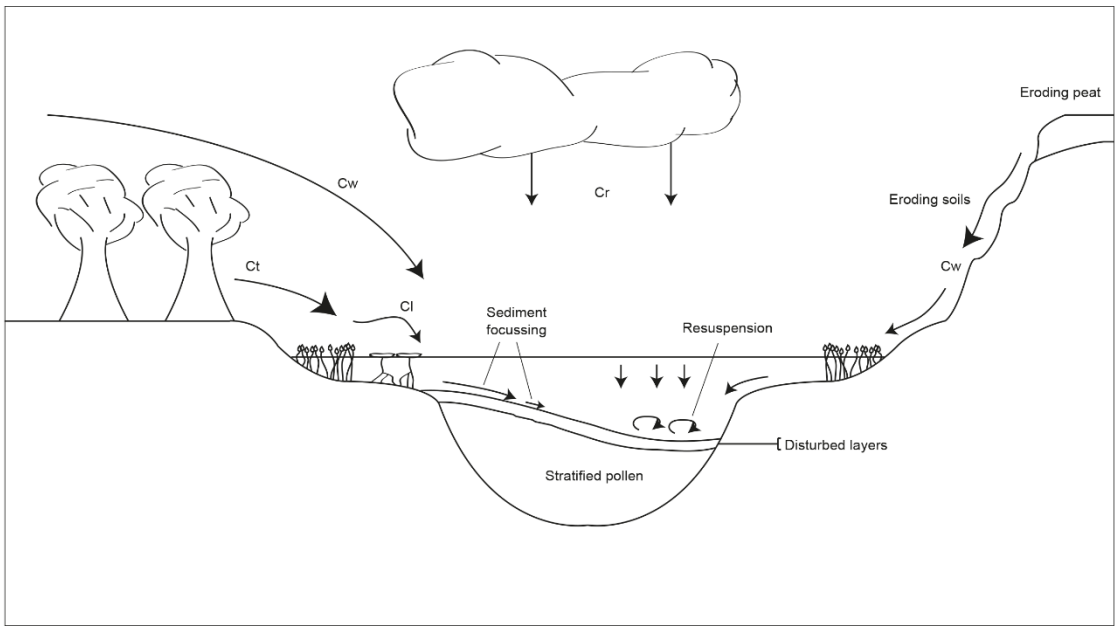

Figure 4.1 Taphonomical considerations in the analysis of pollen in inacustrine settings. Prefixes relate to: Cw) secondary sources, Cl) local component; Ct) trunk component; and Cr) rain component. Stratified pollen within lakes can further be re-suspended through lake turnover. Figure from Moore et al. (1991).

the grains of which are produced in the anther of male plants to carry gametophyte genera to the stigma in female plants (Seppä, 2013). Pollen is therefore produced for reproductive purposes, to carry sperm to the ovule, in vast quantities from all seed-bearing plants, which is carried by wind, water, insects, birds and mammals to host plants. However, most pollen grains fall into sediment archives (Figure 4.1) and, as pollen grains are species-specific, can be identified and used to infer vegetation patterns.

Despite the common vegetation inference approach, caveats present difficulties. Importantly, direct vegetation reconstruction is not performed, rather vegetation is inferred. Thus, patterns in vegetation are suggested from the analysis of pollen. Secondly, suggested vegetation patterns do not always reflect vegetation abundances within the landscape (Sugita, 1994). This is a product of the individualistic nature of pollen production and dispersal (Moore et al., 1991), with high pollen producers obscuring the vegetation signal. Allied to this are difficulties in identifying pollen source areas due to the leptokurtic nature of pollen deposition (Prentice, 1985), with most pollen deposited close to the plant source and decreasing with distance. In lake systems, which are presented in this study, potential issues include catchment and lake size, number of inflows, mixing and sedimentation (Figure 4.1). However, these taphonomic issues are well-known and not thought to be problematic.

Additionally, and perhaps key to this research, pollen assessments can be undertaken at much higher resolutions than other biotic indicators (plant macro-fossils). In carbonate

sediments, which the study sites contain, pollen will be abundant; this abundance is not mirrored in plant macro-fossils. Further, whilst a plethora of pollen-based vegetation studies exist for the British Isles, many do not use a high-resolution approach to reveal vegetation variability. The use of pollen to infer local and regional vegetation histories at high-resolution is therefore justified.

4.3.1.1 Pollen sub-sampling strategy

To observe vegetation response to climatic events, sediments were analysed for pollen at high-resolution (Table 4.4). At Quoyloo Meadow, contiguous 1 cm samples were obtained from the sequence barring the central minerogenic sediments lithostratigraphically correlated to the Loch Lomond Stadial, where the resolution was reduced to 2 cm. At Tirinie, a 1 cm contiguous sampling resolution was obtained across key lithostratigraphic and isotopic transitions, with the remainder between 2-4 cm. The sites containing longer sediment sequences, Llangorse and Palaeolake Flixton, were not analysed at a contiguous resolution because of the assumption that the time-averaged difference between the samples would be similar to the first two sites. As a result, Llangorse was analysed at a 4 cm resolution, increasing to 12 cm during the central minerogenic phase, with the main Palaeolake Flixton sequence, Star Carr Core B, analysed between 4-16 cm resolution, higher over key transitions. However, as Palaeolake Flixton is a large and complex site, an additional sequence was analysed for pollen to investigate differences between pollen representation; Star Carr Core C. The resolution of Core C is variable between 4-12 cm.

4.3.1.2 Pollen sample preparation

All pollen samples were processed following standard Royal Holloway, University of London procedures (Figure 4.2). These procedures followed Fægri and Iversen (1989); and Moore et al. (1991) with the addition of *Lycopodium* to estimate pollen concentrations. Cubic centimetres of sediment were extracted, placed into glass beakers, and disaggregated over a hot plate (ca 70°C) using 1 % Tetrasodium Pyrophosphate (TSPP) ($Na_4P_2O_7$) to break down clay sediments. Each pollen sample was subsequently wet-sieved, using di-ionised water, over a 125 µm sieve and 10 µm mesh to separate fine and coarse particles from pollen bearing sediment. Residues on the finer mesh were collected in centrifuge tubes. All samples then underwent treatment with 10 % HCl, to remove calcium carbonate, and were rinsed in a centrifuge.

In recent decades, it has been recognised that density separation procedures can be fruitful in isolating organic remains from the minerogenic sediment fraction in organic sediments (e.g. Forster and Flenley, 1993; Nakagawa et al., 1998). Therefore, for most

Table 4.4 Pollen sub-sampling strategy for each of the sites forming this research. Within Palaeolake Flixton Core C, sediments were sampled for pollen from a newer sequence for the base of the record. The sediments at the base of the original record were poorly preserved

Site	Sequence	Depth (cm)	Resolution	Researcher
Tirinie	TIR 2012; Composite	354.5-323.5	1 cm	This study
		323.5-292.5	4 cm	
		292.5-282.5	2 cm	
		282.5-258.5	1 cm	
		258.5-242.5	2 cm	
		242.5-209.5	1 cm	
		209.5-198.5	4 cm	
Quoyloo Meadow	QM; Composite	212.5-195.5	1 cm	This study
		195.5-181.5	2 cm	
		181.5-123.5	1 cm	
Palaeolake Flixton	B 2012; Composite	509.5-333.5	8 cm	This study
		333.5-301.5	16 cm	
		301.5-205.5	4 cm	
Palaeolake Flixton	C 2010; composite	699.5-561.5	6 cm	This Study
		561.5-381.5	12 cm	
		381.5-281.5	4 cm	
	C 2017	711.5-687.5	4 cm	
Llangorse	LlaN 14; Composite	650.5-486.5	4 cm	This study
		486.5-402.5	12 cm	
		402.5-248.5	4 cm	

palynological extraction approaches in this research, Hydroflouric acid (HF) treatment was substituted for density separation using Sodium Polytungstate (SPT) ($Na_6[H_2W_{12}O_{40}]$) at a specific gravity of 2.0 g/ml^{-3}. After separation, the organic residue was poured into conical centrifuge tubes and both fractions rinsed for SPT recycling. To ensure adequate pollen recovery, all SPT approaches were employed twice.

Prior to the final stages of preparation, samples were dehydrated using glacial acetic acid (CH_3COOH). Once dehydrated the samples were exposed to Erdtman's acetolysis (Erdtman, 1934), using an acetic anhydride ($(CH_3CO)_2O$): sulphuric acid (H_2SO_4) mixture at 9:1, and boiled at 100°C for three minutes and 30 seconds. This step cleaned the pollen grains, making them easier to observe, through the removal of grain surface

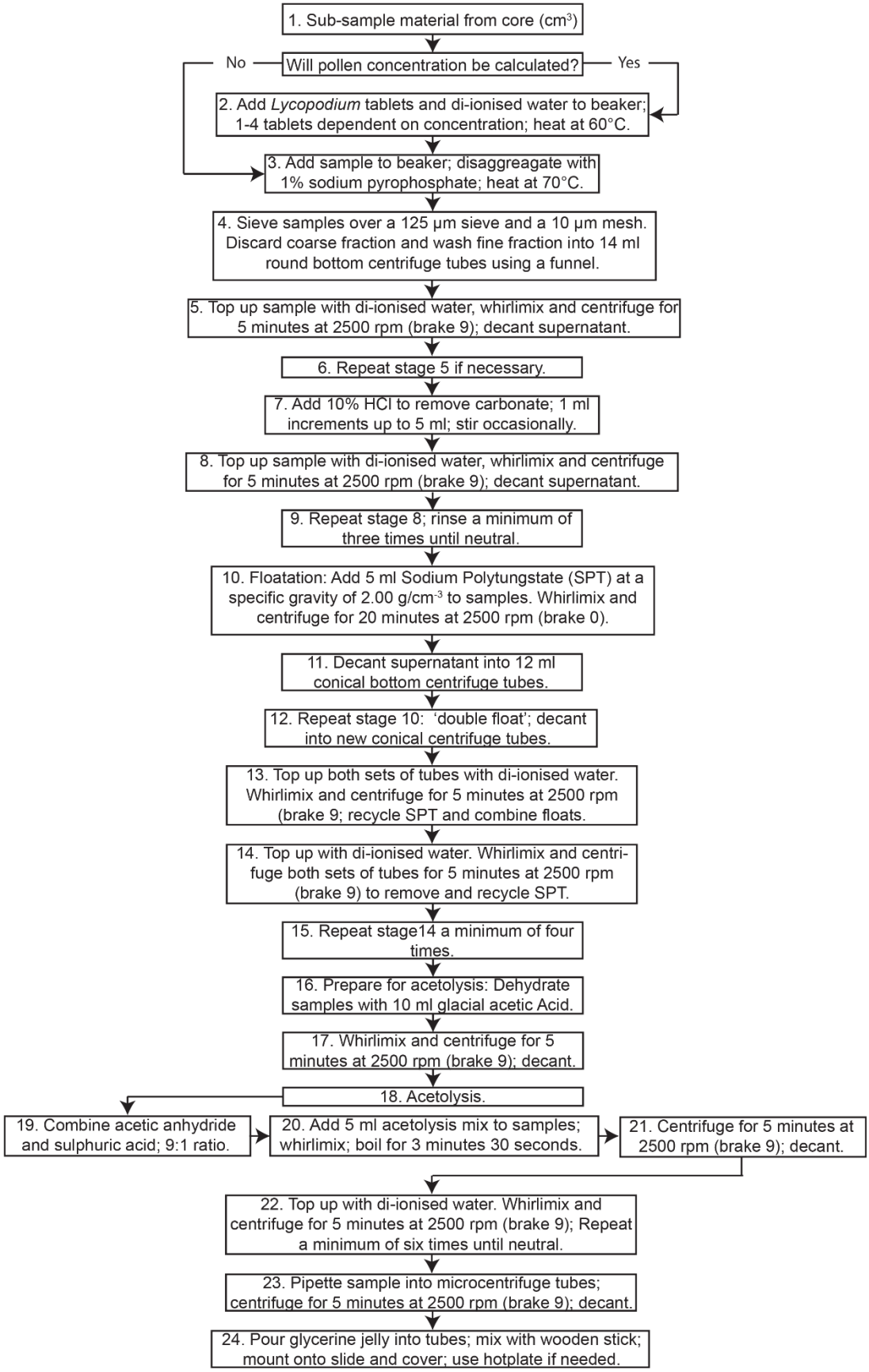

Figure 4.2 The pollen preparation method employed during this research. All pollen samples were treated using this method prior to any additional hydroflouric acid treatment.

polysaccharides (cellulose) and carbohydrates present in the sediments (Bennett and Willis, 2001). All pollen residues were transferred to 1.5 ml microcentrifuge tubes and mounted using glycerine jelly.

4.3.1.3 Density separation vs Hydroflouric acid (HF)

Most pollen preparation followed the method outlined in Section 4.3.1.2; however, under certain circumstances the SPT 'floatation' method was exchanged in favour of HF treatment. Hydroflouric acid treatment of pollen samples was introduced by Assarsson and Granlund (1924) and has been routinely used in pollen preparations until the observations by Forster and Flenley (1993) and Nakagawa et al. (1998) (Section 4.3.1.2). Where density floatation separates organic remains from the minerogenic component, HF treatment digests mineral/siliceous material (Fægri and Iversen, 1989; Moore et al., 1991) leaving pollen grains largely unaltered. Predominantly, the method employed depended on the sedimentological characteristics of each site in question; although all samples underwent density separation as a standard practice. However, at Llangorse, a conspicuous lack of palynological material was observed within organic residues for basal clay-rich samples.

At Llangorse, both SPT and HF were used. The organic and silt/clay sediments were treated with SPT; whilst deeper minerogenic silts and clays, between 650-594 cm, were subsequently retreated with HF. The decision to resample and treat with HF, resulted from the lack of palynological material obtained from density separation but also the observation of considerable quantities of pollen and *Lycopodium* present in the minerogenic residue following SPT treatment. It is likely that the specific nature of the lowermost sediments, largely dominated by fine grained clayey silts, prevented the 'floating' of organic residues. Quoyloo Meadow also contains sediments at the base of the sequence that appear devoid of pollen. However, it was decided to not resample sediments from this site because of three key reasons: 1) there were abundant quantities of *Lycopodium* present on the pollen slides; 2) the minerogenic residues contained no palynomorph materials and; 3) work undertaken by Bunting (1994) at Quoyloo Meadow showed a similar lack of pollen at the base of the sequence after HF treatment.

The method adopted within this research for HF treatment followed modified procedures outlined in Moore et al. (1991) (Figure 4.3). All treatment occurred after the HCl stage but prior to acetolysis. A three stage HF treatment first subjected the samples to 5 ml of concentrated, 40 %, cold HF with samples being stirred to resuspend the material and left overnight. Samples were then rinsed and a further 5 ml of concentrated HF added. The second HF treatment involved placing the samples in a water bath at 100°C for 15

minutes and rinsing. This hot stage was employed to remove all soluble materials (Bennet and Willis, 2001). Once complete, samples were exposed to one final cold HF treatment overnight, rinsed and treated with HCl. The final HCl treatment ensured that no silicoflourides were present following the HF procedure.

Retreatment with HF at Llangorse greatly increased the number of pollen grains present on the pollen slides. This has implications for the methodological approaches deemed suitable for pollen preparation. It is clear then, a lack of palynomorph materials following density separation should not be deemed reflective of a lack of pollen within sediments. At Llangorse, relying on one method of preparation, would have led to erroneous interpretations regarding the nature of the vegetation assemblages surrounding the basin during specific time-periods.

4.3.1.4 Pollen identification

Pollen slides were inspected using an Olympus CX-41 transmitted light binocular microscope. Magnification was provided by a 10x magnification eyepiece and; 20x, 40x and 100x objective lenses. All slides were traversed systematically travelling up and down the slide using the 40x magnification objective for pollen count purposes. The lower magnification objective was used for slide scanning whilst the higher objective was used, with immersion oil, to reveal specific morphological features on hard-to-distinguish pollen grains. Pollen grain morphology, including shape, surface texture and number of apertures were the principal components in distinguishing different pollen types (Moore *et al*., 1991).

These three distinguishing features of pollen grains, shapes, aperture and sculpturing elements, need to be carefully scrutinised; and are therefore key to successful pollen identification. However, grain identification is largely dependent on the user and time invested in understanding and delineating specific morphological configurations of different grains. The many additional components present on pollen slides (e.g. mineral fragments, detrital organic remains, non-pollen palynomorphs) provide barriers to identification, as grains can often be obscured making identification problematic. Nevertheless, for this research, pollen identifications were conducted using the reference collection at Royal Holloway, University of London, and identification keys and photographs within Fægri and Iversen, (1989) and Moore et al. (1991). Additional tools used included Reille (1992) and Punt et al. (2007). Pollen nomenclature and taxonomy follows Godwin (1956); Moore et al. (1991) and Stace (1992).

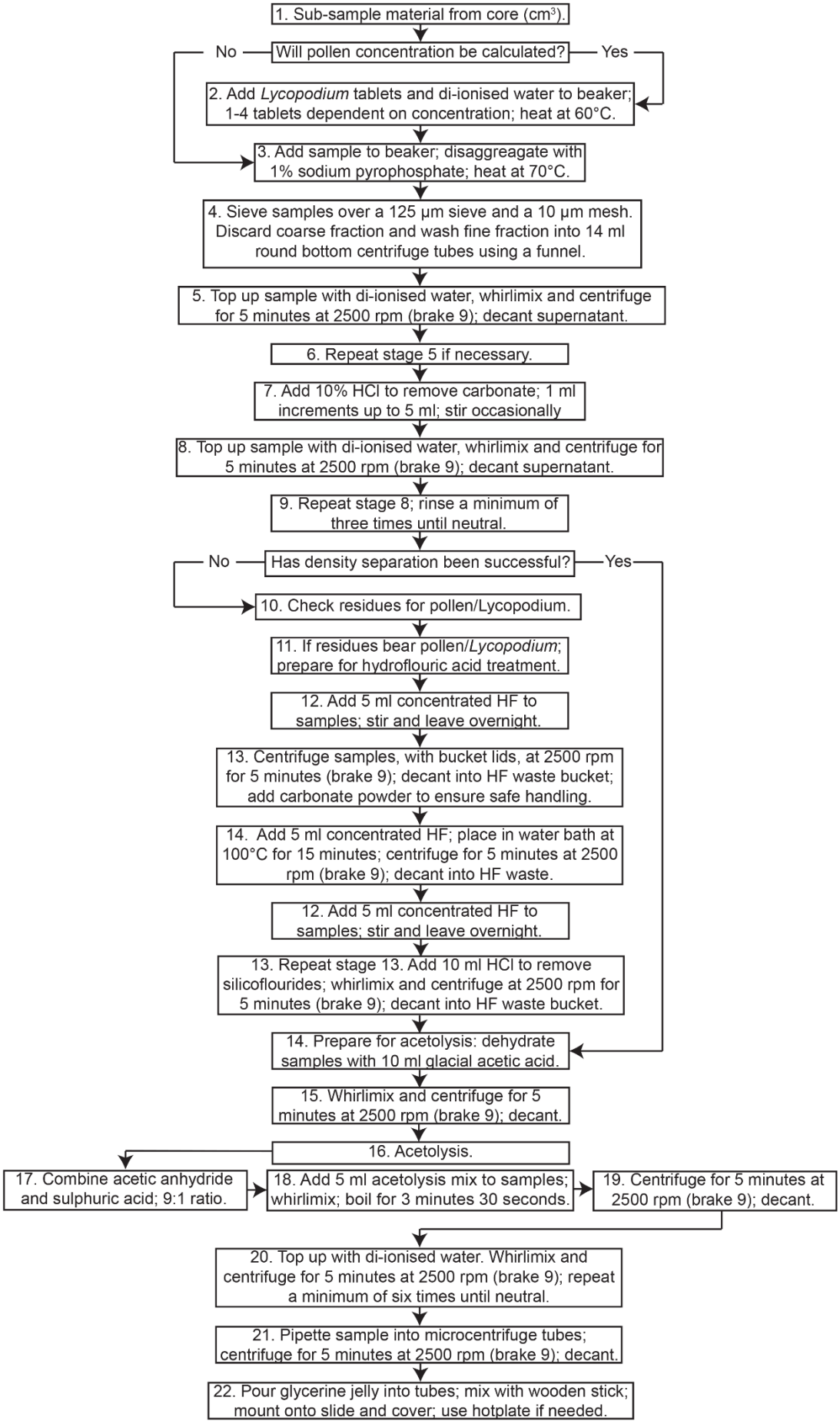

Figure 4.3 The modified hydroflouric acid treatment used at Llangorse. The modified approach used both cold and hot HF to digest as much soluble material as possible.

All pollen analyses were subject to counts of 300 total land pollen (TLP) per sub-sample with aquatic pollen and spores counted alongside this sum. However, samples with very low pollen concentrations were analysed to a minimum of 100 TLP. Occasionally this was not possible and certain levels at certain sites, for example Palaeolake Flixton and Quoyloo Meadow, pollen sums were dependent on the total number of pollen observed across multiple pollen slides (see individual results sections).

4.3.1.5 Data analysis

For each site, taxon-specific percentages and concentrations were calculated. Pollen percentages were calculated as a percentage of TLP. For aquatics and pteridophytes percentages were expressed as a percentage of the TLP plus sum of either aquatics or pteridophytes respectively. For individual pollen taxa this is expressed as:

$$\%\ Pollen = \left(\frac{\Sigma Pollen\ taxon}{\Sigma TLP}\right) * 100$$

For aquatics and pteridophytes this is expressed, using aquatics as an example, as:

$$\%\ Aquatics = \left(\frac{\Sigma Aquatics}{\Sigma Aquatics + \Sigma TLP}\right) * 100$$

As an exotic marker grain of known concentration was added during the processing stage, individual pollen concentrations were calculated. Pollen concentration is defined as the number of grains per unit volume or mass of wet sediment in cm^{-3} or g^{-3} and is an absolute measure of quantifying pollen present within sediments. The calculation for pollen concentration is expressed as:

$$Concentration = \frac{\left(\left(\frac{Ls}{Lc}\right) * Tc\right)}{Wt}$$

Where Ls is *Lycopodium* added to the sample; Lc is *Lycopodium* counted; Tc reflects taxa counts; and Wt is the weight or size of the sample.

Pollen percentage and concentration data were presented stratigraphically using C2 V. 1.7.7 (Juggins, 2016). The curves for individual taxa are represented by histograms with each horizontal line reflecting a sample point. Although the samples are joined in the histogram, no attempt has been made to interpolate between sample points (Moore et al., 1991). The pollen taxa are arranged into groups: trees, shrubs, herbs, aquatics and

pteridophytes, with rare taxa and those with continuously low percentages and concentrations given an exaggeration line (10 x). Summary diagrams of specific groups of taxa are presented as cumulative curves.

4.3.1.6 Pollen diagram zonation

Each pollen diagram was subjected to zonation into Local Pollen Assemblage Zones (LPAZ). Diagram zonation is a conventional practice that allows for both the visual splitting of pollen diagrams into distinctive biostratigraphic units, based on the relative proportions of changes in major taxa, and efficient diagram summation and interpretation. Pollen diagram zonation, using untransformed pollen data, was assisted by Constrained Incremental Sum of Squares Cluster Analysis (CONISS) (Grimm, 1987). However following CONISS, it was noted that variability in the pollen data was not adequately defined, therefore, additional zones were added to individual pollen diagrams. Individual LPAZ's have not been incorporated into regional pollen assemblage zones (e.g. Jessen, 1935; West, 1970).

4.3.1.7 Numerical analyses

In any community ecological study, additional evidence may be required that substantiate the claims from ecological count data and subsequent diagrammatic representation. Within this research, numerical/statistical approaches were applied to confirm the existence of structures or cycles within the collected pollen data.

As all pollen data are multivariate, including counts for both samples and species, approaches were chosen to examine all variables simultaneously (Gauch, 1982). Specific approaches used within this research were indirect ordination techniques including Principal Components Analysis (PCA); Correspondence Analysis (CA); Detrended Correspondence Analysis (DCA); Principal Curve Analysis (PC) and; Rate of Change Analysis (RoC). Indirect gradient analysis uses the data without measured environmental variables; hypothetical environmental gradients are then inferred from species compositions and their placement along axes of variation (ter Braak and Prentice, 1988). Therefore, ordination allows the exploration of a dataset by finding underlying structures, patterns or trends and reducing the dimensionality of the data.

The ordination techniques were applied to pollen percentage data in this study. Whilst it is accepted that percentage data incorporates unit-sum problems (Aitchison, 1986; Pollard et al., 2006), with taxon change not independent of each other, the above techniques are routinely applied to pollen percentage data (e.g. Simpson and Birks, 2012) which justifies the approach used here. Equally, CA was used as a secondary

analysis tool as it assumes a Gaussian response, as opposed to a linear response in PCA, which is expected with vegetation data. Therefore, CA's do not suffer from the 'arch effect', as is common with PCA; where variations along one axis have spread to other axes; removing interdependency (Gauch et al., 1977).

In performing the statistical analyses, the pollen data were square-root transformed to reduce the data skew, and detrended by segments. For all statistical approaches, all rare taxa were down-weighted with the analyses performed on taxa whose abundances were greater than 5 %. As standard, *Pediastrum* (medium and large cell clusters) were removed from the analysis whilst at certain sequences additional taxa were removed (Chapter 5-8). Down-weighting and taxa less than 5 % abundance was performed to remove the effects of data skew and, with *Pediastrum*, to remove the effects of limnological processes as opposed to shifts in the environmental gradient. The results from the analyses are presented as: 1) DCA tabular outputs; 2) biplots of PCA axis one and axis two species scores; 3) stratigraphic plots for sample scores of axis one from the PC, based on PCA or CA modelled outputs; 4) stratigraphic RoC analyses; and 5) individual species response curves, where taxa are modelled along the gradient of the PC. All statistical analyses were undertaken using the computer programming software 'R' and the 'Rioja', 'Vegan' and 'Analogue' packages (Juggins, 2017; Oksanen, 2018).

The principal curve method proved to have the most discriminating power in determining change across the pollen data sets with the extracted gradient routinely capturing >70% of the total variability in the data. PCs have only recently been applied in palynological studies; and may be defined as smooth one-dimensional curves fitted via regression through the multi-dimensional data space. PCs are iteratively generated using smoothing splines to achieve the best fit to the data and use a smoothing parameter to define the flexibility of the curve. Fit is usually assessed by the variation explained, the reduction of residuals away from the regression line and the ability for the model to converge (subsequent iterations become stable) (Simpson and Birks 2012). Within this thesis the gradient defined by the data usually had open ground taxa and closed woodland as each end member permitting assessment of landscape change.

4.3.2 Micro-charcoal analysis

Pollen slides contain numerous additional components alongside pollen, including micro-charcoal. Micro-charcoal here is defined as being smaller than 125 μm. Small particles of charcoal are likely to reflect extra-local or regional fire inputs as small fragments can be wind transported to the basin (Carcaillet et al., 2001). To understand micro-charcoal frequencies; all black, opaque, angular fragments greater than 5 μm were tallied

alongside counts of pollen. Charcoal concentrations were constructed using the pollen concentration equation (Section 4.3.1.5) substituting taxon for charcoal counts. On occasion, charcoal counts were not made alongside pollen counts. Subsequent micro-charcoal concentration estimates across these levels were obtained by traversing the slide until an appropriate number of *Lycopodium* and charcoal were obtained. This is not thought to be problematic however, as macro-charcoal counts have been made alongside micro-charcoal counts which better reflect local fire histories (Carcaillet et al., 2001).

4.3.3 $\delta^{18}O$ and $\delta^{13}C$ stable isotope analysis

The proliferation in stable isotopic research, specifically $\delta^{18}O$ and $\delta^{13}C$, in different sedimentary archives has increased our understanding of climatic variability through the late Quaternary (e.g. Dansgaard et al., 1993; Marshall et al., 2002; Steffensen et al., 2008). Within lacustrine carbonates this is observed through abrupt shifts in $^{18}O/^{16}O$ isotopic ratios (e.g. Marshall et al., 2002; Candy et al., 2016). However, to understand these isotopic changes, it is first necessary to assess the controls on lacustrine isotopic values.

The primary controls on the isotopic signal within lacustrine carbonates are complex (Figure 4.4). However, in hydrologically-open lakes oxygen isotopes reveal climatological variability due to the linear relationship between the $\delta^{18}O$ of the sedimentological carbonate ($\delta^{18}O_{carb}$) and the $\delta^{18}O$ of lake waters (Leng and Marshall, 2004). The $\delta^{18}O$ of lake waters is largely controlled by the $\delta^{18}O$ of precipitation ($\delta^{18}O_{water}$). This is mainly a function of air temperature and 'Rayleigh Fractionation' whereby $\delta^{18}O_{water}$ values are modulated by temperature dependency of vapour condensation under equilibrium processes (e.g. Dansgaard, 1964; Gat, 1980). Also, the 'amount effect'; the trajectory of air masses (continentality) and; seasonality of rainfall (Rozanski et al., 1992; 1993; Gionfantini et al., 2001) with greater incidence of the above phenomena increasing loss of heavy $\delta^{18}O$, which acts to deplete lacustrine carbonates. Additionally, in temperate mid-latitudes, a shift in temperature can influence $\delta^{18}O_{water}$ by 0.59 ‰ / 1°C (Rozanski et al., 1992); which is further regulated by temperature dependent offsets during carbonate mineralisation of approximately 0.24 ‰ / 1°C (Leng and Marshall, 2004), therefore, a 1°C temperature may explain a 0.3 ‰ shift in $\delta^{18}O_{carb}$. Nonetheless authigenic lacustrine carbonates, due to annual averaging of the signal have, in the past been used as a proxy for mean annual temperature (Marshall et al., 2002; Candy et al., 2011; 2015; 2016)

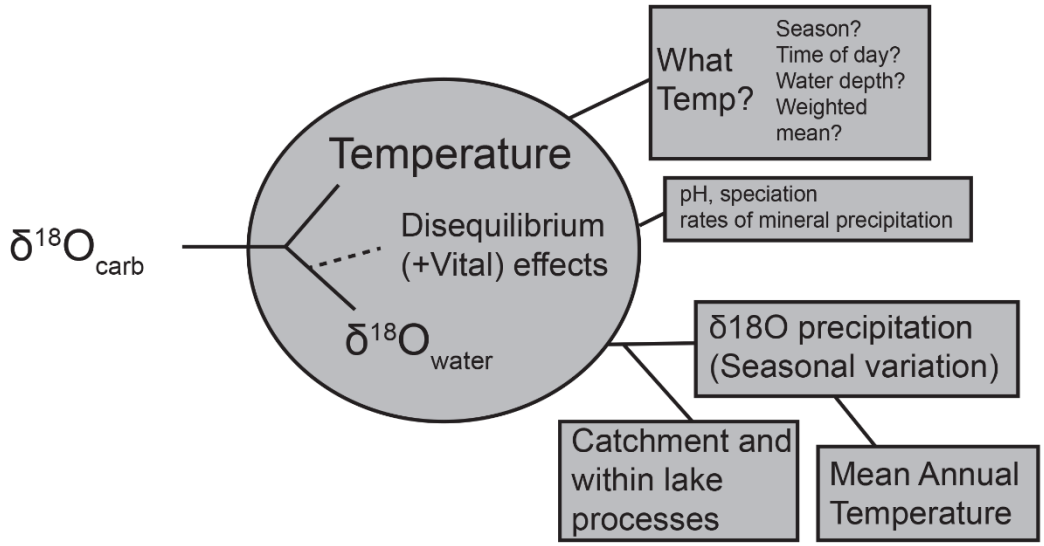

Figure 4.4 Major controls on the oxygen isotopic composition of lacustrine carbonates. Modified from Leng and Marshall (2004).

$\delta^{13}C$ is indirectly related to climate, in that the ratio reflects the variable inputs of atmospheric and plant respired CO_2 into lake waters modifying the Dissolved Inorganic Carbon (DIC) budget in the lacustrine environment (Cerling and Quade, 1993; Leng and Marshall, 2004).

Both $\delta^{18}O_{carb}$ and $\delta^{13}C_{carb}$ can be further modified by detrital contamination and, if under certain conditions, the lake becomes hydrologically-closed. These two features can modify the isotopic ratio of lake waters and carbonates and therefore warrants further explanation (e.g. Mangili et al., 2010). Detrital contamination can arise from a variety of sources, principally, geological carbonate that formed under different climatic conditions and biogenic carbonates (ostracod tests; bivalves). The latter of these contain vital offsets, which produce different isotopic signals through disequilibrium processes (Leng and Marshall, 2004). Detrital contamination can be guarded against through sedimentological analysis or methodological considerations whilst sample processing, such as removal of the biogenic fraction. Further, an assessment of geologic carbonate within study regions should be made alongside authigenic carbonates as a measure of contamination. Isotopic modification is more difficult to ascertain, as during periods of aridity, the lake may become a closed system, with evaporitic modification enriching the isotopic signal through the preferential loss of $\delta^{16}O$, $\delta^{12}C$ and equilibration between DIC and atmospheric CO_2 (Hammarlund et al., 2003; Leng and Marshall, 2004). Often employed to ascertain detrital influences and basin hydrology is covariance testing between $\delta^{18}O_{carb}$ and $\delta^{13}C_{carb}$ (Hammarlund et al., 2003; Mangili et al., 2010). Where greater covariance exists, it is possible that one or more of the processes above has occurred.

Nevertheless, if it can be demonstrated that the carbonates are authigenic, the isotopic values, through rapid propagation of the atmospheric-terrestrial system (Candy et al., 2015; 2016), can be applied to reveal dominant climatic regimes.

4.3.3.1 $\delta^{18}O$ and $\delta^{13}C$ sampling and preparation

Samples for isotopic analysis were extracted from all calcium carbonate bearing sediments by cutting 0.5 cm^3 of material at variable resolutions through each of the sites (Table 4.5). All samples were placed into glass beakers and disaggregated using 0.5 % Sodium Hexametaphosphate (SHMP) ($(NaPO_3)_6$). Samples were wet-sieved over a 63 µm mesh, with di-ionised water, to separate the coarse fraction and any biological carbonate sources from authigenic calcite. The fine fraction was placed in a drying cabinet, at 40°C, dried and treated with 10% hydrogen peroxide (H_2O_2). Treatment with H_2O_2 removes any organic materials from the endogenic calcite fraction. Samples were subsequently re-dried, homogenized, and weighed using a Cahn C-31 Microbalance. Sediment volumes between 400-600 µg were used for isotopic analyses. $\delta^{18}O$ and $\delta^{13}C$ values were measured by analysing CO_2 liberated from a sample reaction with phosphoric acid (H_3PO_4) at 90°C using a VG PRISM series 2 mass spectrometer. Internal (RHBNC-PRISM) and external (NBS-19, LSVEC) standards were run every ten samples to ensure machine calibration. All stable isotopic values are quoted with reference to the Vienna Pee Dee Belemnite (VPDB) international reference standard.

4.3.4 Biomarker analyses

A key aim of this research was to understand how vegetation responds to palaeoclimatic shifts. In this regard, deuterium (δD) isotopic lipid biomarker reconstructions, a novel approach in palaeoclimatic research (e.g. Sachse et al., 2004; 2009; 2012; Garcin et al., 2012; Rach et al., 2014), were sought to infer palaeohydrologic signals.

Lipid biomarkers are molecular markers in plant cell membranes that are produced by all plant organisms. The primary functions of plant lipids are for energy storage, the prevention of water loss and to aid in structure (Quinn and Williams, 1978; Eglinton and Eglinton, 2008). However, δD values of hydrocarbons (*n*-alkanes) in plant leaf waxes have been shown to record δD of precipitation (δD_{precip}) either directly through meteoric waters or a mixed lake water signal (Sachse et al., 2012). Whatever the meteoric water source, precipitation is ultimately the only source of hydrogen for different lipids. In this respect shorter hydrocarbons with lower *n*-alkane chain lengths are prescribed to submerged aquatic plants (*n*-C_{21}: *n*-C_{25}) with longer hydrocarbons attributed to higher terrestrial plants (*n*-C_{25}: *n*-C_{31}) (Sachse *et al*., 2006). Therefore, these two classes should provide a measure of precipitation δD.

Table 4.5 Isotopic sample details for different sites within this study.

Site	Sequence	Depth (cm)	Resolution	Researcher
Tirinie	TIR 2012; Composite	354.5-327.5	<1 cm	Candy (2016)
		290.75- 261.75	1 cm	This study
		261.75-198.75	3-8 cm	Francis (2013)
Quoyloo Meadow	QM; Composite	191.5-155.5	0.5 cm	Abel and Timms (2016)
Palaeolake Flixton	Star Carr B 2012	515.5-445.5	1 cm	Candy (2017)
		445.5-295.5	1-6 cm	
		295.5-197.5	1-2 cm	
Palaeolake Flixton	Star Carr C 2010	730-692	3-6 cm	Darvil (2011) and Candy (2017)
		692-656	2 cm	
		656-600	2-4 cm	
		600-520	10 cm	
		520-440	20 cm	
		440-283.5	1.5-8 cm	
Llangorse	LlaN 14; Composite	639.5-510.5	4-12 cm	Palmer (ongoing)
		37.5-219.5	1-4 cm	

Much like the $\delta^{18}O$ and $\delta^{13}C$ isotopic controls, δD_{precip} is mediated by temperature (Rayleigh fractionation), the 'amount' of precipitation, evaporation and changes in moisture source (Craig, 1961; Dansgaard, 1964). With changes in each of these parameters enriching or depleting the isotopic signal through preferential loss of the heavier or lighter isotope. For example, in polar regions temperature change has been shown to influence δD_{precip} by up to 5 ‰ / 1°C (Alley and Cuffey, 2001). However, the δD biomarker signal within specific compounds is offset from δD_{precip} (Figure 4.5). This is due to biosynthetic fractionation offsets during lipid synthesis (Sachse et al., 2012). These offsets are approximately -82 ‰ for submerged aquatic *n*-alkanes (Aichner et al., 2010) and approximately -157 ‰ for higher terrestrial plants (Sachse et al., 2012). Whilst a linear relationship between δD_{precip} and aquatic *n*-alkanes exists, terrestrially derived *n*-alkanes have been shown to be affected by increased δD enrichment through evaporative processes (Kahmen et al., 2013) and preferential loss of the lighter hydrogen isotope. However, this evaporative enrichment is not observed for aquatic *n*-alkanes.

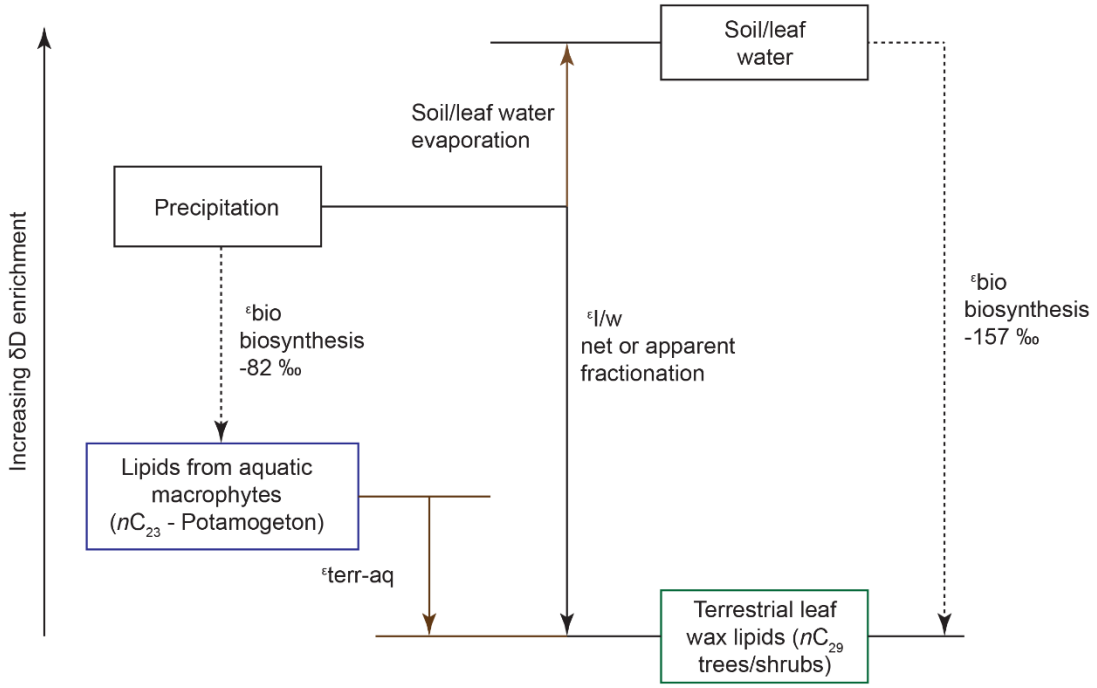

Figure 4.5 Relationships between source water δ*D* and leaf wax δ*D* from submerged aquatic macrophytes (*n*-C_{23}) and terrestrial plants (*n*-C_{29}). Modified from Sachse et al. (2006). From Rach et al. (2014).

Therefore, differences in isotopic values between terrestrial and aquatic *n*-alkanes can be used to provide a record of evapotranspiration or aridity (e.g. Rach et al., 2014; 2017).

These are not the only controls however, and plant specific offsets may exist (Rach et al., 2014). Fractionation of hydrogen during lipid synthesis has been shown to vary between plants and their life stage (Liu et al., 2006; Sachse et al., 2012). Therefore, δ*D* variability may result from changing vegetation. However, in this research this is guarded against by performing biomarker analyses alongside high-resolution pollen analysis.

4.3.4.1 Biomarker sub-sampling strategy

For this research, three sites were analysed for biomarkers (Table 4.6). Unfortunately, due to time constraints, Llangorse was not studied. At Quoyloo Meadow, 30 contiguous samples at 1 cm resolution, were selected spanning the two organic units and the central minerogenic unit. At Tirinie, 80 samples were selected, at contiguous 1 cm intervals over key climatostratigraphic/lithostratigraphic transitions and increased to 4 cm intervals within certain areas of the sequence. Contrastingly, at Palaeolake Flixton two sequences were studied for biomarkers. The first sequence, Star Carr Core B 2017, contained a variable resolution between 4 cm and 12 cm, whereas for the second sequence, Star Carr Core C 2017, an 8 cm and 24 cm resolution was adopted. Both sequences were analysed due to the presence of a hiatus, in the Core B record (Chapter 7) resulting in 61 samples across both sequences. Unfortunately owing to time constraints and

Table 4.6 Biomarker sample details for different sites within this study.

Site	Sequence	Depth (cm)	Resolution	Researcher
Tirinie	TIR 2012; Composite	354.5-317.5	1 cm	This study
		317.5-301.5	2-4 cm	
		301.5-266.5	1 cm	
Quoyloo Meadow	QM; Composite	209.5-179.5	1 cm	Maas (2016); This study
Palaeolake Flixton	B 2017	473.5-245.5	4-12 cm	This study (not presented)
Palaeolake Flixton	C 2017	669.5-301.5	8-24 cm	This study (not presented)

laboratory issues, the Palaeolake Flixton biomarker data have not been analysed. However, all materials have been sampled and prepared.

4.3.4.2 Biomarker preparation and identification

All biomarker preparation was undertaken following procedures at the Organic Surface Geochemistry Laboratory, GFZ Potsdam (Figure 4.6). All core material for centimetre samples was extracted; ranging in dry weight between ca 1.4 – 7.0 g and placed into combusted glass vials. Prior to weighing, samples were frozen then freeze dried to remove all moisture. Total Lipid Extracts (TLE) were obtained using a Dionex accelerated solvent extraction 350 system (ASE) using a Dichloromethanol (DCM; CH_2Cl_2): Methanol (MeOH; CH_3OH) mixture, 9:1, at 100°C. Samples were concentrated and dried using dry nitrogen gas and transferred to 4 ml glass vials. For *n*-alkane quantification the concentration of a known standard, Androstane, was added. TLE's were split into aliphatic, aromatic and alcohol/fatty acid fractions by solid phase extraction (SPE) in 8 ml glass columns filled with silica gel using hexane (C_6H_{14}); hexane: DCM (1:1); and DCM: MeOH (1:1) respectively. The aliphatic fractions were analysed for *n*-alkanes using an Agilent Technologies 5975C series Gas Chromatography Mass Spectrometer (GC-MS) coupled to a flame ionising detector (FID).

Through the GC-MS outputs it was clear that certain samples required cleaning (Figure 4.7). To desulphurise further column chromatography, using copper powder in a pipette column, was performed. Samples were collected with hexane. Equally, purification was sought on samples that contained a mix of both saturated and unsaturated compounds and those that co-elute. Here, samples were purified using activated silver nitrate ($AgNO_3$) and flushed with hexane then DCM to separate the two compound classes.

4.3.4.3 Data analysis

To identify *n*-alkanes present within each GC-MS output, each baseline separated peak in the chromatogram, with no co-elution, was assessed for vaporization time and the molecular ion in the mass spectrum (M/Z). *n*-Alkane determination was also assisted by an elemental compound library at the GFZ. To calculate the abundance of each *n*-alkane present within each sample the area of each alkane peak was calculated from the GC output; concentrations of each alkane were then extracted based on the known concentration of the standard, Androstane. Concentrations are provided in µg/g by the following equation:

$$Alkane\ concentration\ = \frac{\left(\frac{\left(\frac{Cn}{Cs}\right)}{As}\right)}{V\ or\ Wt}$$

Where Cn is the abundance of the n-alkane; Cs is the concentration of the standard; As is the abundance of the standard; V is the volume of sample used for measurement and Wt is weight. Using only the bracketed component, concentration is provided in µg; whereas, using the whole equation, concentration is provided in µg/µl or µg/g.

As a first approximation in data analyses, Average Chain Length (ACL) indices were used. ACL is an averaging of the chain lengths for each sample in a sequence. As different carbon atom lengths of sedimentary *n*-alkanes are produced by different source vegetation types (e.g. *n*-C_{17} and *n*-C_{19} from algae; *n*-C_{21}, *n*-C_{23} and *n*-C_{25} from submerged aquatics and *n*-$C_{25:31}$ from higher terrestrial plants (Sachse et al., 2006)), the ACL can inform, in a crude way, significant vegetation shifts during periods of change. ACL indices were calculated as follows:

$$ACL = \frac{(\Sigma Cn * n)}{(\Sigma Cn)}$$

Where Cn is the abundance of any alkane; n is the chain length of the alkane and; Σ reflects the summation of all $Cn * n$ or $odd\text{-}even\ Cn$ alkanes in a sample.

4.3.4.4 Compound-specific deuterium isotopic biomarker analyses

Compound specific hydrogen isotope ratios were measured using a Thermo Scientific Delta V Plus Isotope Ratio Mass Spectrometer coupled with an Agilent 6890N GC at the GFZ Potsdam. The samples were measured on a 50 m HP ultra 1 column (Rach et al., 2014). All samples were measured with the following GC-temperature program:

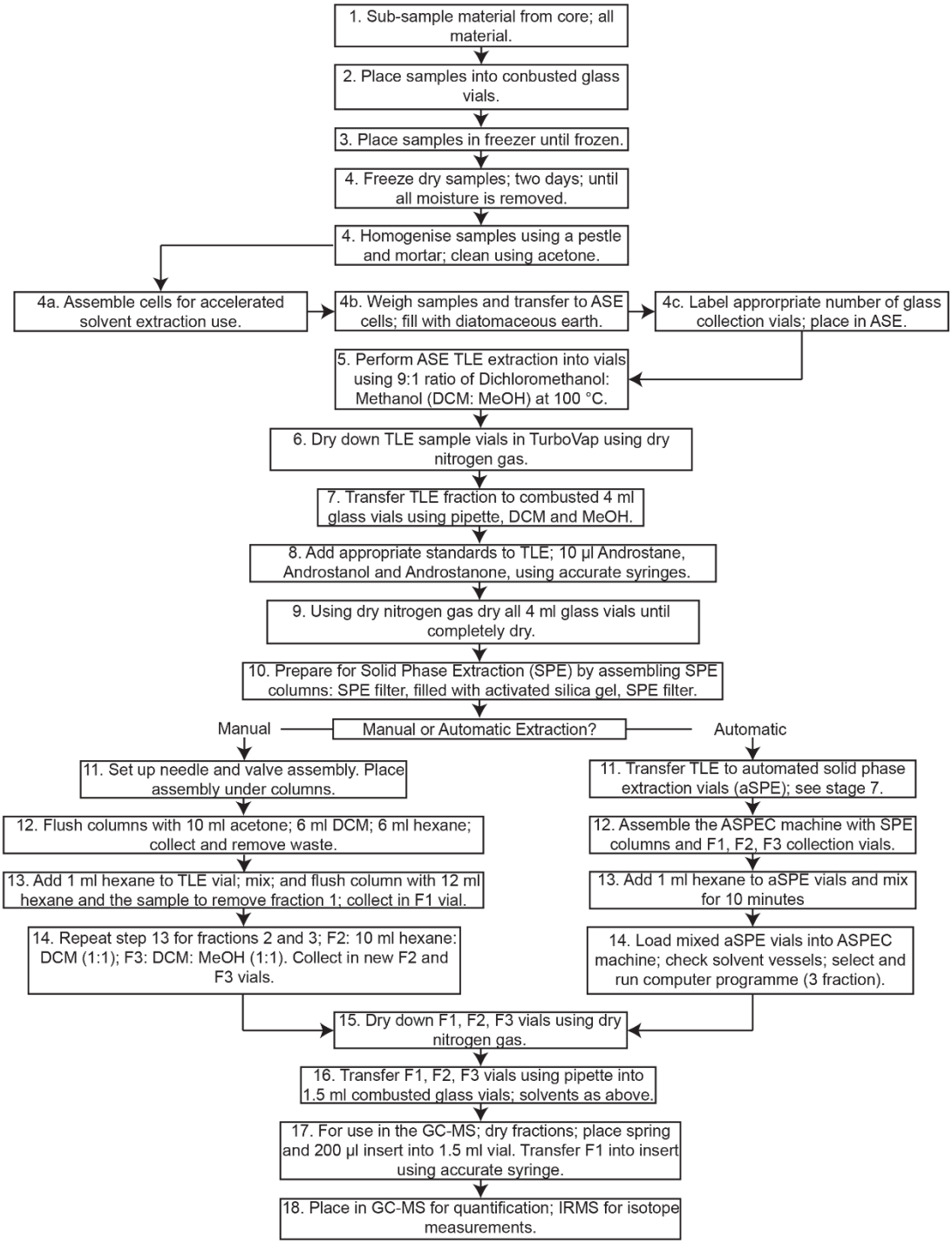

Figure 4.6 The methodological procedure for biomarker extraction from sediments. The method highlights where procedures can take a manual or automatic approach depending on preference. There is no advantage, other than laboratory time, in using the automatic method.

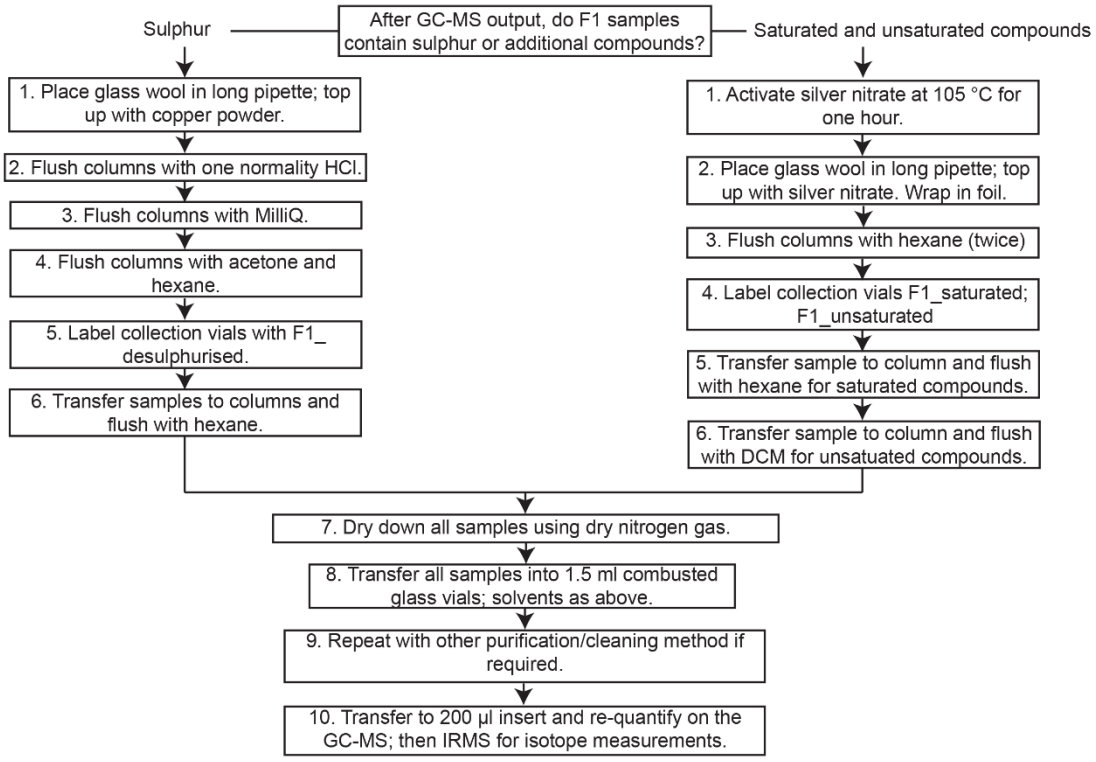

Figure 4.7 The performed method for cleaning and purifying biomarker samples. The two differing methods depend on whether the samples contain a mix of compounds and/or sulphur.

temperature was held for 2 minutes at 70°C, then heated to 180°C at a rate of 20°C per minute. Subsequently, oven temperature was increased to 320°C at 5°C per minute and the final temperature was held for 15 minutes 30 seconds. The alkane standard mix was measured over the same programme. Every sample in this research was measured in duplicate and quoted in reference to Vienna Standard Mean Ocean Water (VSMOW).

4.3.5 Macro-charcoal analysis

As well as micro-charcoal analyses sediments were also assessed for macro-charcoal (Table 4.7). Predominantly the observation and identification of charcoal within lake sediment cores reflect incidences of burning around the catchment of the lake (Carcaillet et al., 2001). As a result, macro-charcoal analysis has been used as a proxy for fire history and fire frequency across different study sites (Whitlock and Larsen, 2001). The purpose of pursuing additional macro-charcoal analyses was to differentiate between extra-local/regional charcoal, smaller fragments incorporated into pollen slides from distal fires and larger charcoal fragments which are likely a product of local fire (Carcaillet et al., 2001). Charcoal analysis was used to provide an additional constraint over what may be affecting vegetation assemblages; namely if landscape burning has any influence over the vegetation. Within this research all charcoal greater than 125 µm is considered macro-charcoal and no greater size differentiation has been conducted.

Table 4.7 Sample depths and resolutions obtained from macro-charcoal analyses from sites within this research.

Site	Sequence	Depths	Resolution	Researcher
Tirinie	TIR 2012;	346.5-323.5	1 cm	This Study
	Composite	323.5-292.5	4 cm	
		292.5-282.5	2 cm	
		282.5-258.5	1 cm	
		258.5-242.5	2 cm	
		242.5-209.5	1 cm	
		209.5-198.5	4 cm	
	Core 4 2017	330.5-339.5	1cm	
Quoyloo	QM;	212.5-195.5	1 cm	This study
Meadow	Composite	195.5-181.5	2 cm	
		181.5-123.5	1 cm	
Palaeolake	B 2012;	509.5-333.5	8 cm	This study
Flixton	Composite	333.5-301.5	16 cm	
		301.5-205.5	4 cm	
Llangorse	LlaN 14;	582.5-486.5	4 cm	This study
	Composite	486.5-402.5	12 cm	
		402.5-248.5	4 cm	

Four sites were analysed for macro-charcoal at variable resolutions matching the resolution of the pollen records. Of the two Palaeolake Flixton sequences studied for pollen, only the most resolved in terms of proxy data, was selected for macro-charcoal analysis, Core B 2012. Owing to a lack of material, the basal sediments at Llangorse were not analysed.

Samples for analysis were extracted and processed following a selection of the methods outlined in Carcaillet et al. (2007) (Figure 4.8). As charcoal splinters easily, a non-destructive water displacement method was used to estimate 1 cm^3 of sediment. All samples were disaggregated in 5 % SHMP ($(NaPO_3)_6$) and gently sieved using di-ionised water over a 125 µm sieve. Due to the paucity of organic remains from 10 test samples, further size differentiation was not pursued. The resultant organic residues were bleached in solution, using 12 % sodium hypochlorite (NaClO), to aid in charcoal identification, and re-sieved over a 63 µm mesh. For each sample, all charcoal fragments were counted and tallied using a low powered binocular stereomicroscope.

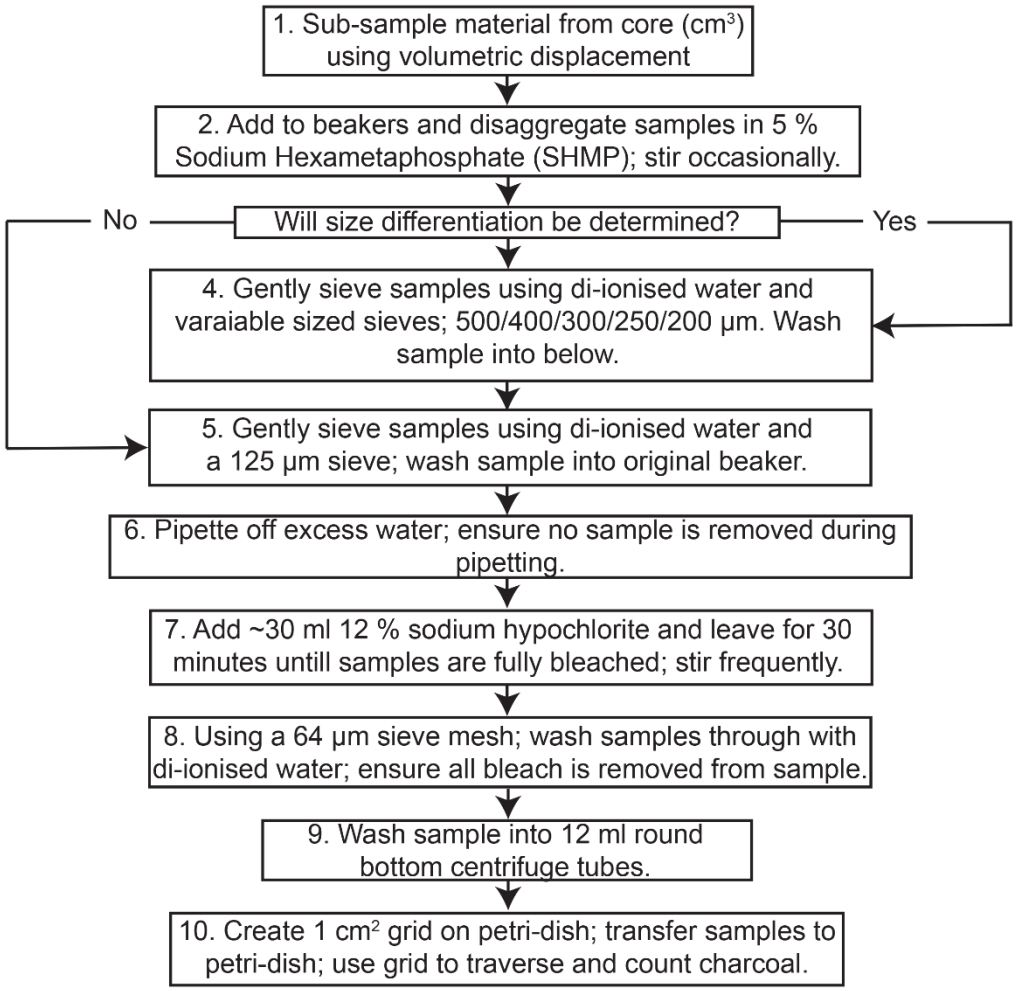

Figure 4.8 Macro-charcoal processing method performed within this research. As charcoal size differentiation is normally performed, the method has been included within this diagram.

4.3.6 Abrupt event definition and detection

In climatological and environmental research exactly what constitutes the defining of an abrupt event has been a matter of debate. In ice-core research, an 'event' is demarked by abrupt changes in the isotopic signature, with the onset of the event taken to reflect an abrupt change in the climatic record which act as pinning points in the NGRIP stratigraphy (Rasmussen et al., 2014). However, a suitable term to adequately define abrupt 'events' in terrestrial records is lacking. To better define both climatic events and palynologically-inferred vegetation revertence a series of criteria was devised (Table 4.8). From a climatic perspective, events are given more certainty where multiple climatic parameters are reconstructed, thus one of the criteria states that oscillations must be outside of the error range of the technique and recorded across multiple parameters. Where multiple parameters are not constructed, the former criterion is considered sufficient for the later chapters but caveats surrounding the nature of the event are noted.

Table 4.8 Criteria for defining a climatic event or vegetation revertence in terrestrial records (Watts, 1970; Edwards and Whittington, 2010). If not all of these criteria are met climatic events and revertences can still be defined if both climatic and vegetation proxies are changing concomitantly

Environmental construct	Criteria	Term if criteria met
Climate	1) Evidence across multiple climatic parameters (where possible)	Palaeoclimatic 'event'
	2) Changing climatic proxy outside of predictive error	
	3) Greater than one sample point (if no other criteria are met)	
Vegetation	1) Pollen flora identified to a good modern standard	Palynologically-inferred vegetation revertence
	3) Vegetation revertence clearly identified in a number of pollen spectra	
	4) Relative changes in sedimentology or other stratigraphic indicators.	
	5) Evidence for a short-lived climatic deterioration; changes in quantified palaeoclimatic reconstructions.	

From a palynological perspective the Watts (1970) criteria can be used. Despite this being previously used to define climatic variability, the criteria can actually be used to infer phases of vegetation change. Using these criteria, palynological change across multiple taxa gives with a greater degree of certainty evidence for inferring landscape vegetation change. Equally, the formulation of the PC, which treats all subject pollen taxa to a modelling approach, is a powerful tool to define potential vegetation variability (Section 4.3.1.7). A further addition to these criteria, is through the multi-proxy approach. If both climatic change and inferred vegetation change are broadly coeval, then climatic and vegetation change is clear. Therefore, henceforth, the terms 'event' and 'palynologically-inferred vegetation revertence' are conditioned to relate to changes in climatic structure and vegetation respectively.

4.4 Geochronological methods

4.4.1 Radiocarbon dating

The principal geochronological method used in this research was radiocarbon dating. Radiocarbon chronologies are constructed, with Advanced Mass Spectrometry (AMS)

techniques, by the direct measurement of the radionuclides or ^{14}C, within plant materials, for example wood, leaf fragments and seeds. In principal, upon atmospheric ^{14}C production, oxidation processes form $^{14}CO_2$ in the atmosphere, and through photosynthetic mechanisms ^{14}C is incorporated into plants (van der Plicht, 2007). As it is assumed that at the time of death ^{14}C:^{12}C ratios of organisms are the same as the atmospheric ratio, there is no diagenetic alteration of the ^{14}C signal and that beta decay occurs with time (^{14}C half-life: 5730 years); directly measuring the ratio of radioactive and stable carbon within sedimentary macro-fossils can reveal the time of death of the organism (Lowe, 1995). There are complications however, including variations in atmospheric ^{14}C production, variable reservoir effects and mineral carbon contamination; which highlight the need for effective calibration (e.g. Reimer et al., 2013) and scrutiny in sample selection (Lowe and Walker, 2000). Nonetheless, radiocarbon dating is the most frequently applied method in generating site chronologies during the LGIT (e.g. Lowe and Walker, 2000; Walker et al., 2000; Walker et al., 2012), with advancements in AMS techniques offering greater precision over bulk analyses.

Within this research, only Tirinie and Palaeolake Flixton were radiocarbon dated. Further, Palaeolake Flixton has been tied to a radiocarbon chronology and Quoyloo Meadow contains abundant tephra horizons (Timms et al., 2017; Blockley et a., 2018). To generate a chronology from Llangorse, bulk dates were transferred from the published literature using sequences proximal to the site across biostratigraphic ties (Chapter 8), whilst it is acknowledged that this is problematic it formed the basis for a provisional chronology. For radiocarbon determination at Tirinie, individual 1 cm slices were extracted from 10 cm diameter Russian cores and all core material was used. Samples for AMS radiocarbon dating were selected from key lithostratigraphic boundaries and where important pollen assemblage shifts were identified. The outer edges of the sample were cleaned to reduce carbon contamination and samples were picked for plant macro-fossil remains. Where required, samples were combined following a lack of identifiable plant remains. The lack of macro-fossil yielding sediments meant that only a select number of age determinations could be made throughout the profile. Samples were dated at the Scottish Universities Environmental Research Centre (SUERC) at the University of Glasgow, following standardised SUERC procedures.

4.4.2 Bayesian age modelling

To compare sequences across wide areas precise age-depth models are required (Lowe et al., 2008). One method, using Bayesian statistics allows for the generation of robust depositional models. For this reason, the flexibility of Bayesian models in incorporating prior information related to sediments, and their routine use in LGIT studies (e.g.

Matthewes et al., 2011; Bronk Ramsey et al., 2015), Bayesian age-modelling techniques were used in this thesis.

Age modelling was undertaken using radiocarbon dated horizons and well dated tephra layers. At Palaeolake Flixton age modelling was performed through the linking of key pollen horizons between the well-dated Monolith 1 archaeological sequence (e.g. Dark, 1998a) and lake records within Palaeolake Flixton (e.g. Candy et al., 2015; Palmer et al., 2015). See Blockley et al. (2018) for a detailed assessment of the procedures in creating this model.

Age models were constructed using OxCal V. 4.3 (Bronk Ramsey, 2009) using the IntCal13 calibration curve presenting calibrated ages before AD1950 (Remier et al., 2013). OxCal both calibrates radiocarbon ages and allows for the creation of age-depth models based on the incorporation of successively dated horizons into a Bayesian framework. All models use the *p_sequence* depositional model function within OxCal; a Poisson depositional function that states that depositional events are random, to allow for variable sedimentation rates (Bronk Ramsey, 2008). Secondly, the *k_parameter*, which sets accumulation events per unit depth, was kept variable to allow for better interpolation of dates between undated samples (Bronk Ramsey and Lee, 2013). All tabulated ages are presented as the mean with a 2 σ age range barring Palaeolake Flixton where reported errors are presented as 1 σ (Blockley et al., 2018). Ages in text use μ ± σ.

Chapter 5. Results from Quoyloo Meadow

Quoyloo Meadow is a former lake basin in west Mainland, Orkney. Two sites in the Orkney Islands exhibit calcareous sediments in close proximity, Quoyloo Meadow and Crudale Meadow (Whittington et al., 2015; Timms et al., 2017). Within the British Isles these currently are the most northerly sites displaying calcareous sedimentation, making them rare archives that permit the investigation of the expression of abrupt climatic events and associated palynological responses. Crudale Meadow was subject to recent high-resolution palynological and isotopic investigations (e.g. Whittington et al., 2015), and therefore it was decided that Quoyloo Meadow would be the Orcadian focus for this thesis.

Quoyloo Meadow has previously been the subject of a palynological investigation (Bunting 1994). Despite the relatively high stratigraphic sampling interval, the sequence perhaps still demonstrates unsuitable resolutions to detect palaeoenvironmental shifts both during the Windermere Interstadial and within the early Holocene. Equally, there is a gap within the pollen record during the earliest Holocene where one might expect to identify shifts in vegetation. From the Crudale Meadow site, where the resolution in the two periods is much higher, palynological shifts have been identified. Thus, in light of Quoyloo Meadow being recently chronologically constrained using tephrochronology it represents one of the sites, with associated climatic data, containing the highest chronological precision in the United Kingdom, especially within the early Holocene (Timms et al*.,* 2017). Re-evaluation of the vegetation history is therefore permitted. All data presented within this chapter can be found in Appendix B.

5.1 Basin stratigraphy and sedimentology

The Quoyloo Meadow basin was sampled in February 2014 by members of the Centre for Quaternary Research, Royal Holloway, University of London (Timms, 2016). In total nine boreholes were tested but owing to time constraints a complete basin-wide survey was not undertaken. To identify the best area of the basin to extract a core sequence 1.0 m Russian rods were used to depth sound the basin every 10-15 m following a NNE-SSW transect (Timms, 2016). The transect ran parallel with a drainage ditch identified on the Quoyloo mire surface with boreholes being spaced approximately 20 m away from the drainage system (Timms, 2016). The deepest location along the transect was identified at (59.066417, -3.309333) which became the focus of the core sequence retrieved from the basin. Duplicate cores were obtained adjacent to this borehole.

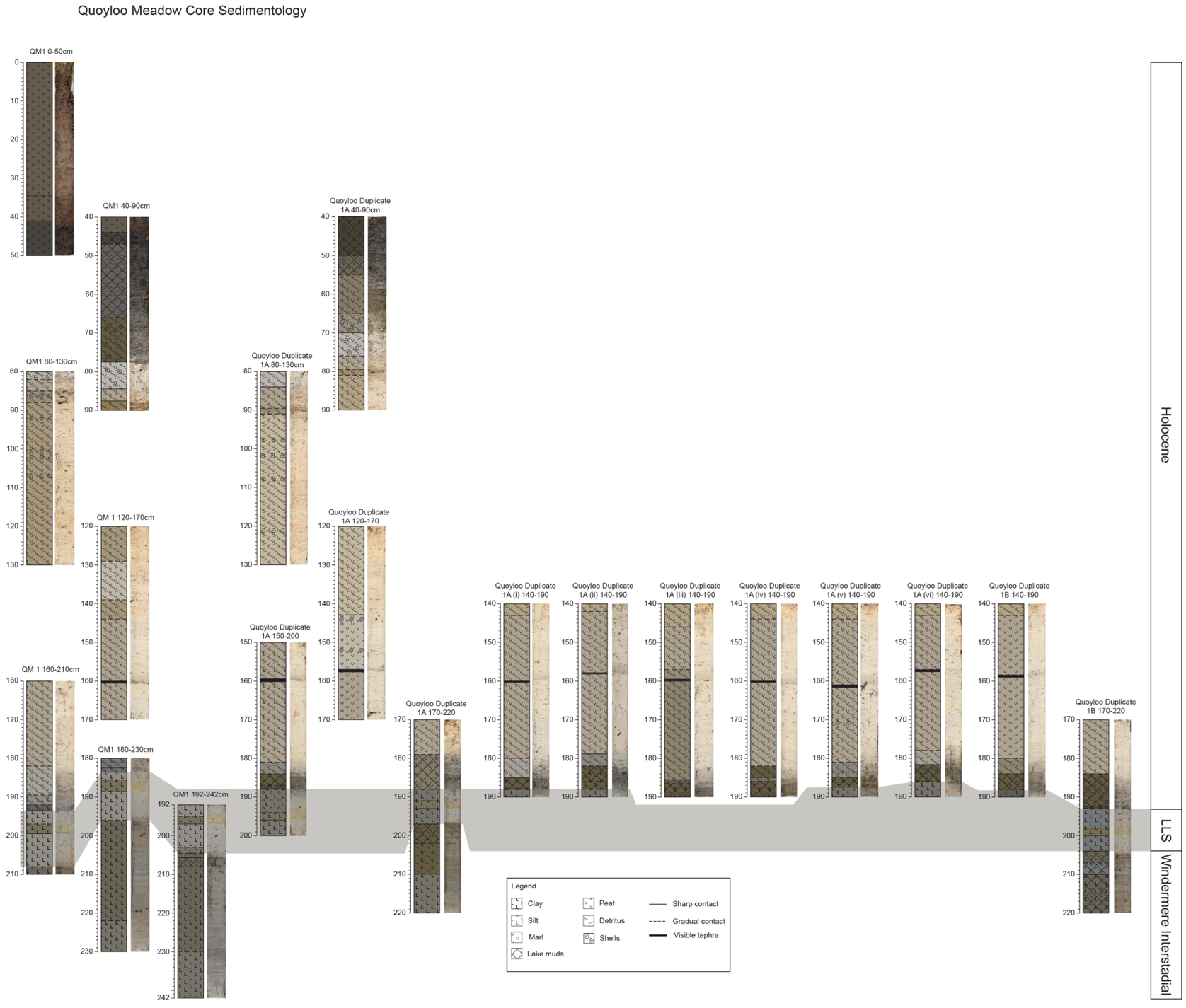

Figure 5.1 Quoyloo Meadow basin sediment stratigraphy. The sequence presented here is a combination of all sediment cores extracted from the basin at Quoyloo Meadow. The cores highlight significant changes within the sedimentology of Quoyloo, with the sequence displaying structures associated with the LGIT; shown by the grey shaded box. Broad climatostratigraphic zones have been shown here to assist in visualising the sequence. A clear feature of this sequence is the visible tephra layer observed within the calcium carbonate sediments. Figure from Timms (2016).

The cores retrieved from Quoyloo Meadow are presented in Figure 5.1. Although the deepest sequence is presented by the QM1 cores, owing to ongoing research, a subset of cores from Figure 5.1 are used within this thesis. These have been compiled into a composite profile, QM2, based on visual stratigraphy and key marker horizons (Figure 5.2). To facilitate comparisons between the QM1 and QM2 profiles, the former containing all palaeoclimatic and geochronological data, core alignment has been performed. The lower sedimentological units are stratigraphically comparable. However, the upper units of QM2 appear approximately 1 cm shorter, based on the position of the visible tephra layer. To allow for data comparison, between the last point of stratigraphic correlation and the ash layer, a linear scaling has been applied. In assuming the sedimentation rate has not changed above the ash layer, scaling continues to the top of the profile. As the QM2 depths have been placed onto QM1, for brevity, the presented sedimentology will focus on QM1 (Table 5.1; Figure 5.2) and all data will be placed onto this profile. Sedimentological differences (Figure 5.2) stem from subjectivity in sediment attribution.

The basal units from the sequence, units 1a and 1b, are characterised by silty clay sediments with a gradual increase in organic components. Unit 1a is characterised by organic percentages of <4 %; whereas, 1b organic percentages are <10 %. The final unit within the lower basal profile, unit 1c, is still characterised by silts and clays, however a greater organic influence is noted, with Loss on Ignition (LOI) values increasing to 17 %.

Throughout units 2a to 2c silt and clay sedimentation dominates. However, a shift to a dark grey colour is noted from the underlying units. This may reflect the reduction in organic sedimentological constituents; shown by a reduction in the LOI profile to <5 %. Furthermore, a two-centimetre light brown staining can be observed, attributed to unit 2b, which has been postulated to reflect sediment staining from a basaltic component of a known tephra horizon (Timms et al., 2017).

For the first time in the QM1 stratigraphy, fully organic sediments are observed in units 3 to 5. The colouration and high carbonate content denote marl sedimentation. Unit 3a and 3b exhibit increases in $CaCO_3$, from 3 to 31 %, and an increase in organic components, up to 13 %. Continued increases in $CaCO_3$ are observed within unit 3c, alongside a sequence high of 26 % within the LOI profile. In contrast, unit 3d exhibits a sequence high for $CaCO_3$, at 96 %, but a reduction in organics to 3 %. Unit 4 is characterised as a visible tephra layer (Timms et al., 2017). Overlaying unit 4, unit 5 returns to high percenatges for $CaCO_3$, between 84-90 %, and steadily rising LOI percentages.

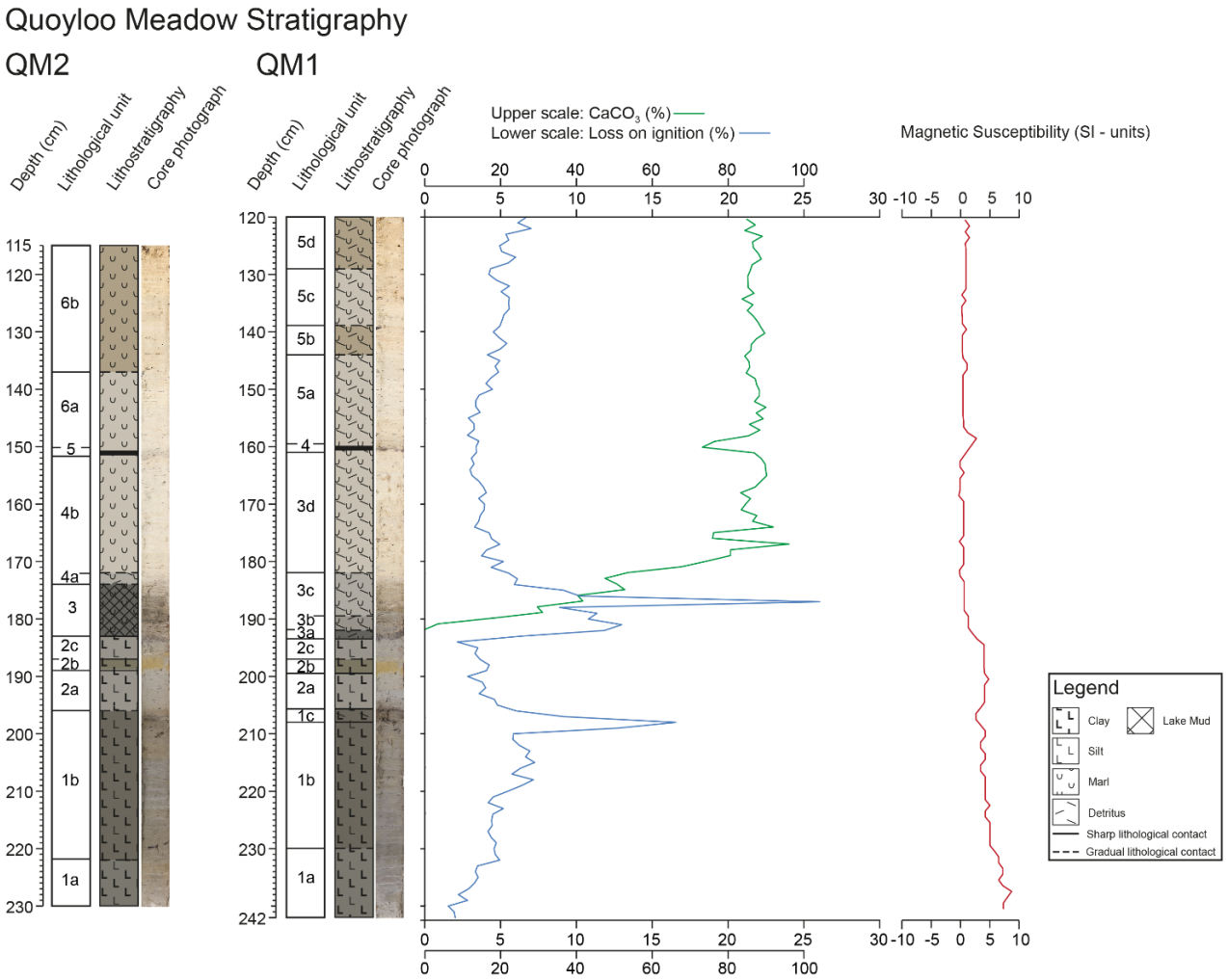

Figure 5.2 Stratigraphy of the QM1 and QM2 sequences from Quoyloo Meadow. LOI, calcimetry and magnetic susceptibility values are shown from the QM1 profile. The two sequences are largely identical being recovered at the same time from the same location. Modified from Timms et al. (2017).

Table 5.1 Lithostratigraphy of the QM1 sediment sequence presented within this research. Shown here are the major lithological units with descriptors.

Unit	Depth (cm)	Troels-Smith	Classification	Munsell colour
5d	120-129	Lc3, Ag1, Dg+	Marl	10YR 6/3 Pale Brown
5c	129-139	Lc3, Ag1, Dg+	Marl	2.5Y 7/2 Light Grey
5b	139-144	Lc3, Ag1, Dg+	Marl	10YR 6/3 Pale Brown
5a	144-159	Lc3, Ag1, Dg+	Marl	2.5Y 6/2 Light Brownish Grey
4	159-160	N/A	Tephra	10YR 2/1 Black
3d	161-182	Lc3, Ag1, Dg+	Marl	2.5Y 6/2 Light Brownish Grey
3c	182-189	Lc3, Ag1, Dg+	Marl	2.5Y 4/2 Dark Greyish Brown
3b	189-192	Lc2, Ag1, Dg1	Detrital Marl	2.5Y 4/2 Dark Greyish Brown
3a	192-193.5	Lc2, Ag1, Dg1	Detrital Marl	2.5Y 3/1 V. Dark Grey
2c	193.5-197	As3, Ag1	Silty Clay	5Y 4/1 Dark Grey
2b	197-199.5	As3, Ag1	Silty Clay	5Y 4/1 Dark Grey
2a	199.5-206.5	As3, Ag1	Silty Clay	2.5Y 4/2 Olive Grey
1c	206.5-208	As2, Ag1, Ld1, Dg+	Silty Clay	2.5Y 3/2 V. Dark Greyish Brown
1b	208-230	As3, Ag1	Silty Clay	2.5Y 3/1 Dark Greyish Brown
1a	230-242	As3, Ag1	Silty Clay	5Y 4/1 Dark Grey

5.2 Palynological results

Quoyloo Meadow was analysed for pollen at a contiguous 1 cm resolution within sedimentological unit 1 and units 3 to 5 (resampled so units 3:5 appear greater than 1 cm); increasing to 2 cm within unit 2. In total 112 samples were processed. Unfortunately, between 223-242 cm the sediment contained minimal pollen but abundant *Lycopodium*; suggesting either a limited vegetation presence surrounding Quoyloo, or taphonomic preservation issues. It was concluded not to continue counting these levels. Equally, within the lower countable samples the pollen was sparse. Hence, certain levels contain pollen counts to 100 TLP only despite using all available pollen residues. The same is also true at other levels in the profile (Table 5.2). From 83 final pollen samples; 11 local pollen assemblage zones have been defined (QMP-*n*) based on changes in principal taxa. Only the small *Pediastrum* fraction will be discussed in text.

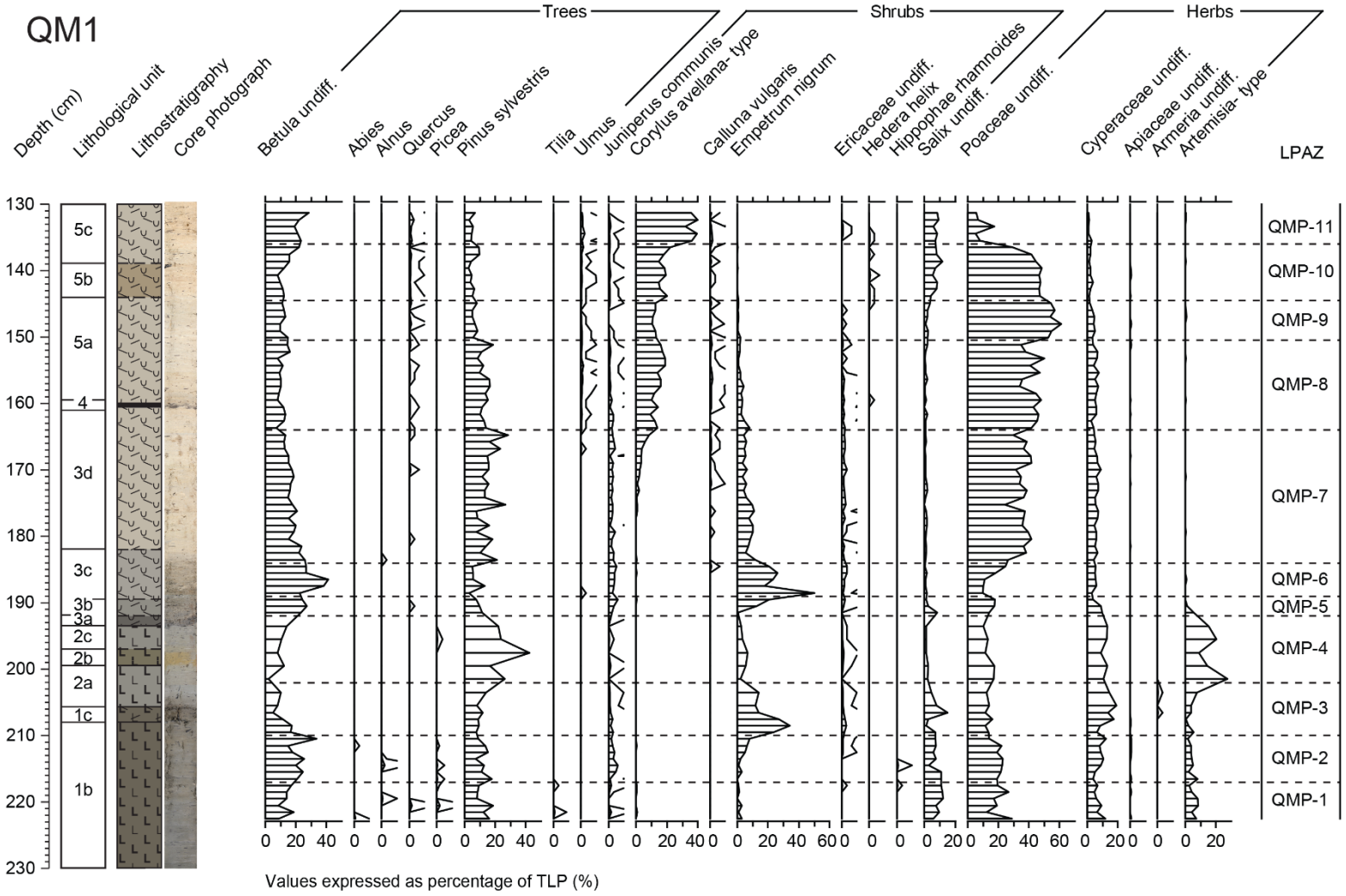

Figure 5.3 Pollen percentage profile presented from Quoyloo Meadow. All values are presented against TLP.

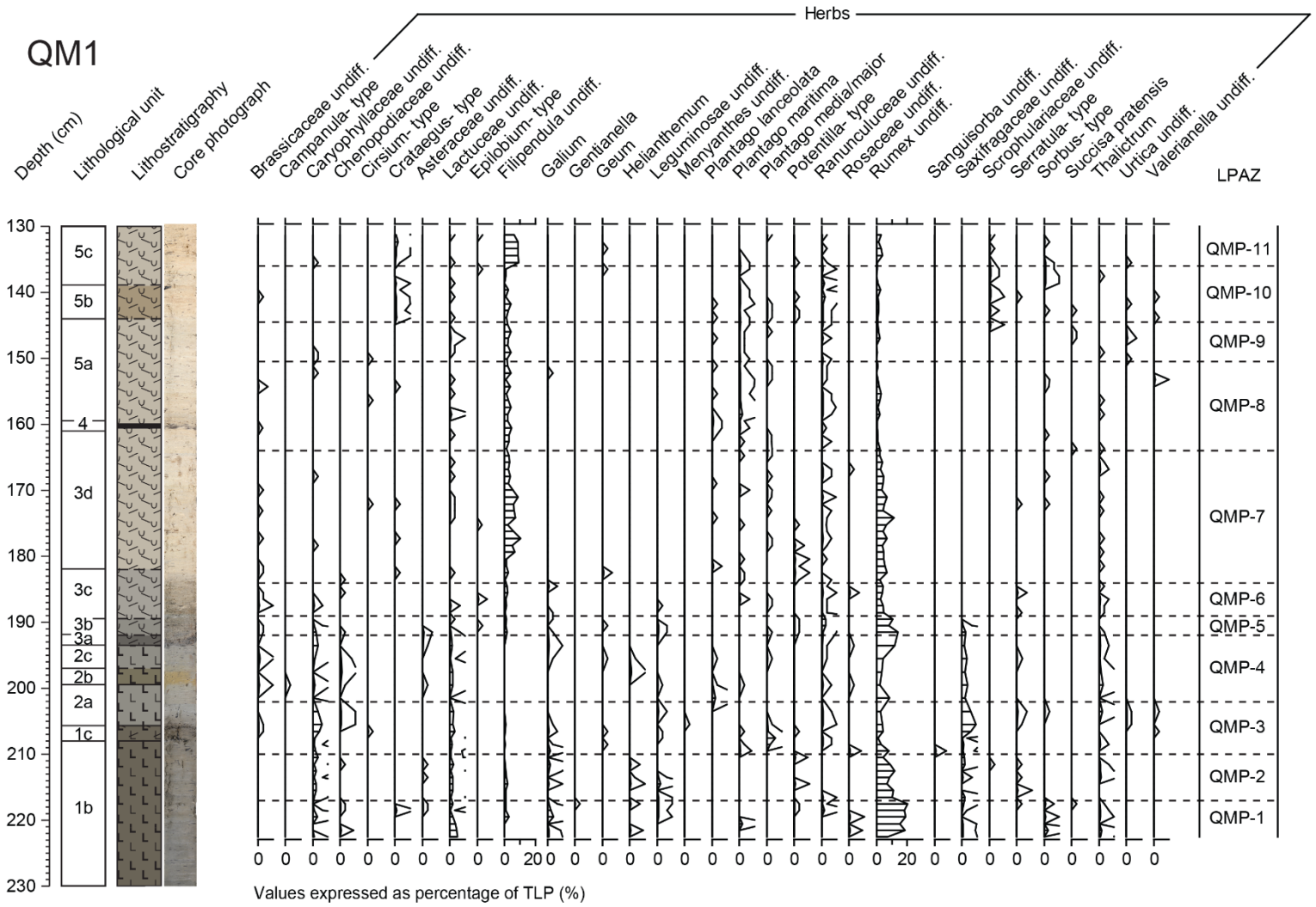

Figure 5.3 (Cont.) Pollen percentage profile presented from Quoyloo Meadow. All values are presented against TLP.

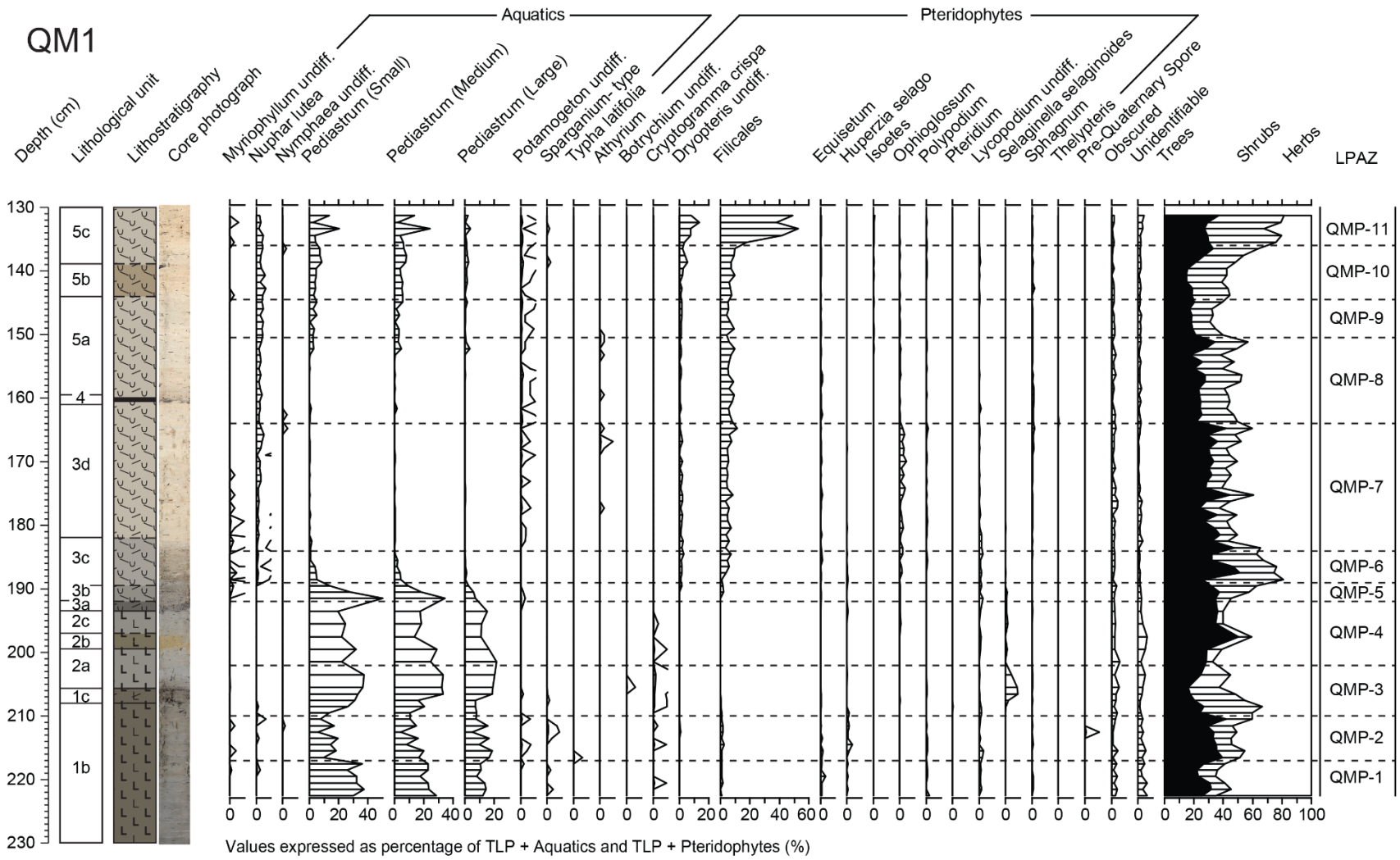

Figure 5.3 (Cont.) Pollen percentage profile presented from Quoyloo Meadow. Values are presented as TLP + Aquatics and TLP + Pteridophytes.

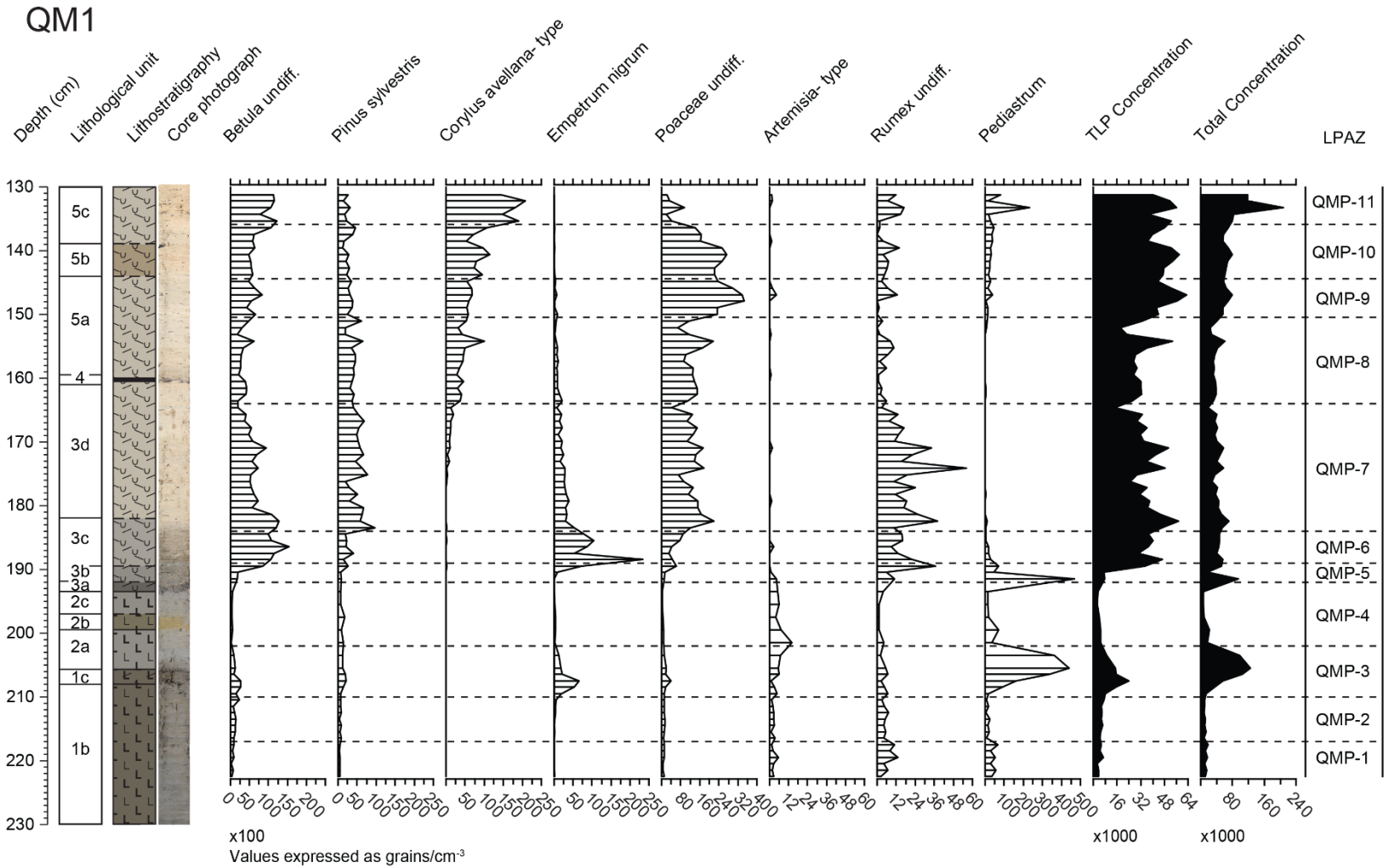

Figure 5.4 Summary pollen concentration data from Quoyloo Meadow showing key pollen taxa. All values multiplied by 100 unless stated.

Table 5.2 Quoyloo Meadow pollen zone information. Also provided are the zones from the QM2 stratigraphy and the new resampled zones within the QM1 profile.

LPAZ	QM2 Depth (cm)	QM1 Depth (cm)	Key Taxa
QMP-11	128-123	136-131	Filicales, *Corylus*, *Betula*
QMP-10	136-128	144.5-136	Poaceae, *Corylus*, *Betula*
QMP-9	142-136	150.5-144.5	Poaceae
QMP-8	155-142	164-150.5	Poaceae, *Corylus*, *Pinus*
QMP-7	174-155	184-164	Poaceae, *Pinus*, *Betula*
QMP-6	179-174	189-184	*Empetrum*, *Betula*, Poaceae
QMP-5	182-179	192-189	*Pediastrum*, *Betula*, *Empetrum,* Poaceae
QMP-4	192-182	202-192	*Pinus*, *Artemisia*, *Pediastrum*
QMP-3	200-192	210-202	*Empetrum*, *Pediastrum,* Cyperaceae
QMP-2	207-200	217-210	*Betula*, Poaceae, *Pediastrum*
QMP-1	213-207	223-217	*Pediastrum*, Poaceae, *Rumex*

Zone QMP-1. QM1 depth: 223-217 cm.

Zone QMP-1 is dominated by herbaceous taxa. Poaceae values start high at the base, decrease, and then rise towards the top of the zone, between 12-29 %. *Rumex* percentages are low at the start of the zone before increasing to moderate percentages, 18-20 %, at the end of the zone. Additional herbaceous taxa include Cyperaceae, *Artemisia*, Compositae: Lactuceae, and Saxifragaceae. These taxa contain percentages of less than 10%. *Salix* is the main shrub taxa with a high of approximately 12 %. Percentages of *Pediastrum* are high, >26 % throughout with a high of 36 %.

Pollen concentrations are low throughout this basal zone characterised by TLP concentrations with a maximum of 6851 grains/cm^{-3} at 219.5 cm. Total concentrations, which peak at 19,090 grains/cm^{-3} at 217.5 cm, reflect the increased aquatic component within this zone. The majority of pollen concentrations do not rise above 1000 grains/cm^{-3}.

Zone QMP-2. QM1 depth: 217-210 cm.

Zone QMP-2 demonstrates for the first time an increase in arboreal pollen types. The major arboreal pollen constituent is *Betula*, increasing from 21 to 33 % throughout the zone. However, *Betula* percentages drop from 25 to 15 % at 211.5 cm. The other dominant arboreal taxa, *Pinus*, oscillates between 7 and 18 % throughout. Poaceae is also recorded with percentages between 14 and 23 %. Equally, *Pediastrum* and *Rumex* are present albeit in lower percentages. Where percentage drops in *Betula* are observed higher *Pediastrum* and *Rumex* values are recorded, from 6 to 17 % and 7 to 12 % respectively. Shrub-type pollen include *Juniperus*, *Empetrum* and *Salix*. Additional herbaceous types include Cyperaceae, *Artemisia*, Caryophyllaceae and Compositae: Lactuceae. Filicales and *Huperzia selago* complete the pteridophyte components. Pre-Quaternary spores are also observed for one sample at 211.5 cm.

In accordance with the basal zone, TLP concentrations are low throughout with a maximum concentration at the end of the zone of 7126 grains/cm^{-3}. Higher total concentrations similarly reflect the aquatic components. There is a general decrease in concentration at 211.5 cm; however, *Pediastrum* increases in this sample.

Zone QMP-3. QM1 depth: 210-202 cm.

This zone demonstrates considerable variation in principal taxa. A peak in *Empetrum* is noted at the zone onset and rapidly decreases from 34 to 14 %. A peak in *Salix*, 15 %, occurs directly after *Empetrum*. Contrasting with QMP-2, *Betula* percentages follow a downward trend with *Pinus* percentages stable but rising. Cyperaceae values increase from 6 % at the base to 19 % near the top of the zone. Like QMP-1, *Pediastrum* percentages are high throughout; peaking with 37 % at 203.5 cm. Throughout the zone there is increased representation of herbaceous types; including *Aretmisia*, Caryophyllaceae and *Saxifragaceae*. *Rumex* is once more present along with *Cryptogramma* and increasing percentages of *Selaginella*.

TLP concentrations peak at 207.5 cm at 24,141 grains/cm^{-3} before decreasing. In contrast, where TLP concentrations decrease, total concentrations are rising to 125,105 grains/cm^{-3} at 205.5 cm. Although most concentrations are decreasing, *Artemisia* increases to a zone high of 686 grains/cm^{-3} at 203.5 cm with increasing values for Caryophyllaceae. *Rumex*, *Selaginella* and Saxifragaceae concentrations appear at their

highest towards the middle of the zone. *Pediastrum* exhibits a 26-fold increase from 1648 grains/cm^{-3} to 44,160 grains/cm^{-3} throughout QMP-3.

Zone QMP-4. QM1 depth: 202-192 cm.

QMP-4 shows a marked change from the previous zones. *Pinus* is the principal arboreal pollen taxa peaking at 42 % towards the middle of the zone. The second major component of QMP-4, *Artemisia*, demonstrates an oscillatory trend; whereby successive percentages of 29, 9 and 20 % are observed. Percentages of *Pediastrum* are high throughout the zone although to a lesser extent than QMP-3. Poaceae and Cyperaceae percentages fluctuate between 15 and 20 %. Additional taxa closely resemble that of the upper levels of QMP-3 with *Empetrum*, Caryophyllaceae, *Rumex* and Saxifragaceae all present.

Concentrations are as low as QMP-1 with a TLP average of 4119 grains/cm^{-3}. Highest concentrations are observed at the base of the zone. The offset between TLP and total concentration is reduced within QMP-4. *Pinus* and *Artemisia* are the only taxa that demonstrate concentrations above 1000 grains/cm^{-3}; mirroring the respective peaks in the percentage data.

Zone QMP-5. QM1 depth: 192-187 cm.

Zone QMP-5 is dominated by the aquatic taxon *Pediastrum*. It peaks abruptly at the onset of the zone, up to 50 %, and falls to 14 % at the zone terminus. *Betula* percentages are moderate throughout with a high of 27 %. From <1 % *Empetrum* increases considerably throughout the zone with percentages of 21 % reached by 189.5 cm. Poaceae and *Juniperus* percentages increase to 18 % and 6 % respectively. *Rumex* percentages are more elevated than QMP-4, with highest values observed from the base of the zone. Additional taxa include *Artemisia*, Ranunculaceae and *Myriophyllum*.

TLP concentrations are higher than QMP-4 and increase to 35,110 grains/cm^{-3} at 189.5 cm. Contrastingly, total concentrations are highest at the base of the zone, 94,524 grains/cm^{-3}, reflecting the high *Pediastrum* values, 46,920 grains/cm^{-3}.

Zone QMP-6. QM1 depth: 189-184 cm.

QMP-6 is characterised by high values of shrub-type pollen. *Empetrum* rises sharply to a sequence high of 50 % at 188.5 cm and then falls as abruptly to 18 %. Subtle increases

in percentages are then seen through the remainder of QMP-6. The arboreal component is provided by *Betula*, which further peak to a sequence high of 41 % at 186.5 cm. Poaceae demonstrates increases throughout; increasing to 25 % towards the end of the zone. Further components of the pollen spectra include *Juniperus*, Cyperaceae, *Filipendula*, *Rumex* and Filicales all of which are below 7 %.

Land pollen concentrations are high at 186.5 cm, 46,819 grains/cm^{-3}, and between 30-40,000 grains/cm^{-3} through the remainder of QMP-6. The discrepancy between total and land pollen concentrations is further reduced within this zone. Concentrations of *Empetrum*, 23,487 grains/cm^{-3}, and *Betula*, 15,358 grains/cm^{-3}, are high.

Zone QMP-7. QM1 depth: 184-164 cm.

Zone seven is predominantly characterised by moderate to high percentages of Poaceae, between 24 and 42 %. *Betula* percentages are decreasing from 25 % at 183.5 cm to 12 % at 165.7 cm whereas *Pinus* is increasing, from 10 % at 182.5 cm to 28 % at 164.7 cm. The *Pinus* spectrum also demonstrates added complexity with a peak at 174.1 cm. This peak is associated with reductions in *Filipendula* and *Empetrum*, from 6 to 2 % and 9 to 4 % respectively, and increases in *Rumex*, from 4 to 12 %. Pollen that continue to be present throughout the zone include *Filipendula*, *Rumex* and *Juniperus*; with aquatic and pteridophytes consisting of *Nuphar*, Filicales and *Ophioglossum*.

The percentage peaks of *Pinus*, *Rumex* and Poaceae are all associated with concentration increases to 5950 grains/cm^{-3}, 5443 grains/cm^{-3} and 10,486 grains/cm^{-3}. *Filipendula* decreases from 3729 grains/cm^{-3} to 573 grains/cm^{-3} during this phase. Holistically, these changes result in total land pollen concentration increases to 53,156 grains/cm^{-3}. From this high, TLP concentrations fluctuate then decrease to 14,470 grains/cm^{-3} by the end of QMP-7.

Zone QMP-8. QM1 depth: 164-150.5 cm.

QMP-8 is dominated by Poaceae. Percentages are high at the base of the zone, between 42 and 48 %, but oscillate between 34 and 50 % towards the top of the zone. For the first time in the sequence *Corylus* is represented between, 9 and 19 %. *Pinus* and *Betula* exhibit low percentages. Herbaceous taxa include Cyperaceae, *Filipendula* and *Rumex*.

Throughout the zone TLP concentrations are variable with elevated and depressed

values of 53,550 grains/cm^{-3} and 18,160 grains/cm^{-3} at the top of the zone. A peak in Poaceae, 21,801 grains/cm^{-3}, is observed at 154.3 cm; mirrored across dominant taxa.

Zone QMP-9. QM1 depth: 150.5-144 cm.

Zone QMP-9 is characterised by an increase in herbaceous pollen types. The dominant taxon throughout is Poaceae, with percentages greater than the previous zone, up to 61 % which are the greatest taxon percentages recorded. Other herbaceous taxa include *Artemisia*, albeit at less than 1 % over two levels, small increases in *Rumex*, up to 2 %, Compositae: Lactuceae and *Plantago maritima*. *Filipendula* is continually recorded with percentages between 2-4 %. *Pinus* and *Corylus* percentages are generally lower than the previous zone, whereas, *Betula* percentages are similar. Aquatic taxa are represented by *Pediastrum* and *Nuphar* and pteridophytes by Filicales.

Pollen concentrations are largely higher than the previous zone, with a TLP peak of 63,053 grains/cm^{-3} mid-zone. Poaceae pollen is high throughout ranging from 23,243 grains/cm^{-3} at the base to 34,693 grains/cm^{-3} towards the centre of the zone. Concentrations of additional taxa are generally lower than or comparable to the previous zone (e.g. *Betula*, *Pinus*, *Corylus*) although *Salix*, *Filipendula* and to a lesser extent *Rumex*, attain higher concentrations.

Zone QMP-10. QM1 depth: 144.5-136.5 cm.

Poaceae is again the dominant taxon, with percentages of 47 %. These high percentages decrease to 29 % at the top of the zone. *Betula* and *Pinus* are represented by fluctuating percentages and *Corylus* reaches elevated values towards the middle of the zone. *Salix* percentages also rise, peaking at 12 % at the top of the zone. Only Cyperaceae, *Filipendula* and *Rumex* demonstrate percentages >2 %. *Pediastrum* values climb throughout, with Filicales fluctuating between 6-10 %.

TLP concentrations are high, peaking at 58,269 grains/cm^{-3}; a function of high values for Poaceae, 27,186 grains/cm^{-3}. Across other horizons, taxon specific values are high, e.g. *Salix* with 4233 grains/cm^{-3} at 138.6 cm. *Corylus* and *Betula* increase throughout.

Zone QMP-11. QM1 depth: 136-131 cm.

The final zone in the sequence is dominated by *Corylus*. *Corylus* doubles in percentage from 22 % from the previous zone to 40 % at the top of QMP-11. The taxon being

replaced is Poaceae. For one sample at 133.4 cm Poaceae returns to moderate values. Coinciding with this peak, *Pediastrum* rises abruptly to 20 %. *Betula* percentages are moderate to high; between 19 and 29 % throughout. Additional arboreal components include *Pinus*, *Quercus* and *Ulmus*. The dominant herbaceous taxon is *Filipendula*, with values between 6 and 9 % throughout. High values are recorded for Filicales.

Absolute TLP concentrations are similar to the previous zone. Highs of 56,256 grains/cm^{-3} are observed at 133.4 cm, reflecting increased concentrations of Poaceae with lower concentrations of *Betula* and *Corylus*. Similarly, total concentration abruptly peaks at 133.4 cm; predominantly reflecting the influence of Filicales, 78,237 grains/cm^{-3} and *Pediastrum*, 27,383 grains/cm^{-3}.

5.3 Statistical analyses

Statistical analyses were performed on a reduced Quoyloo Meadow dataset where all taxa were selected with an abundance of greater than 5 %. A 5 % cut off was deemed suitable as this excluded the influence of rare taxa within the dataset. A detrended correspondence analysis (DCA) was first employed to establish the lengths of the primary axes (Table 5.3). These lengths (>1.5-3 SD) demonstrated that both Principal Components Analysis (PCA), Correspondence Analysis (CA) and therefore Principal Curves (PC) were suitable for data exploration at Quoyloo Meadow.

The PCA was preferred for exploring the variation due to short axes lengths. The results of the PCA are presented in Figure 5.5. The results along the two axes in ordination space show axis one as representing 33.6 % of the variation in the data and axis two representing 15 % of the variation. Taxa that plot negatively along axis one include: *Corylus* (the most significant contributor), Filicales, *Dryopteris*, *Nuphar*, *Filipendula* and Poaceae. Contrastingly, taxa plotting positively along the axis include: *Pediastrum*, Saxifragaceae, Caryophyllaceae, Cyperaceae, *Artemisia* and *Rumex*. Intermediate taxa, and those that show a stronger axis two component, in either direction, include: *Salix*, *Juniperus*, *Empetrum* and *Betula*.

Table 5.3 Preliminary DCA analyses on the reduced Quoyloo Meadow dataset highlighting the greater variation explained by axis 1.

	DCA1	**DCA2**	**DCA3**	**DCA4**
Eigenvalue	0.3319	0.12307	0.10736	0.09799
DCA value	0.3348	0.09539	0.04324	0.02464
Axis length	2.1710	1.90586	1.37306	1.36359

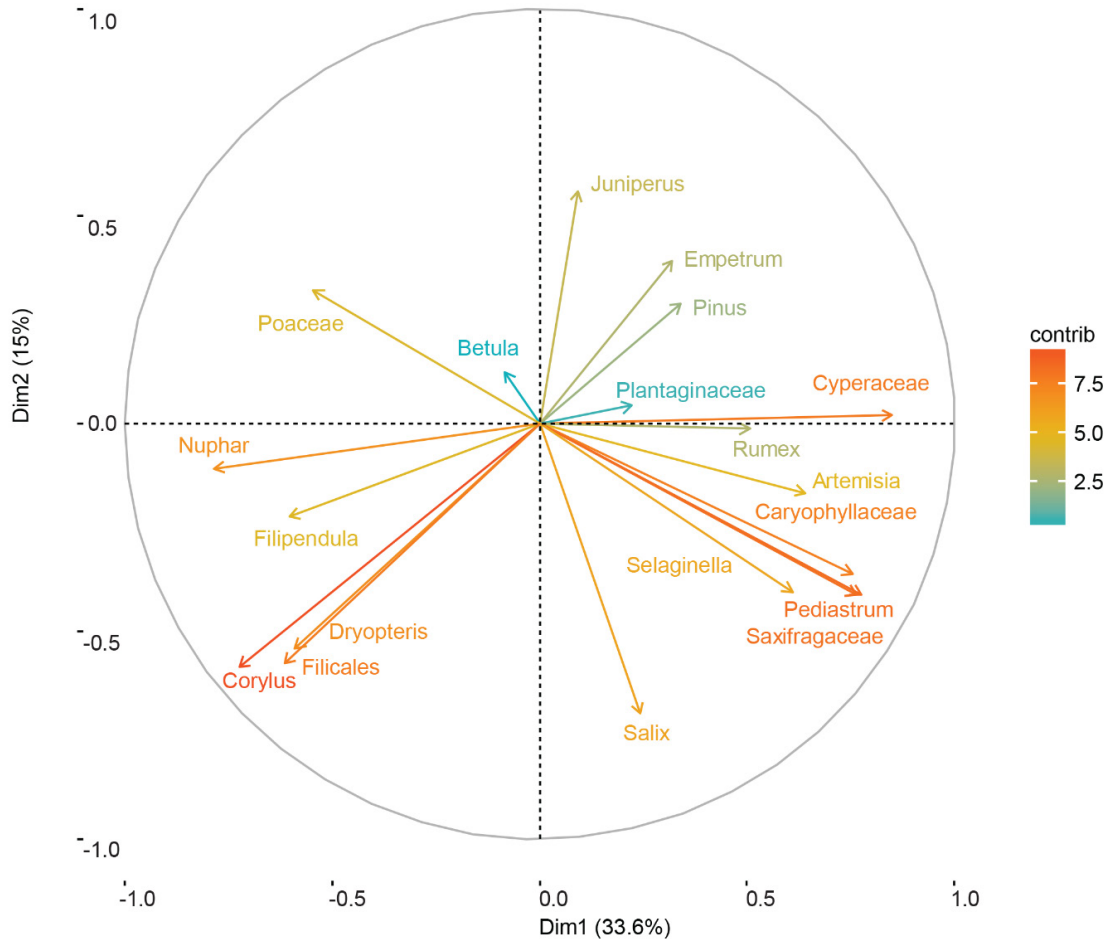

Figure 5.5 Results of the PCA output from Quoyloo. The data are presented as a biplot showing the two principal components, axis 1 and 2, with taxa placed along the axes relative to their importance. The length of the arrow and the variable colour indicates the dominant taxa along the axis. Plotting positively along axis one with greater importance are open herbaceous taxa; whereas negative values are composed of shrub and tree-type taxa. Certain tree and shrub type taxa also demonstrate an association with axis 2.

To explore the relationship between pollen and stratigraphy, axis 1 scores were plotted for both the PCA and CA solutions. This was subsequently modelled using the PC which explained the most variation in the data (Figure 5.6). The final PC solution has been calculated on a CA-based output as the CA-based output explained more variation within the data with similar penalty values applied to the regression. This suggests the PCA is less successful in capturing the variation within the data:

- PCA based output: 80.0 %
- CA based output: 81.1 %

Changes within the PC data are confined to a single major oscillation, and five additional oscillations in the curve. These may be defined as: 1) increased variance in the distance along the gradient and; 2) a pause in the general shift towards lower values. Additional locations are confined to single data points that demonstrate sight deviations from the

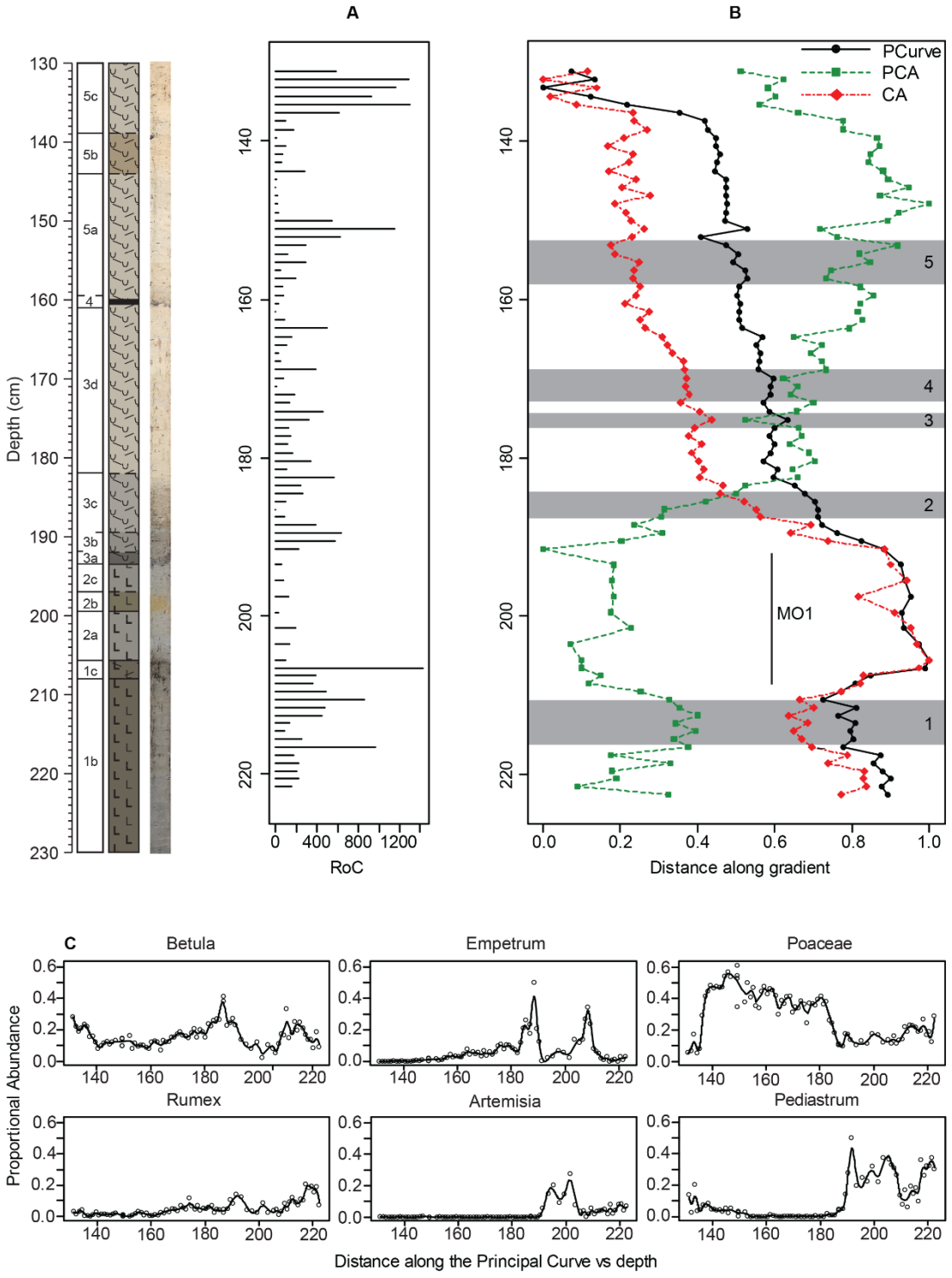

Figure 5.6 Results of different statistical tests applied to the Quoyloo pollen data. A) Rate of change analysis. The values for the analysis are arbitrary and an exaggeration multiplier has been applied to demonstrate where significant periods of compositional change are inferred. The greater the length of the bar the more significant the compositional change. B) The overlain output from three tests applied (PCA, CA and PC). This highlights the clear differences between the PCA and CA based output with both having a different start point. The PC will be discussed from this point. The data show rapid short oscillations (grey boxes) and a longer oscillation termed (MO1). C) Individual taxa response curves modelled on the gradient of the PC. These key taxa demonstrate what may be driving the changes in the PC from B). The stratigraphy is shown on the composite profile within this study, however the statistical modelling has been placed on the master profile from Timms (2016).

trend, and hence, their significance is difficult to reconcile. Nevertheless, they have been shaded on Figure 5.6 and presented as follows:

- Major Oscillation 1: 206.5-189.5 cm
- Oscillation 1: 216.5-210.5 cm
- Oscillation 2: 188.5-185.5 cm
- Oscillation 3: 175.2 cm
- Oscillation 4: 173.09-168.91 cm
- Oscillation 5: 158.45-154.27 cm

These shifts can be identified in the rate of change analysis (RoC) where increases in RoC demonstrate palynological compositional change against stratigraphic resolution. To visualise which taxa may be driving the changes observed in the principal curve, individual taxa response curves have been generated. *Artemisia*, identified concurrently with taxa in a similar ecological group, exerts significant influence over the PC within Major Oscillation 1. Additional taxa can be shown to influence the PC at various points in the stratigraphy and compared to other sequences, do not follow the established pattern of vegetational change observed throughout the LGIT period. The statistical data will be discussed in the context of vegetation history in Section 5.6

5.4 Micro- and macro-charcoal

Micro- and macro-charcoal analyses were undertaken at the same resolutions as the pollen profile, resulting in 83 samples. Micro-charcoal analyses were conducted alongside pollen counts and presented as charcoal concentrations, whereas macro-charcoal identification was undertaken separately and are presented as raw counts. There is considerable variation between each sample, however, amongst this variation there are also phases where clear peaks in micro- and macro-charcoal can be observed. Therefore, for each of the graphs presented in Figure 5.7 an average of the charcoal counts are represented by a horizontal line. Values occurring above this average are deemed significant, whereas values below are prescribed to background variation. The average value for concentration data is 27,478 shards/cm^{-3} whereas for macro-charcoal the average is 11.70 fragments/cm^{-3}.

Micro-charcoal

Micro-charcoal concentrations range from 5166 shards/cm^{-3} to 107,592 shards/cm^{-3}. Within this record four peaks in charcoal have been identified. The first exists towards the base of the sequence. More prominent peaks in charcoal concentration exist in the

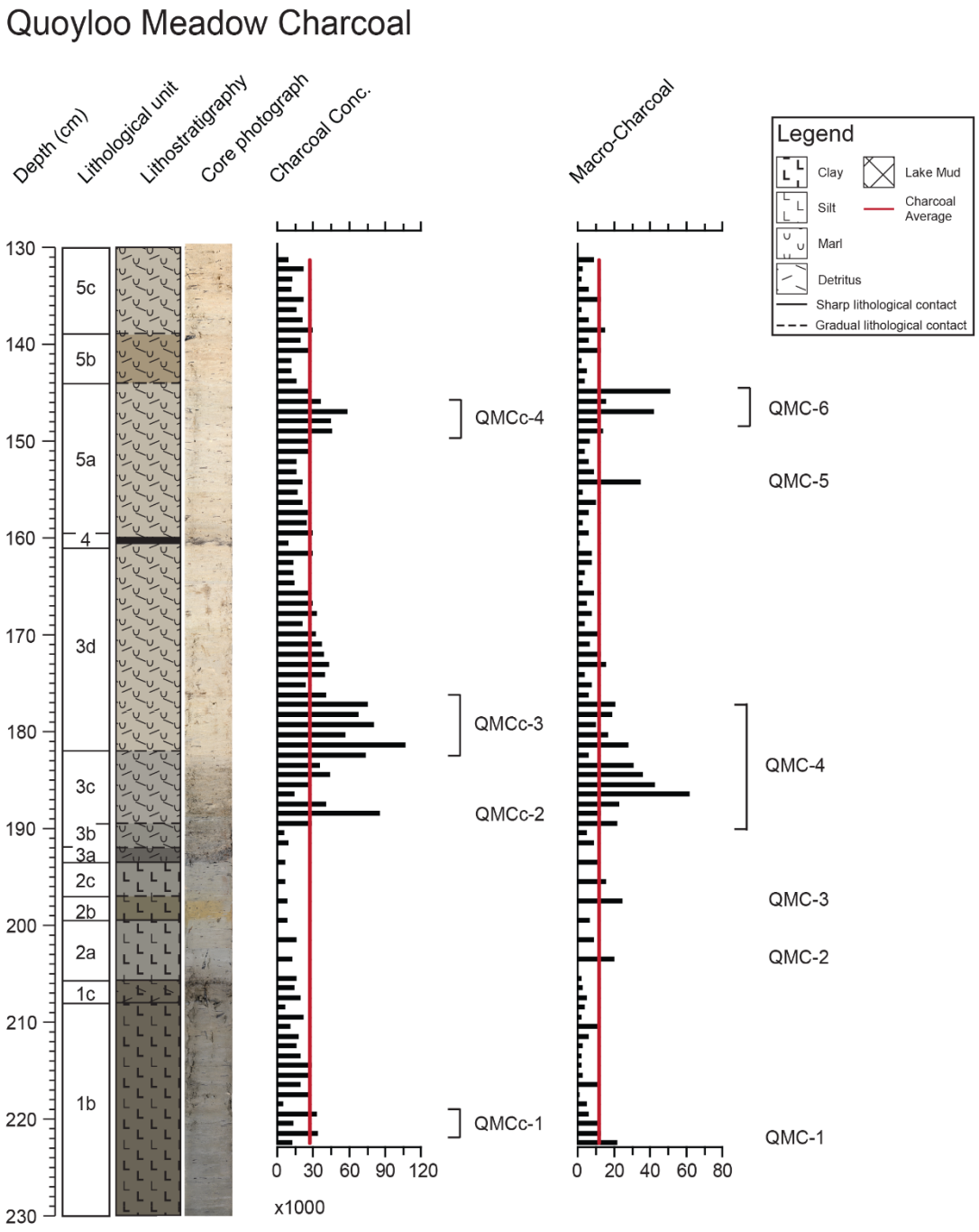

Figure 5.7 Micro-charcoal concentration (left) and Macro-charcoal counts (right) for the Quoyloo Meadow sequence are presented against the composite depth and the master stratigraphy. Significant peaks are labelled using QMCc for concentration values and QMC for raw counts. Average charcoal is presented on the figures to aid in identifying charcoal peaks. Both graphs exhibit similarities and differences with regards to abundance of the major peaks and their positioning. Considerable variation is further noted between QMCc-2:3 and QMC-4.

marl sediments however. The first of these, QMCc-2 at 186.5 cm, contains 85,861 shards/cm^{-3}. This peak is clearly separated from QMCc-3, which spreads between 183.5-176.2 cm. This peak is the most significant throughout the sequence, with 107,592 shards/cm^{-3}. Charcoal identifications either side of this peak are generally greater than other areas throughout the sequence. It is currently unclear whether the small increases in charcoal post QMCc-3 represent a secondary peak. It was concluded that, as only one sample falls beneath the average between the two sets of values and concentrations are lower than the main peak of QMCc-3, these values reflect a long tail of QMCc-3. Additional support is provided by successive decreases in charcoal concentrations following this peak. One final peak is identified within QMP-9, where charcoal concentrations reach 58,683 shards/cm^{-3}. It is noted that very little charcoal is observed between 205.5-189.5 cm.

Macro-charcoal

Marco-charcoal counts through the profile range from lows of 1 fragment/cm^{-3} to highs of 62 fragments/cm^{-3}. Six macro-charcoal peaks have been identified throughout the sequence. At the base of the record, a peak of 20 fragments is observed, termed QMC-1. At 203.5 and 197.5 cm two successive increases of charcoal can be observed, classified as QMC-2 and QMC-3, containing 20 and 25 charcoal fragments respectively. Like the micro-charcoal record, the greatest abundances of macro-charcoal are recorded in the carbonate sediments. The most significant peak in the record, QMC-4, sits within a complex of charcoal between 189.5-177.3 cm. This complex contains a maximum abundance of 62 charcoal fragments. Within the complex, high count numbers surrounding the main peak are acknowledged. The penultimate charcoal peak, QMC-5, is demarked by a single sample with a total of 35 fragments identified. The final charcoal peak within the sequence, QMC-6, sits between 149-144.9 cm and contains 51 charcoal fragments.

5.5 Additional site data

The data provided here includes data compiled alongside this thesis. Stable isotopic data were compiled by Rhys Timms; chironomid-inferred temperature data by Agnieska Mroczkowska and Rhys Timms; and biomarker data compiled by David Maas (Preface; Chapter 4). The biomarker data presented here are therefore confined to compound specific isotopic analyses for *n*-C_{23} and *n*-C_{29} only. Most palaeoclimatic data were extracted from the master profile of Timms et al. (2017) however, like the pollen profile, the biomarker analyses were performed on a separate core (QM1 170-220). Owing to a 1 cm offset between QM1 170-220 and the QM1 stratigraphy (Figure 5.1), biomarker data have been scaled, resampled and presented against QM1 (Table 5.4).

Table 5.4 Example of the scaling process used for biomarker data at Quoyloo Meadow. Linear scaling has been applied assuming a constant sedimentation rate up to the location of the offset in the core. Scaling was stopped following core alignment.

Biomarker Sample	Core Depth (cm)	QM1 (cm)
13	197.5	197.5
12	198.5	198.5
11	199.5	199.5
10	200.5	200.67
9	201.5	201.83
8	202.5	203
7	203.5	204.17
6	204.5	205.33
5	205.5	206.50
4	206.5	207.5
3	207.5	208.5

5.5.1 $\delta^{18}O$ and $\delta^{13}C$ stable isotopes

Owing to the nature of core materials retrieved, isotopic analyses were only applied to sedimentary units 3 and 5 in the QM1 profile. This resulted in 85 isotopic measurements at 0.5 cm resolution. Throughout the reconstructed profiles, there is a considerable noise between samples. To smooth this variation a three-point moving average has been applied to the raw values and overlain within Figure 5.8; which will be the basis for discussion.

Throughout the profile there is slight evidence of co-variation between oxygen and carbon with an R^2 value of 0.54. The carbon isotopic record is characterised by enriched values at the base of the profile, 3.07 ‰ at 194.25 cm, dropping to 1.20 ‰ at 150.25 cm. The average carbon values are given as 1.86 ‰, 1σ=0.51. Contrastingly, the oxygen isotopic profile is relatively depleted at the base of the carbonate sequence, -4.16 ‰ at 194.25 cm, becoming more enriched towards the top of the profile, -3.29 ‰ at 150.25 cm. The average oxygen isotopic value throughout is presented as -3.49 ‰, 1σ=0.41. Superimposed on this trend are a series of oxygen isotopic depletions which have been labelled QMO-1:6 in Figure 5.8. QMO-1 at the base of the profile demonstrates a subtle depletion with minimum values of -4.18 ‰ observed at 191.25 cm. QMO-2 is more pronounced with values of -3.90 ‰ and -3.88 ‰ separated by depleted values of -4.14 ‰ at 186.25 cm. More enriched isotopic values bounding QMO-3; -3.14 ‰ and -3.05 ‰

at 173.5 cm and 167.25 cm respectively, are punctuated by values of -3.51 ‰ at 170.75 cm. Like QMO-1, QMO-4 is not as pronounced as the other depletions identified throughout the sequence. It features subtle drops from -3.03 ‰ at 165.25 cm to -3.26 ‰ at 163.75 cm before returning to -2.93 ‰ at 159.25 cm. Contrastingly the subsequent depletion in the isotopic record, QMO-5, exhibits the greatest depletion observed in the sequence. Enriched values of -2.93 ‰ at 159.25 cm and -3.03 ‰ at 154.75 cm delimit the phase with depleted values of -3.44 ‰ observed at 156.75 cm.

5.5.2 Chironomid-inferred temperatures

The C-IT reconstruction from Quoyloo Meadow is shown in Figure 5.8 using 35 chironomid samples. Temperature reconstructions were obtained using a modern Norwegian calibration dataset (Brooks and Birks, 2001). A two-component, weighted averaging-partial least squares regression (WA-PLS) model was selected leading to a root mean squared error of prediction (RMSEP) of 1.137°C, a coefficient of determination (R^2_{JACK}) of 0.89 and a maximum bias of 1.1°C.

The data suggest that mean July temperatures were high at the base of the record, between 237.5 and 208.5 cm, with reconstructed temperatures of 10.6-12.6°C. Elevated temperatures are punctuated by a short cooling phase. This occurs within one sample, centred on 214.5 cm, with a temperature decline of 1.86°C and a minimum reconstructed temperature of 10.64°C. Significant cooling is observed between 207.5-191.5 cm where temperatures drop abruptly to 5.06°C, the coldest temperatures recorded throughout the Quoyloo Meadow sequence. Within this phase, there is an increase in temperature, at 199.5 cm, where temperatures are elevated to 9.01°C. Subsequently temperatures return to colder values with a recorded temperature of 5.35°C.

In association with the inception of carbonate sedimentation; elevated temperatures are recorded. Reconstructed values, between 10.31-13.86°C, are observed throughout the remainder of the sequence, excluding three phases whereby subtle temperature declines are observed. These samples centred at 174.5 cm, between 159.5 and 152.5 cm and at 130.5 cm, show temperature declines of 0.68°C, 2.34°C and 1.34°C respectively.

5.5.3 Biomarkers

Quoyloo Meadow was analysed for *n*-alkanes at a contiguous 1 cm resolution (resampled so the resolutions are greater) resulting in 30 analyses. Owing to concentrations being below the integration threshold for two samples within the aquatic end-member (197.5 and 199.5 cm) 28 analyses for *n*-C_{23} were obtained.

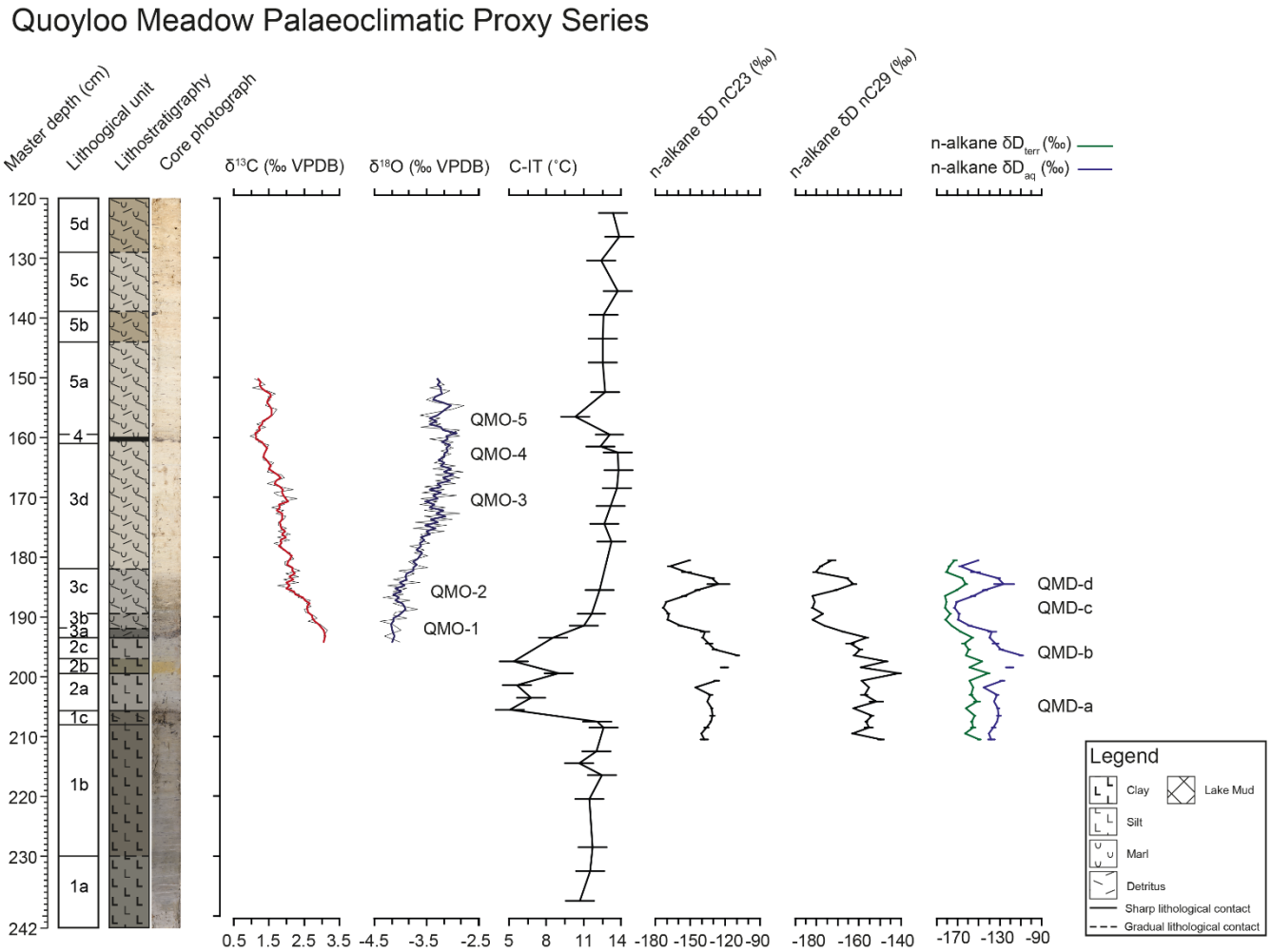

Figure 5.8 The complete suite of palaeoclimatic data from the Quoyloo Meadow sequence. The graphs presented from left to right are: Carbon and Oxygen isotopic data; chironomid-inferred temperatures, compound specific Deuterium isotopes from nC23 and nC29 alkanes. Labels are presented where discussed in text.

5.5.4 Compound specific isotopic reconstructions

Compound specific deuterium isotopic reconstructions are presented in Figure 5.8. There are considerable variations between absolute reconstructed values of *n*-C_{23} and *n*-C_{29} between individual samples, however, similar trends are observed between the two end-members. The deuterium isotopic profile throughout the basal units, 1b to 1c, are confined to six samples. Over these levels the *n*-C_{23} alkane exhibits enrichment from -140.29 ‰ to -130.95 ‰; labelled QMD-a. In contrast, *n*-C_{29} values demonstrate considerable noise between -163.05 ‰ and -149.40 ‰ but are largely stable.

A change in *n*-C_{23} is observed between 201.83-192.5 cm. Here values are rapidly enriched to a sequence high of -109.42 ‰ at 196.5 cm before falling with the same rapidity to values observed earlier in the sequence. This trend is somewhat mirrored in the *n*-C_{29} curve, although values are not as enriched and appear, like lower in the sequence, more variable. However, peak enrichment is observed at 199.5 cm displaying -141.06 ‰. This enriched phase is termed QM-Db.

The remainder of the sequence assessed for biomarkers is oscillatory in nature. Within the *n*-C_{23} alkane, between 192.5-187.5 cm, significant deuterium depletion is observed with a sequence low of -173.07 ‰ at 188.5 cm. Immediately succeeding this, rapid enrichment is observed, up to -125.90 ‰ at 184.5 cm. Over this phase of the record, enriched maximum values and depleted minimum values for *n*-C_{29} mirror *n*-C_{23}. These depletion and enrichment phases are labelled QM-Dc and QM-Dd (Figure 5.8).

5.5.5 Chronology

No radiocarbon dates were sought from Quoyloo Meadow owing to the abundant tephra horizons presented from the sequence (Timms et al., 2017). Published ages of these tephra horizons were used to construct an age model (Table 5.5; Figure 5.9) using a p_sequence depositional model and the IntCal13 calibration curve (Reimer et al., 2013) in OxCal V. 4.3 (Bronk Ramsey, 2008; 2009) (Chapter 4). No boundaries were added to the model over areas of lithostratigraphic change to allow the model greater flexibility. However, the model was constrained by boundaries to extend modelling to the base and top of the proxy data series.

Of note, Timms et al. (2017) did not place two tephra (QM 218; QM 213) into a tephrochronological framework, despite being chemically indistinguishable from the Borrobol and Penifiler Tephras. The decision not to define the tephra was largely stratigraphic (Timms et al., 2017). However, using palaeoclimatic and biostratigraphic data presented in this thesis, which provide more credible evidence that these tephras

are the Borrobol and Penifiler Tephras, they have been incorporated into the age model. Further the Hovdahargi/An Druim Tephras have been combined in this model owing to their co-identification at the same depth within Timms et al. (2017). Combining these tephra produced a better agreement index in the final age model (Rhys Timms, Pers. Comm 2018).

The model produced good model agreement across the sequence and was therefore used to provide calendar age ranges for the reconstruction presented in Section 5.6. The model suggests that sediments were deposited in the basin between 15.22±0.85 and 9.04±0.64 Cal. ka BP (Table 5.9) The complete age model (Figure 5.9), alongside the rest of the data in this chapter, is presented in Appendix B.

Table 5.5 Summary of the tephra, depth, unmodeled input range and modelled output range (2 σ age range) and mid-point age with 1σ error at Quoyloo Meadow.

Name	Depth (cm)	Unmodelled range (Cal. ka BP)	Modelled range (Cal. ka BP)	μ ± σ	Reference
Boundary	120		9.78-7.80	9037±639	
An Druim Tephra	133	9.80-9.53	9.80-9.53	9666±66	Timms et al. (2017)
Fosen Tephra	155	10.40-10.0	10.27-10.04	10,165±56	Lind and Wastegård (2011)
Saksunarvatn Ash	160	10.28-10.14	10.28-10.15	10,214±34	Lohne et al., 2014
Askja-S Tephra	188	10.92-10.73	10.94-10.74	10,837±55	Kearney et al. (2018)
Hässeldalen Tephra	193	11.66-11.12	11.67-11.10	11,385±144	Ott et al. (2016)
Vedde Ash	198	12.11-11.94	12.11-11.93	12,020±45	Bronk Ramsey et al. (2015)
Penifiler Tephra	213	14.07-13.82	14.08-13.82	13,951±66	Bronk Ramsey et al. (2015)
Borrobol Tephra	218	14.19-14.00	14.18-13.99	14,084±48	Bronk Ramsey et al. (2015)
Boundary	242		16.99-14.08	15,221±848	

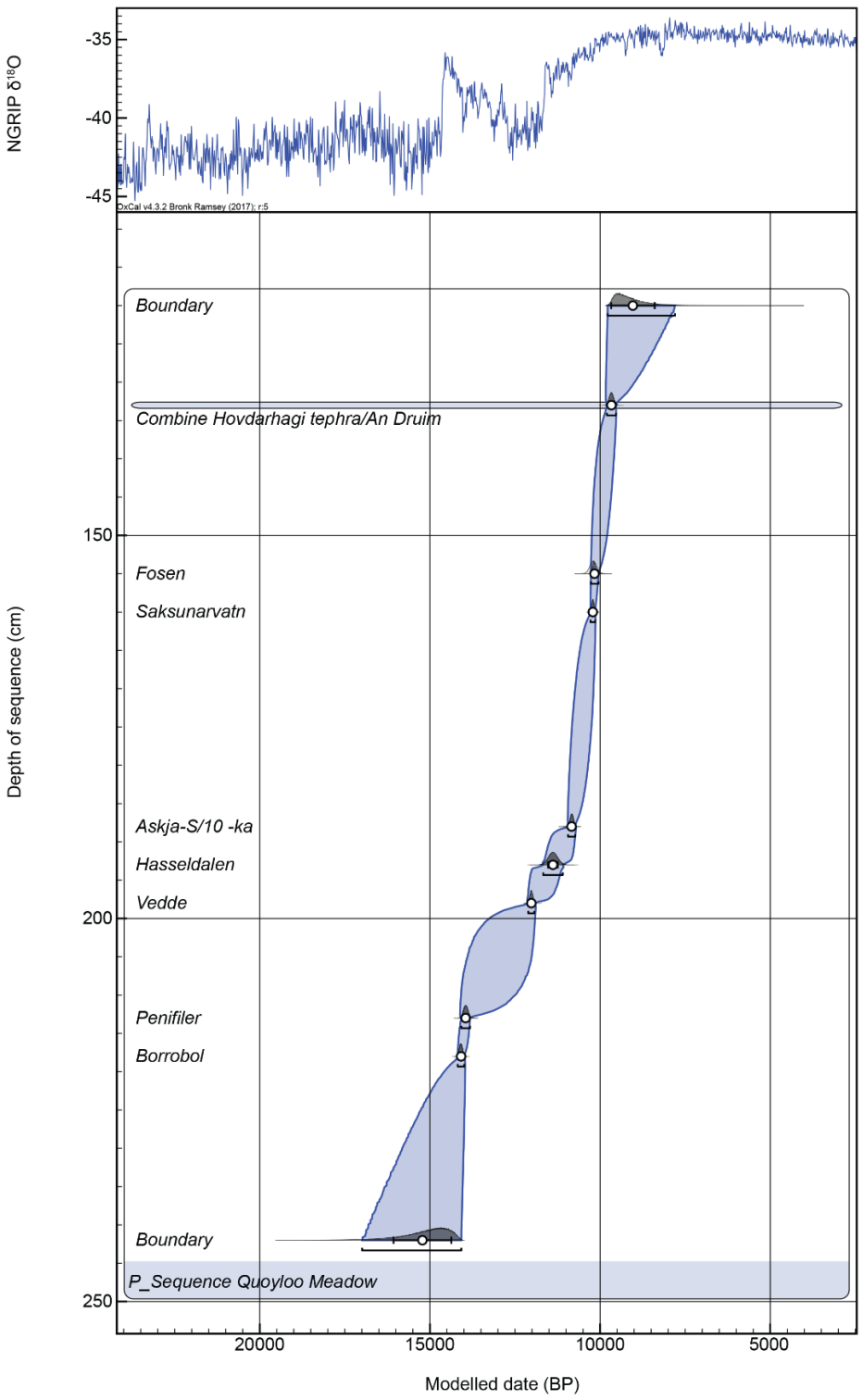

Figure 5.9 Age-depth, p_sequence model for Quoyloo Meadow, with age uncertainties plotted μ and 1 σ, whilst the complete range is shown at 2 σ. Boundaries have been added at the top and bottom of the sequence for interpolation.

5.6 Palaeoclimatic and palaeoenvironmental interpretation

The presented palaeoclimatic and palaeoenvironmental data will used here to reconstruct the climatic and environmental history of Quoyloo Meadow. All palaeodata (Figure 5.10; Figure 5.11) will be discussed chronologically. The pollen data will be discussed here to infer vegetation development and change. Whilst it is acknowledged that this is an assumption, based on available data and the plethora of palynological studies that utilise this approach (e.g. Walker, 1975; Lowe and Walker, 1986; Tipping, 1991; Bunting, 1994; Whittington et al., 2015) it is justified. Nonetheless, based on the age modelling applied to this study, sediment unit 1 can be attributed to the Windermere Interstadial (WI); sediment unit 2 to the Loch Lomond Stadial; and sediment units 3 to 5 to the early Holocene (EH). No Dimlingston Stadial sediments are proposed (DS)

Isotopic considerations

The isotopic analyses performed across sediment units 3 to 5 provide some evidence of covariation (R^2= 0.547; Figure 5.12). Covariation might be taken to reflect significant phases of artificial isotopic enrichment, including evaporitic modification or phases of detrital contamination (Chapter 4). From Quoyloo Meadow, it is thought unlikely that evaporitic modification has affected the signal as: 1) units 3 to 5 present carbonate sedimentation throughout which appears continuous; 2) $\delta^{13}C$ becomes progressively depleted with no phases of continued isotopic enrichment, as would be expected following evaporitic modification (Hammarlund et al., 2003); and 3) whilst $\delta^{18}O$ does become enriched throughout the profile, the enrichment is tracking increases in C-ITs, which would be expected if $\delta^{18}O$ is predominantly reflecting changes in temperature (Leng and Marshall, 2004). Disentangling the influence of detrital carbonates is difficult as Devonian-aged Orcadian basin carbonates have oxygen isotopic ranges of -7.5 ‰ and 0 ‰ with the Devonian 'fish beds' between -9.0 ‰ and +1 ‰ (Duncan and Hamilton, 1988). These values overlie the reconstructed values from Quoyloo Meadow. Further, the noisy nature of reconstructions may also suggest sequential contamination. However, it is unlikely that detrital carbonates impact the Quoyloo Meadow sequence as no $CaCO_3$ is recorded from sediments attributable to the WI or LLS, where, if detrital contamination were a factor, increased carbonate would be expected. It is thought that increased noise in the data stems from the 0.5 cm sampling strategy employed and the recording of greater temporal variability. Therefore, as minimal evidence of detrital contamination exists at Quoyloo Meadow and isotopic modification through evaporation is negligible, Quoyloo remained an open lacustrine system during phases of carbonate precipitation with authigenic carbonates forming in equilibrium with climate.

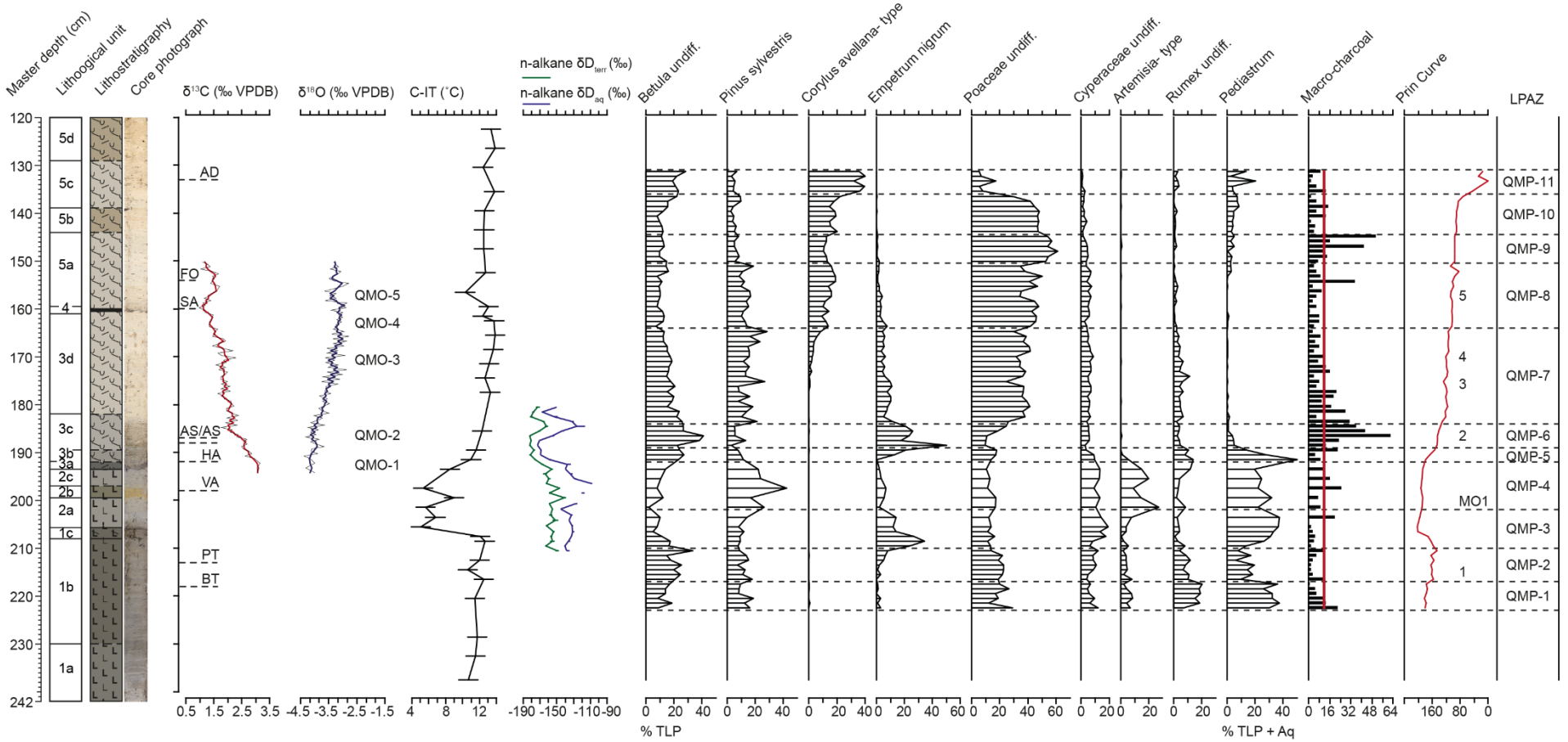

Figure 5.10 Summary of palaeodata presented from Quoyloo Meadow. The principal pollen taxa have been included. The position of the tephra (BT: Borrobol; PT: Penifiler; VA: Vedde; HA: Hässeldalen; AS/AS: Askja-S; SA: Saksunarvatn; FO: Fossen; AD: An Druim/Hovdarhagi) are highlighted to the of the figure. Also shown are the oxygen isotopic depletions and oscillations in the principal curve.

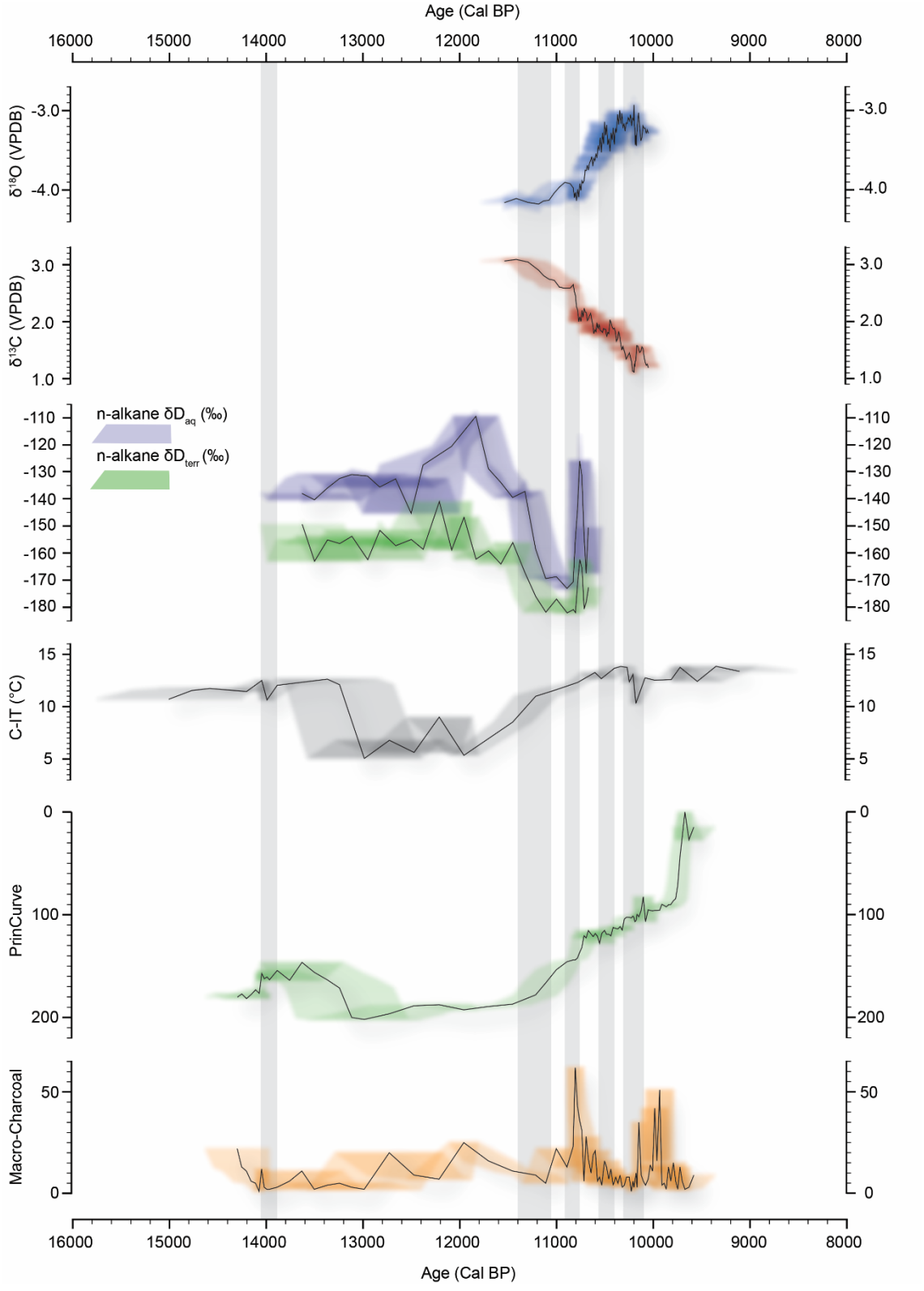

Figure 5.11 Comparison of all proxy data from Quoyloo Meadow placed against age. Shown are $\delta^{18}O_{carb}$, $\delta^{13}C_{carb}$, δD_{aq} and δD_{terr}, chironomid-inferred temperatures, the principal curve from the pollen data and macro-charcoal counts. Also shown on the diagram are key phases discussed in text. Whilst not all represent climatic events or vegetation revertences, they are shown here. These are evidenced by grey shaded bars.

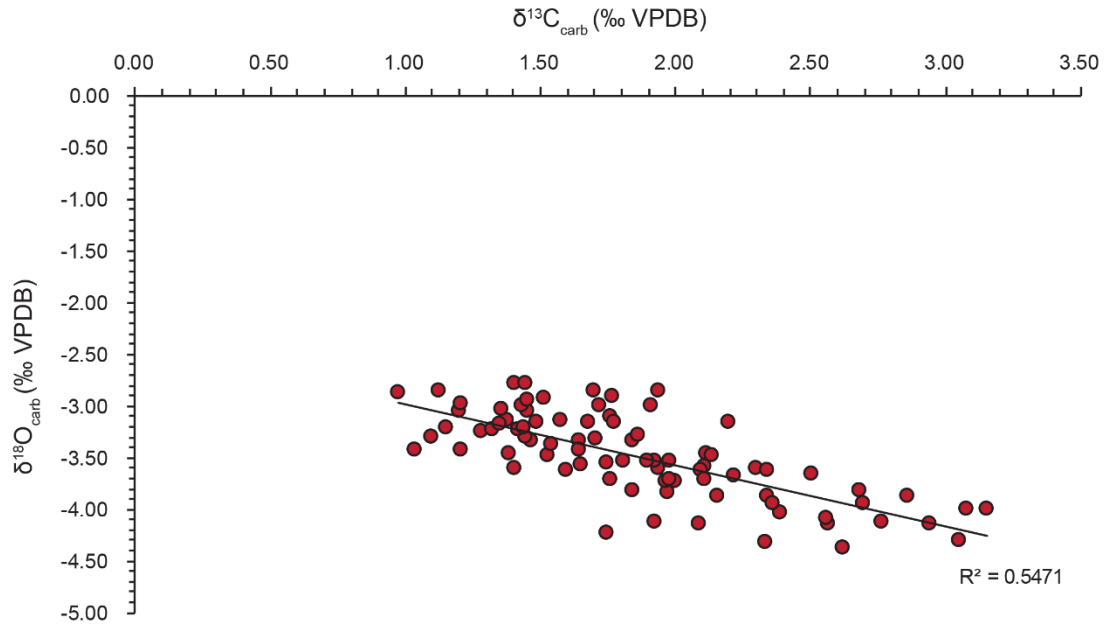

Figure 5.12 Comparison of $\delta^{18}O$ and $\delta^{13}C$ from Quoyloo Meadow. Throughout the profile moderate evidence exists for covariation between the two measured isotopes.

Attributing a source for the *n*-C_{23} and *n*-C_{29} compound classes is important to understand biomarker δD values (Chapter 4). However, few aquatic taxa were identified in the pollen record. Those identified include *Potamogeton*, *Myriophyllum* spp., *Sparganium*, *Nuphar lutea* and *Typha latifolia*. Emergent macrophytes frequently produce longer chain length *n*-alkanes, closer to those of higher terrestrial plants (e.g. Cranwell, 1984; Ficken et al., 2000; van den Bos et al., 2018). It is therefore unlikely that the *n*-C_{23} homologue was affected by the latter three taxa (e.g. Aichner et al., 2018) with *Potamogeton* and *Myriophyllum* the most likely sources for *n*-C_{23}. Considering both taxa have similar reconstructed δD values (e.g. Liu et al., 2018) and biosynthetic fractionation offsets, a combined source attribution is likely, but not thought problematic. Concerning *n*-C_{29}, dominant higher plant pollen identified throughout the sequence include *Betula* undiff., *Pinus sylvestris*, *Salix* undiff. and Poaceae undiff. However, *P. sylvestris* observations likely reflect long distance transport. Equally gymnosperms do not produce significant quantities of *n*-alkanes (e.g. Diefendorf et al., 2011). Therefore, as with other studies, the source for the *n*-C_{29} alkane is likely to be attributed to *Betula* and *Salix*, with further contributions from Poaceae and additional herbaceous plants (e.g. Rach et al., 2014; Aichner et al., 2018).

Based on these considerations the $\delta^{18}O_{carb}$ is interpreted in terms of the $\delta^{18}O$ of precipitation which is influenced by temperature dependent fractionation during vapour condensation. Due to lacustrine mixing, the signal is interpreted to reflect mean annual temperatures. Biomarker δD reconstructions are affected by the same atmospheric

processes as $\delta^{18}O_{carb}$ thus can be interpreted in terms of changing temperature (Chapter 4). Equally however, terrestrial leaf waxes over aquatic leaf waxes can be affected by evaporitic modification, thus the two can be used to infer changes in aridity (Chapter 4).

Early Windermere Interstadial- 15.01±0.75 - 14.05±0.07 Cal. ka BP

The base of the sequence shows relatively warm C-ITs (10.71°C). Like many records from the British Isles, no climatic amelioration is recorded from terminal DS/WI sediments (e.g. Brooks et al., 2016). This suggests that the onset of the WI may not be recorded at Quoyloo Meadow. Unfortunately, the analysis of a deeper sample (241-242 cm) revealed no chironomid head-capsules to test this. Nevertheless, the early Interstadial (unit 1) was dominated by minerogenic sedimentation. This relates to significant catchment erosion and the break-down of skeletal soils and mineral lithologies, or the lack of soil formation in a chaotic environment. Evidence is gained through the lack of pollen between 15.22±0.85 to 14.3±0.33 Cal. ka BP. No pollen is recorded through the earliest WI suggesting that: 1) conditions were not favourable for pollen production; 2) taphonomic issues prevented pollen preservation; or 3) no vegetation was present on the landscape. Firstly, the warm temperatures of the early WI suggest that thermal conditions were favourable for plant flowering, with colder temperatures in the high Arctic not being a barrier to flowering (Birks, 2015). Secondly, taphonomic issues can be discounted based on the presence of chironomid head capsules within the sediments, which are less structurally resistant than pollen grains, and abundant *Lycopodium* within the samples. Therefore, it is more likely that the absence of pollen indicates that there was limited or no catchment vegetation surrounding Quoyloo Meadow during the earliest Interstadial, which prohibited landscape stabilisation. Bunting (1994) encountered a similar scenario at Quoyloo Meadow providing greater evidence to the assertion of a lack of vegetation. Erosivity and minerogenic sedimentation are thought related to the strong wind action on Orkney in an unvegetated landscape (Bunting, 1994). However, this could be related to a combination of enhanced snow-melt and greater seasonality with colder winter temperatures increasing the effect of periglacial activity. The latter cannot be quantified at this stage; however, it is probable that greater snow-melt occurred during the earliest WI under warm conditions. Therefore, a combination of strong wind regimes and enhanced snow-melt likely caused continued minerogenic sedimentation during warm climates of the WI.

Climatic warmth continued throughout the early WI (unit 1b) with summer temperatures ranging between 10.64°C to 12.63°C. Open tundra grassland communities developed in the catchment after 14.30±0.33 Cal. ka BP (QMP-1), dominated by Poaceae, *Rumex, Salix*, Cyperaceae, *Artemisia*, Compositae: Lactuceae with some occurrence of

Caryophyllaceae and Saxifragaceae. This grassland community reflects the colonisation of substrates by pioneering taxa (positive values on the PCA; Figure 5.5) with increased LOI revealing either greater organic input and/or enhanced lake productivity. Low pollen concentrations suggest the vegetation coverage was sparse and silt and clay sedimentation indicates that landscape erosion and instability continued throughout the early WI leading to high sedimentation rates within the basin. Constant in-washing of sediments likely led to increased nutrient supply to the lake and algal blooming, as inferred from high *Pediastrum* abundances (Weckström et al., 2010).

It is certain that, as other records attributed to the WI, *Pinus* is reflective of long-distance transport (e.g. Birks et al., 2005; Paus, 2010; Whittington et al., 2015). Low concentrations reveal the lack of pine present on Orkney despite the elevated percentages recorded at Quoyloo (19 %). Elevated percentages of far-travelled components have been shown by Birks et al. (2005) to result from low local pollen production, which is confirmed during the early Interstadial on Orkney by the lack of vegetation. The same scenario may be true for *Betula* undiff (Birks et al., 2005). However, the relative contribution of *B. nana* to the pollen spectrum cannot be overlooked, suggesting that *B. nana* may have grown locally 14.30±0.33 Cal. ka BP, although this is unconfirmed without macro-fossil evidence (Birks and Birks, 2000).

Early Windermere Interstadial- 14.05±0.07 – 13.89±0.21 Cal. ka BP

Whilst C-ITs were relatively high during the earliest WI (unit 1b), the subsequent phase reveals a short-lived climatic event. Between 14.05±0.07 and 13.89±0.21 Cal. ka BP summer temperatures declined by 1.86°C (12.5-10.64°C). Whilst this decline is fairly small, it is outside of the predictive error of the technique (Chapter 4) and can be considered as an event. Further, the Borrobol and Penifiler Tephras bracket this event, which has been noted from other locales in Britain (e.g. Matthews et al., 2011; Candy et al., 2016). Specifically, the Penifiler Tephra is frequently identified in association with amelioration following an early WI climatic event (Matthews et al., 2011). On this basis, the C-IT oscillation can be attributed to an early Interstadial climatic event.

Prior to the early WI summer temperature decline, open habitat vegetation continued to dominate (QMP-2), with increases in *Betula* pollen, alongside decreases in *Rumex* suggesting a greater colonisation of *B. nana*. This coincided with a general reduction in *Pediastrum*, indicating a slowing of erosive input into the Quoyloo basin. Nevertheless, coeval with the climatic event, a reversion towards higher values in the PC is observed (Oscillation one; Figure 5.10; 5.11). Through this phase, small increases are observed in *Pediastrum*, Poaceae, Cyperaceae, *Rumex*, *Artemisia*, Compositae: Lactuceae and

Caryophyllaceae, perhaps suggesting increased populations of open ground vegetation revealing greater landscape instability. These small increases in the above taxa are taken to reflect a short palynologically-inferred vegetative revertence during the early WI. Of these taxa, Poaceae, *Rumex*, *Artemisia* and *Pediastrum* all show increased proportional abundance within the individual taxa response curves (Figure 5.6) suggesting that these taxa are driving the PC in response to the observed summer cooling. There is no evidence of fire throughout this climatic event as the peak falls below the demarked line (Figure 5.10). Whilst a palynologically inferred vegetation revertence is suggested, the magnitudes of change are likely small owing to the open nature of vegetation throughout the early WI. As both evidence of climatic driver and palynological response is noted, more confidence in identifying this event is gained.

Mid-late interstadial- 13.89±0.21 – 13.12±0.58 Cal. ka BP

The remainder of the Interstadial was characterised by warm summer temperatures (12.04-12.63°C) with biomarker δ*D* suggesting a relatively wet climate based on the substantial difference between δD_{aq} and δD_{terr} (Chapter 4). As δD_{aq} values sit above δD_{terr} and as the two indices track each other, the same moisture source affected both end-members, with negligible isotopic enrichment in δD_{terr}. Therefore, moist and humid conditions are suggested towards the mid-late WI (QMD-a). These climatological conditions were favourable for a significant phase of vegetation development surrounding Quoyloo Meadow (QMP-3). Initially reductions in *Betula* pollen are noted with increases in *Empetrum nigrum*. This change is mirrored by concomitant increases in the LOI profile. It is supposed that increased *E*. *nigrum* pollen reflects colonisation and proliferation of heathland at Quoyloo, reflective of the relatively moist conditions (Bell and Tallis, 1973) as revealed by biomarker δ*D*. The spread of heathland may also reflect the development of increasingly mature, well drained, albeit base poor soils (Birks, 1970). Continued presence of Poaceae and Cyperaceae suggest incomplete heathland coverage with *Betula* and *Salix* indicating areas of dwarf-shrub heath.

The importance of *Empetrum* at Quoyloo Meadow should not be overlooked. Its occurrence following an early WI climatic event is important as heathland spread is common during the mid-Interstadial in Scotland (e.g. Pennington et al., 1972; Walker and Lowe, 1986). The spread of heathland provides further evidence of the rapidly accumulating sediments of the early Interstadial and the later positions of the Borrobol and Penifler Tephra. However, this has implications for the remainder of the sequence, suggesting that the basin at Quoyloo during the late WI was characterised by very low sedimentation rates, leading to a compressed latter part of the record. Given the small catchment and low relief surrounding Quoyloo Meadow, once vegetation had stabilised

the landscape, it may have starved the delivery of sediments to the basin. Whilst clastic sediments reduced, organic loading and autochthonous lacustrine productivity increased as shown by the large increase in LOI. Therefore, the late Interstadial record is highly compressed at Quoyloo Meadow.

Loch Lomond Stadial- 13.12±0.58 – 11.54±0.24 Cal. ka BP

Sedimentation during the LLS (units 2a to c) was dominated by silt and clay, caused by increased erosion from the catchment, and cessation of organic input, shown by reduced LOI values. At the same time as the sedimentological change, mean July temperatures fell abruptly by 7.04°C to 5.05°C. This shift in summer temperature is comparable to other sequences presented in this thesis, and other high latitude sequences in Britain (Brooks et al., 2012; Brooks et al., 2016) although absolute values are colder, likely relating to the northerly latitude of the sequence (e.g. Birks et al., 2014) and proximity to the Atlantic where southwardly migrating sea-ice may have a cooling effect (Renssen and Isarin, 1998).

At the onset of the LLS the vegetation changed markedly (QMP-3) and large compositional turnover occurred (as inferred from the PC and RoC (Figure 5.10; 5.11)). *Pediastrum* became more abundant thought to reflect landscape erosion and the input of nutrient-rich soils from the WI (Weckström et al., 2010) likely through mass wasting processes under severely cold climates. At the same time cover of woody vegetation declined, namely *Empetrum* and *Betula*, and *Selaginella selaginoides*, Saxifragaceae, Cyperaceae, Caryophyllaceae and *Salix* populations increased. These changes suggest the loss of widespread heath and expansion of open grassland at the onset of the LLS. The presence of taxa that can survive on disturbed and unstable soils (Caryophyllaceae and *Salix*), and the appearance of *S. selaginoides* reflects a cold climate vegetation assemblage (Heusser and Igarashi, 1994). The increase in *Salix*, coincident with cold reconstructed temperatures points to the incidence of late snow lie or exposed landscapes (Wijk, 1986; Beerling, 1993). The lingering presence of *Empetrum* supports the occurrence of late-snow lie, with moisture and protection derived from continued snow presence. During this phase, macro-charcoal values increased (QMC-2), reflecting the breakdown in the community and increased fuel source on the landscape.

After 12.73±0.56 Cal. ka BP (QMP-4) the landscape was dominated by *Artemisia,* alongside Poaceae, Cyperaceae, Caryophyllaceae, *Rumex* and Saxifragaceae. The addition of *Artemisia* and *Rumex* suggests the establishment of a tundra/steppe community following the onset of the LLS. However, a vegetational change, bracketed by this tundra community, is noted between 12.21±0.34 and 11.96±0.15 Cal. ka BP

which coincides with a 3.38°C increase in summer temperature, between 5.63 and 9.61°C. Over this phase δD_{aq} and δD_{terr} enrichment of 24.72 ‰ (-145.26 to 120.55 ‰) and 17.6 ‰ (-158.66 to 141.06 ‰) is observed. This is succeeded by δD_{aq} enrichment (11.12 ‰ between -120.55 and 109.42 ‰; QMD-b) at 11.83±0.23 Cal. ka BP. Here, reductions in xerophytic taxa, *Artemisia* and *Rumex*, are noted with increased *Pinus* and *Empetrum*. It may be possible that a mid-LLS climatic amelioration favoured a return to a heathland environment. Whilst high percentages of *Pinus* may point to the emergence of pine at Quoyloo Meadow during the LLS, it is highly unlikely. No evidence suggests that *Pinus* was a landscape component during the LLS in Britain, further its presence in Scandinavia has been called into question (e.g. Birks et al., 2005). Under a stadial climatic regime with exacerbated climatic conditions (e.g. Brauer et al., 2008) the increase in a far travelled component may reveal greater apparent dominance over low pollen producing local herbaceous plant types (Birks and Birks, 2000). Low concentrations of pollen are favourable to this explanation.

Observed biomarker δD (QMD-b) enrichment during the LLS is difficult to comprehend as it is unexpected that values would be more enriched than during the WI. To explain this the following scenarios are presented: 1) increased enrichment through evaporitic modification of the lake and leaf/soil water; 2) a moisture source shift with enriched δD_{precip} affecting both the lacustrine and terrestrial environments; and 3) the mid-LLS at Quoyloo was characterised by wetter conditions. Evaporitic effects can be discounted due to secondary enrichment observed in the aquatic over terrestrial end-members. Regarding scenario two, the presence of sea-ice might be a barrier to a moisture source shift during the LLS (Isarin et al., 1998). However, with increased summer temperatures, as recorded by chironomids, it is possible that seasonal sea ice break-up (e.g. Birks et al., 2015) allowed a mechanism where a localised moisture source could affect biomarker δD values. An enriched moisture source is possible with altered atmospheric configurations during the Stadial, through both weakened AMOC (Broecker et al., 1989; Condron and Windsor, 2012) and atmospheric blocking from large ice-sheets (Schenk et al., 2018). It may therefore be feasible that the interplay of different wind regimes (westerlies vs easterlies following the southward migration of the Atlantic Westerly Jet (Isarin et al., 1998; Bakke et al., 2009)) impact moisture delivery to Quoyloo under reduced sea-ice conditions. Moreover, it may be possible that biomarker enrichment and thermal increases did cause locally wet conditions during the mid-Stadial, following the northwards migration of the polar front with sea-ice break up (Bakke et al., 2009). These theories require further testing to understand hydrological change throughout the Stadial. Nevertheless, as the climatic and vegetations changes are co-occurring, a causal link is probable.

Early Holocene- 11.54±0.24 – 10.75±0.12 Cal. ka BP

Carbonate sedimentation characterised the Quoyloo Meadow basin during the early Holocene (EH) (units 3 to 5). Rising $CaCO_3$ values suggest climatic amelioration as the processes concerning calcium and bicarbonate supersaturation and precipitation are temperature dependent (Kelts and Hsu, 1978). Climatic amelioration in the EH is confirmed by rising C-ITs, between 8.54 and 12.31°C and moderate $\delta^{18}O_{carb}$ values. Following enrichment of biomarker δD values during the LLS, a return to depleted values are observed at 11.33±0.18 Cal. ka BP (192.5 cm). This depletion appears counter intuitive, however, following the strengthening AMOC, following sea-ice regression, and removal of blocking effects from the ice sheets (Schenk et al., 2018) under climatic warmth; atmospheric configurations were likely to revert to pre-Stadial modes. Hence similar values compared to the WI.

Climatic amelioration during the EH is clearly recorded in the vegetation (QMP-5). Initially increased *Pediastrum* reflects the erosion of soils under low vegetation densities. Subsequent expansions of *Rumex* and *Salix* demonstrate the re-colonisation of the Quoyloo catchment by pioneering taxa following the loss of the Arctic tundra assemblage from the LLS (Lowe and Walker, 1986). The expansion of *Salix* in this instance points to areas of exposed ground in the catchment (Beerling, 1993). Between 10.95±0.18 and 10.75±0.12 Cal. ka BP (QMP-6) *Empetrum* and *Betula* expansion reflects accelerated soil development, with major increases in concentration, suggesting the establishment of an extensive dwarf-shrub heathland. Extensive heathland coverage also registers with greater LOI percentages (Figure 5.2), suggesting organic allochthonous input at this time. Initially, during the EH, the occurrence of *Betula* is thought to be *B*. *nana*. Local tree birch may have been present; however, owing to the expansion of shade intolerant *Empetrum* (Bell and Tallis, 1973) widespread tree birch colonisation was unlikely. Thus, the establishment of this dwarf-shrub heathland during the EH shared similarities with the mid-WI vegetation assemblage.

Between 11.42±0.17 - 11.11±0.23 Cal. ka BP and 10.91±0.16 - 10.8±0.08 Cal. ka BP two subtle depletions are observed in $\delta^{18}O_{carb}$ values (QMO-1; QMO-2) with a depletion of 0.07 ‰ (from -4.11 to 4.18 ‰), and 0.23 ‰ (from 3.90 to 4.13 ‰) respectively. These subtle depletions are within the uncertainty of measured changes within the entire record, however, a significant depletion in δD_{aq} and δD_{terr} (QMD-c) is observed which exhibits a minor return to enriched values mid-oscillation suggesting commonality with $\delta^{18}O_{carb}$. Total δD_{aq} depletion of 35.87 ‰ (from -137.2 to 173.07 ‰), and δD_{terr} depletion of -25.88 ‰ (from -156.19 to 182.07 ‰) with end-member convergence suggests greater aridity

as the magnitude of δD_{terr} depletion is less than δD_{aq}. An increase in evapotranspiration (ETA) under low atmospheric humidity may lead to greater evaporative enrichment of leaf waters hence the suggestion of aridity. Through this phase, no variability is observed within C-ITs. Therefore, two events are suggested between these two phases with no summer temperature correlatives and minor mean annual change (Chapter 4) however, significant aridity between these two events is suggested.

To enable a mechanism for negligible temperature decline over this period but depletion and aridity in biomarker δD, these changes must be occurring over the growing season. It is postulated that snow melt from winter precipitation could deplete both δD and $\delta^{18}O_{carb}$, equally permafrost melt could have the same effect, alongside depleted North Atlantic waters. However, the first notions are discarded owing to the lack of change in C-ITs, which may be expected through snow and permafrost melt as the influx of cold meltwater would alter species assemblages (e.g. Brooks et al., 2012). Therefore, it is suggested that continual meltwater flux into the North Atlantic following climatic amelioration during the EH, may cool annual temperatures which would also deplete source waters. However, this does not explain identified aridity. One possibility is that a regional cooling during these events (Andresen et al., 2007; Fiłoc et al., 2018) enabled a short-lived period of seasonal sea-ice expansion which continued into the spring. This sea-ice may impact atmospheric configurations during the EH bringing aridity to Orkney following a small southerly migration of the storm track (e.g. Isarin et al., 1998). It is therefore proposed that a combination of isotopically light meltwater influx and sea-ice expansion causes the shifts in biomarker δD and minor effects on isotopic records.

Between 11.42±0.17 - 11.11±0.23 Cal. ka BP, vegetation shows no change, largely a result of the low-lying herbaceous vegetation community present during the EH. However, between 10.95±0.18 - 10.8±0.08 Cal. ka BP a pause is observed in the PC curve (Revertence 2; Figure 5.10; 5.11). It is possible that the PC is identifying small increases in *Pediastrum* and *Pinus* with single sample decreases in *Empetrum* and *Betula*. As woody taxa reductions are confined to single samples; it is difficult to acknowledge the event as a vegetative revertence; nonetheless it is suggested as multiple spectra show variability aligned with palaeoclimatic change (Chapter 4). Further, a charcoal component (QMCc-2; QMC-4) can be observed within the record. The data suggests that, following heathland establishment, small variability in mean annual temperatures and increased aridity may cause greater heathland stress (Bell and Tallis, 1973). Potential drought stress on *Empetrum* heath, increased the fuel source on the landscape leading to local fires. Therefore, whilst no revertence is identified for the first climatic event, the second event reveals a change in landscape conditions.

Early Holocene- 10.75±0.12 – 9.11±0.59 Cal. ka BP

The remainder of the EH at Quoyloo Meadow reveals mean annual warmth through enriched $\delta^{18}O_{carb}$ and biomarker δD values. Like mean annual warmth, elevated C-ITs (between 10.31 and 13.85°C), confirms warm summer temperatures over this period. Where available, enriched values for δD_{aq} and $\delta D_{terr,}$ between 10.75±0.12 and 10.67±0.14 Cal. ka BP, with greater enrichment observed within δD_{aq} depicts a relatively wet climate phase akin to pre-LLS conditions (QMD-d). Rapid enrichment in biomarker δD perhaps reflects the brief cessation of meltwater flux, or the release of heavier isotopes values from sea-ice form the previous phase.

Despite recorded high temperatures, the vegetation dynamic follows a different path to other sequences in Scotland during the early Holocene after 10.75±0.12 Cal. ka BP (QMP-7:11). Reduced populations of dwarf-shrub heathland taxa, *Empetrum* and *Betula*, were favoured by an expansion of Poaceae alongside Cyperaceae, *Filipendula* and the pteridophytes *Dryopteris* and Filicales. These taxa indicate that a tall herbaceous grassland community proliferated at this time, indicative of landscape stability. This is confirmed by the PCA (Figure 5.5) and the disassociation of Poaceae with Arctic/alpine taxa encountered during the LLS. Throughout the grassland phase localised pockets of dwarf-shrub heathland existed, which likely included *Corylus* unimpeded by *Betula*. After 9.73±0.11 Cal. ka BP (QMP-11) *Corylus* emerged in the landscape, which, alongside greater incidences of *Betula* and reduced Poaceae, suggests the beginnings of woodland establishment. The lack of birch woodland prior to phase likely stems from migratory lags to an island location (Birks, 1989) or the out-competing of birch by Poaceae in an environment with strong wind sheer (Bunting, 1996). *Filipendula*, *Salix*, Filicales and *Dryopteris* presence on the landscape in conjunction with woodland development suggest areas of moist well-developed soils in tree clearings.

Superimposed on this general EH sequence; two climatic events may be recorded within C-ITs and multiple within the stable isotopic record (Figure 5.10; 5.11). A small summer temperature decline of 0.58°C (from 13.26 to 12.68°C) at 10.54±0.16 Cal. ka BP appears to have no isotopic comparative. As the decline is within the predictive error of the C-IT technique it is not prudent to classify this minor summer deterioration as an event. Nevertheless, occurring alongside this is a slight inflection in the PC and increase in RoC (Oscillation 3; Figure 5.10; 5.11). Increases in *Pinus* and *Rumex* with a decrease in *Empetrum* may suggest a brief expansion of unstable ground taxa (Walker, 1975) and therefore a revertence. However as both occur for one sample, it is currently difficult to ascertain whether these small changes are indeed a palaeoclimatic event and vegetation

revertence at Quoyloo Meadow or relate to natural variability. Interestingly for 100 years following lower summer temperatures, mean annual shifts are noted between ca 10.5 and 10.4 Cal. ka BP (-0.37 ‰ from -3.14 to -3.51 ‰; QMO-3). However, a small inflection is noted on the PC (Oscillation 4; Figure 5.10; 5.11). Like the suggested phase at 10.54±0.16 Cal. ka BP however, caution is required and formal event/revertence attribution is not given. The same scenario is postulated for a depletion at 10.33±0.12 Cal. ka BP (-0.22 ‰; QMO-4). As before this bears no resemblance to summer temperature change. Whilst small reversions are noted in the PC, these appear to be driven by *Pinus*. As only one taxon is being affected, no vegetation revertence is suggested. Therefore, variability during the Holocene is common at Quoyloo Meadow, however, no high-magnitude climatic or vegetation change is formally defined here between 10.80 and 10.3 Cal. ka BP.

Despite uncertainly with the above climatic events, one clear climatic deterioration is recorded during the EH at Quoyloo Meadow. Between 10.21±0.04 and 10.18±0.5 Cal. ka BP a depletion of -0.52 ‰ (from -2.93 to -3.44 ‰; QMO-5) which coincides with a 2.8°C cooling in summer temperature suggests significant mean annual and summer temperature variability. Based on the positioning of these oscillations, following the deposition of the visible Saksunarvatn Ash (QM1 160), two theories may explain the occurrence of these events; 1) changes in the climatic proxies reflect true climatic shifts; and 2) lacustrine volcanic ash loading has an impact on the biological and chemical proxies employed in this research. Evidence for both scenarios exist, with glacial readvance in the North Atlantic linked to reduced solar forcing at 10.30 Cal. BP (Björk et al., 2001; Dahl et al., 2002) (close to the Saksunarvatn Ash) and studies demonstrating the effects of tephra in influencing the chemistry of the water column; impacting biological lacustrine components (e.g. Urrutia et al., 2007). Considering the identification of 'Erdalen' events across the northern hemisphere at 10.30 Cal. ka BP (Björk et al., 2001; Dahl et al., 2002) and the concurrent multi-proxy change at this time it is perhaps more likely that this is a climatic event at Quoyloo Meadow.

Occurring alongside these shifts in climatic proxies are changes in the vegetation assemblage, and variability in the PC (Oscillation 5; Figure 5.10; 5.11). Broadly coeval with changes in climate are expansions in Poaceae, *Rumex* and *Pinus* with reduced *Empetrum*. Regardless of the cause of this shift, heathland regression with greater open herbaceous grassland coverage during this phase suggests a landscape change. Although a stable grassland community exists prior to the revertence, increased *Rumex* occurrence is indicative of greater landscape instability. With this vegetation change shift, fire seems to be an important component of the landscape (QMC-5). As other climatic

events, fire appears to be important following the modification of vegetation. Thus, fire incidence is a response to climatic change and change in the structure of the fuel source.

5.7 Chapter summary

This chapter summarises the litho-, palyno- and climatostratigraphic findings from Quoyloo Meadow, Orkney. All available data, including chronological information imported form Timms et al. (2017) demonstrate an LGIT attribution for the Quoyloo Meadow sequence.

The Windermere Interstadial at Quoyloo Meadow is defined by warm summer temperatures and following the establishment of vegetation, a transition from open pioneering grassland to a heathland dominated landscape. Continued minerogenic sedimentation at this time demonstrates continued landscape instability. The transition into the Loch Lomond Stadial is shown by a rapid decline in summer temperatures to absolute minima of ca 5°C. Coinciding with this temperature decline is a contraction of heathland and an expansion of an Arctic tundra vegetation assemblage. The transition into the early Holocene is revealed by warm summer and mean annual temperatures and the establishment of a stable, species-rich grassland. Woodland establishment is suggested later in the Holocene with the expansion of *Betula* and *Corylus*.

For the duration of the record, $\delta^{18}O_{carb}$, biomarker δD and C-ITs reveal a number of small-scale changes. During the Interstadial a summer temperature decline appears alongside increased open vegetation. However, mid-Stadial, a brief amelioration is noted, which may suggest a phase of increased moisture availability following the seasonal break up of sea-ice. This then leads to a brief contraction of *Artemisia*. However, during the Holocene, a number of these climatic events are observed, which often show a decline in mean annual and summer temperatures alongside greater aridity, again believed to be a product of changes in the North Atlantic. The affect this has on vegetation is minimal however although brief regressive phases are noted with slight increases in open/disturbed ground taxa. The highest magnitude climatic event throughout the record appears at 10.2-10.3 Cal ka BP which appears following the deposition of the Saksunarvatn Ash. Therefore, whilst events are noted at Quoyloo Meadow, their expression on the landscape is minimal. This is in stark contrast to the results from the rest of this thesis.

Chapter 6. Results from Tirinie

Tirinie is a former lake basin residing within the south-east Grampian Highlands, Scotland. Other than Orkney, Tirinie serves as one of few examples of a high-latitude site with carbonate sedimentation which can be used to test for abrupt climatic events. Furthermore, being at a relatively high-altitude for Britain, 323 m a.s.l, Tirinie offers a rare opportunity to demonstrate whether high-altitude sites reveal greater sensitivity in both palaeoclimatic expression and vegetation response to abrupt events.

The Tirinie palaeobasin has previously been the subject of a palynological investigation as part of a wider research aim (e.g. Lowe and Walker, 1977). This aim differed to that of the present study, whereby sites were analysed to detect both tripartite sedimentation and Late-Glacial pollen spectra to better constrain the limits of the Loch Lomond Stadial (LLS) ice-cap (e.g. Walker and Lowe, 2017; Chapter 3 Section 3.3.2). Lowe and Walker (1977) demonstrated a clear pollen spectrum of LGIT age, with open herbaceous pollen taxa being successively replaced by a low lying *Juniperus* and *Empetrum* heath then *Betula*. The following stages show a shift to disturbed ground and Arctic/alpine communities (e.g. *Artemisia*, *Rumex*, Poaceae) before *Betula* and *Corylus* woodland during the earliest Holocene. Notably, during the Interstadial, cyclicity was observed within the disturbed ground taxa; although this was not explored in more detail.

Furthermore, recent retrieval of sedimentary material, allied with the acquisition of new palaeoclimatic data, has suggested that high-magnitude climatic events can be observed at Tirinie during the Windermere Interstadial (Candy et al., 2016). This therefore permits a re-evaluation of the site to better understand palaeoclimatic and environmental development at high-altitudes in Britain. All data presented can be found in Appendix C.

6.1 Basin sedimentology and stratigraphy

The Tirinie palaeobasin was sampled in the spring of 2012 by members of the Centre for Quaternary Research, Royal Holloway, University of London and during spring 2017 by the author of this thesis. The site was previously assessed to reveal the bathymetry of the basin (Figure 6.1). For the purposes of this research, and for brevity, sediment cores were not retrieved from the deepest area of the basin, rather sediments were extracted towards the western limits of the basin (56.787500, -3.815319) where oscillations in carbonate sediments were previously noted.

Sediment cores from the Tirinie site are presented in Figure 6.2. Assumed climatostratigraphic zones are presented on the figure where changes in lithostratigraphy are observed (Lowe and Walker, 1977).

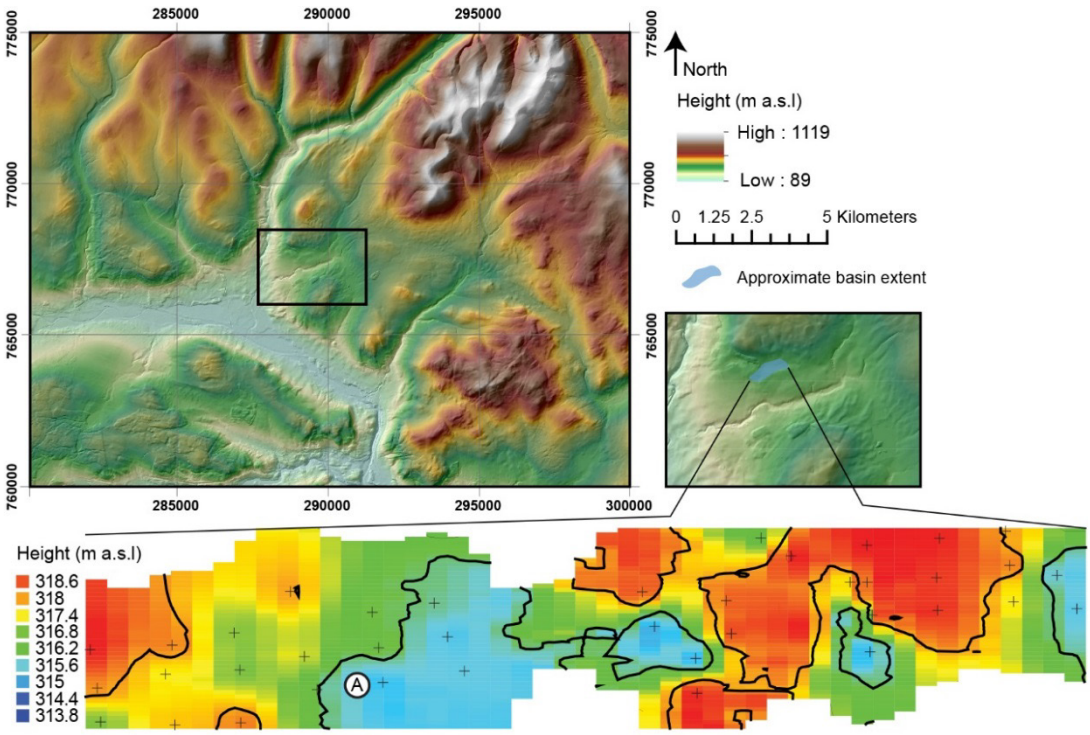

Figure 6.1 A) Digital elevation model of the Tirinie palaeobasin and surrounding highlands. Shown is the approximate extent of the basin and a bathymetric map of the site. The coring location is marked with the letter A.

A composite sedimentological profile was created using key marker horizons and patterns in bulk sedimentology. The composite profile represents the most complete and stratigraphically expanded carbonate sequence from the Tirinie basin. The composite profile exhibits a 355 cm classically tripartite sediment sequence (Walker and Lowe, 2017). Minerogenic sediments are overlain by organic carbonate rich sediments which are further overlain by successive phases of minerogenic and carbonate sedimentation.

Table 6.1 and Figure 6.3 reveal the stratigraphy of the composite profile. The basal unit within the profile, unit 1, is characterised by clay rich sediments with increasing carbonate, 14 to 44 %, and small decreases in TOC, from 9 to 7 %. Subsequently, unit 2 shows changes within the sedimentary make-up as sub unit 2a is characterised as a silty marl where $CaCO_3$ values fall to 25 %. In contrast, unit 2b is characterised by a return to minerogenic, clay dominated sediments and low $CaCO_3$ values, 15 to 13 %.

Unit 3 is characterised by carbonate sedimentation. High $CaCO_3$ percentages, between 70 and 90 %, and low TOC, 4 to 7 %, typify this phase. Within units 4a to 4d marl sediments are replaced with, clay/silt (4a), marl (4b), clay/silt (4c) and silty clay gyttja (4d) with oscillations in carbonate content; troughs of 52 % and 16 % separated by a peak of 90 %. Increased TOC values are noted throughout these sub-units, between 7 and 15 %. Unit 5 represents a shift to marl sedimentation with high $CaCO_3$, 71-84 %.

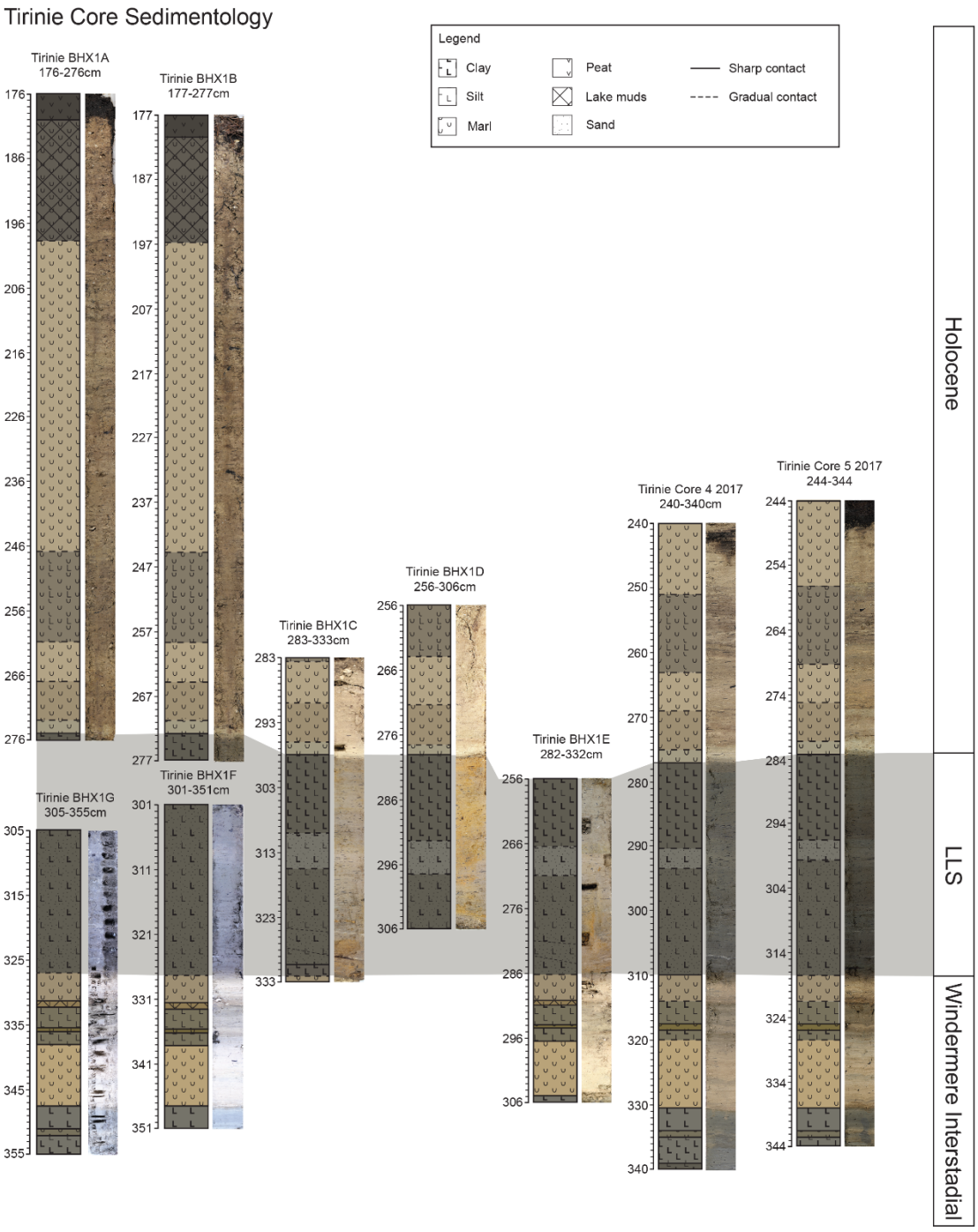

Figure 6.2 Tirinie basin sediment stratigraphy. The sequence presented here is a combination of all sediment cores extracted for this research. The sediment cores presented here demonstrate changes within the sedimentology of the Tirinie basin with all cores collected from proximal locations but displaying markedly different depths. All analysed cores that penetrate the central minerogenic sediment bands detail complex sedimentological characteristics. Cores 4 and 5 2017 were collected for the purposes of chronological control. Broad climatostratigraphic zones have been shown here to assist in visualising the sequence

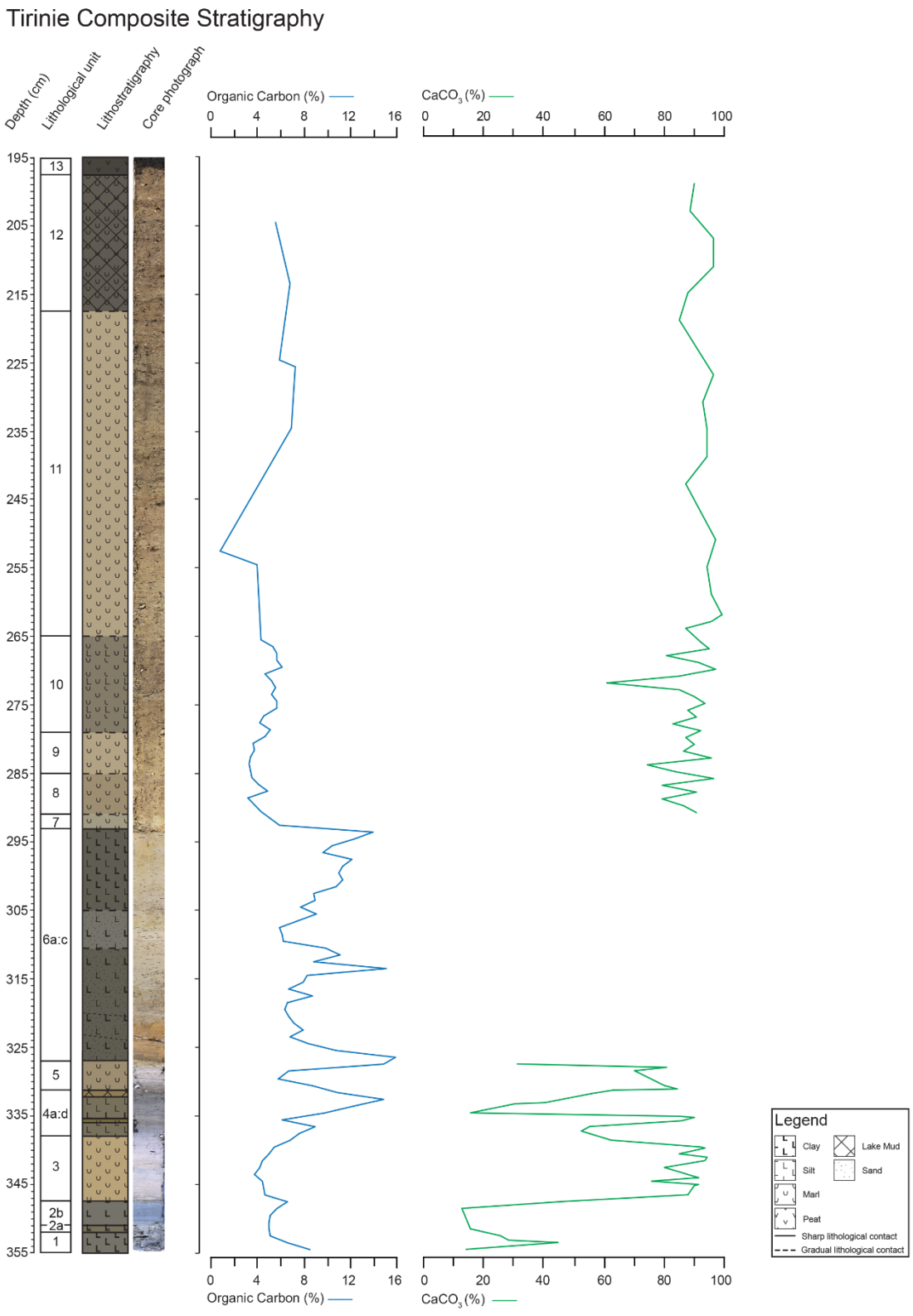

Figure 6.3 The composite stratigraphy for Tirinie BHX1 using four overlapping cores presented in Figure 6.2. Total organic carbon and calcimetry values are shown to highlight the different phases within the Tirinie composite profile. The lack of calcimetry data within the central minerogenic units relate to the lack of carbonate identified throughout this zone. The upper sections of the diagram with fewer sample points demonstrate a coarser resolution.

Table 6.1 General lithological units at Tirinie including the major sedimentological units/sub-units, their descriptors, classification and Munsell colour.

Unit	Depth (cm)	Troels-Smith	Classification	Munsell colour
13	197.5-194	Th4, Dg+	Peat	10YR 2.5/2 Very Dark Brown
12	217.5-197.5	$Lc^4$2, $Ld^4$1, As1, Dg+	Gyttjaeous Marl	10YR 3/2 Very Dark Greyish Brown
11	265-217.5	Lc4, Ag+, As+, Dg+	Marl	2.5Y 6/3 Light Yellowish Brown
10	279-265	Lc 3, Ag1, Dg+	Silty Marl	2.5Y 4/2 Dark Greyish Brown
9	285-279	$Lc^4$4, As+, Dg+	Marl	2.5Y 6/3 Light Yellowish Brown
8	291-285	$Lc^4$4, As+, Dg+	Marl	2.5Y 5/3 Light Olive Brown
7	293-291	$Lc^4$4, Ag+, Dg+	Marl	5Y 6/2 Light Olive Grey
6c	305-293	As3, Ag1, Dg+	Silty Clay	5Y 3/1 Very Dark Grey
6b	310.5-305	Ag2, As1, Ga1, Dg+	Clayey Sandy Silt	5Y 4/1 Dark Grey
6a	327-310.5	Ag2, As1, Ga1, Dg+	Clayey Sandy Silt	5Y 3/1 Very Dark Grey
5	331.1-327	$Lc^4$4, Dg+	Marl	2.5Y 5/3 Light Olive Brown
4d	332.2-331.1	Ld2, Ag1, Ag1, Lc4+, Dg+	Silty Clayey Gyttja	2.5Y 4/4 Olive Brown
4c	335.2-332.2	Ag3, As1, Dg+	Clayey Silt	5Y 4/1 Dark Grey
4b	336.2-335.2	$Lc^4$4, As+	Marl	5Y 4/4 Olive
4a	338-336.2	Ag3, As1, Dg+	Clayey Silt	5Y 4/1 Dark Grey
3	347.5-338	$Lc^4$4, As+, Dg+	Marl	2.5Y 6/3 Light Yellowish Brown
2b	351-347.5	As3, Ag1, Lc4+	Silty Clay	5Y 4/1 Dark Grey
2a	352-351	$Lc^4$2, Ag2, Dg+	Silty Marl	5Y 4/2 Olive Grey
1	355-352	As3, Ag1, Dg+	Silty Clay	5Y 4/1 Dark Grey

Units 6a to 6c are dominated by silts and clays. Units 6a and 6b exhibit coarser sediment fractions with fine sand, which is absent in unit 6c. Throughout, three peaks in TOC are observed at: 326.5 cm, 313.5 cm and 293.5 cm with values of 16 %, 15 % and 14 % respectively. Overlaying unit 6, units 7 to 12 are composed of marl with variable portions of silt (unit 10) and gyttja (unit 12). Nonetheless, $CaCO_3$ is high throughout, between 61 and 99 %. In general, the lowest values are observed within unit 10. Unit 13 is represented by a capping peat.

6.2 Palynological results

The Tirinie profile was analysed for pollen at variable resolutions. Sedimentological units 1 to 5, at contiguous 1 cm resolution, unit 6 at 4 cm resolution and between 1-4 cm for the remainder of the profile. High-resolution sampling was undertaken in areas where vegetation shifts were expected based on changes in sedimentology, leading to 113 pollen samples. Over certain areas of the profile 300 TLP pollen count sums could not be obtained due to low pollen concentrations. For these levels a minimum of 100 TLP was sought except for 320.5 cm where only 95 TLP grains were counted. Within units 6a to 6c the abundance of *Pediastrum* made identifications difficult, thus a 100 TLP sum was adopted. From the Tirinie profile 11 local pollen assemblage zones (TirP-*n*) have been identified based on changes in principal taxa with *Pediastrum* and *Equisetum* included. Figures 6.4 and 6.5 reveal the pollen profile, with zonation details presented in Table 6.2.

Zone TirP-1. Composite depth: 355-351 cm.

Cyperaceae, 27 %, and Poaceae, 23 %, dominate TirP-1. Both taxa increase at 353.5 cm before reducing to 21 % and 27 % respectively. Contrastingly, *Rumex* percentages are high in the basal sample, 11 %, then fluctuate for the remainder of the zone. Elevated percentages of *Empetrum* are reached at 351.5 cm, from 0 to 19 %. Additional taxa within this zone include *Betula*, *Pinus* and *Pediastrum*. The former contains stable percentages throughout whereas the latter show increased percentages at the base.

Pollen concentrations throughout TirP-1 are low. TLP concentrations demonstrate an increase from 4472 grains/cm^{-3} to 8254 grains/cm^{-3} at the top of the zone.

Zone TirP-2. Composite depth: 351-348 cm.

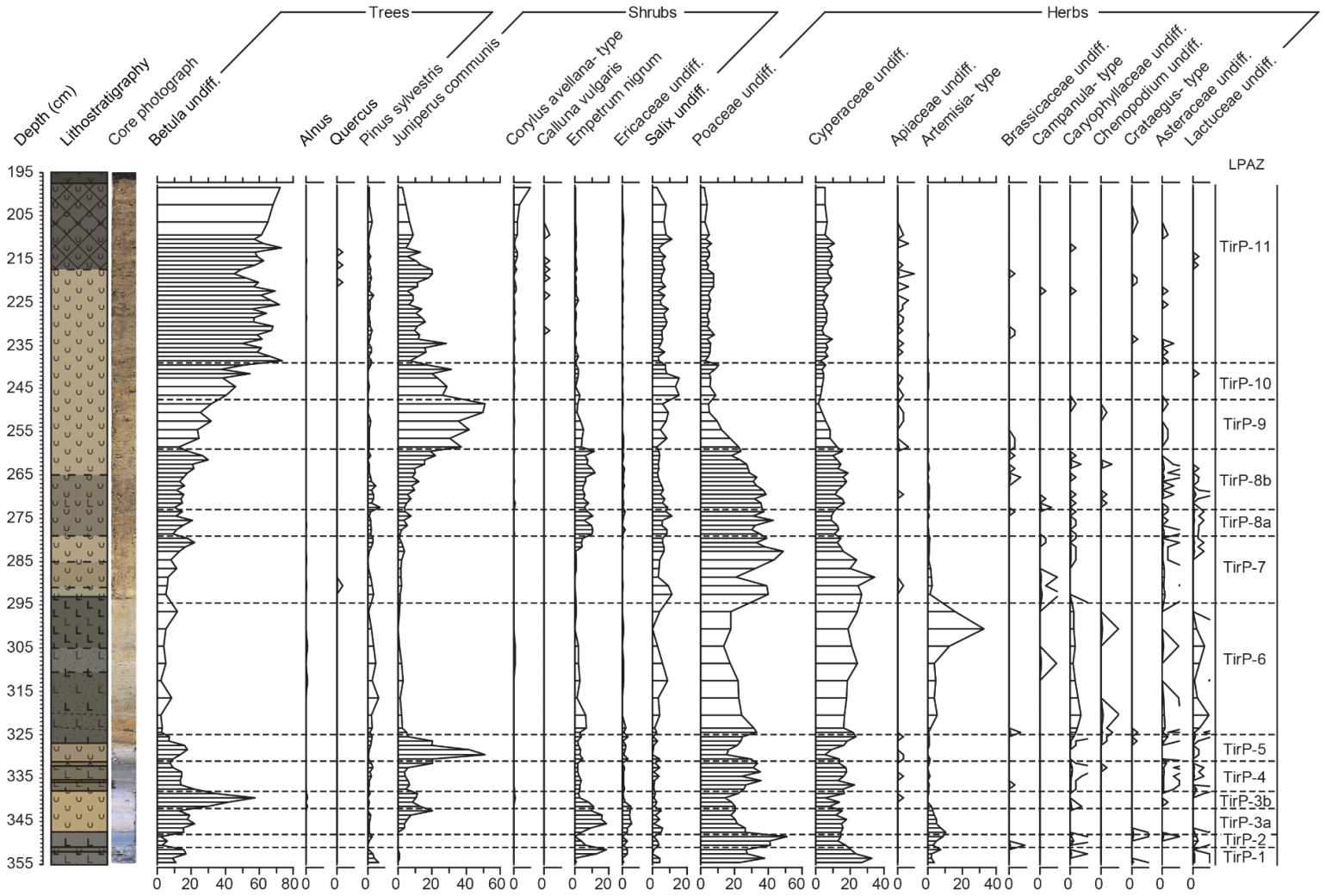

Figure 6.4 Pollen percentage profile from Tirinie. All values are presented as percentages of TLP.

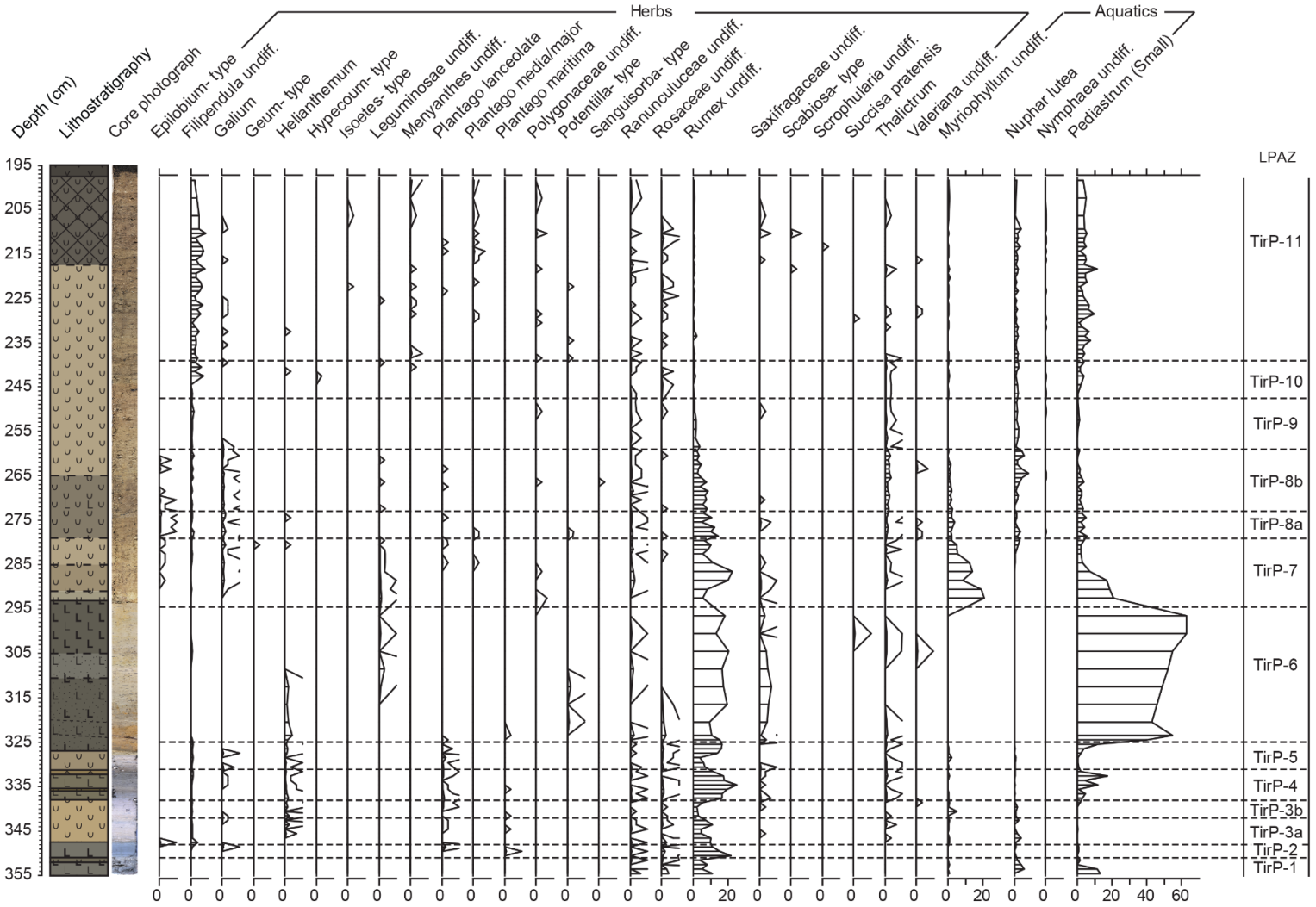

Figure 6.4 (Cont.) Pollen percentage profile of Tirinie. All values are presented as percentages of TLP and TLP + Aquatics

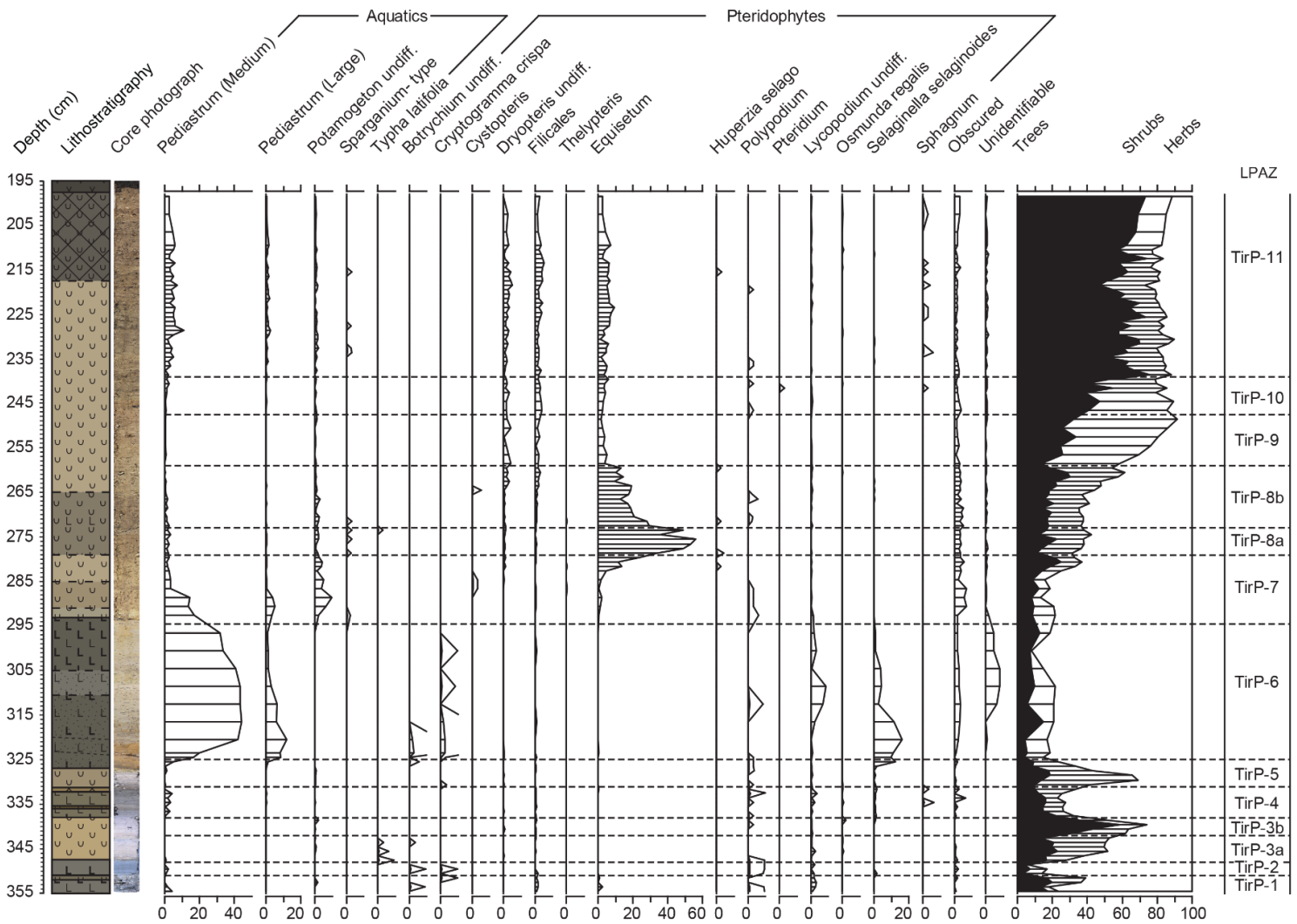

Figure 6.4 (Cont.) Pollen percentage profile of Tirinie. All values are presented as percentages of TLP + Aquatics and TLP + Pteridophytes.

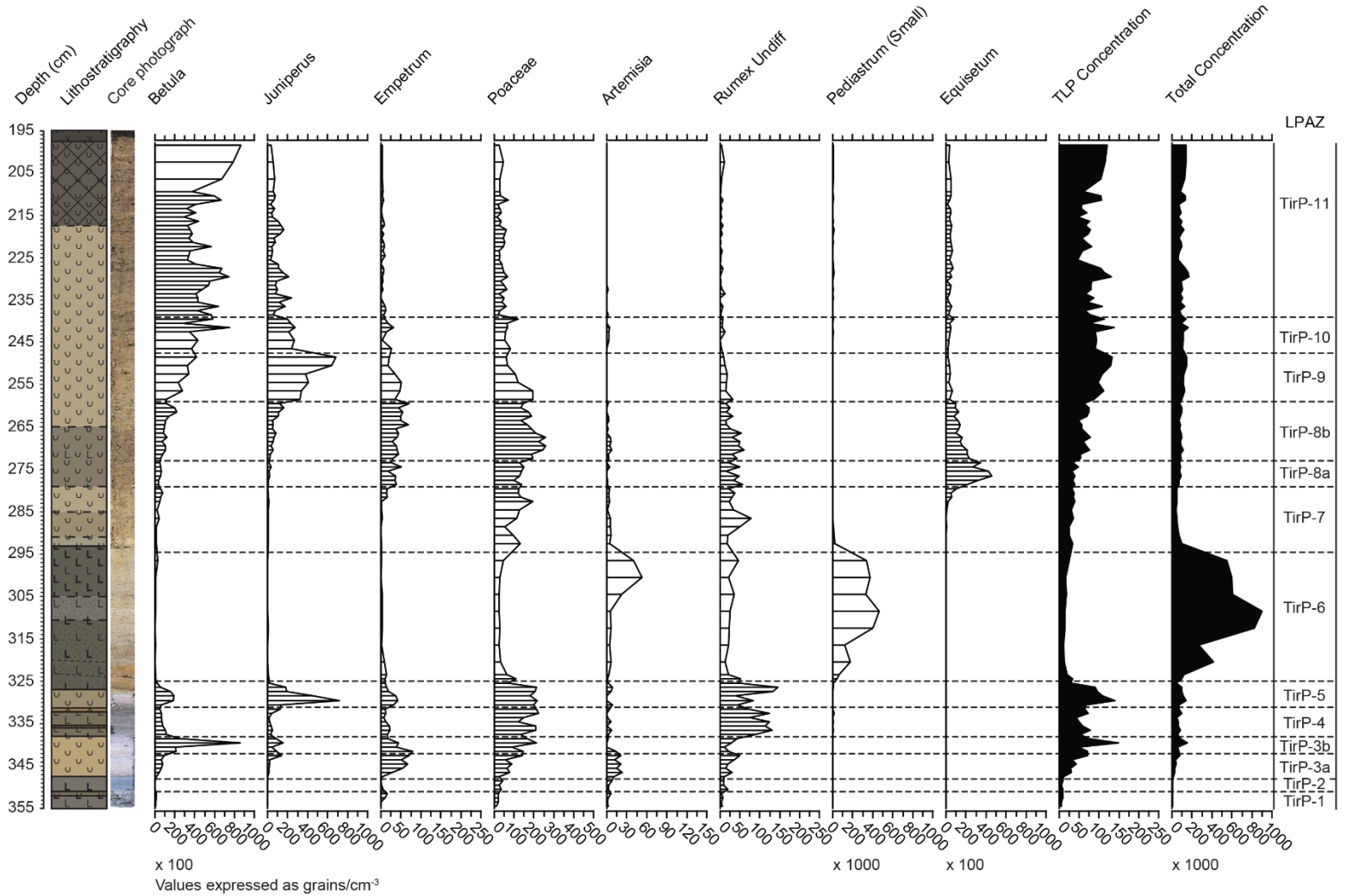

Figure 6.5 Summary pollen concentration data from Tirinie showing key pollen taxa. All concentration values multiplied by 100 unless stated.

Table 6.2 Tirinie pollen zone delineation and key information. The names of the zones are provided alongside the composite depth and the key taxa observed within each zone.

LPAZ	Composite Depth (cm)	Key Taxa
TirP-11	239-198	*Betula*
TirP-10	247.5-239	*Betula, Juniperus*
TirP-9	259-247.5	*Juniperus, Betula*
TirP-8b	273-259	*Equisetum*, Poaceae, Cyperaceae
TirP-8a	279-273	*Equisetum, Poaceae, Rumex*
TirP-7	294.5-279	Poaceae, Cyperaceae, *Rumex*, *Myriophyllum*
TirP-6	325-294.5	Poaceae, Cyperaceae, *Artemisia*, *Rumex*, *Pediastrum*, *Selaginella*
TirP-5b	328-325	*Poaceae*, *Rumex*
TirP-5a	331-328	*Juniperus*, *Betula*
TirP-4	338-331	Poaceae, *Rumex*, *Pediastrum*
TirP-3b	342-338	*Betula*, *Juniperus*
TirP-3a	348-342	*Juniperus*, *Betula*, *Empetrum*
TirP-2	351-348	Poaceae, *Rumex*, *Artemisia*
TirP-1	355-351	Poaceae, Cyperaceae, *Rumex, Empetrum*

TirP-2 is characterised by a reduction in woody-type pollen with replacement by herbaceous taxa. Within TirP-2, the most significant observation is the reduction in *Betula*, from 16 % within TirP-1, to 2 % in zone 2. This reduction is mirrored by decreases in *Empetrum*, from 19 % in TirP-1, to 0 % at the top of this zone. These taxa are replaced by Poaceae, increasing to 51 % by the top of the zone and *Rumex*, with highs of 21 % within the zone. Throughout TirP-2 *Artemisia* also increases. Additional herbaceous components of this zone include Cyperaceae and Compositae: Lactuceae.

Pollen concentrations are similar to the upper levels of the previous zone. However, at 349.5 cm, TLP concentrations drop to low values of 5885 grains/cm^{-3}. Poaceae is the greatest contributor to pollen concentrations with 2413 and 4223 grains/cm^{-3} in the upper levels.

Zone TirP-3. Composite depth: 348-338 cm.

The third zone in the sequence is characterised by successive increases first in the shrub-type pollen of *Empetrum* and *Juniperus*, then by *Betula*. From the previous zone *Empetrum* rises to a joint sequence high of 19 % at 345.5 cm. Following this peak, *Empetrum* tails off and is replaced by the increases in *Juniperus*, 20 % at 342.5 cm. For the remainder of the zone *Juniperus* percentages are declining, whereas, from lower percentages, *Betula* peaks to a zone high of 58 % at 339.5 cm. Throughout the zone Poaceae percentages fluctuate around 20 %. *Rumex* percentages are lower than the previous zone, despite a minor peak at 343.5 cm. Further, highest *Artemisia* percentages are observed at the base of the zone before falling to 0 % at the top of the zone. Aquatic components consist of *Myriophyllum* and *Nuphar;* albeit in low percentages.

Owing to complexity, TirP-3 has been split into two sub-zones:

TirP-3a: 348-342 cm. Peaks in both *Empetrum* and *Juniperus*.
TirP-3b: 342-338 cm. Reduction in *Empetrum*/*Juniperus*, Peak in *Betula*.

Generally, TLP concentrations are increasing throughout the zone from 10,070 grains/cm^{-3} at the zone onset, to a sequence high of 148,310 grains/cm^{-3} at 339.5 cm. In the first sub-zone, *Empetrum*, Poaceae and *Juniperus* provide the main concentration values before *Betula* is dominant in sub-zone 3b with a concentration of 85,582 grains/cm^{-3}.

Zone TirP-4. Composite depth: 338-331 cm.

TirP-4 is markedly different from the previous zone and bears close resemblance to TirP-2. Within TirP-4 tree- and shrub-type taxa decrease and are replaced by herbaceous pollen. The two taxa that display the greatest increases are Poaceae and *Rumex*. Poaceae increases to a zone high of 36 % at 335.5 cm and percentages are sustained at >24 % for the remainder of the zone. *Rumex* and Cyperaceae exhibit a similar structure with the former exhibiting percentages of 25 % at 334.5 cm and sustained percentages > 11 % to 331.5 cm. The aquatic component is dominated by *Pediastrum* with percentages rising to a high of 17 % at the top of the zone. Equally at the top of the zone there is a return to increased *Juniperus* percentages, 20 %. Contributing taxa include: *Artemisia*, Caryophyllaceae, Asteraceae, *Filipendula*, *Helianthemum* and *Thalictrum*.

TLP and total concentrations in TirP-4 are higher than TirP-2 and TirP-3a. However, they do not reach highs of TirP-3b with zone low concentrations recorded of 48,940 grains/cm^{-}

^{3} and 42,471 grains/cm^{-3} at 333.5 cm respectively. Basal and upper zone concentration values are comparable to the upper levels of the previous zone. All concentration values of key taxa decrease at 333.5 cm and all but *Rumex* have zone high concentrations at 332.5 cm.

Zone TirP-5. Composite depth: 331-325 cm.

TirP-5 shows a return to high percentages of *Juniperus*, a joint sequence high of 51 % at 329.5 cm, and moderate percentages of *Betula*, zone highs of 18 % at 328.5 cm. For the remainder of the zone these two taxa decrease in percentage. Contrastingly, Poaceae and *Rumex* increase from 328.5 cm to the terminus of the zone with percentages of 25 % and 16 % respectively. Towards the top of the zone taxa including *Pinus*, Caryophyllaceae, Compositae: Lactuceae, *Helianthemum* and *Thalictrum* all increase. *Pediastrum* and *Selaginella* increase throughout, both containing percentages of 12 % at 325.5 cm.

Concentration values are high throughout the zone with a peak in TLP concentration of 140,158 grains/cm^{-3}. *Juniperus*, 71,948 grains/cm^{-3}, Poaceae, 21,491 grains/cm^{-3} and *Betula*, 18,688 grains/cm^{-3} are the primary contributors. At 325.5 cm however, concentration declines to 27,829 grains/cm^{-3}. Concentrations of *Pediastrum* are rising throughout the zone.

Zone TirP-6. Composite depth: 325-294.5 cm.

Zone TirP-6 is markedly different from any previous zone within the Tirinie profile. Poaceae starts the zone at elevated percentages, 33 %, and follows a downward trajectory to 14 % at 304.5 cm, whereas, Cyperaceae is generally stable between 16 and 25 % throughout. Percentages of *Rumex* increase to a zone maximum of 20 % at 304.5 cm. The greatest change in percentage is observed within *Artemisia*, with percentages rising until the taxa peaks at 33 % at 300.5 cm. Increased percentages are also observed in *Pinus*, *Salix*, Caryophyllaceae, Compositae: Lactuceae and *Saxifraga*. The aquatic component is dominated by *Pediastrum* with percentages >40 % throughout. The principal pteridophyte component is composed of *Selaginella* with percentages of 16 % at 320.5 cm.

For most of the zone, TLP concentrations are low. Higher concentrations are observed at 324.5 cm and 296.5 cm with 33,358 grains/cm^{-3} and 25,271 grains/cm^{-3} respectively, with lows of 10,701 grains/cm^{-3} at 316.5 cm. Concentrations of all taxa are lower during

TirP-6, barring *Artemisia* which peaks 5235 grains/cm^{-3} at 300.5 cm. Total concentrations are much higher than TLP concentrations which relates to the increase in concentration of *Pediastrum*, with totals of 63,799 grains/cm$^{-3.}$

Zone TirP-7. Composite depth: 294.5-279 cm.

The seventh zone demonstrates considerable variability. Percentages of Poaceae peak at two points through the zone with 40 % and 49 % at 292.5 cm and 282.5 cm. Contrastingly, Cyperaceae peaks towards the centre of the zone alongside *Rumex*, 34 % and 22 %, respectively. Percentages of *Salix* are greater than at any previous stage, 11 % towards the base of the zone. Following from TirP-6, zone seven shows high but falling percentages of *Pediastrum*. The main aquatic taxa within this zone is Myriophyllum with 21 % and 19 % between 292 cm and 290 cm.

Concentrations within TirP-7 are greater than the previous zone. TLP concentrations increase throughout to 36,742 grains/cm^{-3} at 280.5 cm.

Zone TirP-8. Composite depth: 279-259 cm.

The major taxon within TirP-8 is *Equisetum*. Values rise towards the top of the previous zone and peak with high values of 56 % at 275.5 cm. Whilst slightly lower, values for Poaceae are between 18 % and 43 %. At the zone onset, *Rumex* percentages are 14 %, and whilst the taxon is continually recorded, values are reduced throughout the remainder of the zone. Further, *Betula* percentages at the beginning of the zone are largely lower than the previous zone, until values begin to rise at 264.5 cm. *Empetrum* percentages are greater at the start and end of the zone, with reductions to <7 % between 272.5 cm and 265.5 cm. Around this phase, *Pinus* and *Salix* percentages are elevated.

Similar to other zones in the sequence TirP-8 has been split into two subzones:

TirP-8a: 279-273 cm. Peak in *Equisetum* and slight peak in *Rumex*
TirP-8b: 273-259 cm. High *Equisetum*, troughs in *Betula* and *Empetrum*.

Concentration values are generally increasing throughout the zone. High TLP values are observed at 267.5 cm with 77,203 grains/cm^{-3}. Total concentration values are principally controlled by high concentrations of *Equisetum*; with 45,724 grains/cm^{-3} at 276.5 cm. Concentrations of *Pinus*, Poaceae and Compositae: Lactuceae peak towards the middle

of TirP-8, between 272.5 cm and 266.5 cm. Whereas, high *Thalictrum* values appear throughout.

Zone TirP-9. Composite depth: 259-247.5 cm.

Within TirP-9 *Juniperus* values rise and peak at 51 % TLP at 248.5 cm. Coincident with high vales for *Juniperus*, *Betula* percentages rise from 13 % to 32 % throughout the zone. In contrast to previous zones, Poaceae, Cyperaceae, *Empetrum*, *Rumex* and *Equisteum* percentages are all either falling or considerably lower that TirP-8.

Concentration data for the zone depict increasing concentrations of *Juniperus* and *Betula* with peaks of 67,998 grains/cm^{-3} and 42,125 grains/cm^{-3} at the top of the zone respectively. This is mirrored by the high values for TLP between 87,290 grains/cm^{-3} at 258.5 cm and 132,575 grains/cm^{-3} at 248.5 cm.

Zone TirP-10. Composite depth: 247.5-239 cm.

The main differences between TirP-10 and the preceding zone is the reversal between *Betula* and *Juniperus*. Low percentages of *Juniperus* are encountered at the top of the zone with values of 17 %, whereas, *Betula* percentages rise from 38 % to 51 % throughout. *Salix* percentages rise to a sequence high of 16 % at 242.5 cm. *Filipendula* percentages also increase, although values are <7 % throughout the zone.

TLP concentration values are oscillatory throughout the zone. The base of the zone is characterised by concentration values of 93,586 grains/cm^{-3}, which are lower than the previous zone. Two higher values of, 138,235 grains/cm^{-3} and 114,206 grains/cm^{-3} towards the top of the zone are separated by a lower value of 75,005 grains/cm^{-3}. Concentrations are largely controlled by *Betula*, *Juniperus*, and Poaceae.

Zone TirP-11. Composite depth: 239-198 cm.

Betula percentages are very high, >50 % throughout, barring one sample at 218.5 cm where percentages drop to 45 %. At this point *Juniperus* percentages rise to 20 %. Additionally, *Corylus* increases to 10 % by the top of the zone. The aquatic spectrum is composed of *Nuphar* and small increases in *Pediastrum* with pteridophytes composed by *Dryopteris*, Filicales and *Equisetum*.

TLP concentrations are moderate, with higher concentrations observed at 229.5 cm, 130,835 grains/cm^{-3}, and at the top of the zone 119,904 grains/cm^{-3}. *Betula* is the primary source of high concentration values. Contrastingly, where decreases in TLP concentrations are observed, variable increases in *Juniperus* are noted, rising to 15,897 grains/cm^{-3} at 218.5 cm.

6.3 Statistical analyses

All statistical analyses were performed on a reduced Tirinie dataset using all taxa with an abundance of greater than 5 %. This cut-off was chosen to better characterise the trends within the principal taxa throughout the pollen sequence. Detrended Correspondence Analyses (DCA) were employed to establish the lengths of the primary axes (Table 6.3). These lengths (>1.5-3 SD) demonstrate that Principal Components analysis (PCA), Correspondence Analysis (CA) and Principal Curves (PC) were suitable for data exploration at Tirinie.

A PCA (Figure 6.6) was selected to explore variation in taxa owing to the axis lengths provided in Table 6.3. Axis one explains 29.5 % of taxon variability, whilst axis two explains 14.8 %. Clear differences within taxa plotting along axis one can be observed. Taxa plotting negatively along axis one includes *Betula*, which is the most significant contributor, *Filipendula*, *Corylus* and *Juniperus*. In contrast, taxa plotting positively along the axis include Caryophyllaceae, *Pediastrum*, Saxifragaceae, *Selaginella* , Compositae: Lactuceae, *Rumex* and *Artemisia*. The remaining taxa plot in intermediate space with aquatics and pteridophytes showing greater affinity with axis two.

Table 6.3 Preliminary decorana analyses on the reduced Tirinie dataset highlighting that axis 1 explains more variation than the remaining axes and the short axis lengths.

	DCA1	**DCA2**	**DCA3**	**DCA4**
Eigenvalue	0.3823	0.12135	0.09436	0.10099
DCA value	0.3825	0.09782	0.04655	0.02776
Axis length	2.4482	1.66785	1.22593	1.24586

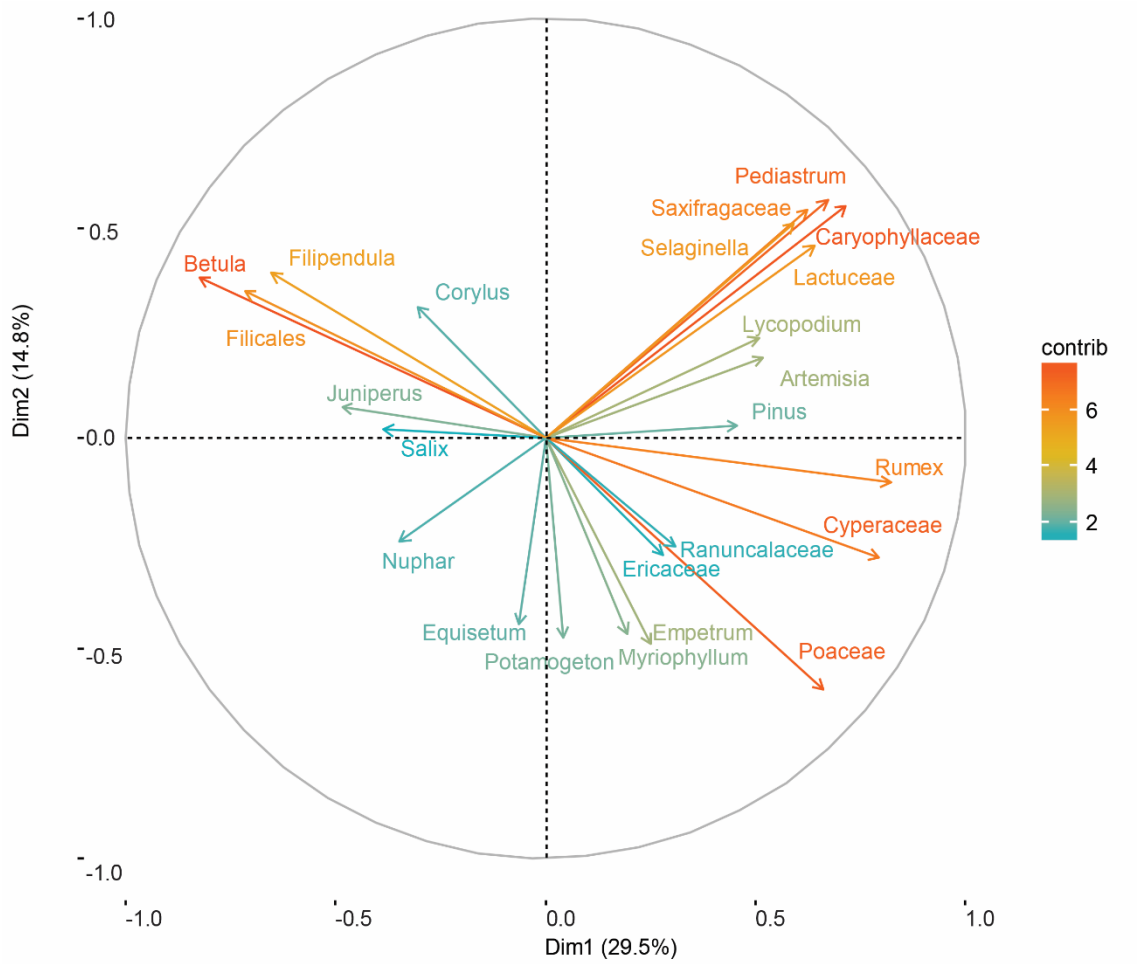

Figure 6.6 Results of the PCA output from Tirinie. The data are presented as a biplot showing the two principal components, axis 1 and 2, with taxa placed along the axes relative to their importance. The length of the arrow and the variable colour indicates the dominant taxa along the axis. Plotting positively along axis one with greater importance are open herbaceous taxa; whereas negative values are composed of shrub and tree-type taxa.

To demonstrate the relationship between palynological change and stratigraphy axis one scores for PCA and CA are plotted (Figure 6.7). This was subsequently modelled in n-dimensions with a PC (Figure 6.7). The PC data from Tirinie has been modelled on a PCA-based output owing to convergence in fewer iterations (six versus nine), under similar penalty values applied to the regression. Both approaches explain similar variances within the data:

- PCA based output: 88.0 %
- CA based output: 88.4 %

Variance within the output (Figure 6.7) have been inferred by rapid switches to more positive values. From this output, one major and potentially four minor revertences can be observed. The shorter are shaded in Figure 6.7 and are as follows:

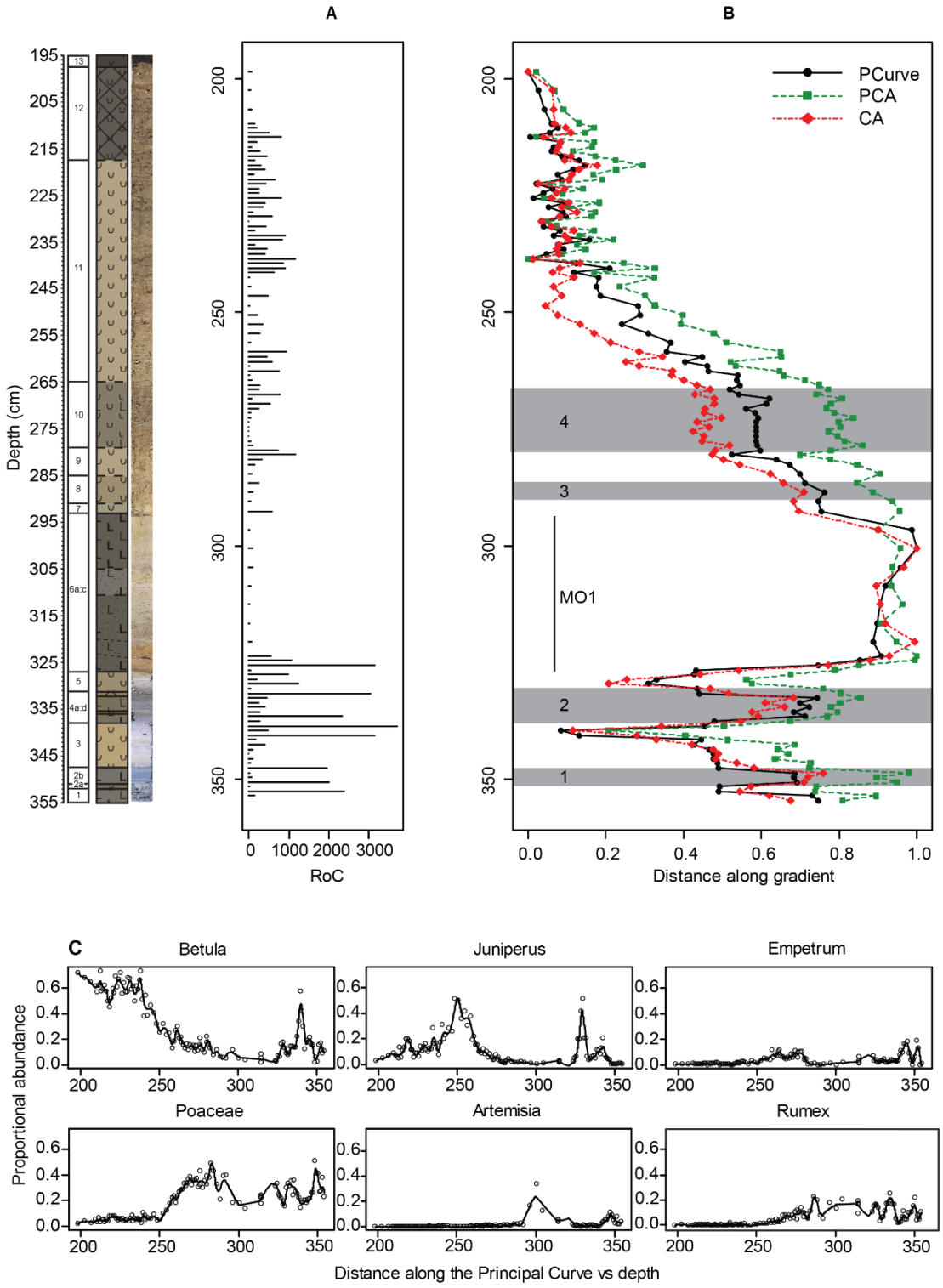

Figure 6.7 Results of different statistical tests applied to the Tirinie pollen data. A) Rate of change analysis. The values for the analysis are arbitrary and an exaggeration multiplier has been applied to demonstrate where significant periods of compositional change are inferred from the pollen data. The greater the length of the bar the more significant the compositional change. B) The overlain output from three tests applied (PCA, CA and PC). This highlights the similarity of the three tests and the PC will be discussed from this point. The data show rapid short revertences (grey boxes) and a longer revertence termed (MO1). C) Individual taxa response curves modelled on the gradient of the PC. These key taxa demonstrate what may be driving the changes in the PC from B).

- Major Oscillation 1: Samples between 327.5-293.5 cm
- Oscillation 1: Samples between 350.5-347.5 cm
- Oscillation 2: Samples between 337.5-330.5 cm
- Oscillation 3: Sample at 288.5 cm
- Oscillation 4: 279.5-266.5 cm

These variances occur alongside peaks in the rate of change analysis (RoC); indicating large-scale compositional change within the vegetation data over short stratigraphic distances. For assistance in interpretation, individual taxa response curve are modelled using proportional abundances along the gradient of the PC (Figure 6.7). Using this approach, key taxa can be shown to drive variance in the PC at different points in the stratigraphy. For example, increases in *Rumex* and *Artemisia* with Poaceae as *Betula* and *Juniperus* become less influential.

6.4 Micro- and macro-charcoal

Micro- and Macro- charcoal analyses were undertaken at the same resolutions as the pollen reconstruction resulting in 113 data-points. Micro-charcoal analyses were undertaken alongside pollen identifications with micro-charcoal data presented as pollen concentrations. Macro-charcoal data is presented as raw counts per cubic centimetre of sediment (Figure 6.8). For ease of interpretation and better delineation of a phase of charcoal accumulation, an average line for charcoal concentrations and macro-charcoal counts is presented as a horizontal line on Figure 6.8. The average value for charcoal concentration is 236,151 shards/cm^{-3}, whereas, for macro-charcoal the average value is 8.16 fragments/cm^{-3}.

Micro-charcoal

Micro-charcoal concentration ranges from 8472 shards/cm^{-3} to 922,000 shards/cm^{-3}. Throughout this record eight significant peaks or significant charcoal accumulations have been identified. The first observation, TirCc-1, is characterised by a single sample peak of 642,020 shards/cm^{-3} at 346.5 cm. Two further phases of increased charcoal concentrations can be identified from the first carbonate phase, TirCc-2 and TirCc-3, which are shown by peaks of 401,336 shards/cm^{-3} and 320,904 shards/cm^{-3} at 332.5 cm and 327.5 cm respectively. With the former existing as a complex of charcoal spread over 4 cm. Within sediment unit 10 a further complex of charcoal exists between 274.5-262.5 cm with a sequence high of 922,000 shards/cm^{-3}. Bracketing this complex, elevated values are observed at 282.5 cm and 256.5 cm. Throughout the remainder of the record further peaks in charcoal concentration can be observed. These centre on 250.5, 241.5, 226.5 and 218.5 cm.

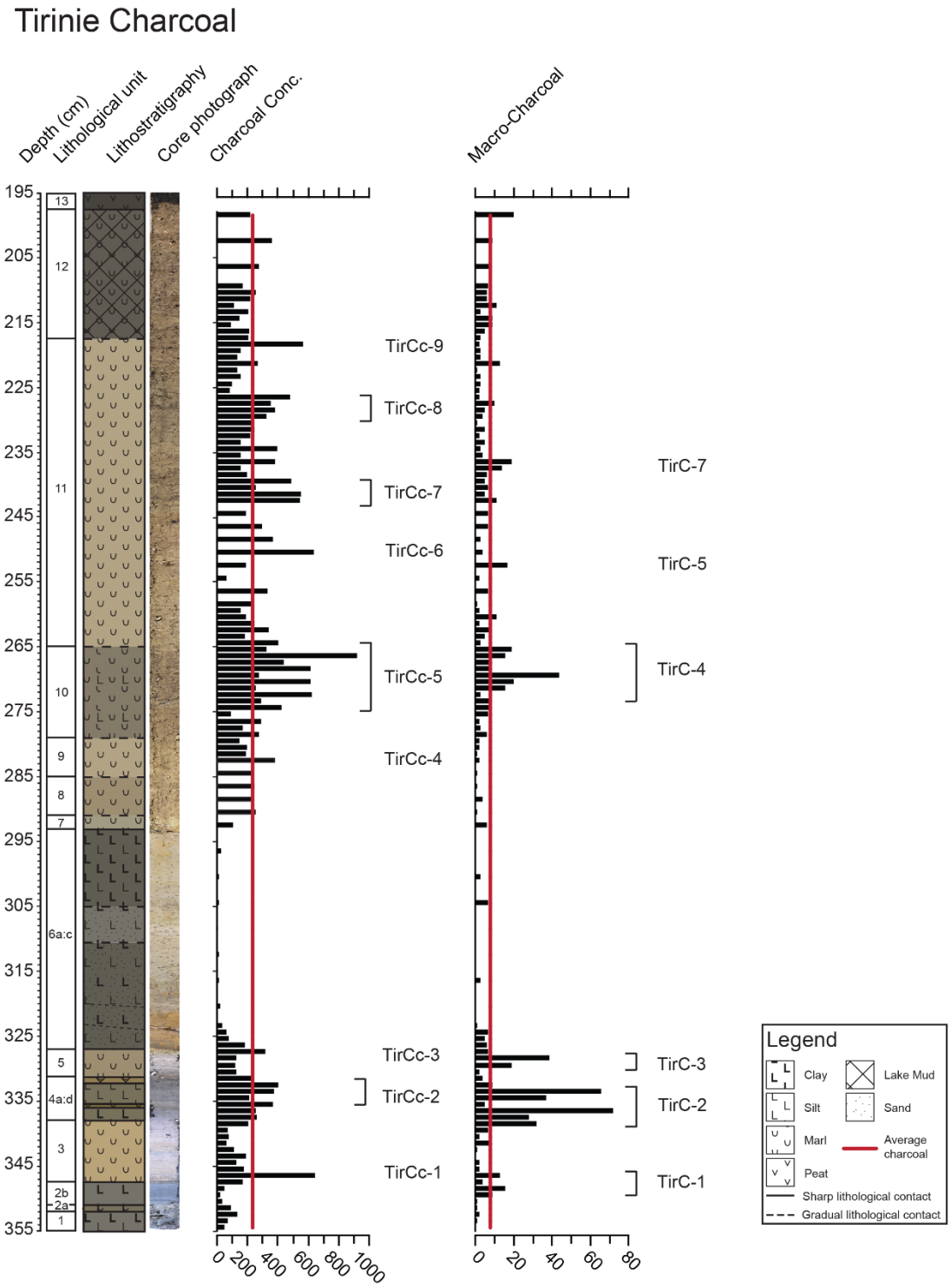

Figure 6.8 Results of the charcoal analysis at Tirinie. Presented are the micro-charcoal concentrations from Tirinie (left) and the macro-chacoal counts (right). Presented on the figure are average lines for charcoal abundance to assist in peak identification with key peaks given presented with the prefix TirCc (micro-charcoal) and TirC (macro-charcoal).

Macro-charcoal

Macro-charcoal counts range from 0 to 72 fragments/cm^{-3}. In contrast to the concentration data, six significant areas of increased macro-charcoal abundance can be observed. Three of these phases occur towards the base of the record. TirC-1, between 349.5-346.5 cm, is characterised by a charcoal count of 16 fragments. TirC-2, between 338.5-332.5 cm, contains consistent values above background counts and comprises a sequence high of 72 fragments. TirC-3, a more confined charcoal accumulation between 329.5-328.5 cm contains 38 charcoal fragments. The most significant period in the upper carbonate units sits between 271.5-265.5 cm and is shown as containing successive peaks, grouped as a complex, of 44 fragments and 19 fragments respectively. Charcoal is consistently recorded throughout the remainder of the profile and increased abundance is noted at 252.5 and 236.5 cm.

6.5 Biomarker analyses

Tirinie was analysed for the presence of *n*-alkanes at variable resolutions. Over sediment units 1 to 5 and 7 to 11 a contiguous approach was adopted. However, within unit 6a to 6c the resolutions attained were variable, with key transitions being sampled at contiguous intervals. This approach provided a provisional 80 biomarker samples. Owing to Androstane (standard) not being identified in five samples (351.5, 343.5, 321.5, 318.5 and 298.5 cm) manual integration was performed. As the integration uses the Gas Chromatogram (GC) 'peak area' to calculate abundances and as no peak was detected, the final calculated *n*-alkane concentrations were higher than stratigraphically adjacent samples. Furthermore, two additional samples (325.5 and 284.5 cm) proved problematic; the former sample looked to be contaminated on the GC-MS output (Dirk Sachse, pers. comm. 2017) and the latter contained no biomarker data. Therefore, seven samples were removed from the analysis, producing a total of 73 samples which are presented in Figure 6.9 as concentrations of µg/g dry weight of sediment. Total average chain lengths and terrestrial average chain lengths are also presented. An aquatic origin for alkanes of *n*-C_{21}, *n*-C_{23} has been previously shown (e.g. Aichner et al., 2010; Sachse et al., 2012) however, the incomplete alkane record for *n*-C_{21} Tirinie precludes its use as a sole aquatic member, therefore *n*-C_{23} is presented. Further, it is noted that the mid-chained *n*-C_{25} alkane contains both aquatic and terrestrial components (e.g. Sachse et al., 2012) but has been included here.

6.5.1 *n*-Alkane concentrations

Typical *n*-alkane concentrations range from 0.27 to 103.4 µg/g per dry weight of sediment. There is considerable variability between successive samples and between different n-alkane members, however, all analysed n-alkanes show similar patterns

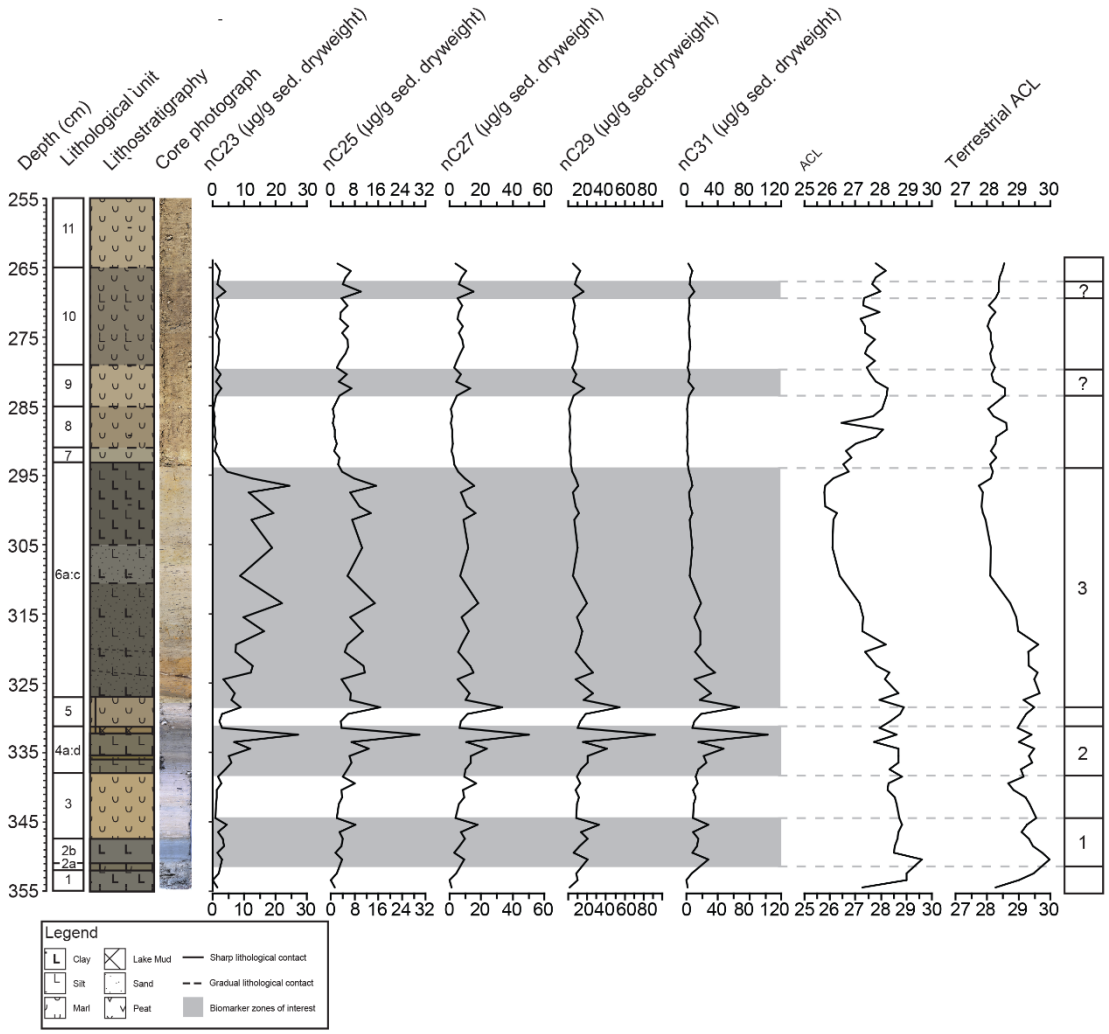

Figure 6.9 Concentrations of *n*-alkane data from the biomarker analyses. Concentrations in µg/g dry weight of sediment are shown for the principal odd chained n-alkanes identified covering 355-255 cm. Odd numbered chain lengths have been plotted as these are integral components of leaf waxes. ACL and Terrestrial ACL are also shown here. Grey shading relates to areas of interest where changes in concentration can be observed.

throughout the sequence. Notwithstanding, three zones of increased concentration can be identified and are shown in Figure 6.9. The first, between 350.5 and 345.5 cm, is initially recorded in *n*-C_{31}. However, by 345.5 cm, *n*-C_{25} to *n*-C_{31} all demonstrate increases. The greatest contributors at this depth are *n*-C_{29} and *n*-C_{31} with concentrations of 32.59 and 28.27 µg/g respectively. The second zone of greater concentration, between 338.5 and 332.5 cm, increases in can be observed across all members. All concentrations follow an upward trend towards sequence high values at 322.5 cm. Individual values include, 26.32 µg/g for *n*-C_{23}; 29.95 µg/g for *n*-C_{25}; 0.18 µg/g for *n*-C_{27}; 92.46 µg/g for *n*-C_{29} and 103.4 µg/g for *n*-C_{31}. The final zone in the sequence demonstrates stratigraphic differences between different *n*-alkane members. Initially, concentrations in the mid- and longer-chained alkanes increase to zone highs between

328.5 and 323.5 cm; with the dominant member being *n*-C_{31} at 66.61 µg/g. The mid- and longer-chained members subsequently reduce in concentrations. In contrast, the *n*-C_{23} member, shows the reverse trend with concentrations increasing throughout this zone. At 296.5 cm, zone high concentrations are observed with 24.43 µg/g. Throughout the remainder of the sequence not discussed here, concentrations are much lower across all members. There is a possibility that subtle increases in concentration can be observed in the upper sections of the sequence. These are however, confined to single samples and as a result have not been defined into formal units.

6.5.2 Average chain lengths

Values for total average chain length (TACL) vary between 25.79 and 29.62. Similarly, whilst more constrained, terrestrial average chain lengths (tACL) vary between 26.74 and 29.96. From the highest ACLs at the base of the sequence, 350.5 cm, the two series follow different trajectories. The TACL curve drops to lower values and is stable, albeit with subtle variations, until sedimentological unit 6. Contrastingly, the terrestrial ACL data shows a two-step decline and subsequently follows a rising trend. Increases in tACL are noted between 339.5 and 331.5 cm before the curve drops to preceding values.

During unit 6 TACL values fall; and the lowest values are reached at 296.5 cm. During the same phase, tACL's are initially high, until 319.5 cm; before falling akin to the total ACL curve. Absolute tACL minima are observed at 296.5 cm. The subsequent phase of the record shows increased ACL values for both spectra. Within sedimentological units 7 to 11 considerable variations are observed, specifically at 286.5 cm and between 282.5 and 265.5 cm. Whilst both curves demonstrate this complexity, variability within the TACL data are more pronounced.

6.5.3 Compound specific isotopic reconstructions

Like the issues encountered during *n*-alkane quantification, certain samples were omitted from the isotopic reconstruction. Other than the contaminated sample at 325.5 cm and lack of data at 284.5 cm, three additional samples failed to return isotopic data: 345.5, 339.5 and 284.5 cm. Whilst the *n*-C_{29} alkane produced the greatest return in deuterium values for each sample; measurements from *n*-C_{21}, *n*-C_{23}, *n*-C_{25}, *n*-C_{27} and *n*-C_{31} were not always successfully obtained (Table 6.4).

Figure 6.10 displays the deuterium isotopic concentrations of individual compound classes. There are considerable variations between and within all compound classes, with greatest variability shown within the *n*-C_{23} and *n*-C_{31} classes. As the errors of the isotopic values are considerable within the *n*-C_{27} and *n*-C_{31} classes, the *n*-C_{21} values

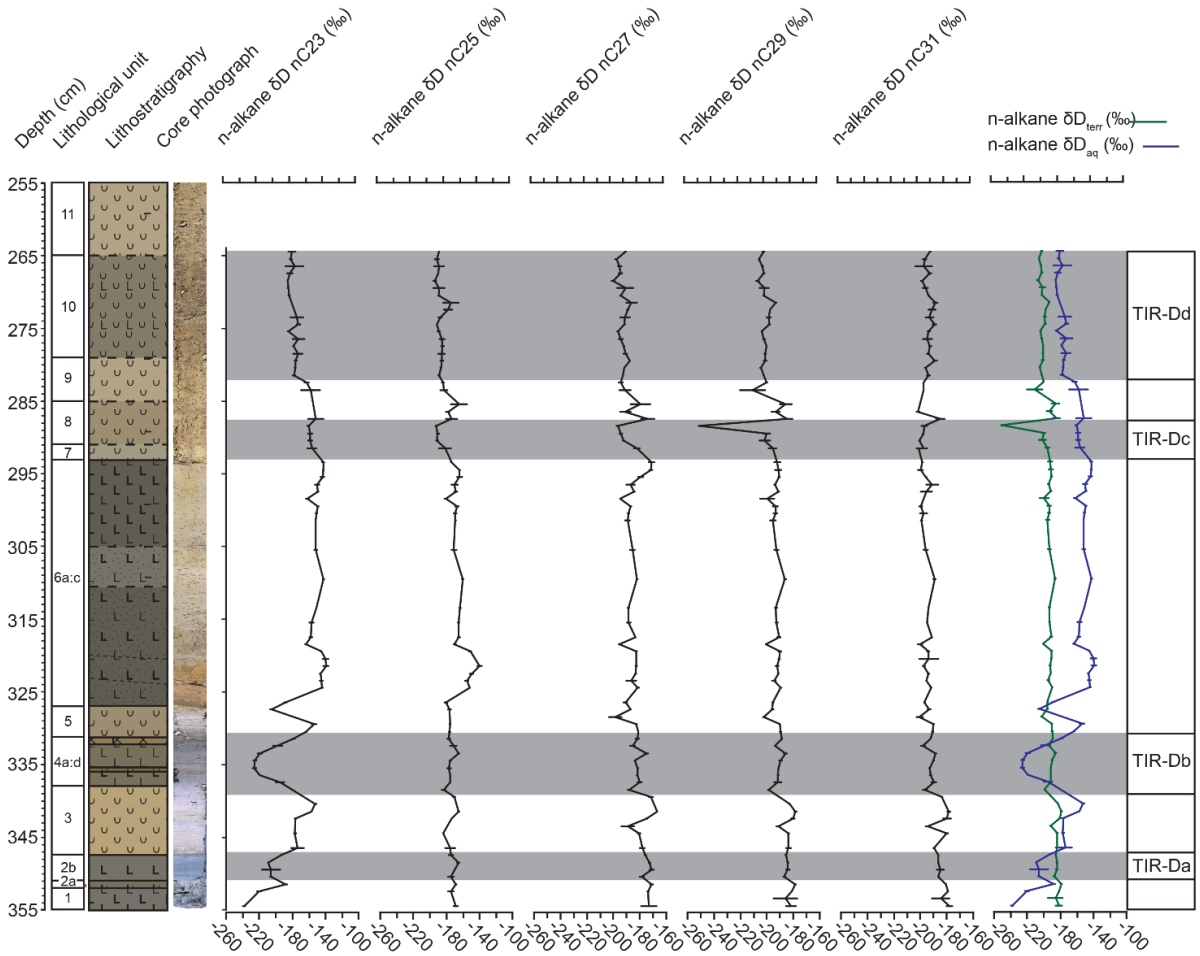

Figure 6.10 Deuterium isotopic reconstructions for the commonly identified n-alkanes throughout the Tirinie sequence. δD_{terr} (*n*-C_{29}) and δD_{aq} (*n*-C_{23}) have been overlain assist in interpretation. Grey shading highlights phases, principally within *n*-C_{23}, where significant depletions are observed. All isotope values are quoted against Vienna Standard Mean Ocean Water (VSMOW).

Table 6.4 Highlighting the differences in the δ*D* measurements from the Tirinie sequence. *n*-C_{29} contains the most measurements with shorter-chained n-alkanes displaying fewer measurements.

Compound Class	No. of Measurements
***n*-C_{21}**	47
***n*-C_{23}**	67
***n*-C_{25}**	70
***n*-C_{27}**	73
***n*-C_{29}**	75
***n*-C_{31}**	74

contain fewest samples and a common origin (aquatic vs. terrestrial) cannot be precluded from *n*-C_{25}; the results will focus on *n*-C_{23} and *n*-C_{29} alkanes.

The deuterium isotopic profile of *n*-C_{23}, throughout units 1 to 5, displays considerable variation. From depleted values at the base of the sequence, -238.26 ‰ at 354.5 cm, two significant episodes of depletion can be identified. One termed TIR-Da between 350.5 and 348.5 cm, where isotopic values fall to a low of -208.98 ‰. And a second, TIR-Db between 337.5 and 331.5 cm where isotopic values fall from -152.16 ‰ to lows of -225.74 ‰. Between these events isotopic values are relatively enriched with peaks of -152.16 ‰ at 340.5 cm and -152.72 ‰ at 329.5 cm. Contrastingly, the isotopic reconstruction from *n*-C_{29} throughout the same phase is relatively stable, with subtle variations occurring throughout but without the same depletion and enrichment profile.

Within the minerogenic units, 6a to 6c, following an initial trough on the boundary between unit 5 and 6, *n*-C_{23} exhibits enrichment between 324.5 and 319.5 cm with values between -139.33 ‰ and -145.95 ‰. Subsequently, values fall and remain stable until 299.5 cm where subtle increases to enriched values can be observed. Throughout units 6a to 6c *n*-C_{29} again remains stable, with isotopic values between -200.82 ‰ and -186.21 ‰.

The final phase of the diagram is characterised by a largely downward trending isotopic profile for *n*-C_{23} with perhaps two phases of increased depletion. One centred at 288.5 cm, TIR-Dc, with lows of -160.30 ‰ and the second, TIR-Dd, between 281.5 and 264.5 cm with lows of -185.59 ‰. *n*-C_{29} follows a similar trend to *n*-C_{23} albeit with a phase of significant depletion within TIR-Dc, where values reach -250.90 ‰. A short period of

enrichment follows with the onset of isotopic depletion within TIR-Dd occurring earlier than *n*-C_{23}. A small reversion to more positive values can be observed at 271.5 cm.

6.6 Additional site data

The data presented within this section includes all data that were completed alongside this thesis, representing a combination of data compiled by both the author of this thesis and colleagues from the Centre for Quaternary Research at RHUL. The stable isotopic data were compiled by Ian Candy, Finella Elliot, Christopher Francis and Ashley Abrook; the chironomid data was compiled by Lucy Turner and Christopher Francis (Preface; Chapter 4). This section also contains the chronological methods employed at Tirinie.

6.6.1 $\delta^{18}O$ and $\delta^{13}C$ isotope stratigraphy

Across the sedimentological units associated with carbonate sedimentation (units 1 to 5 and 7 to 12) a total of 78 isotopic analyses were performed at variable resolutions (Figure 6.11). In contrast to the Quoyloo Meadow sequence no smoothing has been applied to the isotopic profile. Owing to phases of a lack of calcium carbonate production within the lake, between 351.5 and 348.5 cm and within unit 6, no isotopic data was generated.

The lower carbonate phase demonstrates no evidence for co-variance between the $\delta^{18}O$ and $\delta^{13}C$ datasets (R^2=0.13). The $\delta^{13}C$ values at the base of the record are high, 2.39 ‰ at 354.5 cm and largely follow a declining trend, -3.70 ‰ at 327.5 cm. Average values for $\delta^{13}C$ are given as -0.91 ‰, 1σ=2.22 ‰. In contrast, the oxygen isotopic record oscillates between high and low values throughout. Average values for $\delta^{18}O$ are -7.52 ‰, 1σ=0.86 ‰. Within this phase the $\delta^{18}O$ record oscillates between major peaks TIR-O1, -6.71 ‰; at 353.5 cm; TIR-O3, -6.05 ‰; at 344.25 cm; TIR-O5, -6.82 ‰; at 328 cm; and troughs TIR-O2, -9.03‰; at 351.5 cm and TIR-O4, -9.35‰; at 334.5 cm (Candy et al., 2016).

The upper carbonate phase shows a moderate relationship between oxygen and carbon (R^2= 0.425). At the base of this phase, the $\delta^{13}C$ values show increased depletion than the values in the lower carbonate units, -2.63 ‰ at 290.75 cm but follow the same declining trend -5.35 ‰ at 198.75 cm. Average carbon values are presented as -3.60 ‰, 1σ=0.87. The oxygen isotopic signature from the upper carbonate section does not peak and trough with the same regularity, although the reconstruction contains the same range of values, with an average of -8.13 ‰, 1σ=0.54. The record can be split into a primary phase of 'relative' isotopic enrichment between 290.75 and 278.75 cm, a depleted phase between 277.75 and 264.75 cm and the remainder of the record where $\delta^{18}O$ values are declining between 263.75 and 198.75 cm with a switch to enriched values at the top of

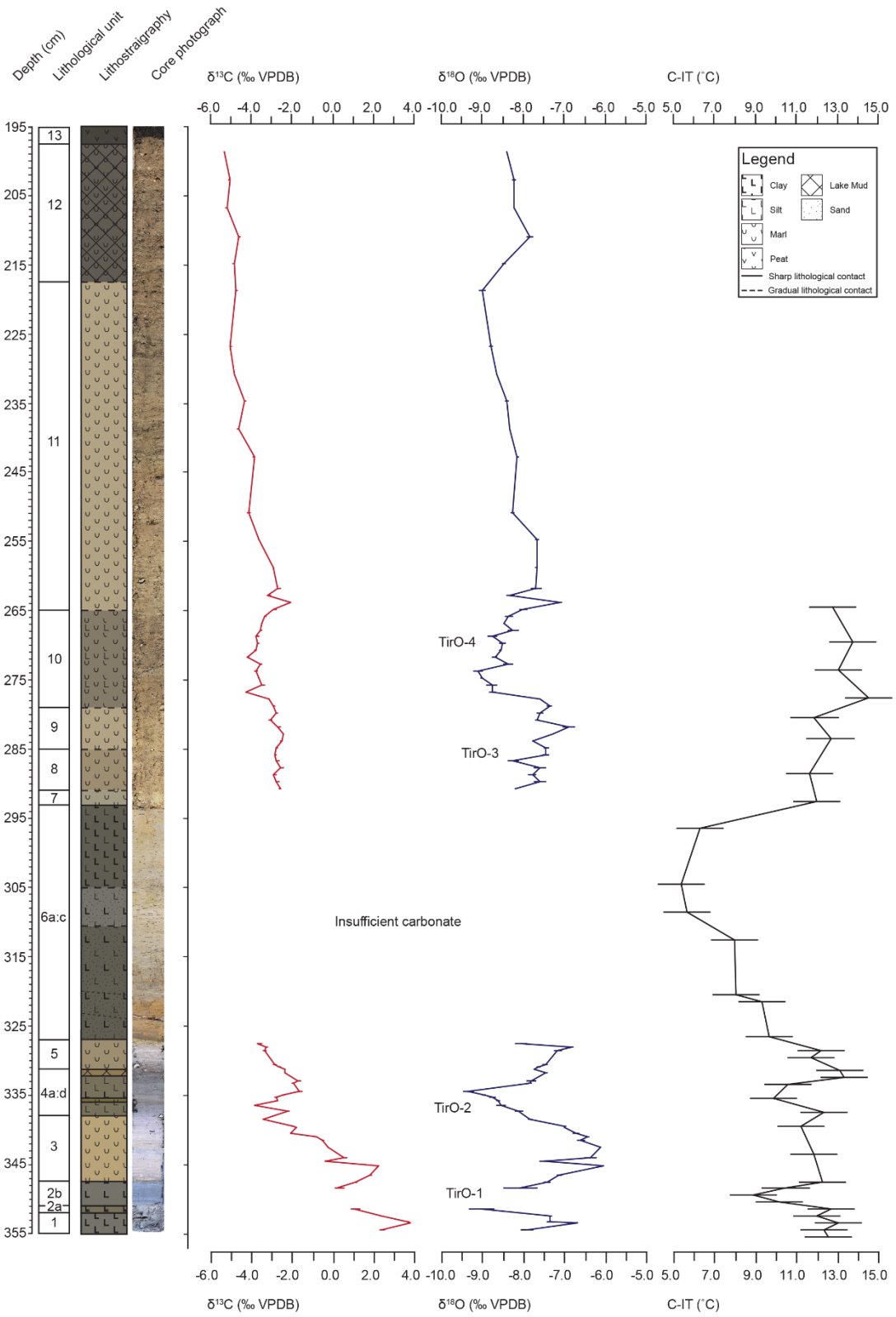

Figure 6.11 Oxygen and carbon isotope stratigraphy alongside a chironomid-inferred temperature reconstruction from Tirinie. All isotope data are presented against Vienna Pee Dee Belemnite (VPDB) with temperature data presented as degrees Celsius. Clear depletions can be observed in both the oxygen isotopic data and the C-IT.

the sequence. During this phase, two episodes of isotopic depletion are formally identified, TIR-O6, -8.26; at 286.75 cm and TIR-O7, where values fall from -7.38 ‰ at 278.75 cm to lows of -9.11 ‰ at 273.75 cm. Reduced resolution towards the top of the record prevents an understanding of significant isotopic complexes between 261.75 and 198.75 cm.

6.6.2 Chironomid-inferred temperatures

The C-IT reconstruction for the Tirinie sequence is shown in Figure 6.11. In total 33 samples were obtained for chironomid analysis, with temperature reconstructions generated using a modern Norwegian calibration dataset (Brooks and Birks, 2001). A three-component, weighted averaging-partial least squares regression (WA-PLS) model was selected leading to a root mean squared error of prediction (RMSEP) of 1.128°C and a coefficient of determination of (R^2_{JACK}) of 0.892 and a maximum bias of 0.82°C. Owing to the lack of core materials present, the lowest samples were obtained from Core 4 2017. Core matching was performed by stratigraphic alignment, which was deemed appropriate as the two stratigraphies are identical. As Core 4 records a greater portion of the basal materials the stratigraphy extends to 356 cm, not 355 cm as per the base of all other proxy records.

The data suggest that mean July temperatures were high from sediment units 1 to 5; between 11.2-13.3°C. These high temperatures were punctuated by two events during this phase. The former event centres on 349.5 cm and has minimum reconstructed temperatures of 8.87°C. The second event centres on at 335.5 cm and exhibits a minimum reconstructed temperature of 9.83°C. More pronounced cooling is observed within sediment unit 6 where temperatures decline throughout. The lowest temperatures, 5.35°C, are recorded within the second half of the unit. Temperatures rise towards the end of unit 6, and are high in the second carbonate phase with a maximum reconstructed summer temperature of 14.49°C.

6.6.3 Chronology

A total of 5 AMS radiocarbon samples were prepared for analyses from Tirinie using Cores 4 and 5 2017. These cores were sampled and assessed for plant macro-fossils, and where required, were combined to amalgamate enough sample material. These cores were aligned to the master sequence based on key lithostratigraphic marker horizons within the stratigraphy. Upon macro-fossil extraction the samples were sent to SUERC, unfortunately however, only one sample yielded enough carbon for radiocarbon measurement. To construct the age model this sample was combined with known tephra horizons presented in Candy et al. (2016) using published ages for the tephra (Table 6.5;

Figure 6.12). To constrain the model at the top of the sequence, the position of the *Corylus* rise was imported from Kelly et al. (2017) with the knowledge that *Corylus* (50 %) occurs stratigraphically after the upper samples from Tirinie (10 %). The date of the An Drium Tephra, from Timms et al. (2017) was also incorporated as this tephra occurs following the *Corylus* rise in Kelly et al. (2017). Therefore, the model was constrained with the caveat that the top of the sequence was deposited before the *Corylus* rise and the An Drium Tephra. Whilst this is not ideal, it was necessary to provide better chronological control across units 7 to 12.

Using this data, a p_sequence depositional model was constructed using the IntCal13 calibration curve (Reimer et al., 2013) in OxCal V. 4.3 (Bronk Ramsey, 2008; 2009) (Chapter 4). No boundaries were added to the model over areas of lithostratigraphic change to allow the model greater flexibility. However, the model has been constrained by boundaries at its upper and lower limits to extend modelling throughout the proxy data series.

The model produced good model agreement across the sequence and was therefore used to provide calendar age ranges for the reconstruction presented in Section 6.7. The model suggests that sediments were deposited in the basin between 14.16±0.41 and 10.03±0.60 Cal. ka BP (Table 6.5). The complete age model is presented in Appendix C.

Table 6.5 Summary of the all chronological constraints at Tirinie, including: depth information, unmodeled input range and modelled output range (2 σ age range) and mid-point age with 1σ error.

Name	Depth (cm)	Unmodelled range (Cal. ka BP)	Modelled range (Cal. ka BP)	μ ± σ	Reference
Boundary	197		11.25-9.27	10,026±601	
Before Corylus Before An Druim Tephra	198	9.78-9.56	9.78-9.56	9671±53	Timms et al. (2017)
Vedde Ash	309	12.11-11.94	12.12-11.94	12,029±43	Bronk Ramsey et al. (2015)
SUERC-78788	334.5	13.13-13.01	13.13-13.01	13,072±30	
Penifiler Tephra	348	14.06-13.82	14.05-13.81	13,927±61	Bronk Ramsey et al. (2015)
Boundary	355		15.03-13.77	14,166±415	

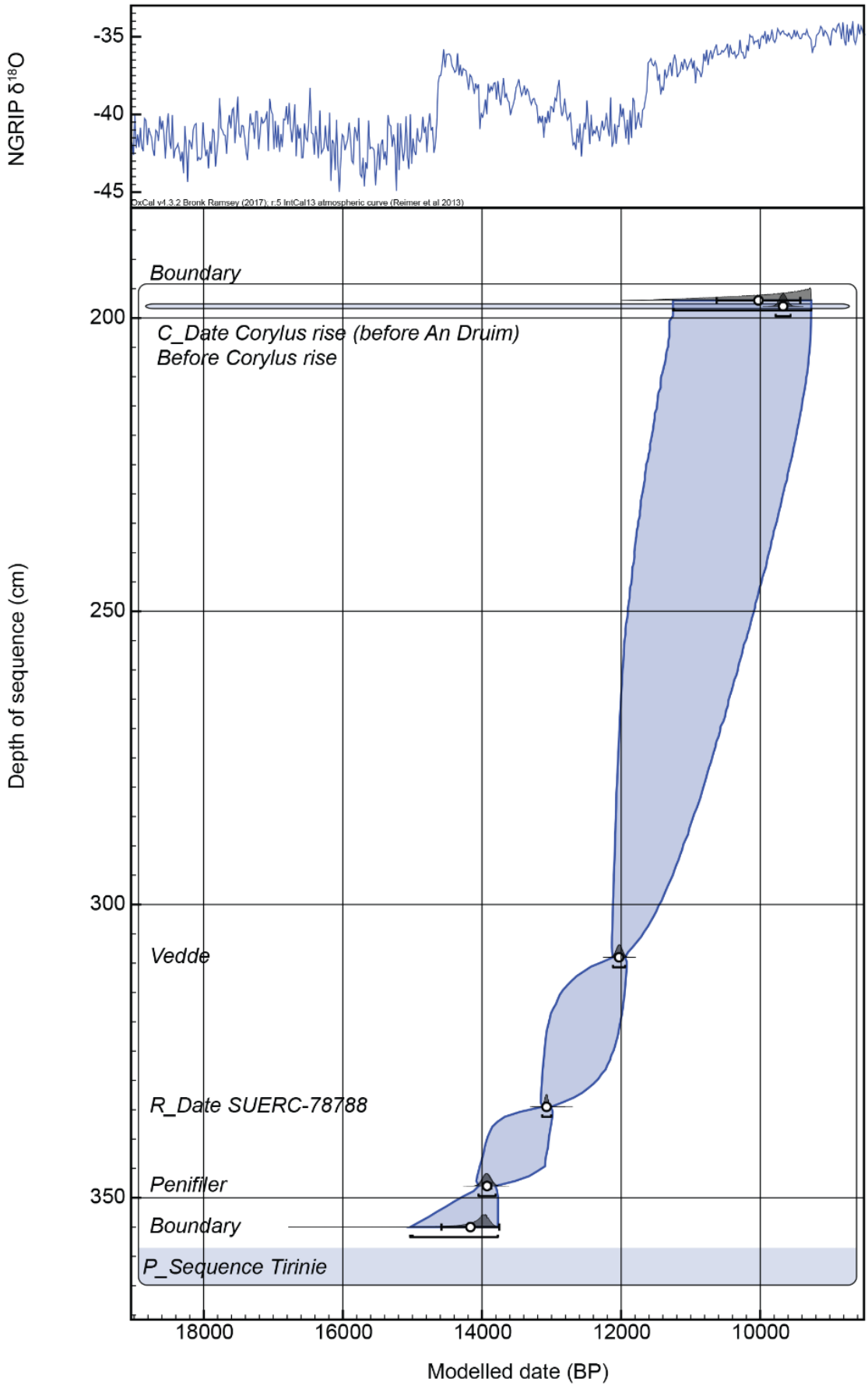

Figure 6.12 Age-depth, p_sequence model for Tirinie with age uncertainties plotted, μ and 1 σ, whilst the complete range is shown at 2 σ. Boundaries have been added at the top and bottom of the sequence for interpolation.

6.7 Palaeoclimatic and palaeoenvironmental interpretation

The presented palaeoclimatic and palaeoenvironmental data will be used here to reconstruct the climatic and environmental history of Tirinie. All palaeodata (Figure 6.13; 6.14) will be discussed against chronology, with the pollen data used here to infer vegetation development. As Chapter 5, it is acknowledged that this is an assumption but follows the traditional approach in palynological investigations. Based on the age model applied sediment units 1 to 5 can be attributed to the Windermere Interstadial (WI); sediment unit 6 to the Loch Lomond Stadial; and sediment units 7 to 12 to the early Holocene (EH). Terminal Dimlington Stadial (DS) sediments are not recorded at Tirinie.

Isotopic considerations

Across all stable isotopic analyses, minimal evidence for covariation exists (R^2= 0.13 and 0.425; between sediment units 1 to 5 and 7 to 12 (Figure 6.15)). This is important as higher covariance may suggest hydrological changes with waters affected by evaporitic modification (Hammarlund et al., 2003). Basement carbonates from different members of the Darladian Supergroup, namely the Argyll and Appin groups, those underlying Tirinie, reveal complex $\delta^{18}O$ and $\delta^{13}C$ relationships. Whilst an overlap is noted, $\delta^{13}C$ values range from +9.34 to -12.31 ‰, whereas $\delta^{18}O$ values range from -4.41 to -24.77 ‰ (mainly -10 to -15 ‰) (Lowry and Grassineau, 2009; Prave et al., 2009; Moles et al., 2015). Despite the overlap Tirinie is not thought to be affected by detrital contamination due to: 1) the measured isotopic values for both oxygen and carbon are remarkably smooth with no abrupt jumps in reconstructed values; 2) $\delta^{18}O$ and $\delta^{13}C$ are broadly in line, increased $\delta^{13}C$ depletion is broadly comparable to shifts in *Betula*, indicating an increase of plant respired CO_2 into ground waters; and 3) under phases whereby increased carbonate influence would be expected, units 6a to 6c, carbonate content falls to zero. As minimal evidence for detrital contamination and covariation exists, it is likely that Tirinie remained an open system (see caveat below for units 6a:c) with stable isotopic measurements performed on authigenic carbonate.

Regarding biomarker isotopic measurements, an important step is to identify a source for the *n*-C_{23} and *n*-C_{29} alkanes (used as δD_{aq} and δD_{terr}) as plant specific fractionation offsets may occur with different plant sources (Chapter 4). Previous studies have attributed the *n*-C_{23} alkane to *Potamogeton* (e.g. Aichner et al., 2010; Rach et al., 2014). From the palynological record *Potamogeton* is recorded throughout the sequence barring TirP-6. However, aquatic pollen is also recorded throughout for *Nuphar* and *Myriophyllum*. It is noted that *Nuphar lutea* predominantly produces *n*-C_{27} and *n*-C_{29} homologues (e.g. van den Bos et al., 2018). However, *Myriophyllum* does produce both

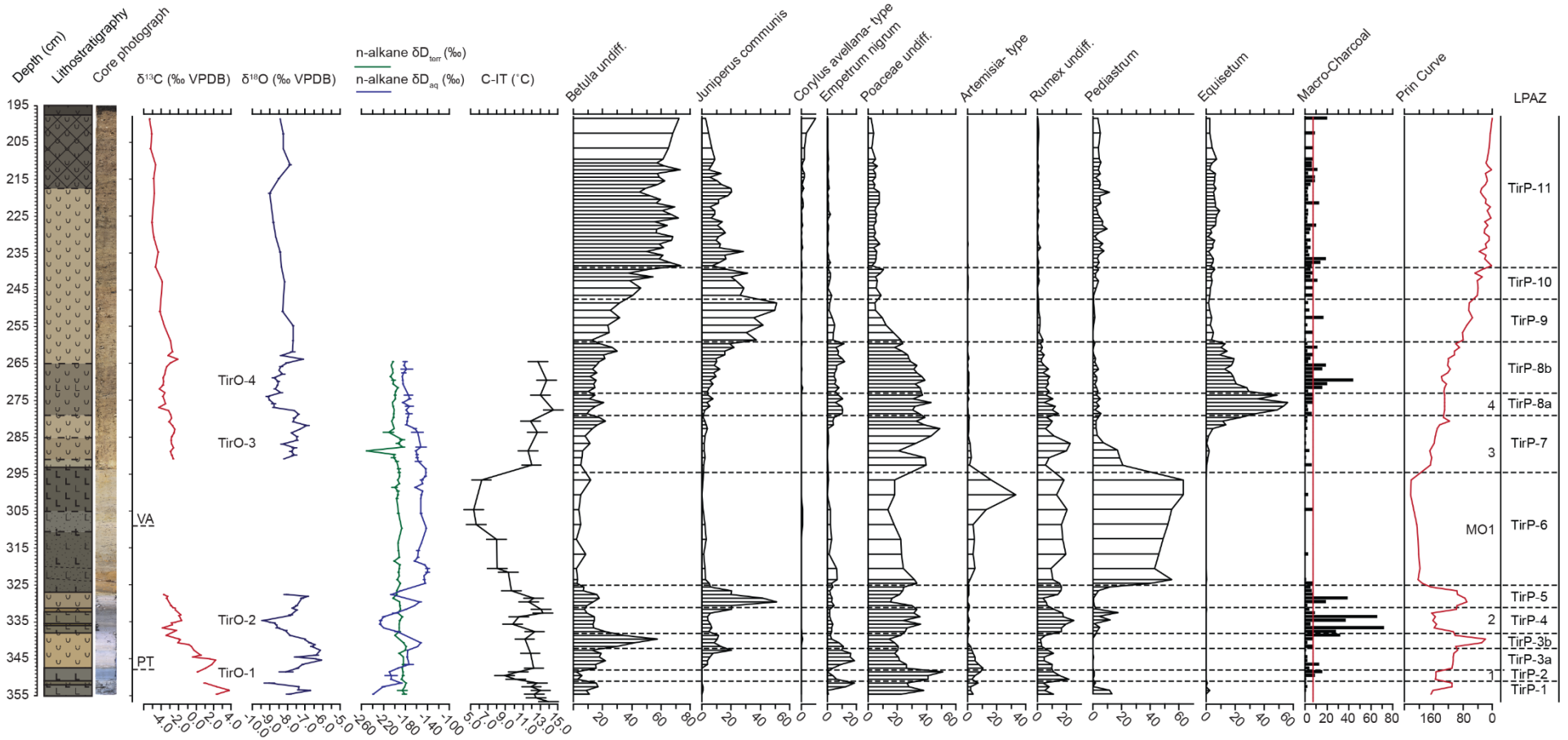

Figure 6.13 Summary of palaeodata presented from Tirinie. The principal pollen taxa have been included. The position of the Penifiler tephra at 348 cm and the Vedde Ash at 308-310 cm has been placed on to the diagram for ease of interpretation. Individual *n*-alkane concentrations have not been included here. Shown are oxygen isotopic depletion phases and oscillations as shown by the principal curve.

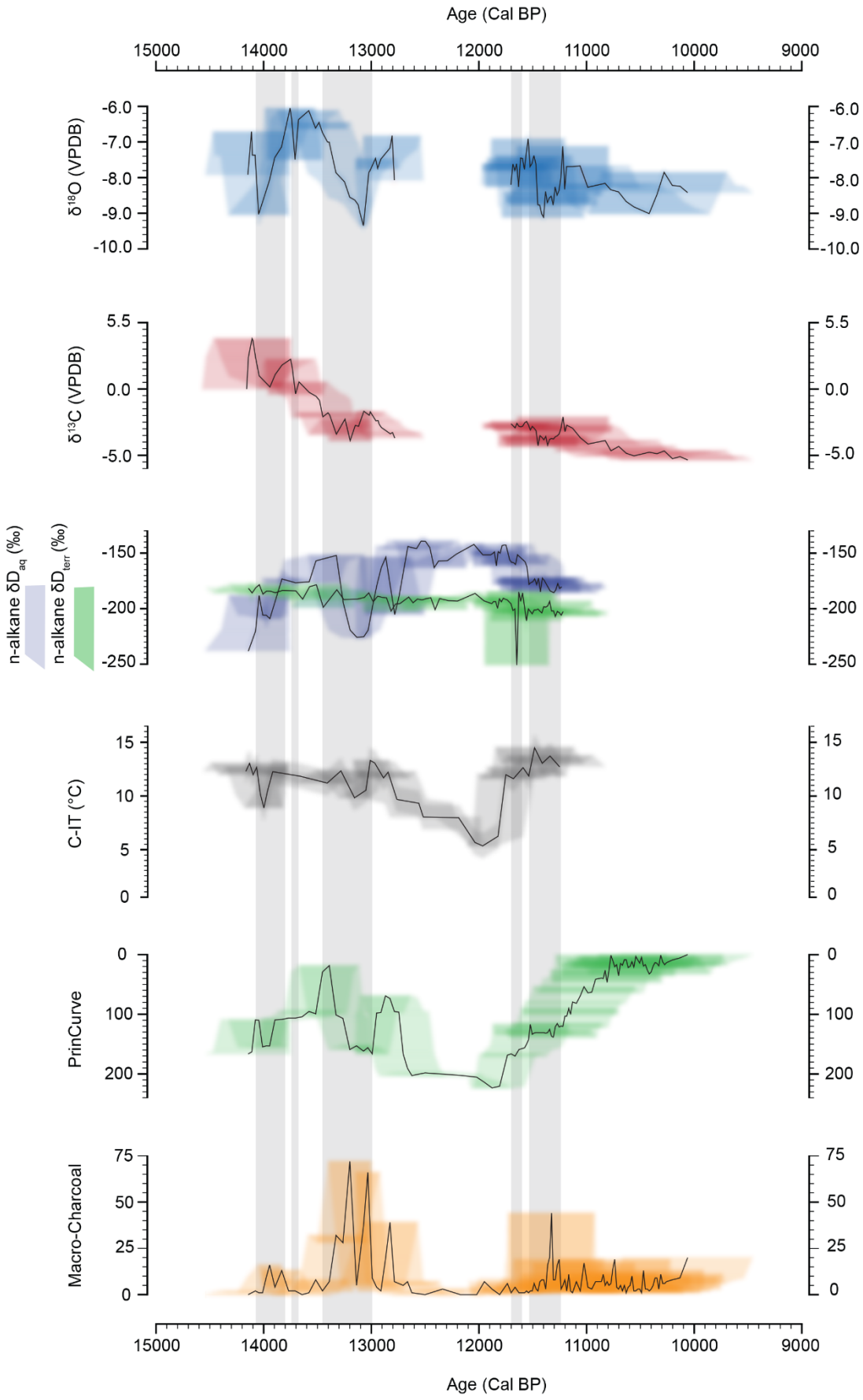

Figure 6.14 Comparison of all proxy data from Tirinie placed against age. Shown are $\delta^{18}O_{carb}$, $\delta^{13}C_{carb}$, δD_{aq} and δD_{terr}, C-ITs, the principal curve and macro-charcoal counts. Also shown on the diagram are phases discussed in text. Whilst not all represent climatic events or vegetation revertences, they are shown here in grey.

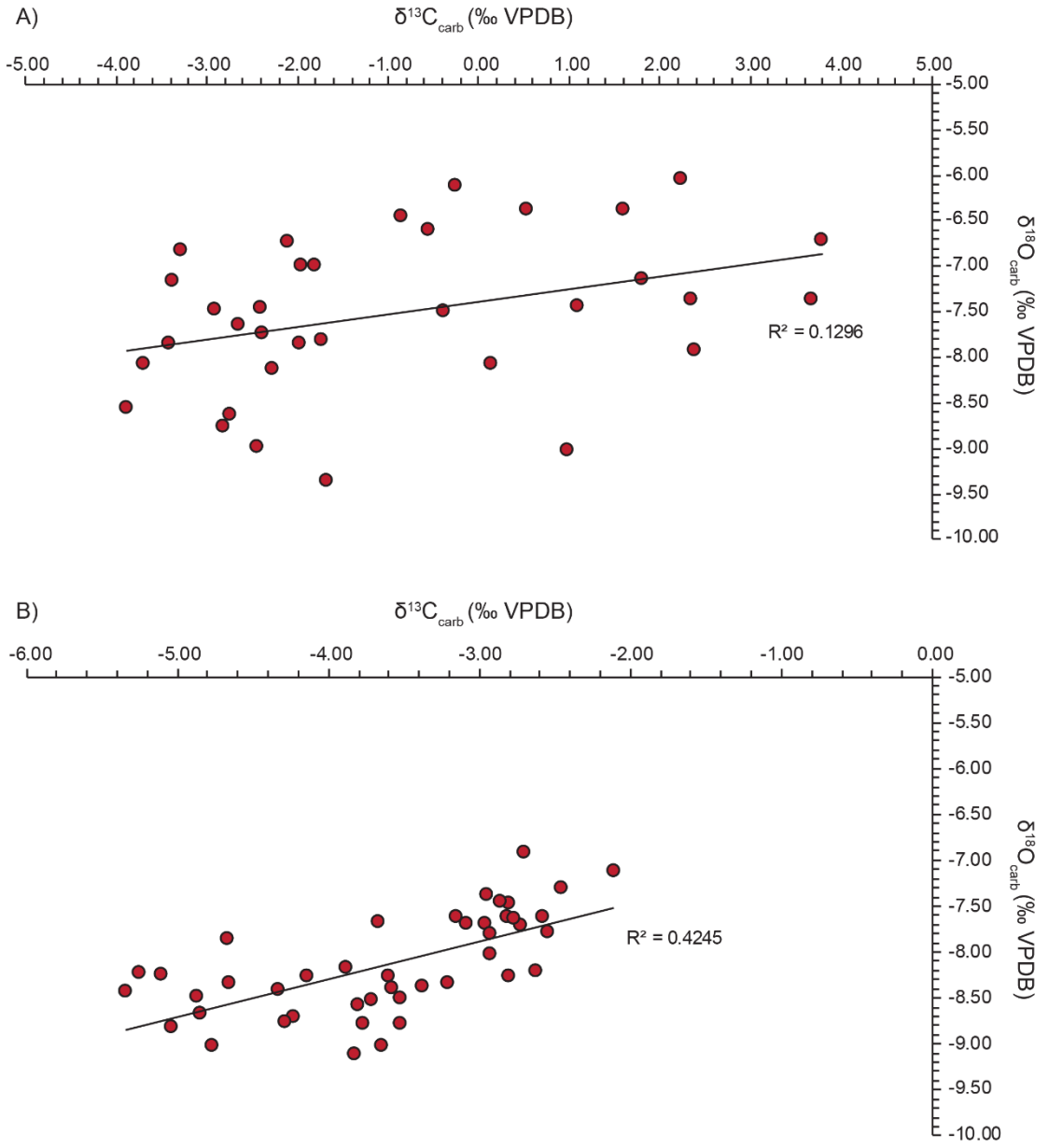

Figure 6.15 Co-variation between $\delta^{18}O$ and $\delta^{13}C$. The record has been split in this instance to demonstrate the regression differences between the two isotopic datasets between the different carbonate sedimentological units. A) Scatter plot showing co-variation of isotopic values from carbonates attributed to sediment units 1:5. B) Plot showing co-variation in the upper carbonate units; 7-12.

n-C_{23} and *n*-C_{25} homologues (Aichner, 2009; Liu and Liu, 2016). Based on evidence from Liu et al. (2018) reconstructed δD values for *Myriophyllum* *n*-C_{23} homologues overlap with that of *Potamogeton* (−169 ‰ (n=1) Myriophyllum; −164 ‰ (n=39) *Potamogeton*). As per other aquatic n-alkane records (e.g. Rach et al., 2014) *Potamogeton* is suggested to be the principal source for *n*-C_{23} with additions from *Myriophyllum*. For *n*-C_{29}, commonly attributed source organisms are *Betula* and *Salix* (Rach et al., 2014). This is favourable with observations from Tirinie, with *n*-C_{29} likely attributable to *Betula* and *Salix*.

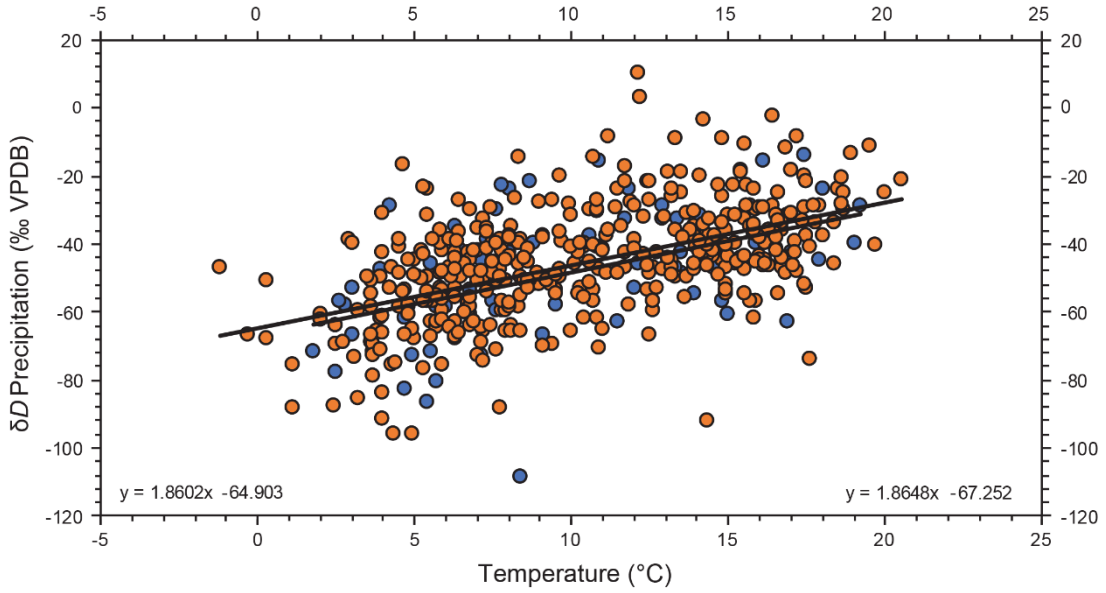

Figure 6.16 Sensitivity of monthly mean precipitation δ*D* values to air temperature from southern Britain. The isotopic data is generated from monitoring stations at Keyworth, Nottinghamshire (blue dots) and Wallingford, Oxfordshire (orange dots). Data generated from IAEA/WMO (2018).

Following delineation of the source and controls of the isotopic data, the $\delta^{18}O_{carb}$ can be interpreted in terms of the $\delta^{18}O$ of lake waters, influenced by mean annual temperature, and biomarker δ*D* values through the influence of temperature and precipitation (Chapter 4). A 1°C temperature change is expected to explain a 0.3 ‰ shift in $\delta^{18}O_{carb}$. In high-latitude polar regions temperature change has been shown to influence the δD_{precip} by up to 5 ‰ / °C (Alley and Cuffey, 2001) and data from IAEA/GNIP stations from southern Britain suggest offsets of ca 1.9 ‰ / 1°C (Figure 6.16) (IAEA/WMO, 2018). A change of 1°C is therefore expected to have between a 1.9-5 ‰ shift in δD_{precip}. This δ*D* signal is then further influenced by plant specific biosynthetic fractionation offsets for biomarker δ*D* plus any evaporitic modification directly from the leaf of the plant or soil (Sachse et al., 2012).

Early Windermere Interstadial- 14.16±0.41 – 14.06±0.30 Cal. ka BP

Mineral sediments dominated the early WI suggesting considerable erosivity in the catchment. Enriched $\delta^{18}O_{carb}$ and high C-ITs (-6.7 ‰ and 13°C respectively) suggest that warm climates prevailed. Warm temperatures suggest that the onset of the WI is not recorded at Tirinie. In accordance with other palaeoclimatic reconstructions from the BI (e.g. Brooks and Birks, 2000a; Watson et al., 2010; van Asch et al., 2012a; Lincoln, 2017) rising values in both proxies would be indicative of amelioration from the terminal DS/WI boundary. The modelled age for the onset of sediment accumulation appears late when compared with NGRIP (Rasmussen et al., 2014). This suggests that the Tirinie basin

was not competent before this, perhaps due to continued ice presence at high-altitude in proximity to the sequence (e.g. Walker and Lowe, 2017).

Nevertheless, the vegetation during the early WI (TirP-1) was dominated by open grassland communities (e.g. Poaceae, Cyperaceae, *Rumex*, and *Artemisia*) These pioneering taxa reflect the colonisation of deglaciated substrates and bear little resemblance to the warm climates suggested by the C-ITs and $\delta^{18}O_{carb}$. Whilst *Betula* and *Pinus* are recorded, it is probable that *Pinus* reflects a far travelled component (e.g Birks et al., 2005), with *Betula* (likely *B*. *nana*) existing sporadically in the catchment. Complete *B*. *nana* coverage is not presumed as minerogenic sedimentation was still ongoing (van Dinter and Birks, 1996). Throughout this initial phase enriched $\delta^{13}C$, demonstrates poor vegetative development with greater incorporation of atmospheric CO_2 with lake waters.

Owing to the biosynthetic fractionation offsets between δD_{aq} (enriched -82 ‰ Aichner et al., 2010) and δD_{terr} (depleted -157 ‰ Sachse et al., 2006) considerable depletion observed in δD_{aq} early during the WI indicates two scenarios: 1) a coupled moisture source between δD_{aq} and $\delta D_{terr,}$ with δD_{terr} artificially enriched through the loss of light δH from leaf water. This scenario suggests greater evapotranspiration (ETA) under low atmospheric humidity, thus increased aridity; or 2) a decoupled system with isotopically light meltwater affecting δD_{aq} values. Given the warm thermal conditions as suggested by C-ITs and $\delta^{18}O_{carb}$ at this time it is likely that the early WI was characterised by greater effective moisture. Further, as remnant ice from the last British Ice Sheet (BIS) was likely present from the DS throughout the WI in areas of Scotland (e.g. Bradwell et al., 2008) climatic amelioration would increase glacial melt; influencing the δ*D* ratio of aquatic systems. Scenario one can therefore be discarded.

From a vegetative view-point, following colonisation by pioneering taxa landscape compositional change is suggested by the establishment of an *Empetrum nigrum* heathland at 14.44±0.28 Cal. ka BP. The continued presence of open-habitat taxa reveals incomplete heathland coverage; suggesting a grassland/heathland mosaic. Whilst pollen concentrations are low, common in pioneering communities with low landscape densities (Birks et al., 2005), the presence of *E*. *nigrum*, with associations with moisture (Brown, 1971; Bell and Tallis, 1973) confirms moisture availability during the early WI. Thus with more certainty, the second scenario above is accepted.

Early Windermere Interstadial- 14.06±0.30 – 13.83±0.18 Cal. ka BP.

Reduced $CaCO_3$ and a shift to depleted $\delta^{18}O_{carb}$ (TirO-1; Figure 6.13; Figure 6.14) with

secondary summer temperature and δD_{aq} reductions are noted between 14.06±0.30 – 13.83±0.18 Cal. ka BP. These observations suggest a climatic event occurred early during the WI at Tirinie. If $\delta^{18}O_{carb}$ depletions are taken to reflect annual temperature change, the onset of $\delta^{18}O_{carb}$ depletion which occurs prior to changes is C-ITs (mean July temperature) may reflect heightened seasonality; with winter temperature changes controlling the initial isotopic shifts. Secondary C-IT declines of 3.8°C (from 12.7 to 8.9°C) and further $\delta^{18}O_{carb}$ depletion of 1.66 ‰ (from -7.4 to -9.0 ‰) suggest a slightly lagged summer climate response to initial depletion in $\delta^{18}O_{carb}$. Nevertheless, all proxy evidence suggests a climatic event with a suppression of summer and mean annual temperatures during the early WI. As both δD_{aq} and δD_{terr} demonstrate depletion, albeit with the former more depleted than the latter, aridity is proposed with δD_{terr} enrichment through evapotranspirative losses (Rach et al., 2014).

Against a backdrop of climatic change, a vegetation revertence is suggested by the PC (Figure 6.13; 6.14) and RoC (Figure 6.7) analyses, indicating landscape compositional change (Simpson and Birks, 2012). The deviation to more positive values of the PC and the increase in RoC over a short stratigraphic distance (Figure 6.7) demonstrates that this revertence was abrupt. Losses in *E. nigrum* suggest that the heathland community was replaced by herbaceous open-habitat grassland with greater abundances of Poaceae, Cyperaceae and disturbed ground indicators including *Rumex* and *Artemisia* (TirP-2). Increased ACL and tACL values confirm this shift to a grassland dominated community alongside increased concentrations of n-C_{31}; commonly attributed to grasses (Rach et al., 2014). Therefore, these taxa, common to Arctic/alpine environments appear as a response to early WI climatic cooling and hydrological change. The loss of *Empetrum* from the landscape and increased xerophytic herbaceous taxa, including *Artemisia* spp., further signified a reduction in available moisture (Walker, 1975) during this climatic event.

Charcoal is prevalent during this phase suggesting greater fire occurrence. However increases in macro-charcoal (TirC-1; Figure 6.13), suggesting the occurrence of local fires occur following the vegetation revertence. It is possible that fires occurred in the Tirinie catchment following a shift in climatic conditions, perhaps through greater aridity, but once an appropriate fuel source existed on the landscape. In this instance *E*. *nigrum*. Low pollen concentrations throughout this phase, coupled with a return to mineral sedimentation, suggests erosivity following landscape destabilisation with increased sedimentation rates at this time.

Mid- Windermere Interstadial- 13.83±0.18 – 13.48±0.29 Cal. ka BP.

The mid-WI was characterised by a switch to lacustrine marl sedimentation in the Tirinie basin inferred from high percentages of $CaCO_3$. A return to less depleted $\delta^{18}O_{carb}$ and a return to warm C-IT's (11.2 to 12.3°C), suggest that a phase of climatic warmth followed the early Interstadial climatic event. The increase in δD_{aq} and stable δD_{terr} values indicate that moist conditions prevailed with δD_{aq} more enriched than δD_{terr} for the first time in the sequence. Lower δD_{terr} perhaps points to greater atmospheric humidity during this time. Enhanced moisture is further confirmed with the re-expansion of *Empetrum* heathland between 13.83±0.18 and 13.64±0.27 Cal. ka BP.

The expansion of *Juniperus* and reduction in herbaceous taxa between 13.64±0.27 and 13.58±0.28 Cal. ka BP (TirP-3a) highlights the replacement of open ground taxa with a *Juniperus* scrub, likely reflecting greater soil maturation (Preston et al., 2002). *Juniperus*, being heliophilic, provides further evidence of *Betula* being of *B*. *nana* type as *Juniperus* will not flower under shaded conditions (Huntley and Birks, 1983). Occurrences of *Typha latifolia* demonstrate that summers were at least 13°C (Isarin and Bohncke, 1999) during the mid-WI. Whilst these plant indicator temperatures are slightly higher than C-ITs, 13°C is within error of the chironomid technique. Further, as chironomid resolution is reduced at this time it is possible that higher temperatures would be identified if analysed in greater detail.

Increased *Betula* undiff. between 13.58±0.28 and 13.39 ±0.28 Cal. ka BP (TirP-3b) are likely due to greater colonisation of *B*. *nana*, however, the identification of a tree birch fruit (Ian Matthews, pers. comm. 2017) points the development of stands of local tree birch in the Tirinie catchment. Summer temperatures of 12°C are required to sustain tree birch (Birks, 1994). Temperatures between 11.2-12.3°C therefore reveal favourable conditions for tree birch growth and flowering, coinciding with a reduction of the shade intolerant shrubs *Empetrum* and *Juniperus*. tACL values close to 29 (Figure 6.9) indicate greater contributions of *Betula* at this time. Lower $\delta^{13}C$ values (-3.41 ‰) through a greater supply of plant respired ^{13}C depleted CO_2 into the lake body (Leng and Marshall, 2004) and higher pollen concentrations in lake sediments provide further evidence of greater vegetation development and soil maturation in the catchment during the mid-WI

At 13.52±0.29 Cal ka BP depleted $\delta^{18}O_{carb}$ values may suggest a phase of reduced mean annual temperatures. However, there is no coeval response in additional proxy sources (Chapter 4) and it does not meet the criteria for delineating an event outlined in this thesis.

Late Windermere Interstadial- 13.45±0.29 - 13.02±0.12 Cal. ka BP.

During the mid- late WI, a phase of $\delta^{18}O_{carb}$ depletion (Tir-O2) suggests a second WI climatic event. The onset of $\delta^{18}O_{carb}$ depletion (Figure 6.14) occurrs at 13.45±0.29 Cal. ka BP, with depletion from -6.45 to -9.35 ‰. This occurred prior to declines in summer temperature (Figure 6.14). As per the early WI climatic event this depletion relative to summer temperature change suggests greater seasonal temperature variability. Which, in light of the continued presence of tree birch on the landscape, was not sufficient to directly affect the vegetation assemblage. Tracking the $\delta^{18}O_{carb}$ depletion, albeit slightly delayed, is the onset of depletion in δD_{aq} suggesting a common origin. It is only following enhanced δD_{aq} depletion (from -152.56 to -225.74 ‰), greater than depletion in δD_{terr}, at 13.26±0.24 Cal. ka BP are summer temperature declines observed (12.3 to 9.8°C). δD_{aq} depletion, more so than $\delta D_{terr,}$ suggests a phase of evaporitic enrichment in a coupled hydrological system; thus, a phase of aridity. From the available data a clear sequence of events is presented. Initially mean annual temperature declines occurred, with a subsequent δD_{aq} depletion, relative to δD_{terr}, interpreted as the onset of drying. Finally, summer temperature changes occurred alongside a greater shift in aridity and a coeval strengthening of mean annual temperature change. The collection of multi-proxy data suggests a major climatic event at Tirinie at this time.

Occurring before summer temperature declines, in conjunction with shifts in δD_{aq}, is a shift to higher values in the PC and RoC analysis suggesting widespread compositional turnover and a vegetative revertence (Revertence 2). During this phase woody vegetation contracted and open ground herbaceous vegetation expanded (TirP-4), dominated by Arctic/alpine taxa. Key vegetation in the Tirinie catchment throughout this revertence phase included: Poaceae and *Rumex* but also larger populations of Caryophyllaceae, Asteraceae, Compositae (Lactuceae), Saxifragaceae, *Thalictrum* and *Selaginella selaginoides*. Whilst the reduction of woody vegetation percentages could indicate a reduction in flowering ability under a period of climatic stress, the Arctic-alpine community identified here is more indicative of wholescale landscape replacement under a background of significant climatic change. Further, if a reduction in flowering ability were to occur, this might be expected to be instantaneous, however, *Betula* concentrations are rising through this phase, showing the opposite effect. From the climatic data presented it appears that seasonal temperatures and aridity are important factors in initiating the vegetation revertence. Summer temperature changes may then act as a secondary factor modulating vegetation relative to climate.

Similar to the early WI climatic event and vegetation revertence, increases in macro-charcoal (TirCc-2, TirC-2; Figure 6.13; 6.14) indicate greater wildfire prevalence in the

Tirinie catchment during this climatic deterioration but only after the vegetation change occurred, suggesting that fire was an important component of the landscape, but only after climatic and vegetation change.

Higher *n*-alkane concentrations across all compound classes reflects in-washing of molecular structures following the break-down of soils under cold climates. Further, the increase in TOC throughout this period, suggests both allochthonous and autochthonous basin loading following a likely resumption of periglacial activity. Small increases in ACL and tACL values throughout the late WI climatic event (Figure 6.9) highlight the change to a grassland dominated landscape, whilst, lower pollen concentrations, coupled with minerogenic sedimentation, are suggestive of increased sedimentation rates. Reduced concentrations are also a result of lower pollen production rates of open-habitat taxa compared to the *Betula* dominated landscape in the preceding phase (Andersen, 1967).

Late Windermere Interstadial- 13.02±0.12 – 12.74 ± 0.28 Cal. ka BP.

The late-WI was characterised by a return to warm climates (Figure 6.13; 6.14). $\delta^{18}O_{carb}$ and δD_{aq} enrichment allied to greater carbonate precipitation indicates warm mean annual temperatures with significant moisture availability. Peak C-ITs (13.3°C) further suggests a warm climate. These climatic changes coincided with the loss of open-habitat assemblages and a return to a Juniper scrub dominated landscape (TirP-5). Reduced percentages of *Betula spp*. compared to the Mid-WI (TirP-3b), and significant *Juniperus* scrubland suggest considerable light availability with *Betula* attributed to *B*. *nana*. Although sufficiently warm (Birks, 1994), it is not likely that tree birch migrated back into the Tirinie catchment late in the Interstadial. High pollen concentrations during this time suggests that the late-WI was characterised by greater vegetation densities or, at least in the case of *Juniperus,* greater flowering under warm climates in open vegetation (Broström et al., 2008).

Loch Lomond Stadial- 12.74±0.28 – 11.74±0.26 Cal. ka BP.

Whilst no oxygen isotopic data exists between this date range, large-scale climatic and environmental changes are inferred from the C-IT data and sedimentology (units 6a to 6c). Stepped decreases in C-ITs, from 12.2°C to sequence minima of 5.4°C, indicates a high-magnitude climatic event. The reconstructed values are comparable to summer temperature changes observed during the LLS elsewhere in Scotland (e.g. Brooks and Birks, 2012). Further, the identification of the Vedde Ash (Candy et al., 2016), dated to 12,023±46 (Bronk Ramsey et al., 2015) confirms the LLS attribution of these sediments. Whilst the sediments were sampled for radiocarbon, the lack of datable material prevented a more robust assessment of the onset and termination of this phase.

Nevertheless, minerogenic sedimentation, which has widely been used to demark the LLS in Scotland (e.g. Pennington et al, 1972; Walker, 1975; Walker and Lowe, 1990; 2017), with coeval reductions in $CaCO_3$ suggest catchment instability and allogenic sediment loading into the basin. Three phases of heightened TOC, at 12.74±0.28 12.21±0.23 and 11.75±0.26 Cal. ka BP, roughly equating to the early, mid and late LLS show pulsed nutrient loading likely in response to small changes in environmental conditions throughout the LLS.

In association with the reduction in temperature, woody vegetation in the catchment markedly reduced. The vegetation of this interval (TirP-5; TirP-6) was characterised by a species-rich open grassland, dominated by A*rtemisia*, *Rumex* and Poaceae, occurring alongside Cyperaceae, Caryophyllaceae, Compositae: Lactuceae, *Helianthemum*, Saxifragaceae, *Thalictrum* and the pteridophytes *Cryptogramma crispa* and *Selaginella selaginoides*. Many of these taxa occur in present day steppic/tundra environments, on barren ground and on soils prone to solifluction or cryoturbation (Birks and Matthewes, 1978; Brysting et al., 1996). Saxifragaceae in particular suggests the establishment of snow-bed vegetation (Walker, 1975), with these beds providing a mechanism for mass wasting processes. The establishment of *Artemisia* further suggests arid continental climates throughout the LLS (Birks and Matthewes, 1978). Minimal evidence of burning exists during the LLS, but fires may have been a possibility at the onset of the LLS (TirCc-3, TirC-3), which appear to have coincided with a loss of thermophilic vegetation. It is proposed that cold/arid climates and a changing vegetation assemblage allowed for greater fire incidence on the landscape.

Some shrub and tree taxa were present during the LLS, including *Salix*, *Betula*, and *Pinus sylvestris*. The incidence of *Pinus sylvestris* is likely reflective of long distance transport under stronger wind regimes (e.g. Isarin et al., 1997; Brauer et al., 2008) with *Betula* of *B*. *nana* type. Continued presence of *Salix* and *Empetrum* may indicate greater protection from harsh climatic conditions, either in sheltered localities or within seasonal snow-beds, also acting as a moisture supply. The cold climatic conditions of the LLS indicted that at least seasonally, snow cover was likely (Isarin et al., 1998). Continued presence of shrub taxa may indicate why ACL and tACL shifts to lower average chain lengths during the LLS. However, lower average chain lengths may also be a product of a reduced growing season as angiosperm plants produce shorter n-alkanes under shorter flowering seasons (Piasentier et al., 2000; Sachse et al., 2009). Late increases in *Artemisia* after ca 12.0 Cal. ka BP appear to coincide with the coldest temperatures of the LLS; which, with reductions in other taxa may demonstrate greater spatial expansion (Birks and Matthewes, 1978). Being xeric, the late-WI was probably drier. This is a

possibility in the lee of the West Highland Ice-Field which may have built up late during the LLS (Palmer et al., 2010; MacLeod et al., 2011) with effective rain-shadow effects from the ice. The vegetation assemblage presented here is common across comparative stratigraphies within Britain (e.g. Pennington et al., 1972; Walker and Lowe, 1990; Edwards and Whittington, 2010) further cementing LLS associations.

Holistically the vegetation changes observed during the LLS are shown to have the greatest influence over the PC throughout the record (Figure 6.13; 6.14). Response curves show greater influences of Poaceae, *Rumex* and *Artemisia*. An interesting facet of the PC curve is the structure held throughout this stage which, as already postulated, reflects the significant contribution of *Artemisia* during the second half of the LLS coinciding with the coldest temperatures recorded from the sequence (Chapter 11).

Despite aridity suggested by *Artemisia*, the biomarker δ*D* record during this phase warrants further explanation as data are markedly different than observed from other Stadial sequences (e.g. Rach et al., 2014; Muschitiello et al., 2015). The values are enriched with no suggestion of convergence, therefore aridity. Enriched δD_{aq}, alongside increases in the concentration of *n*-C_{23} could be explained by the following processes: 1) a relatively moist Stadial at Tirinie; 2) changes in source moisture tracks (e.g. Bakke et al., 2009); and 3) shifts in the aquatic source organism, with enrichment reflecting different biosynthetic fractionation offsets of different species. The former can be discounted on the evidence of *Artemisia* presence and limited growth of the West Highland Ice Field (Golledge et al., 2008). If the Stadial was moist then, this ice-field would likely have grown much larger (Golledge et al., 2008). The second scenario can be discounted based on the lack of comparative enrichment within $\delta D_{terr.}$ Unless moisture sources between the biomarker end-members were decoupled, under different moisture regimes and an enriched vapour source, both series should reveal similar enrichment. The latter is more difficult to explain as the only aquatic identified at this time is *Pediastrum*. During the LLS, percentages and concentrations of *Pediastrum* coenobia increase markedly, thought to reflect significant nutrient loading form in-washing soils (Weckström et al., 2010). Further reflected by greater concentrations of *n*-alkanes at the onset of minerogenic sedimentation and pulsed TOC observations.

Pediastrum and other green algae have a primary composition of *n*-C_{17}/*n*-C_{19} (Blokker et al., 1998; Sachse et al., 2012) but also mono-unsaturated *n*-C_{21}/*n*-C_{23} homologues (Blokker et al., 1998) and significant fatty acid components (Blocker et al, 1998; Zhang and Sachs, 2007). These are unlikely to be recorded at Tirinie as saturated and unsaturated compounds were separated, minimal *n*-C_{17} was recorded and fatty acid

fractions were not run. Furthermore, a shift in source organism is difficult to reconcile with increases in *Pediastrum* during the late WI climatic event; whereby δD_{aq} depletion is observed. The latter argument can therefore be discounted. It may be possible that lake hydrology is modulating the change in δD_{aq}. Continued high abundance *Pediastrum* may further indicate lake level lowering under low effective moisture (Sarmaja-Korjonen et al., 2006). It is therefore possible that evaporitic enrichment of the δD_{aq} signal has occurred which would explain considerable enrichment of δD_{aq} relative to δD_{terr}. Interpreting the biomarker record climatically is therefore difficult, however, if the biomarker δD is reflecting lake water isotopic enrichment then the climatic must have been arid throughout the LLS.

Early Holocene- 11.74±0.26 – 11.14±0.44 Cal. ka BP

A return to carbonate sedimentation coincided with rising summer temperatures and enrichment in $\delta^{18}O_{carb}$ (12°C and -7.6 ‰ respectively), indicating climatic amelioration following the LLS. The vegetation assemblage at this time (TirP-7) was characterised by subtle changes from the Arctic/alpine communities of the LLS with the disappearance of *Artemisia*, Compositae: Lactuceae, Saxifragaceae and *Selaginella selaginoides* from the landscape. However, some LLS taxa persisted, which, like the early-WI (TirP-1), indicates that pioneering taxa continued to be present on the landscape into the early Holocene. The increase in *Salix* likely relates to increased flowering potential under warm conditions, but also greater landscape abundances following the LLS, within which the taxon was restricted to sheltered localities. Further, the increase in the oligotrophic *Myriophyllum spp*. (Edwards and Whittington, 2010) and reduction in *Pediastrum* demonstrates higher lake levels and a reduced allogenic input at this time. Low *n*-alkane concentrations and increasing ACL and tACL indices suggest the prevalence of an open grassland community.

Warm climates throughout the early Holocene were punctuated by two phases of lower mean annual temperatures, as revealed by oxygen isotopic depletions (TirO-3 and TirO-4; Figure 6.13; 6.14) both of which occur in conjunction with subtle changes in basin sedimentology, increased TOC and decreased carbonate content at 11.63±0.31 and between 11.49±0.35 - 11.24±0.42 Cal. ka BP. In contrast to the events from the WI, where summer temperature declined, C-ITs do not suggest a summer temperature change with temperatures between 11.6-14.5°C throughout this phase. However, $\delta^{18}O_{carb}$ depletions of 0.6 ‰ and 1.5 ‰ are observed which perhaps indicate a climatic deterioration manifest by increased seasonality. Whilst it is acknowledged that the resolution of the C-ITs is not sufficient throughout the isotopic depletion(s), samples were taken from the most depleted $\delta^{18}O_{carb}$ sediments suggesting no significant summer

temperature response. This is contrasting to other early Holocene events observed from elsewhere in Britain (e.g. Blockley et al., 2018).

For each of these events minor depletions in δD_{aq} are observed, ca 17.5 ‰ and 27.7 ‰ respectively, with a convergence of δD_{aq} and δD_{terr} between 11.54±0.34 - 11.24±0.42 Cal. ka BP. The convergence of the end-members suggests a drying phase; greater evapotranspiration within δD_{terr}, increasing overall enrichment. It is important to note that, whilst this drying may have had an effect on the basin hydrology, lake water recharge must have been constant as without constant replenishing, under drier conditions, residence times would increase making the waters susceptible to evaporitic isotopic modification. This process is not observed here with depletion not enrichment observed in $\delta^{18}O_{carb}$ and δD_{aq}.

Whilst the vegetation surrounding Tirinie was characterised by low lying herbaceous vegetation during the early Holocene, the pollen suggests a brief phase of variability at 11.63±0.31 Cal. ka BP. This variability (Oscillation 3; Figure 6.13) is characterised by an increase in the disturbed ground indictor, *Rumex*, and increased littoral, open-habitat vegetation, e.g. Cyperaceae, suggesting increased open ground indicators. Further a pause is observed in the down-trending *Pediastrum* curve, which alongside reduced oligotrophic *Myriophyllum spp*. may indicate a brief phase of allogenic inwash, combined with the change sedimentology. Despite this, the suggested climatic and environmental changes at this time appear minor and occur over one sample. As the early Holocene was characterised by significant environmental change following the LLS it is unknown whether this is a product of natural variability or a real climatic/environmental event in the record.

However, the latter climatic event between 11.50±0.35 - 11.24±0.42 Cal. ka BP (Figure 6.14) is much clearer and is formally attributed. Here increases in *Equisetum*, elevated Poaceae and *Rumex*, and fluctuating *Empetrum* percentages are observed. The vegetation surrounding the lake at this time was characterised by an open heathland with grasses and sedges occupying areas of incomplete heath coverage, and significant colonisation of *Equisetum* in the littoral zone.

The expression of this early Holocene event appears to share associations with both the vegetation surrounding Tirinie and the littoral environment. In this instance, it is probable that drying, as perceived by changes in δD_{aq} and δD_{terr}, lowered the lake level allowing the proliferation of *Equisetum*. This is suggestive of fenland development. However, the terrestrial environment, with contracting *Empetrum*, and expanding *Rumex* may be

responding to increased seasonal change and aridity shifts. The lack of coeval expansion of typical cold climate taxa and the presence of *Myriophyllum* suggests summer temperatures of at least 9°C (Isarin and Bohncke, 1999), which is confirmed by the C-ITs. Whilst pollen concentrations are low, increases in Poaceae between 11.3 and 11.2 Cal. ka BP (TirP-8b) reflects increased grassland dominance.

Contrasting to other vegetation-based events throughout the sequence, the principal curve demonstrates a pause between 11.49±0.35 - 11.24±0.42 Cal. ka BP (Figure 6.14). This pause is thought to reflect greater abundances of *Equisetum* with minor increases in low lying open-habitat taxa as opposed to wholescale vegetation shifts as observed during the WI. This pause relates to a pause in successional development in the catchment. This is further shown by reduced compositional turnover within the RoC analyses. Similar to other intervals during the LGIT at Tirinie, fire appears to be a significant component of the landscape (TirCc-5; TirC-4; Figure 6.14) but only once lake level reductions and heathland opening occurred. Again, reflecting increased fuel sources on the landscape.

Later early Holocene- <11.14±0.44 Cal. ka BP

The lack of high-resolution palaeoclimatic data throughout the remainder of the Tirinie sequence does not permit assessments of changing climatic regimes. In terms of vegetation, the remainder of the sequence is characterised by a typical successional sequence in Britain. Initially *Empetrum* heath gives way to extensive *Juniperus* scrub. The loss of *Empetrum* as Juniper proliferates may reflect increasing soil development and richer base status (Huntley and Birks, 1983). Increasing *Betula* undoubtedly reflects colonisation of tree birch and the development of an open birch woodland. Alongside *Betula* it is probable that willow is also present; although pollen differentiation was not undertaken on *Salix* spp. grains. The continued occurrence of *Juniperus* demonstrates the open nature of the birch woodland. The increase in *Filipendula* alongside *Betula* suggests the development of damp fertile soils (Birks and Matthewes, 1978) with *Filipendula* and *Juniperus* indicating the establishment of meadow communities in woodland openings (Hormata, 1995). The final stage depicts the first occurrence of *Corylus* in the Tirinie catchment. Full *Betula*/*Corylus* woodland (e.g. Walker, 1975; Whittington et al., 2015) however, is not depicted at Tirinie. Nevertheless, continually depleted $\delta^{13}C$ demonstrates greater vegetation development and significant input of plant respired CO_2 into vadose waters and into the lake.

At 10.42±0.56 Cal. ka BP a possible shift in vegetation is noted (TirP-11). Subtle variability in the PC (Figure 6.14) are manifested as reduced *Betula* and increased

Juniperus percentages. These observations suggest greater opening of the landscape which is replicated in concentration data. This event is not formally defined at Tirinie however, as the change only occurs across two taxa with no additional indicators. Increases in charcoal concentrations are noted (TirCc-9; Figure 6.13) but their presence in the macro record are insignificant; suggesting no local fire input at this time.

6.8 Chapter summary

This chapter summarises the litho-, palyno- and climatostratigraphic findings from Tirinie, Grampian Highlands, Scotland. All data indicates the sequence was deposited during the LGIT. Millennial-scale climatic and vegetation development follows that of all other sequences in Scotland (Chapter 2) with climatic warmth and moist conditions leading to the development of woody vegetation. During the LLS summer temperatures cool with a phase of aridity postulated (evaporitic biomarker signal) leading to the development of an open-habitat community. During the early Holocene, a dominant successional sequence is observed whereby grasslands are replaced by birch woodland.

However, superimposed on this millennial-stratigraphy, Tirinie demonstrates a series of mean annual and summer temperature declines, with heightened aridity, during the Interstadial and Holocene. These changes appear to affect the vegetation surrounding Tirinie which is clearly demarked in the pollen reconstruction but also the Principal Curve. During the WI vegetation-based changes show the replacement of woody vegetation with Arctic/alpine and disturbed ground indicators (*Rumex* and Poaceae); it is only following these vegetation shifts that fire becomes important in the landscape. During the early Holocene, mean annual temperature declines are noted alongside greater aridity, however summer temperatures do not change, suggesting a more seasonal signal. These changes appear to promote littoral and marginal taxa alongside small contractions of woody taxa. Whilst a vegetation response is observed, they do not appear as major as those during the Windermere Interstadial.

Chapter 7. Results from Palaeolake Flixton

Sequences from around Star Carr comprise a suite of basins within Palaeolake Flixton, Vale of Pickering, north-east England, containing calcareous infills. These locations, as a mid-point within the transect of sites studied as part of this research and on the eastern coast of the England, make an ideal location to investigate the expression and landscape response of abrupt climatic events during the LGIT. It is supposed that the palaeoclimatic expression of abrupt events will differ compared to other sites, due in part to the altitudinal/latitudinal setting and distance from oceanic source; where abrupt events are likely to originate (e.g. Rohling and Pälike, 2005; Muschitiello et al., 2015). Therefore, the vegetation response to events at Palaeolake Flixton may differ from other sites.

Palaeolake Flixton has been palynologically analysed at various times during the past 60 years. The most recent of these assessments came in 1998 when Petra Dark examined both lake edge and lake centre sequences, to understand the palaeobotany and phytogeography of Palaeolake Flixton (Dark, 1998a, b, c). The longer of these sequences, which spans the LGIT, exhibits a series of revertences whereby reductions in *Betula*, are replaced by concomitant increases in first Poaceae, then *Juniperus*, and certain open ground taxa (Dark, 1998c). Through the Interstadial two of these vegetation revertences have been observed, with the possibility of at least one more of these events occurring within the early Holocene (Dark, 1998c). These revertences were postulated to reflect short phases of climatic deterioration across Palaeolake Flixton. Nevertheless, evidence of climatic change is based entirely on the nearby site of Gransmoor (e.g. Walker et al., 1993a).

Reinvestigations of Palaeolake Flixton site has led to the recovery of a series of different sequences, two of which will be presented within this chapter, Star Carr Core B and Core C. On-going palaeoclimatological investigations throughout these sequences, permits a reinvestigation of vegetation change at this locale throughout the LGIT. This chapter will present the litho-, palyno-, and climato-stratigraphic results from Star Carr Cores B and C and provide an interpretation of these results based on the current understanding of climatic and vegetation change during the LGIT.

7.1 Basin sedimentology and stratigraphy

A series of research expeditions at Palaeolake Flixton revealed a complex basin bathymetry with a suite of deep basins separated by relatively higher ground (Figure 7.1) From this survey, seven locations were identified, Cores B to H (Palmer et al., 2015), with the focus of this thesis, directed toward to the western edge of the survey using Cores B (54.215919, -0.42034507) and C (54.21695, -0.422318: Figure 7.1)

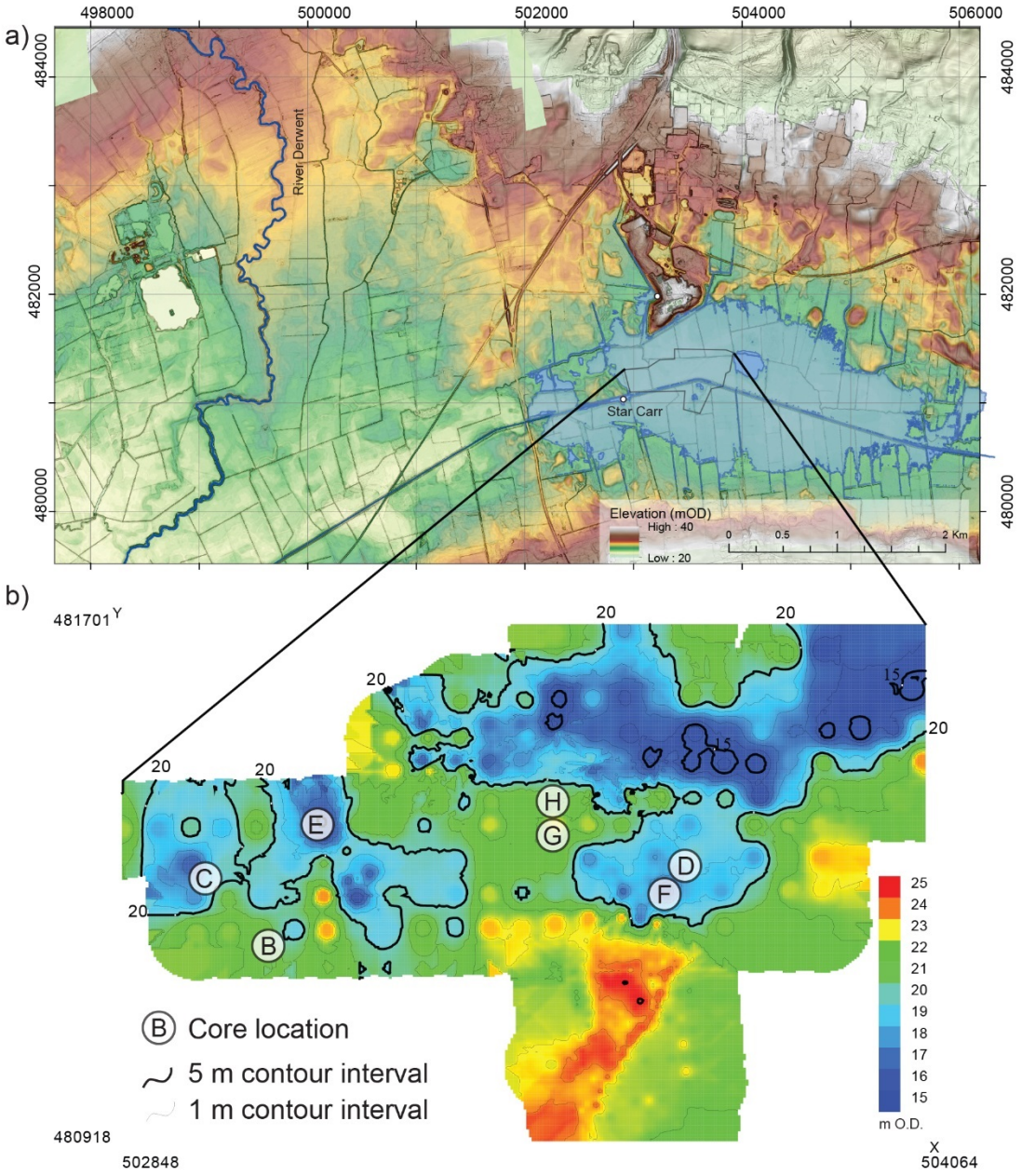

Figure 7.1 A) Hillshade model of the eastern Vale of Pickering and B) bathymetric map of the western periphery of Palaeolake Flixton. Shown are borehole locations B to H. Boreholes B and C will be presented here. Modified from Lincoln (2017) and Palmer et al. (2017).

The lithostratigraphy from Cores B and C are presented in Figure 7.2. Owing to the complex nature of the sediments within both sequences and a lack of key marker horizons, composite profiles from Cores B and C were constructed on depth assessments alone. The shorter Core B, 517 cm at base, does not contain a traditional tripartite sediment sequence, however a layer of sand and gravel at ca 300 cm perhaps points to a hiatus within the record. In contrast, the deeper Core C, 735 cm at base, does not contain a gravel band but does contain an extended sequence of silts and clays, indicating a complete tripartite sequence. This difference, with the knowledge that a full

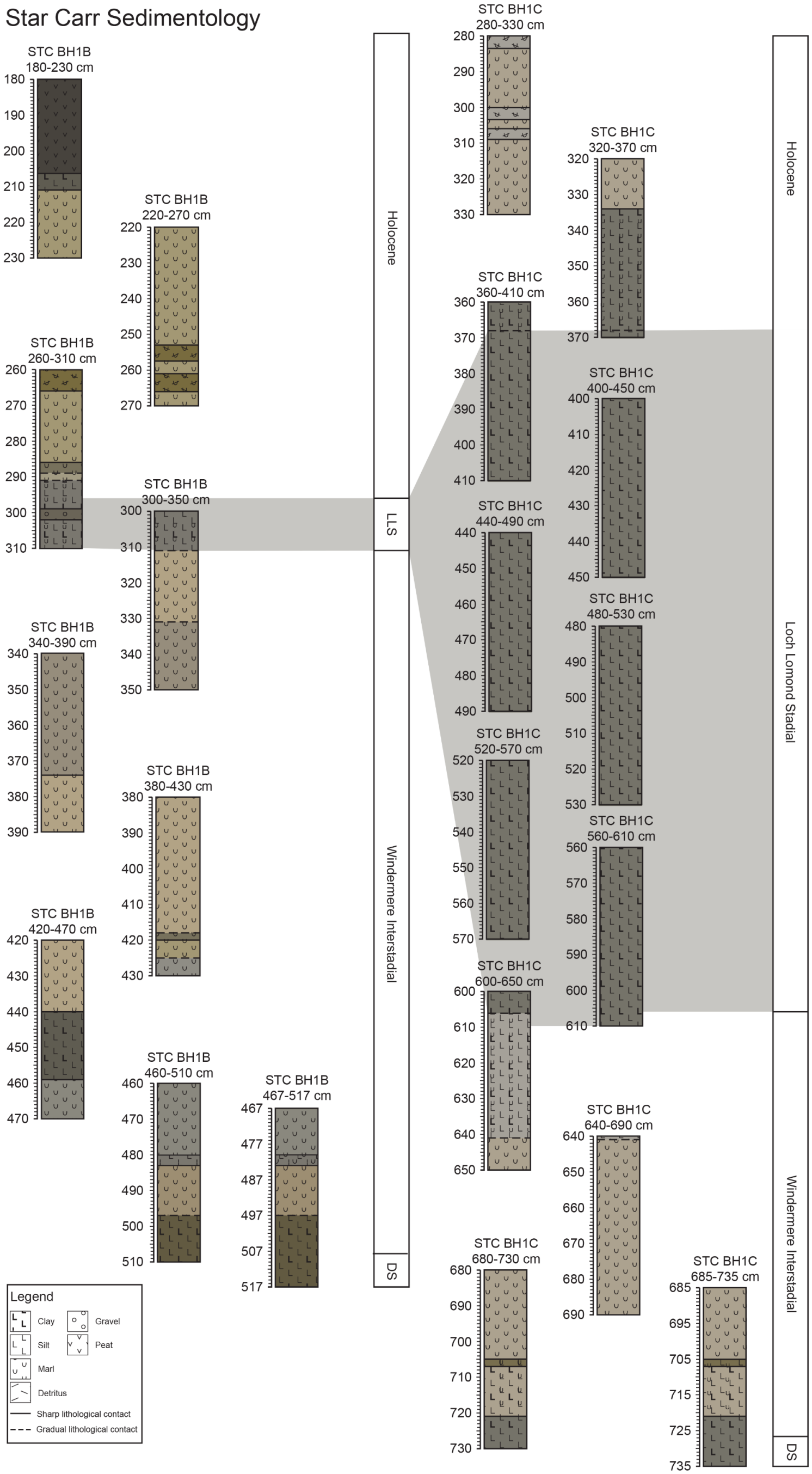

Figure 7.2 Star Carr Core B (left) and Core C (right) sediment stratigraphy. The sequences here are the primary sequences analysed as part of the research from Palaeolake Flixton for this thesis. Discrepancies between the two sequences are shown here, with the extended minerogenic sequence present within Core C but not Core B; despite being taken from proximal locations within the Star Carr fields. Broad climatostratigraphic zones are shown here based on lithostratigraphy.

sequence is not present within Core B, was the reason for analysing these two sequences from Palaeolake Flixton.

Core B

Table 7.1 and Figure 7.3 show the composite sediment profile from the Core B sequence. Unit 1 is characterised by silt and clay dominated sediments with low but increasing carbonate content, up to 62 %. The second unit is dominated by banded marl with an initial increase in $CaCO_3$ to 87 %. A reduction in $CaCO_3$ is observed across unit 2b to 2c coinciding with a greater silt component. A clear sedimentological change is observed within unit 3, with the unit dominated by silt and clay sedimentation, but with some carbonate maintained within the sediment, ca 41 %. Units 4 and 5 show a return to marl sedimentation, with carbonate percentages above 75 %, sub-units coincide with subtle changes in $CaCO_3$.

The greatest sedimentological changes are observed through unit 6. The three sub-units are dominated by mineral sediments. Unit 6a exhibits a reduction in $CaCO_3$, to 78 %. Subsequently, a coarse sand and gravel lens is identified, unit 6b, representing a significant change within the system. Further it has been suggested that unit 6b contains partially sorted sediments (e.g. Palmer et al., 2017) which is not possible to ascertain here. Unit 6c exhibits a return to relatively high carbonate values with a maxima of 76 %.

The second dominant carbonate phase, units 7 to 9e, demonstrates continually high $CaCO_3$ values, between 75 and 97 %. Certain sub-zones in the latter part of the record, however, do reveal variations from the overall trend. For example, units 9b and 9d, contain a detrital input or organics, mainly mosses. A phase of pure clay sedimentation is observed in unit 10, which, like unit 6b suggests a system change. Finally, unit 11, reveals a capping peat to the record presented here. Both units 10 and 11 demonstrate a reduction in carbonate percentage from 12 to 66 %.

Core C

The composite profile from the Core C sequence is detailed in Table 7.2 and Figure 7.4; with the key differences between Cores B and C emphasised here. Core C reveals minerogenic sedimentation at the base of the record with low TOC and $CaCO_3$ values but high MS values. Overlying this is a phase of increasing carbonate sedimentation, with values ranging between 13 and 60 %, and falling MS values. Unit 2b exhibits an increase in silt and lower $CaCO_3$ percentages, 48 %. Unit 2c returns to marl sedimentation with values >60 %. In contrast, unit 3 exhibits a continual reduction of $CaCO_3$ from highs of 63 % to lows of 24 %.

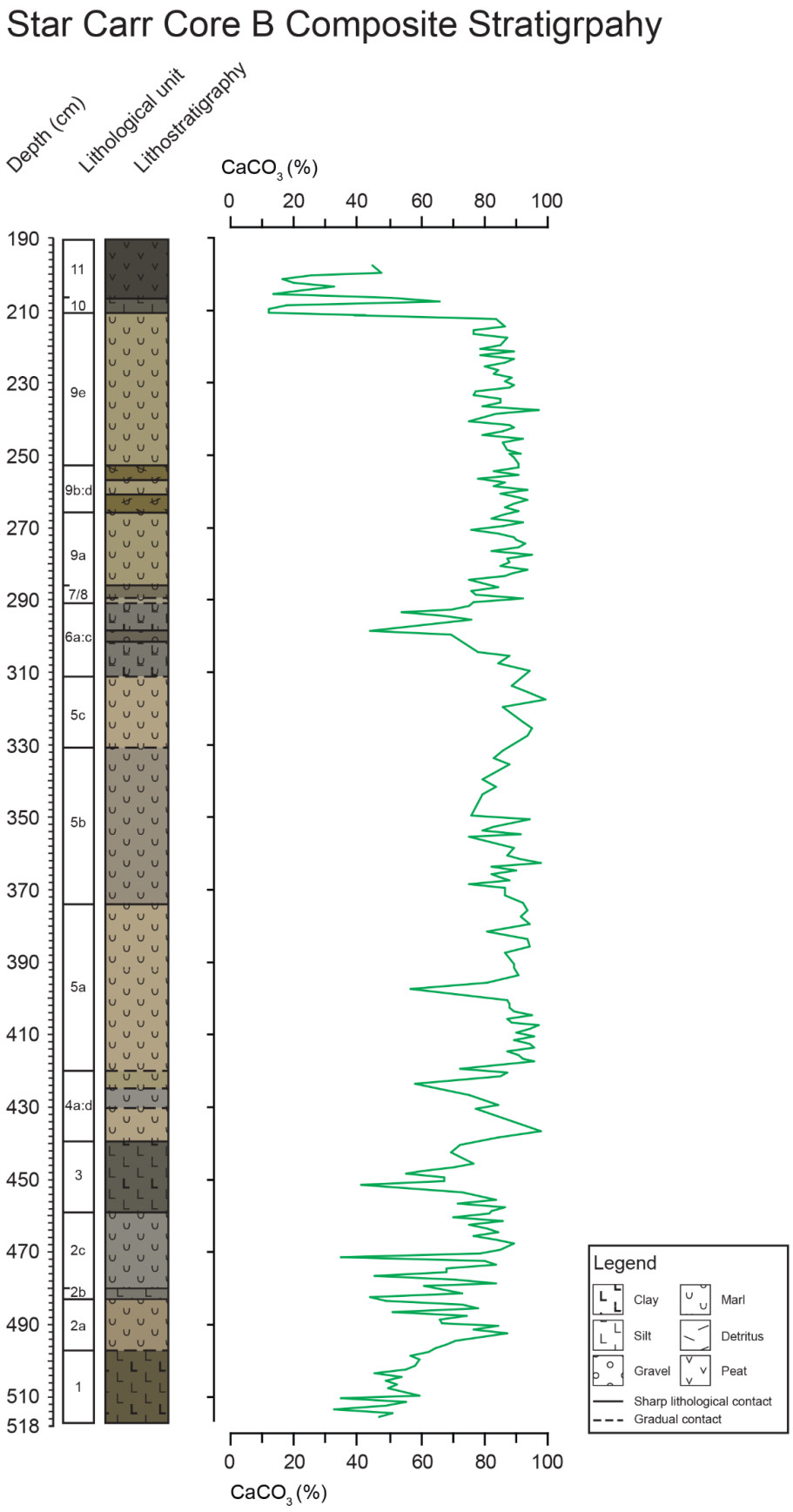

Figure 7.3 The composite stratigraphy for Star Carr Core B, utilising the overlapping cores presented in Figure 7.2. Carbonate values are presented here via mass spectrometry means rather than Bascomb calcimetry data which was not available. Clear shifts in carbonate percentage are generally shown to align with shifts noted within the lithostratigraphy.

Table 7.1 General lithological units within Star Carr Core B. Shown are the major sedimentological units/sub-units, their descriptors, classification and Munsell colour.

Unit	Depth (cm)	Troels-Smith	Classification	Munsell colour
11	206.5-180	Th4, Lc+, Ag+	Peat	2.5Y 2.5/1 Black
10	211-206.5	As4, Ag+, Lc+	Clay	5Y 3/1 Very Dark Grey
9e	253-211	Lc4, Ag+, As+, Dg+	Marl	5Y 6/3 Pale Olive
9d	257.5-253	Lc2, Dg2, Ag+	Detrital Marl	5Y 4/2 Olive Grey
9c	261-257.5	Lc4, Ag+, As+, Dg+	Marl	5Y 6/3 Pale Olive
9b	266-261	Lc2, Dg2, Ag+	Detrital Marl	5Y 4/2 Olive Grey
9a	286-266	Lc4, Ag+, As+, Dg+	Marl	5Y 6/3 Pale Olive
8	289-286	Lc2, Ag1, Dg1	Detrital Marl	5Y 4/2 Olive Grey
7	291-289	Lc2, As1, Ag1	Clayey Silty Marl	5Y 6/2 Light Olive Grey
6c	299-291	Ag2, As1, Lc1	Clayey Silt	2.5Y 4/1 Dark Grey
6b	302-299	Gs2, Ga2, As+, Ag+	Sand and Gravel	2.5Y 3/2 Very Dark Greyish Brown
6a	311-302	Ag2, As1, Lc1	Clayey Silt	2.5Y 4/1 Dark Grey
5c	331-311	Lc4, Ag+ As+	Marl	2.5Y 6/3 Light Yellowish Brown
5b	374-331	Lc4, Ag+, Dg+	Marl	2.5Y 5/2 Greyish Brown
5a	418-374	Lc4, Ag+, As+, Dg+	Marl	2.5Y 6/3 Light Yellowish Brown
4d	420-418	Lc3, Ag1, As+, Dg+	Silty Marl	5Y 4/2 Olive Grey
4c	425-420	Lc4, Ag+, As+	Marl	5Y 6/3 Pale Olive
4b	430-425	Lc3, Ag1, As+	Silty Marl	2.5Y 5/2 Greyish Brown
4a	440-430	Lc4, Ag+ As+ Dg+	Marl	2.5Y 6/3 Light Yellowish Brown
3	459-440	Ag2, As1, Lc1	Clayey, Marly Silt	5Y 3/2 Dark Olive Grey
2c	480-459	Lc3, As1, Ag+, Dg+	Silty Marl	5Y 8/2 Pale Yellow
2b	483-480	Ag2, Lc2, As+	Marly Silt	2.5Y 4/2 Dark Greyish Brown
2a	497-483	Lc4, Ag+ Dg+	Banded Marl	2.5Y 5/3 Light Olive Brown
1	517-497	Ag2, As2	Clay and Silt	5Y 3/2 Dark Olive Grey

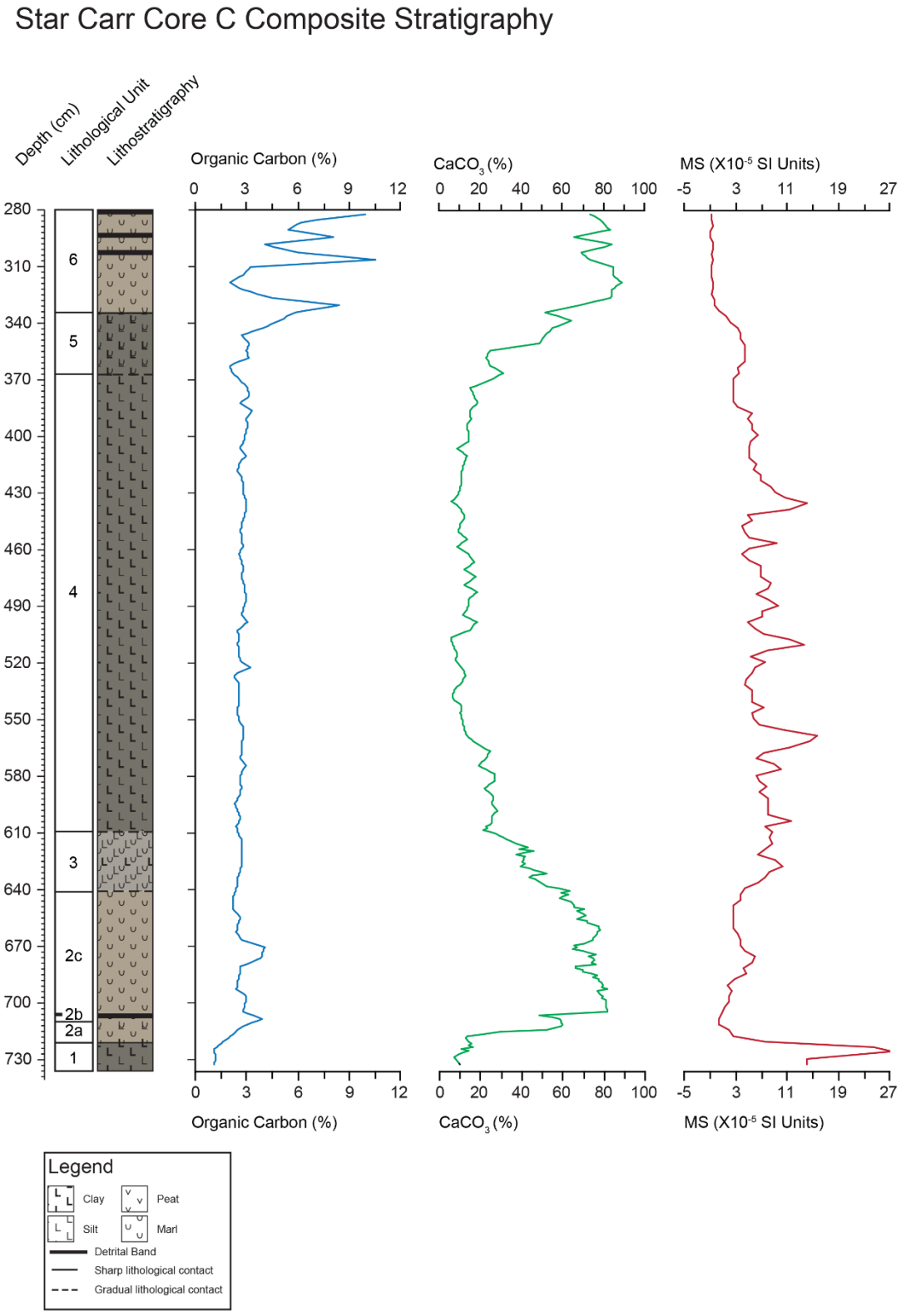

Figure 7.4 Composite stratigraphy from Star Carr Core C. Total organic carbon, calcimetry and magnetic susceptibility values are shown to highlight the different phases within Core C profile. Clearly shown are the transitional phase of unit 3 and greater MS values within unit 4, highlighting greater ferromagnetic input into the basin. Each spike in values signifies gravel clasts present in the system.

Table 7.2 General lithological units within Star Carr Core C. Shown are the major sedimentological units/sub-units, their descriptors, classification and Munsell colour.

Unit	Depth (cm)	Troels-Smith	Classification	Munsell colour
6	334-280	$Lc^4$4, Ag+, Dg+	Marl	2.5Y 6/2 Light Brownish Grey
		In part: $Lc^4$2, Dg2, Ag+	Detrital Marl	In part: 2.5Y 6/1 Grey
5	368-334	Ag2, As1, $Lc^4$1	Marly Silt	5Y 4/1 Dark Grey
4	609-368	Ag2, As1, $Lc^4$1	Silts and Clay	5Y 4/1 Dark Grey
3	641-609	$Lc^4$3, Ag1, Dg+	Silty Marl	2.5Y 6/2 Light Brownish Grey
2c	705-641	$Lc^4$4, As+, Dg+	Marl	2.5Y 6/2 Light Brownish Grey
2b	707-705	$Lc^4$2, Ag2, Dg+	Silty Marl	5Y 4/3 Olive
2a	721-707	$Lc^4$2, Ag2, Dg+	Silty Marl	2.5Y 6/2 Light Brownish Grey
1	735-721	As4, Ag+	Clay	5Y 4/1 Dark Grey

Unit 4 is dominated by dark, oxidising silts and clay. This extensive unit, ca 275 cm long, contains low TOC values of <4 %, and low carbonate percentages, between 6 and 28 %. Throughout this phase, a background of greater MS values is observed with a further series of higher values, coinciding with the presence of isolated gravel clasts throughout the unit. Towards the top of the unit, and within unit 5, increases in $CaCO_3$ and TOC values are observed allied to reduced MS values, although minerogenic sediments are still recorded.

Unit 6 is characterised by a return to marl, with $CaCO_3$ values of >88 %. During this phase, three detrital bands are observed which feature extensive moss remains. At these points, a series of TOC peaks are observed with values of 11, 8 and 10 %. Whilst peat does cap this sequence, the cores analysed here do not reveal a capping peat unit.

7.2 Palynological results

Cores B and C were analysed for pollen at different resolutions (Chapter 4). Both sequences were analysed between 4-8 cm but not greater than 16 cm resulting in a total of 49 analyses for Core B and 70 analyses from Core C. Analyses were performed with a minimum of 300 TLP barring basal samples from C. Unfortunately, as Core C was recovered prior to the commencement of this thesis, the lowest 35 cm had been

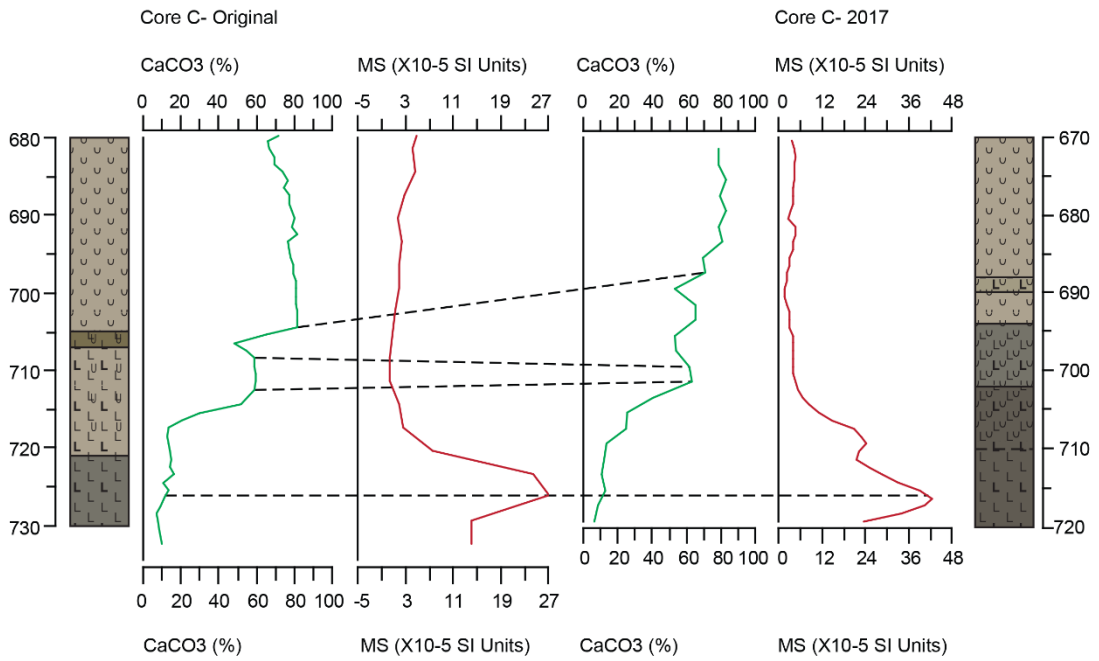

Figure 7.5 Tie points used between the original Core C profile and a new sequence recovered in 2017. Peaks in MS and calcimetry have been used to tie the cores together. As greater complexity is observed within the 2017 sequence, samples throughout have been linearly scaled to fit the original profile. The basal samples from Core C therefore appear to show greater resolution.

intensively sampled. To overcome this a basal core from a new sequence, extracted from the same location, was tied to the original sequence (Figure 7.5). This was deemed appropriate to enable a complete palynological assessment of the Core C sequence.

Nine local pollen assemblage zones have been identified within Core B (STCBP-1:9) and seven from Core C (STCCP-1:7). As both sequences contain significant abundances of *Pediastrum*, this taxon has been included in the zonation. The pollen profiles are presented in Figures 7.6 to 7.9 and Tables 7.3 and 7.4. Elements of the palynological descriptions are extracted *verbatim* from Blockley et al. (2018).

Core B

Zone STCBP-1. Composite depth: 510-465.5 cm.

The basal sample contains high percentages of Poaceae, 48 % and pre-Quaternary spores, 50 %. Herbaceous taxa, including *Artemisia* and *Rumex* are also recorded. Throughout, values for the above taxa decrease with replacement by *Juniperus* and *Betula*. The former increases to 11 % at 477.5 cm with the latter increasing from 5 % at the base of the zone to 33 % at 469.5 cm. Cyperaceae and *Pinus* are present throughout.

TLP concentrations are low at the base of the zone, 9096 grains/cm^{-3} at 509.5 cm but increase throughout. Total concentrations are higher than TLP throughout the zone, which reflects high values for pre-Quaternary spores at 509.5 cm; 10,512 grains/cm^{-3}.

Zone STCBP-2. Composite depth: 465.5-433.5 cm.

Zone 2 shows marked decreases of *Betula*; from 33 % at the top of the preceding zone to 9 % at 445.5 cm. Increasing herbaceous taxa at the expense of *Betula* include Poaceae, to 44 % by 445.5 cm, and Cyperaceae, to 20% by 453.5 cm. Marked increases in *Pediastrum* are noted from a zone low of 2 % at 461.5 cm, to 17 % at 453.5 cm. Other taxa include *Artemisia*, *Rumex* and *Thalictrum* with small increases in pre-Quaternary spores.

TLP concentrations are similar to STCBP-1, where the highest concentrations recorded throughout are 16,911 grains/cm^{-3} at 445.5 cm. Between 453.5 and 445.5 cm, total concentrations are considerably higher than TLP; at 24,900-30,001 grains/cm^{-3}, which reflects increased concentrations of *Pediastrum* and pre-Quaternary spores.

Zone STCBP-3. Composite depth: 433.5-409.5 cm.

All tree taxa remain low throughout, with a minor increase in *Betula* centred at 421.5 cm. In contrast to STCBP-2, percentages of Poaceae and Cyperaceae decrease to 21 % and 7 % respectively at the top of the zone alongside decreases in *Pediastrum* and pre-Quaternary spores. To account for the reductions in Poaceae and Cyperaceae, *Juniperus* increases to a sequence high of 57 % at 429.5 cm.

TLP concentrations are moderate with highest values recorded near the base of the zone, 56,941 grains/cm^{-3}. Concentrations of *Juniperus* are high, between 14,303 and 32,402 grains/cm^{-3}.

Zone STCBP-4. Composite depth: 409.5-369.5 cm.

Zone 4 exhibits an expansion in percentages of *Betula*, from 44 % at 405.5 cm to 53 % at 373.5 cm. In contrast to the previous zone, percentages of *Juniperus* decrease and by 373.5 cm contains <5 % TLP. *Salix* percentages increase, to >10% at 389.5 cm, which is contemporaneous with initial increases in *Filipendula*. Percentages of Poaeceae and Cyperaceae are comparable to STCBP-3. During this zone the aquatic component is composed of *Myriophyllum*.

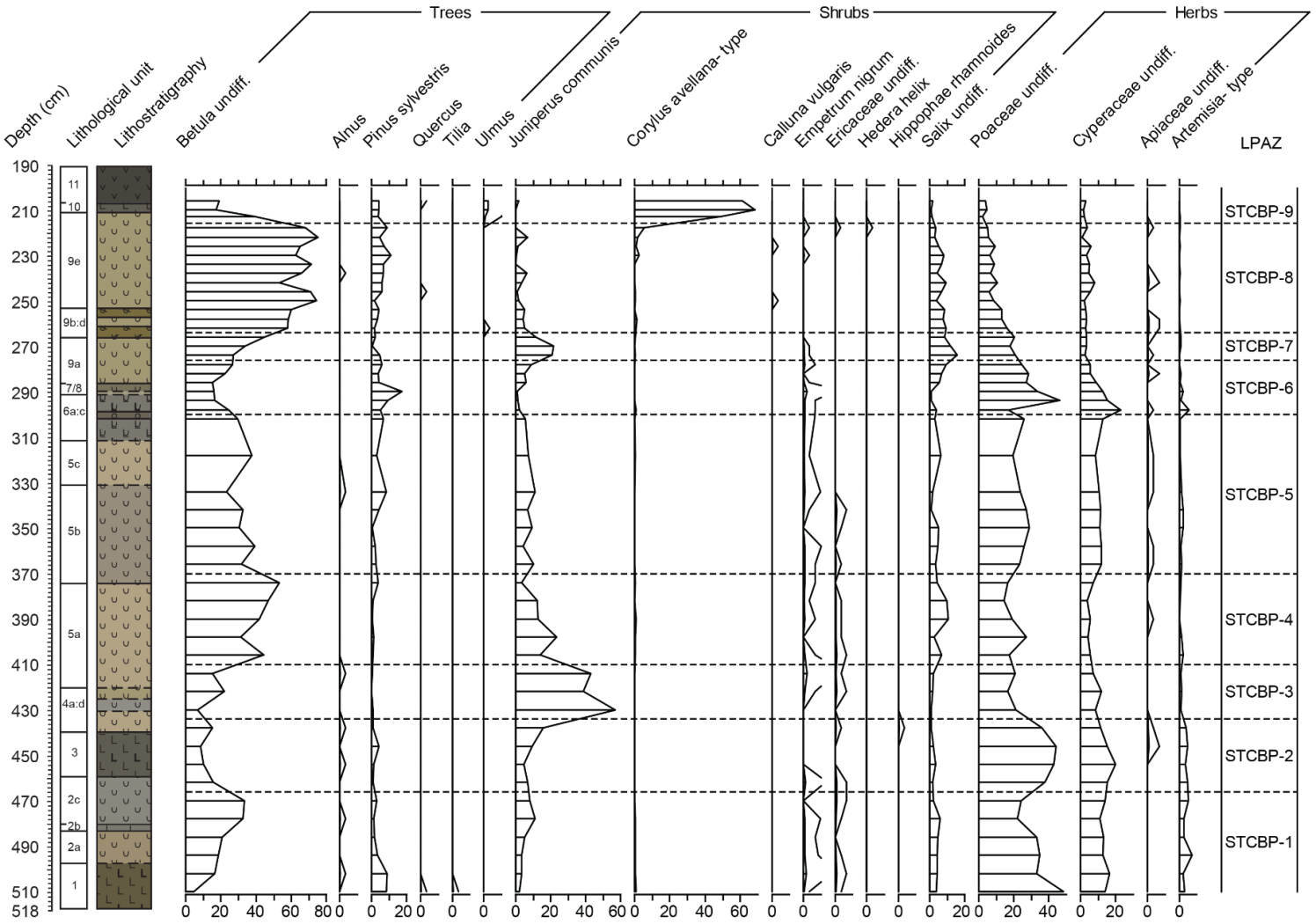

Figure 7.6 Pollen percentage profile of Star Carr Core B. All values are presented as percentages of TLP.

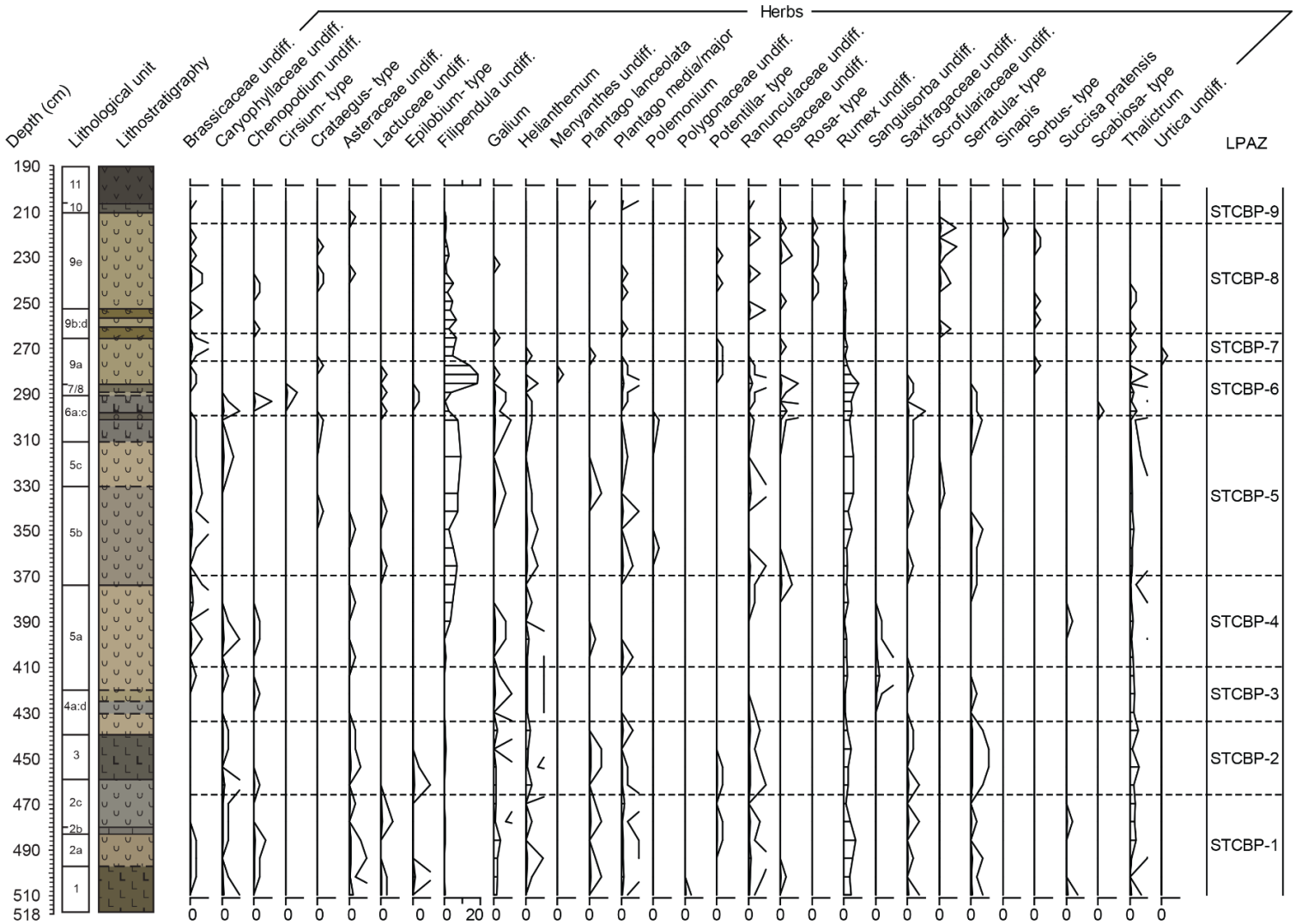

Figure 7.6 (Cont.) Pollen percentage profile of Star Carr Core B. All values are presented as percentages of TLP.

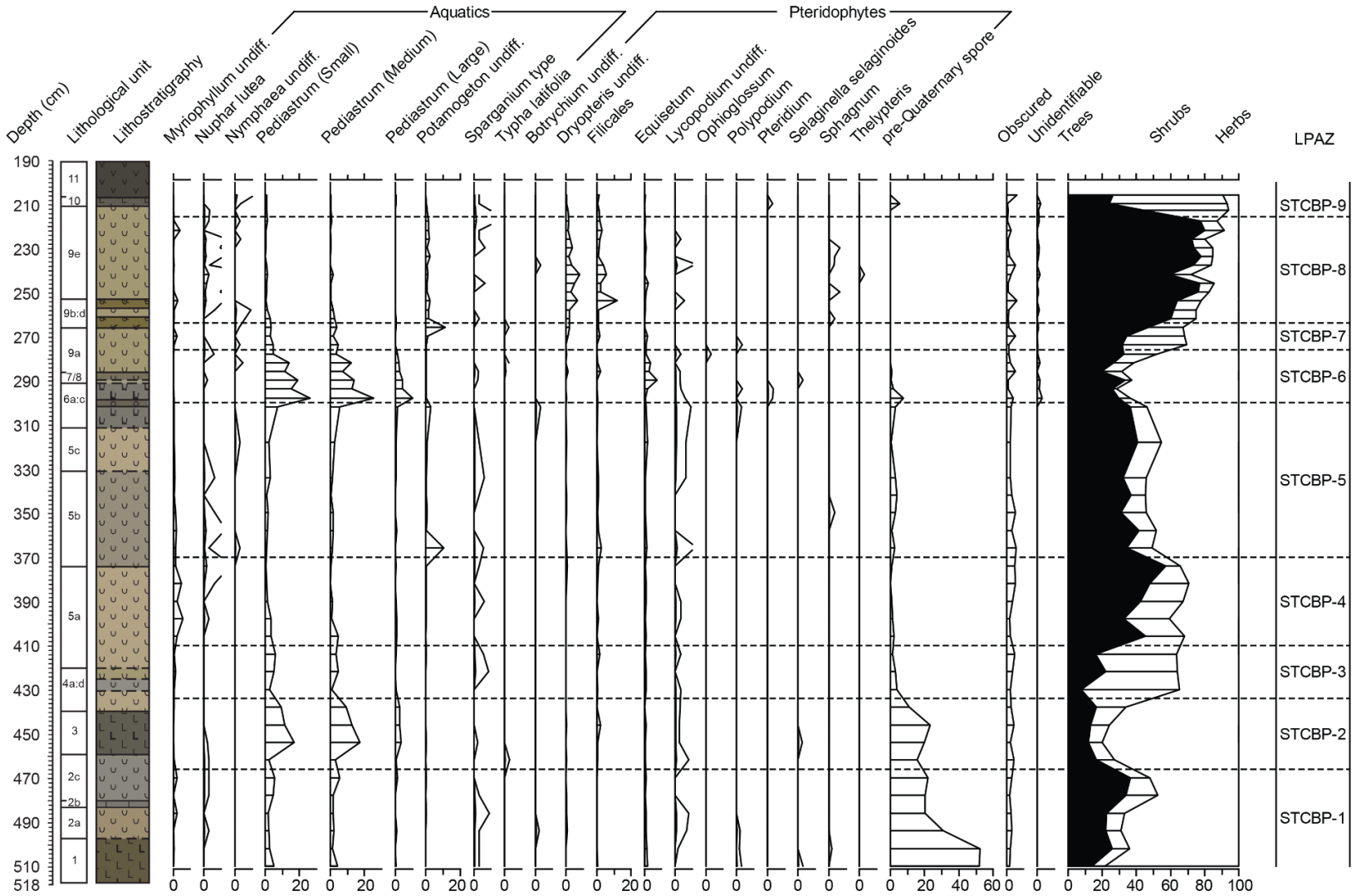

Figure 7.6 (Cont.) Pollen percentage profile of Star Carr Core B. All values are presented as percentages of TLP + aquatics and TLP + pteridophytes.

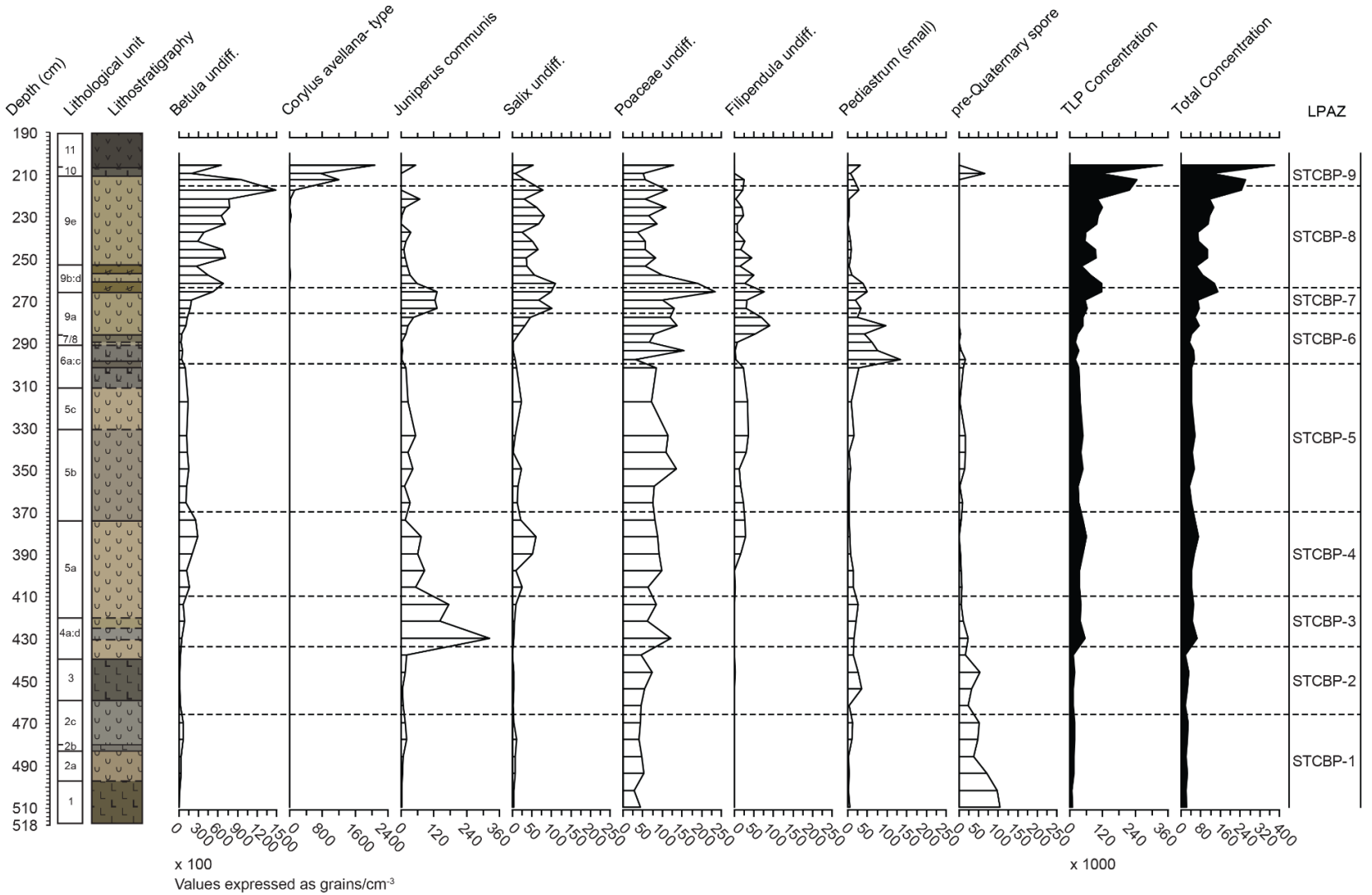

Figure 7.7 Summary pollen concentration data of key taxa from Star Carr Core B. All concentration values multiplied by 100 unless stated.

Table 7.3 Star Carr Core B pollen zone delineation and associated information. The names of the zones are provided alongside composite depths and key taxa observed within each zone.

LPAZ	Composite Depth (cm)	Key Taxa
STCBP-9	215.5-205	*Corylus*
STCBP-8	263.5-215.5	*Betula*
STCBP-7	275.5-263.5	*Juniperus*, *Betula*, *Salix*
STCBP-6	299.5-275.5	*Pediastrum*, Poaceae, Cyperaceae, *Filipendula*
STCBP-5	369.5-299.5	*Betula*, Poaceae, *Filipendula*
STCBP-4	409.5-369.5	*Betula*, *Juniperus*, Poaceae
STCBP-3	433.5-409.5	*Juniperus*, Poaceae, Cyperaceae
STCBP-2	465.5-433.5	Poaceae, *Pediastrum*, Cyperaceae
STCBP-1	510-465.5	Poaceae, pre-Quaternary spore, *Betula*, *Artemisia*

Both TLP and total concentrations are comparable to the previous zone with greatest concentrations observed at 381.5 cm; 60,919 and 69,780 grains/cm^{-3} respectively. From this horizon *Betula* exhibits moderate concentrations; 28,597 grains/cm^{-3}.

Zone STCBP-5. Composite depth: 369.5-299.5 cm.

Percentages of *Betula* appear moderate but are lower than zone 4 between 23 and 40 %. *Juniperus* and *Filipendula* are similar to the previous zone with Poaceae and Cyperaceae displaying greater percentages, up to 29 % and 13 % respectively. Within the second half of the zone, *Rumex* increases to a maximum of 6 %.

At the onset and termination of the zone, TLP concentrations are lower than STCBP-4. However, between 349.5-333.5 cm concentrations approach those of the previous zone, with a zone maximum of 48,112 grains/cm^{-3} at 333.5 cm.

Zone STCBP-6. Composite depth: 299.5-275.5 cm.

STCBP-6 is markedly different than the previous zones. Distinctive changes are observed with rapid increases in *Pediastrum* and Poaceae. *Pediastrum*, increases from 7 % in the upper sample from the previous zone to 24 % 297.5 cm, whereas Poaceae

increases to 46 % at 293.5 cm. In contrast, *Betula* percentages decrease to a zone low of 15 % at 285.5 cm. The dominant arboreal pollen taxa recorded during STCBP-6 is *Pinus*, recorded at 18 % at 289.5 cm. Additional herbaceous taxa recorded throughout the zone include *Rumex*, which peaks at 285.5 cm, and *Filipendula* which has a sequence high of 18 % at 285.5 and 281.5 cm.

TLP concentrations are low at the base of the zone, 19,199 grains/cm^{-3} but rise to 48,582 grains/cm^{-3} at the top of the zone. Considerable increases are present in total concentration, 54,370 grains/cm^{-3} at the base of the sequence, due to concentrations of *Pediastrum*. By the top of the zone where aquatics and pteridophytes are less frequently recorded however, total concentrations are comparable to TLP concentrations.

Zone STCBP-7. Composite depth: 275.5-263.5 cm.

Zone 7 appears similar to STCBP-3. The main taxon, *Juniperus*, increases to zone highs of 22 % at 269.5 cm. This rise is mirrored in *Betula* which is increasing throughout the zone. *Salix* reaches a sequence high during STCBP-7 with percentages of 16 % at 273.5 cm. Taxa that are present throughout the zone but at lower percentages than STCBP-6 include Poaceae, *Filipendula* and *Pediastrum*.

Concentrations throughout STCBP-7 are higher than at any previous point within the sequence. Highest TLP concentrations are recorded at 265.5 cm with 115,776 grains/cm^{-3}. *Juniperus* and *Betula* are the main controlling taxa with highs of 13,264 and 51,919 grains/cm^{-3} respectively.

Zone STCBP-8. Composite depth: 263.5-215.5 cm.

The most dominant taxon across all spectra within STCBP-8 is *Betula*. Percentages of *Betula* are high throughout at >53 %. *Pinus* represents the only other notable tree taxa to be recorded with highs of 11 % at 229.5 cm. *Salix* is continually present, between 3 and 10 %. For the first time in the sequence *Dryopteris* percentages increase, up to 8 % by 241.5 cm, with associated increases in Filicales.

TLP concentrations are moderate to high throughout the zone, however, a reduction in concentration is observed in the centre of the zone to 54,514 grains/cm^{-3}. High values are observed at 217.5 cm with a concentration of 218,327 grains/cm^{-3}.

Zone STCBP-9. Composite depth: 215.5-205 cm.

The final zone within Core B is characterised by increases in Coryloid shrubs. From first appearance during the preceding zone, *Corylus* expands to a zone and sequence high of 68 % at 209.5 cm. The only other notable taxa within this zone is *Betula*, however and percentages are lower than the previous zone between 17 and 39 %. Remaining taxa (e.g. *Pinus*, *Ulmus*, Poaceae, Cyperaceae) are all recorded at <5 %.

TLP concentration values are high throughout with the highest values recorded at 205.5 cm with 340,444 grains/cm^{-3}. Within STCBP-9 there is a considerable drop in concentration at 209.5 cm where concentration falls from 244,911 to 110,617 grains/cm^{-3}.

Core C

Zone STCCP-1. Composite depth: 722-706.3 cm.

STCCP-1 demonstrates considerable variation amongst principal taxa. The basal samples contain high percentages of both pre-Quaternary spores and *Pinus*, 68 % and 49 % respectively. Over these basal horizons, herbaceous taxa including *Artemisia*, 14 % at 719.5 cm and *Rumex*, 5 % at 715.5 cm are present. Where peaks in *Rumex* are identified, Poaceae increases to 48 %; further coinciding with a reduction in *Betula*. In the successive sample, 711.5 cm, *Juniperus* peaks at 20 %. Across these depths, *Pediastrum* increases to 13 %.

TLP concentrations are low in the basal samples, 4456 grains/cm^{-3} but increase significantly to 61,353 grains/cm^{-3}. This increase is due to considerable concentrations of Poaceae, 18,315 grains/cm^{-3} at 711.5 cm. Whilst total concentrations are high due to large concentrations of *Pediastrum* and pre-Quaternary spores. Highs of 91,064 grains/cm^{-3} at the top of the zone.

Zone STCCP-2. Composite depth: 706.3-654.5 cm.

Zone two is dominated by *Betula*. From low values in the previous zone, *Betula* percentages increase to 49 % by 703.5 cm and fluctuate between 30-45 % for the remainder of the zone. Poaceae and Cyperaceae are moderate with highs of 26 % and 17 % respectively. Whilst low, Filipendula is recorded throughout with highs occurring in conjunction with the former two taxa; 9 % at 681.5 cm. Continually recorded taxa include *Pinus*, *Juniperus* and *Salix*.

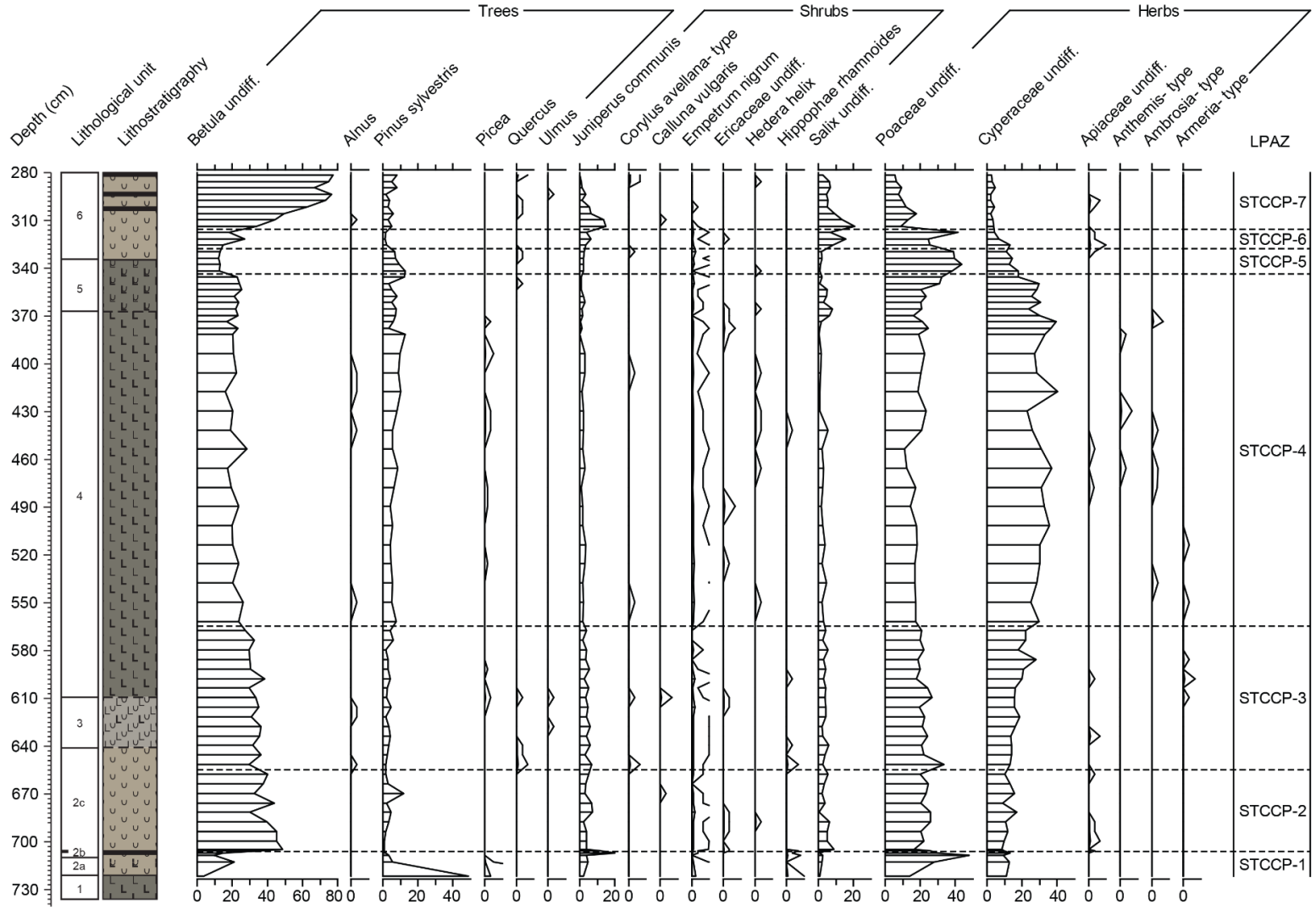

Figure 7.8 Pollen percentage profile of Star Carr Core C. All values are presented as percentages of TLP.

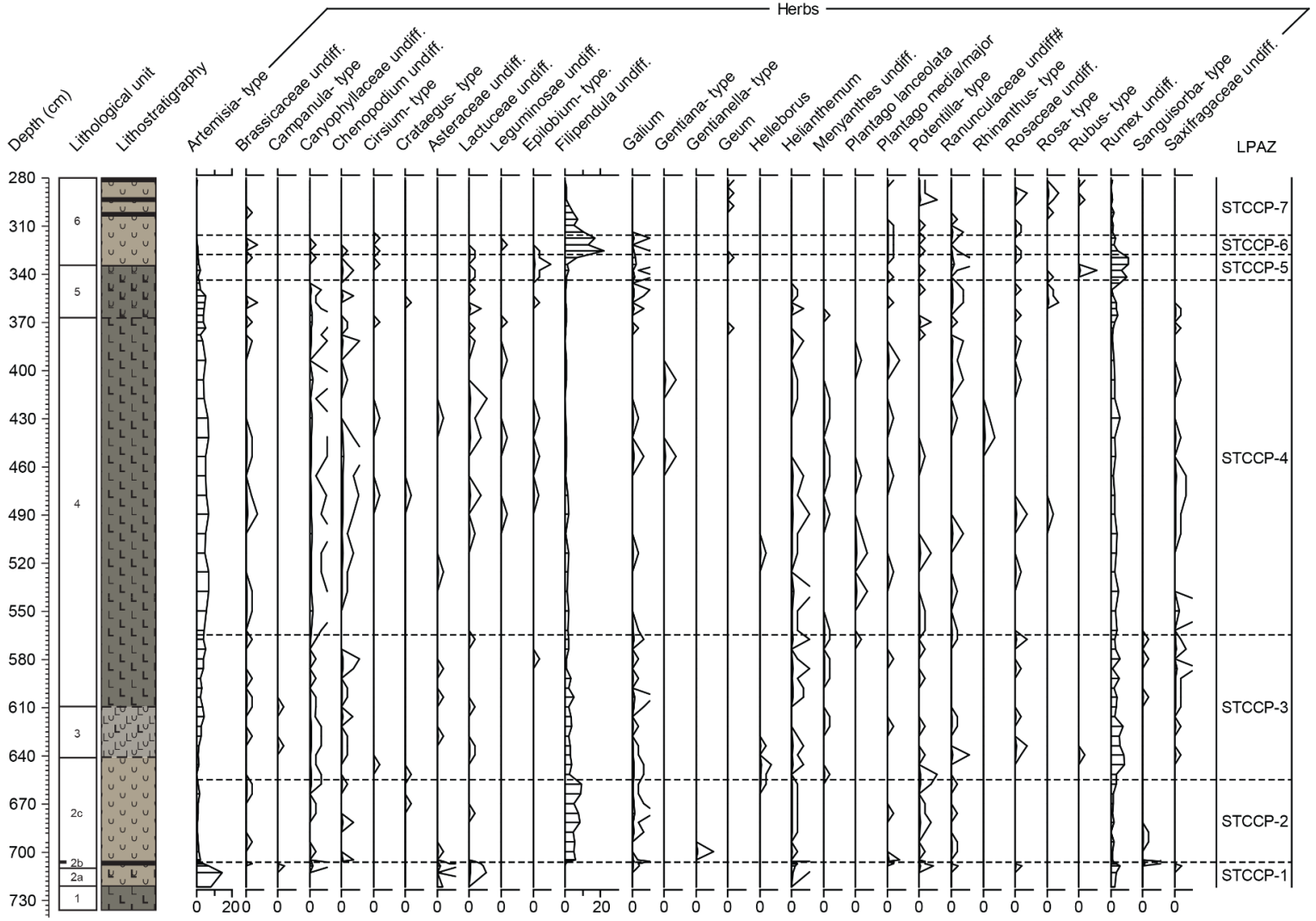

Figure 7.8 (Cont.) Pollen percentage profile of Star Carr Core C. All values are presented as percentages of TLP.

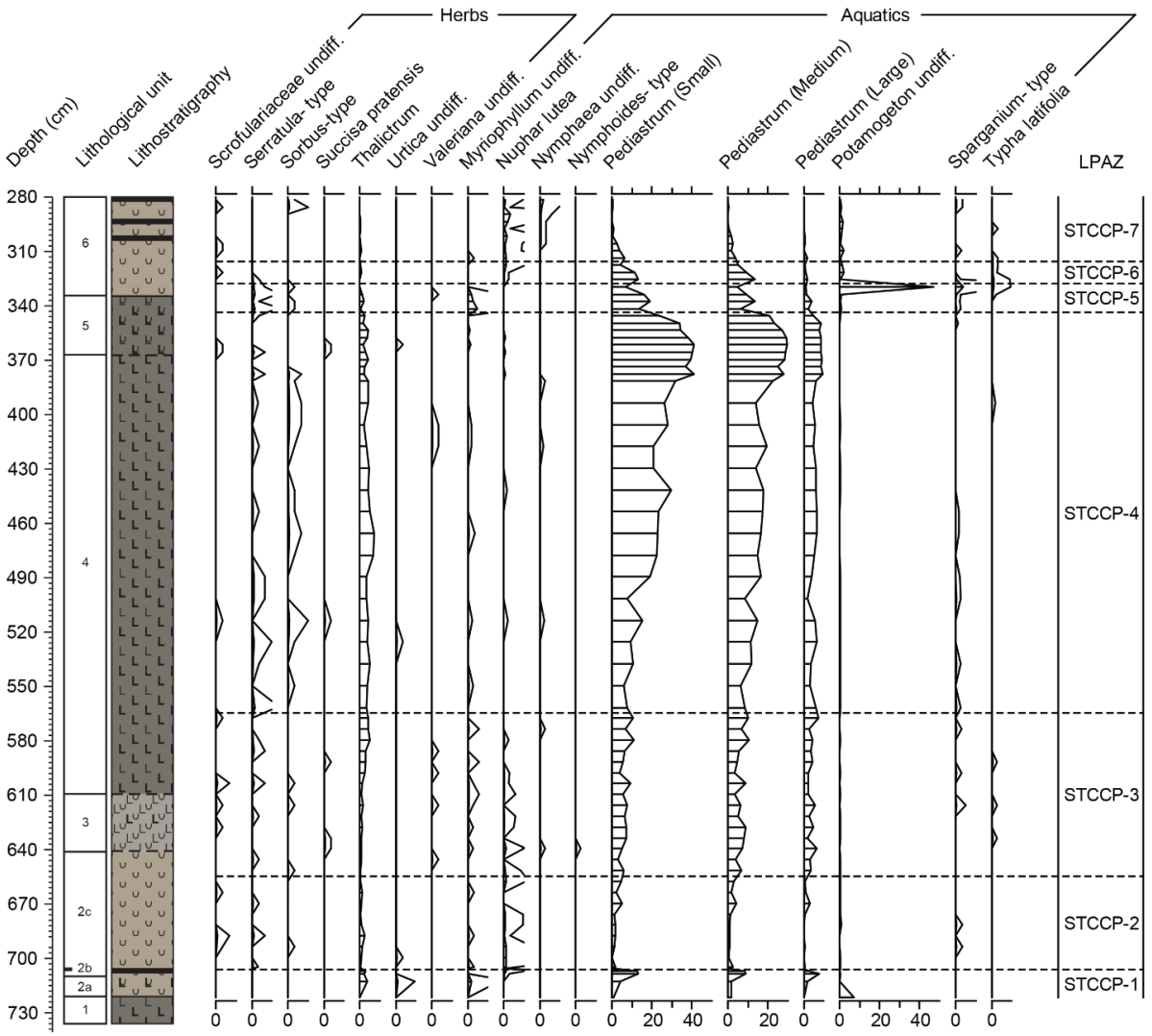

Figure 7.8 (Cont.) Pollen percentage profile of Star Carr Core C. All values are presented as percentages of TLP and TLP + aquatics.

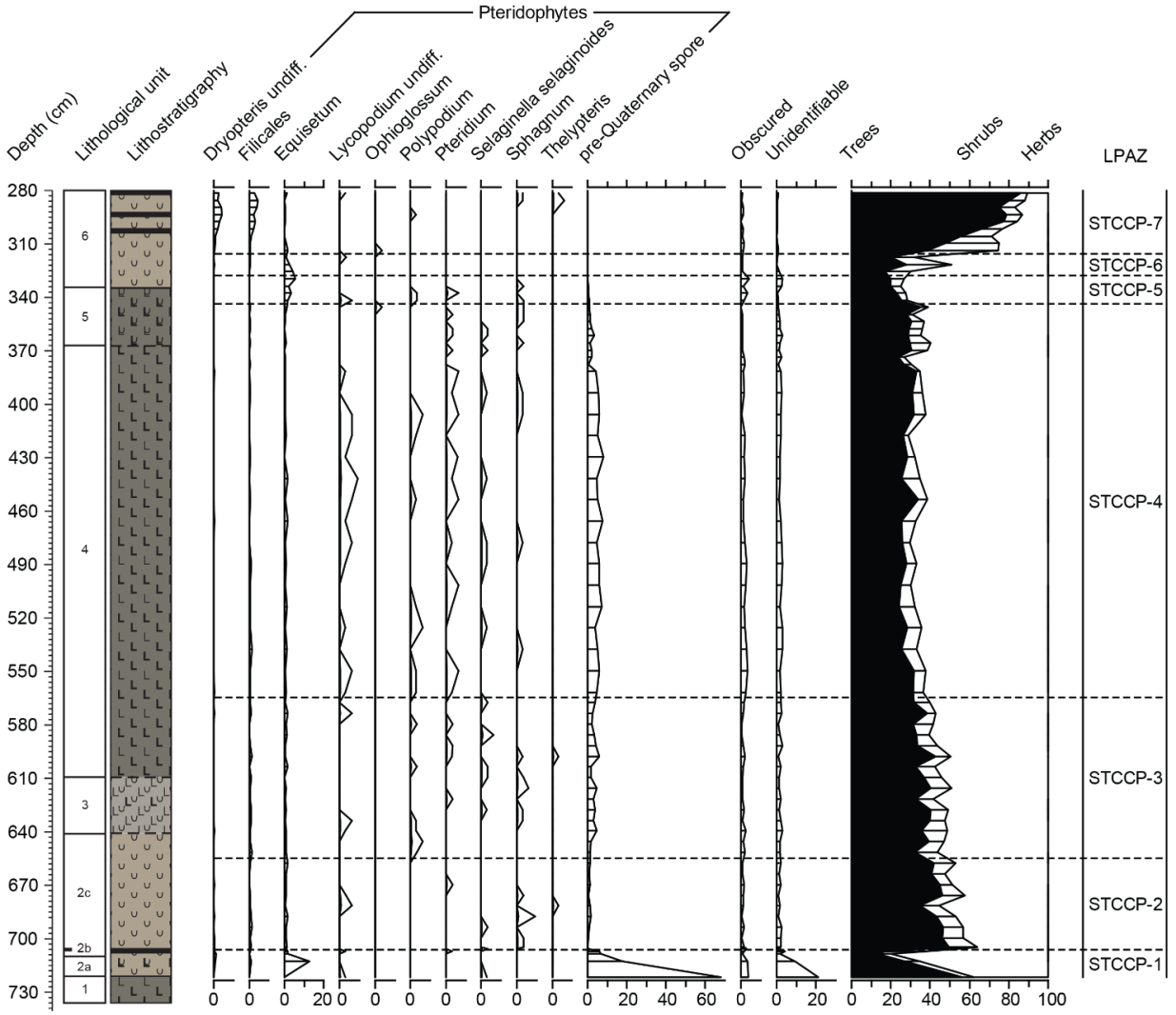

Figure 7.8 (Cont.) Pollen percentage profile of Star Carr Core C. All values are presented as percentages of TLP and TLP + pteridophytes.

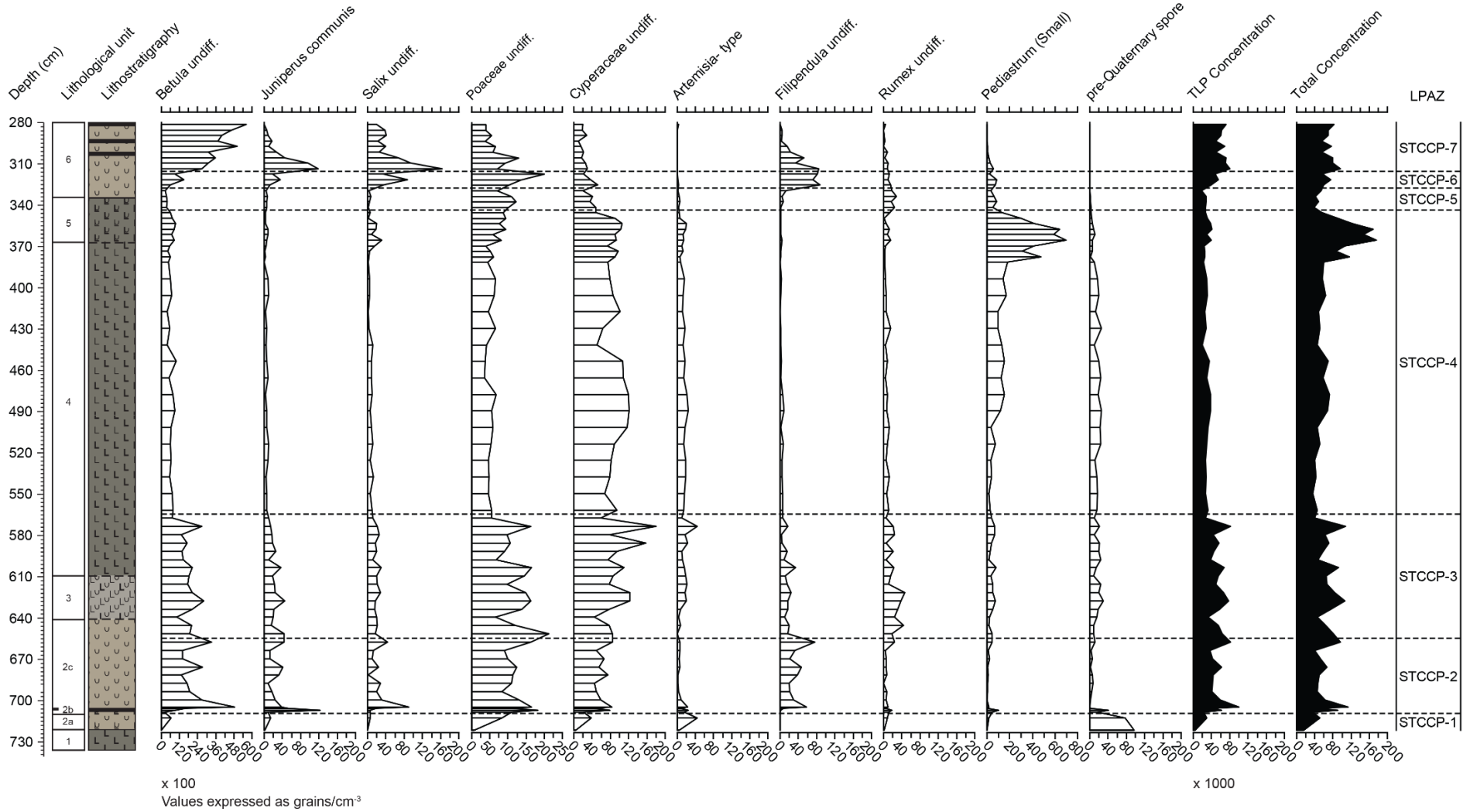

Figure 7.9 Summary pollen concentrations from Star Carr Core C showing principal taxa. All concentration values multiplied by 100 unless stated.

Table 7.4 Star Carr Core C pollen zone delineation and associated information. The names of the zones are provided alongside composite depths and key taxa observed within each zone.

LPAZ	Composite Depth (cm)	Key Taxa
STCCP-7	315.5-281	*Betula*, *Juniperus*, *Salix*
STCCP-6	327.5-315.5	Poaceae, *Filipendula*, *Salix*
STCCP-5	343.5-327.5	Poaceae, *Pinus*, *Rumex*, *Potamogeton*
STCCP-4	564.5-343.5	*Pediastrum*, Cyperaceae, *Betula*, Poaceae
STCCP-3	654.5-564.5	*Betula*, Poaceae, Cyperaceae
STCCP-2	709.5-654.5	*Betula*, Poaceae, Cyperaceae, *Filipendula*
STCCP-1	728-709.5	pre-Quaternary spore, *Pinus*, Poaceae, *Juniperus*

TLP concentrations are greater than STCCP-1 with highs of 99,721 grains/cm^{-3} at 703.5 cm. *Betula* contributes approximately 50 % to this with a concentration of 48,652 grains/cm^{-3}.

Zone STCCP-3. Composite depth: 654.5-564.5 cm.

STCCP-3 is similar to STCCP-2 albeit with lower percentages of *Betula*, between 28-39 %. Poaceae percentages are similar however Cyperaceae percentages increase to between 13-28 %. *Filipendula* percentages are reduced compared to the previous zone with increases in *Rumex* and *Artemisia* noted. Percentages of *Rumex* are higher at the base of the zone, between 645.5-639.5 cm, whereas *Artemisia* percentages are greater towards the middle and end of the zone. Additionally, *Thalictrum* and *Pediastrum* are both recorded.

TLP concentrations appear variable throughout, between 26,494-82,093 grains/cm^{-3}. Discrepancies between TLP and total concentration are due to increases in *Pediastrum* and pre-Quaternary spores.

Zone STCCP-4. Composite depth: 564.5-343.5 cm.

Zone 4 is characterised by increasingly elevated percentages of *Pediastrum*. *Pediastrum* increases from 6 % at 549.5 cm to 26 % at 393.5 cm. However, a greater increase is observed between 393.5-349.5 cm where percentages are sustained at >31 %.

Coincident with this increase are elevated percentages of Cyperaceae with Poaceae and *Betula* also displaying moderate percentages. Whilst percentages are low, <10 %, *Artemisia*, *Rumex* and *Thalictrum* are continually present. Additional taxa include *Pinus*, *Salix*, Caryophyllaceae and *Filipendula*.

TLP concentrations are lower than most of the previous zones. Low values are observed at 441.5 cm, with 19,758 grains/cm^{-3}, highest values are observed at 357.5 cm with 40,226 grains/cm^{-3}. Total concentrations are high towards the top of the zone. This undoubtedly reflects high concentrations of *Pediastrum* which peak at 70,008 grains/cm^{-3} at 365.5 cm.

Zone STCCP-5. Composite depth: 343.5-327.5 cm

Compared to the previous zone, percentages of *Betula* decrease with an increase in *Pinus* to 13 % by 341.5 cm. The most substantial increases within zone 5 are those of Poaceae; with percentages >37 % throughout. Occurring alongside the increases in Poaceae are increases in *Rumex*, with a two-fold increase to 10 % at 329.5 cm. At this point there is a significant spike in *Potamogeton*, from 1-47 %.

Concentrations are comparable to the previous zone, although the lowest TLP concentrations are recorded at 329.5 cm with 18,189 grains/cm^{-3}.

Zone STCCP-6. Composite depth: 327.5-315.5 cm.

Percentages of Poaceae are reduced at zone onset, 26 % at 325.5 cm, after which they increase sharply to 41 % at 317.5 cm. Within zone 6, *Filipendula* increases to a sequence maximum of 22 % at 325.5 cm before reducing to lower percentages. *Salix* also demonstrates moderate percentages of 16 % within the successive level. *Pediastrum*, whilst not as well represented is also recorded.

TLP concentrations are greater than the previous zone increasing from 39,970-55,441 grains/cm^{-3} between 325.5-321.5 cm. Poaceae is the main component with 20,046 grains/cm^{-3} at 317.5 cm.

Zone STCCP-7. Composite depth: 315.5-281 cm.

Zone 4 is initially characterised by moderate percentages of *Juniperus*, 15 %, and a sequence high for *Salix*, 21 %, at 313.5 cm. Percentages of both subsequently decline

throughout the remainder of the zone. In contrast to these declining trends, the zone is further characterised by increasing percentages of *Betula*, from 34 % at 313.5 to 77 % at 281.5 cm. The pteridophyte component is composed of *Dryopteris* and Filicales.

TLP concentrations are further increased throughout this zone and are considerably higher than any zone following minerogenic sedimentation. Highest concentrations are observed at 313.5 cm with a total of 79,697 grains/cm^{-3}, which reflects high concentrations of *Juniperus* and *Salix*. Throughout the zone *Betula* becomes dominant with a high of 56,074 grains/cm^{-3} recorded at 281.5 cm.

7.3 Statistical analyses

All statistical analyses were performed on reduced Core B and Core C datasets, utilising all taxa greater than 5 % abundance. Owing to the significant abundances of *Corylus* identified in the upper three samples of Core B, up to 68 %, these samples were removed from the analysis. As *Corylus* obscures subtle vegetation change and has a negative impact in the statistical approaches used to assist identifying potential vegetation revertences, owing to *Corylus* being identified in the upper samples only, the removal of this taxon is justified. Detrended Correspondence Analyses (DCA) were employed to establish the lengths of the primary axes (Table 7.5). These lengths (>1.5-3 SD) demonstrate that Principal Components analysis (PCA), Correspondence Analysis (CA) and Principal Curves (PC) were suitable for data exploration across Palaeolake Flixton.

Table 7.5 Preliminary DCA analysis on the reduced Core B pollen dataset.

	DCA1	**DCA2**	**DCA3**	**DCA4**
Eigenvalue	0.3000	0.1171	0.07132	0.08008
DCA value	0.3042	0.1202	0.03362	0.01941
Axis length	1.9197	1.5584	0.90933	1.07167

Table 7.6 Preliminary DCA analysis of the reduced Core C pollen dataset.

	DCA1	**DCA2**	**DCA3**	**DCA4**
Eigenvalue	0.2151	0.07487	0.08128	0.03318
DCA value	0.2155	0.05301	0.03890	0.02062
Axis length	2.2555	1.27513	1.30272	0.90121

Statistics- Core B

The PCA was preferred for exploring the variation due to short axes lengths and lack of an arch effect (e.g. Gauch, 1982) (Figure 7.10). Axis one represents a considerable proportion of the variation in the dataset, 33.5 %. Clear differences are observed with taxa plotting across axis one. Those plotting positively include, in order of greatest contribution: Cyperaceae, Poaceae, *Thalictrum*, *Artemisia*, *Rumex* and *Pediastrum*. In contrast, taxa that plot negatively along the axis include *Betula*, *Dryopteris Salix*, Filicales and *Corylus*. The remaining taxa, including *Pinus*, *Equisetum*, *Juniperus* and *Filipendula* plot within intermediate space with a greater affinity to axis two.

To explore the relationships between pollen and stratigraphy, axis 1 scores were plotted for both the PCA and CA solutions. This was subsequently modelled using the PC (Figure 7.11). The PC data for Core B are modelled on a CA output. Whilst both PCA and CA methods converge in nine iterations, the CA output explains more variation under the same penalty values. Variation expressed with the different approaches are summarised as:

- PCA based output: 78.5 %
- CA based output: 86.1 %

Within Figure 7.11 variance in the data is shown where the PC curves shifts to more positive values. From these observations, one significant major oscillation is observed, however, it is not significantly expanded in the sequence and entirely different from other sequences presented in this thesis. Additionally, four additional points of variation can be picked out with the PC. The first oscillation is clear, however the remaining three are not significant compared to this first oscillation. Oscillations two and four are both represented by a single sample point, although considerable variability is suggested by the second oscillation. Further, oscillation 4 is subtle suggesting only minor variability within the pollen data. From the PC data oscillations are proposed at:

- Major Oscillation 1: Samples between 301.5-285.5 cm
- Oscillation 1: Samples between 469.5-429.5 cm
- Oscillation 2: Samples between 405.5-389.5 cm
- Oscillation 3: Sample between 373.5-317.5 cm
- Oscillation 4: Samples between 277.5-269.5 cm

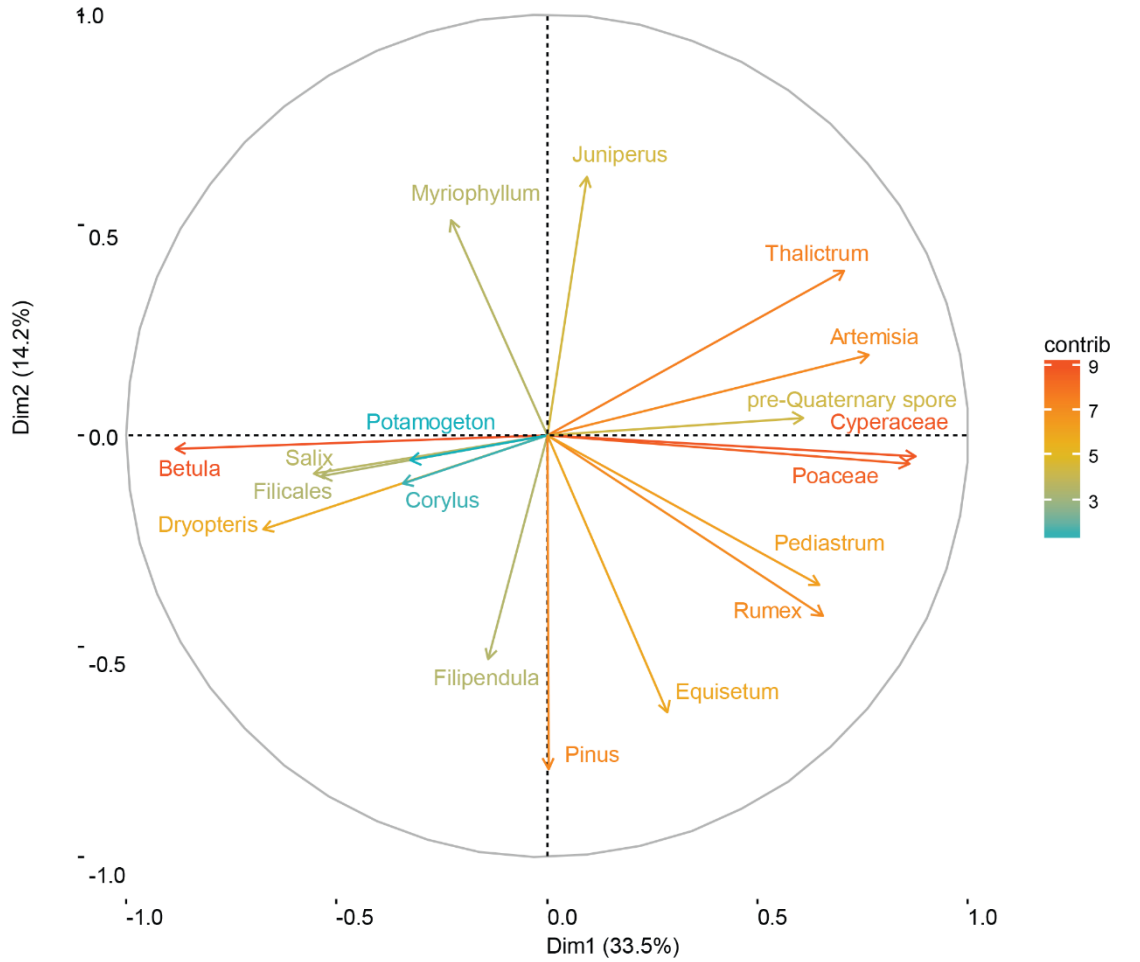

Figure 7.10 Results of the PCA output from Core B. The data are presented as a biplot with principal components one and two. Plotting positively along axis one with greater importance are open herbaceous taxa and certain spores; whereas negative values are composed of shrub and tree- type taxa.

These variances in the PC data can be observed in the Rate of Change Analyses (RoC). At each point increases in RoC reveals phases of compositional turnover. However, compared to other sequences Core B demonstrates less compositional turnover than elsewhere. The greatest change is suggested between 301.5-285.5 cm. This encompasses the gravel band and might be expected to reveal considerable change between pollen samples. Furthermore, key taxa have been modelled along the gradient of the PC. Using this approach, changes in taxa within Figure 7.11 clearly demonstrate what is driving the change in the PC over different events. For example, large increases in Poaceae and Cyperaceae are modelled at ca 300 cm; whereas the change in the PC between 469.5-429.5 cm is the result of increasing Poaceae and *Juniperus* with decreasing *Betula*.

Statistics- Core C

Like Core B, the PCA was preferred to explore the variation in Core C due to short axes lengths (e.g. Gauch, 1982) (Figure 7.12).

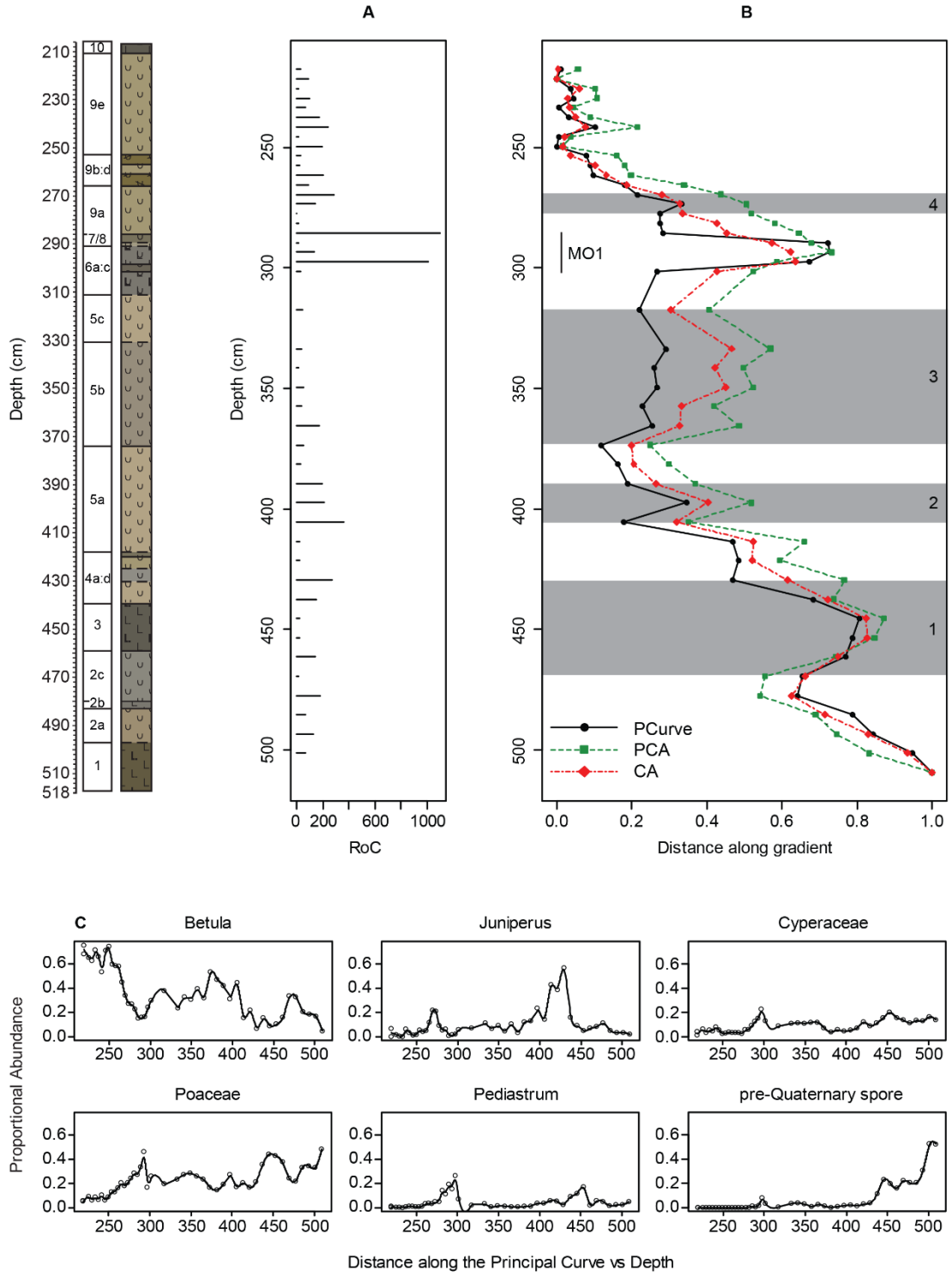

Figure 7.11 Results of different statistical tests applied to the Core B pollen data. A) Rate of change analysis (RoC). All values are arbitrary, with an exaggeration multiplier applied to demonstrate significant periods of compositional change. The greater the length of the bar the more significant the compositional change. B) The overlain output from three tests applied (PCA, CA and PC). With the PC, the data show rapid short oscillations (grey boxes) and a longer oscillation termed (MO1). C) Individual taxa response curves modelled on the gradient of the PC. These key taxa demonstrate what may be driving the changes in the PC from B).

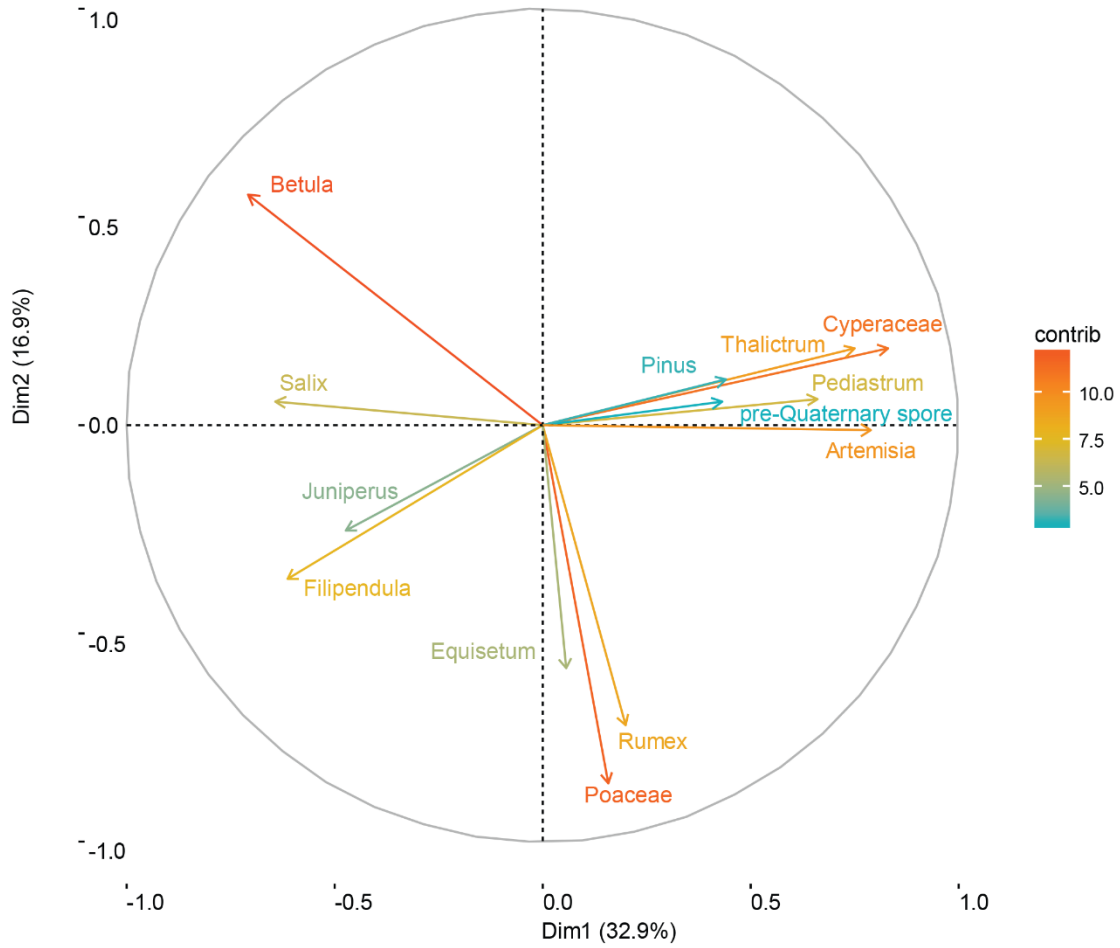

Figure 7.12 Results of the PCA output from Core C. Data are presented as Core B. Plotting positively along axis one with greater importance are open herbaceous taxa, with pre-Quaternary spores, *Pediastrum* and *Pinus*. Taxa plotting negatively include shrub and tree- type taxa. Axis two is represented by *Rumex* and Poaceae.

Axis one explains 32.9 % of the variation whereas axis two represents 16.9 % of the variation. Taxa plotting positively along axis one include: Cyperaceae, *Artemisia*, *Thalictrum* and *Pediastrum*. Whereas those plotting negatively include *Betula*, *Filipendula*, *Salix* and *Juniperus*. Poaceae, *Rumex* and *Equisetum* show a greater relationship with axis two.

Different statistical approaches to assist in event delineation have been plotted within Figure 7.13. Like B, the Core C vegetation data are modelled on a CA based output. To allow convergence of the PC, penalty values for both PCA and CA approaches had to be set very low (0.5). This gives the PC considerable flexibility however it may also significantly overfit the data; rendering assessments redundant. Nevertheless, the data have been modelled on a CA-based output which explains considerably more variation:

- PCA based output: 76.0 %
- CA based output: 88.4 %

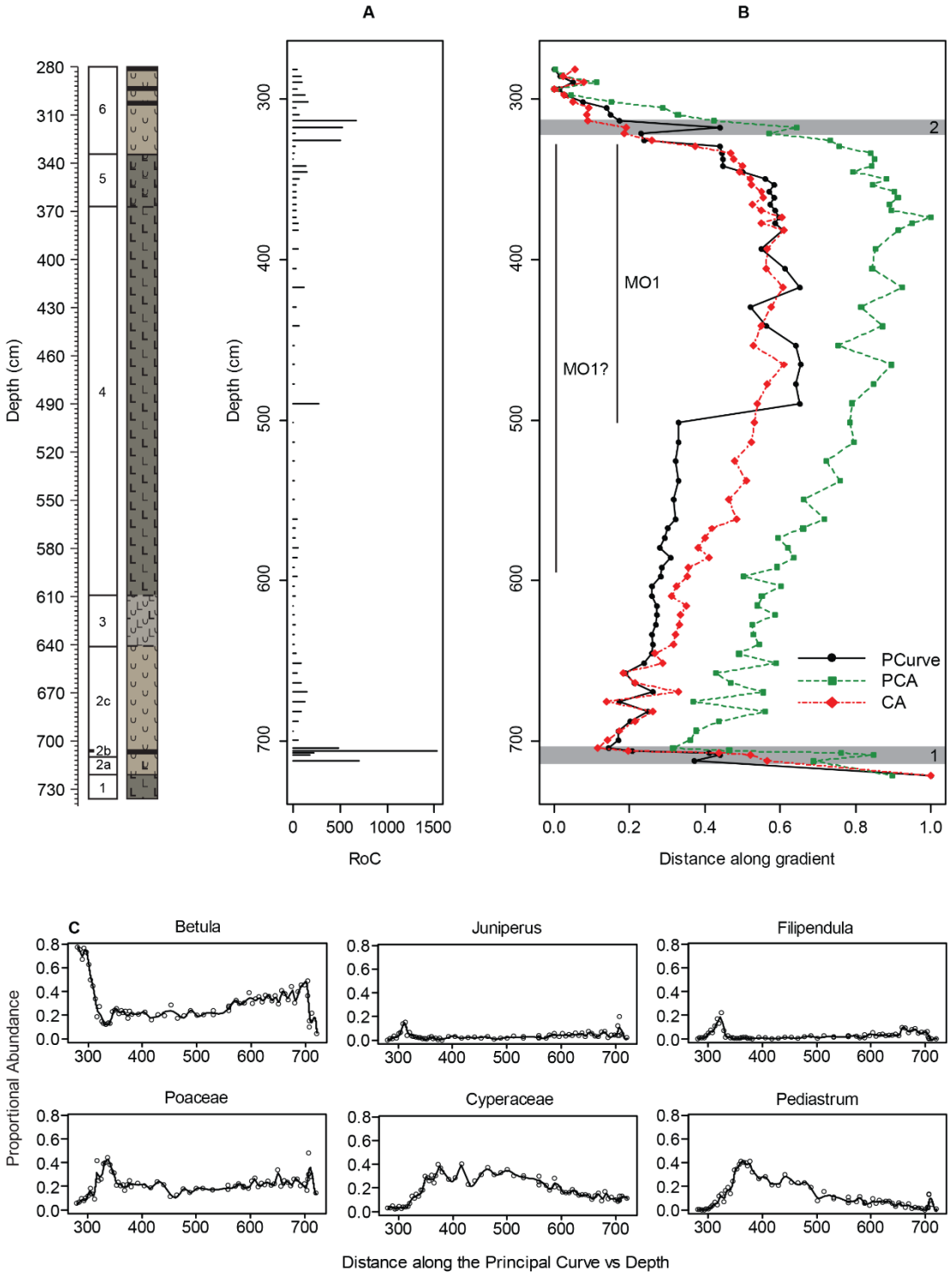

Figure 7.13 Results of the statistical approaches within the Core C pollen data. A) Rate of change analysis. All values are arbitrary, with an exaggeration multiplier applied to demonstrate significant periods of compositional change. The greater the length of the bar the more significant the compositional change. B) The overlain output from three tests applied (PCA, CA and PC). The different ordination approach clearly influences the output; however, a significant change is noted at 501.5 cm not observed in other approaches. With the PC, the data show rapid short oscillations (grey boxes) and a longer oscillation termed (MO1) (see main text for a note of caution) C) Individual taxa response curves modelled on the gradient of the PC.

Demarking increases in variance from the PC output (Figure 7.13) should be taken with caution. One major episode of variance is noted between 501.5-325.5 cm. However, due to overfitting and effects of localised taxa, for example Cyperaceae and *Pediastrum* occurring in greater percentages post 501.5 cm, caution is required. Actual increases in taxa that associate with this oscillation occur at deeper points (*Artemisia* and *Thalictrum* increases between 615.5-560.5 cm) suggesting that the episode starts before 501.5 cm. Nevertheless, two additional phases of greater variance are observed, which are confined to one or two sample points:

- Major Oscillation 1: Samples between 501.5-325.5 cm (615.5-325.5 cm)
- Oscillation 1: Samples between 708.5-704.5 cm
- Oscillation 2: Sample at 317.5 cm

RoC analysis suggests considerable vegetation change over the oscillations above with greatest change at the base of the sequence and within oscillation 2. Greater confidence is given to the placement of major oscillation 1 lower in the record, as minor increases in RoC are suggested. Individual taxa response curves demonstrate where points of change are indicated throughout the PC and Poaceae is the main plant taxon driving changes over the short oscillations outlined above. Again however, substantial increases in *Pediastrum* and Cyperaceae clearly influence the curve over major oscillation 1.

7.4 Micro- and macro-charcoal

Micro- and macro-charcoal analyses were undertaken matching the resolutions of the palynological assessment. However, due to time constraints Core C was not assessed for macro-charcoal. As a result, Core B contains 49 analyses of micro and macro-charcoal whereas Core C contains 70 analyses of micro-charcoal only. Average values for Core B charcoal concentrations are 210,753 shards/cm^{-3} whilst macro-charcoal concentrations are 26.53 fragments/cm^{-3}. In contrast Core C average concentrations are 131,826 shards/cm^{-3} (Figure 7.14).

Core B- Micro-charcoal

Charcoal concentrations range from 24,039 shards/cm^{-3} to 817,363 shards/cm^{-3}. Throughout Core B, five significant areas of increased charcoal accumulation are recognised. The first of these, STCBc-1, occurs in unit 4c and is characterised by a single peak of 429,592 shards/cm^{-3}. The second peak is shown by a spread of micro-charcoal between 405.5-373.5 cm with the greatest concentrations observed at 389.5 cm.

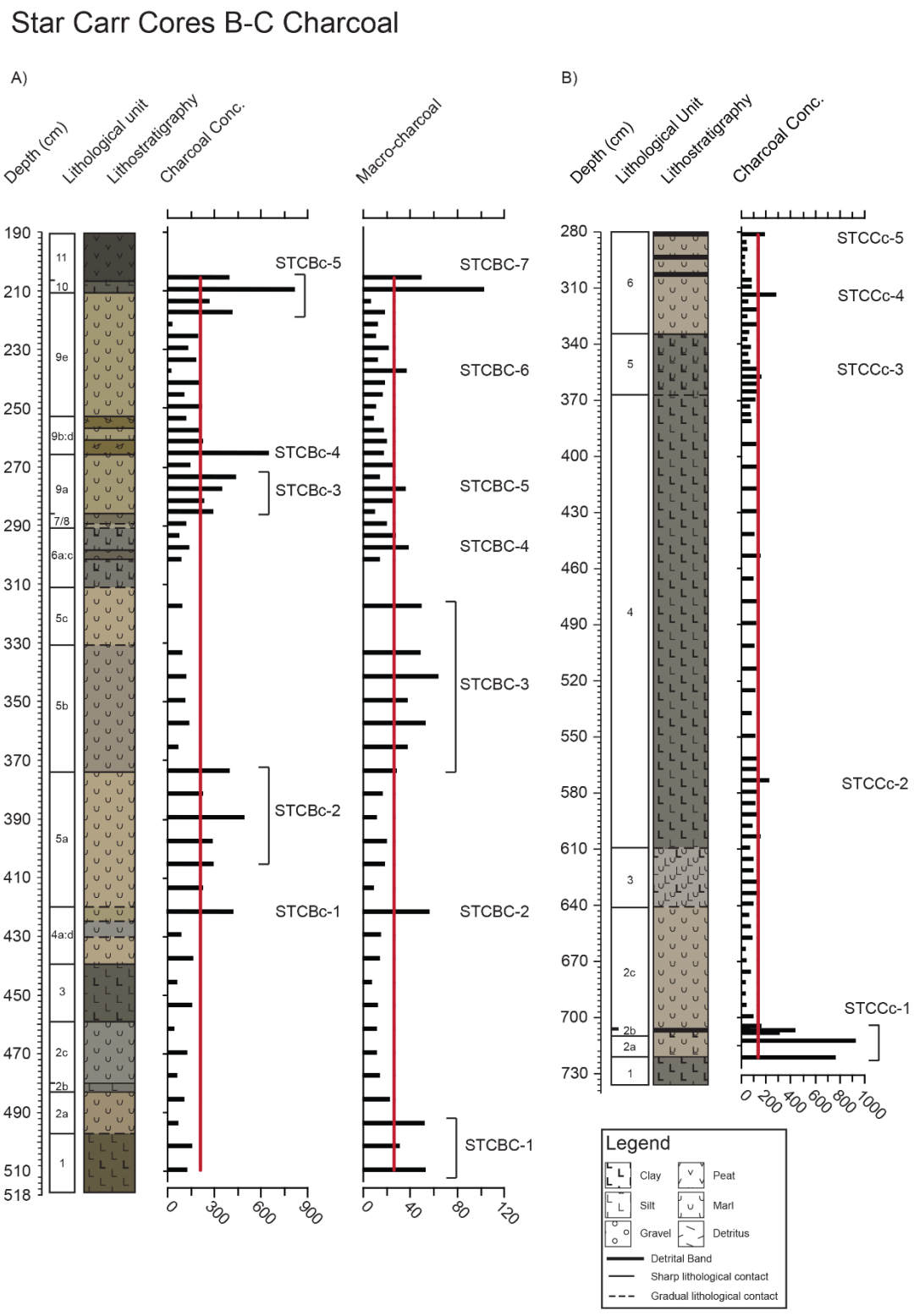

Figure 7.14 Results of the charcoal analysis from Core B (A) and Core C (B). Charcoal concentrations and macro counts from Core B exhibit both similarities and differences in peak locations. Further clear peaks can be observed within the concentration data for Core C. Average charcoal abundance is placed on the figure to assist in peak identification. Key peaks are presented with the prefix STCBc (concentration; B) STCBC (macro; B) and STCCc (concentration; C).

Subsequent peaks in micro-charcoal are not observed until after the gravel band. Between 289.5-273.5 cm, a clear increase in charcoal above the baseline can be observed. Bar the first point in the sequence, charcoal rises within successive samples to a high of 438,775 shards/cm^{-3}. The subsequent peak has not been included in STCBc-3 as charcoal concentrations are low at 269.5 cm. From this low concentration, charcoal abruptly increases to 648,438 shards/cm^{-3} at 265.5 cm. The final peak in the sequence contains the greatest concentrations. The STCBc-5 complex, spread over 16 cm has a peak centred on 209.5 cm with 817,363 fragments/cm^{-3}.

Core B- Macro-charcoal

Macro-charcoal observations range from 7 to 103 fragments/cm^{-3}. In contrast to the concentration data, seven significant macroscopic charcoal peaks or amalgamations are identified. The first of these are at the base of the sequence and are characterised by peaks of 53 and 52 fragments respectively. Subsequently, STCBC-2, displays a singular peak at 421.5 cm with 57 fragments identified. The next phase in the sequence displays a spread of charcoal between 373.5-317.5 cm. As all count data between these levels are high and above the average, this spread has not been split into multiple peaks. Furthermore, the most significant charcoal peak is observed within the middle of the complex, with 64 fragments at 341.5 cm. Units 7 to 11 display four additional phases of increased charcoal, STCBC-4 to 7, separated stratigraphically. Whilst STCBC4 to 6 are only marginally above average values, STCBC-7 contains the highest number in the sequence with 103 fragments.

Core C- Micro-charcoal

Within Core C micro-charcoal concentrations range from 26,712 shards/cm^{-3} to 926,782 shards/cm^{-3}. Throughout this sequence there appears to be a constant background signal with a minimal number of observations above the average. As a result, minor concentrations above this average have not been formally assigned, resulting in four significant charcoal peaks. The first, exists as a complex between 721.5-707.5 cm, with greatest concentrations of 926,782 shards/cm^{-3} occurring at 712.5 cm. Despite the increase in concentration at ca 707 cm, the complex has not been split. The remaining peaks throughout the sequence appear stratigraphically variable and are centred upon 573.5, 357.5, 313.5 and 281.5 cm. Concentrations of these peaks are 228,444; 161,171; 281,052; and 194,102 shards/cm^{-3} respectively.

7.5 Additional site data

The data presented within this section of the thesis includes all data from Cores B and C compiled alongside this thesis. In part this relates to an ERC funded POSTGLACIAL

project led by Professor Nicky Milner (University of York) with paleoclimatic data generated by collaborators at RHUL and the University of Southampton. Core B isotopic reconstructions were compiled by Ian Candy and Rebecca Kearney; with Core C determinations lead by Ian Candy and Christopher Darvill. Chironomid-inferred temperatures for both Star Carr sequences were compiled by Peter and Cathy Langdon (Preface; Chapter 4). This section also contains chronological information relating to the sequences.

7.5.1 $\delta^{18}O$ and $\delta^{13}C$ isotope stratigraphy

Within Core B, 244 stable isotopic analyses were performed; compared to 96 analyses from Core C (Figures 7.15; 7.16). Repeat measurements through unit 4 from Core C demonstrated considerable scatter between different measurements of $\delta^{18}O$. This scatter, which for certain data-points is more enriched than any other point throughout the isotopic reconstruction, may be the result of the measurement of different carbonate fractions. Under cold climatic conditions, which is unfavourable for authigenic carbonate production, the source of carbonate may be allogenic, i.e. material transported into the site from calcareous basement lithologies. As the Kimmeridge and Speeton Clays underlie the site and as the carbonates within are more positively enriched in $\delta^{18}O$ (Candy et al., 2015); detrital carbonate contamination affected the determinations in unit 4. From these observations, all unreliable measurements have been excluded from the reconstruction, totalling 79 samples (Figure 7.16).

Within Core B, across units 1 to 6a there is limited co-variation between $\delta^{18}O$ and $\delta^{13}C$ (R^2=0.39). At the base of the record $\delta^{13}C$ values are high (2.91 ‰) and follow a decreasing trend to a low of 0.44 ‰ at 453.5 cm. An oscillatory pattern is then observed between relatively enriched and depleted values prior to the gravel band. Depleted phases are centred at 373.5 (-1.16 ‰) and 315.5 cm (-1.54 ‰). Average $\delta^{13}C$ values over this phase are given as 1.00 ‰, 1σ=1.06. The $\delta^{18}O$ record peaks and troughs in the same manner as the $\delta^{13}C$ record. STCBO-1 is characterised by low $\delta^{18}O$ values of -6.81 ‰ at 492.5 cm, whereas STCBO-2, which is greater in magnitude, follows a trend of isotopic depletion to a low of -8.12 ‰ at 445.5 cm. Three additional isotopic depletions are noted. Average values are presented as -6.49 ‰, 1σ=0.61.

Within units 7 to 11 evidence for co-variation between $\delta^{18}O$ and $\delta^{13}C$ is negligible (R^2= 0.03). Initially, $\delta^{13}C$ values are enriched, up to 1.25 ‰ at 294.5 cm with a short phase of depletion between 294.5-280.5 cm. A general trend towards depleted values is observed

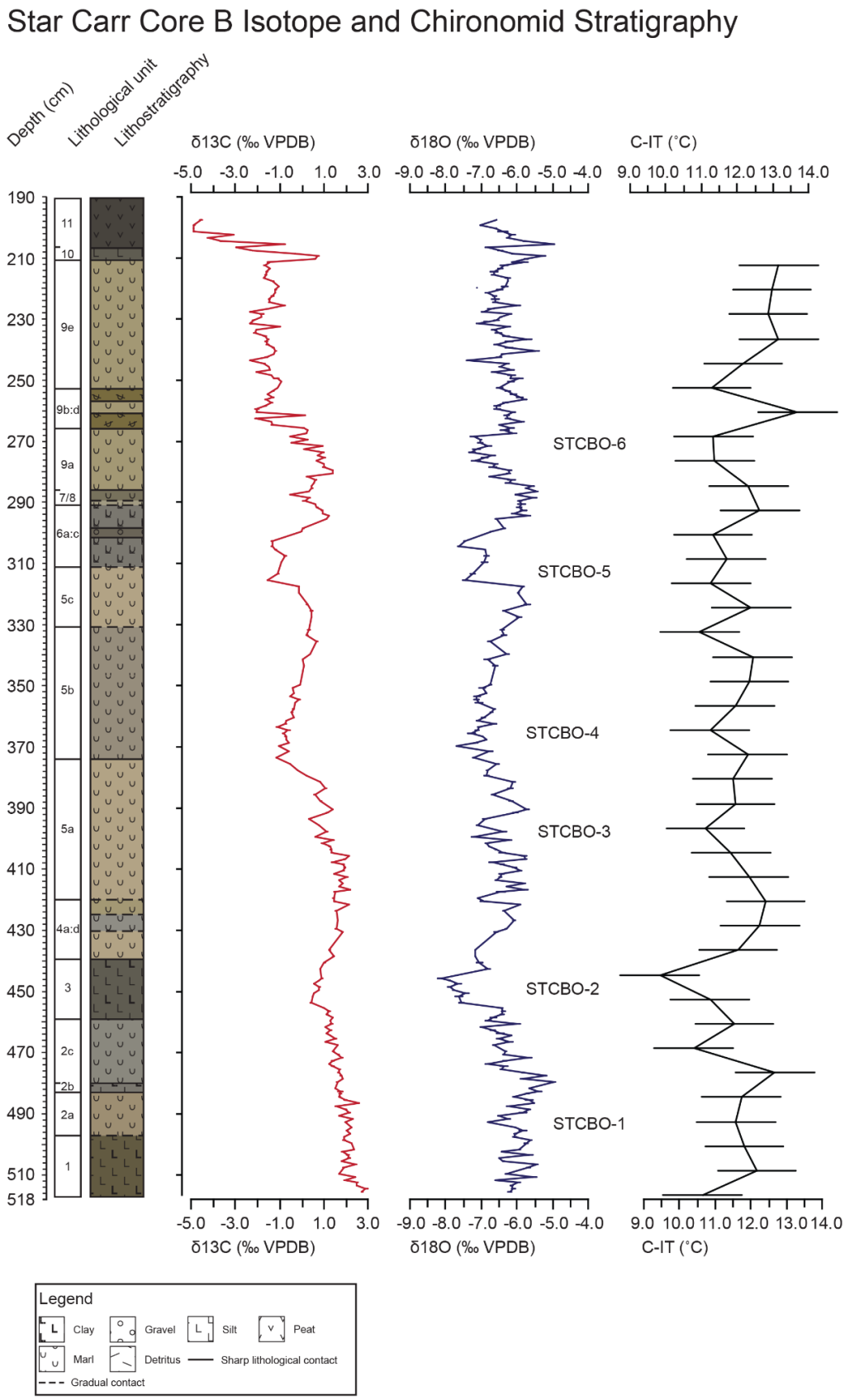

Figure 7.15 Oxygen and carbon isotopic stratigraphy alongside a chironomid-inferred temperature reconstruction from Core B. All isotope data are presented against Vienna Pee Dee Belemnite (VPDB) with temperature data presented as degrees Celsius. Clear oscillations can be observed in both the oxygen isotopic data and the C-IT. These events are labelled on the isotopic stratigraphy and are prominent throughout the sequence.

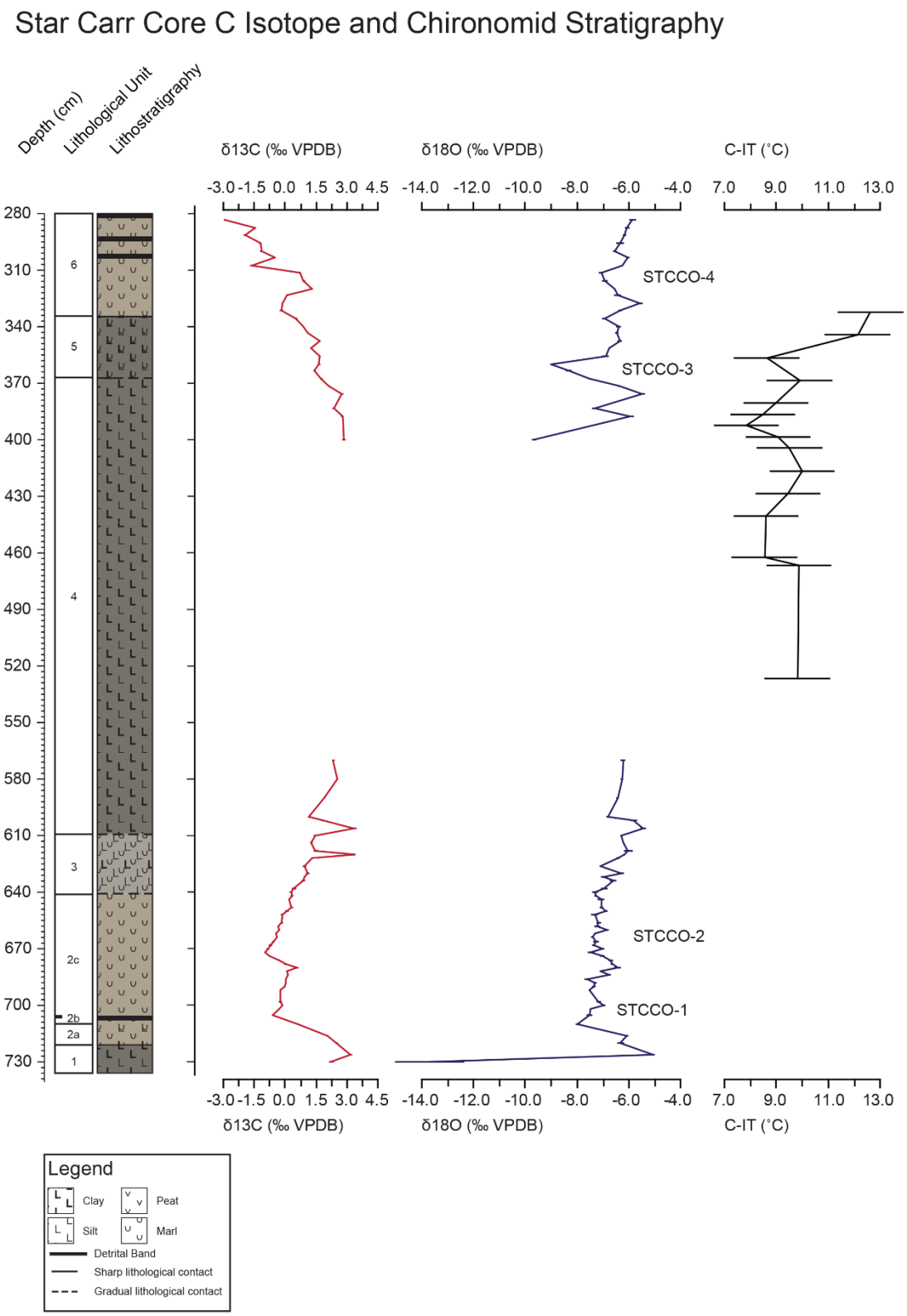

Figure 7.16 Oxygen and carbon isotopic stratigraphy alongside a chironomid-inferred temperature reconstruction from Core C. All isotope data are presented against Vienna Pee Dee Belemnite (VPDB) with temperature data presented as degrees Celsius. Depletions can be observed in the $\delta^{18}O$ record at the base of the sequence and both $\delta^{18}O$ and C-IT's at the top of the profile.

punctuated by a phase of enrichment between 280.5-265.5 cm. Average $\delta^{13}C$ values throughout this phase are -0.99 ‰, 1σ=1.06. Throughout this interval, considerable $\delta^{18}O$ depletions are lacking. However, coinciding with $\delta^{13}C$ enrichment, one depletion (STCBO-6) is observed between 286.5-267.5 cm; exhibiting a maximum depletion of -7.27 ‰ (Figure 7.15). Average oxygen isotopic values after the gravel band are -6.33 ‰, 1σ=0.45.

Throughout Core C there are varying degrees of covariation. Between units 1 to 3 there is minimal evidence of covariation (R^2=0.32). However, between 672-560 cm evidence for covariation increases (R^2= 0.76). With that in mind, $\delta^{13}C$ values at the base of the sequence are high, 3.16 ‰ at 726 cm. These values then drop to absolute lows of -1.00 ‰ at 672 cm. The remainder of the unit depicts a remarkably smooth trend towards increasingly enriched values. Average values for this phase are 0.66 ‰, 1σ=1.17. In contrast, the $\delta^{18}O$ signal is very depleted at the base of the sequence -13.71 ‰ and rapidly increases to -5.06 ‰ at 726 cm (Figure 7.16). Subsequently a depletion is observed, STCCO-1, between 716-684 cm, with maximum depletion of -8.00 ‰ at 710 cm. The remainder of the profile is characterised by a similar trend to the $\delta^{13}C$, albeit with a further depletion potentially identified between 680-630 cm. Average $\delta^{18}O$ values for this phase of the record are -7.02 ‰, 1σ= 1.18.

Within units 5 to 6 evidence for co-variation is reduced (R^2=0.18). From enriched values, 2.79 ‰ at 387.5 cm, $\delta^{13}C$ follows a trend of isotopic depletion with the most depleted values throughout the sequence observed at 283.5 cm. At this time oxygen values are more variable, with two depletions identified, STCCO3-4, centred at 360 cm and 311.5 cm respectively (Figure 7.16). The former is much greater in magnitude with a depletion of -9.01 ‰ whilst the latter displays depletion of -7.06 ‰. Average $\delta^{13}C$ and $\delta^{18}O$ values throughout this phase are 0.65 ‰, 1σ=1.57; and -6.72 ‰, 1σ=0.97 respectively.

7.5.2 Chironomid-inferred temperatures

C-IT's from the two sequences are shown in Figures 7.15 and 7.16. Core B contains a total of 39 July temperature analyses, spanning the complete sequence; whereas Core C contains 15 samples from units 4:5. Summer temperature inferences were generated using a WA-PLS regression model with a modern Norwegian calibration dataset (Blockley et al., 2018). Owing to the data not being generated by the author of this thesis, diagnostic information is not available here.

Prior to the sand and gravel band, summer temperatures are warm, between 11.0-13.1°C. However, throughout this phase, a series of temperature deteriorations can be

observed. The first, between 508.5-476.5 cm, is shown by a temperature reversion of 0.6°C, albeit within error of the technique. The largest reversion however, between 476.5-436.5 cm, exhibits a temperature decline from 13.1°C to 9.8°C. The final clear temperature reduction, before the sand and gravel band, is centred at 396.5 cm with lows of 11.1°C. Perhaps greater summer temperature variability exists during this phase. However, these reversions are confined to single sample-points and, barring the temperature estimate at 364.5 cm, are all within predictive error. Following the hiatus, high summer temperatures are noted, however between 292.5-260 cm summer temperatures decline from 12.6 to 11.3 °C.

Within Core C, summer temperatures are moderate, ca 10°C before increasing to >12°C at 344.5 cm. Throughout this record however, short small reversions in temperature have been noted with summer temperature changes of 1.3, 2.2 and 1.3°C respectively.

7.5.3 Chronology

To place both datasets into a chronological framework, chronological data has been used from Blockley et al. (2018). Within this framework, the upper organic sediments from both Cores B and C, and Monolith 1 (an extensively dated sequence from Palaeolake Flixton; Dark, 1998a) have been matched using biostratigraphic tie points, with the chronologies transferred. For a complete description of the chronological construction and age model see Blockley et al. (2018). Further chronological control was not obtained for the Core C sequence. However, to construct a chronology for the lower organic marls of Core B, available tephra data and radiocarbon analyses were combined with data from Wykeham Quarry, a site proximal to Palaeolake Flixton (Lincoln, 2017), where possible. Wykeham Quarry has a constraining radiocarbon date, OxA-32400, which has been incorporated as a *terminus post quem*, as the isotopic data within Lincoln (2017) suggest depleted values occurring before the values recorded in Core B. Further, a modelled date from a sand bed across Wykeham Quarry is proposed to link with the hiatus in Core B, therefore, the model has incorporated this boundary with sedimentation in Core B ceasing before Wykeham Quarry. The tephra in Core B is the Penifiler Tephra (Ian Matthews, pers. comm. 2018).

To construct the age model these data were combined (Table 7.7; Figure 7.17) and modelled using a p_sequence depositional model, using the IntCal13 calibration curve (Reimer et al., 2013), in OxCal V. 4.3 (Bronk Ramsey, 2008; 2009) (Chapter 4). The model produced good agreement across the sequence and was used to provide calendar age ranges. The model suggests sedimentation between 14.35±244 and 12.72±154. The complete age model from both Core B and C is presented in Appendix D.

Table 7.7 Summary of the all chronological constraints at Palaeolake Flixton Core B. Including: depth information, unmodeled input range and modelled output range (2 σ age range) and mid-point age with 1σ error.

Name	Depth (cm)	Unmodelled range (Cal. ka BP)	Modelled range (Cal. ka BP)	μ ± σ	Reference
Boundary Before Wykeham	300	12.86	13.01-12.42	12,724±154	Lincoln (2017)
OxA-32404	388	13.07-12.81	13.08-12.84	12,978±65	
Penifiler Tephra	435	14.07-13.81	14.05-13.79	13,923±65	Bronk Ramsey et al. (2015)
Boundary	518		14.84-14.01	14,354±244	
Boundary OxA-32400	518	15.13-14.31			Lincoln (2017)

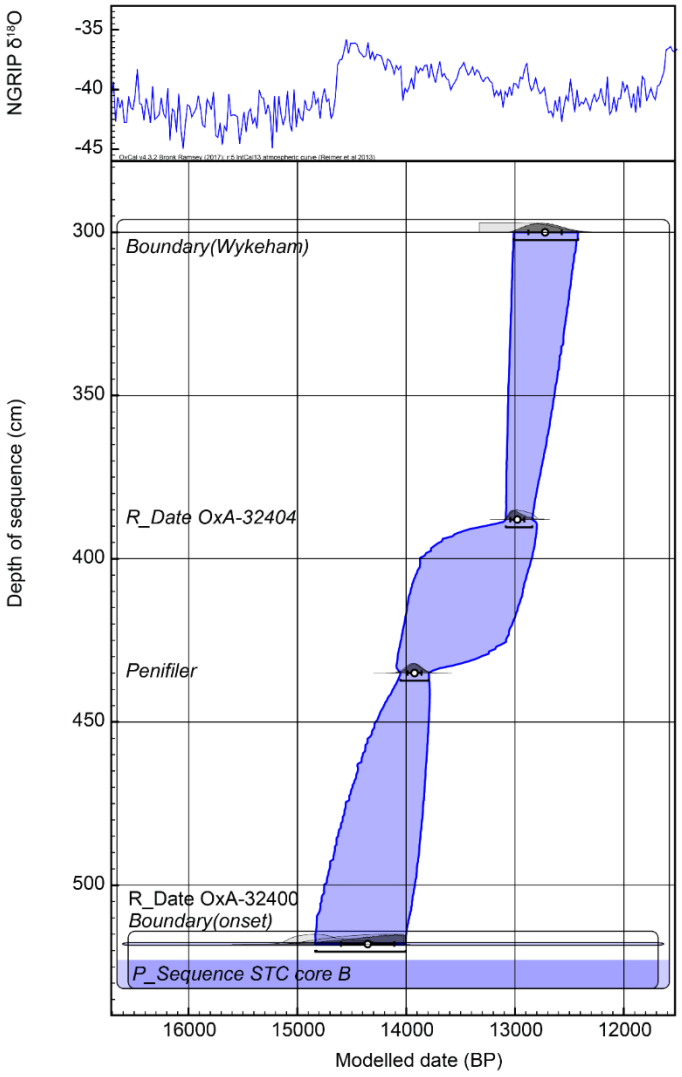

Figure 7.17 Age-depth, p_sequence model for Star Carr Core B, lower organic sediments, with age uncertainties plotted μ and 1 σ, whilst the complete range is shown at 2 σ. Boundaries have been added at the top and bottom of the sequence for interpolation.

7.6 Palaeoclimatic and palaeoenvironmental interpretation

The presented palaeoclimatic and palaeoenvironmental data is used here to reconstruct the climatic and environmental history in the vicinity of Palaeolake Flixton (PF). All palaeodata (Figure 7.18; 7.19; 7.20) will be discussed chronologically with vegetation-based interpretations and reconstructions based on the palynological profile. Whilst no chronology exists for lower sediments of Core C a holistic interpretation will be provided because both sequences can be tied using biostratigraphy, lithostratigraphy and sit in the landscape ca 30 metres from each other. The chronology, from the lower carbonates of Core B has therefore been transferred to Core C where possible. Based on the age modelling applied to this study, sediment units 1 to 5 (Core B) and units 1 to 3 (Core C) can be attributed to the Windermere Interstadial (WI); sediment unit 6 (Core B) and 4 (Core C) to the Loch Lomond Stadial; and sediment units 7 to 11 (Core B) and 5 to 6 (Core C) to the early Holocene (EH).

Isotopic considerations

The two presented sequences contain varying degrees of $\delta^{18}O$ and $\delta^{13}C$ covariation (Figure 7.19). Within Core B, sediment units 1:6 exhibit moderate covariation, R^2= 0.392; with no covariation observed in units 6c to 11, R^2= 0.027. In contrast, units 1 to 3 in Core C exhibit significant correlations, R^2= 0.673, with units 4 to 6 displaying minimal evidence, R^2= 0.184. From both Core B and Core C, covariation is higher in the lowest marl sediments attributable to the WI. Understanding this covariation is important as it may provide an insight into isotopic controls, for example evaporitic modification or detrital contamination. Potential contamination stems from detrital carbonate sources in the Kimmeridge, Speeton and Oxford Clay Formations but also the Ravenscar Group. For comparison, carbonate values from these groups are shown alongside isotopic values presented within this thesis (Figure 7.22). It is not thought that detrital contamination affects the isotopic values gained from PF because of 1) the lack of overlap with the main carbonate geological sources from the Vale of Pickering (Figure 7.22); and 2) the similarity of drilled calcite isotopic values, from thin sections, and bulk measurements from Core B (Candy et al., 2015), suggesting a dominant calcite source in the bulk isotopic measurements. Therefore, it is likely that PF, from which the Star Carr sequences originate, remained an open system with stable isotopic analyses performed on authigenic carbonates. Despite this generality, certain phases may have been affected by isotopic enrichment (369.5-302.5 cm; Core B; 672-570 cm; Core C; Figure 7.21) which will be discussed below. These considerations notwithstanding, the $\delta^{13}C$ can be interpreted based on the $\delta^{13}C$ of dissolved inorganic carbon (DIC) related to groundwaters, plant respired CO_2 and associated vegetative inputs and atmospheric CO_2 equilibration (Talbot, 1990; Leng and Marshall, 2004).

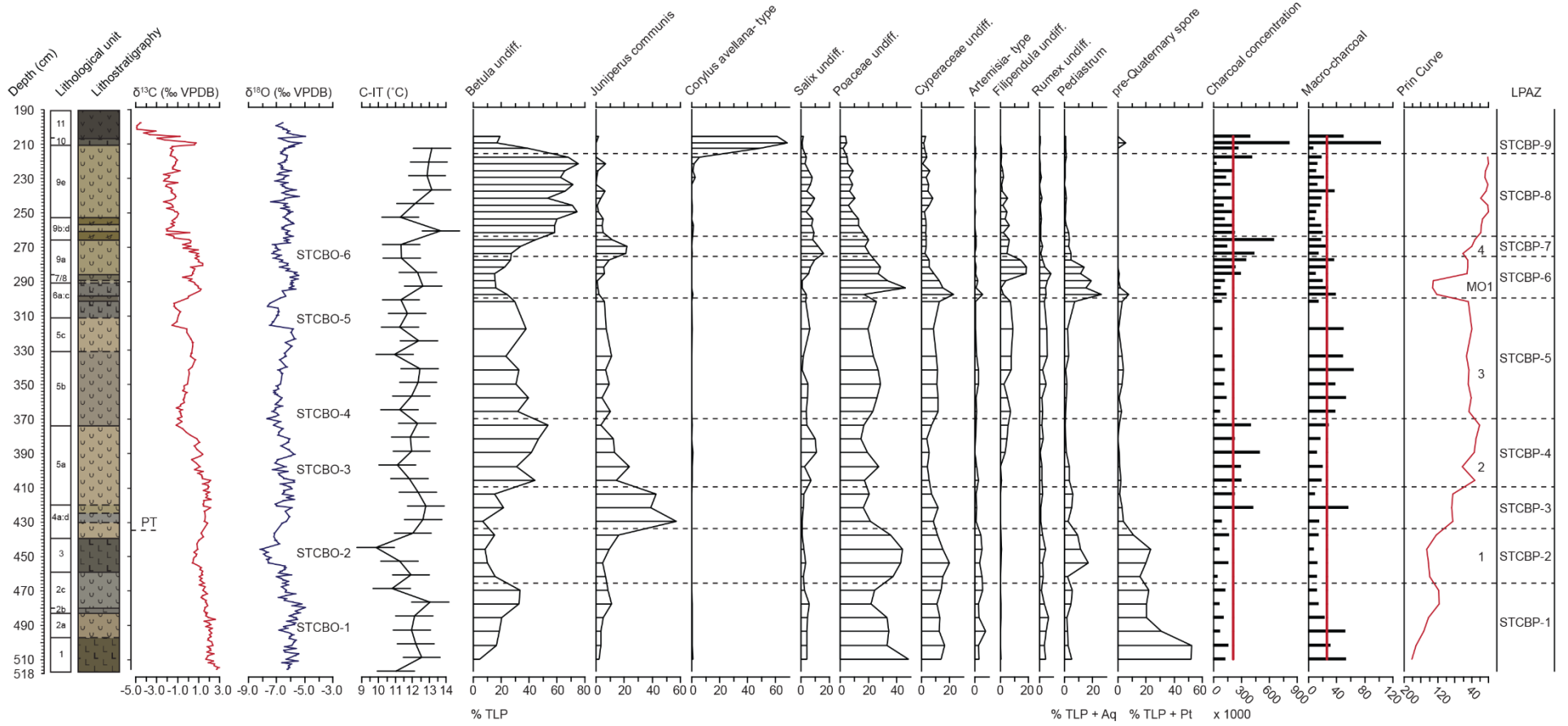

Figure 7.18 Summary of palaeodata presented from Star Carr Core B. The palaeoclimatic data are to the left of the series, and the environmental data to the right; only principal pollen taxa have been included here. As both charcoal concentrations and macro-charcoal exhibit both similarities and differences, they have both been included within this summary.

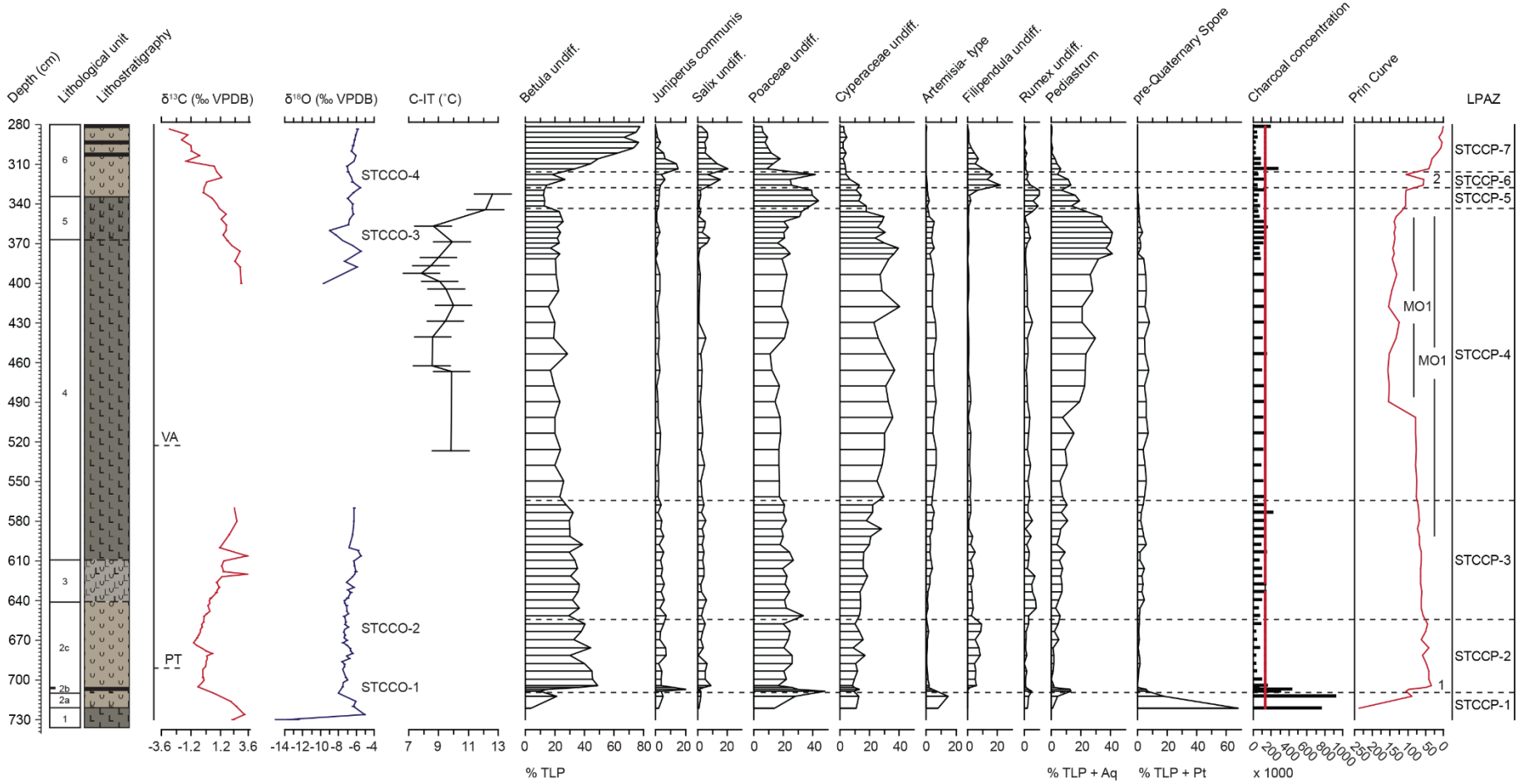

Figure 7.19 Summary of palaeodata presented from Star Carr Core C. The palaeoclimatic data are to the left of the series, and the environmental data to the right; only principal pollen taxa have been included here. Only charcoal counts alongside pollen counts were conducted for this sequence. The position of two tephra horizons are highlighted. The Penifiler Tephra, sits within the lower carbonates and the Vedde Ash, lies within the central silts and clays.

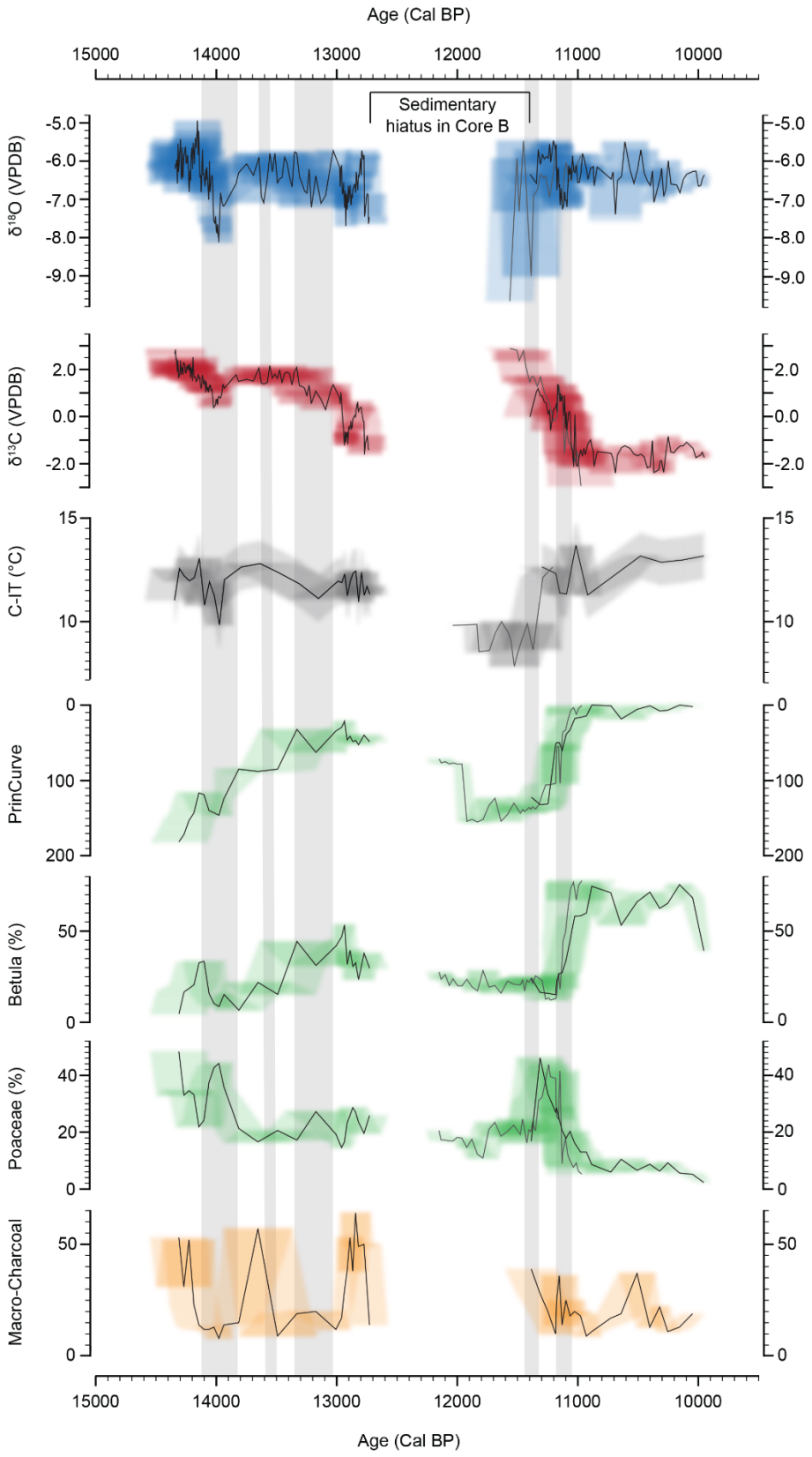

Figure 7.20 Comparison of all proxy data from Palaeolake Flixton. Core B (black lines) and Core C (grey lines) are amalgamated and placed on a common age to reveal overlaps in climatic events and stratigraphy. Shown are $\delta^{18}O_{carb}$, $\delta^{13}C_{carb}$ and chironomid-inferred temperatures. The principal curve is shows from the from the pollen data, with Poaceae and *Betula* percentages for comparison on the PC. Macro-charcoal counts are also presented. As macro-charcoal was not undertaken for Core C, and concentrations are on a different scale, micro-charcoal concentrations have not been added. Climatic deterioration episodes are shown on the diagram by grey shaded boxes.

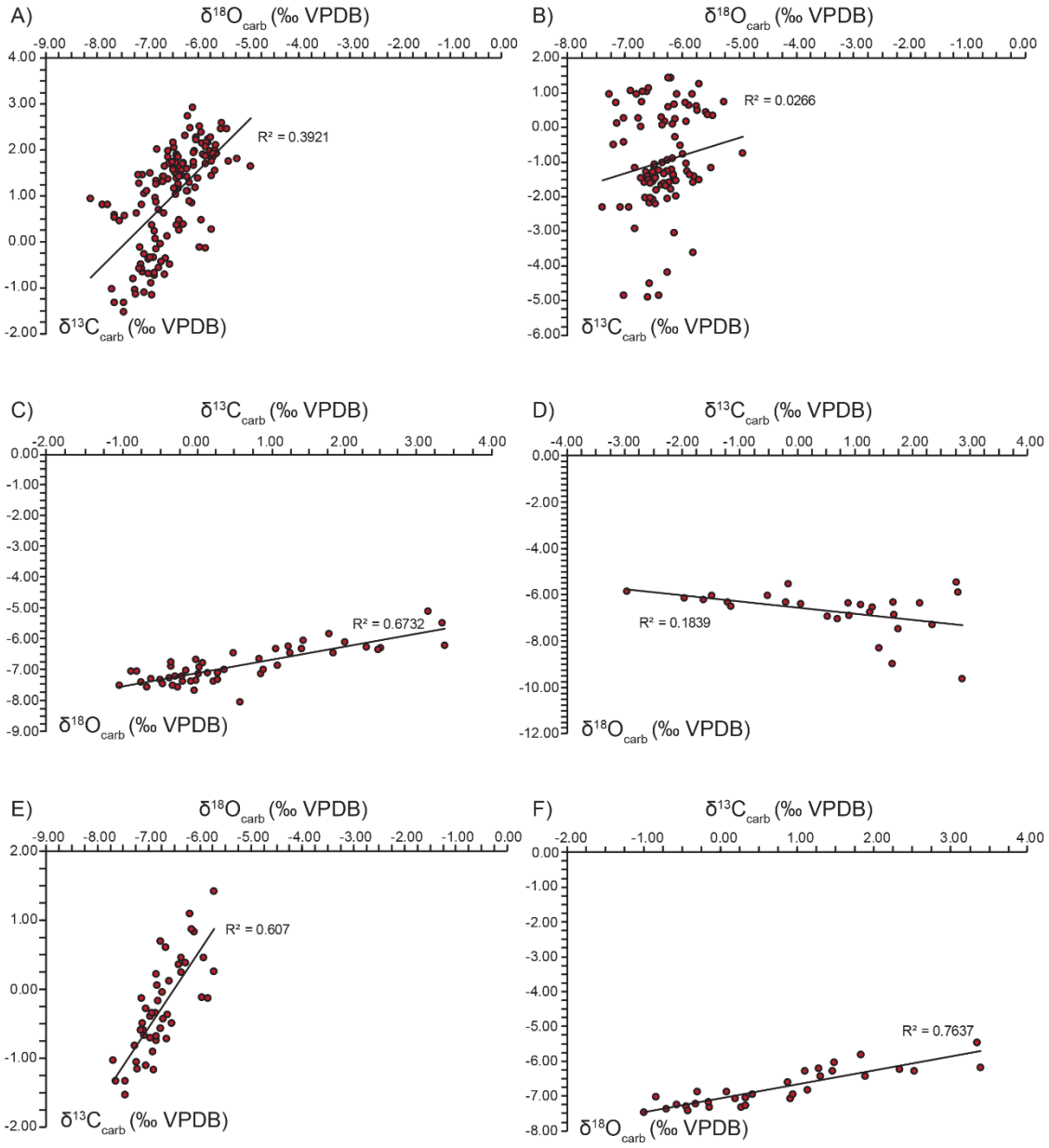

Figure 7.21 Series of scatter plots from both the Core B and Core C sequences with regression models applied to the $\delta^{18}O$ and $\delta^{13}C$ datasets to test for co-variation. A) from the lower carbonates of Core B; B) from the upper carbonates of Core B; C) from the lower carbonates of Core C; D) the upper carbonates of Core C; E) Model of co-variation between 390.5-302.5 cm; Core B and; F) regression model applied to sediments between 672-570 cm; Core C. The lower carbonate series from both sequences appears to demonstrate greater co-variation than the upper. This is pulled out by graphs E) and F) which demonstrates considerable co-variation between $\delta^{18}O$ and $\delta^{13}C$.

The $\delta^{18}O$ record can be interpreted in terms of the temperature dependency of carbonate mineralisation and the $\delta^{18}O$ of lake waters. The latter is then influenced by the $\delta^{18}O$ of precipitation, which is controlled by mean annual temperature, the amount effect and seasonality of rainfall (Chapter 4) (Leng and Marshall, 2004). As per other studies (e.g. Marshall et al., 2002; Whittington et al., 2015; Candy et al., 2016) the isotopic data from PF are interpreted as reflecting the influence of temperature on vapour condensation. Consequently, these data can be used to infer mean annual temperature change.

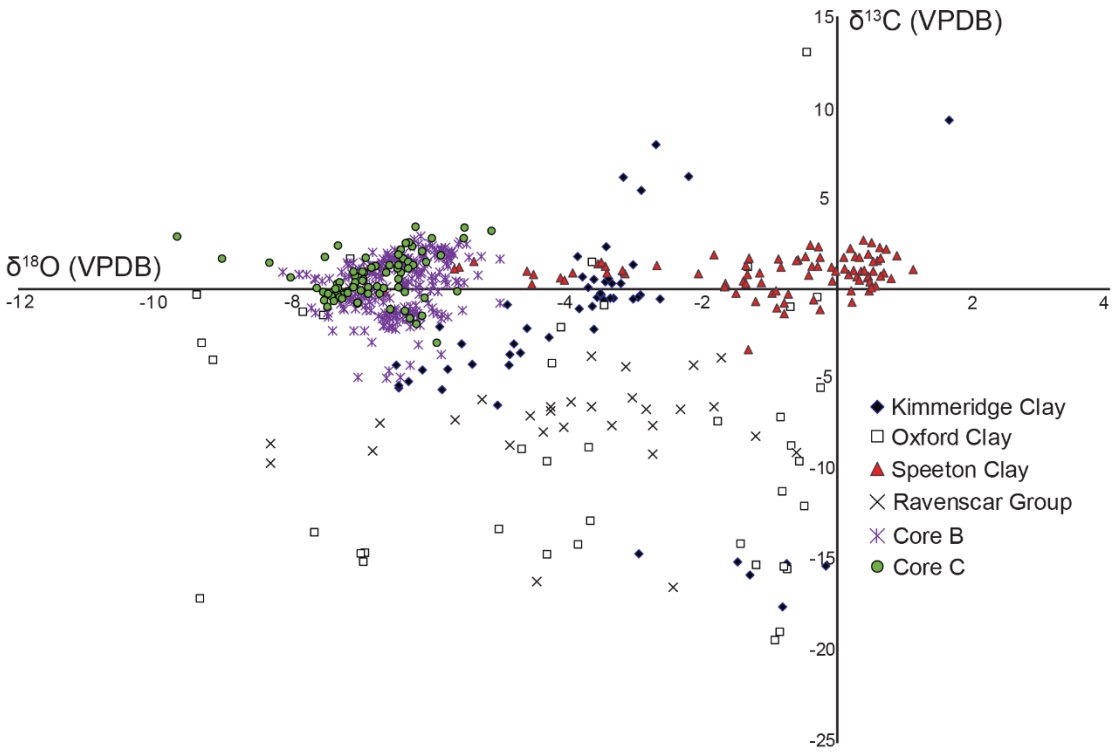

Figure 7.22 Evidence for the lack of an impact of geologic carbonates. $\delta^{18}O$ and $\delta^{13}C$ isotopic data from basement lithologies of the Vale of Pickering have been plotted alongside stable isotopic data within this thesis. In general there is minimal overlap between isotopic data from PF and geological carbonates. Data used from previously published sources (Irwin et al., 1977; Hudson, 1978; Astin and Scotchman, 1988; Kantorowicz, 1990; Price, 1998; Price et al., 2000). Modified from Candy et al. (2015).

Early Windermere Interstadial- 14.35±0.34 - 14.14±0.17 Cal. ka BP

The early-WI was dominated by minerogenic sedimentation that denotes erosivity in an unstable landscape. The presence of pre-Quaternary spores (52 % Core B; 68 % Core C) suggests erosion of glacial deposits in the catchment of PF. It is thought that pre-Quaternary spores are derived directly from the incorporation of Carboniferous palynomorphs in till sediments deposited by the North Sea Ice Lobe (NSIL) in the Vale (e.g. Busfield et al., 2015). Reworking of till material into the basin allows palynomorphs to be concentrated in the early-WI sediments at PF. This is also postulated to reflect greater charcoal incidence at this time (STCBC-1, STCCc-1) as these till members have previously been shown to contain abundant charcoal (Busfield et al., 2015).

The change from minerogenic to organic sedimentation across PF, is shown by the increase in $CaCO_3$ values. Following supersaturation of lake waters, $CaCO_3$ precipitation is either biologically mediated or controlled by physical chemical processes (Kelts and Hsu, 1978). Crucially, both processes are likely to be affected by enhanced climatic warmth with biologic and physical processes removing CO_2 from the water column, increasing alkalinity resulting in $CaCO_3$ precipitation (Kelts and Hsu, 1978). Climatic

warmth is suggested by enriched $\delta^{18}O_{carb}$ values from both sequences (-5.43 ‰ Core B; -5.06 ‰ Core C) via reduced poleward isotopic fractionation gradients with heightened temperatures. One sample from Core C (-13.71 ‰; 730 cm) is anomalously depleted for Britain (e.g. Marshall et al., 2002; Candy et al., 2016). Whilst this might be expected if analysed from DS sediments, it appears too depleted. The sample is derived from low carbonate-bearing sediments, and although the carbonate is not detrital (expected positive $\delta^{18}O$ values), the amount of CO_2 liberation may be insufficient leading to significant measurement error. Thus, the sample may be erroneous. Warm temperatures are suggested from C-ITs at this time (11.03-13.06°C; Core B). Owing to these heightened temperatures it is suggested, as with other sequences, the onset of the WI is not recorded within these two Star Carr sequences. Principally, the transition from low temperatures that characterised the DS to relative warmth during the WI is not observed. At this time high $\delta^{13}C$ values reflect greater atmospheric CO_2 exchange as both sequences are broadly in the range expected under atmospheric equilibrium +1 and +3 ‰ (Leng and Marshall, 2004).

During the early WI, the landscape was dominated by open herbaceous grassland taxa (Poaceae, Cyperaceae, *Artemisia spp* and *Rumex spp;* STCBP-1; STCCP-1). These taxa are interpreted as pioneering taxa that colonised the landscape surrounding PF, bearing little resemblance to suggested climatic warmth. Low pollen concentrations suggest incomplete colonisation and sparse vegetation coverage by an open, low-lying herbaceous grassland. The increase in woody taxa throughout the early-WI, shown by *Betula* undiff. and *Juniperus*, indicates that the landscape gradually stabilised, with the expansion of a *Betula* scrub, potentially coinciding with greater soil maturity. At this time the occurrence of *Betula* is presumed *B*. *nana*, which is often shown during the early-WI (Day, 1996; Mayle et al., 1997) as colonisation of tree birch was delayed due to the lack of suitable soils (Pennington, 1986).

High percentages of *Pinus* (9 % Core B; 48 % Core C) reflect a far travelled component with no incidence of *Pinus* identified in N Europe during the early-WI (Birks et al., 2005). However, the greater contribution of *Pinus* within Core C perhaps reflects three scenarios: 1) the onset of sedimentation was earlier within Core C; 2) the different positions of the sequences within Palaeolake Flixton and 3) deeper sampling within Core C. The lack of datable material from the base of both sequences hampers any assessment of the first scenario; however, if sedimentation began earlier under a sparsely vegetated catchment, greater pollen flux would be derived from a far-travelled component (e.g. Sugita, 1994). Palmer et al. (2015) detailed the undulations in the bed form of PF and depth discrepancies between multiple sequences. It is possible that the

shallower Core B exhibits greater sediment focussing and thus greater sensitivity towards local palynological incorporation; the deeper location of C may therefore reflect a greater far travelled component under reduced sedimentation. Due to sedimentation rate discrepancies, it is not possible to constrain sampling variability. A combination of these three scenarios may therefore explain the differences during the earliest WI.

Between 14.30±0.23 and 14.22±0.21 Cal. ka BP, a depletion in $\delta^{18}O_{carb}$ of 0.97 ‰ (STCBO-1; -5.84 to -6.81 ‰) is observed. This depletion may also be recorded by a 0.59°C shift in C-IT's. However, the lower sampling resolution in the C-ITs precludes formal attribution. Nonetheless a short duration climatic deterioration may have occurred. As the isotopic depletion is greater than suggested by the summer temperature decline (0.3 ‰ / °C; Leng and Marshall, 2004) it is possible that greater annual temperature change influenced the $\delta^{18}O_{carb}$ record. Alternatively, greater depletion relative to C-IT change is a product of changing source water $\delta^{18}O$ values. Following considerable influx of isotopically light meltwater into the N Atlantic during the early phases of the WI, this is a plausible mechanism. Freshwater influx into the Atlantic does however provide a further mechanism for a brief weakening of Atlantic Meridional Overturning Circulation (AMOC; Chapter 2), and thus it is currently uncertain whether a climatic event occurred at 14.2 Cal. ka BP. If an event did occur at this time, no vegetation response is observed, which is assumed to reflect basic vegetation development during the early-WI.

Early Windermere Interstadial- 14.14±0.19 – 13.89±0.17 Cal. ka BP.

Following marl accumulation, a shift in sedimentation style is noted across PF, shown in Core B by mineral sediments and a detrital band in Core C. Reductions in $CaCO_3$ and increased TOC (Core C) highlights a phase of renewed landscape erosion. These events are characterised by depletion in $\delta^{18}O_{carb}$, of 3.18 ‰ (STCBO-2; Core B) and 2.94 ‰ (STCCO-1; Core C), suggesting a phase of mean annual temperature change. Coeval with these changes, summer temperatures fall by 3.23°C, as inferred by C-ITs. These downturns are suggestive of a significant climatic deterioration during the early Interstadial. Despite lower C-IT resolutions, and as shifts in both proxies co-occur, it is likely that this deterioration affected the whole climatic system. Therefore, a temperature component is clearly recorded within the $\delta^{18}O_{carb}$ values, although, at present it is not possible to quantify the impact of greater mean annual change. The magnitudes of this climatic event will be discussed in Chapter 9. Throughout this event $\delta^{13}C$ becomes progressively depleted. As $\delta^{13}C$ has a minimal temperature fractionation offsets, continued depletion may result from the breakdown of organic matter with a greater incorporation of isotopically light CO^2 within groundwaters (e.g. Leng and Marshall, 2004; Talbot, 1990). The incorporation of light CO_2 would therefore deplete $\delta^{13}C$.

In association with this climatic event, vegetation changes are observed (STCBP-2 and within STCCP-1) from 14.10±0.17 Cal. ka BP. This assumption is supported by the changes in the PCs (Oscillation 1; Figure 7.20). Both sequences reveal similar changes in assemblage, however, sedimentation rates appear greater within Core B, owing to greater sediment focussing in proximity to the shore of PF, giving the appearance of an expanded stratigraphic phase. Reductions in *Betula* undiff. and *Juniperus* suggests a replacement of scrubland with Poaceae and greater colonisation of the marginal zone by Cyperaceae. Additional replacing taxa include: *Artemisia*, Asteraceae, Caryophyllaceae, *Helianthemum*, *Rumex,* and *Thalictrum*. These taxa, all associated with open-habitats, suggest a vegetative revertence early during the WI (Figure 7.20). Continued presence of *Artemisia* and increases in *Rumex* suggest areas of broken and disturbed ground; whilst *Helianthemum* suggests colonisation of bare rock/ground (Curtis et al., 1985). Low pollen concentrations at this point do not suggest widespread expansion, although increases in concentration of Poaceae are observed suggesting greater grassland abundance. Increases in pre-Quaternary spores alongside mineral sediments suggests reinvigorated breakdown and transport of tills in the Vale to PF (Busfield et al., 2015). Increases in *Pediastrum* coincident with these two observations likely reflected the in-washing of nutrient-rich soils, developed during the preceding phase, into the basin. Following this event, charcoal is abundant across PF (STCBC-2; STCCc-1). Greater charcoal production is likely to be due to greater fuel availability (Millspaugh and Whitlock, 1995) in the catchment and associated increased occurrence of fire and reworked charcoal bearing carboniferous deposits (e.g. Bisfield et al., 2015).

The taxa described above are clustered together within the PCA plots (Figure 7.10; 7.12). From Core B, a spread of taxa can be observed towards more positive values for axis one. In contrast, Core C demonstrates a cluster of taxa plotting positively on axis one. However, a secondary cluster of Poaceae and *Rumex* is observed showing greater affinity with axis two. These different clusters perhaps reflect a landscape stability gradient across axis one. With axis two in Core C perhaps demonstrating open landscapes.

Mid- Windermere Interstadial- 13.89±0.17 – 13.35±0.31 Cal. ka BP.

During the mid-WI a return to marl sedimentation with high carbonate values (98 %) is coupled with enrichment in $\delta^{18}O_{carb}$ (-6.30 ‰; Core B; -6.74 ‰ Core C) and warm summer temperatures, 12.8°C; confirming climatic amelioration from the preceding event. $\delta^{13}C$ also becomes more enriched, comparable to enrichment during the earlier WI,

suggesting a greater atmospheric CO_2 input. Allied to continued carbonate sedimentation enriched $\delta^{18}O_{carb}$ and high C-ITs suggest continued favourable climatic conditions.

In conjunction with this amelioration are considerable increases in *Juniperus* at 13.81±0.20 Cal. ka BP. Increasing *Juniperus*, decreasing open-habitat vegetation and low *Betula* undiff. reflects the colonisation of the landscape surrounding PF by a *Juniperus* scrubland. The increase in thermophilic *Juniperus* is surprising given its affinity for mature soils (Lowe and Walker, 1986). Whilst climatic warmth is suggested, soils are likely to be immature considering the types of vegetation present and suggestion of soil movement during the preceding event. However, low percentages of *Betula* coupled with high *Juniperus* percentages may reflect the pioneering abilities of Juniper (Branch, 1999) and the lack of competition from woody vegetation. Increased concentrations of *Juniperus* clearly demonstrates the widespread establishment of this plant taxon. The establishment of this taxon, a shade intolerant shrub (Walker, 1975), suggests that *Betula* was predominantly *B*. *nana*. At 13.49±0.32 Cal. ka BP (STCBP-4; STCCP-2) *Juniperus* populations and herbaceous vegetation abundance decreased, suggesting the loss of *Juniperus* scrub. At this time *Betula* undiff. appears to replace the scrubland. During the mid-WI it is possible that *Betula* is both *B*. *nana* and tree birch. Whilst macrofossils were not identified across these sequences, *Betula pubescens* fruits have been identified at comparable stratigraphic positions at this site by Dark, (1998c). Expansions of stands of *B*. *pubescens* would likely outcompete *Juniperus* following the establishment of suitable soils (Pennington, 1986). Increases in *Filipendula* and *Salix* throughout both zones point to establishment of moist, fertile soils under a moderately humid climate (Hormata, 1995).

Late Windermere Interstadial- 13.35±0.31 – 13.01±0.18 Ca ka BP.

During the late-WI an event is recorded at PF, however, it is only identified within the Core B climatic record. A depletion of 1.45 ‰ (STCBO-3) is observed within $\delta^{18}O_{carb}$ suggestive of a period of reduced mean annual temperatures. Further a summer temperature decline is observed with declines of 1.22°C. The data suggests that summer temperatures are the first to change, during the mid-WI, however, this is likely a product of the sampling resolution attained. At 13.35±0.31 Cal. ka BP, the PC (Figure 7.20) and RoC analyses reveal an inversion in the vegetation record (Oscillation 2; Core B). From the pollen and individual taxon response curves, declines in *Betula* and *Salix* occur alongside increases in Poaceae and *Juniperus* (STCBP-4; STCCP-2). The replacement of these taxa suggests a partial landscape opening, with replacement of *Betula* woods, and a reversion to a *Juniperus* scrub-open grassland mosaic. The re-expansion of *Juniperus* may point to an increase in habitat availability following landscape opening. In

close association with this inferred vegetation revertence is an increase in charcoal concentrations (STCBc-2). The changes in climate and vegetation are not accompanied by an increase in the macro-charcoal record, suggesting there was not an increase in local fire incidence in the catchment of PF. Instead, it is assumed that greater micro-charcoal concentrations at this time reflects an increase in far-travelled charcoal input; or greater in-washing with microscopic charcoal in soils. The lack of any sedimentological change and paucity of taxa previously interpreted as reflecting greater soil movement (e.g. *Pediastrum* and pre-Quaternary spores) is at odds with the latter suggestion. A greater far-travelled input therefore appears more likely. Whilst depleted $\delta^{18}O_{carb}$ is noted within Core C (STCCO-2) a comparable isotopic structure to Core B is not observed. Coupled with no evidence of vegetation change, it is not thought that a second WI event exists within the Core C WI record.

Late Windermere Interstadial- 13.01±0.18 – 12.74±0.15 Cal. ka BP.

The remainder of the isotopic profile from the WI appears problematic. Principally, the $\delta^{18}O$ and $\delta^{13}C$ data across both sequences exhibits considerable covariation (R^2= 0.607 core B; R^2= 0.764 Core C; Figure 7.21). Covariation has been inferred to reflect either detrital contamination (e.g. Mangili et al., 2010) or potential isotopic modification. Detrital contamination can be disregarded based on the lack of overlap with detrital carbonates from the Vale (Figure 7.22). Following initial depletion at 12.92±0.09 Cal ka BP, both $\delta^{18}O$ and $\delta^{13}C$ reveal smooth enrichment across both sequences. Enriched $\delta^{13}C$ values are unexpected at this time, due to greater inputs of plant-respired CO_2 into vadose waters; with plant respired CO_2 depleted relative to $\delta^{13}C$ (Cerling and Quade, 1993). In contrast, aquatic plant respiration/photosynthesis would increase $\delta^{13}C$ through assimilation of the lighter $\delta^{12}C$ (Hammarlund et al., 1997). However, these effects working in opposite directions would not cause the observed enrichment. Therefore, initial depletion may reflect a climatic perturbation with subsequent enrichment a result of evaporitic modification. If this were true, an initial climatic deterioration may impact lake levels, which, by association may impact lake water residence times. Greater residence times increase the potential for evaporitic modification of the isotopic signal. Regardless, the structure of the isotopic data reveals decoupling from the climatic regime. Therefore, the proposed depletions (STCBO-4; STCCO-2) cannot be related to a climatic event. Further, C-ITs are inconsistent but do not fall beneath 11.0°C, suggesting minimal summer temperature change.

Throughout this phase the pollen records are variable. Across both records (STCBP-5) and (STCCP-2/3) losses of *Betula* are noted alongside increased Poaceae, Cyperaceae, *Rumex,* and *Artemisia*. This is suggestive of a shift in assemblage although a contraction

in Betula populations may not have occurred. However, increases in the xerophytic *Artemisia* may suggest aridity. The continued presence of *Filipendula* alongside *Artemisia* is surprising given the affinity of *Filipendula* for moisture and damp fertile soils (Birks and Matthewes, 1978; Hormata, 1995). It is postulated that continued summer warmth may exert greater control than moisture over the mesophilic *Filipendula* (Edwards and Whittington, 2010). Across both PC's, there are subtle changes (Figure 7.18; 7.19; Oscillation 3; Core B) however, as major changes in vegetation are not observed a revertence has not been formally placed.

The terminal WI across PF perhaps therefore demonstrates a transitional phase. This may help explain the complex isotopic and C-IT signals and the apparent mis-match between the presence of woody/thermophilic taxa alongside Poaceae, *Rumex* and *Artemisia*. A transition may also explain continued carbonate sedimentation across both sequences, albeit reducing in Core C, and the presence of charcoal (STCBC-3) despite no directional climatic change.

Loch Lomond Stadial- 12.74±0.15 – 11.50±0.21 Cal. ka BP.

In Core B, the deposition of a gravel lens suggests a sedimentary hiatus. Comparatively, Core C reveals an expanded phase of predominantly silt and clay sedimentation comprised of low organic carbon, $CaCO_3$ values and increases in MS. It has been postulated (e.g. Palmer et al., 2017) that a hydroclimatic shift lowered the water table and consequently the lake level across PF. Owing to the undulating bathymetry across PF (Figure 7.1) a reduced lake level would leave the shallower basin exposed with the potential to accumulate sands and gravel under greater landscape erosion and the deeper basin would retain lake water but at a lower level.

The length of the minerogenic unit suggests that the small, relatively deep Core C basin experienced substantially higher sedimentation rates throughout this phase. Three lines of evidence support this: 1) inwash of clastic material would have been enhanced by the steep relief immediately around the basin; 2) the presence of the Vedde Ash (Core C, 522.5 cm; modelled to 12.023±0.05 Cal. ka BP; confirming LLS attribution), which is characterised by a long upward tail structure (Darvill, 2011) suggests sedimentological loading and considerable reworking of material from the lake margins, where tephra was deposited originally on the land surface; and 3) continued carbonate presence alongside high MS values, with peaks coinciding with isolated coarse gravel clasts. A continued carbonate presence throughout the LLS, alongside discarded isotopic data (Darvill, 2011), is taken to reflect reworking of geological carbonates, under heightened periglacial activity. Taken together, all three pieces of evidence suggest increased

energy in the system during the LLS and heightened erosivity with continued landscape instability.

Summer temperatures in association with the deposition of the Vedde Ash were relatively cold, 9.82°C. Towards the end of the Stadial however, summer temperatures fall to 7.84°C. The prior warmer temperatures do not provide a mechanism from which extensive landscape erosion could force minerogenic sedimentation. To enable this sedimentation style, temperatures may have been much cooler during winter months signifying greater seasonality and a continental climate. From this dataset alone however, this can only be postulated.

The direct placement of the LLS, from a biostratigraphic view is problematic and issues are borne out in the PC (Figure 7.19). The greatest period of change in the PC occurs at 11.96±0.06 Cal. ka BP (Figure 7.20) however, this is post deposition of the Vedde Ash and cannot therefore be the vegetative expression of the LLS. The preferred scenario for the onset of the LLS lies with initial increases in *Artemisia* (STCCP-3) at approximately 12.74±0.15 Cal. ka BP (Figure 7.18). Unfortunately, this phase of Core C is not chronologically constrained. Throughout this phase, *Betula* undiff. is continually recorded, albeit with trends towards lower percentages, suggesting reduced *Betula* populations on the landscape. Given the 12°C threshold for tree birch growth (e.g. van Dinter and Birks, 1996) some of the *Betula* in the catchment were likely *B. nana*. However, a fraction of the *Betula* pollen identified are amorphous (e.g. Lowe and Lowe, 1989). Physically abraded pollen (e.g. Cushing, 1964; 1967) suggests that a subset of the identified *Betula* pollen are reworked. Nonetheless, thermophilous plant taxa, including *Juniperus* and *Filipendula*, also follow a falling trend. Replacing these taxa are plant types from open-habitat or disturbed ground assemblages including Poaceae, Cyperaceae, *Rumex*, *Artemisia* and *Thalictrum*. Therefore, following the onset of the LLS, an open grassland vegetation community dominated the landscape surrounding PF. Vegetation densities are suggested to be low with low pollen yields throughout the LLS.

At the point of greatest change within the PC (11.96±0.06 Cal. ka BP; Figure 7.20) increased abundances of *Pediastrum* and Cyperaceae are noted. *Pediastrum* blooming has previously been inferred to reflect nutrient loading into the basin (e.g. Birks, 2000; Sarmaja-Korjonen, 2006). However, the potential for greater *Pediastrum* abundance is increased with shallow lake waters (Weckström et al., 2010). The same scenario is true for Cyperaceae, with lake level lowering increasing habitat availability and an expansion of the littoral zone in proximity to PF. Therefore, despite continued minerogenic

sedimentation, nutrient loading and resuspension, littoral and algal dominance is reflective of continued lake level adjustment. Which, by association is being recorded in the PC. At this point therefore, the PC is not reflecting dominant terrestrial vegetation change. This is confirmed by the RoC analysis where minimal compositional turnover is suggested. Thus, owing to the presence of these taxa, the dominant vegetation assemblage was open grassland, but also typical of a littoral fen-type environment, under considerable lake level adjustment.

Early Holocene- 11.50±0.21 – 11.12±0.16 Cal. ka BP

The earliest Holocene is recognised within Core C. Whilst still dominated by minerogenic sedimentation, increasing $CaCO_3$ and reduced MS suggests a reduction in erosivity, with lacustrine carbonate production occurring with climatic amelioration (Kelts and Hsu, 1978). Increased mean annual warmth is suggested with a transition to enriched $\delta^{18}O_{carb}$ values, from -9.66 to -5.47 ‰. Although these isotopic samples are derived from mineral-rich sediments, that may be fraught with issues of detrital contamination, the reconstructed values are deemed to be reflective of authigenic carbonate production as: 1) the $\delta^{18}O_{carb}$ and $\delta^{13}C_{carb}$ values are within the range expected for carbonates during the EH (e.g. Marshall et al., 2002); 2) absolute values are comparable to peak enrichment observed during the WI; and 3) the $\delta^{18}O_{carb}$ and $\delta^{13}C_{carb}$ data do not co-vary; which is characteristic of detrital contamination or isotopic modification (Leng et al., 2010; Mangili et al, 2010). Enriched $\delta^{13}C$ again suggest greater atmospheric CO_2 input into the DIC pool during the EH, under sparsely vegetated landscapes. Occurring alongside greater mean annual temperatures, summer temperatures increased (to between 7.84 and 9.9°C). However, summer temperatures were still depressed suggesting full climatic amelioration had not yet occurred (Blockley et al., 2018), or that enrichment in $\delta^{18}O_{carb}$ reflects increased seasonal temperatures.

Floristically, the earliest Holocene revealed no change from the terminal LLS. A result of the continued presence of pioneering, open- and disturbed-ground indicators. Taxa present on the landscape included: Poaceae, Cyperaceae, *Salix* and *Artemisia* (STCCP-4). High percentages for Cyperaceae and *Pediastrum* reflect continued restriction of the lake body during the earliest Holocene, suggesting continued low moisture availability. This further, provides evidence for the lack of sedimentation within the Core B basin. At 11.41±0.23 Cal. ka BP, increased pollen concentrations, suggests greater vegetation development (STCCP-4). In conjunction with this view however, greater concentrations of *Salix*, *Pediastrum*, Cyperaceae, Poaceae and to a lesser extent *Betula*, may indicate a reduction in sedimentation rates, therefore reduced minerogenic sedimentation.

Superimposed upon this ameliorating climatic signature is evidence of two early Holocene climatic deteriorations. Two are identified within Core C with one identified in Core B. The former, between 11.45±0.22 and 11.37±0.24 Cal. ka BP (STCCO-3) is characterised by isotopic depletion of 3.54 ‰ (from -5.47 to -9.01 ‰). Co-occurring with this depletion is a reduction in C-ITs by 1.26°C (from 9.9 to 8.6°C). Unfortunately, the resolution of the C-IT data is not sufficient to reveal whether this deterioration was manifest by greater seasonal change. This former event is not present in Core B, owing to continued depressed lake levels and no competent basin at this time. Nevertheless, the data suggests a climatic event at PF with reductions in mean annual and summer temperatures.

Occurring alongside this climatic event *Salix*, *Rumex* and *Pediastrum* abundances increased (STCCP-4). Together, these may reflect a period of landscape instability with *Salix* requiring continued disturbance or exposure, but also perhaps later snow lie in the Vale (Wijk, 1986; Beerling, 1993), and *Pediastrum* reflecting turbid lacustrine conditions (Weckström et al., 2010). However, as these frequently increase in abundance during the EH in Britain (e.g. Day, 1996) this is difficult to establish. Further, no decrease in woody taxa occurred, which might be expected given the magnitude of isotopic depletion, using the early WI as an analogue. Throughout this phase the principal woody taxon, *Betula*, continued to persist on the landscape although it is likely attributable to *B*. *nana*, which was common to the EH in N Europe (Birks and Birks, 2014). Further, as minimal response is suggested by the PC, a vegetation revertence, if present, is minor.

The second early Holocene climatic event at PF can be matched across both sequences through the structure of the isotopic record and chronological constraints (e.g. Blockley et al., 2018). Between 11.18±0.14 and 11.05±0.14 Cal. ka BP, isotopic depletions of 1.80 ‰ (STBO-6; Core B) and -1.50 ‰ (STCCO-4; Core C) are recorded. Broadly synchronous with isotopic depletion, within Core B a C-IT decline of 1.31°C is further observed. Therefore, between 11.18±0.14 and 11.12±0.16 Cal. ka BP an abrupt climatic event is suggested that exhibited reduced mean annual and summer temperatures. Unfortunately, the C-IT record, is not sufficiently resolved to confidently identify changing parameters of the climatic system however, depressed isotopes and C-ITs across both events likely displays similar causality.

The latter climatic event appears to reveal a vegetation revertence across both sequences (Figure 7.20). However, reductions in *Betula* are not thought to be the expression of this event (STCBP-6) rather are thought to be related to: 1) taphonomy and the cessation of sediment redeposition, and 2) a shift in landscape conditions

whereby *B. nana* is being replaced by tree birch. Across both sequences this phase occurs in association with the transition from clastic to marl sediments, shown by lithostratigraphy and greater carbonate percentages. The cessation of mineral sedimentation is a mechanism for the reduction in redeposition and resuspension of *Betula* pollen, which is confirmed by fewer degraded *Betula* pollen grains. Equally, a transition between different *Betula* plant types may not be seamless; a period of intermediary vegetation change is likely. Therefore, the fall in Betula pollen is a response to a series of complex factors and unlikely to be climatically driven in this instance.

However, vegetative responses to the second event are manifest by a pause in the expansion of *Betula*, reduced abundances of *Filipendula*, continued presence of Poaceae and increases in *Salix* (STCBP-6/7; STCCP-6). Both sequences further display increased abundances of *Pediastrum*. The greater incidence of open herbaceous vegetation points to a pause in *Betula* development with increased *Salix* reflective of greater landscape exposure (Beerling, 1993). The reduction in *Filipendula* is related to subdued temperatures and perhaps greater aridity (Walker et al., 1993a). Further increased *Pediastrum* is, at this time, thought to relate to enhanced nutrient loading as opposed to a lake level variability. PC data across both sequences reveal reversions to greater values which statistically confirm the evidence of a vegetative revertence. Further, the taxa present are confined to positive clusters within both PCAs (Figures 7.10; 7.12). Considering inversions in the PC occur with summer and mean annual climatic change, this revertence is clearly in response to a climatic event. These vegetation changes occur alongside increases in charcoal (STCBC-5; STCCc-4), suggesting greater fire occurrence in the landscape. Despite the recording of these climatic and vegetation episodes, the events are not sufficient to cause widespread ecological change, typified by a pause or slight reduction in *Betula* pollen. Thus, early Holocene vegetation changes appear muted when compared to the events within the WI.

Early Holocene- <11.13±0.13 Cal. ka BP

Whilst variable, the remainder of the early Holocene is characterised by warm annual and summer temperatures as suggested by enriched isotopic data and elevated C-ITs. Progressive depletion in $\delta^{13}C$ reveals the greater input of depleted plant/soil respired CO_2 into the DIC pool with greater catchment vegetation densities (e.g. Hammarlund et al., 1997; Andrews, 2006; Leng and Marshall, 2004). After the amelioration from the preceding climatic events the vegetation was dominated by an increasingly woody flora. Principally, the expansion of *Juniperus* at 11.13±0.15 Cal. ka BP may be taken to reflect a change in edaphic conditions following the climatic event, as *Juniperus* avoids moist

soils (Huntley and Birks, 1983). The sequence observed at PF suggests the establishment of a shrubland mosaic with increasing *Juniperus* alongside stands of tree birch and *Salix*. High percentages of *Betula,* at 10.98±0.14 Cal. ka BP suggests the establishment of open birch woodland within the catchment, a common feature of all British pollen diagrams from this region (e.g. Bartley et al., 1976; Pennington et al., 1972; Lowe, 1982; Walker and Harkness, 1990) at this stage during the EH. Poaceae, Cyperaceae, *Salix*, *Filipendula*, *Dryopteris* and Filicales reveal a distinctive and rich understory vegetation and suggesting humid conditions persisted in an open woodland.

The final phase broadly coincides with clay sedimentation and peat initiation across PF at 9.95±0.05 Cal. ka BP. Clay sedimentation is taken to reflect suspension settling within a small undisturbed pool prior to peatland formation. Floristically, the record is dominated by *Corylus* (STCBP-9). High pollen percentages suggest the emergence of hazel as a canopy species (Birks, 1970) and the establishment of a *Corylus* woodland at PF.

7.7 Chapter summary

This chapter summarises the litho-, palyno- and climatostratigraphic findings from two sequences from Star Carr, Palaeolake Flixton, eastern England. These sequences show considerable complexity in depositional history although both can be attributed to the LGIT. Climatic warmth is revealed during the Windermere Interstadial with the pollen data, and evidence of birch fruits from previous analyses (Dark, 1998c), suggesting birch woodland development, following a period of expansive *Juniperus* scrub. The Loch Lomond Stadial is variably represented. Within Core C mineral sedimentation and the deposition of the Vedde Ash confirms Stadial attribution. Although a hiatus within Core B precludes the identification of this phase. Nonetheless the Stadial environment is dominated by Cyperaceae, *Pediastrum*, *Artemisia*, Caryophyllaceae, *Rumex*, *Thalictrum* and pre-Quaternary spores. During the Holocene, carbonate sedimentation and rising mean annual and summer temperatures are observed with vegetation dominated by at first an early successional pioneering community, then extensive scrubland, open birch woodland and finally a birch-hazel woodland.

Superimposed on these trends are a series of centennial-scale climatic events as recorded in oxygen isotopic data and C-ITs. At least two can be observed in the Interstadial, alongside a further two during the Holocene. During the Interstadial, vegetation responses to these events appear to show woodland/landscape opening with a proliferation of grassland communities. In contrast, negligible vegetation responses are noted for the first Holocene event (11.4 ka), but a response is noted for the latter (11.1

ka) whereby a pause in the expansion of *Betula* is noted with an expansion of open grassland. Thus, as elsewhere vegetation response during the Holocene appears muted.

Chapter 8. Results from Llangorse

Llangorse is an extant lacustrine basin, north-east Brecon Beacons, south Wales. The calcareous sediments within the basin, some of the most southerly within Wales, provide a unique opportunity to study the expression of abrupt climatic events from this locale. The vegetation dynamic, at lower latitudes, is expected to contrast to that from higher latitudes. Therefore, any vegetation revertences observed may be somewhat different from sites to the north.

The Llangorse basin has previously been the subject of a palynological assessment (e.g. Walker et al., 1993b) however, the focus of this investigation was to understand vegetation change within the marl sediments beneath a crannog within the lake. From this location, this investigation was the first to robustly reconstruct the vegetation history of Llangorse during the earliest Holocene (Walker et al., 1993b). Furthermore, Walker et al. (1993b) postulated a vegetative revertence within sub-zone 3a whereby *Juniperus* percentages were replaced by Poaceae and open ground herbaceous taxa including: *Artemisia*, *Thalictrum*, *Helianthemum* and Caryophyllaceae. The authors suggest this is a vegetative response to a short-lived climatic oscillation within the early Holocene. Despite this observation, there was no palaeoclimatic data from the sequence.

Recent reinvestigations of the Llangorse basin, including the retrieval of carbonate sediments from the north-west of the present lake (e.g. Walker et al., 1993b) has demonstrated, for the first time, sedimentological associations throughout the LGIT. The purpose of this chapter is to present to litho-, palyno- and climatostratigraphic results within this project and provide a detailed interpretation of the results presented. All results from this chapter are presented in Appendix E.

8.1 Basin sedimentology and stratigraphy

The north-west basin of Llangorse lake was sampled in the summer of 2014 by members of the Centre for Quaternary Research, Royal Holloway, University of London. Sediments were retrieved from the location of (51.930930, -3.2625103) which became the focus of the present Llangorse project.

The cores retrieved from the sampling location are presented in Figure 8.1. Broad climatostratigrpahic zones are presented on the diagram based on changes in lithostratigraphy and bulk sedimentology. A composite profile was created using key marker horizons and patterns in the bulk sedimentology between individual cores. This composite therefore represents the most complete sedimentary profile from Llangorse.

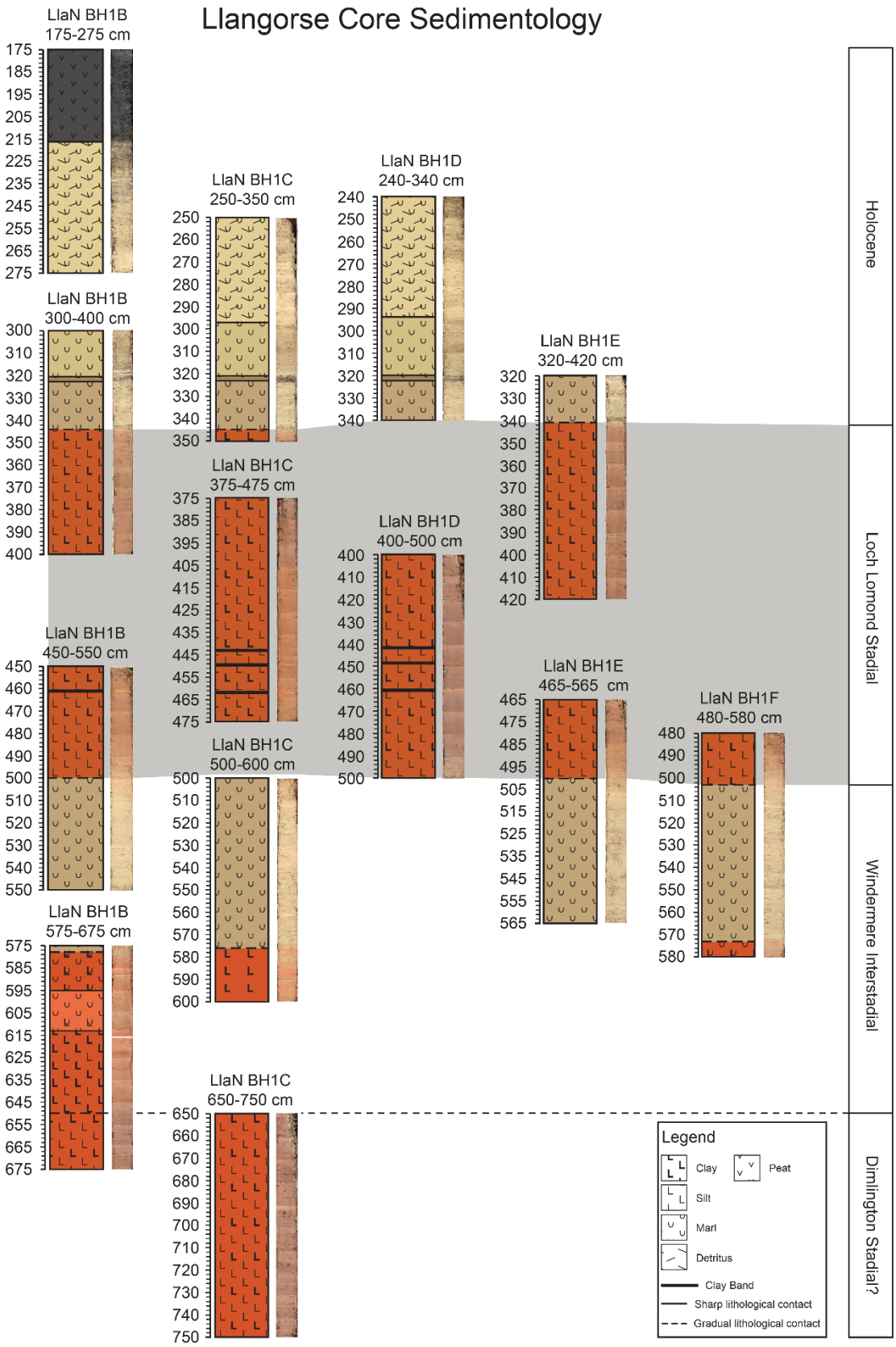

Figure 8.1 Llangorse basin sediment stratigraphy. The sequence presented here contains all cores extracted from the sampling location within the northern-western sector of Llangorse. The sediment cores presented here demonstrate remarkable consistency regarding sedimentological associations between different sediment units, especially with the duplicate cores (D-F).

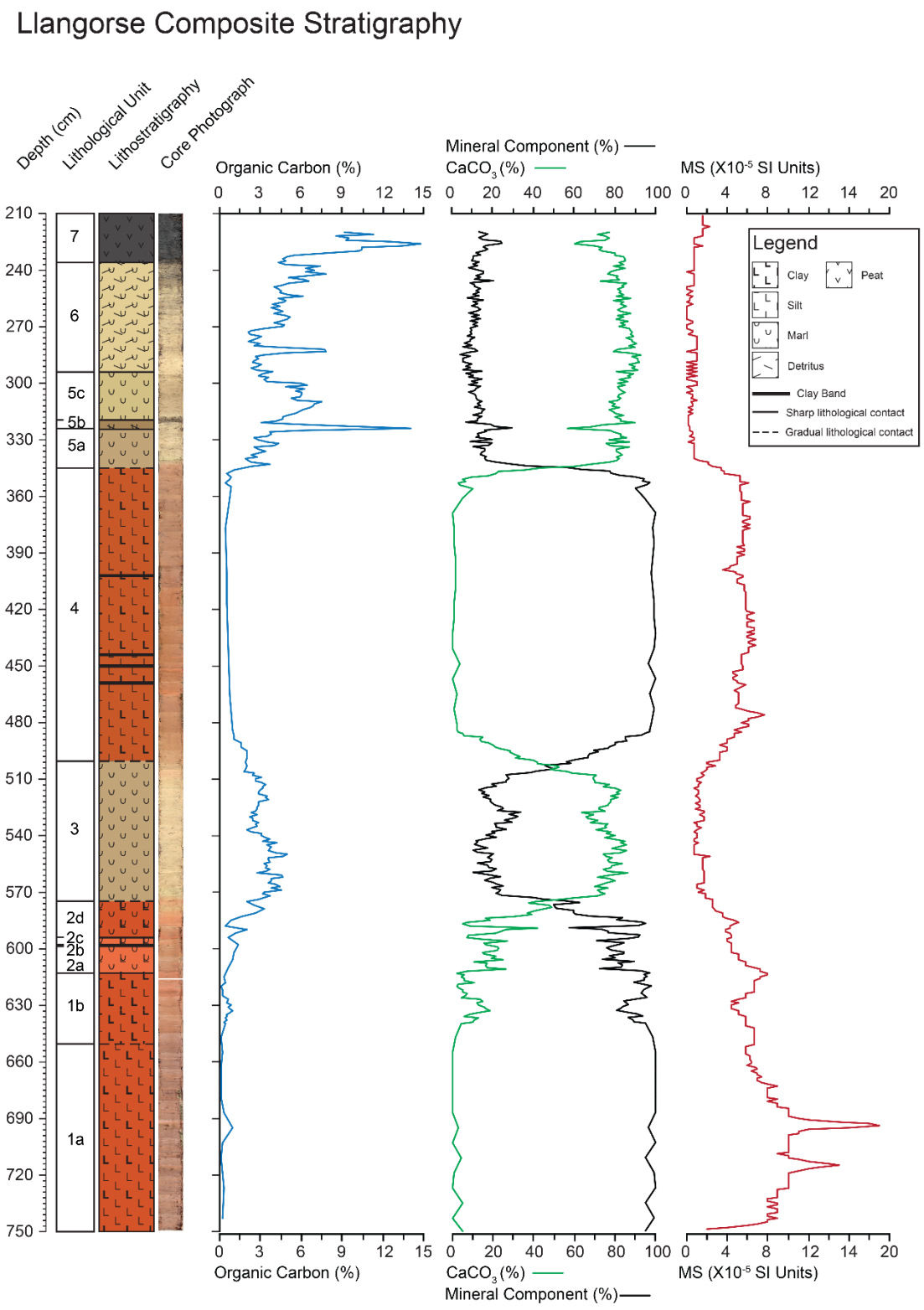

Figure 8.2 The composite stratigraphy for Llangorse. Shown are TOC, calcimetry values, mineral component and magnetic susceptibility. The relationships between the different data sources are clear to see with increased mineral components and MS values during the central minerogenic phase coinciding with reduced $CaCO_3$. Oscillations in $CaCO_3$ may point to the impact of climatic events on the sediments at Llangorse.

The composite profile, 750 cm at base, is shown by a classically tripartite sequence (e.g. Walker and Lowe, 2017) whereby minerogenic sediments are successively overlain by organic sediments and a secondary minerogenic phase. At Llangorse this secondary minerogenic phase is overlain by further organic sediments.

Table 8.1 Lithostratigraphy of the Llangorse composite sedimentary profile within this research. Shown here are the major sedimentological units and sub units, their Troels-Smith descriptors, classification and Munsell colour. What is not shown in this table are the diffuse transitional sections between units and detailed observations. For example, diffuse sedimentological associations between units 3 and 4 and 4 and 5a and a series of clay bands within unit 4.

Unit	Depth (cm)	Troels-Smith	Classification	Munsell colour
7	236-210	Th3, Dh1	Peat	5Y 2.5/1 Black
6	294-236	Lc3, Dg1	Marl (with detritus)	2.5Y 6/2 L. Brownish Grey
5c	321-294	$Lc^4$4, Dg+	Marl	2.5Y 4/3 Olive Brown
5b	324-321	$Lc^4$2, Dg2	Marl (with detritus)	2.5Y 3/2 V. D. Greyish Brown
5a	345-324	$Lc^4$4, Dg +	Marl	2.5Y 5/2 Greyish Brown
4	500-345	Ag3, As1, Ga+, Dg+	Clayey Silt (with sand)	5YR 3/3 Reddish Brown
3	574-500	$Lc^4$4, As+, Dg+	Marl	2.5Y 5/2 Greyish Brown
2d	595-574	As3, Lc1	Marly Clay	2.5YR 4/3 Reddish Brown
2c	597-595	As2, $Lc^4$2	Clayey Marl	2.5YR 4/2 Weak Red
2b	598-597	As4	Clay	2.5YR 4/3 Reddish Brown
2a	613-598	As2, Ag1, $Lc^4$1	Silty, Marly Clay	2.5YR 4/2 Weak Red
1b	650-613	As3, Ag1, Lc^4+	Silty Clay	2.5YR 4/3 Reddish Brown
1a	750-650	Ag3, As1	Clayey Silt	2.5YR 4/3 Reddish Brown

Table 8.1 and Figure 8.2 show the stratigraphy of the core sequence from Llangorse. Unit 1a is characterised by silt and clay sedimentation containing high magnetic susceptibility (MS) values, up to 19 $x10^{-5}$ SI units, and high mineral components, 99 % (Figure 8.2). Unit 1b is shown by a shift from silt to clay sedimentation, with reduced MS values and higher percentages of both calcium carbonate, between 1-18.4 %, and organic contents, up to 1 %. The subsequent complex, units 2a to 2d, demonstrates an oscillatory pattern between increased/reduced carbonate and clay. Peaks in $CaCO_3$, 23 % and 42 % are interspersed with troughs of 7 % and 5 %. Within the low $CaCO_3$ values, MS peaks are observed.

Clear changes are observed in unit 3 with lacustrine marl sedimentation. High $CaCO_3$ values, 50-86 %, characterise the unit with concomitant increases in TOC, between 2-5 %. However, contrary to this trend, variations are noted between 540-520 cm; whereby reduced carbonate percentages are noted, from 80-64 %, with coeval declines in TOC.

Sedimentological unit 4, reveals a distinctive shift from marl sedimentation to the deposition of red silts and clays. This minerogenic sedimentation is comprised of reduced carbonate percentages, <5 %, the initial transition into the unit notwithstanding, increased MS values, 7.6 $x10^{-5}$ SI units, and a greater mineral presence, >95 %. Further, at 461-463 cm; 449-451 cm; 443-441 cm and 402-402.5 cm bands of pure clay can be observed. Whilst comprised of clastic sediment, increases in carbonate content and TOC are noted at the top of unit 4.

Unit 5a to 5c, 6 and 7 exhibit a return to organic sediments. Units 5 and 6 reveal marl sedimentation with varying degrees of detrital input. These two units contain high carbonate percentages, between 44 and 93 %, and high but variable TOC, between 2 and 14 %. A detrital moss band, unit 5b, is shown by a large peak in organic carbon, and reduced carbonate. Finally, unit 7 is the capping peat unit to this sequence, which shows elevated TOC values, up to 15 %.

8.2 Palynological results

The Llangorse palaeobasin was analysed for pollen at variable resolutions. Across most of the profile, between 655.5-486.5 cm and 402.5-248 cm sediments were analysed for pollen at 4 cm resolution. Between 486.5-402.5 cm a greater resolution of 12 cm was obtained. A total of 88 samples were processed with resolutions hoped to be sufficient to detect abrupt vegetation shifts. The sediments beneath 594.5 cm were re-processed using a HF procedure as density separation at this depth provided poor palynological yields. Furthermore, the basal three samples, 650.5 cm; 644.5 cm and 640.5 cm

contained minimal pollen and the count sum was curtailed to 100 TLP. For two levels in the sequence, 620.5 cm and 614.5 cm a lack of pollen was identified using both approaches, hence were discarded. From 88 pollen samples a total of 11 local pollen assemblage zones have been defined (LlaP-*n*). In contrast to Quoyloo Meadow, pollen zonation did not include *Pediastrum* as at Llangorse the values are considerably lower. Percentages of the small *Pediastrum* fraction will be discussed only.

Zone LlaP-1. Composite depth: 651-638.5 cm.

Zone LlaP-1 is dominated by high percentages of *Pinus* pollen. *Pinus* reaches percentages of 27 % and, other than *Betula*, represents the only arboreal taxon. The herbaceous pollen spectrum is composed of elevated percentages of Poaceae, 19 to 27 %, *Artemisia,* 6 to 9 %, and *Rumex,* 11 %. A key feature of this zone are high percentages of unidentifiable pollen. A maximum peak of 40 % is observed at 650.5 cm. It is noted, whilst not recorded, the unidentifiable grains are amorphous. Moderate percentages of pre-Quaternary spores are also shown with highs of 12 %.

Total land pollen concentration is low throughout this zone, with a maximum concentration of 5735 grains/cm^{-3}.

Zone LlaP-2. Composite depth: 638.5-596.5 cm.

The second zone is characterised by high percentages of herbaceous pollen. The dominant taxon is Poaceae, with high percentages at the base of the zone, 41 %, decreasing to a low of 26 % by the top of the zone. *Rumex* and *Artemisia* are constant throughout and exhibit a small peak at 628.5 cm. A secondary peak in *Rumex* is observed at 602.5 cm where percentages increase to 16 %. The arboreal pollen spectrum is primarily characterised by rising values of *Betula*. Additional taxa noted throughout the zone include *Pinus*, *Salix*, Cyperaceae and Compositae: Lactuceae with *Pediastrum* forming the bulk of the aquatic input.

TLP concentrations are generally increasing through the early phases of LlaP-2 from 9813 grains/cm^{-3} to 22,052 grains/cm^{-3}. However, at 624.5 cm, concentration drops significantly to 7850 grains/cm^{-3} before increasing to 35,170 grains/cm^{-3} at the top of the zone. At comparable percentage peaks in *Artemisia* and *Rumex*, both taxa increase in concentration to 3234 grains/cm^{-3} and 3455 grains/cm^{-3} respectively. A concomitant peak is also observed in Poaceae with 6983 grains/cm^{-3}.

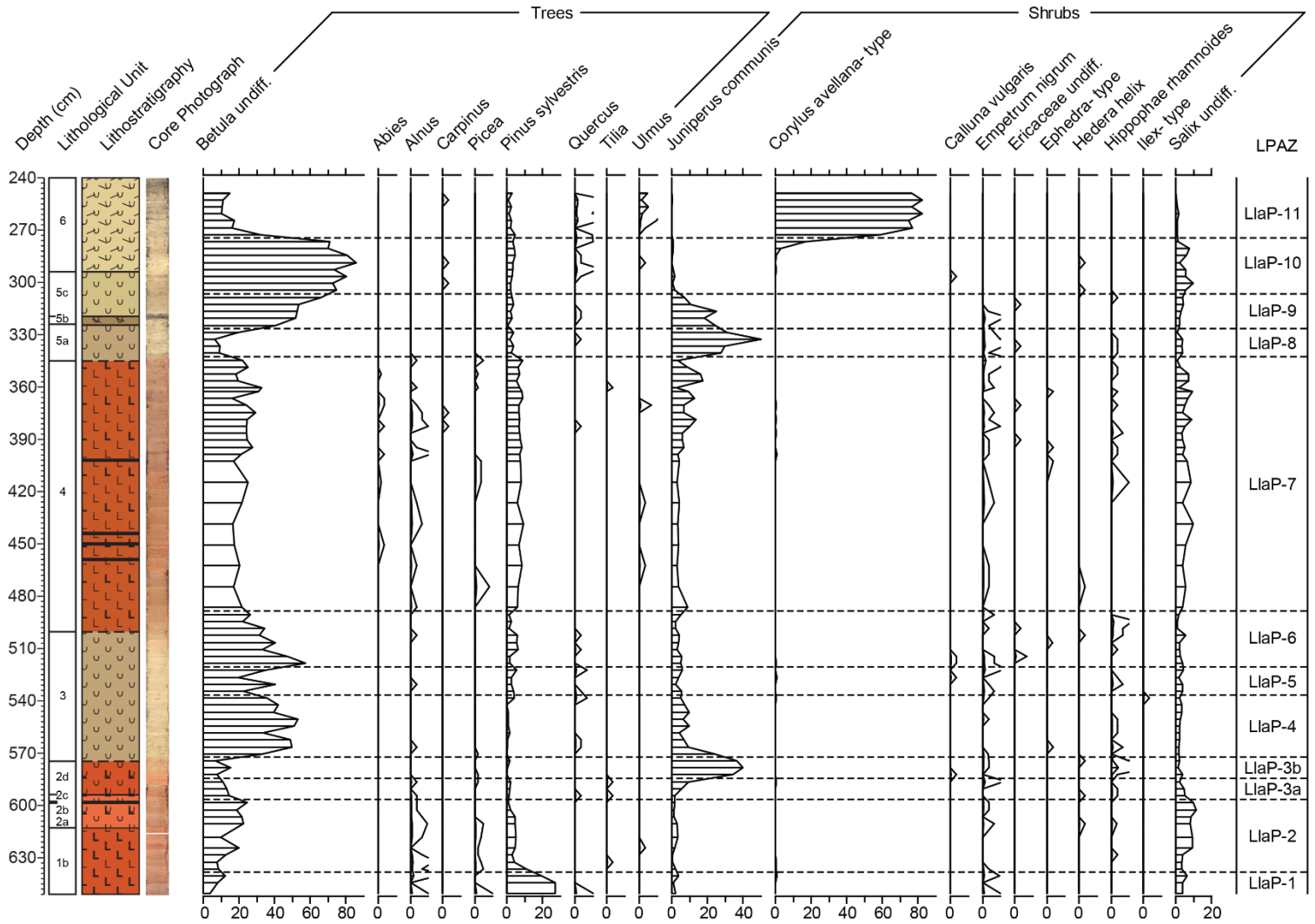

Figure 8.3 Pollen percentage profile of Llangorse. All values are presented as percentages of TLP.

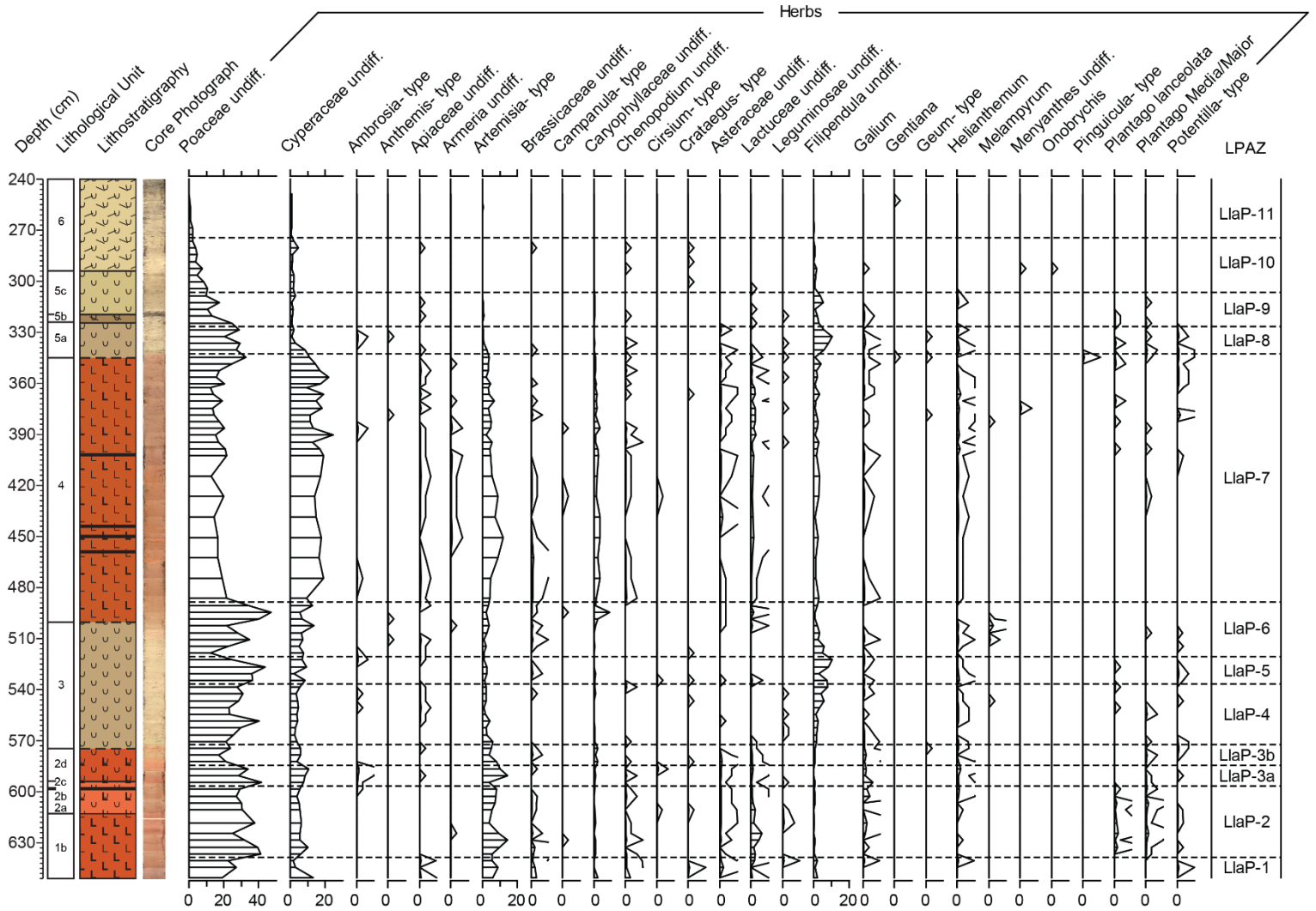

Figure 8.3 (Cont.) Pollen percentage profile of Llangorse. All values are presented as percentages of TLP.

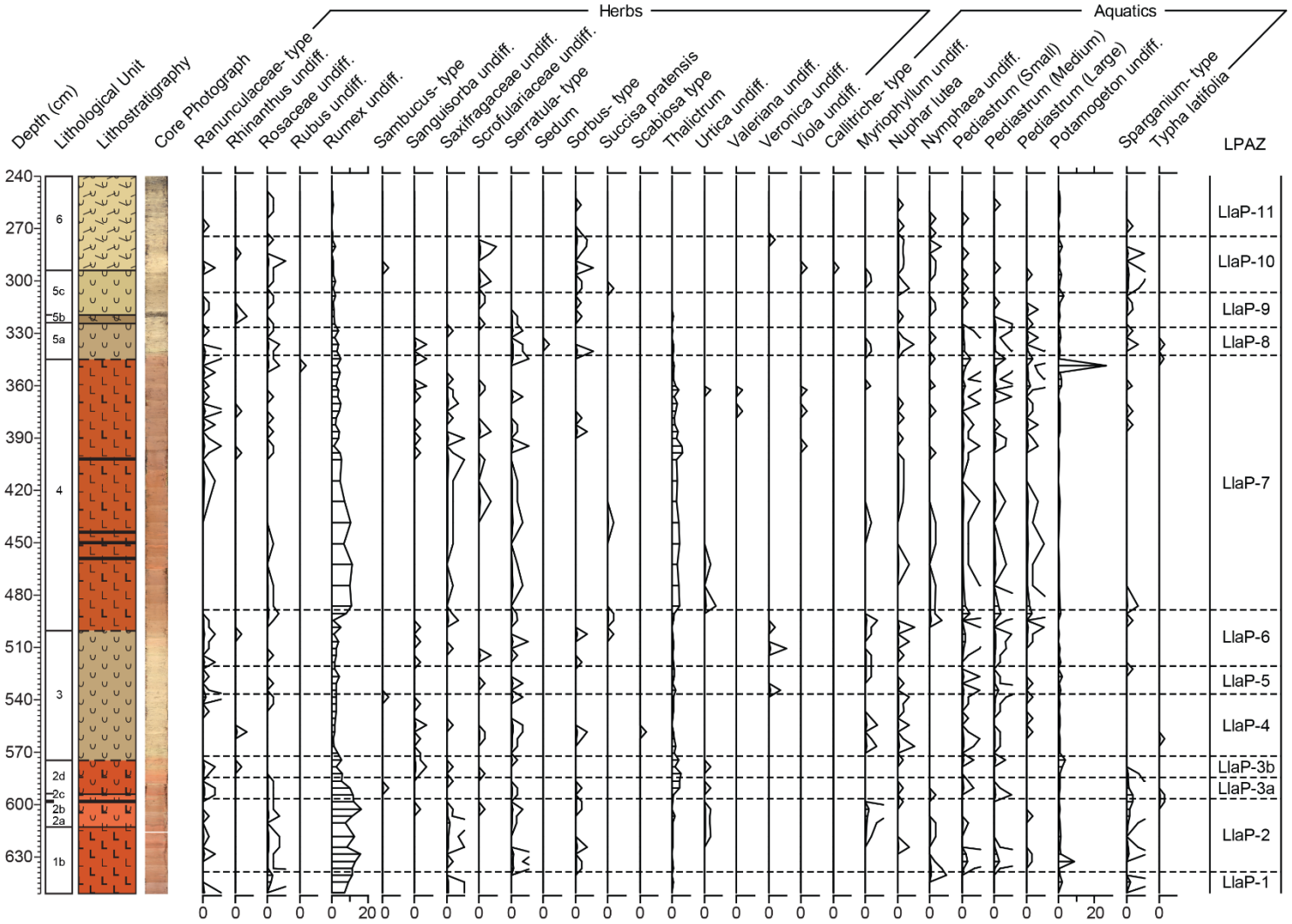

Figure 8.3 (Cont.) Pollen percentage profile of Llangorse. All values are presented as percentages of TLP.

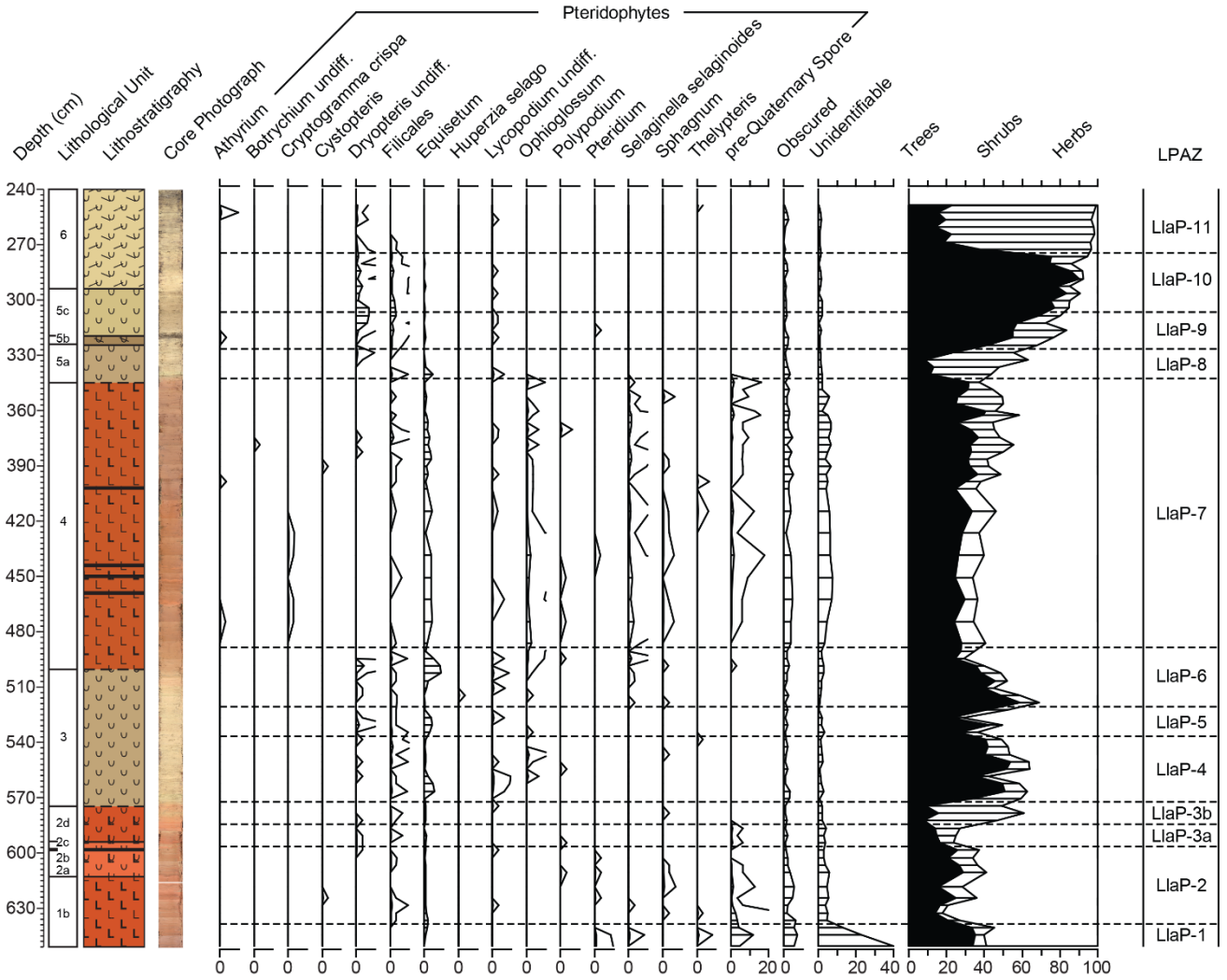

Figure 8.3 (Cont.) Pollen percentage profile of Llangorse. All values are presented as percentages of TLP.

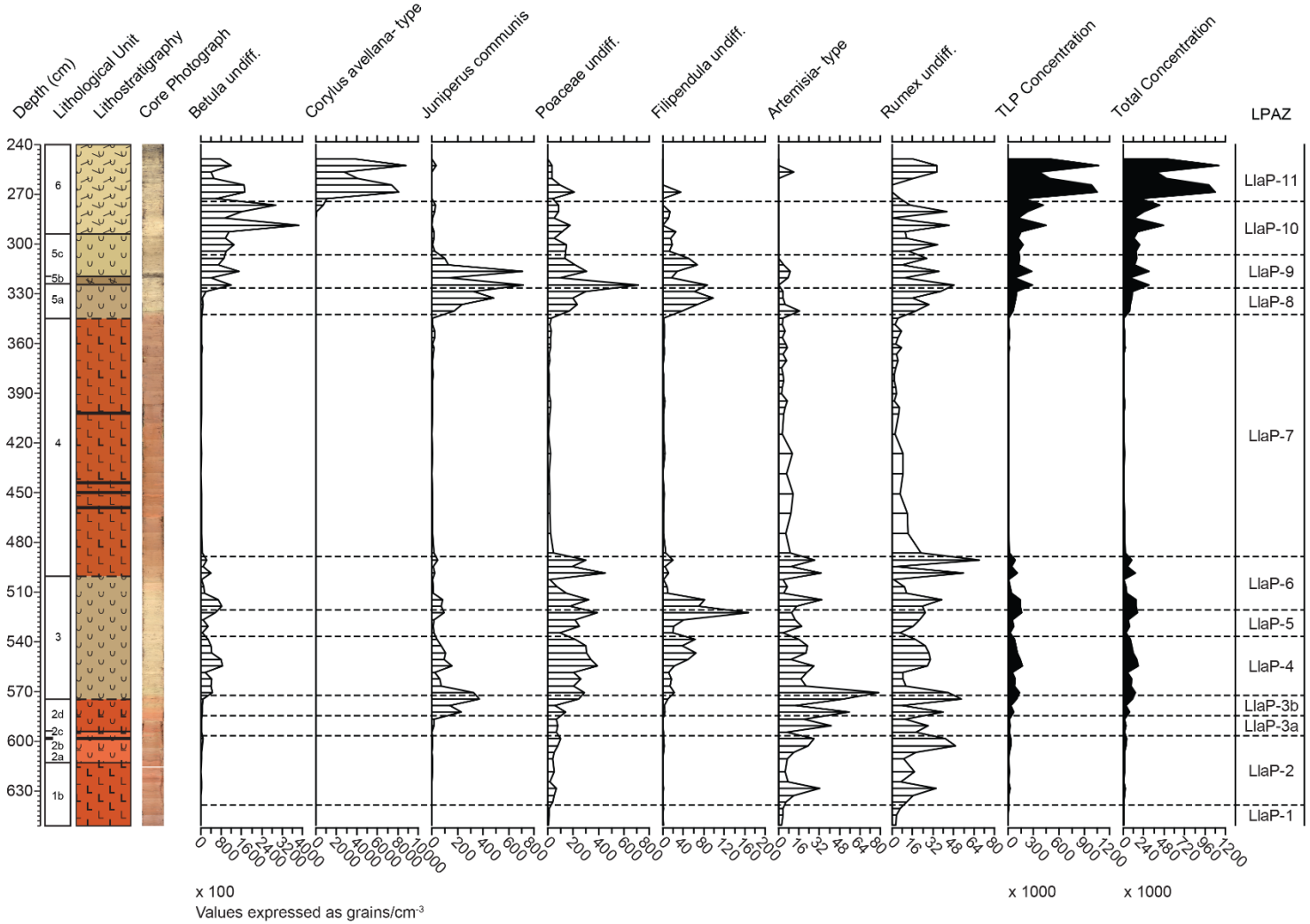

Figure 8.4 Summary pollen concentration data from Llangorse. All concentration values multiplied by 100 unless stated.

Table 8.2 Llangorse pollen zone delineation and key information. The names of the zones are provided alongside the composite depth and the key taxa observed within each zone.

LPAZ	Composite Depth (cm)	Key Taxa
LlaP-11	274.5-248	*Corylus*
LlaP-10	306.5-274.5	*Betula*
LlaP-9	326.5-306.5	*Betula*, *Juniperus*, Poaceae
LlaP-8	342.5-326.5	*Juniperus*, Poaceae, *Filipendula*
LlaP-7	488.5-342.5	*Betula*, Poaceae, Cyperaceae, *Artemisia*, *Rumex*
LlaP-6	520.5-488.5	*Betula*, Poaceae, Cyperaceae
LlaP-5	536.5-520.5	Poaceae, *Betula*, *Filipendula*
LlaP-4	572.5-536.5	Poaceae, *Betula*, *Juniperus*
LlaP-3b	584.5-572.5	*Juniperus,* Poaceae
LlaP-3a	596.5-584.5	Poaceae, *Artemisia*, *Rumex*
LlaP-2	638.5-596.5	Poaceae*, Rumex, Betula, Artemisia*
LlaP-1	651-638.5	*Pinus,* Poaceae

Zone LlaP-3. Composite depth: 584.5-572.5 cm.

LlaP-3 is characterised by varying proportions of herbaceous and shrub-type pollen. Key taxa include Poaceae, with high pollen percentages at the base of the zone, 42 %, declining to 17 %; *Artemisia* whose values peak at 590.5 cm with 15 %; and *Rumex* with moderate values at the base of the zone, 12 %, and decrease throughout. Additional herbaceous pollen includes Cyperaceae, Caryophyllaceae, *Galium* and *Thalictrum.* An abrupt peak in *Juniperus*, 40 %, is observed at 578.5 cm. Additional shrub taxa include *Hippophae* and *Salix*. *Betula* is recorded but in much lower percentages, from 25 to 7 %.

Due to the complexity of the pollen-stratigraphic record for the zone has been split:

LlaP-3a: 596.5-584.5 cm. Troughs in *Betula* and peaks in Poaceae.
LlaP-3b: 584.5-572.5 cm. Troughs in *Betula* and the peak of *Juniperus*.

TLP concentrations through the zone are generally rising; from low values of 16,048 grains/cm^{-3} at the onset of the zone, to 102,595 grains/cm^{-3} at the end of the zone. The increase in concentration is driven here by increases in *Juniperus*, maximum of 37,307

grains/cm^{-3} at 574.5 cm, and Poaceae, maximum of 24,419 grains/cm^{-3} at 574.5 cm. Concentrations of *Artemisia* and *Rumex* increase throughout. *Betula* concentrations are lower than the previous zone, with a high of 7122 grains/cm^{-3} towards the top of the zone.

Zone LlaP-4. Composite depth: 572.5-536.5 cm.

For the first time in the sequence *Betula* percentages rise to 53 % at 550.5 cm and are greater than 33 % throughout. In contrast, *Juniperus* percentages are markedly lower, dropping to 5 % at 538.5 cm. Poaceae percentages are moderate-high, 21 % at the base of the zone and 40 %, mid-zone. Additional taxa include *Filipendula* and Cyperaceae. For one sample, 558.5 cm, a subtle oscillation is observed. This oscillation includes a reduction in *Betula*, from 49 % to 34 %, and an increase in Poaceae, from 30 % to 40 %. During this horizon, increases in *Artemisia* from 2-4 % and *Rumex* are observed.

Land pollen concentrations are high with a maximum of 167,360 grains/cm^{-3} at 554.5 cm comprised predominantly of high *Betula* concentrations 85,613 grains/cm^{-3}. In contrast, *Juniperus* concentrations are high at the base of the zone, 32,952 grains/cm^{-3}. The oscillation in percentage data is matched across concentrations with all land pollen taxa decreasing in concentration; minus *Artemisia* which increases to 2185 grains/cm^{-3}.

Zone LlaP-5. Composite depth: 536.5-520.5 cm.

At the onset of the zone, percentages of Poaceae are high, 36 %, peak with a maximum of 43 % at 526.5 cm and decline towards the top of the zone. The arboreal component is dominated by *Betula* although percentages are low; 20 % at 526.5 cm. Throughout LlaP-5, *Filipendula* is the only additional taxa that surpasses 10 % TLP; reached towards the top of the zone. Additional components include: *Pinus*, *Juniperus*, *Salix*, Cyperaceae, *Artemisia*, *Heliantheumum*, *Rumex* and *Thalictrum* all with values less than 10 %. Aquatics are low, and the pteridophytes consist of Filicales and *Equisetum.*

Concentration indices are variable throughout. At the onset, all concentration values are considerably lower than the previous zone, with TLP demonstrating 26,737 grains/cm^{-3} at 534.5 cm. However, by the end of the zone, high concentrations of TLP are observed, 159,620 grains/cm^{-3}, which is largely controlled by herbaceous taxa. Concentrations of Poaceae and *Betula* increase throughout LlaP-5.

Zone LlaP-6. Composite depth: 520.5-488.5 cm.

At the onset of LlaP-6, *Betula* dominates with a zone high of 57 % at 518.5 cm. For the remainder of the zone however, *Betula* percentages decline to a zone low of 22 % at 494.5 cm. In contrast, at the onset of the zone Poaceae percentages are moderate, with a zone low of 12 % at 518.5 cm before increasing significantly to 47 % at 494.5 cm. Cyperaceae percentages fluctuate throughout the zone with highest percentages observed at 502.5 cm. Taxa also recorded within this zone include *Pinus*, *Juniperus*, *Salix*, *Artemisia*, Caryophyllaceae, *Filiendula*, *Rumex*, *Pediastrum* and *Equisetum*. Of these taxa Caryophyllaceae and *Rumex* are increasing in percentages to a maximum of 9 % and 8 % respectively; whereas *Equisetum* peaks to a maximum of 9 %.

TLP concentration values are initially high, 145,473 grains/cm^{-3} at 514.5 cm, fall to a zone low of 9048 grains/cm^{-3} at 502.5 cm and oscillate between these high and low values for the remainder of the zone. Like the percentage data, *Betula* is high at the base, 81,100 grains/cm^{-3}, and Poaceae is high towards the top of the zone 45,356 grains/cm^{-3}. Herbaceous taxa increase within the upper phases of LlaP-6 with increases in *Artemisia* and *Rumex*, to highs of 3346 grains/cm^{-3} and 6823 grains/cm^{-3} respectively.

Zone LlaP-7. Composite depth: 488.5-342.5 cm.

LlaP-7 is characterised by a multitude of taxa, all of which are continuous and stable throughout. The dominant taxon is *Betula* with percentages between 17 % and 33 %. The two other dominant taxa are Poaceae and Cyperaceae with percentages between 13 and 33 %, and 9 and 24 % respectively. *Artemisia* and *Rumex* are also key components with percentages of 12 % and 11 % towards the base of the zone and recorded throughout. *Pinus* and *Salix* are continually recorded with elevated percentages. Additional herbaceous taxa include: Caryophyllaceae, Compositae: Lactuceae, *Filipendula*, *Helianthemum*, *Saxifragaceae* and *Thalictrum*. *Equisetum*, *Ophioglossum*, and pre-Quaternary spores are also recorded. Towards the top of the zone, *Juniperus* percentages begin to increase from 3 % to a maximum of 17 % at 356.5 cm.

Land pollen concentration is low throughout the zone with all levels below 20,000 grains/cm^{-3}. Herbaceous taxa exert the most influence over the totals throughout.

Zone LlaP-8. Composite depth: 342.5-326.5 cm.

Zone LlaP-8 is dominated by both shrub- and herb-type pollen. Percentages of *Juniperus* are high and peak with 50 % at 332.5 cm. Similarly, percentages of Poaceae are higher

than the previous zone, between 21 and 29 % throughout. In contrast, arboreal pollen taxa decrease in percentage with *Betula* dropping from 33 to 6 % at 332.5 cm and *Pinus* dropping from 9 to 2 % at the same depth. *Filipendula* percentages are moderate throughout with a maximum of 10 % towards the upper levels of the zone.

TLP concentrations are rising throughout the zone, increasing from 62,803 grains/cm^{-3} to 104,945 grains/cm^{-3}. Poaceae values are generally moderate, whereas, *Betula* values are low and increase to 20,713 grains/cm^{-3} at the top of the zone.

Zone LlaP-9. Composite depth: 326.5-306.5 cm.

Zone LlaP-9 is characterised by high and increasing percentages of *Betula* pollen. Whilst high at zone onset, 40 %, *Betula* reaches a zone maximum of 66 % at 308.5 cm. Increasing percentages of *Betula* replace the high percentages of *Juniperus* and Poaceae from the previous zone. Although *Juniperus* briefly returns to greater percentages, 25 %, at 316.5 cm. Taxa that additionally contribute to the zone include *Salix*, Cyperaceae, *Filipendula* and *Rumex*. The aquatic pollen assemblage is principally composed of *Potamogeton*, with pteridophytes primarily composed of *Dryopteris*; where percentages reach a joint sequence high of 7 % at 308.5 cm.

Pollen concentrations are higher than previous zones. Maximum land pollen concentrations are observed at 324.5 cm with 291,430 gains/cm^{-3}. The upper sections of the zone are lower in concentrations, barring 320.5 cm. *Betula* peaks in concentration with 149,133 grains/cm^{-3} at 316.5 cm as *Juniperus* and Poaceae show increased values of 70,884 grains/cm^{-3} and 30,379 grains/cm^{-3}.

Zone LlaP-10. Composite depth: 306.5-274.5 cm.

Zone LlaP-10 is characterised by very high percentages of *Betula* at the expense of all shrub- and herb-type pollen. *Betula* percentages throughout this zone are >70 % with peak percentages of 86 % observed at 288.5 cm. Further, *Corylus* is increasing towards the top of the zone, with a high of 17 % at 276.5 cm. *Salix* percentages are less than 10 % and Poaceae values are higher at the base than for the remainder of the zone. All other pollen percentages, barring *Dryopteris* (7 %) do not exceed 5 %.

TLP concentrations are high throughout the zone. Where horizons of lower concentration are present, e.g. 292.5 cm; 284.5 cm; they are surrounded by higher values >400,000 grains/cm^{-3}. *Betula* values peak with 385,153 grains/cm^{-3} at 288.5 cm.

Zone LlaP-11. Composite depth: 274.5-248 cm.

LlaP-11 is dominated by *Corylus*. Percentages increase from 58 % at the onset of the zone to 82 % towards the top of the zone. *Corylus* replaces *Betula*, whose percentages decrease from 32 % to between 10 to 15 %. Very few pollen of herbaceous type have been identified within this zone. Those that are identified: Poaceae, Cyperaceae, *Rosaceae* and *Rumex* are all <5 %.

Concentrations of observed taxa are high. Two peaks in land pollen concentration are observed at 268.5 cm and 252.5 cm with values of 1,054,473 grains/cm^{-3} and 1,072,047 grains/cm^{-3} respectively. Concentrations of *Corylus* are high throughout and peak at the same levels with 811,944 grains/cm^{-3} and 882,242 grains/cm^{-3} respectively.

8.3 Statistical analyses

Statistical analyses were performed on a reduced Llangorse pollen percentage dataset, utilising all taxa with abundances greater than 5 %. Owing to significant *Corylus* values identified in the upper eight samples, up to 82 %; which both obscured vegetation change within the pollen diagram and had a negative impact in the potential statistical delineation of vegetation revertence detection; the uppermost eight samples were removed. As *Corylus* is rarely observed beneath these upper eight samples, and as vegetation that occurs in association is fragmentary, the statistical methods predict that the effect of *Corylus* is inverse to what would be suggested by its ecology. This inversion occurs irrespective of *Corylus* being a dominant component of the successional sequence in Britain (e.g. Boyd and Dickson, 1986; Tallantire, 2002) and is a product of the statistical approach. The removal of the *Corylus* bearing upper eight samples is therefore justified.

Table 8.3 Preliminary decorana analyses on the reduced Llangorse dataset. The axis lengths here are short, which perhaps reflects the influence of Betula, but also the reduction of taxa through the sequence.

	DCA1	DCA2	DCA3	DCA4
Eigenvalue	0.2073	0.1217	0.05152	0.04088
DCA value	0.2111	0.1206	0.04191	0.02548
Axis length	1.8374	1.4802	1.02009	1.06572

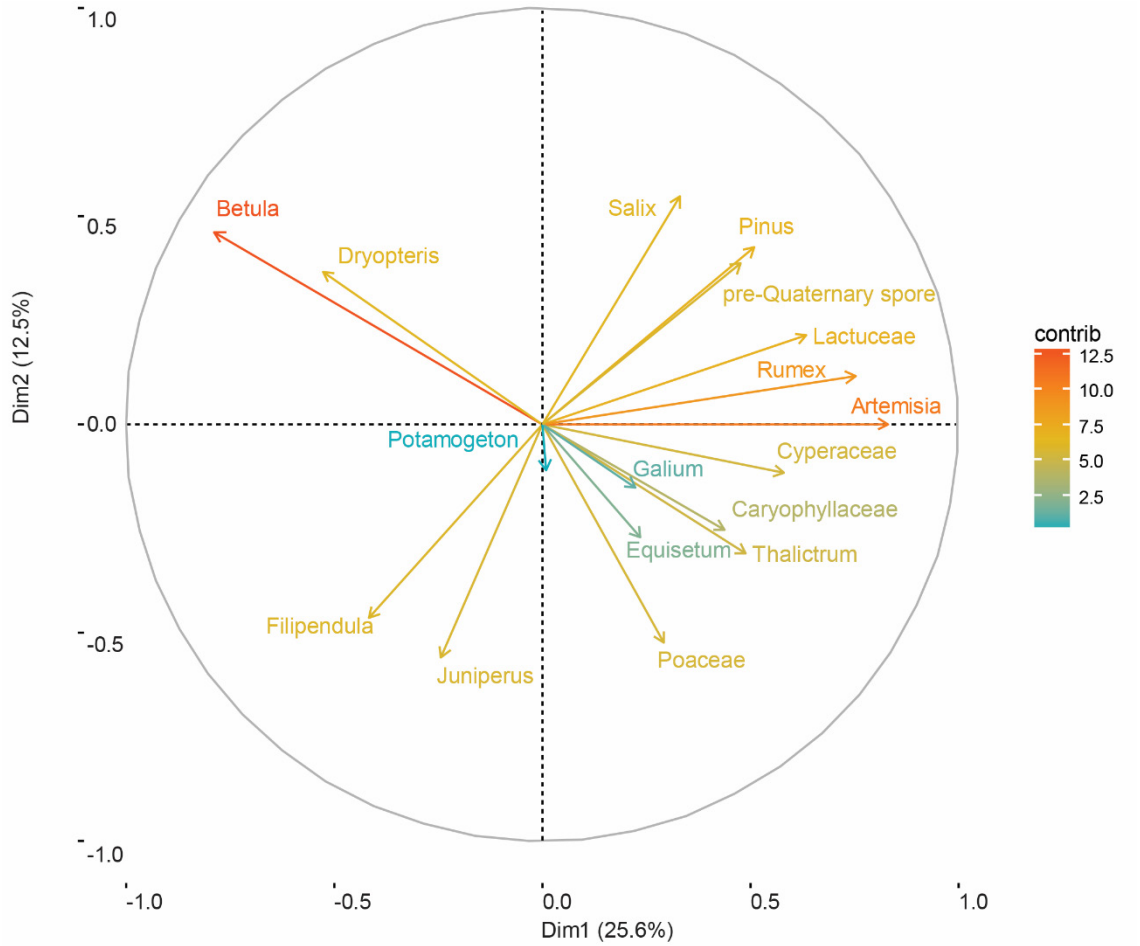

Figure 8.5 Results of the PCA output from Llangorse. The data are presented as a biplot showing the two principal components, axis 1 and 2, with taxa placed along the axes relative to their importance. The length of the arrow and the variable colour indicates the dominant taxa along the axis. Plotting positively along axis one with greater importance are open herbaceous taxa (and *Pinus*); whereas negative values are composed predominantly of *Betula* and *Dryopteris*.

Detrended Correspondence Analyses (DCA) was employed to establish the lengths of the primary axes (Table 8.3). These lengths (>1.5-3 SD) demonstrate that Principal Components analysis (PCA), Correspondence Analysis (CA) and Principal Curves (PC) were suitable for data exploration within Llangorse.

The PCA was preferred for exploring taxa variation owing to the short axis lengths (Figure 8.5). Axis one explains the most variation, 25.6 %, with axis two representing 12.5 %. Herbaceous taxa plot positively along axis one, with the inclusion of shrub (*Salix*) and tree (*Pinus*) taxa. These taxa include, in order of greatest influence: *Artemisia*, *Rumex*, Compositae: Lactuceae, Cyperaceae, *Thalictrum* and Caryophyllaceae. Taxa that plot negatively include *Betula* and *Dryopteris*. Taxa that show more affinity to axis two in either direction include *Juniperus*, Poaceae, *Filipendula* and *Salix*.

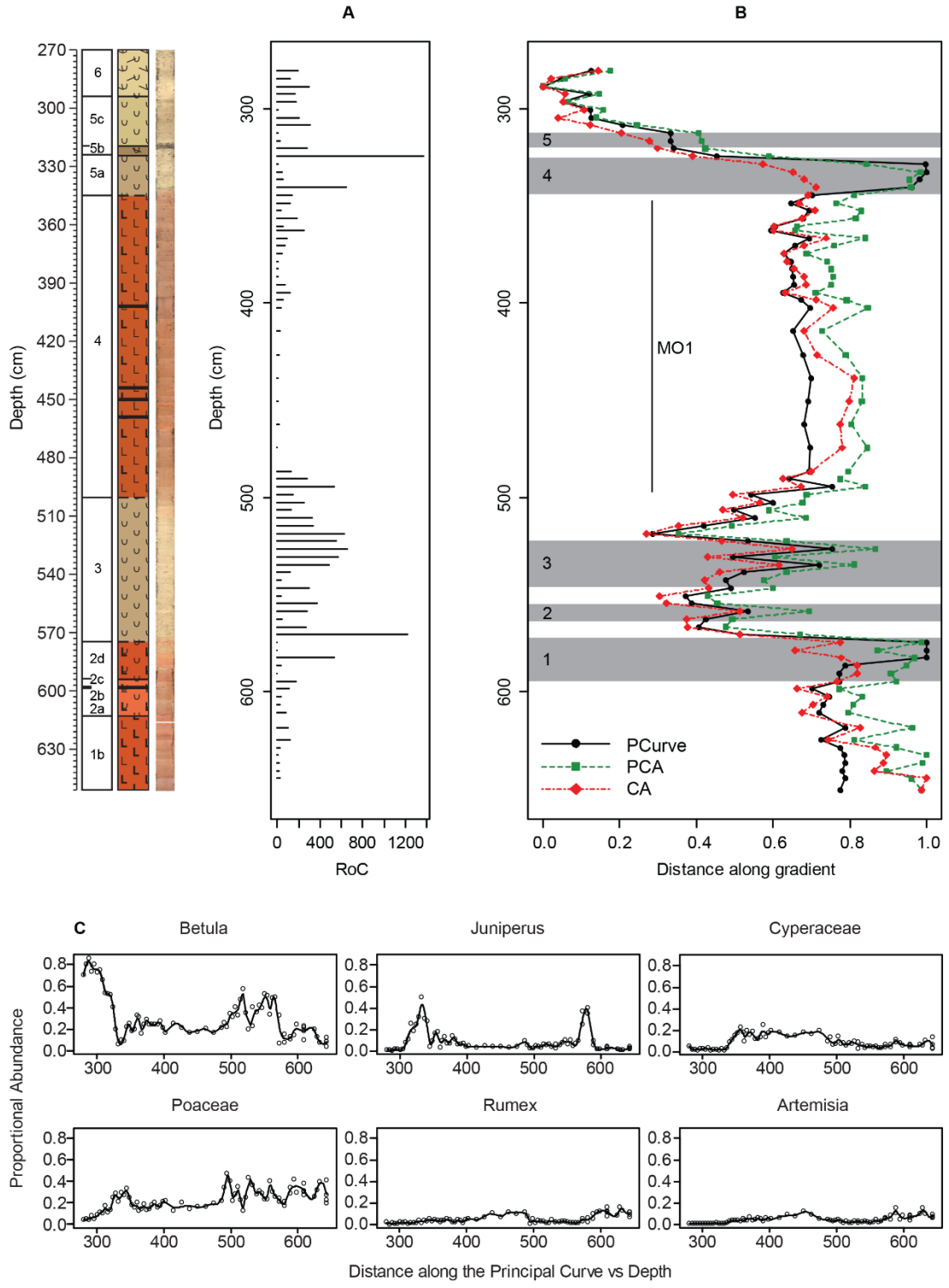

Figure 8.6 Results of different statistical analyses applied to the Llangorse pollen dataset. A) Rate of change analysis. The values for the analysis are arbitrary and an exaggeration multiplier has been applied to demonstrate where significant periods of compositional change are inferred from the pollen data. The greater the length of the bar the more significant the compositional change. B) The overlain output from three tests applied (PCA, CA and PC) highlighting the similarity of the output of the three tests. The data show rapid short oscillations (grey boxes) and a longer oscillation termed (MO1). C) Individual taxa response curves modelled on the gradient of the PC. These key taxa demonstrate what may be driving the changes in the PC from B).

To explore the relationship between pollen and stratigraphy, axis 1 scores were plotted from PCA and CA-based solutions. This was subsequently modelled in multiple dimensions using a PC (Figure 8.6). The PC data from Llangorse was modelled on a PCA-based output. Whilst both PCA and CA methods converge in nine iterations, the CA output explains slightly more variation within the pollen. However, to force convergence in the CA-based solution, the penalty value had to be set much lower. This reduced penalty allows the curve to be more flexible and whilst encompassing more variation, could potentially overfit the data. Variation expressed with the different approaches are summarised as:

- PCA based output: 78.5 %
- CA based output: 86.1 %

Variance within the data (Figure 8.6) is inferred where the PC curve shifts to more positive values. From this, a major oscillation is not immediately obvious; though its presence is noted. Additionally, three oscillations are observed within sediment units 2a to 3, although one is represented by a single sample, and two appear within sediment unit 5. The inflection in the curve towards more positive values between 582.5-574.5 cm and 344.5-324.5 cm appears a high magnitude revertence. However, caution is needed owing to the interplay between different vegetation types. These have been added as events and caveats will be discussed in Section 8.6. From this PC data oscillations are suggested at:

- Major Oscillation 1: Samples between 506.5-362.5 cm
- Oscillation 1: Samples between 598.5-570.5 cm
- Oscillation 2: Sample at 558.5 cm
- Oscillation 3: Samples between 542.5-518.5 cm
- Oscillation 4: Samples between 348.5-324.5 cm
- Oscillation 5: Samples between 320.5-312.5 cm

Variance in the PC can be observed in the Rate of Change Analyses (RoC). During each PC inflection, the RoC reveals phases of compositional turnover. Whilst greater changes are noted for the oscillations above, the greatest change is observed between 598.5-570.5 cm and 344.5-324.5 cm. As previously stated, compositional change here may not be wholly representative of vegetation-based events. Further, key taxa have been modelled along the gradient of the PC. Using this approach, changes in taxa in Figure 8.6 are shown to be driving the PC during different phases. For example, losses of *Betula*

appear most strongly felt; however, increases in Poaceae, *Juniperus* and *Rumex* across different events, all exert differential control.

8.4 Micro- and macro-charcoal

Charcoal analyses were undertaken at the same resolution as the palynological investigation. However, the lack of core materials between 586-650 cm truncated the macro-charcoal assessment. Micro-charcoal analyses were undertaken alongside the pollen counts and are presented as micro-charcoal concentrations (88 analyses) whereas macro-charcoal analyses are presented as raw counts (71 analyses). Considerable variability exists between counts; however, a series of peaks can be observed above background values. To discriminate between peaks and background variability, an average has been placed across each of the graphs in Figure 8.7. The average micro-charcoal concentration is 97,580 shards/cm^{-3} whereas average macro-charcoal counts are 28.66 fragments/cm^{-3}.

Micro-charcoal

Within the micro-charcoal record concentrations range from 10,126 shards/cm^{-3} to 313,927 shards/cm^{-3}. Throughout the record nine peaks are identified. The first is characterised by the greatest concentration of charcoal fragments throughout the sequence at 313,927 shards/cm^{-3}. Greater separation between peaks is noted within sediment units 2a to 4. LlaCc-2 is shown by a peak spread across four samples with a maximum concentration of 208,356 shards/cm^{-3}. The subsequent accumulation is clearly separated from the preceding peak by 44 cm containing low background concentrations. LlaCc-3 is spread over five samples with a maximum peak abundance of 195,799 shards/cm^{-3} at 550.5 cm. The clustering of charcoal around these five samples negated further splitting. LlaCc-4 and LlaCc-5 are centred at 514.5 and 498.5 cm with 252,283 and 204,101 shards/cm^{-3} respectively.

The second carbonate phase in the record is characterised by complex sedimentological-charcoal relationships. Following LlaCc-6, the next clear peak within the sequence is shown by an abrupt increase in concentration between 328.5 cm and 324.5 cm. LlaCc-7 is characterised by a maximum concentration of 306,412 shards/cm-3. Within the subsequent phase, it is difficult to discriminate between individual peaks as most concentrations are above background level. Therefore, between these horizons, a charcoal complex has been denoted where a series of events may exist. With individual elevated levels a clear downward trend is observed. The final clear peak in the charcoal concentration data, LlaCc-9, exists for one sample at 252.5 cm; with a maximum concentration of 295,252 shards/cm-3.

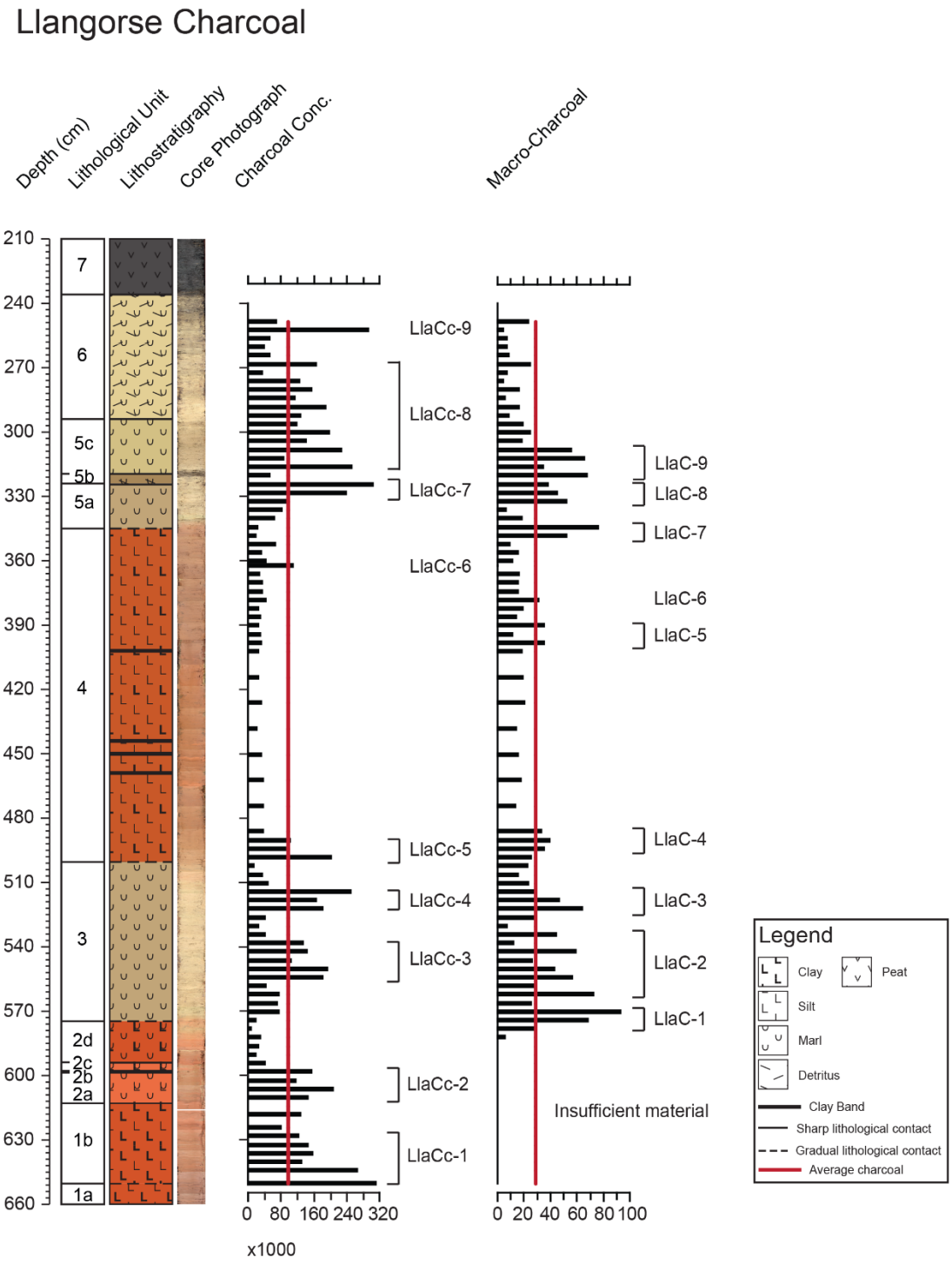

Figure 8.7 Micro-charcoal concentration (left) and Macro-charcoal counts (right) from Llangorse are presented against composite stratigraphy. Significant peaks are labelled as LlaCc (concentration) and LlaC (raw counts). Average charcoal is presented on the within the figure to aid peak identification. Peak position between the two graphs are largely similar, albeit with some differences within sediment units 5a:7. Unfortunately owing the a lack of core materials, macro-charcoal counts for the basal units were not conducted.

Macro-charcoal

Macro-charcoal counts throughout the sequence vary from 1 to 94 fragments/cm^{-3}. Nine significant macro-charcoal peaks have been identified with the caveat that the whole sequence was not sampled. LlaC-1 sits between 578.5-570.5 cm and is characterised by a peak of 94 fragments. As no real tail structure exists around the subsequent accumulation, a complex of charcoal is suggested between 562.5-534.5 cm. The highest peak is characterised by 73 fragments and the lowest peak by 44 charcoal fragments. Two subsequent peaks can be identified within sediment units 3 to 4. LlaC-3 is characterised by peak values of 65 fragments at 522.5 cm whereas, LlaC-4 contains 40 fragments at 490.5 cm.

With respect to other peaks throughout the sequence, LlaC-5:6 contain low charcoal sums with 36 and 32 fragments respectively. Between sediment units 4 to 5a, an abrupt increase in charcoal is noted containing a maximum of 77 fragments (LlaC-7). The final complex of charcoal has been split, as two distinct phases of increased charcoal input can be observed. The first, LlaC-8, demonstrates a maximum of 53 fragments at 332.5 cm whereas the second, between 320.5-308.5 cm, contains a peak abundance of 68 fragments. All values within the complex lie above the background values.

It is clear from the charcoal reconstructions that over phases of the record micro- and macro- values are similar, but at points, disparities exist. The largest differences appear where individual peaks lie. As the charcoal record has not been sampled contiguously it may be that taphonomic considerations are important at Llangorse. Nevertheless, encouragement is taken from the similarity of the records during certain phases.

8.5 Additional data

Data presented here centres on stable isotopic data derived from the Llangorse sequence collected alongside this thesis. All stable isotopic data was compiled by Adrian Palmer and analysed in the department of Earth Sciences at Royal Holloway, University of London (Preface; Chapter 4). This section also contains the chronological model constructed for Llangorse.

8.5.1 $\delta^{18}O$ and $\delta^{13}C$ isotope stratigraphy

At Llangorse, a total of 81 preliminary stable isotopic analyses were performed at variable resolutions. The highest resolutions attained, at the time of writing, are within units 5a to 5c. Like Tirinie, isotopic analyses over phases containing minimal carbonate were not sought. Hence the gap in the isotopic stratigraphy within unit 4. Further, one isotopic result looked spurious as the values reconstructed for the sample centred on

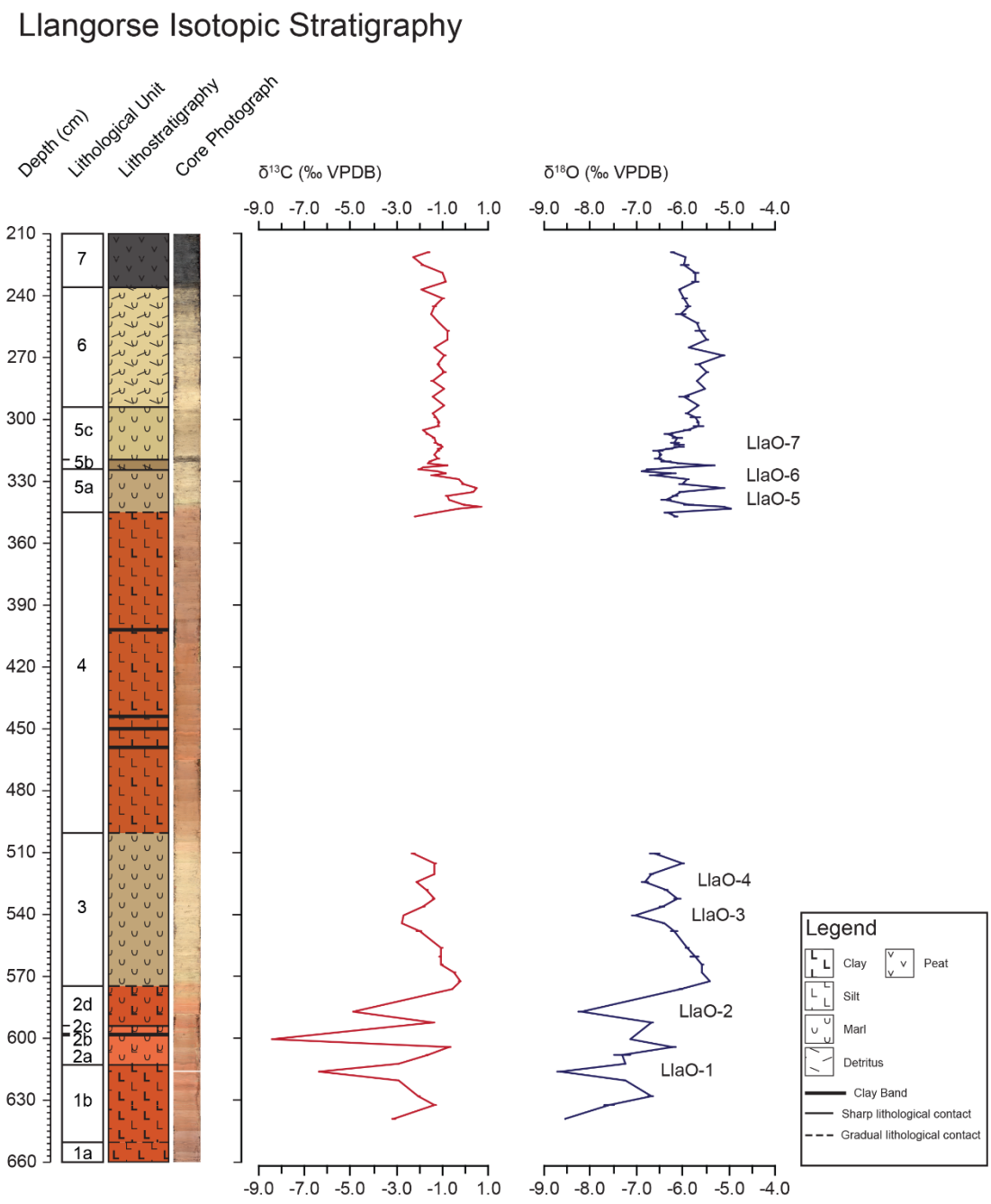

Figure 8.8 Preliminary oxygen (left) and carbon (right) isotope stratigraphy for Llangorse. All isotope data are presented against Vienna Pee Dee Belemnite (VPDB). Within the oxygen isotopic data, a series of oscillations are observed, labelled LlaO-1:7. These events appear significantly stronger within the basal carbonates than the upper carbonates. Due to insufficient carbonates, isotopic analyses were not performed within sedimentological unit 4.

553.25 cm were 5.00 ‰ greater in reconstructed $\delta^{18}O$, and 2.00-3.00 ‰ greater in $\delta^{13}C$. This sample then, either demonstrates measurement error, or the influence of detrital carbonate. In this instance, the influence of detrital carbonate can be discounted based on: 1) the greater values recorded within this sample compared to values in the region for basal limestones (<-1.9 ‰; Leslie et al., 1992) and 2) the observation that carbonate percentages fall to <2 % during unit 4; demonstrating the lack of detrital carbonate input under a phase of minimal authigenic carbonate formation. It is therefore likely that the 553.25 cm sample displays significant measurement error. As a result, 553.25 cm has been removed from the reconstruction.

Between units 1b to 3, some evidence exists for $\delta^{18}O$ and $\delta^{13}C$ co-variation (R2= 0.45). Nevertheless, $\delta^{13}C$ values exhibit significant depletions centred on 616.25, 600.25 and 587.25 cm. The second of these shifts exhibits maximum depletion to -8.40 ‰. $\delta^{13}C$ is more enriched between 576.25-556.25 cm with values -1.09 to -0.24 ‰. Further depletion is observed at 544.25 cm, before a stepped enrichment. Average $\delta^{13}C$ values throughout the basal units are -2.20 ‰, 1σ= 1.81. In contrast, $\delta^{18}O$ values follow a rising trend from low values recorded at the base of the sequence (-8.55 ‰) with a series of depletions punctuating this general trend. Four depletions are centred at 617.25, 587.25, 540.25 and 520.25 cm with depleted values of -8.65, -8.21, -7.03 and -6.82 ‰ respectively. The average $\delta^{18}O$ value throughout the basal profile is -6.68 ‰, 1σ= 0.86.

The magnitude of the isotopic shifts within units 5a to 7 are not as great as the depletions within units 1b to 3. Further, there is minimal covariation between $\delta^{18}O$ and $\delta^{13}C$ (R2= 0.23). $\delta^{13}C$ increases from -2.19 ‰ at 347.25 cm to a sequence high of 0.67 ‰ at 342.25 cm. Barring two samples, enriched values are recorded until 336.25 cm, after which values show depletion to the top of the sequence. Average $\delta^{13}C$ values over the secondary phase are -1.10 ‰, 1σ= 0.61. Whilst not as great $\delta^{18}O$ demonstrates shifts between relatively enriched and depleted values. Initial values rise to peak enrichment of -4.97 ‰, but between 343.25 and 303.25 cm three depleted phases ore observed. LlaO-5, between 343.25-334.25 cm, exhibits maximum depletion of -6.37 ‰ between peaks of -5.14 ‰. LlaO-6, between 334.25-323.25 cm, shows depletion of -6.87 ‰ between -5.14 ‰ and -5.36 ‰. Finally, LlaO-7, between 323.25-304.25 cm, has maximum depletion of -6.55 ‰ between peaks of -5.36 ‰ and -5.64 ‰. Average $\delta^{18}O$ values over this phase are -5.95 ‰, 1σ= 0.41.

8.5.2 Chronology

Radiocarbon measurements from Llangorse are ongoing but outside of the timeframe of this thesis. To place the data into a chronostratigraphic framework an age model was constructed through tephra analyses and through importing radiocarbon dates from sequences proximal to Llangorse where biostratigraphic tie points exist.

The tephra identified at Llangorse has not been geochemically characterised however its position in the stratigraphy would suggest a Borrobol tephra attribution (Ian Matthews, pers. comm. 2018). Furthermore, radiocarbon dates have been extracted from Llangorse (Chambers, 1999), Traeth Mawr (Walker, 1982) and Craig-Y-Fro (Walker, 2007). Whilst not optimal, due to bulk radiometric dating (Lowe and Walker, 2000), it is deemed appropriate here in the absence of a chronology. Further dates were selected from areas where pollen signals could be matched; suggesting common regional significance. Thus, the influence of local pollen and vegetation was minimised.

The constructed age model, using the published Borrobol Tephra age and biostratigraphic tie-points (Table 8.4; Figure 8.9) were combined in a p_sequence

Table 8.4 Summary of the tephra and radiocarbon data used in this chronology. Including: depth, unmodeled input range and modelled output range (2 σ age range) and mid-point age with 1σ error.

Name	Depth (cm)	Unmodelled range (Cal. ka BP)	Modelled range (Cal. ka BP)	μ ± σ	Reference
Boundary	219		9.41-7.94	8812±436	
SRR 2383 Before *Quercus*	248.5	9.41-8.78	9.46-8.82	9179±139	Chambers (1999)
SRR 2384 EH 60 % *Betula*	276.5	10.13-9.54	10.12-9.53	9735±139	Chambers (1999)
Craig-Y-Fro EH peak *Juniperus*	332.5	11.97-11.25	11.69-11.22	11,411±126	Walker (2007)
SRR 1560 EH peak Poaceae	344.5	11.96-11.20	11.74-11.25	11,476±136	Walker (1982)
SRR 1561 Late IS peak *Betula*	506.5	12.74-12.9	12.73-12.40	12,590±96	Walker (1982)
SRR 1562 Early IS peak *Juniperus*	578.5	13.82-13.23	13.82±13.24	13,544±148	Walker (1982)
Borrobol Tephra	605	14.19-14.00	14.19-13.99	14,093±92	Bronk Ramsey et al. (2015)
Boundary	651		15.70-14.03	14,663±527	

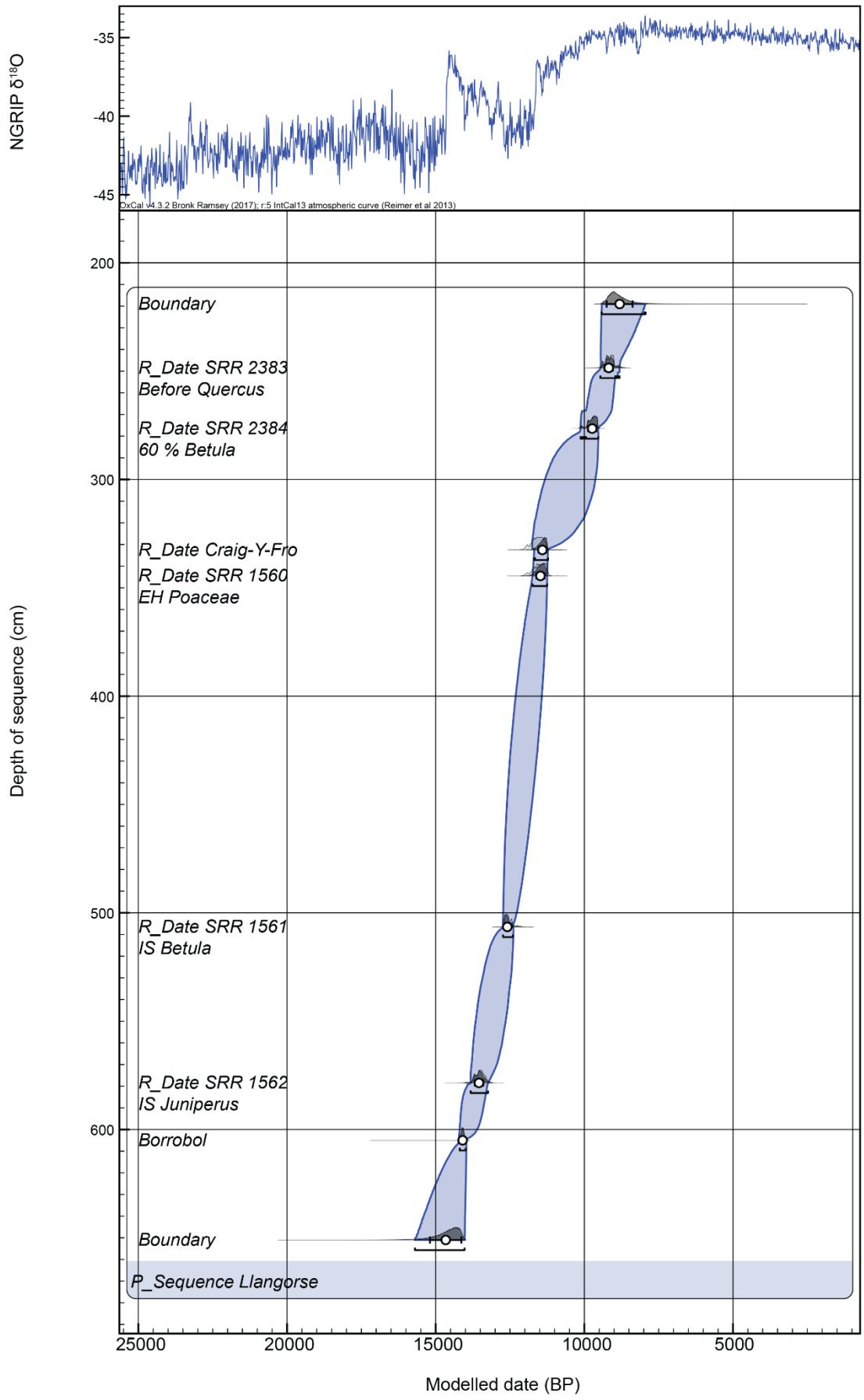

Figure 8.9 Age-depth, p_sequence model for Llangorse, the with age uncertainties plotted at μ and 1 σ, whilst the complete range is shown at 2 σ. Boundaries have been added at the top and bottom of the sequence for interpolation.

depositional model using the IntCal13 calibration curve (Reimer et al., 2013) in OxCal V. 4.3 (Bronk Ramsey, 2008; 2009) (Chapter 4). No boundaries were added to the model over areas of lithostratigraphic change to allow the model greater flexibility, however the model has been constrained by boundaries to extend modelling to the base and top of the proxy data series.

The model produced good model agreement across the sequence and was therefore used to provide calendar age ranges for the reconstruction presented in Section 8.6. The model suggests that sediments were deposited in the basin between 14.66±0.53 and 8.81±0.44 Cal. ka BP. However, this model does not capture sedimentation beneath this basal modelled age, therefore sediment accumulation in the basin began before this modelled date. The complete age model is presented in Appendix E.

8.6 Palaeoclimatic and palaeoenvironmental interpretation

The presented palaeoclimatic and palaeoenvironmental data will be used here to reconstruct the climatic and environmental history surrounding Llangorse, south Wales (Figure 8.10; 8.11). All palaeodata will be discussed chronologically, with the pollen data used here to infer vegetation development. As Chapter 6, it is acknowledged that this is an assumption but follows the traditional vegetation reconstruction approach. Based on the age model, unit 1a can be attributed to the Dimlington Stadial (DS), units 1b to 3 to the Windermere Interstadial (WI), unit 4 to the Loch Lomond Stadial (LLS) and units 5 to 7 to the early Holocene.

Isotopic considerations

The presented sequence contains varying degrees of covariation. Sediment units 1b to 3 exhibit moderate $\delta^{18}O$ and $\delta^{13}C$ covariation (R^2=0.452; 640.25-511.25 cm; Figure 8.12). Whereas, the latter carbonate units do not show covariation (R^2=0.228; 348.25-220.25 cm; Figure 8.12). Understanding covariation is important to understand the predominant controls on the isotopic dataset. Greater covariation may reflect either detrital contamination (e.g. Leng et al., 2010; Mangili et al, 2010) or isotopic modification. Disentangling a detrital carbonate influence is difficult as basement isotopic data from south Wales are lacking. However, where available, $\delta^{18}O$ and $\delta^{13}C$ data from Carboniferous limestone range from -14 to -1.9 ‰, and -12 to +3.54 ‰ respectively (Searl, 1989; Leslie et al., 1992; Brasier et al., 2014). This is clearly overlapping with the $\delta^{18}O$ and $\delta^{13}C$ values presented within this thesis. However, reconstructed values are not thought to be affected by detrital contamination as: 1) during phases where the influence of detrital carbonate contamination would be most felt, through greater catchment inputs (unit 4), carbonate percentages are negligible (<3.5 %); and 2) sieving at 64 µm removed any identified biogenic components from the bulk carbonate pool. Whilst covariation is noted at certain points in the stratigraphy (Figure 8.12); the isotopic signal is not thought to be affected by isotopic modification (e.g. evaporation) as this would increase both the $\delta^{18}O$ and $\delta^{13}C$ values through preferential loss of the lighter $\delta^{16}O$ and $\delta^{12}C$ isotopes. Phases of enrichment are thought to reflect climatic improvement immediately following a climatic downturn. Therefore, it is likely that Llangorse remained an open water body for the duration of the LGIT; with stable isotopic analyses performed on authigenic carbonates. Whilst these modifying effects can be disregarded, evaporative enrichment may affect certain phases of the record. Where these phases occur in the stratigraphy they will be discussed.

The $\delta^{13}C_{carb}$ record can therefore be interpreted based on the $\delta^{13}C$ of dissolved inorganic carbon (DIC); related to DIC of groundwaters, plant respired CO_2 and associated

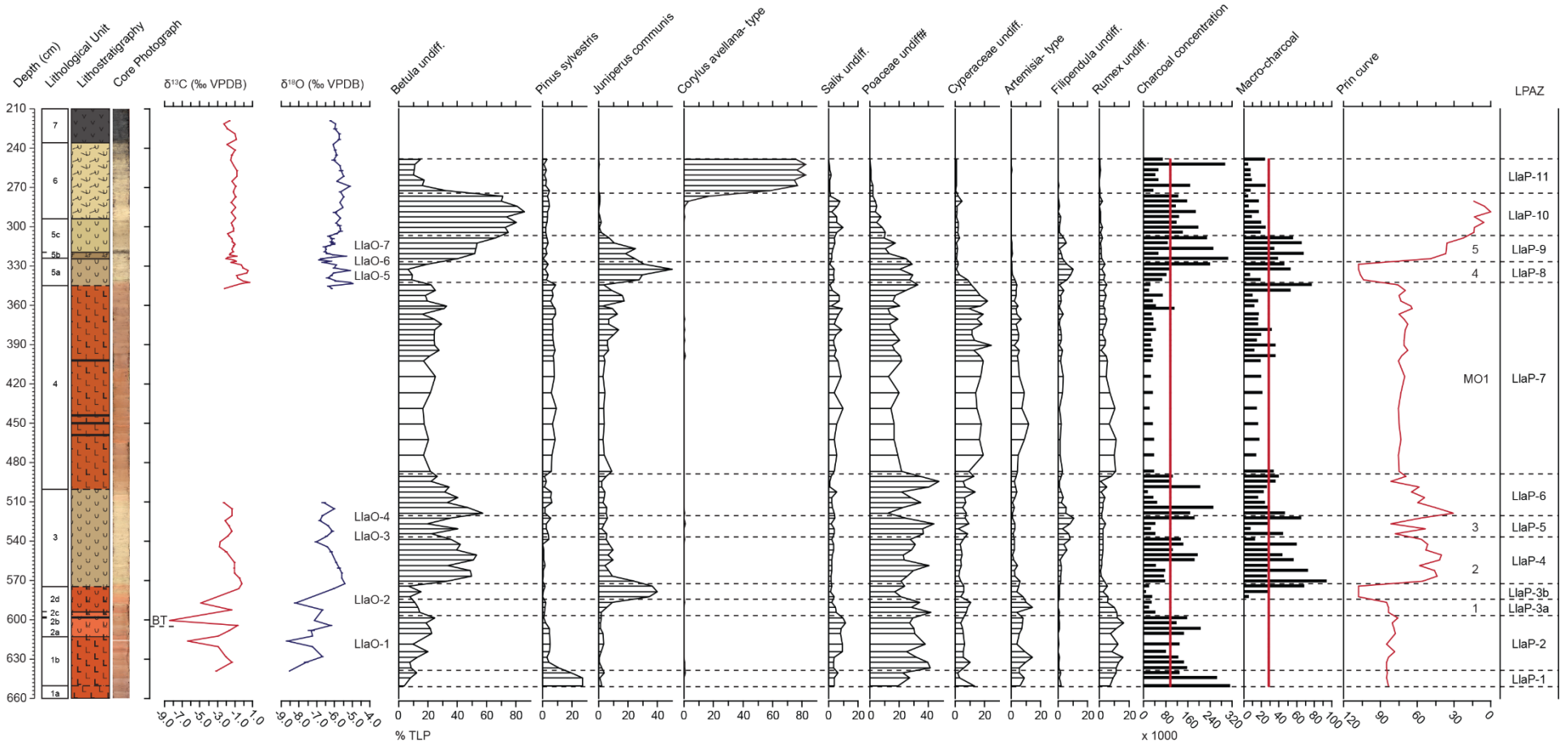

Figure 8.10 Summary of palaeodata presented from Llangorse. All principal pollen taxa have been included. The position of the Borrobol tephra (BT) at 605 cm has been placed on to the diagram for ease of interpretation. Both charcoal indices have been included due to potential differences in abundance.

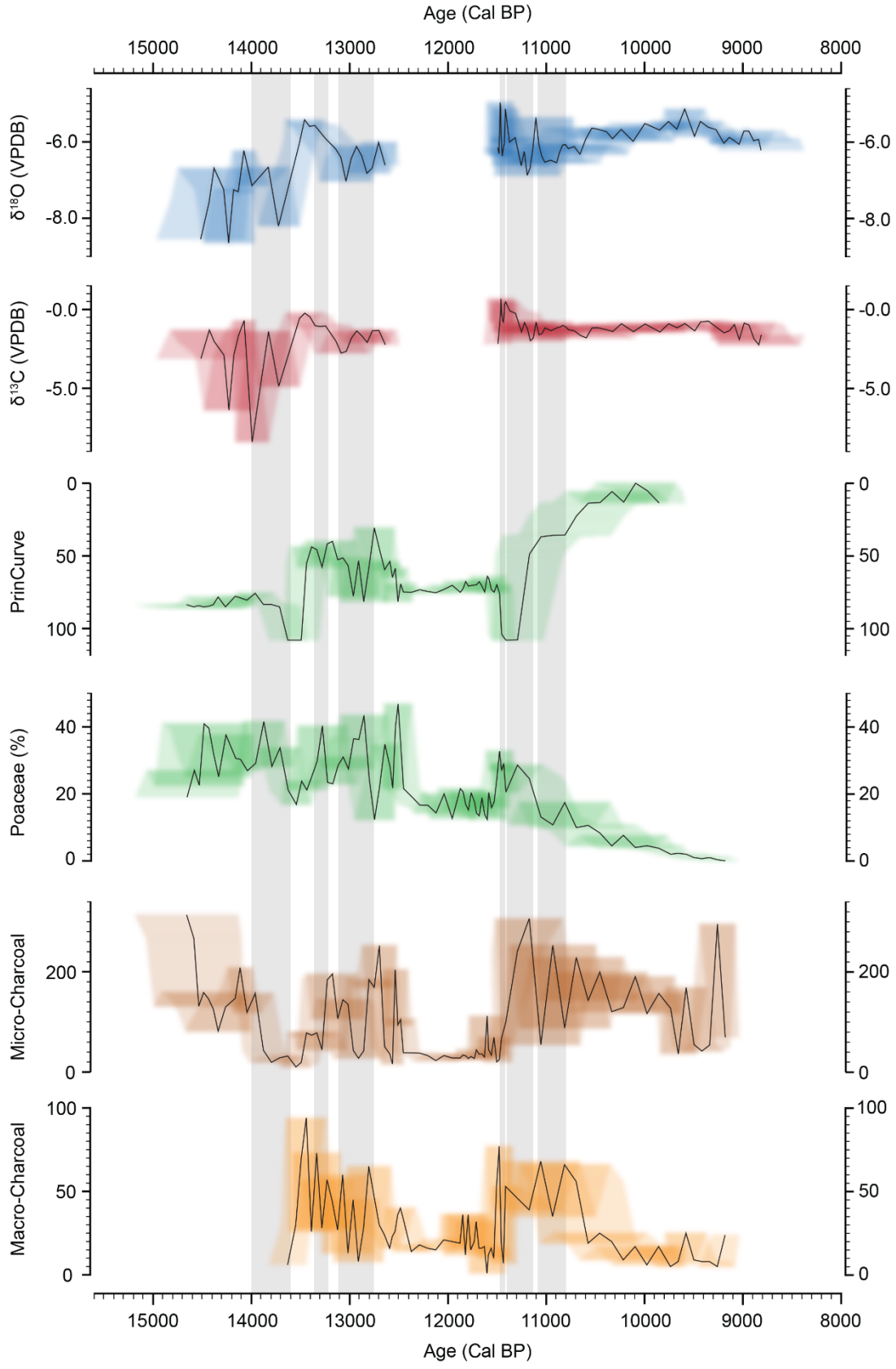

Figure 8.11 Comparison of all proxy data from Llangorse placed against age. Shown are $\delta^{18}O_{carb}$ and $\delta^{13}C_{carb}$. The principal curve is shown alongside the Poaceae curve to highlight areas of vegetation revertence. Macro-charcoal counts are presented where they are available, although as charcoal concentrations are presented throughout the sequence they are also included. Climatic deterioration episodes are shown on the diagram by grey shaded boxes.

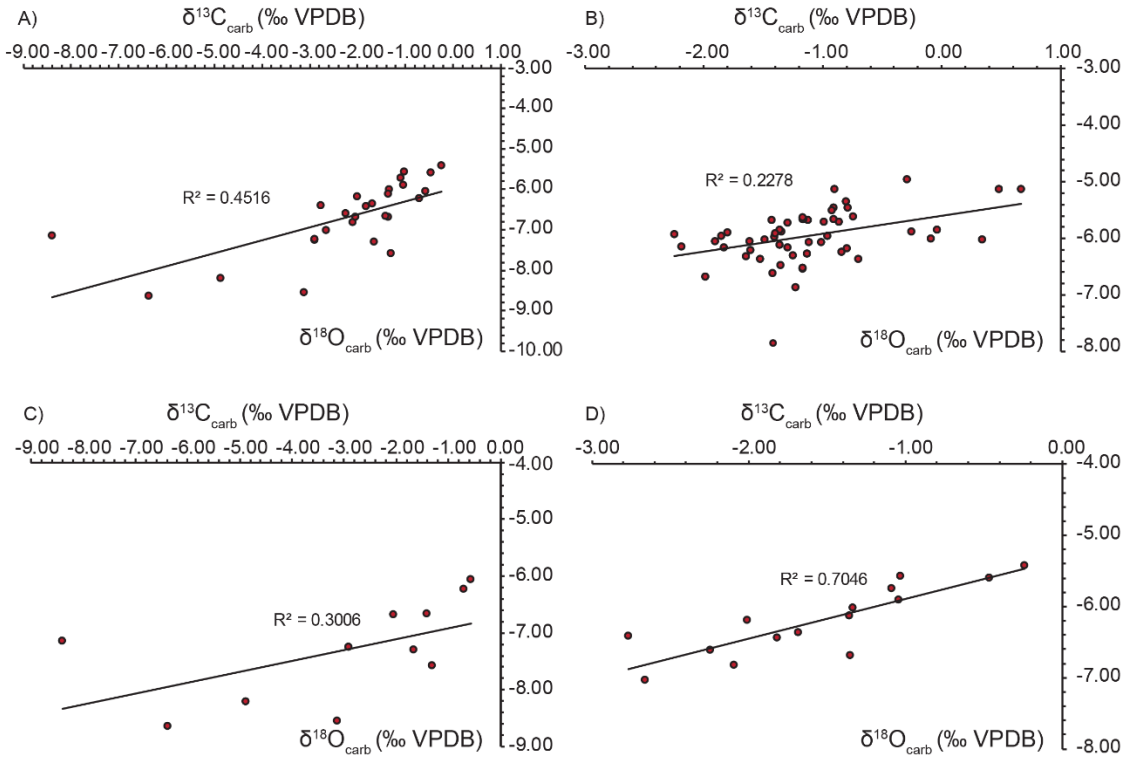

Figure 8.12 Series of scatter plots from the carbonate bearing sediments of Llangorse with regression models applied to the $\delta^{18}O$ and $\delta^{13}C$ datasets to test for co-variation. A) from the lower WI carbonates; B) from the early Holocene carbonates; C) From the carbonates between 639.25-576.25 cm; and D) from carbonates between 572.25-510.25 cm. The WI carbonates appear to show greater covariance. With strong covariance observed within the highest WI sediments.

vegetative inputs, and lacustrine equilibration with atmospheric CO_2 (Talbot, 1990; Leng and Marshall, 2004). The $\delta^{18}O_{carb}$ record can be interpreted in terms of the temperature of lake waters during carbonate mineralisation and the $\delta^{18}O$ of lake waters. The $\delta^{18}O$ of lake water is predominantly influenced by the $\delta^{18}O$ of precipitation, controlled by mean annual air temperatures, the amount of precipitation and distance from moisture source (Leng and Marshall, 2004; Chapter 4). In keeping with stable isotopic studies from carbonates within Britain (e.g. Marshall et al., 2002; van Asch et al., 2012a; Whittington et al., 2015; Candy et al., 2016) the isotopic data from Llangorse are interpreted as reflecting the temperature dependency of vapour condensation hence mean annual temperature.

Dimlington Stadial- >14.66±0.53 Cal. ka BP.

Sediment unit 1a is dominated by minerogenic, clay and silt, sediments. Carbonate and TOC values are low, <5 % and <1 % respectively, whilst MS and mineral components are high, up to 19 $x10^{-5}$ SI units and up to >99 % respectively. High MS values, with minerogenic sedimentation and a high clastic component, with no palynological material, suggests considerable erosivity in the catchment in an unvegetated landscape during

the DS. Further, low carbonate percentages suggest cold climates. Calcium Carbonate will precipitate out of solution if lake waters become super saturated with calcium and bicarbonate (Kelts and Hsu, 1978). The precipitation process is predominantly controlled by climatic warmth as: 1) warm lake waters decrease the solubility of CO_2 resulting in CO_2 loss; and 2) warmth leads to greater macrophyte abundances from which photosynthesis and respiration further removes CO^2 (Kelts and Hsu, 1978). Both processes increase the alkalinity of lake waters, allowing carbonate to precipitate. Thus, the dominance of clastic input via meltwater to the basin and lack of marl precipitation is indicative of lake sedimentation under cold climate conditions. In combination with the tephra identified in the overlying sediments suggests deposition during the DS.

Early Windermere Interstadial- 14.66±0.53 – 14.08±0.11 Cal. ka BP.

Minerogenic sedimentation continued into the early-WI. This, with high percentages of amorphous unidentifiable pollen, indicating physical abrasion (e.g. Cushing 1964; 1967), suggests continued erosivity. The prevalence of pre-Quaternary spores (LlaP-1) is thought to be derived from the erosion of a complex of Brecon Beacons glacial deposits (e.g. Bowen et al., 2002; Evans et al., 2005; Clark et al., 2012). Greater prevalence of microscopic charcoal (LlaCc-1) may confirm reworking, following incorporation of charcoal from geologic deposits. Alongside greater organic and carbonate percentages, $\delta^{18}O_{carb}$ enrichment, from -8.55- to -6.69 ‰, and $\delta^{13}C_{carb}$ enrichment, from -3.12 to -1.31 ‰, are postulated to reflect climatic amelioration. Caution is required however as isotopic analyses were performed on low carbonate-bearing sediments. Nevertheless, samples are taken from progressively increasing carbonate percentages, suggesting authigenic carbonate precipitation under a favourable climatic regime. Combined enrichment across both $\delta^{18}O_{carb}$ and $\delta^{13}C_{carb}$ would be expected with climatic amelioration due to 1) the temperature dependency of $\delta^{18}O$ in precipitation; with reduced poleward fractionation gradients associated with climatic warmth; and 2) greater $\delta^{12}C$ removal from lake water DIC, through increased photosynthesis/respiration with increased concentrations of aquatic plants (Leng and Marshall, 2004).

During the early WI (LlaP-1) the landscape was characterised by open-habitat herbaceous vegetation dominated by Poaceae, *Artemisia*, *Rumex* and *Salix*. These taxa are interpreted to reflect colonisation of the catchment by pioneering vegetation. *Salix* presence, likely in its dwarf form, is not surprising given the requirement for regular disturbance (e.g. Beerling, 1993). Low pollen concentrations suggest low catchment vegetation densities, which, aligned with continued minerogenic sedimentation demonstrates landscape instability. High *Pinus* pollen during the earliest WI demonstrate a far travelled component as no Pinus has been identified growing at this time in northern

Europe (e.g. Birks et al., 2005). Plant diversity increased after 14.50±0.44 Cal. ka BP (LlaP-2) with occurrences of *Betula* undiff. (*B*. *nana* confirmed through macro-fossils*;* Paul Lincoln, pers. comm. 2018), Cyperaceae, Compositae: Lactuceae, *Galium*, *Helianthemum*, *Plantago spp*., Saxifragaceae and *Urtica*. However, vegetation densities were still low as shown by low pollen concentrations. Thus, at Llangorse, the early WI was characterised by an open grassland thriving on unstable substrates but following 14.50±0.44 Cal. ka BP, greater species richness and the development of a *B*. *nana* scrubland indicates greater landscape stability and maturing soils.

At 14.23±0.25 Cal. ka BP an isotopic depletion is observed (LlaO-1). Depletions of 1.96 ‰ (from -6.69 to -8.65 ‰) characterise the $\delta^{18}O_{carb}$ record, whereas a depletion of 5.07 ‰ (from -1.31 to -6.38 ‰) is exhibited by $\delta^{13}C_{carb}$. Two scenarios could account for these patterns: 1) The isotopic data reflect a climatic event; and 2) the patterns of isotopic depletion are a product of detrital contamination. Following continued meltwater release during the earliest WI, North Atlantic freshening may weaken AMOC and retard heat transport to the northern hemisphere (e.g. Clark et al., 2001); resulting in a phase of cold climate and $\delta^{18}O_{carb}$ depletion. It is difficult to explain the high-amplitude $\delta^{13}C_{carb}$ depletion as $\delta^{13}C$ is weakly temperature dependent (Romanek et al., 1992). It is unlikely at this point that depleted $\delta^{13}C_{carb}$ resulted from a greater input of plant/soil respired CO_2 as catchment vegetation densities were low. However, if a more seasonal rainfall regime existed during this phase, aquifer/groundwater residence times may be reduced, resulting in reduced equilibration with atmospheric CO_2, minimal dissolution from geologic carbonates and more negative $\delta^{13}C_{carb}$ values (e.g. Hammarlund, 1993; Hammarlund et al., 1997; Andrews, 2006). In contrast, observed depletion may result from detrital contamination (e.g. Searl, 1989; Leslie et al., 1992; Brasier et al., 2014). As the isotopic values overlap with the main carbonate bearing materials from the basement lithology, this is a possibility. However, with the presented data, a climatic event may be more plausible.

It is not clear whether a palynologically inferred vegetative change in response to this climatic event can be identified. However, an inflection in the PC is observed. This appears to be driven by decreases in *Betula* and increases in Poaceae and Compositae: Lactuceae. Owing to the open, pioneering nature of vegetation early during the WI, it is not definitive whether this is a vegetative revertence. Further, as these observations are characterised by a single datapoint within the PC, less certainty is gained. To better characterise this event a higher sampling resolution is required.

Early Windermere Interstadial- 14.08±0.11 – 13.49±0.19 Cal. ka BP.

The subsequent phase of the record reveals an oscillatory $CaCO_3$ pattern and an increase in MS values. This pattern is further reflected by depletion in $\delta^{18}O_{carb}$ between 14.08±0.11 and 13.73±0.21 Cal. ka BP (from -6.23 to -8.21 ‰; LlaO-2) (Figure 8.11). At the point of oxygen isotopic depletion, two episodes of $\delta^{13}C_{carb}$ depletion are observed; 7.69 ‰ (from -0.71- to -8.40 ‰) and 3.47 ‰ (from -1.41 to -4.88 ‰) respectively. It is proposed that oxygen isotopic depletion reflects a cold climatic oscillation and a change in mean annual temperatures. However, $\delta^{13}C_{carb}$ depletion may be explained by 1) changes in the $\delta^{13}C$ of groundwaters; and 2) lacustrine modification of the isotopic signal. Detrital contamination can be disregarded based on minimal evidence of covariation (R^2=0.301; Figure 8.12).

Regarding scenario one, a cold climatic oscillation would increase the potential for increased periglacial activity, greater soil degradation and therefore transport. As mature soils are likely, through greater *Betula* undiff., the release and incorporation of isotopically depleted CO_2 from the decomposition of humic substances (Håkansson, 1985) into groundwaters would act to deplete the $\delta^{13}C_{carb}$ lacustrine signal. The former of these shifts may be expected to be greater under initial soil break-down, whereas, a secondary phase might be expected with event intensification, which may be observed with the $\delta^{18}O$ record. Notwithstanding, a change in lacustrine conditions may also impact the $\delta^{13}C$ ratio (e.g. Hammarlund et al., 2003). For example, a lake level change may lead to areas of Llangorse experiencing palustrine sedimentation. Palustrine conditions may reduce lake water residence times with concomitant decreases in groundwater residence times under a changing precipitation regime. These effects would reduce the level of atmospheric CO_2 equilibration with groundwater DIC and reduce dissolution of geologic carbon (Andrews, 2006). The groundwaters entering the waterbody would therefore be depleted in respect to $\delta^{13}C$; indeed, $\delta^{13}C_{carb}$ values presented are outside the range (+3 to -3 ‰) for lacustrine carbonates (Talbot, 1990). Support for this lake level change is given by increases in Cyperaceae undiff and *Sparganium spp*, an emergent macrophyte, that does not survive in water depths greater than 1 metre (Cook, 1962). Further evidence is derived from other sequences across the Llangorse basin where WI and LLS sediments appear missing, possibly due to hiatus' across the Llangorse site (e.g. Walker et al., 1993b). Whilst it is likely that a climatic oscillation may be the ultimate cause of both scenarios, it is not currently possible to decipher which is more plausible. Further research is therefore required.

In association with these climatic events, vegetational changes are suggested by an oscillation in the PC (Figure 8.11; LlaP-2; LlaP-3). Prior to major vegetation shifts, the

pollen data suggests that *Rumex* expands on the landscape at 14.04±0.14 Cal ka BP. Subsequently decreases in *Betula* and increases in *Artemisia*, Poaceae, Cyperaceae, Asteraceae, Compositae: Lactuceae and *Thalictrum* are noted between 13.96±0.19 and 13.79±0.22 Cal. ka BP. Reductions in *Betula* suggest a removal of *B*. *nana* scrubland and an increase in low lying herbaceous vegetation on the landscape. These taxa indicate a phase of vegetative revertence. Continued *Artemisia* and *Rumex* suggests greater colonisation of these taxa on areas of broken and disturbed ground and greater Poaceae indicates a greater grassland presence. The assemblage presented all have Arctic/alpine affinities confirming the evidence from the isotopic reconstruction that this phase of the record was characterised by mean annual temperature changes, which owing to *Artemisia* presence may have been arid and more seasonal (Birks and Birks, 2014).

From 13.67±0.20 Cal. ka BP, a further vegetation assemblage change occurs (LlaP-3b). Arctic/alpine and open grassland taxa are replaced by *Juniperus*. The significant expression of *Juniperus*, demonstrates the colonisation of Llangorse by an extensive *Juniperus* scrub. The presence of *Juniperus*, with thermophilic tendencies (e.g. Whittington et al., 2015) is proposed to reflect the terminus of the climatic episode thriving on immature, well-drained soils with a lack of competition from other woody plant taxa. High *Juniperus* concentrations demonstrates widespread colonisation, although increased concentrations of *Artemisia* and *Rumex* points to continued areas of open ground. Coincident with *Juniperus*, are significant abundances of charcoal (LlaC-1). It appears that increased woody vegetation accompanied by a return to climatic warmth provides a means for increased fire prevalence, with evidence suggesting that fire prevalence can in some cases be linked with *Juniperus* (Thomas, 2007; Lincoln, 2017).

The Arctic/alpine vegetation assemblage are clustered towards positive values within the PCA (Figure 8.5). Axis one may therefore be representative of a landscape stability gradient. However, multiple signals are recorded within the PC and RoC data, suggesting variability in the vegetation assemblage (Figure 8.11). Initially, the palynological change is recorded by increases in the PC owing to reduced *Betula* and increased *Rumex* and Poaceae. Subsequently, the greatest change in the PC is recorded in association with *Juniperus*. This change is supplemented by greater RoC values, indicative of major compositional turnover with respect to stratigraphy, thus rapid vegetational change. However, *Juniperus* is proposed to reflect climatic amelioration, which is not *per se*, a vegetative response to a climatic deterioration. Thus, at Llangorse, the abundance of *Betula* and *Juniperus*, may have important controls over the PC at this time, rendering the different signals present within the PC difficult to interpret.

Mid-Windermere Interstadial- 13.49±0.19 - 13.23±0.26 Cal. ka BP.

Marl sedimentation with high carbonate values alongside enriched $\delta^{18}O_{carb}$ values reveal warm climates during the mid-WI. Elevated TOC values suggest greater organic input or greater lacustrine productivity at this time. From 13.49±0.19 Cal. ka BP*,* increased *Betula* pollen suggests that tree birch was present in the Llangorse catchment (LlaP-4). This assertion has subsequently been confirmed with evidence of tree birch macro-fossils (Paul Lincoln, pers. comm. 2018) during radiocarbon processing. The presence of tree birch demonstrated greater soil maturation during the mid-WI with minimum summer temperatures of at least 12°C (Birks, 1994; van Dinter and Birks, 1996). The emergence of *Filipendula* on the landscape further confirms climatic warmth (Walker et al., 1993b; Edwards and Whittington, 2010) but also suggests moist climatic conditions and the development of moist nutrient rich soils (Birks and Matthewes, 1978). Despite evidence of birch woodland within the Llangorse catchment, the woodland remained open as suggested by the continued presence of Poaceae. Throughout the mid-WI a constant influx of charcoal is observed (LlaC-2) which suggests continued fire prevalence despite relatively moist climates. The mosaic of *Betula* woodland alongside grassland, with less positive PC values, suggests a phase of landscape stability during the mid-WI.

However, within the PC a vegetative change is suggested (Oscillation 2) at 13.28±0.25 Cal. ka BP. Reduced *Betula* populations alongside increases in Poaceae and *Rumex* characterise this phase. It is possible that following a climatic perturbation, a landscape opening caused increased incidence of grassland. However, as this is confined to few stratigraphic levels, the event may be of short duration, or a product of natural variability. Equally, no evidence of a climatic downturn is provided by the isotopic data. Whilst the event may be present within the PC, it is currently difficult to reconcile with the available data.

Late Windermere Interstadial- 13.23±0.26 – 12.80±0.22 Cal. ka BP.

Reduced $CaCO_3$ alongside reduced TOC is noted during the late WI suggestive of cooler climatic conditions and reduced organic or lacustrine productivity. Throughout this interval, a multi-phase depletion is observed within $\delta^{18}O_{carb}$ and $\delta^{13}C_{carb}$ (LlaO-3 to 4). From the onset of isotopic depletion during the Mid-WI, $\delta^{18}O_{carb}$ is characterised by successive depletions of 1.61 ‰ (from -5.42 to -7.03 ‰) and 0.70 ‰ (from -6.12 to -6.82 ‰). These phases are separated by enrichment of 0.91 ‰ (from -7.03 to -6.12 ‰) at 12.93±0.26 Cal. ka BP. These depletion events suggest a period of climatic deterioration, with reduced mean annual temperatures during the late WI at Llangorse. Comparable $\delta^{13}C_{carb}$ trends indicate either a greater input of soil-respired CO_2 following breakdown of

soil, or a late WI lake level shift towards paludal conditions (e.g. Garnet et al., 2004; Andrews, 2006). Nonetheless, as the isotopic event appears multi-phased, the series may reveal two individual climatic events (LlaO-3; laO-4); or one single event with enrichment a product of isotopic modification (Figure 8.10).

Whether this phase relates to two climatic deteriorations is difficult to ascertain, as the resolution of the isotopic profile is not currently sufficient. Multiple late WI climatic events are not a feature common to lacustrine records in Britain (e.g. Tipping, 1991a; Whittington et al., 2015; Candy et al., 2016). However, lake Meerfelder Maar does contain a late Interstadial climatic deterioration interspersed between the Gerzensee Oscillation and the Younger Dryas (e.g. Engels et al., 2016). Therefore, multiple events during the late WI are plausible. However, greater covariance in the isotopic dataset is recorded throughout (R^2=0.705). Thus, the two depletions proposed may be interspersed by a period of isotopic modification. If Llangorse experienced reduced lake levels, through greater aridity, then the system would be susceptible to evaporitic enrichment through the preferential loss of the lighter $\delta^{16}O$ and $\delta^{12}C$ isotopes. This scenario provides further credence for the $\delta^{13}C$ signal recording autochthonous palustrine change (e.g. Andrews, 2006). Equally, the pollen signal, with greater presence of *Pediastrum*, *Sparganium* and littoral *Equisetum*, suggest a contraction of the lake body (e.g. Cook, 1962; Sarmaja-Korjonen et al., 2006). Further, the $CaCO_3$ profile does not support a multi-event terminal WI record with a single reversion to lower percentages, if amelioration was recorded, it would be expected that $CaCO_3$ percentages would increase. Thus, the late WI at Llangorse is complex but proposed to show a single episode of climatic change with aridity postulated following reduced lake levels.

Coeval to $\delta^{18}O_{carb}$ depletion, between 13.14±0.27 and 12.80±0.22 Cal. ka BP (LlaP-5) a palynologically-inferred vegetation revertence is observed; confirmed by the PC (Oscillation 3) and greater values in RoC analyses. From the pollen and taxa response curves, the vegetative response appears manifest as reduced *Betula* alongside increased Poaceae. The increase in Poaceae reflects greater habitat availability following the partial removal of *Betula* from the catchment as opposed to reduced *Betula* flowering ability under unfavourable conditions (Walker, 1982). Reduced pollen concentrations may indicate increased sedimentation rates, however increasing Poaceae concentrations suggest increased open herbaceous grassland as opposed to sedimentation rate changes. Additional components of the landscape present during this phase include: *Pinus*, *Salix*, Cyperaceae, *Artemisia*, *Helianthemum*, *Rumex* and *Thalictrum*. The presence of *Filipendula*, a thermophile with moderate moisture requirements (e.g. Bunce, 1968; Walker et al., 1993a) would not be expected within a

cold, arid climatic event. However, *Filipendula* can survive depressed temperatures, to 8-9°C (Hormata, 1995). Perhaps therefore, summer temperatures were not sufficiently reduced to impact this plant taxon. Given a temperature gradient across Britain, which may have been exacerbated buring this phase (Chapter 9) it is not surprising that the impact of a climatic event is less felt in south Wales. Throughout this phase, the taxa on the landscape are commonly associated with a steppic community. This alongside a lack of tree *Betula*, as observed during the preceding stage, suggests landscape instability.

A feature of this climatic deterioration is increased charcoal abundance (LlaC-2:3). As charcoal occurs with the shift in *Betula*, it may be that fire impacts vegetation during this climatic event. However, the first increase in charcoal occurs after the onset of isotopic depletion after initial declines in *Betula*. Therefore, increased local fire incidence is a result of greater fuel availability on the landscape perhaps in conjunction with the establishment of aridity. Equally latter increases (LlaC-3) reflect greater fire incidence after the climatic event. Therefore, whilst fire may impact vegetation and drive vegetation change at Llangorse, wildfire incidence appears in response to a climatic event.

Late Windermere Interstadial- 12.80±0.22 – 12.51±0.14 Cal ka BP.

The late-WI is characterised by climatic warmth as suggested by greater $CaCO_3$ percentages, and enriched $\delta^{18}O_{carb}$. This amelioration is favourable with an initial loss of open-habitat assemblages and a return to a tree birch dominated landscape (LlaP-6). Concomitant decreases in *Filipendula* and Poaceae undiff. demonstrate the loss of an open meadow habitat. The loss of littoral and aquatic taxa with increases in *Myriophyllum* points to a rise in lake levels and oligotrophic lacustrine conditions (Edwards and Whittington, 2010). Towards the end of this phase, in conjunction with reducing $CaCO_3$, losses of *Betula* are observed with increases in Poaceae. *Artemisia*, Caryophyllaceae and increased fire prevalence (LlaC-4). This is taken to reflect a transitional phase into a period of climatic severity.

Loch Lomond Stadial- 12.51±0.14 - 11.73±0.21 Cal. ka BP.

A shift to minerogenic sedimentation, with low $CaCO_3$, TOC and high MS values, indicates active catchment erosion. Whilst no palaeoclimatic data currently exists, the sedimentation style is indicative of major climatic and environmental change. Greater MS values at the onset of this period may suggest more substantial sediment input. Nonetheless, elevated and stable MS values for the remainder of the record show continued clastic sediment supply with massive silts and clays constantly suppled to the lake system for a prolonged period. Anomalous to this situation are four separate periods of clay deposition, where a decrease in the energy of allogenic input and relatively still

lake waters allowed clay to settle from suspension. The cessation of coarse sediment supply may relate to freezing of the water body during the entire year. The sedimentology and chronology of this unit demonstrates a Loch Lomond Stadial (LLS) association.

The vegetative expression of the LLS (LlaP-7) is clear and shown with higher values in the PC (Figure 8.10; 8.11). Percentage decreases in Poaceae reflects the greater variety of herbaceous taxa present on the landscape during the LLS; which may not be reflective of considerable vegetative biome change. Further, whilst *Betula* is reduced compared to the WI, elevated *Betula* percentages throughout this phase are observed. For example, it is expected that summer temperatures are beneath 12°C during the LLS. Given this threshold for tree birch (van Dinter and Birks, 1996) it is probable that many of the *Betula* grains identified are of *B*. *nana* type. A secondary complication is that many of the *Betula* pollen grains were amorphous (e.g. Cushing, 1964; 1967). Physically abraded pollen demonstrates a reworked component. Hence, the elevated percentage of *Betula*, relate to a combination of the persistence of *B*. *nana* on the landscape and reworked pollen. This directly affects the PC and RoC analyses which at present are not suggestive of greater landscape instability than the vegetation revertences identified throughout the WI. Therefore, taphonomical issues may be prevalent throughout the LLS at Llangorse and whilst use of the PC is still valid caution is required.

During the LLS, the landscape was dominated by open, low lying herbaceous vegetation, with Cyperaceae, *Artemisia*, *Rumex*, *Salix*, *Pinus*, Caryophyllaceae, Compositae: Lactuceae, *Thalictrum* and *Selaginella selaginoides*. These taxa, with heliophilic associations (Whittington et al., 2015) are common in Arctic/alpine environments. *Artemisia* and *Rumex* demonstrate disturbed soils, with incidences of *Salix*, a chionophilic taxon, suggestive of greater seasonal snow lie and areas of landscape exposure (Walker, 1975; Beerling, 1993). *Pinus* reflects a greater far travelled component in an open landscape (Birks et al., 2005) confirmed by low concentrations (Appendix E). Greater abundance of the marginal taxa Cyperaceae may suggest lower lake levels throughout the LLS. Whilst aridity is likely during the LLS in Britain (e.g. Golledge et al., 2008) palaeohydrological data are required to fully appreciate aridity in south Wales. Low pollen concentrations highlight increased sedimentation rates, low landscape densities and low abundances of fewer pollen producing taxa. Thus, the LLS vegetation assemblage is depicted by a diverse grassland common to steppic/tundra environments in a period of major climatic deterioration.

Early Holocene- 11.73±0.21 - 10.64±49 Cal. ka BP.

Vegetation development in response to early Holocene climatic amelioration occurred

as the basin was still collecting clastic sediments (LlaP-7). As no climatic data exists during this phase, the demarcation of the early Holocene is proposed due to increased abundance of *Juniperus* a thermophilic taxon (Lowe and Walker, 1986) and elevated $CaCO_3$ with increased carbonate precipitation under warm climates. The fragility of *Juniperus* pollen confirms local plant growth and its occurrence is not a product of reworking. It is also expected that the landscape would be dominated by pioneering taxa during the earliest Holocene, bearing no resemblance to suggested climatic warmth (Walker et al., 1993b). Continued presence of *Artemisia* and *Rumex* confirms this view. Further, increases in charcoal (LlaC-5 and 6; LaCC-6) suggests greater fire occurrence, possibly caused by greater fuel availability with increased vegetation densities with ameliorating climates. However, caveats are noted, 1) lithostratigraphic evidence suggests continued landscape erosion and instability; 2) unidentifiable pollen indicates continued pollen reworking; and 3) pollen concentrations are low. Nonetheless, these effects are possible under a warm climatic regime, with incomplete landscape stabilisation, continued sediment delivery and high sedimentation rates. Thus, a disconnect is possible with the local vegetation signature and minerogenic sedimentological style during the earliest Holocene.

Enriching $\delta^{18}O_{carb}$ values, up to -4.97 ‰ between 11.48±0.14 and 11.47±0.14 Cal. ka BP denotes climatic warmth. The vegetation throughout this phase exhibits a greater abundance of Poaceae and *Juniperus* on the landscape at the expense of *Betula*. *Betula* declines are reflective of: 1) reduced *Betula* pollen redeposition; occurring in conjunction with marl sedimentation; and 2) a change in landscape conditions whereby tree birch is replacing *B. nana* which is not instantaneous (Walker et al., 1993b). During the early Holocene, an extensive *Juniperus* scrubland existed surrounding Llangorse. Alongside *Juniperus*, greater abundances of *Filipendula*, which has thermophilic associations, suggests that its occurrence in the landscape at this time was likely a product of greater moisture availability and the generation of damp fertile soils (Birks and Matthewes, 1978).

Superimposed on these trends are a suite of $\delta^{18}O_{carb}$ depletions. LlaO-5 exhibits a depletion of 1.41 ‰; between 11.47±0.14 and 11.45±0.13 Cal. ka BP; LlaO-6 shows a depletion of 1.74 ‰; between 11.42±0.13 and 11.19±0.33 Cal. ka BP; and LlaO-7 has a depletion of 1.18 ‰; between 11.11±0.38 and 10.89±0.45 Cal. ka BP. These depletions are proposed to reflect decreases in mean annual temperatures. However, it is uncertain whether these isotopic depletions are truly representative of three climatic deteriorations, a product of natural variability or potential intra-depletion enrichment. If, as revealed during the late WI, a phase of aridity occurred during one of these events then it is

possible that the isotopic signal could be modified. Whilst no covariation exists within the upper carbonates (R^2=0.228) reductions in $CaCO_3$, increased TOC and a detrital band is noted; suggesting greater allochthonous input. This may lend weight to the isotopic signal being modified between LlaO-6 and LlaO-7, although two episodes of open vegetation rather discounts isotopic modification; confirming at least two centennial-scale climatic deteriorations during the EH at Llangorse.

Across these proposed climatic oscillations, the vegetation record appears variable. Within the PC data there is the suggestion of a vegetation revertence (Oscillation 4), which appears more significant than the vegetation changes during the LLS. However, as the early WI, mono-specific taxon responses are masking potential signals of landscape instability; arising from variability in *Betula* and the widespread *Juniperus* scrub. Therefore, as the early WI caution is required when using the PC at Llangorse. Regardless, the first isotopic depletion (11.47±0.14 to 11.45±0.13 Cal. ka BP) exhibits no vegetation response, with falling Poaceae and increasing Filipendula. Due to the shortness of the event, the lack of vegetation response and only being observed in this climatic proxy (Chapter 4) this depletion is not proposed as a climatic event. Increased charcoal frequencies (LlaC-7) suggest local fires were prevalent at this time. The rapid and abrupt spread of the fire-sensitive *Juniperus* is proposed to reflect low intensity wildfires (Thomas et al., 2007) as *Juniperus communis* regrowth will not occur following large intense fires (Quevedo et al., 2007). Nonetheless, the spread of *Juniperus* in the British Isles reflects part of a successional sequence and like the WI, may be reflective of greater habitat availability with losses in *B. nana*.

Between 11.42±0.13 and 11.19±0.33 Cal. ka BP reduced *Juniperus* and the moisture sensitive *Filipendula* (Hormata, 1995) with increased open grassland taxa are proposed as the vegetative response to a cold, arid climatic event. This event is masked in the PC. Whilst climate may be the ultimate control, increased charcoal (LlaC-8) occurring within the onset of isotopic depletion, may have a secondary effect. A greater fuel source, e.g. *Juniperus*, with arid climatic conditions may suggest increased fire intensity potential (Power et al., 2008). Therefore, for this vegetation revertence it is probable that climatic deterioration influences fire occurrence which both work to remove *Juniperus* from the catchment. The final isotopic depletion 11.11±0.38 and 10.89±0.45 Cal. ka BP is manifest by a pause in the PC (Figure 8.11) suggesting a brief pause in vegetation development. This is confirmed by a pause in the *Betula* curve, and an increase in Poaceae; suggesting an expansion of grassland with slowed woodland development. Like the former climatic event, fire may have a secondary control with increased charcoal abundance (LlaC-9) at this time. Taken together, the vegetative responses to early

Holocene climatic events at Llangorse appear highly complex. In contrast to the events during the WI, vegetation responses to EH climatic events appear muted despite comparable forcing. Furthermore, the influence of fire during the early Holocene cannot be discounted.

Later early Holocene- <10.64±49 Cal. ka BP.

The later early Holocene record at Llangorse is characterised by climatic warmth as inferred from enriched $\delta^{18}O_{carb}$ and a constant $\delta^{13}C_{carb}$ signal. High percentages and concentrations of *Betula* undiff. with the paucity of additional pollen (LlaP-10) indicates the establishment of dense birch woodland. After 9.70±0.16 Cal. ka BP Betula woodland was replaced by a *Corylus* dominated woodland (LlaP-11). The continued presence of *Betula*, suggests that birch stands existed in the catchment of Llangorse throughout the *Corylus* phase. Increases in *Ulmus* and *Quercus* during the later early Holocene indicates the encroachment of deciduous trees into the catchment.

8.7 Chapter summary

This chapter summarises the litho-, palyno- and climatostratigraphic findings from Llangorse lake, south Wales. The tripartite sequence, alongside the Borrobol Tephra and chronological information imported from Llangorse (Chambers, 1999), Traeth Mawr (Walker, 1982) and Craig-Y-Fro (Walker, 2007) confirm that the sequence was deposited during the LGIT. Whilst the modelled age range was started from the onset of the Windermere Interstadial, clastic sediments beneath show a Dimlington Stadial attribution. The onset of the Windermere Interstadial is characterised by continued minerogenic sedimentation highlighting catchment erosivity. However, the trend towards enriched isotopic values highlights warm mean annual temperatures. The vegetation appears to develop from open pioneering communities to an open birch woodland throughout this phase. The Loch Lomond Stadial is characterised by a return to clastic sedimentation and the development of a grassland community with continued presence of *Betula nana*. Renewed organic sedimentation and isotopic enrichment depicts the climatic amelioration during the early Holocene. The vegetation during this phase is characterised by an open herbaceous grassland, *Juniperus* scrub, *Betula* then *Corylus* woodland.

Throughout the sequence the $\delta^{18}O_{carb}$ profile reveals a series of climatic events and associated vegetation responses. Three clear depletions are observed in the Windermere Interstadial and possibly two during the Holocene. The initial depletion in $\delta^{18}O_{carb}$ is not classified as a climatic event. However, the second (14.08-13.73 ka) and third depletion (13.23-12.80 ka) reveals a contraction of thermophilic woody vegetation

and expansions of open-habitat grassland communities. Interestingly the $\delta^{13}C$ record may indicate a period of lake level change in association with the early Windermere event. In contrast to the Windermere Interstadial, isotopic depletion in the Holocene is lower in magnitude, with muted vegetation responses. Of the three potential events, the first does not generate a vegetation response whilst the latter two exhibit differential responses. The second event is characterised by the loss of *Juniperus* and *Filipendula* and increases in grasses, whereas the latter reveals a pause in *Betula* development and an increase in Poaceae. In association with these climatic events, fire appears a locally important feature of the environment which may have a secondary effect in modulating vegetation responses.

Chapter 9. Synthesis of climatic variability during the Last Glacial-Interglacial transition (LGIT)

The series of sites presented within this thesis provide evidence for both palaeoclimatic events and associated vegetation responses. It achieves this via mean annual and summer temperature reconstructions using isotopic and chironomid-inferred temperatures (C-ITs). It reconstructs moisture availability using compound-specific deuterium isotopic biomarker data. It considers catchment stability via physical core data and sedimentological characteristics. Vegetation responses are characterised using high-resolution palynological data. Finally, the potential influence of fire is characterised using charcoal (micro-macro) records. This chapter synthesises the climatic data from each site; with all climatic proxies presented on absolute timescales (see Chapters 5 to 8) and considers millennial and centennial-scale climatic change. Here the term abrupt event is conditioned to relate to specific episodes of climatic deterioration. Further, this chapter seeks to present a climatic framework from which highly resolved and dated records from Britain and Europe can be compared to.

9.1 Chronological uncertainty

The age models from Tirinie and Quoyloo Meadow are relatively secure. Quoyloo Meadow contains the most robustly dated stratigraphy in Britain using tephrochronological horizons alone (Timms et al., 2017). However, at Tirinie from the Vedde Ash to the top of the sequence no datable material was identified, therefore the chronological uncertainty is relatively large from ca 12.00 Cal. ka BP onwards. The two Star Carr sequences, hereafter termed Palaeolake Flixton (PF), yielded little terrestrial macrofossil material however, a robust age model for the Holocene could be constructed from Core B and from the Vedde Ash in Core C (see Blockley et al., 2018). The Interstadial age model is robust but has been tied to the proximal Wykeham sequence (Lincoln, 2017). These two age models were combined to form the basis of the model from PF. Llangorse is most likely the least robust of the chronologies presented within this thesis (Section 8.5.2) but it is expected that as the other sites, the absolute chronology is correct within centennial timescales.

While these chronological limitations are acknowledged, it is thought that a clear set of climatic forcing mechanisms will have impacted all sequences to a varying degree. A case in point are the Greenland ice-core records, from which the regional stratotype for the North Atlantic during the LGIT (GICC05; Rasmussen et al., 2014) reveals that forcing and connections between the dominant ocean state and atmosphere are coherent. The individual severity, internal structure, duration and subsequent local landscape response is potentially variable and that is what is being explored here.

9.2 Synthesis of millennial-scale climatic variability during the LGIT

The climatic records are presented in Figure 9.1. Across each sequence the general climatic trends are clear, with climatic warmth during the Windermere Interstadial (WI), cold climatic conditions during the Loch Lomond Stadial (LLS) followed by a return to warm climates during the early Holocene (EH). Superimposed on these general trends are short-lived abrupt centennial-scale climatic deteriorations (Section 9.3).

9.2.1 Windermere Interstadial ca 15.01-12.51 Cal. ka BP

The basal modelled ages from each of the sequences are based on the first occurrence of palaeoclimatic data. From these records the onset of sedimentation appears variable, with warm C-ITs (10.71°C) at Quoyloo Meadow ca 15.01 Cal. ka BP, enriching $\delta^{18}O_{carb}$ (-8.55 ‰) at Llangorse ca 14.52 Cal. ka BP, warm C-ITs (11.02°C) at PF ca 14.35 Cal. ka BP and warm C-IT's (12.31°C) and enriched $\delta^{18}O_{carb}$ (-7.92 ‰) at Tirinie 14.14 Cal. ka BP. Climatic warmth reveals that the transition from DS-WI is not recorded at the three higher latitude sequences. This might not be the case from Llangorse, although palaeoclimatic data is not recorded beyond 651 cm, where laminated clastic DS sediments are present (Palmer et al., 2008). Therefore, QM, Tirinie and PF were unlikely to exist as competent palaeobasins during the DS. Due to the modelling approach employed, the basal ages contain wide errors. Equally as Quoyloo Meadow appears to be dominated by rapid sedimentation with an expanded stratigraphy during the early WI, the onset of sedimentation at Quoyloo Meadow appears much older (ca 300 years) than modelled ages in lower latitude sequences. This is clearly at odds with the other sequences and the onset of the WI in the regional stratotype, NGRIP (ca 14.7 Cal. ka BP; Rasmussen et al., 2014). Which perhaps reflects the lack of constraint in the age model. In contrast, the late onset of sedimentation at Tirinie may reflect a lingering presence of ice within this locality (Walker and Lowe, 2017) which may have caused a barrier to sedimentation. This is plausible with recent suggestions that Scotland was ice-free between 14.30-13.90 Cal. ka BP (Walker and Lowe, 2017). Regardless of the onset of sedimentation within basins, the transition from cool climates of the Dimlington Stadial is not recorded.

Throughout the WI across all sequences, barring Quoyloo Meadow, a transition from clay to carbonate-dominated sediments reveals climatic warmth. This is not the case at Quoyloo Meadow which is characterised by continued mineral sedimentation, suggesting erosivity in the Quoyloo Meadow catchment. Favourable climates are recorded across the three carbonate bearing sequences through enriched $\delta^{18}O_{carb}$ values, revealing warm mean annual temperatures, and elevated C-ITs indicating warm

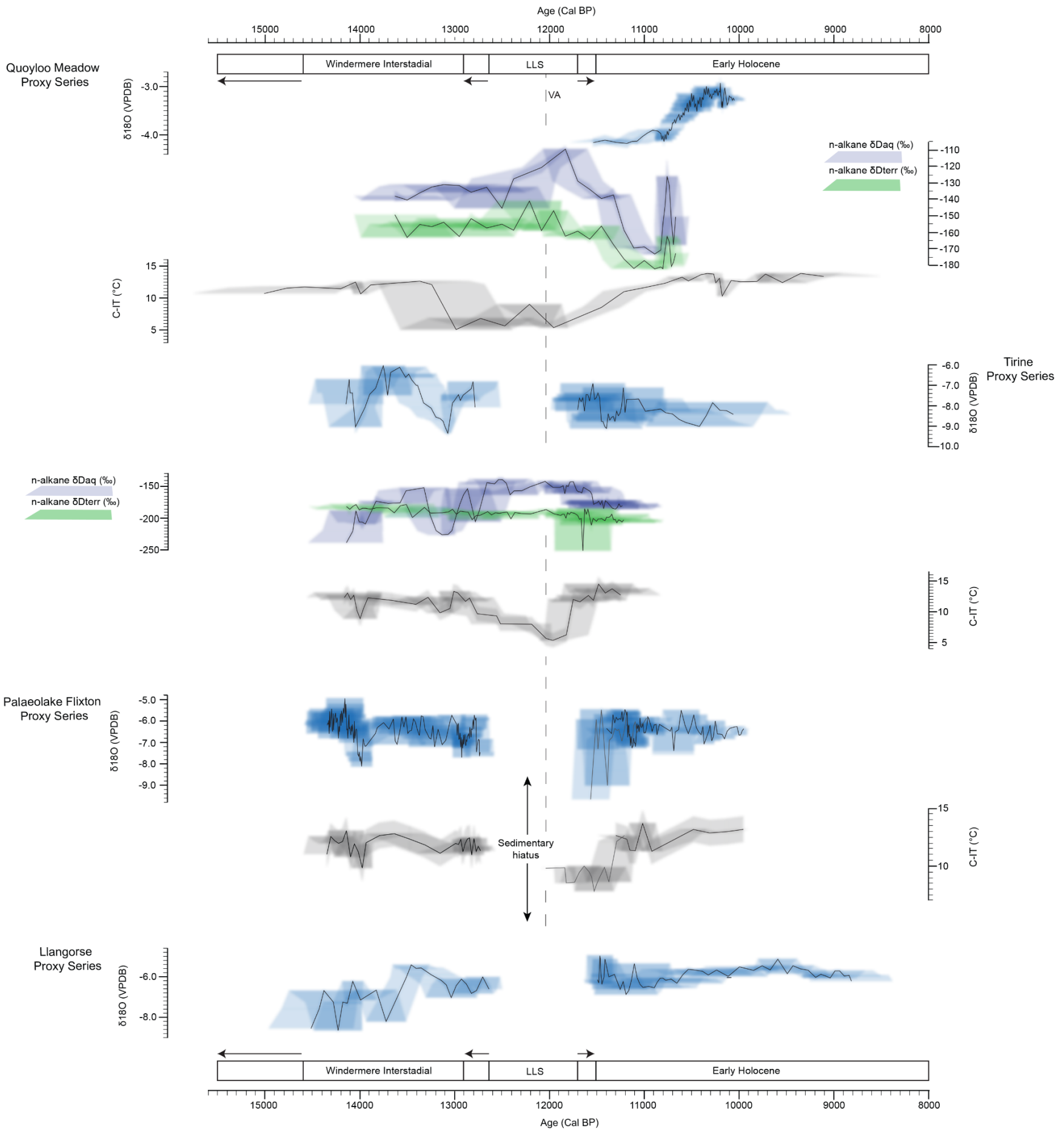

Figure 9.1 Showing all climatic proxy data on common age scale. The top of the figure reveals climatic proxy data from Quoyloo Meadow, with successive sections showing data from Tirinie, Palaeolake Flixon and finally Llangorse. Different colours reveal different proxy evidence with blue representing $\delta^{18}O_{carb}$; grey representing chironomid inferred temperatures; dark blue representing δD values of n-C_{23} (aquatic plants); and green representing δD values of n-C_{29} (higher terrestrial plants). Shading within each proxy along the x-axis reveal 95 % chronological uncertainty bounds. Also highlighted are the major millennial phases within the proxy record with arrows indicating their minimum/maximum chronological extent and the Vedde Ash (dashed line; 12,023 ± 43 Cal. ka BP; Bronk Ramsey et al., 2015) indicating that Quoyloo Meadow, Tirinie and Palaeolake Flixton are tied records.

summer temperatures. Whilst carbonates are not deposited at Quoyloo Meadow, climatic warmth is denoted by elevated C-ITs alone.

The individual proxy sources reveal variability across Britain (Figure 9.1). At Tirinie and Llangorse, the mean annual thermal optimum during the WI is suggested between 13.75-13.46 Cal. ka BP (-6.05 ‰ and -5.42 ‰), whilst at PF this optimum occurs at 14.15 Cal. ka BP (-4.94 ‰). Over the same period peak summer temperatures appear variable suggesting differential climatic development. At Quoyloo Meadow and Tirinie, peak summer temperatures are recorded at 13.37-12.99 Cal. ka BP, whilst at PF this occurs earlier during the WI at 14.14 Cal. ka BP. Outside of these peak temperatures, the WI appears stable with no clear cooling trends observed (e.g. Brooks and Birks, 2000a; Rasmussen et al., 2014). Although negligible, average summer temperature records from PF are warmer compared to high-latitude sequences (11.83°C at PF; compared to 11.63°C and 11.7°C at Tirinie and Quoyloo Meadow). However, it remains to be seen whether the full range of temperatures are observed owing to non-contiguous sampling. Further, the biomarker δ*D* records indicate, at least after ca 13.50 Cal. ka BP and not withstanding climatic events, the high-latitudes of Britain were characterised by moisture availability. Therefore, the WI in Britain is characterised by warm mean annual and summer temperatures, and relatively wet conditions.

9.2.2 Loch Lomond Stadial ca 13.12-11.52 Cal. ka BP

The transition from warm to cold climates of the LLS is well represented, however the onset appears to be latitudinally variable. The onset at Tirinie and PF ca 12.74-12.73 Cal. ka BP splits the earlier onset at Quoyloo Meadow ca 13.12 Cal. ka BP and later onset at Llangorse ca 12.51 Cal. ka BP respectively (Figure 9.1). This difference is a product of the modelling approach, with wide errors across the latter two sequences attributed to: 1) the lack of chronological constraint following the deposition of the Penifiler Tephra (Quoyloo Meadow); and 2) a lack of precision following the potential incorporation of a mixed carbon source from bulk radiocarbon dates (Llangorse) (e.g. Wohlfarth, 1996; Lowe and Walker, 2000). Alternatively, the onset of the LLS could be time-transgressive across Britain (Muschitiello and Wohlfarth, 2015) with higher latitudes experiencing an earlier onset. This might be supported by evidence of a period of ice-rafting in the North Atlantic towards the end of the Interstadial with freshwater flux weakening Atlantic Meridional Overturning Circulation (AMOC) (Klitgaard-Kristensen et al., 2001; Muschitiello and Wohlfarth, 2015). With a dominant oceanic climatic regime in the northern latitudes, it might be expected that oceanic perturbations would be first registered in the higher latitudes as the polar front migrates south (Ruddiman and

McIntyre, 1981). However, as atmospheric reorganisation occurs within 1-3 years at the onset of the Stadial (Steffensen et al., 2008) a ca 500-year difference between Quoyloo Meadow and Llangorse may be improbable, based on the observed ca 290-year lag across Europe (Muschitiello and Wohlfarth, 2015). Therefore, these differences likely result from dating imprecision during the onset of the Stadial in Britain.

At the inception of the LLS, organic sediments are replaced by minerogenic silts and clay, highlighting the shift in erosivity and environmental conditions. Coeval with lithostratigraphic change, all four sites exhibit a shift in palaeoclimatic data. Whilst isotopic reconstructions were not possible due to the lack of carbonate sedimentation, C-ITs reveal cooling by 7.04°C at Quoyloo Meadow (12.1-5.0°C) and 6.8°C at Tirinie (12.26-5.35°C). In contrast PF reveals cool temperatures, although they are not as cold as presented from the Scottish sites (minimum reconstructed temperature of 7.84°C). This may highlight a latitudinal climatic gradient across Britain (Figure 9.8; Brooks and Langdon, 2014) in the expression of cold events. Biomarker δD from Tirinie suggests LLS aridity is held within a complex evaporitic signal. This is favourable to models suggesting that starvation of moisture is required to 'force-stop' LLS glaciation (e.g. Golledge et al, 2008; Bromley et al., 2018) in Scotland. Alternatively, with Tirinie in the lee of the West Highland glacier complex aridity would also dominate.

At Quoyloo Meadow, the minimum reconstructed temperatures are inferred during the earliest phase of the LLS, likely due to the cooling effect of sea-ice (Renssen and Isarin, 1998), whilst at Tirinie, coldest temperatures arise during the latter half of the Stadial. A similar feature is observed at Loch Ashik (Brooks et al., 2012). Increased winter precipitation, suggested by the expansion of ice over Croftamie, north of Glasgow, at a later point during the Stadial (MacLeod et al., 2011) is argued for increased incidence of long-lasting snow-beds on the Isle of Skye (Brooks et al., 2012). The melting of these snow beds proximal to Loch Ashik, in the spring and summer months, decrease water temperatures and influence the C-IT reconstruction (Brooks et al., 2012). Being at a higher altitude than Loch Ashik, in the lee of the West Highland glacier complex (Bickerdyke et al., 2018) this mechanism in entirely plausible to explain the late LLS cold summer temperatures at Tirinie. The LLS across Britain is the most severe climatic deterioration episode during the LGIT. This is expressed through large climatic downturns and the effect this has on the environment in Britain (Chapter 10).

9.2.3 Early Holocene ca 11.74-8.8 Cal. ka BP

Enriched $\delta^{18}O_{carb}$ (-4.00 ‰) at Quoyloo Meadow ca 11.54 Cal. ka BP; warm C-IT's (11.99°C) at Tirinie ca 11.74 Cal. ka BP; enriched $\delta^{18}O_{carb}$ (-5.93 ‰) from PF ca 11.50

Cal. ka BP; and expansion of *Juniperus* at Llangorse ca 11.73 Cal. ka BP reveal climatic amelioration during the Holocene. At each sequence, the onset of the early Holocene (EH) appears inconsistent. The variable onset is likely to be a product of sampling resolution and availability of sediments for proxy reconstruction (e.g. carbonate and isotopes) as no apparent latitudinal pattern in climatic amelioration is observed. Nevertheless, within age errors all proxies reveal a broad contemporaneous warming.

9.3 Synthesis of centennial-scale climatic variability during the LGIT

Whilst the general pattern of millennial-scale climatic development is clear, across each sequence a series of short-lived, high-magnitude centennial-scale climatic events are observed. Two, potentially three climatic events can be observed during the WI, with evidence of climatic variability during the LLS, and a series of lower magnitude events during the EH (Figure 9.2). This section is conditioned to relate to observed climatic events across multiple sequences only.

9.3.1 Early Windermere Interstadial ca 14.14-13.73 Cal. ka BP.

All climatic data demonstrate a high-magnitude, centennial-scale climatic event early within the WI between 14.14-13.73 Cal. ka BP (Figure 9.2; Table 9.1). Within chronological uncertainties this climatic deterioration is synchronous across Britain. Nonetheless, the duration of climatic deterioration appears greater towards the lower latitudes, ca 400 years at Llangorse, compared with an intermediate and shorter duration at higher latitudes, ca 300 and 150 years at Tirinie, PF and Quoyloo Meadow respectively. The longer duration at Llangorse is most likely a product of the low sampling resolution and lack of stratigraphic constraint as opposed to a longer period of climatic severity, which is improbable following a southerly migration of the polar front (Hogg et al., 2016). Mean annual temperature change is recorded by $\delta^{18}O_{carb}$ depletions of 2.33 ‰ at Tirinie; 3.18 ‰ at PF and 1.98 ‰ at Llangorse. This mean annual change is mirrored by summer temperature declines of 3.8°C; 3.23°C and 1.86°C at Tirinie, PF and Quoyloo Meadow. Across all sequences, the early WI climatic event is the largest amplitude centennial-scale event (Figure 9.2) suggesting that the perturbation to the climatic system was severe enough to cause wide-spread changes in different climatic parameters across Britain (e.g. Marshall et al., 2002; Leng and Marshall, 2004; Brooks et al., 2012; van Asch et al., 2012a). This deterioration is most pronounced at Tirinie followed by PF and Llangorse (Figure 9.2; Table 9.1). Although summer temperature changes are large at Tirinie, the lack of carbonate production during this event represents minimum isotopic depletion, thus minimum annual temperature change. Why Tirinie should experience a greater climatic response to this event is discussed in more detail in section 9.4. The variability between sequences in absolute reconstructions perhaps

Table 9.1 Climatic event timing and the different depletion within oxygen and deuterium isotopic data and summer temperature change at each site for A) the Windermere Interstadial; and B) the Early Holocene. Dashes represent where no data exists at a particular sequence with the proxy data and N/O represents where a climatic deterioration or depletion is not observed.

A) Windermere Interstadial	**Age (Cal. ka BP)**											
Climatic Event	**14.14-13.73**				**13.60-13.50**				**13.45-12.80**			
Site	**$\delta^{18}O_{carb}$**	**C-IT**	**δD_{aq}**	**δD_{terr}**	**$\delta^{18}O_{carb}$**	**C-IT**	**δD_{aq}**	**δD_{terr}**	**$\delta^{18}O_{carb}$**	**C-IT**	**δD_{aq}**	**δD_{terr}**
Quoyloo Meadow	-	-1.86°C	-	-	-	**N/O**	**N/O**	**N/O**	-	**N/O**	**N/O**	**N/O**
Tirinie	-2.33 ‰	-3.8°C	-20.75 ‰	-8.43 ‰	-1.44 ‰	**N/O**	**N/O**	**N/O**	-3.23 ‰	-2.51°C	-73.57 ‰	-8.58 ‰
Palaeolake Flixton	-3.18 ‰	-3.23°C	-	-	-1.19 ‰ ?	**N/O**	-	-	-1.45 ‰	-1.22°C	-	-
Llangorse	-1.98 ‰	-	-	-	**N/O**	-	-	-	-1.61 ‰	-	-	-
Climatic event	**Yes**				**Uncertain**				**Yes**			

B) Early Holocene	**Age (Cal. ka BP)**											
Climatic Event	**11.45-11.05**				**11.18-10.75**				**10.20-10.10**			
Site	**$\delta^{18}O_{carb}$**	**C-IT**	**δD_{aq}**	**δD_{terr}**	**$\delta^{18}O_{carb}$**	**C-IT**	**δD_{aq}**	**δD_{terr}**	**$\delta^{18}O_{carb}$**	**C-IT**	**δD_{aq}**	**δD_{terr}**
Quoyloo Meadow	-0.07 ‰	**N/O**	-32.25 ‰	-25.64 ‰	-0.23 ‰	**N/O**	-4.32 ‰	-5.07 ‰	-0.74 ‰	-2.8°C	-	-
Tirinie	-2.20 ‰	**N/O**	-22.85 ‰	-25.06 ‰	-	-	-	-	-	-	-	-
Palaeolkae Flixton	-3.54 ‰	-1.26°C	-	-	-1.80 ‰	-1.31°C	-	-	-	-	-	-
Llangorse	-1.74 ‰	-	-	-	-1.18 ‰	-	-	-	-	-	-	-
Climatic event	**Yes**				**Yes**				**Yes**			

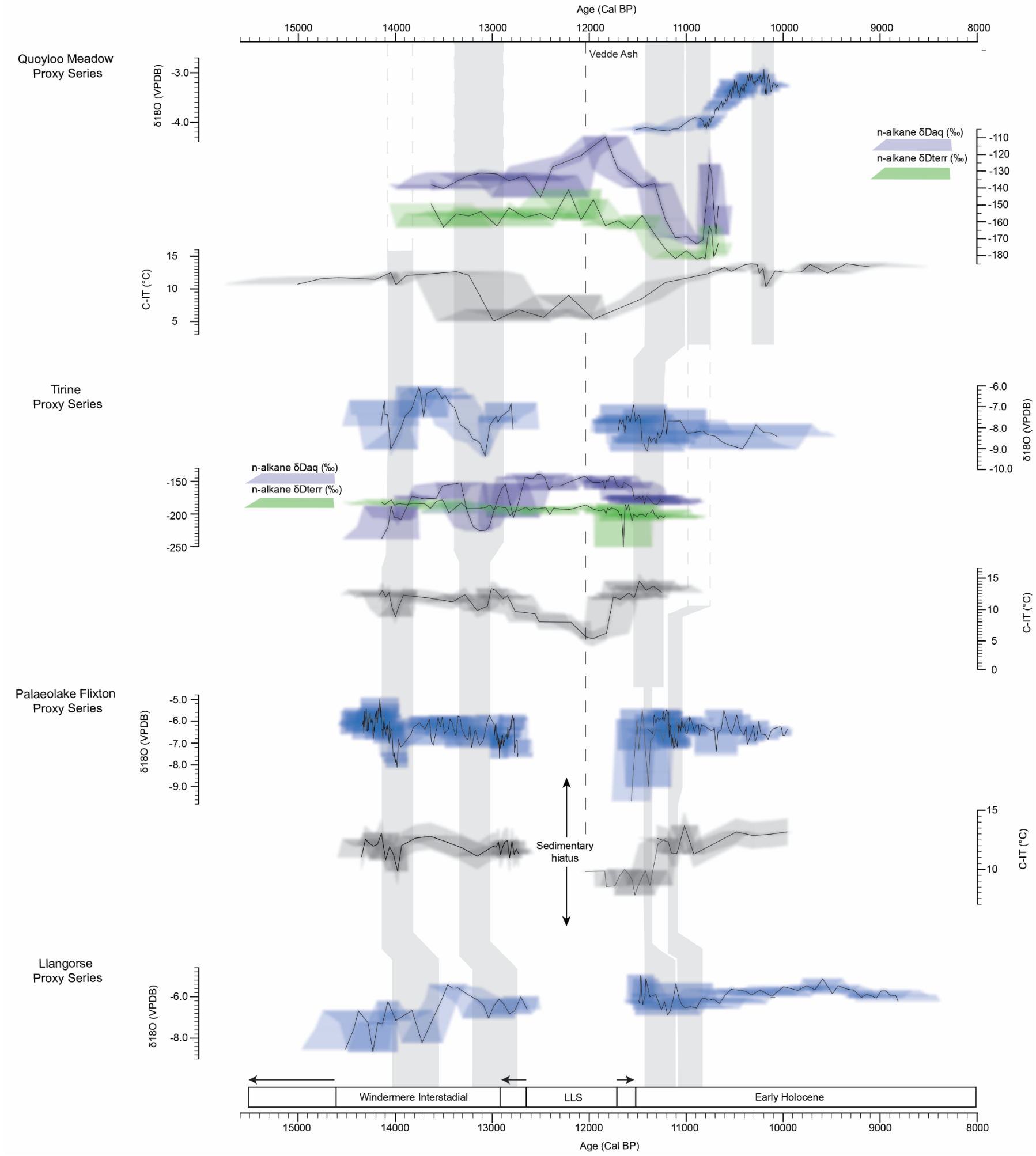

Figure 9.2 Showing all climatic proxy data on common age scale. The top of the figure reveals climatic proxy data from Quoyloo meadow, with successive sections showing data from Tirinie, Palaeolake Flixon and finally Llangorse. Different colours reveal different proxy evidence with 1) blue representing $\delta^{18}O_{carb}$; 2) grey representing chironomid inferred temperatures; 3) dark blue representing δD values of n-C_{23} (aquatic plants); and 4) green representing δD values of n-C_{29} (higher terrestrial plants). Shading within each proxy along the x-axis reveal 95 % chronological uncertainty bounds, and along the y-axis individual proxy measurement/predictive error. The box reveals millennial scale phases, with arrows indicating their minimum/maximum chronological extent and the Vedde Ash (12,023 ± 86 cal. BP; Bronk Ramsey et al., 2015) indicating that Quoyloo Meadow, Tirinie and Palaeolake flixton are tied records. Grey shaded bars reveal the abrupt climatic events at each point within each sequence. The plotting of sequences together allows for an understanding of duration, timing and amplitude of the events.

suggests a climatic gradient across the British Isles (Figure 9.7; Brooks and Langdon, 2014; Moreno et al., 2014) in the expression of cold events, as observed in the LLS.

The Tirinie δ*D* biomarker record reveals depletion in *n*-C_{23} and *n*-C_{29} indicative of reduced temperatures and 'rain out' of the heavier isotope at lower latitudes (e.g. Sachse et al., 2012). However, falls in *n*-C_{23} relative to *n*-C_{29} suggest a phase of aridity with heightened evapotranspiration enriching the *n*-C_{29} δ*D* signal in a coupled system (Rach et al., 2014). It is probable that a similar latitudinal gradient exists between higher and lower latitudes, but further research would be required to confirm this. Therefore, between 14.14-13.73 Cal. ka BP a high-magnitude, centennial-scale climatic event is recorded across all sequences, with mean annual and summer temperatures depressed, and at Tirinie, at least, a phase of aridity.

9.3.2 Mid-Windermere Interstadial ca 13.60-13.50 Cal. ka BP

In contrast to the widely observed early Interstadial climatic event, Tirinie and PF reveal short-lived centennial to sub-centennial isotopic depletion episodes during the mid-Interstadial. Minor $\delta^{18}O_{carb}$ depletions of 1.44 ‰ and 1.19 ‰, are observed with no summer temperature correlatives. During this phase, reductions in mean annual temperature approximate a 100-150-year duration and are of a much lower magnitude compared to the early WI event. As no C-IT variability is noted, it may be that the climatic deterioration is too short-lived, the climatic event does not contain a summer temperature component, the sampling resolution is insufficient or chironomids are insensitive during the mid-WI. However, Whitrig Bog, at an intermediate latitude between Tirinie and PF, reveals a decline at a comparable stratigraphic position (Brooks and Birks, 2000a), suggesting that chironomids do respond to this event. Further, as chironomids are sensitive to changes in summer temperature (Walker et al., 1987) the lack of a response suggests that the sample resolutions employed here are insufficient to fully capture the event. Nonetheless, as this only occurs in one sample for each of these sites, a climatic event has not been formally defined.

9.3.3 Late Windermere Interstadial ca 13.45-12.80 Cal. ka BP

The late WI reveals a climatic deterioration between 13.45-12.8 Cal. Ka BP. The modelled onset of climatic deterioration occurs at ca 13.45, 13.35 and 13.23 Cal. ka BP at Tirinie, PF and Llangorse respectively with the duration of the climatic phase appearing variable, ca 400 years at Tirinie, 350 years at PF and 500 years at Llangorse (Figure 9.2). The age of this oscillation is robust from Tirinie, with a terrestrially dated macrofossil sample giving an age of 13.07±62 Cal. ka BP (SUERC-78788; Chapter 6) after maximal isotopic depletion. Whilst the age of this climatic deterioration appears

younger at Llangorse and contains larger chronological error, within age estimates this event is contemporaneous with other sequences suggesting common climatic forcing. Quoyloo Meadow does not reveal a climatic deterioration at this time as the late WI record is stratigraphically compressed. Nevertheless, $\delta^{18}O_{carb}$ depletion is observed 3.23 ‰; 1.45 ‰ and 1.61 ‰ from Tirinie, PF and Llangorse. The former two records exhibit C-IT declines of 2.51°C (minima of 9.83°C) and 1.22°C to (minima of 11.11°C) respectively. These depletions in $\delta^{18}O_{carb}$ and downturns in C-IT reflect both mean annual and summer temperature change across Britain. Tirinie again exhibits greater change than the lower latitudes. Whilst this may reflect a regional climatic gradient (e.g. van Asch et al., 2012a; Brooks and Langdon, 2014) in the expression of climatic deterioration, site specific factors need to be considered (section 9.4). This event exhibits a reduced magnitude than the early WI climatic event (Table 9.1) which may highlight that between 13.5-12.8 Cal. ka BP, the climatic deterioration is less severe. Alternatively, the mechanism driving the climatic change for these two events may differ.

In contrast to the early WI event δ*D* data reveals greater isotopic depletion in the *n*-C_{23} alkane relative to *n*-C_{29}, suggesting, in a coupled system, greater isotopic enrichment of higher terrestrial plant *n*-alkanes (e.g. Rach et al., 2014; 2017; Muschitiello et al., 2015). Whilst the values are relative and dependent on climatic regime (e.g. Sachse et al., 2012), greater magnitudes suggest that the late WI climatic event was characterised by greater aridity. As per the early WI event, it is unknown if greater aridity is site specific or it extends regionally across Britain. The understanding of aridity is therefore vital to develop theories relating to the propagation of the climatic signal throughout these abrupt events.

9.3.4 Loch Lomond Stadial ca 12.2-12.0 Cal. ka BP

Throughout the LLS subtle changes can be observed in the palaeoclimatic data. However, at Quoyloo Meadow at ca 12.2 Cal. ka BP, immediately preceding the deposition of the Vedde Ash a 3.38°C increase in summer temperature is observed. This broadly coincides with an increase in LOI suggesting greater environmental productivity and in conjunction with enriched δ*D* values suggesting climatic amelioration, a shift to localised precipitation or a change in the moisture source (Rach et al., 2014). Whilst warmer temperatures are recorded from Quoyloo Meadow, coldest temperatures are recorded after the deposition of the Vedde Ash at Tirinie. As posited above, this may reflect localised snow melt at altitude (Brooks et al., 2012). Nonetheless, if snowmelt is affecting lake water temperatures, it is possible that warming is also recorded, but not revealed by the summer temperature proxy. Further evidence for warmer temperatures from lower latitudinal British sequences in the approximate stratigraphic position of the

Vedde Ash is revealed from Whitrig Bog (Brooks and Birks, 2000a) and Hawes Water (Bedford et al., 2004). Thus, it would appear that within the LLS a phase of climatic variability is recorded between 12.2-12.0 Cal. ka BP in Britain.

9.3.5 Early Holocene ca 11.45-11.05 Cal. ka BP

Within the early Holocene a series of abrupt climatic events can be observed. The first is centred between 11.45-11.05 Cal. ka BP (Figure 9.2). The earliest onset of this event is at Tirinie and PF at approximately 11.45 Cal. ka BP. At Quoyloo Meadow and Llangorse the onset of the episode of climatic deterioration occurs at 11.42 Cal. Ka BP. Thus indicating synchroneity across Britain. However, the duration of these events is variable, with the shortest at PF, ca 100 years; and the longest from Quoyloo Meadow, ca 300 years. The events at Tirinie and Llangorse occur for ca 250 years. From all sites $\delta^{18}O_{carb}$ depletions of 0.07 ‰ (QMO-1), 2.20 ‰ (TirO-4), 1.74 ‰ (LlaO-6); 3.54 ‰ (STCCO-3) are recorded from Quoyloo Meadow, Tirinie, Llangorse and PF respectively; suggesting between 1-12°C annual temperature change (Leng and Marshall, 2004). Where available, depletion in biomarker δD: 32.25 ‰ (δD_{aq}) and 25.64 ‰ (δD_{terr}) at Quoyloo Meadow and, 22.85 ‰ (δD_{aq}) and 25.06 ‰ (δD_{terr}) at Tirinie is recorded. The depletion within δD_{aq} and δD_{terr} and convergence of the biomarker end-members from Quoyloo Meadow and Tirinie confirms a period of heightened aridity across the northerly latitudes of Britain. Of the sequences presented only PF reveals a summer temperature decline of 1.26°C; presented by a single data point and within a period of cool summer temperatures. The absence of summer temperature change across the northerly latitudes is presumed to be reliable as chironomid samples are taken from phases of maximal depletion. Therefore between 11.45-11.05 Cal. ka BP a synchronous event is recorded across the four sites that appears to exhibit variable magnitudes (Section 9.4). The event is manifest across Britain by cool mean annual temperatures, relatively unchanged summer temperatures and greater aridity.

9.3.6 Early Holocene ca 11.18-10.75 Cal. ka BP

The second Holocene climatic event, between 11.18-10.75 Cal. ka BP, is revealed across all sequences barring Tirinie, where the resolution of the climatic data is insufficient. Quoyloo Meadow and Llangorse appear to demonstrate the greatest event duration, ca 225-300 years; whilst at PF the duration of the climatic event is ca 150 years. Across Britain, the onset of the event is variable, ca 11.18 and 11.1 Cal. ka BP at PF and Llangorse respectively. However, at Quoyloo Meadow, the onset of Deuterium depletion occurs at ca 11.0 Cal. ka BP, with the greatest shift occurring in $\delta^{18}O_{carb}$ at 10.91 Cal. ka BP reflecting differential phasing between climatic parameters. Across all sequences, depletion in $\delta^{18}O_{carb}$ is revealed by 0.23 ‰ (QMO-2); 1.80 ‰ (STCBO-6) and 1.18 ‰

(LlaO-7) at Quoyloo Meadow, PF and Llangorse respectively. Continued δ*D* depletion is recorded at Quoyloo Meadow and summer temperatures decline by 1.31°C at PF. Akin to the first early Holocene event a short-lived climatic deterioration is observed across Britain. As only PF exhibits small summer temperature change, these climatic deteriorations exhibit greater mean annual or seasonal changes. Like the preceding event, aridity is suggested by the convergence of biomarker end members.

9.3.7 Early Holocene ca 10.20-10.10 Cal. ka BP

The third early Holocene climatic event is recorded from Quoyloo Meadow only (Figure 9.2). Between 10.21-10.18 Cal. ka BP a depletion of 0.52 ‰ (QMO-5) coupled which coincides with a with C-IT decline of 2.8°C. The expected temperature change with isotopic depletion (approximately -2°C) matches with the summer temperature declines, suggesting that summer temperature is an important control on isotopic proxy data in this instance. Nonetheless, inversions in both proxies suggest a phase of mean annual and summer temperature change at least across the northern latitudes of Britain.

9.4 Magnitudes of centennial-scale climatic events

Across all sequences the magnitude of climatic events warrants further discussion (Table 9.1). In Britain, the expression of centennial-scale climatic events appears variable across sequences based on latitudinal position/climatic regime. Generally, the Interstadial events are more pronounced than the early Holocene events. This is not true at Quoyloo Meadow where greater δ*D* depletion is observed with aridity between 11.45-11.05 and 11.00-10.75 Cal. ka BP and mean annual and summer temperature declines at 10.2 Cal. ka BP. Nonetheless, based on the isotopic fractionation between carbonate and meteoric water of ca 0.3 ‰/°C (Leng and Marshall, 2004), the isotopic ($\delta^{18}O_{carb}$ and δ*D*) shifts registered within these four sites would be expected to incur temperature changes between 0.5-2°C (Quoyloo Meadow); 6->11°C (Tirinie); 3-12°C (PF) and 3.5-7°C (Llangorse). With available climatic data, temperature shifts cannot fully explain the climatic oscillations as recorded by isotopic data. It may be that greater mean annual/seasonal change results in the patterns of isotopic depletion observed, however additional isotopic considerations are also likely.

9.4.1 Quoyloo Meadow

The magnitudes of climatic events are smaller at Quoyloo Meadow compared with the other three sites. It is possible that low magnitude events relate to the limited expression of abrupt events within the Orkney archipelago, possibly related to its oceanic location (e.g. Whittington et al., 2003), however, additional arguments include sampling approach and data treatment and the location of the site.

In terms of the sampling approach, for chironomids a contiguous sampling strategy was not adopted. During the WI, a 2 cm resolution was adopted whilst during the EH this increased to 4 cm. Thus, the reported summer temperature changes are minimum estimates only. Further, within the Quoyloo Meadow stratigraphy, the two events between 11.45-11.05 and 11.1-10.75 Cal. ka BP reveal no summer temperature change. Thus, sampling strategy, could be problematic, however, each isotopic depletion contains at least one C-IT sample. These climatic events must then have seasonal variations with minimal summer temperature change. Regarding $\delta^{18}O_{carb}$, a contiguous sampling approach was adopted, so absolute isotopic minima are recorded. However, measurements from Quoyloo Meadow are reported from a three-point moving average. Naturally this underestimates the isotopic signal; although it is necessary for interpretation of the noisy $\delta^{18}O_{carb}$ record. Thus, the moving average signal may mask greater depletion.

Secondly, regarding the location, it has been noted that chironomids may respond to effects other than temperature (e.g. Walker, 1987). Whilst work exists in understanding proxy effects other than climate, Self (2010) and Engels et al. (2014) revealed that continental effects and oceanic proximity may be important in constraining midge populations. Therefore, on Orkney, with an oceanic climate, midge assemblages may be affected by additional effects other than prevailing temperatures. This may dampen the climatic signal. Equally, regarding the isotopic signal, Quoyloo Meadow sits on a low relief archipelago; therefore, it is not affected by altitudinal isotopic effects (e.g. Gonfiantini et al., 2001; Leng and Marshall, 2004) however, proximity to the ocean source may exert influence. Principally, being in proximity to the main heat source for the northern latitudes may act as a buffer against climate change. Thus, even during oceanic perturbations, Quoyloo would still be proximal to a heat supply. Equally, with no continentality, absolute $\delta^{18}O_{carb}$ values and with depletion through a climatic event may be more positive (e.g. van Asch et al., 2012a) due to reduced continental 'rain-out' (Leng and Marshall, 2004). At Quoyloo Meadow therefore, it can be argued that continental effects are more important than latitude. Finally, it may be that the isotopic changes are not only recording temperature or seasonal change but changes in moisture source and precipitation. This is highlighted by the significant shift in δD_{aq} and δD_{terr} during the EH. As the Holocene event is shown to be arid, reduced precipitation may produce less depleted $\delta^{18}O_{carb}$ values, overprinting the $\delta^{18}O_{carb}$ temperature component. However, reduced precipitation would not exhibit significant depletion as observed in δD_{aq} and δD_{terr} so a shift in moisture source isotopic ratios may be important at Quoyloo Meadow.

Therefore, as the magnitudes of centennial-scale climatic events are generally low at Quoyloo Meadow it is postulated that the island location of the site and its oceanic setting are important for the expression of climatic events.

9.4.2 Tirinie

Tirinie presents some of the greatest magnitudes of isotopic shifts throughout the transect. Reasons for the greater magnitudes include: that Tirinie experienced greater magnitudes of climatic change in due to its latitudinal position in Britain; the configuration and altitudinal setting of the site; and that the greater magnitudes of change is an artefact of a change in source water ratios.

Regarding the former scenario, being at a relatively high latitude for Britain, it is possible that Tirinie experienced greater climatic change than other sequences. Support for this is derived from summer temperature variability. The level of summer temperature change is comparable to that of Abernethy Forest (Brooks et al., 2012) and Whitrig Bog (Brooks and Birks, 2000a). However, it is greater than Hawes Water (Bedford et al., 2004) and Fiddaun in Ireland (van Asch et al., 2012a) both of which lie at lower latitudes. The same scenario is true for oxygen isotopic oscillations, with greater change at Tirinie than Hawes Water northern England, Fiddaun in Ireland and Crudale Meadow in Orkney (Whittington et al., 2015; Marshall et al., 2002; van Asch et al., 2012a). Tirinie could therefore represent a greater expression of climatic change than elsewhere suggesting that the mechanism controlling these climatic events and the effects this has, most commonly oceanic forcing and ocean circulation disruption (Section 9.7), is most strongly felt between Tirinie and Whitrig Bog.

Secondly, Tirinie is a small palaeobasin, which is likely to be particularly sensitive to climatic change (e.g. Leng and Marshall, 2004). As water residence times are low, constant lake water recycling means that lake waters will predominantly be composed of $\delta^{18}O$ of precipitation; subsequently reflected in lacustrine carbonates. Thus, at Tirinie the propagation of the dominant climatic regime into lacustrine carbonate is expected to be rapid (Candy et al., 2016). Therefore, variations in dominant seasonal/climatic regime may be more clearly expressed at Tirinie than elsewhere due to the small size of the palaeobasin (Candy et al., 2016). Additionally, an altitudinal component may explain the large isotopic shifts. As Tirinie is relatively high relief for Britain, 323 m a.s.l, heightened vapour condensation with decreasing temperature (e.g. Gonfiantini et al., 2001) may occur with further depletion through greater ‘rain-out’. As Tirinie resides at higher altitudes than any of the sites presented within this thesis, altitudinal effects may exert considerable influence on the recorded isotopic signal. Further, during phases of climatic

severity, greater depletion with altitudinal effects are likely. This is especially true of the Holocene oscillations where no summer temperature change is recorded. It might be unrealistic that seasonal variations of 4-5°C occur, thus site sensitivity and altitudinal position may be a key mechanism to explain observed isotopic depletion during the LGIT at Tirinie.

Finally, $\delta^{18}O_{carb}$ and δD_{aq} ratios have previously been interpreted to reflect a variable moisture source and changing moisture source pathways (e.g. Rach et al., 2014; 2017). If climatic events, as observed throughout these sequences, are terrestrial manifestations of oceanic perturbations (weakening AMOC through freshwater input) changes to the moisture source could explain the magnitude of the events recorded at Tirinie. However, whilst the influx of isotopically light meltwater may induce source water $\delta^{18}O$ dilution in the North Atlantic (e.g. Lewis et al., 2010) baseline source water change would be reflected across all sequences within this thesis, plus site specific isotopic effects. The variable magnitudes of these events across each site are therefore unlikely to reveal a change in source water. It is perhaps more probable that the location of the site, its configuration and the altitudinal setting are far more important in the perceived magnitude of events at Tirinie.

9.4.3 Palaeolake Flixton

At Palaeolake Flixton the amplitudes of climatic change are intermediary between Quoyloo Meadow and Tirinie. This intermediary nature may be a result of: reduced magnitudes of climatic change at Palaeolake Flixton; the size of PF; and greater continentality and enhanced ‘rain out’ across continental Britain.

It is possible that greater mean annual change or increased seasonality may explain the pattern of isotopic depletion relative to summer temperature changes. However, this is difficult to quantify with the reduced resolution of the chironomid dataset across PF. Reduced C-IT resolutions indicate that periods of maximal summer temperature decline may be missing, and a greater resemblance of the two climatic datasets may not be fully appreciated. Nonetheless, the reduced magnitude of summer and mean annual change at PF compared with Tirinie, may be a product of the reduced climatic change experienced at PF. The similarity of reconstructions from north-west England (e.g. Lang et al., 2010) perhaps demonstrates the regional climatic gradient across Britain with Whitrig Bog and Tirinie demonstrating greater magnitudes of change and lower latitude settings experiencing lower magnitudes. Thus, a regional gradient is beginning to show across Britain whereby the higher latitudes may be more susceptible to the dominant forcing mechanisms than the lower latitudes.

Secondly, in direct contrast to Tirinie, PF is a much larger palaeobasin. Whilst this may not influence the chironomid record, the greater size of the basin may influence the isotopes. Greater residence times in large open water bodies would average the isotopic signal between the direct incorporation of the $\delta^{18}O$ of precipitation and hydrologically affected lake water $\delta^{18}O$ (Leng and Marshall, 2004). Thus, the $\delta^{18}O_{carb}$ record may be dampened compared to small sensitive basins. However, the greater isotopic depletion during the early WI event, may be reflective of a contraction of the lake water body, a reduction of lake water residence times and therefore greater sensitivity of the sequence.

Finally, intermediate isotopic depletion across PF may a product of the location of the sequence. Sitting at 24 m.a.s.l altitudinal effects would not affect isotopic values. However, as PF is a considerable distance from the moisture source, which would have been larger with eustatic change following the Devensian glaciation, continentality is a plausible mechanism. With sites further from a moisture source, continental 'rain-out' and loss of $\delta^{18}O$ would result in greater $\delta^{18}O_{carb}$ depletion (Rozanski et al., 1993). Whilst this is known in the modern day (Darling, 2004) it may be exacerbated during periods of climatic severity due to lower latitude vapour condensation, and subsequent depletion in precipitation $\delta^{18}O$ prior to transgression. Sequences farther from the moisture source would thus exhibit greater isotopic depletion following rain out of an already depleted condensate. During a climatic event lower land temperature may further work to enhance the rate of vapour condensation. Therefore, increased distance from a primary westerly moisture source will reveal heightened isotopic expressions of these climatic events relative to dominant isotopic conditions during warm phases. At PF it is probable that a combination of the above three explanations impact the perceived magnitude of the shifts in eastern England.

9.4.4 Llangorse

In comparison to Tirinie and PF, the isotopic depletions at Llangorse appear lower in amplitude. No quantified temperature reconstructions exist from Llangorse. However, Coleopteran Mutual Climatic Range (MCR) estimates exist from Llanilid, south Wales (e.g. Walker et al., 2003). These MCR values are well within the range of isotopic shifts presented from Llangorse ca 4-5°C (Walker et al., 2003). However, as isotopic samples are not contiguous, the full range of isotopic depletion/enrichment may not be realised. Nevertheless, the lower amplitude of these isotopic events in comparison to other sequences may be a product of the lower magnitudes of climatic change at lower latitudes or the size of the basin.

The former of these explanations is difficult to ascertain with the paucity of isotopic and climatic reconstructions from this location. However, within this thesis evidence of greater climatic change at higher latitudes, Tirinie vs PF, is observed. Therefore, it might be expected that abrupt climatic events in south Wales will be of lower magnitude. This may be a product of the climatic expression of Atlantic Meridional Overturning Circulation (AMOC) being less pronounced at lower latitudes (e.g. Lehman and Keigwin, 1992; Clark et al., 2002; Nesje et al., 2004). Therefore, isotopically these climatic events would appear dampened. Llangorse, at the most southerly point of the transect, would also be expected to exhibit more enriched isotopic values as air-masses are less depleted in $\delta^{18}O$ than higher latitudes (Darling, 2004). It is acknowledged that, across Britain, these effects are minimal compared to continent-wide isotopic changes. Nevertheless, the $\delta^{18}O$ data from Llangorse is consistently less depleted than higher latitude sequences, barring Quoyloo Meadow. Therefore, the lower latitudinal position and the role this plays in modulating the $\delta^{18}O_{carb}$ signal is important in understanding the expression of climatic events in south Wales.

Like PF, Llangorse would have been a large lake during the LGIT, with lake waters likely exhibiting longer residence times. The amplitudes of isotopic shifts are therefore dampened due to the greater averaging of lake water $\delta^{18}O$ and precipitation $\delta^{18}O$ (Leng and Marshall, 2004). Furthermore, it is not thought that continentality and altitudinal effects are important at Llangorse. Whilst the sequence sits at a moderate altitude for Britain, 155 m.a.s.l, it is not expected that this altitude would lower temperatures sufficiently to affect vapour condensation rates and impact $\delta^{18}O_{carb}$ values (e.g. Gionfantini et al., 2001). Further Llangorse is relatively proximal to the oceanic source with no real effect of continental 'rain-out' (Rozanski et al., 1993). Thus, at Llangorse the amplitudes of isotopic depletions are reduced owing to the lower latitudinal position of the sequence and the size of the basin.

9.5 Regional comparisons to the British climatic stratigraphy

As the aim of this thesis is to better constrain vegetation responses to abrupt climatic events, comparisons to additional British and regional records are vital. The comparison of climatic signals across a wide area enables an understanding of climatic development, and for comparisons with the regional stratotype the NGRIP isotopic stratigraphy (Lowe et al., 2008; Rassmussen et al., 2014). However, to compare across sequences, criteria need to be outlined and are presented in Table 9.2. Many key published sequences do not conform to these criteria making comparisons problematic. The major issue is the lack of chronological precision plus the piecemeal approach to climatic and environmental reconstruction, with reconstructions often made from the same site using

different sequences, years apart and directly compared. Nonetheless, comparisons are made between sequences that conform to most of these criteria across a wide spatial area with sites shown in Figure 9.3 with reconstructions shown in Figures 9.4; 9.5.

9.5.1 Millennial-scale climatic variability from Britain

Few records from Britain detail the climatic improvement from DS sediments to the WI. Whitrig Bog, south-east Scotland reveals a summer temperature improvement of 6°C (from 6-12°C; Brooks and Birks, 2000a) and Fiddaun, western Ireland shows a strong temperature increase of 8°C (from 6.3-14.3°C; van Asch et al., 2012a; Figure 9.4). No chronology exists from these sequences so the precise timing of these changes cannot be gained. The stronger summer temperature response may be due to the proximity of Fiddaun to the ocean, with the onset of the WI linked to strengthening AMOC following a shutdown in the DS (Denton et al., 2010). Hawes Water north-east England also reveals a 6°C summer temperature rise (7.4-13.4°C) at the onset of the WI (Bedford et al., 2004) perhaps suggesting a greater temperature rise in Ireland than mainland Britain.

Windermere Interstadial/Woodgrange Interstadial

The general Interstadial range in temperature is comparable between sequences; between 12.5-14.3°C at Fiddaun, 11.4-13.4°C at Hawes Water, 10-12.5°C at Whitrig Bog and 11-13.6°C at Abernethy Forest (Brooks and Birks, 2000a; Bedford et al., 2004; van Asch et al., 2012a, Brooks et al., 2012; Figure 9.4). This fits with the range of temperatures presented from sequences in this thesis, 10-13.3°C at Tirinie, 11.4-12.5°C at Quoyloo Meadow and 11-13°C at PF. Generally, warmer temperatures are observed at lower latitudes and coolest temperatures at higher latitudes. However, warmer temperatures at Tirinie and Abernethy Forest are observed. Considering both reside at higher altitude, local site characteristics, including basin size and continentality are likely important controls on the range of summer temperatures (e.g. Lang et al., 2010).

In Britain, peak summer temperatures are recorded at the onset of the Interstadial, with temperature following a downward trend prior to the onset of the LLS. Neither Quoyloo Meadow, Tirinie or PF follow that trend, with reconstructions at higher and lower latitudes being mostly stable. This might be explained through the lower resolutions of the C-IT dataset, where peak summer temperatures are not recorded.

In contrast with the C-IT records, the $\delta^{18}O$ records from across Britain, including: Hawes Water (Marshall et al., 2002) Fiddaun (van Asch et al., 2012a) Crudale Meadow (Whittington et al., 2015) but not PF all reveal peak enrichment mid-Interstadial, and are contrasted with palaeoecological reconstructions (Figure 9.5). As isotopic analyses

Table 9.2 The criteria used to select sequences from across Britain for comparison. In each of the columns a tick is given when the criterion is met and a cross where the criterion is not met. 'In part' relates to the notion that part of the sequence may contain suitable data, whilst 'N/A' is placed where the criteria are unknown. The final column provides the key reference(s) for the site in question. The first element of the table contains only sites from Britain, and the second element extends to other European locations.

Site	High-resolution climatic data	High-resolution vegetation reconstructions	Attributable to the LGIT in part or whole	Contain a robust independent chronology	Palaeodata in same sequence	Reference
Crudale Meadow	✓	✓	✓	×	✓	Whittington et al., 2015
Loch Etteridge	×	✓	×	×	N/A	Walker, 1975; Kelly 2017
Muir Park Reservoir	✓	✓	✓	✓	×	Vasari, 1977; Brooks et al., 2016
Tynaspirit	×	✓	✓	×	N/A	Lowe and Walker, 1977
Pulpit Hill	×	✓	✓	×	N/A	Tipping, 1991b
Loch an Druim	×	✓	✓	✓	N/A	Ranner, 2005; Ranner et al., 2005
Druim Loch	×	✓	✓	✓	N/A	Walker and Lowe, 1990; Pyne O' Donnell, 2007
Whitrig Bog	✓	✓	✓	×	✓	Mayle et al., 1997; Brooks and Birks, 2000a
Lock Ashik	✓	✓	✓	✓	×	Walker and Lowe, 1990; Brooks et al., 2012
Tanera Mor	×	×	✓	✓	N/A	Timms, 2016
Abernthey Forest	✓	✓	✓	✓	×	Birks and Matthewes, 1978; Brooks et al., 2012
Lundin Tower	In Part	✓	✓	×	×	Whittington et al., , 1996
Wester Cartmore Farm	×	✓	✓	✓	N/A	Edwards and Whittington, 2010
Hawes Water	✓	✓	✓	×	In Part	Marshall et al., 2002; Bedford et al., 2004
Tadcaster	×	✓	✓	×	N/A	Bartley, 1962
Thorpe Bulmer	×	✓	✓	×	N/A	Bartley et al., 1976
Wykeham Quarry	✓	✓	✓	✓	✓	Lincoln, 2017
Slubiggin Tarn	✓	✓	✓	×	✓	Lang et al., 2010;
Gransmoor	✓	✓	✓	✓	In Part	Walker et al., 1993a
Llanilid	✓	✓	✓	✓	In Part	Walker and Harkness, 1990; Walker et al., 2003
Sluggan Bog	✓	✓	✓	✓	✓	Walker et al., 2012
Ballybetagh	×	✓	✓	×	N/A	Watts, 1977
Loch Nadourcan	✓	✓	✓	Variable	×	Watts 1977; Watson et al., 2010
Loch Inchiquin	✓	×	✓	✓	N/A	Diefendorf et al., 2006; 2008
Fiddaun	✓	✓	✓	✓	✓	van Asch et al., 2012a; van Asch and Hoek, 2012
Tory Hill	✓	✓	✓	×	✓	O'Connell et al., 1999
Thomastown Bog	✓	✓	✓	×	✓	Turner et al., 2015

Table 9.2 (Cont.) As table 9.2 however, this table focusses on the continental European sequences. In each of the columns a tick is given when the criterion is met and a cross where the criterion is not met. 'In part' relates to the part of the sequence that may contain suitable data, whilst 'N/A' is placed where it is unknown if the criterion is met. The final column provides the key reference(s) for the site in question.

Site	High-resolution climatic data	High-resolution vegetation reconstructions	Attributable to the LGIT in part or whole	Contain a robust independent chronology	Palaeodata in Same sequence	Reference
Moervaart	✓	✓	In Part	In Part	In Part	Bos et al., 2017
Krakeness	✓	✓	✓	✓	✓	Brooks and Birks, 2000b; Lohne et al., 2014
Meerfelder Maar	✓	✓	✓	✓	In Part	Litt and Stebich, 1999; Brauer et al., 2008; Rach et al., 2014; Engels et al., 2016
Gerzensee	✓	✓	✓	×	In Part	Lotter et al., 1992; 2012; van Raden et al., 2012; Ammann et al., 2013
Aegelsee	✓	✓	✓	×	In Part	Lotter et al., 1992
Ammersee	✓	×	✓	×	N/A	von Graffenstein et al., 1999
Soppensee	×	✓	✓	✓	×	Lotter, 1999; Lane et al., 2011
Holzmaar	×	✓	✓	✓	N/A	Litt and Stebich, 1999; Brauer et al., 2001
Hasseldala	✓	✓	✓	✓	In Part	Wohlfarth et al., 2006; Muschitiello et al., 2015
Rieme	×	×	✓	✓	×	Bos et al., 2013
Milheeze	×	✓	✓	✓	N/A	Bos et al., 2006
Slotseng	✓	✓	✓	✓	×	Mortensen et al., 2011; Larsen and Nygaard, 2014
Lake Slone	×	✓	✓	×	N/A	Kulesza et al., 2011
Hamelsee	×	✓	✓	✓	×	Merkt and Muller, 1999; Jones et al., 2018
Trzechowskie	In Part	In Part	✓	✓	✓	Wulf et al., 2013; Słowiński et al., 2017
Hijkermeer	✓	✓	✓	×	✓	Heiri et al., 2007
Lac Loutrey	✓	✓	✓	✓	✓	Heiri and Millet, 2005; Magny et al., 2006
Klein Ven	✓	✓	✓	×	✓	van Asch et al., 2013
Groot ven	✓	✓	✓	×	Not specified	Hoek and Bohncke, 2001
Leysin	✓	✓	✓	×	✓	Schwander et al., 2000; Wick, 2000
Egelsee	In Part	✓	✓	✓	×	Wehrli et al., 2007; Larocque-Tobler et al., 2010
Lake Suchar Wielki	×	✓	✓	×	N/A	Filoc et al., 2018
Usselo	×	✓	✓	✓	×	van Geel et al., 1989

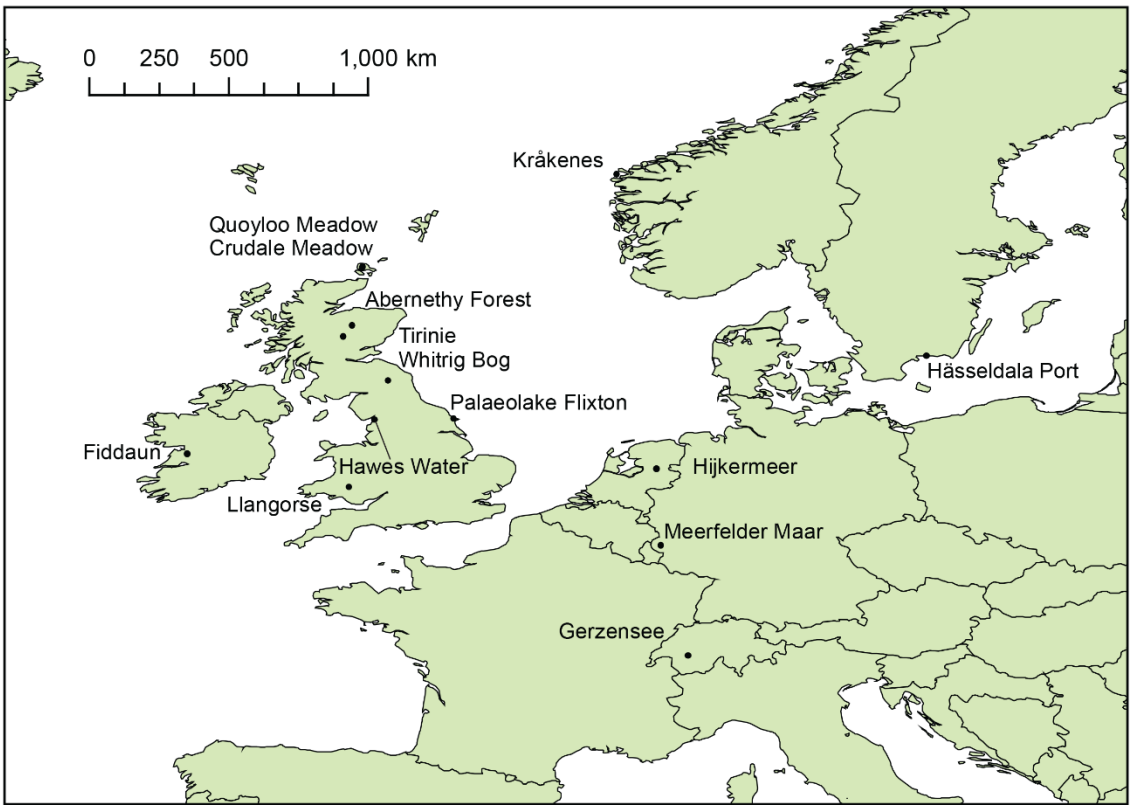

Figure 9.3 The series of sites across Britain and Europe used for comparison with sequences presented in this thesis. Sites presented in Chapters 5-8 are also shown.

from these sequences are performed contiguously or near contiguously, the isotopic trends highlight greater mean annual temperatures during the mid-Interstadial (Figure 9.5). Therefore, in Britain, the WI was characterised by differential mean annual and summer temperature development, a factor that has been debated for several decades (e.g. Atkinson et al., 1987; Coope and Lemdahl, 1995; Coope et al., 1998; Candy et al., 2016).

Loch Lomond/Nahanagan Stadial

Mean annual and summer temperature declines are observed during the LLS (Figures 9.4; 9.5). Predominantly summer temperature minima are observed early in the Stadial: 6.8°C Abernethy Forest. 7.5°C Whitrig Bog, 7.3°C Fiddaun (Brooks and Birks, 2000a; Brooks et al., 2012; van Asch et al., 2012a) (Figure 9.4). These summer temperature estimates map neatly onto reconstructed temperatures from PF, Tirinie and Quoyloo Meadow with colder summer temperatures at higher latitudes. The difference between Tirinie and Abernethy Forest, which are relatively proximal in the Scottish Highlands, can be attributed to altitude with the 1.5°C difference being explained by the ca 100 m altitudinal difference between the two sequences using a lapse rate of ca 0.7°C / 100 m, bringing the two into predictive range of the technique. However, it may be that under cool climatic conditions a steeper lapse rate is observed, which bring the two predictions

closer together (Holden and Rose, 2011). Unfortunately, the lack of carbonate through many of these sequences precludes an understanding of isotopic gradients, nonetheless, at Hawes Water a 2 ‰ shift (minima of -6.4 ‰) is observed whilst at Fiddaun minima of approximately -7.0 ‰ is observed (Figure 9.5).

Temperature variability during the Stadial is also reported. The Fiddaun record does not have sufficient stratigraphic resolution to reveal this variability, however, between the Scottish Highlands and northern England, summer temperature increases between 1.5-2.5°C (Bedford et al., 2004; Brooks et al., 2012; van Asch et al., 2012a) during the latter half of the Stadial (Figure 9.4). The isotopic record at Hawes Water reveals similar climatic variability with a 0.5 ‰ enrichment, producing expected mean annual temperature change of 1.7°C (Figure 9.5) (Marshall et al., 2002). Thus, across all sequences, including Tirinie, where colder summer temperatures are attributed to melting snow packs, and Quoyloo Meadow, Stadial climatic variability is recorded. Unfortunately, the lack of a chronology at these sequences prevents an understanding of regional synchroneity in mid-Stadial transitions, however on stratigraphic positions, they are likely to occur during the latter half of the Stadial.

Early Holocene

All sequences reveal an abrupt transition into the early Holocene shown by heightened summer temperatures and enriched stable isotopic values. However, the Holocene stratigraphy is often under studied. Nonetheless, Abernethy Forest and Crudale Meadow reveal greater summer temperatures and enriched isotopic values later in the Holocene.

9.5.2 Centennial-scale events in Britain

Looking at each of these records in more detail, abrupt, cold centennial-scale events can be observed. As the chronologies are not sufficient at many of the sites, an assessment of synchroneity cannot be made. Whilst an age model exists for Abernethy Forest, the age of the late WI event appears older than at the sequences presented here, which may be result from a lack of precision in the age model later during the WI (Brooks et al., 2012) and modelling on an old calibration curve which may produce greater differences between 12-13.9 Cal. ka BP (Reimer et al., 2013). Therefore, comparisons are largely made on stratigraphic position without a discussion on timing.

The early WI event across many of the sequences is characterised by reductions in mean annual and summer temperatures. At Fiddaun, where the oscillation is constrained by a radiocarbon date (13.9-14.3 Cal. ka BP) a 1.0°C summer temperature decline is observed, which is shown alongside a 1 ‰ depletion in $\delta^{18}O_{carb}$ (Figures 9.4; 9.5). At

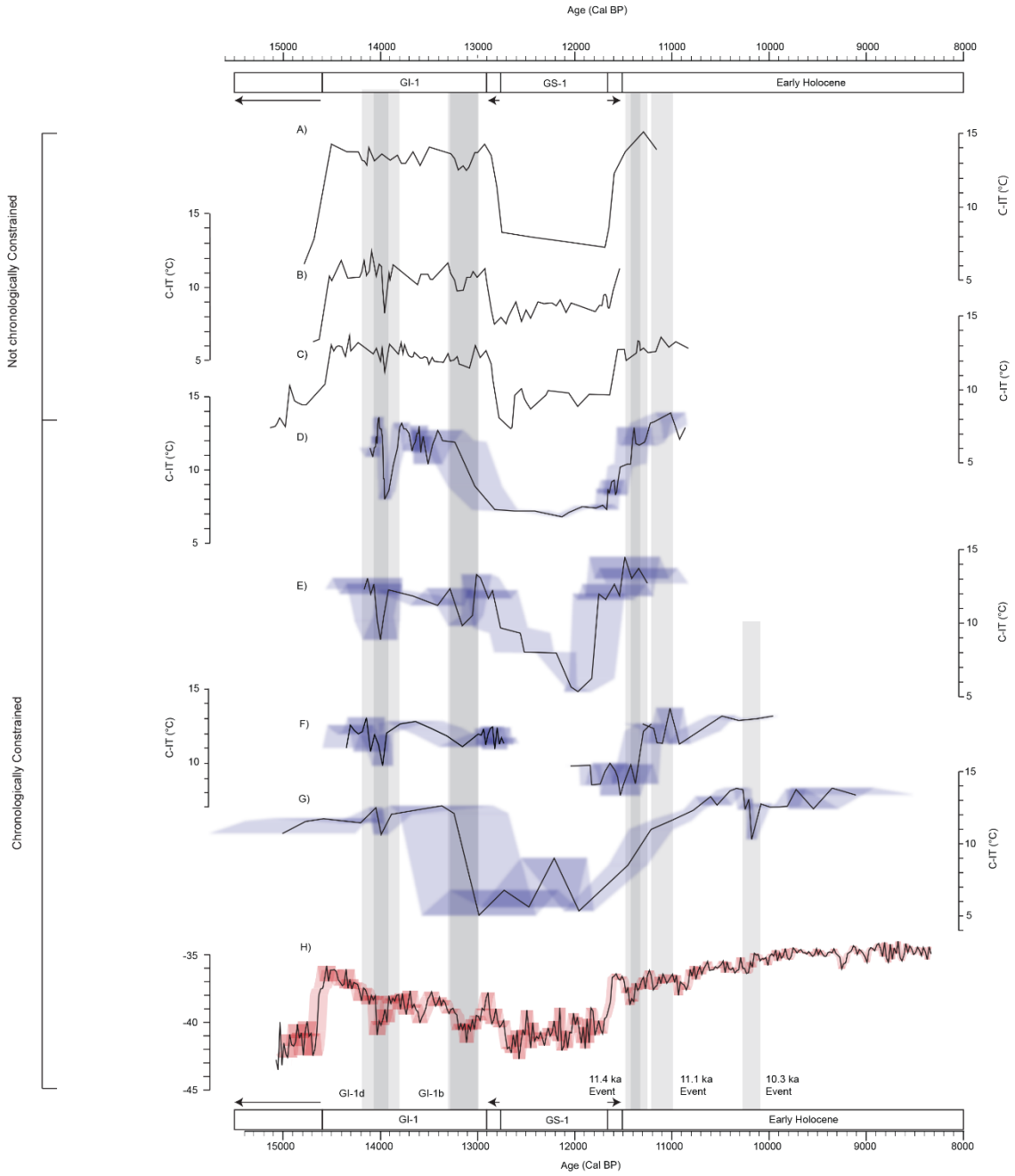

Figure 9.4 Comparisons of summer temperature reconstructions (C-ITs) from the British Isles and the NGRIP $\delta^{18}O$ record from Greenland. A) Fiddaun, Ireland (van Asch et al., 2012a); B) Whitrig Bog, south-east Scotland (Brooks and Birks, 2000a); C) Hawes Water, north-west England (Bedford et al., 2004); D) Abernethy Forest (Brooks et al., 2012); E to G) Sites presented within this thesis, Tirinie, Palaeolake Flixton and Quoyloo Meadow; and H) the NGRIP $\delta^{18}O$ stratigraphy (Rasmussen et al., 2014) converted to a calendar timescale. Where possible, blue shading over the proxy curves represents one-sigma chronological uncertainties. A-C have no chronologies associated with them and are 'wiggle-matched' to NGRIP, therefore they cannot be directly compared to the records presented within D-H as the timing, duration, and synchroneity of climatic oscillations is unknown. They are included for illustrative purposes only. Grey shading is shown to delineate climatic events in each record. Dark grey is given for the duration of the event in Greenland where identified.

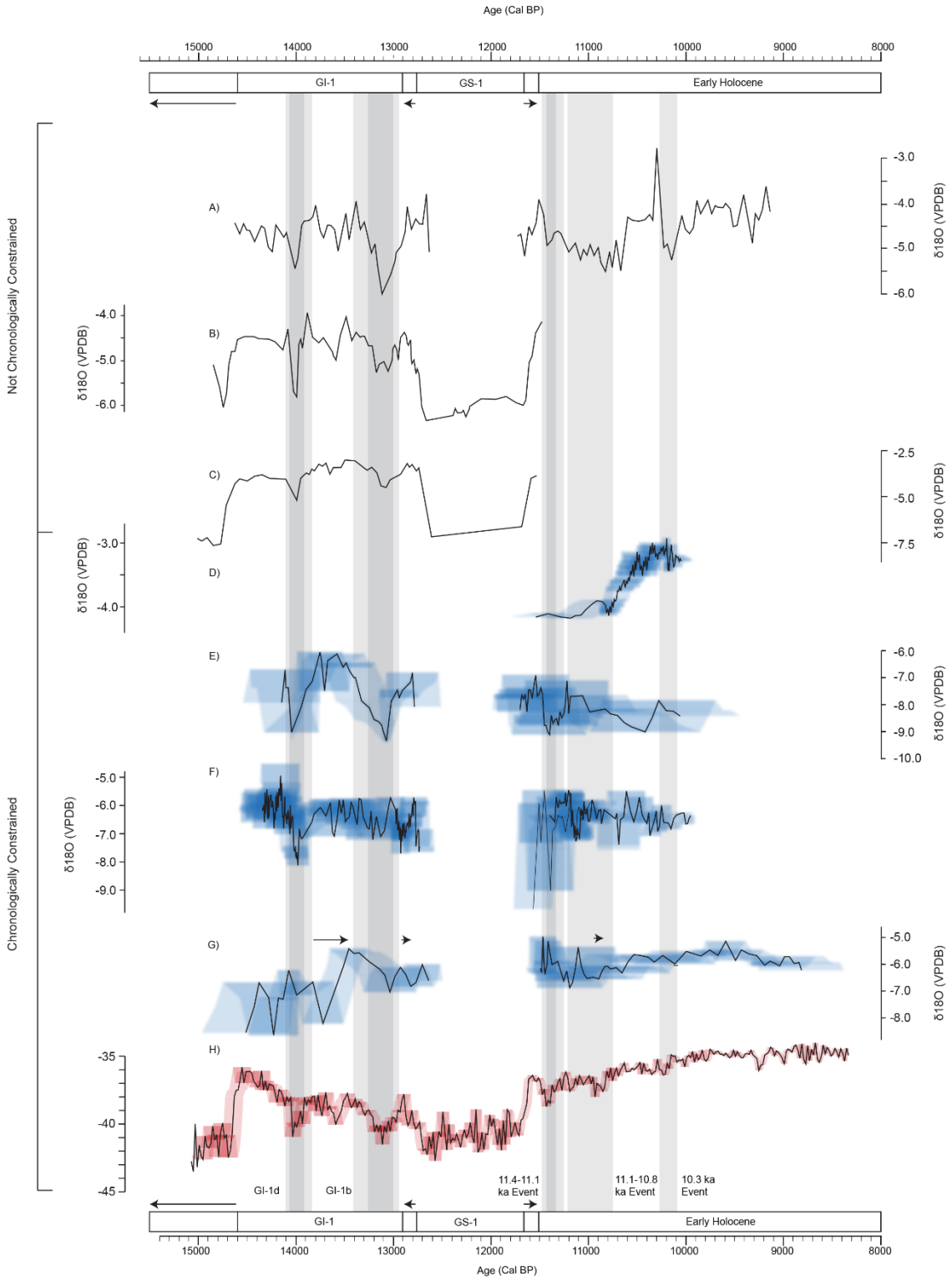

Figure 9.5 Comparisons of $\delta^{18}O_{carb}$ reconstructions from the British Isles and the NGRIP $\delta^{18}O$ record from Greenland. A) Crudale Meadow, Orkney (Whittington et al., 2015); B) Hawes Water, north-east England (Marshall et al., 2002); C) Fiddaun, Ireland (van Asch et al., 2012a); D-G) sites within this thesis, Quoyloo Meadow, Tirinie, Palaeolake Flixton, Llangorse; and H) the NGRIP $\delta^{18}O$ stratigraphy (Rasmussen et al., 2014) converted to a calendar timescale. Where possible, blue shading over the proxy curves represents one-sigma chronological uncertainties. A-C) contain no chronology and are 'wiggle-matched' to NGRIP and cannot be directly compared to sites D-H. They are included for illustrative purposes only. Grey shading is shown to delineate climatic events in each record. Dark grey is given for the duration of the event in Greenland where identified.

Abernethy Forest, the Penifiler Tephra constrains a summer temperature decline of 5.6°C (Matthews et al., 2011; Brooks et al., 2012). The deposition of the Penifiler allows for direct comparison with PF, Tirinie and Quoyloo Meadow where C-IT and $\delta^{18}O_{carb}$ reductions of 3.23°C, 3.8°C, 1.86°C and 3.18 ‰, 2.33 ‰ are observed respectively. Deteriorations at Whitrig Bog and Hawes Water are confined to depletions/temperature decreases of 4.9°C, 1.5°C and 1.5 ‰ (Brooks and Birks, 2000a; Marshall et al., 2002; Bedford et al., 2004; Figures 9.4: 9.5). Across Britain, mean annual and summer temperature variability characterises the early WI climatic event, with the greatest change at the higher latitude site of Abernethy Forest, and reduced magnitudes of change in Ireland and Quoyloo Meadow (Figure 9.6: Figure 9.7). Based on these trends, it is postulated that sites in proximity to the ocean experience a buffering effect from the warm waters of the North Atlantic whilst sites away from the ocean without this buffering experience a greater degree of climatic change

A late WI event is observed across many of the sequences. This event exhibits reduced magnitudes of climatic change in comparison to the early WI event (Figure 9.6: 9.7). The greatest magnitudes of this event are observed in the higher latitudes, with temperature decreases of 2.2°C at Whitrig Bog which is comparable but lower than the 2.5°C summer temperature shift at Tirinie between 13.45-13.02 Cal. ka BP. The lowest magnitudes are observed at Fiddaun and Hawes Water (Figure 9.6).

An exception to this are the $\delta^{18}O_{carb}$ analyses from Crudale Meadow (Whittington et al., 2015) and Fiddaun (van Asch et a., 2012a). Here the late Interstadial event appears more depleted than the former (Figure 9.5). However, At Fiddaun, the authors attribute a reduced response in isotopic values for the early Interstadial oscillation as a result of compression of the sequence and poor stratigraphic resolution between 14.2-13.9 Cal. ka BP (van Asch et al., 2012a). The same may be true of Crudale Meadow, as only one sample reveals the climatic deterioration, highlighting the need for finer temporal resolutions. As these two sequences differ from all British climatic LGIT sequences, local site characteristics may explain the pattern of climatic development. Alternatively, at Crudale Meadow, the greater expression of the late WI event may be a reliable expression of the climatic change.

During the early Holocene, event comparisons are made difficult as the stratigraphy and resolutions of many sequences are insufficient. Further, the chronologies of these sequences are poor due to the paucity of terrestrial macrofossils for AMS radiocarbon measurement and the 600-year long radiocarbon plateau covering the period between 11.45-11.05 Cal. ka BP (Björk et al., 1996; Lowe et al., 1999; Walker et al., 2009).

Nonetheless, at Abernethy Forest, a 1°C summer temperature decline at ca 11.4 Cal. ka BP, is noted. However, at Tirinie, no summer temperature variability exists. Whilst the oscillation may be widespread and just not expressed at Tirinie, the low amplitude of summer temperature change at Abernethy Forest indicates that summer temperature variability was muted compared to the isotopic oscillations observed at Crudale Meadow, Hawes Water and the sequences within this thesis (Figure 9.5). At Hawes Water and Crudale Meadow, depletions of ca 1.0 ‰ are noted for an early Holocene climatic oscillation presumed to reflect the same 11.4-11.1 Cal. ka BP event. A greater depletion for a later early Holocene event at Crudale Meadow (Whittington et al., 2015) is observed possibly related to the 10.2 ka event at Quoyloo Meadow, although this is presently unknown (Whittington et al., 2015). Nonetheless, the magnitudes of summer and mean annual change are comparable to the events that are observed throughout the sites presented within this thesis, with the Holocene being more muted that the WI.

9.6 Comparisons of the British stratigraphy to palaeoclimatic records from northern Europe

The GICC05 NGRIP $\delta^{18}O$ ice-core chronology is the current stratotype for northern Europe covering the LGIT (Lowe et al., 2008; Rasmussen et al., 2014; Chapter 2). The transition from Stadial-Interstadial, termed Greenland Stadial 2-Greenland Interstadial 1 (GS-2 to GI-1), is shown by an enrichment in $\delta^{18}O$ values by 6 ‰ at 14.65 Cal. ka BP (Rasmussen et al., 2014). Whilst none of the climatic datasets presented within this thesis record this transition, the timing of the onset of GI-1 is comparable within errors of the climatic data presented. The suggestion of warmth at Quoyloo Meadow prior to 14.65 Cal. ka BP highlights the inadequacies of the age model, with wide chronological uncertainty placed between 15.01-14.6 Cal. ka BP. The remaining sequences show broad comparability between the onset of the WI in Britain and the onset of GI-1.

Throughout GI-1, which approximately correlates to the Bølling-Allerød biostratigraphic phases in Norway (Mangerud et al., 1974), the record has been subdivided based on periods of climatic variability, forming the North Atlantic event stratigraphy (Lowe et al., 2008; Chapter 2). Three phases of more enriched isotopic values, signalling climatic warmth, are identified, termed Greenland Interstadial events 1e, 1c, 1a (GI-1e; GI-1c; GI-1a). Peak isotopic values are revealed by GI-1e, within the Bølling phase, which correlates to peak summer temperature values recorded across many British sequences, however, this is in contrast to the peak annual temperatures recorded during the mid-WI across Britain. This suggests differential climatic development between the polar latitudes and Britain (e.g. Coope et al., 1998; Brooks and Birks, 2000a; Brooks et al., 2012).

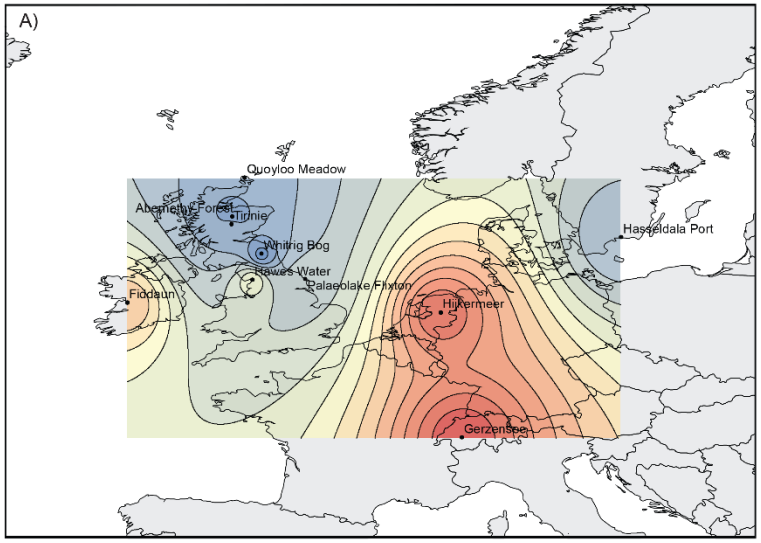
A)
Quoyloo Meadow
Abernethy Forest
Tirinie
Whitrig Bog
Hawes Water
Palaeolake Flixton
Fiddaun
Hijkermeer
Hasseldala Port
Gerzensee
GI-1d C-IT (°C)
(Absolute)
7.5 - 8.0
8.0 - 8.5
8.5 - 9.0
9.0 - 9.5
9.5 - 10.0
10.0 - 10.5
10.5 - 11.0
11.0 - 11.5
11.5 - 12.0
12.0 - 12.5
12.5 - 13.0
13.0 - 13.5
13.5 - 14.0
14.0 - 14.5
14.5 - 15.0

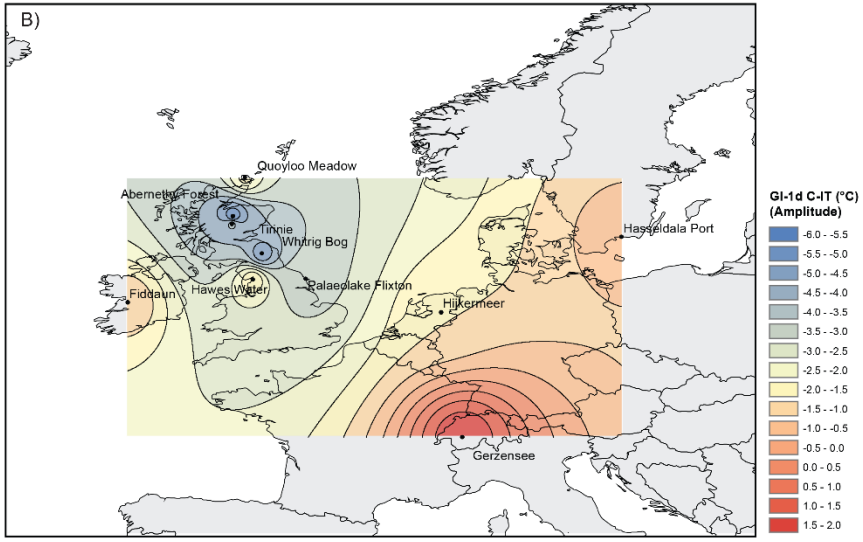
B)
Quoyloo Meadow
Abernethy Forest
Tirinie
Whitrig Bog
Hawes Water
Palaeolake Flixton
Fiddaun
Hijkermeer
Hasseldala Port
Gerzensee
GI-1d C-IT (°C)
(Amplitude)
-6.0 - -5.5
-5.5 - -5.0
-5.0 - -4.5
-4.5 - -4.0
-4.0 - -3.5
-3.5 - -3.0
-3.0 - -2.5
-2.5 - -2.0
-2.0 - -1.5
-1.5 - -1.0
-1.0 - -0.5
-0.5 - 0.0
0.0 - 0.5
0.5 - 1.0
1.0 - 1.5
1.5 - 2.0

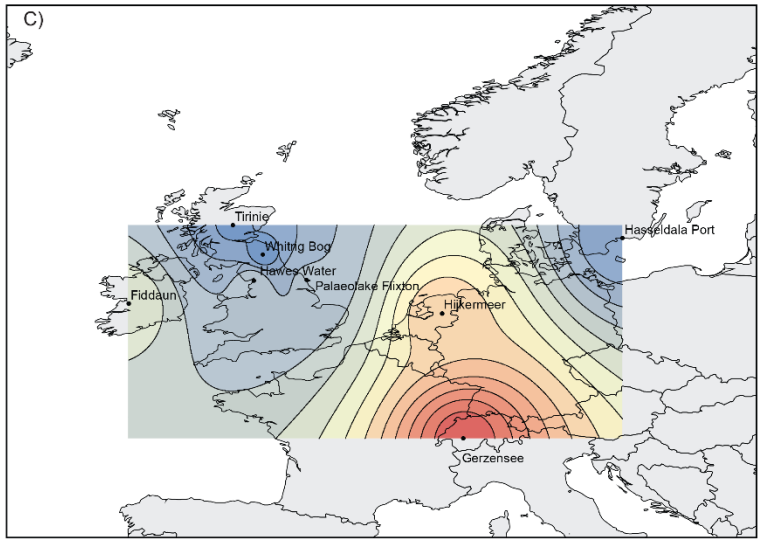
C)
Tirinie
Whitrig Bog
Hawes Water
Palaeolake Flixton
Fiddaun
Hijkermeer
Hasseldala Port
Gerzensee
GI-1b C-IT (°C)
(Absolute)
9.5 - 10.0
10.0 - 10.5
10.5 - 11.0
11.0 - 11.5
11.5 - 12.0
12.0 - 12.5
12.5 - 13.0
13.0 - 13.5
13.5 - 14.0
14.0 - 14.5
14.5 - 15.0
15.0 - 15.5
15.5 - 16.0
16.0 - 16.5

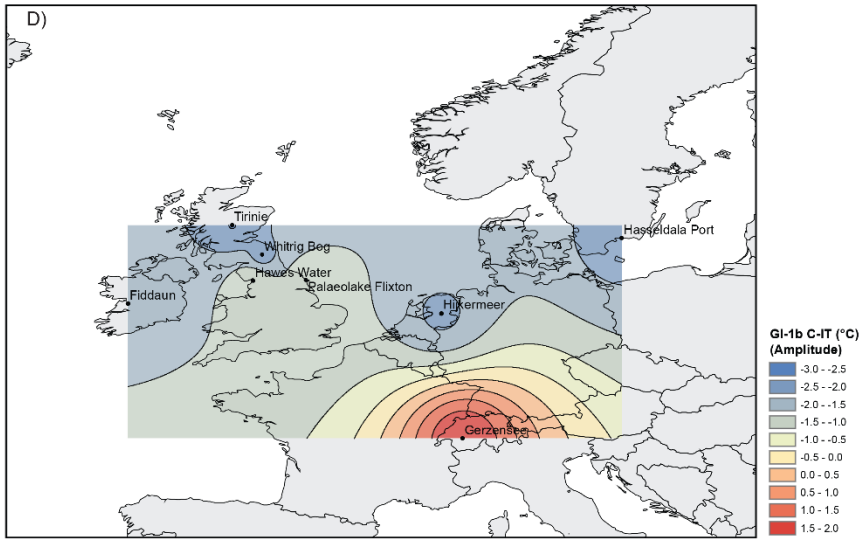
D)
Tirinie
Whitrig Bog
Hawes Water
Palaeolake Flixton
Fiddaun
Hijkermeer
Hasseldala Port
Gerzensee
GI-1b C-IT (°C)
(Amplitude)
-3.0 - -2.5
-2.5 - -2.0
-2.0 - -1.5
-1.5 - -1.0
-1.0 - -0.5
-0.5 - 0.0
0.0 - 0.5
0.5 - 1.0
1.0 - 1.5
1.5 - 2.0

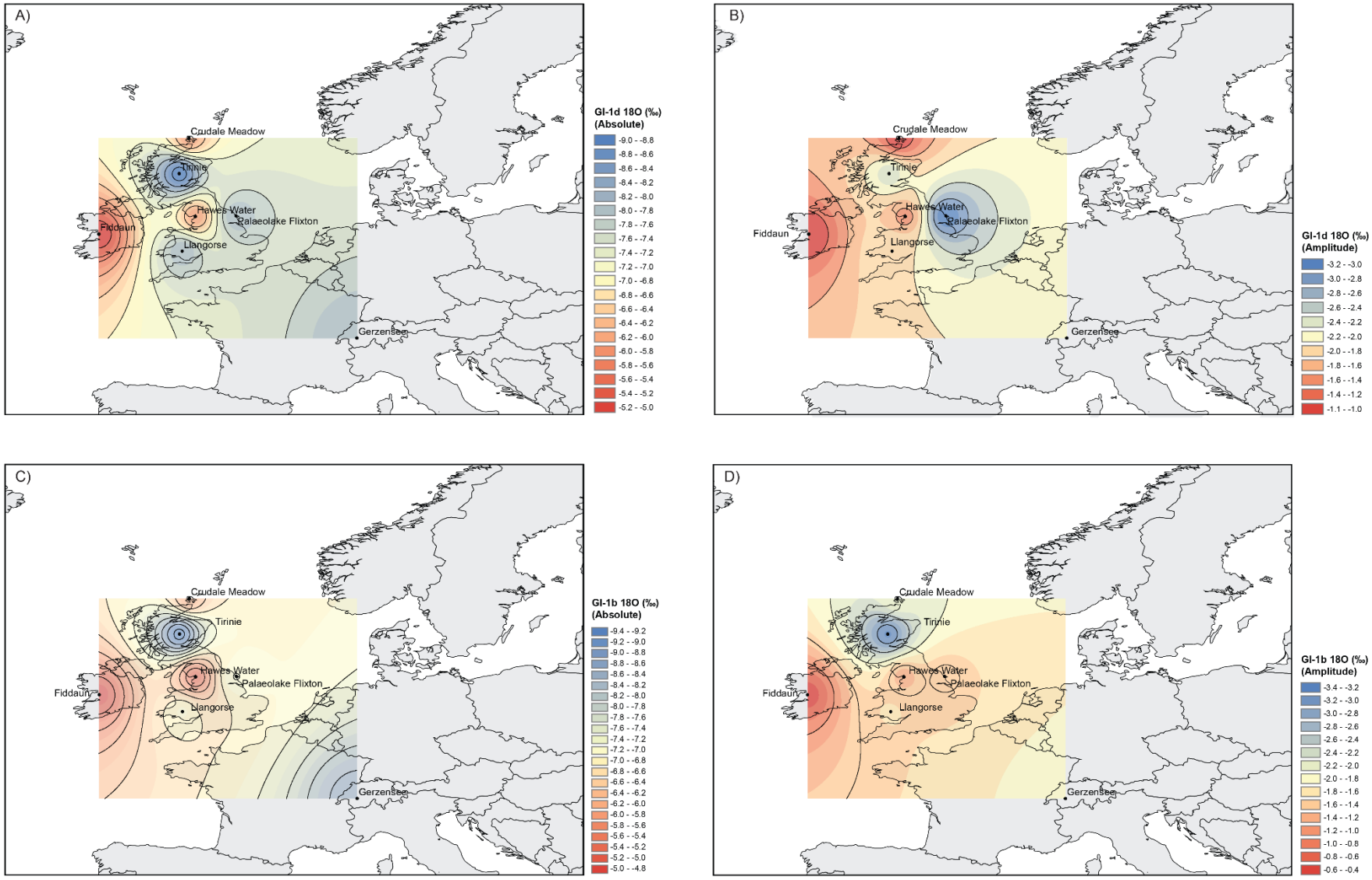
A)
Crudale Meadow
Tirinie
Hawes Water
Palaeolake Flixton
Fiddaun
Llangorse
Gerzensee
GI-1d 18O (‰)
(Absolute)
-9.0 - -8.8
-8.8 - -8.6
-8.6 - -8.4
-8.4 - -8.2
-8.2 - -8.0
-8.0 - -7.8
-7.8 - -7.6
-7.6 - -7.4
-7.4 - -7.2
-7.2 - -7.0
-7.0 - -6.8
-6.8 - -6.6
-6.6 - -6.4
-6.4 - -6.2
-6.2 - -6.0
-6.0 - -5.8
-5.8 - -5.6
-5.6 - -5.4
-5.4 - -5.2
-5.2 - -5.0
B)
Crudale Meadow
Tirinie
Hawes Water
Palaeolake Flixton
Fiddaun
Llangorse
Gerzensee
GI-1d 18O (‰)
(Amplitude)
-3.2 - -3.0
-3.0 - -2.8
-2.8 - -2.6
-2.6 - -2.4
-2.4 - -2.2
-2.2 - -2.0
-2.0 - -1.8
-1.8 - -1.6
-1.6 - -1.4
-1.4 - -1.2
-1.1 - -1.0
C)
Crudale Meadow
Tirinie
Hawes Water
Palaeolake Flixton
Fiddaun
Llangorse
Gerzensee
GI-1b 18O (‰)
(Absolute)
-9.4 - -9.2
-9.2 - -9.0
-9.0 - -8.8
-8.8 - -8.6
-8.6 - -8.4
-8.4 - -8.2
-8.2 - -8.0
-8.0 - -7.8
-7.8 - -7.6
-7.6 - -7.4
-7.4 - -7.2
-7.2 - -7.0
-7.0 - -6.8
-6.8 - -6.6
-6.6 - -6.4
-6.4 - -6.2
-6.2 - -6.0
-6.0 - -5.8
-5.8 - -5.6
-5.6 - -5.4
-5.4 - -5.2
-5.2 - -5.0
-5.0 - -4.8
D)
Crudale Meadow
Tirinie
Hawes Water
Palaeolake Flixton
Fiddaun
Llangorse
Gerzensee
GI-1b 18O (‰)
(Amplitude)
-3.4 - -3.2
-3.2 - -3.0
-3.0 - -2.8
-2.8 - -2.6
-2.6 - -2.4
-2.4 - -2.2
-2.2 - -2.0
-2.0 - -1.8
-1.8 - -1.6
-1.6 - -1.4
-1.4 - -1.2
-1.2 - -1.0
-1.0 - -0.8
-0.8 - -0.6
-0.6 - -0.4

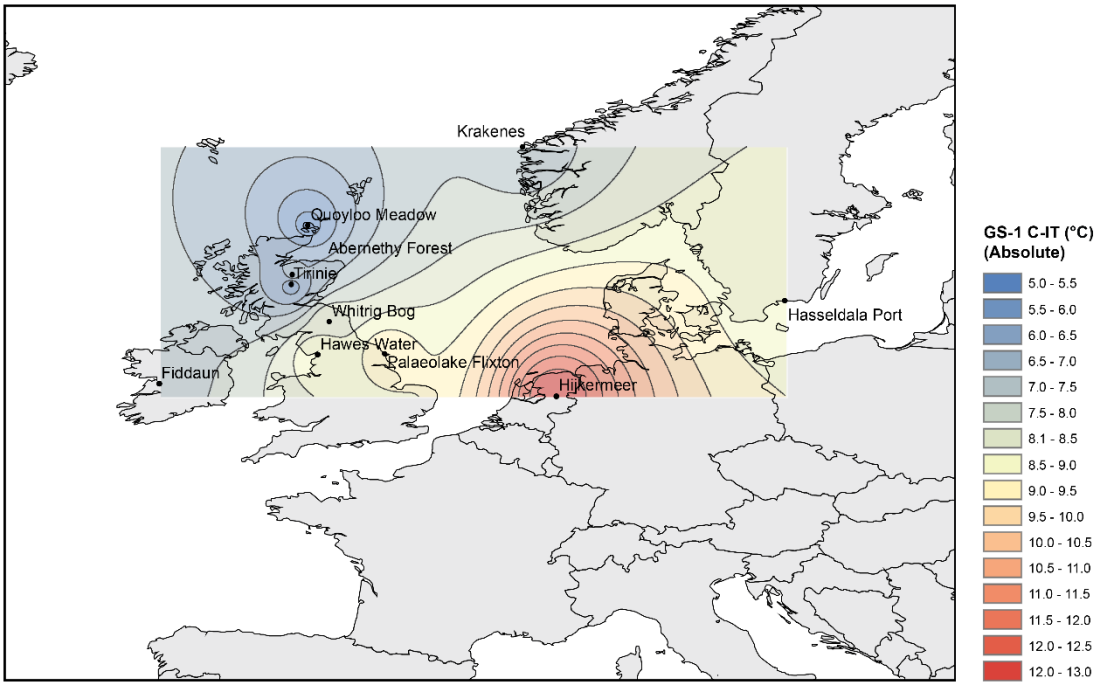

Figure 9.8 Inverse Distance weighted model of C-IT in close association with the Vedde Ash (12,023±43 Cal. ka BP; Bronk Ramsey et al., 2015). Where the Vedde Ash is not present (Fiddaun, Hawes Water, Hijkermeer, Hässeldala) temperatures have been taken at a mid-point in the stratigraphy. Sites used to construct the model are displayed in the figure and referred to in text. Whilst this is not ideal as sedimentation rates likely changed during the Stadial, without a chronology this task is difficult. A clear difference is observed from the figure in that the coldest absolute temperatures are observed in higher latitude regions whilst Hijkermeer in Europe was much warmer during GS-1. This may highlight the approximate location of the polar front during mid-GS-1.

Figure 9.6 (Page 328) Inverse Distance weighted models of absolute values and amplitudes of summer temperature change in Britain and Europe for the GI-1d and GI-1b climatic oscillations. To calculate amplitudes of change, minimum values from each climatic event have been subtracted from peak values immediately preceding the climatic event within GI-1e. A) Absolute C-IT minima within GI-1d; B) Amplitudes of C-IT change within GI-1d; C) Absolute C-IT minima within GI-b and; D) Amplitudes of C-T change within GI-1d. Sites used to construct the model are displayed in the figure and referred to in text.

Figure 9.7 (Page 329) Inverse Distance weighted models of absolute depletion and magnitudes of depletion in $\delta^{18}O$ across Europe for GI-1d and GI-1b. To calculate amplitudes of change, minimum values from each climatic event have been subtracted from peak values immediately preceding the climatic event. A) Absolute minima of $\delta^{18}O$ for GI-1d; B) Amplitudes of $\delta^{18}O$ depletion within GI-1d; C) Absolute minima of $\delta^{18}O$ for GI-b and; D) Amplitudes of $\delta^{18}O$ depletion within GI-1d. Sites used to construct the model are displayed in the figure and referred to in text.

In continental Europe, peak summer warmth during the Interstadial is identified within GI-1c (Allerød) at ca 13.4 Cal. ka BP from Hässeldala Port and Hijkermeer with temperatures of 13°C and 18°C respectively (Heiri et al., 2007; Wohlfarth et al., 2017). In contrast, peak summer warmth, 16°C, is suggested later in the Allerød (GI-1c/b) ca 13.2 Cal. ka BP at Gerzensee, and at ca 13.0 Cal. ka BP from Kråkenes (GI-1a) albeit with cooler temperatures (Brooks and Birks, 2000b; Lotter et al., 2012). These differences may in part be due to site factors, including the lack of GI-1e sediments at Kråkenes due to the presence of ice loading within the Kråkenes basin during GI-1e (Birks et al., 2000) and the lack of GI-1a climatic reconstructions from Gerzensee (Lotter et al., 2012). Nonetheless, regional differences in peak warmth may be a result of true differences in climatic development across Europe with variations due, in part, to latitudinal, longitudinal and altitudinal variability between the sequences (e.g. Lang et al., 2010).

Superimposed on the general climatic pattern are two abrupt climatic events, termed GI-1d and GI-1b. The former, GI-1d correlated with the Older Dryas or Aegelsee Oscillation (Lotter et al., 1992), is characterised by a -2.9 ‰ depletion in $\delta^{18}O$ between 14.02-13.9 Cal. ka BP (Lowe et al., 2008; Rasmussen et al., 2014). The early WI event in Britain can therefore be correlated with GI-1d in Greenland. The second high-magnitude event, termed GI-1b, correlated with the Gerzensee Oscillation or the Inter-Allerød Cold Period (Lotter et al., 1992; Hughen et al., 1996), exhibits depletion of -2.55 ‰ between 13.26-13.04 Cal. ka BP (Lowe et al., 2008). This event is less abrupt and continues for a longer duration. This GI-1b event is comparable to the abrupt late WI event in Britain, which demonstrates the same structural characteristics and exhibits the same chronological range. This is not true at Abernethy Forest where the event appears too old. The lower magnitude GI-1cii event, 13.61-13.55 Cal. ka BP is likely to represent the short event covering the same period from Crudale Meadow, Whitrig Bog and Hawes Water. It has not been classified in this thesis as it does not meet the criteria outlined in Chapter 4.

These abrupt climatic deteriorations are present across Europe, however they are not defined at Kråkenes due to the lack of climatic data prior to 13.5 Cal. ka BP, reduced resolutions of the proxy series surrounding the GI-1b oscillation and insensitivities in western Norway to changing climatic structure (Brooks and Birks, 2000b). The event coeval with GI-1d, exhibits a 1.5°C and 0.5-1°C temperature reversion at Hijkermeer and Hässeldala Port respectively (Figure 9.6). Whilst at Gerzensee, a 2 ‰ shift in $\delta^{18}O_{carb}$ is noted (Figure 9.7). In contrast, the oscillation congruent to GI-1b exhibits greater summer temperature declines in Europe than the former deterioration (Figure 9.6). This is in contrast to Britain where the GI-1d oscillation is the most pronounced. Coupled, with the

observation of multiple events during GI-1, compound specific deuterium biomarker data from Hässeldala Port and Meerfelder Maar reveal two phases of aridity between 14.1-13.9 and 13.2-12.9 Cal. ka BP (Rach et al., 2014; Muschitiello et al., 2015). The latter of these phases at Hässeldala Port exhibits broad correspondence with the latter phase of aridity at Tirinie, suggesting that the GI-1b oscillation is more arid than the former event (Wohlfarth et al., 2017). The abrupt climatic events during the Interstadial can therefore be traced across northern Europe, however, in an apparent difference to structure of the events presented from Britain, the magnitudes of change are greater for the GI-1b event than the GI-1d event in continental Europe.

Following the Interstadial, Greenland Stadial 1, which broadly corresponds to the Loch Lomond and Younger Dryas Stadials between 12.84-11.65 Cal. ka BP, is characterised by a rapid,1-3-year shift in δ*D*, related to a change in the source of precipitation following atmospheric reorganisation (Steffensen et al., 2008) and a longer duration -3.73 ‰ shift in $\delta^{18}O$ approximating 200 years (Steffensen et al., 2008). All records show a transition from warm to cool conditions with the coldest summer temperatures inferred from Kråkenes, ca 4.5°C (Brooks and Birks, 2000b); 8°C at Hässeldala Port (Muschitiello et al., 2015) and 13°C from Hijkermeer (Heiri et al., 2007). Mean coldest temperatures vary with latitude and longitude but compare favourably to reconstructed coldest temperatures from Britain (Figure 9.8). Differences in temperature appear to result from a genuine climatic gradient across Europe, with central European climate regimes more continental than the British Isles (Figure 9.8).

Throughout GS-1, cooling is suggested at Meerfelder Maar (MFM) with depletion and convergence of lipid biomarker δ*D* values suggesting aridification ca 170 years after the onset of GS-1 in Greenland (Rach et al., 2014). This is also revealed at Hässeldala Port which provides evidence of a lagged response in hydroclimatic shifts (Rach et al., 2014; Muschitiello et al., 2015). Within the Stadial however, at 12.2-12.0 Cal. ka BP a reduction in varve thickness at MFM (Brauer et al., 2008) is correlated with variability in the Ti record from Kråkenes (Bakke et al., 2009). Reduced varve thickness suggests that the latter half of GS-1 was stable, whilst greater Ti strength suggests greater instability from the proximal glacier margin at Kråkenes (Bakke et al., 2009). These sedimentological and glaciological shifts are suggested to result from climatic variability and changing positions of the frontal systems (Lane et al., 2013). These changes are positively correlated with summer or mean annual temperature variability in Britain, with ties to the deposition of the Vedde Ash at 12.02 Cal. ka BP. This suggests that Britain does equally record the northward migration of the polar front during the mid-Stadial.

Amelioration in the early Holocene is shown by an abrupt 3 ‰ and 4.45 ‰ enrichment of δ*D* and $\delta^{18}O$ at 11.65 Cal. ka BP (Walker et al., 2009) in NGRIP signalling a further atmospheric reorganisation and a change in the precipitation source regions (Masson-Delmotte et al., 2005). Again however, superimposed on this rising Holocene trend are a series of abrupt climatic events that appear muted. These are termed the 11.4 ka event, between 11.47-11.35 Cal. ka BP, and the 11.1 ka event (Fiłoc et al., 2018; Blockley et al., 2018). Interestingly this 11.1 ka BP event has not been defined in Greenland but appears elsewhere in Europe. Crucially, it is apparent that these early Holocene events exhibit reduced magnitudes compared to the GI-1d climatic oscillation in Greenland but may be more comparable to the GI-1b event.

Deciphering modes of climatic variability during the early Holocene is difficult, as many of the sequences are truncated after GS-1. Nonetheless the records presented from the British Isles, demonstrate a lack of summer temperature change, compared to oscillations in mean annual temperature and phases of aridity. However, at Hijkermeer, summer temperature declines of 1-1.5°C are noted (Heiri et al., 2007). Further, a 0.5 ‰ $\delta^{18}O$ depletion in Greenland, related to the 11.4 Cal. ka BP event, has been suggested to correlate to the pre-Boreal oscillation (Björk et al., 1997) originally defined using palaeobotanical measures. Thus, although limited in extent it appears that summer temperature oscillations are felt in Europe during the early Holocene (e.g. Heiri et al., 2007; Brooks et al., 2012). The convergence of δ*D* at MFM and Hässeldala, coupled with a depleted isotopic signal, signifies a change in climatic conditions and rising aridity between 11.4-11.2 Cal. ka BP (Rach et al., 2014). This then matches with phases of aridity defined at Quoyloo Meadow and Tirinie between 11.4-11.1 Cal. ka BP suggesting that, like the Interstadial, continent-wide connections can be observed with the state of the climate system across multiple parameters.

9.7 Mechanisms of climatic change

Through the observation of both millennial and centennial-scale climatic events during the LGIT, a discussion centred around the mechanisms of climatic change is required. Whilst the climatic events reveal broad synchroneity across Europe, the centennial-scale deteriorations, GI-1d, GI-1b and 11.4 ka exhibit different magnitudes dependent on site latitude and longitude. Here potential mechanisms behind these variable magnitudes will be examined.

Millennial climatic mechanisms

Many of the longer-term millennial-scale climatic shifts, including the transition into GI-1, GS-1 and the Holocene have often been argued to relate to freshwater flux into the North

Atlantic and the role this has on weakening (strengthening) AMOC controlled heat transport to the northern latitudes (e.g. Broecker et al., 1989; Clark et al., 2001; Standford et al., 2011; Denton et al., 2010; Chapter 2). The onset of the Interstadial, 14.65 Cal. ka BP, is recorded across the North Atlantic region (Fleitman et al., 2009; Denton et al., 2010). Whilst a northern or southern hemisphere source is debated (Stanford et al., 2011; Deschamps et al., 2012; Golledge et al., 2014), either through a southern hemisphere meltwater pulse, meltwater pulse 1a (Deschamps et al., 2012) or the release of freshwater, preconditioning the Nordic seas (Stanford et al., 2011), North Atlantic Deep Water (NADW) formation and resumption of AMOC generates heat transfer to the northern latitudes at both at the onset and during the Interstadial, bringing favourable conditions to Europe.

In contrast, GS-1 is considered to reflect a catastrophic input of freshwater into the North Atlantic from either glacial lake Agassiz (Broecker et al., 1985) or the Laurentide ice-sheet (Broecker et al., 1989), the northern Arctic (Tarasov and Peltier, 2005) or the Fennoscadian ice-sheet (Muschitiello et al., 2015). This flux of freshwater was substantive to reduce (NADW), weaken AMOC, and cause the expansion of sea-ice in the Nordic seas (Cabedo-Sanz et al., 2013). The result of this freshwater perturbation caused the southward deflection of the polar front, following sea-ice build-up, bringing severely cold and dry climates across Europe. This climate shift is observed across all sequences presented within this thesis. Whilst the source of meltwater is disputed, the modelling of freshwater fluxes, with associated feedbacks including radiative cooling through heightened atmospheric dust loads, confirms that meltwater can explain the GS-1 climatic phenomenon (Condron and Windsor, 2012; Renssen et al., 2015).

Much like the onset of the Interstadial, the onset of the present Interglacial, is largely explained by a further strengthening of AMOC and a rapid northward migration of the polar front and concurrent decline in sea-ice cover (Lowe and Walker, 2014). As observed within Greenland, this shift was rapid owing to the 1-3-year increase in δD values (Steffensen et al., 2008) at the transition between GS-1 and the Holocene with major reorganisation of atmospheric circulation bringing higher temperatures and greater effective moisture to Europe. This rapid shift is not only identified in the Greenland records but also manifest as a rapid increase in temperature and precipitation proxies across Europe.

Centennial climatic mechanisms

During GI-1, the differences in timing of peak warmth between Greenland, Britain and continental Europe, points to different phases of climatic development between maritime

and continental regions. However, as ocean-atmosphere connections are shown to be strong in modulating the dominant climatic signals across Europe, the abrupt cold GI-1d and GI-1b events, may have an oceanic source. These abrupt centennial events have in the past been suggested to relate to freshwater flux in the North Atlantic, causing a temporary weakening or slowdown of AMOC (Clark et al., 2001; Thornally et al., 2010; Chapter 2) typically from the rerouting of meltwater from the Laurentide ice-sheet. This results in the cessation of northward heat and moisture transport, an increase in sea-ice, and the southward migration of westerly storm tracks, similar to GS-1 (e.g. Lane et al., 2013). In all sequences coincident with GI-1d, a freshwater flux and rapid weakening of AMOC is suggested by rapid depletion in isotopic values and chironomid inferred-temperatures, supporting an almost instantaneous response in sensitive proxies. The difference in magnitude of events in Europe compared to Britain, demonstrate the continentality, latitudinal and altitudinal position of different sequences are key in the expression of these events (Figures 9.6; 9.7). Sites close to the source of the oceanic perturbation, Fiddaun and Quoyloo Meaodow, exhibit lower magnitudes of change perhaps due to the dominantly maritime climate buffering against cool conditions as these sites are close to the ocean where warmer waters may buffer against the effects of climatic change. However, at mid-latitudes and high-altitudes the effects are felt more strongly. Whilst it might be expected that the event would be strongly felt at sites proximal to the ocean, it is not, and further many of the ocean proximal sites reside at lower latitudes where the expression of this climatic event would be less felt, Fiddaun and Llangorse for example. Thus, the GI-1d climatic oscillation is likely to be meltwater forced. This may differ for the GI-1b event however.

In Britain, the GI-1b event exhibits a reduced magnitude of climatic variability compared to the GI-1d event, Whereas, in continental Europe the opposite is observed (Figure 9.6 9.7). If both GI-1d and GI-1b are meltwater driven, and the latter event exhibits greater climatic change than the former, this should be observed in both Britain and continental Europe. However, this is not the case, and an alternative explanation must be sought. Equally, the structure of the GI-1b event is markedly different than the GI-1d event where rapid depletion to the inferred coldest point is not observed. This may be expected at the point of meltwater flux. Coinciding with the lead into GI-1b is a period of reduced solar activity, centred between 13.45-13.2 Cal. ka BP, as observed by greater ^{10}Be concentrations in Greenland (Adolphi et al., 2014). Reduced solar activity, may enable a mechanism whereby a period of atmospheric blocking, not too dis-similar to mechanisms of negative phase NAO, cause greater temperature and precipitation change over Europe than Britain (e.g. Bond et al., 2001). Recent simulations of the Maunder Minimum using a transient simulation model revealed that annual and winter temperature change

is more strongly felt in continental Europe than it is in Britain (Shindell et al., 2001). Further, the recent suggestion that atmospheric blocking was a possibility during the latter phases of the last glaciation, owing to the presence of the Laurentide ice-sheet (Rivière et al., 2010; Adolphi et al., 2014), reveals that NAO-like variability could be possible during GI-1. Further evidence is found from greater aridity at Tirinie and Hässeldala Port (Muschitiello et al., 2015). Presently a negative NAO causes greater aridity over Europe through the different trajectory of the westerly jet, with less frequent storm events and reduced precipitation over Britain and Europe (Hurrell and Deser, 2010). In a period where atmospheric circulation is different to today, solar variability may exacerbate these conditions. Therefore, the aridity observed at ca 13.2 Cal. ka BP, may be a product of an NAO-like oscillation, linked to solar variability. However, as meltwater re-routing has been identified for the GI-1b oscillation (Clark et al., 2001) it may be that meltwater forcing is overprinted onto reduced solar output. Where rapid depletion in oxygen isotopes is observed in Greenland, this may be the manifestation of changes in oceanicity through meltwater flux. Thus, both solar variability and meltwater flux may be invoked to explain the differences in magnitudes and structure of the two climatic oscillations in Europe during the Interstadial.

Climatic variability within GS-1, shown through warm climates in close association with the Vedde Ash in Britain, greater Ti counts at Kråkenes and reduced varve thickness at MFM suggests a mid-Stadial climatic amelioration, the strengthening of AMOC and the northwards migration of polar frontal systems, following the retreat of sea-ice (Bakke et al., 2009). This occurs principally at MFM and as the polar front migrates, slight warming is observed over Britain, then in the northern high latitudes. Differences in timing between south-north Europe highlight the time-transgressive nature of the northward migration of the polar front (Lane et al., 2013). Nonetheless, the close approximation of climatic proxies from Britain and sedimentological proxies from across Europe, demonstrate Stadial climatic variability on a large geographic scale.

Like the Interstadial, climatic events within the early Holocene have been shown to relate to different forcing mechanisms, principally solar variability (Bond et al. 2001; Hu et al., 2003) or the influx of meltwater from the northern hemisphere ice-sheets at 11.4, 11.1, 10.3, 9.3, 8.2 ka BP (Björk et al., 1997; Fisher et al., 2002). It appears that for each of the events identified in Greenland or elsewhere, a period of meltwater flux is followed by a phase of reduced solar activity (van der Plicht et al., 2004; Magny et al 2007). As per other abrupt events within the North Atlantic, greater freshwater flux weakens AMOC and retards heat and moisture transport to northern Europe, approximately coinciding with identified climatic deteriorations. Further, reduced solar irradiance, perhaps

generating NAO-like variability, may exacerbate aridity over continental Europe and Britain, and generate greater summer temperature change in continental Europe. As PF and Hijkermeer are more continental than the northern latitudes of Britain, summer temperature changes may be more expressed under reduced solar forcing (Shindell et al., 2001). Therefore, owing to phases of meltwater flux and solar variability, Europe experiences EH centennial-scale climatic oscillations, that demonstrate differences in climatic development across wide spatial scales at 11.4, 11.1-10.8 and 10.3 Cal. ka BP. Equally as the magnitudes are reduced compared to Interstadial oscillations reduced freshwater fluxes are probable, which is compounded by the minor changes to solar irradiance.

9.8 Chapter summary

The palaeoclimatic records within this thesis represent some of the most detailed records revealing abrupt climatic events during the Last Glacial-Interglacial Transition (LGIT). Principally, the sequences provide evidence of both mean annual and summer temperature change throughout the LGIT across both millennial- and centennial-scale climatic transitions. This greatly improves our understanding of latitudinal/longitudinal climatic gradients across Britain. The reconstruction of compound specific δ*D* measurements from lacustrine and terrestrial biomarkers (e.g. Rach et al., 2014) has provided, for the first time in Britain, a highly resolved hydroclimatic record throughout the LGIT. Crucially, this chapter highlights episodes of centennial-scale climatic variability across Britain, revealing that within age error, these climatic episodes are synchronous. However, it is clear that the magnitudes of these climatic events are diachronous across Britain, with proximity to the ocean, and latitudinal, and altitudinal differences key to the expression of the climatic signal. As a result, the greatest magnitudes of change are observed from Tirinie whilst the lowest magnitudes are observed at Quoyloo Meadow.

Through the comparison of the records presented here, with other highly resolved climatic data from the British Isles and across Europe, the centennial climatic events are shown to be spatially complex but can be correlated with abrupt events identified within the NGRIP ice-core stratigraphy. The centennial events are therefore shown to be terrestrial correlatives of the GI-1d and GI-1b climatic deteriorations and potentially analogous to events between 11.4-11.1, 11.1-10.8 and ca 10.3 Cal. ka BP. Through comparing the climatic events with those from continental Europe, it is apparent that the GI-1d-type oscillation is most strongly felt in Britain and Greenland, whilst in continental Europe the GI-1b event is stronger, reflecting differences in stages of climatic development but also potential differences in forcing mechanisms. Across all sequences

the early Holocene climatic events are of reduced magnitudes than the climatic events during the Interstadial. The close parallels with the events in Britain and those from Greenland suggest that the event stratigraphy is a good stratotype from which to compare terrestrial sequences; although differences in timing still need to be reconciled.

The chapter concludes by providing mechanisms of climatic change, both in terms of millennial climatic development and centennial climatic events. For the latter, the effects meltwater forcing and solar variability are considered as potential triggers for the differences in event magnitude across Europe. The GI-1b-type event is postulated as registering NAO-like variability imprinting on a meltwater signal. In setting the background climatic variability, the subsequent chapter will demonstrate how palynologically-inferred vegetation changes across Britain and Europe vary according to climate.

Chapter 10. Synthesis of vegetation responses to abrupt climatic events during the Last Glacial-Interglacial Transition (LGIT)

The generation of highly-resolved climatic data, either within or alongside this thesis, has allowed for a better understanding of millennial and centennial-scale climatic trends within the British Isles during the Last Glacial-Interglacial Transition (LGIT; Chapter 9). The comparison of these data, with published highly-resolved climatic data from Britain and Europe, allows for a better understanding of regional climatic gradients and spatial and temporal variability within different climatic parameters. However, despite the multitude of environmental reconstructions, of which most are based on palynological data, most do not produce reference climatic data at comparable resolutions from the same sequence. Therefore, many vegetation-based reconstructions are correlated with regional climatic datasets and the NGRIP record (Rasmussen et al., 2014), without assessments of local climatic variation (e.g. Walker et al., 2012). This, coupled with disparate vegetation controls, disequilibrium theory (autogenic drivers: migration lags, differential seed dispersal and population dynamics) and dynamic equilibrium theory (allogenic drivers: climatic change, edaphic conditions and fire; Prentice et al., 1991; Seddon et al., 2015), demonstrates that the correlation of vegetation change with local climatic development has largely not been undertaken. This highlights the importance of this thesis, where not only are localised climatic datasets generated for sequences presented (Chapters 5-8), where possible vegetation reconstructions are made from the same stratigraphic sequence (Chapters 5-8), enabling more robust comparisons. This chapter synthesises the ecosystem/landscape responses from each site and considers both millennial-scale vegetation development and centennial-scale vegetation revertences. These changes are then compared to sequences across Europe and the phase relationships between driver and response variables are discussed.

10.1 Millennial-scale ecosystem development during the LGIT

The PCs and charcoal records for each sequence are presented together on absolute timescales in Figure 10.1; 10.2. From these records, three clear phases of vegetation development are observed: Phase 1: vegetation development associated with the Windermere Interstadial (WI); Phase 2: a transition and reversed vegetation development during the Loch Lomond Stadial (LLS); and Phase 3: a return to similar vegetative development as observed during the WI within the Holocene, where vegetation succession continues beyond the level of the WI. Within this framework, each site reveals differences in vegetative development which will be discussed here. Whilst fire appears locally important at each site, fire incidence appears confined to phases of greater woody vegetation development or in association with the climatic deteriorations discussed in Chapter 9 and will be discussed in detail in Section 10.2.

10.1.1 Windermere Interstadial ca 15.01-12.51 Cal. ka BP

At the onset of the WI, the PCs from all sequences reveal low values. These low values represent pioneering vegetation communities colonising the landscape, which was composed of low-lying herbaceous vegetation including *Rumex*, *Artemisia*, Poaceae, and Cyperaceae (Walker and Lowe, 2017). Across all sequences concentrations of these taxa are low, reflecting low vegetation densities within the landscape. The climatic reconstructions for this interval indicate climatic warmth (Chapter 9). This pioneering community was therefore out of phase with climatic regime, suggesting that Britain was characterised by a tundra community during the earliest WI with minimal fire frequencies.

Prior to ca 14.0 Cal. ka BP, decreasing PC values across all sequences reflects the gradual replacement of open herbaceous taxa with woody vegetation common to all four sites, representing the encroachment of *Betula cf. nana* into catchments following the establishment of well-drained albeit skeletal soils (van Dinter and Birks, 1996). Greater changes are noted at Tirinie and Palaeolake Flixton (PF) which perhaps reflects more abundant communities dominated by *Betula cf. nana*. At Llangorse, the continued presence of a tundra grassland (Poaceae and *Artemisia*) stifles PC variability. Whilst the same decreasing PC trend is observed at Quoyloo Meadow, this decrease is associated with a change in lacustrine process, reduced nutrient loading and reduction in *Pediastrum* from the system (Birks et al., 2000; Weckström et al., 2010) in conjunction with *Betula cf. nana* development, therefore the underlying process from which the PC identifies is different between these sites.

At all sites, a period of woodland/scrub development during the WI is observed at different stages. If it is acknowledged that Quoyloo Meadow is stratigraphically compressed during the late WI (Chapter 5), higher latitude sites (Quoyloo Meadow and Tirinie) display variability in woodland development compared to PF and Llangorse (as observed by the PC; Figure 10.1). During the WI, lowest PC values, taken here to reflect the greatest phase of *Betula* woodland development, or at Quoyloo heathland development (as observed from the gradient defined by PC which has open ground taxa and closed woodland as each end member; Chapter 4), are observed at 13.63 Cal. ka BP and 13.39 Cal. ka BP at Quoyloo Meadow and Tirinie respectively. This is contrasted with PF and Llangorse where greatest woodland development occurs at 12.93 Cal. ka BP and 12.74 Cal. ka BP (Figure 10.1). This appears late at Llangorse and is later than the onset of GS-1 in Greenland: 12.84 Cal. ka BP (Rasmussen et al., 2014), which may relate to low precision of biostratigraphically tied bulk radiocarbon dates (Walker et al., 2001).

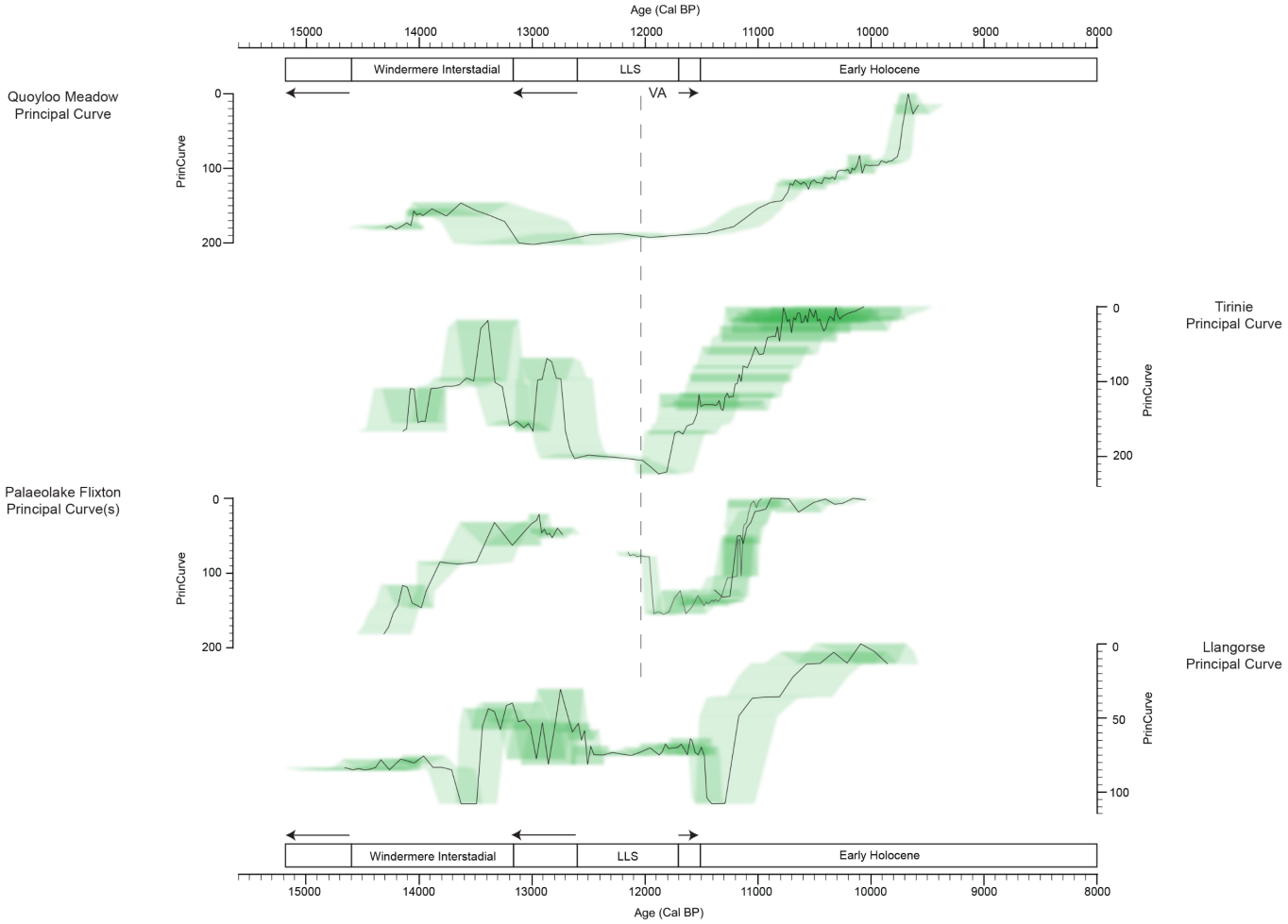

Figure 10.1 Showing all pollen data within the principal curves from each site studied as part of this thesis on a common age scale: Quoyloo Meadow, Tirinie, Palaeolake Flixon and Llangorse. Shading within graph about the x-axis reveal 95 % chronological uncertainties. Also highlighted are the major millennial phases within the vegetation record with arrows indicating their minimum/maximum chronological extent. The Vedde Ash (12,023±43 cal. BP; Bronk Ramsey et al., 2015) shows that Quoyloo Meadow, Tirinie and Palaeolake Flixton are tied records.

From the pollen data, variability in the PC appears to be driven by the increase in woody taxa, principally, *Juniperus communis* and *Betula cf. pubescens/pendula* at Tirinie, PF and Llangorse; and *Betula cf. nana and Empetrum* at Quoyloo Meadow. Ultimately, variations in peak mean annual and summer temperature may have an impact on vegetation development. However, at each sequence optimal climatic conditions, mean annual or summer, are out of phase with woodland vegetation or scrub development at Quoyloo Meaodow (Chapter 9), although greater woodland development at Tirinie coincides with an inferred phase of low aridity. Therefore, during favourable climatic conditions of the WI (Chapter 9; Marshall et al., 2002; Brooks et al., 2012; Whittington et al., 2015), climate exerts a secondary control in providing suitable conditions for the growth and spread of vegetation (warm summer/winter temperatures, enhanced growing seasons, greater effective moisture) but the dominant controls appear to be autogenic (rates of migration, seed dispersal ability, and the dominant successional sequence; Webb, 1986; Prentice et al., 1991). The late WI climatic event, correlated with GI-1b in Greenland at ca 13.3-13.05 Cal. ka BP (Lowe et al., 2008; Rasmussen et al., 2014) affects vegetation assemblages in Britain (Chapter 9 and Section 10.2) and has a direct influence on fire regimes. This climatic deterioration is bound by a phase of woodland and scrub expansion at Tirinie, PF and Llangorse (Figure 10.1). Whilst climatic amelioration produces a means for the re-establishment of woody vegetation following a climatic event climate is not solely responsible. It is likely that the latitudinal and refugial positions of outwardly migrating taxa are key in this instance alongside increased competition following the replacement of grassland communities (e.g. Tipping, 1991a; Wick and Tinner, 1997). At Llangorse and PF, due to the lower latitudinal position and lower expression of climatic events (Chapter 9), thermophilic taxon displacement is reduced or pollen production may be curtailed (e.g. Hoek, 1997). Thus, following a phase of climatic amelioration, thermophilic taxa would start to produce pollen or migrate into lower latitude catchments more rapidly than at higher latitudes, where the displacement would have been greater. Whilst it may appear that these lower latitude sequences are more resilient (e.g. Scheffer et al., 2009), it may be that the period associated with GI-1a is of insufficient duration to allow the re-expansion of woody vegetation at higher latitudes. Therefore, the PC reveals differences across each sequence, inferred to reflect vegetation development, which are postulated to reflect the latitudinal position of the site and the proximity to refugia following a climatic event.

10.1.2 Loch Lomond Stadial ca 13.12-11.52 Cal. ka BP

The transition into the LLS is represented at all sites with a transition from thermophilous vegetation from the preceding GI-1a stage to disparate cold-adapted vegetation communities associated with Arctic/alpine environments (Pennington et al., 1972;

Tipping, 1991b; Walker et al., 2003). This transition is observed in the PCs reflecting widespread compositional turnover, and through reduced pollen concentrations reflecting both the reduction in landscape biomass and increased sedimentation rates. A lithostratigraphic shift from organic to minerogenic sediments at this time highlights greater landscape instability with increased catchment erosion.

The onset of the shift in vegetation follows the dominant change in climatic conditions during the LLS (Chapter 9). Variability is shown in the onset of the biostratigraphic stadial, with the transition at Quoyloo Meadow between 13.24-12.98 Cal. ka BP, at Tirinie 12.74-12.62 Cal. ka BP, and at Llangorse between 12.74-12.5 Cal. ka BP. The timing of the Stadial onset cannot be robustly derived for PF owing to the sedimentological hiatus in Core B due to falling water table elevations (Palmer et al., 2017) and the age model being unconstrained below the Vedde Ash. Although the age models of these sequences are imprecise at this time, the transition is first recorded in the northern high-latitude sites, and later in north-east England and south Wales, perhaps revealing a vegetation gradient responding to the expansion of sea-ice and the southerly migration of the polar front during the LLS cold stage (e.g. Muschitiello and Wohlfarth, 2015). A review by Muschitiello and Wohlfarth (2015) suggests that vegetation at lower latitude sites, between 56-54°N respond earlier than higher latitude sequences between 60-58°N, hence the earlier onset of the biotic Stadial. Muschitiello and Wohlfarth (2015) further suggest that the earlier change is a result of greater regional cooling at lower latitudes following late Interstadial warming but also more resilient vegetation at higher latitudes, in response to short Interstadial growing seasons and increased buffering to seasonal changes that characterised the Stadial. Whilst elements of this may be true, no assessment of the local climatic conditions are made within Muschitiello and Wohlfarth (2015). The sites presented here, whilst they may not be as chronologically precise, show vegetation change following earlier climatic deteriorations in the high latitudes and oppose that of Muschitiello and Wohlfarth (2015) perhaps in relation to the migrating polar front. Therefore, LLS vegetation changes in Britain are first identified in the northern latitudes then in the southerly latitudes, not the opposite as would be expected under the Muschitiello and Wohlfarth (2015) model.

Across the three sequences, the amplitudes of the palynologically inferred vegetation responses vary during the LLS. Whilst site PC data are relative, the underlying values of the curves can be used to reveal site-specific changes. The greatest changes for the LLS are observed at Tirinie, with a percentage shift along the PC gradient of 48 %. At Llangorse and Quoyloo Meadow these shifts are shown by a percentage change of 47 % and 15 % respectively. This demonstrates a vegetation gradient across Britain, with

the greatest shifts in central Scotland. Three potential explanations are proposed to account for this 1) the nature of vegetation prior to the LLS cold reversal; 2) the nature of vegetation within the LLS; and 3) characteristics of the site.

The first and second scenario offer the best explanations as similar LLS vegetation communities exist at Tirinie and Quoyloo despite late Interstadial vegetation discrepancies across all sequences. For example, at Quoyloo Meadow the transition from heathland to grassland is not as marked as at Llangorse, where a transition from *Betula* woodland to a landscape dominated by a mosaic of *Betula nana* and open grassland is observed. At Tirinie, however, whole-scale landscape replacement is suggested by the pollen data. As a modulating effect, the greater altitude of Tirinie may be responsible for the sensitivity of vegetation. At higher altitudes taxa are likely to be closer to ecological limits, therefore the severe climatic perturbation of the LLS (Chapter 9) would generate a greater magnitude of inferred vegetation change (Davis and Shaw, 2001). The altitude of the site is also proposed as to why the transition into the LLS vegetation assemblage is rapid. At Quoyloo Meadow and Llangorse the transition is ca 200 years whilst at Tirinie this transition is ca 100 years. Therefore, the proximity to ecological boundaries precludes a rapid shift in dominant vegetation state; taxa thriving in warm conditions are rapidly replaced by taxa that undergo range expansion when climates cool (Davis and Shaw, 2001). Across Britain therefore, vegetative transitions into the LLS are driven by dynamic equilibrium theory (Prentice et al., 1991) with a latitudinal gradient revealing the time-transgressive nature of climatic change (e.g. Muschitiello and Wohlfarth, 2015). However, the rates and magnitudes of change appear modulated by autogenic factors between sequences and exacerbated by local site characteristics.

10.1.3 Early Holocene ca 11.74-8.8 Cal. ka BP

Due to different vegetative controls, the Holocene palynological records appear out of phase with dominant climatic regimes (Chapter 9). Further the transition out of the LLS into the Holocene from each site is not as abrupt as those into the LLS. This is likely a product of the lag in vegetation reorganisation following a climatic perturbation (Pennington, 1986) in part due to soil status. However, using the PC, an initial shift at Tirinie and PF does appear to be abrupt, this reflects the loss of local/aquatic taxa reflecting a change in the system rather than a change in regional vegetation. For example, the PC shift at Tirinie, between 11.8-11.73 Cal. ka BP, reflects the reduced abundances of *Pediastrum* from the lacustrine environment with the shift at PF between 11.32-11.14 Cal. ka BP reflecting the same losses of *Pediastrum* alongside a contraction of the littoral Cyperaceae. This trend highlights the importance of local process, for

example loss of erosivity and increasing lake water level (Lincoln, 2017; Palmer et al., 2017), as opposed to changes in catchment vegetation. The same scenario is postulated at Quoyloo Meadow, between 11.45-10.89 Cal. ka BP. In contrast, owing to mono-specific taxon change at Llangorse influencing the PC (Chapter 8) this abrupt change is not observed.

Across Britain, there are no apparent latitudinal trends in vegetation responses to the climatic amelioration during the Holocene, although the vegetation changes at Tirinie and Llangorse occur ca 200-400 years prior to PF and Quoyloo Meadow. As per vegetation shifts during cold phases, with the onset of climatic warmth (Chapter 9) vegetation at high altitudes may initially respond quicker than sequences at lower latitudes due to a lack of environmental buffering and greater sensitivity of higher altitude locations (e.g. Candy et al., 2016).

At Tirinie and Llangorse vegetation development surpasses that of WI levels at ca 10.8 Cal. ka BP whilst at PF this occurs earlier at ca 11.0 Cal. ka BP (Figure 10.1) although within chronological errors. Scrutiny of the pollen data reveals that this is reflective of the widespread migration of *Betula* woodland across Britain almost synchronously. It is proposed that the earlier spread of *Betula* at PF is a product of the land-bridge connection with central Europe. Therefore, the spread of *Betula* reflects migration across Dogger Bank, the now inundated area of the southern North Sea basin, from central Europe (Krüger et al., 2017). Credence for this hypothesis is gained through the understanding of radial *Betula* spread across Britain as observed in regional pollen maps (Birks, 1989). These maps also justify the approximately synchronous timing of *Betula* migrations between central Scotland and southern Wales.

In contrast to the spread of *Betula*, the PC from Quoyloo Meadow surpasses values during the WI following the establishment of a species-rich grassland at ca 10.8 Cal. ka BP. This trend highlights that tree Birch was not a part of the landscape during the earliest phases of the Holocene, likely to be a product of the ecotonal setting, harsh climatic conditions and issues of seed dispersal to an island location (Bunting, 1994). Therefore, in contrast to the lower latitude sites, the establishment of grassland is taken to reflect a period of landscape stability with minimal competition from woody taxa. Continued vegetation development across all sequences, follows the dominant successional sequence in Britain (e.g. Lowe and Walker, 1986; Edwards et al., 2018). Therefore, from the available data environmental stability is denoted during Holocene.

10.2 Centennial-scale vegetation revertence episodes

Superimposed on the general millennial-scale vegetation trends, centennial-scale palynologically inferred vegetation revertences are observed. These revertences can be directly correlated with phases of climatic deterioration highlighting a response to climatic forcing; hence conforming to dynamic equilibrium hypotheses (Prentice et al., 1991). As in Section 10.1 the PC will be the major tool used to elucidate vegetation responses to abrupt climatic change, however, criteria outlined in Watts (1970) and Chapter 4 will also be consulted (Table 10.1) to better show variable responses (Table 10.2). Further, fire appears to be an important response variable during phases of climatic deterioration and will be discussed in the following sections.

10.2.1 Early Windermere Interstadial vegetation revertence 14.14-13.73 Cal. ka BP (GI-1d climatic event)

Across all sequences clear palynological revertences are shown by Table 10.1; 10.2 and by inflections in PC values (Figure 10.2); all of which are correlated with climatic deteriorations (Chapter 9). These higher PC values are taken to reflect a period of landscape instability. At Quoyloo Meadow the onset of the revertence occurs at 14.04 Cal. ka BP and is characterised by increased *Pediastrum*, Poaceae, *Rumex*, and *Artemisia.* In comparison, Tirinie, 14.03 Cal. ka BP, exhibits losses of *Betula cf. nana*, *Empetrum nigrum* and increased open-landscape vegetation, Poaceae and Cyperaceae, with increased disturbed ground indicators *Rumex* and *Artemisia*. These two higher latitude sites display differences to PF, 14.10 Cal. ka BP, and Llangorse, 13.96 Cal. ka BP. Whilst both demonstrate revertences, the pollen derived from these low latitude sites suggest a proliferation of open grassland, or opening of the landscape, as opposed to ecosystem change suggested by Arctic tundra disturbed ground indicators at higher latitudes. Whilst the onset of these revertences appear variable, within chronological uncertainties they are synchronous. Although the onset of vegetation change appears earlier at PF, this likely relates to the reduced resolution of the palynological dataset. It might be expected that time-transgressive climatic change will produce temporal variability in vegetation responses, however, it is improbable that the onset of the revertence occurs prior to the shift in climatic conditions in Greenland.

In conjunction with this early WI vegetation revertence, fire appears to be an important landscape component. For this early WI climatic event however, fire appears within the record following a shift in vegetation (Figure 10.2). Thus, fire does not appear to be a parameter driving the shift in assemblage, rather it is a response variable following climatic and vegetation change (Millspaugh and Whitlock, 1995). It seems plausible that, as defined through a palynological means, a shift in vegetation assemblage, produces a

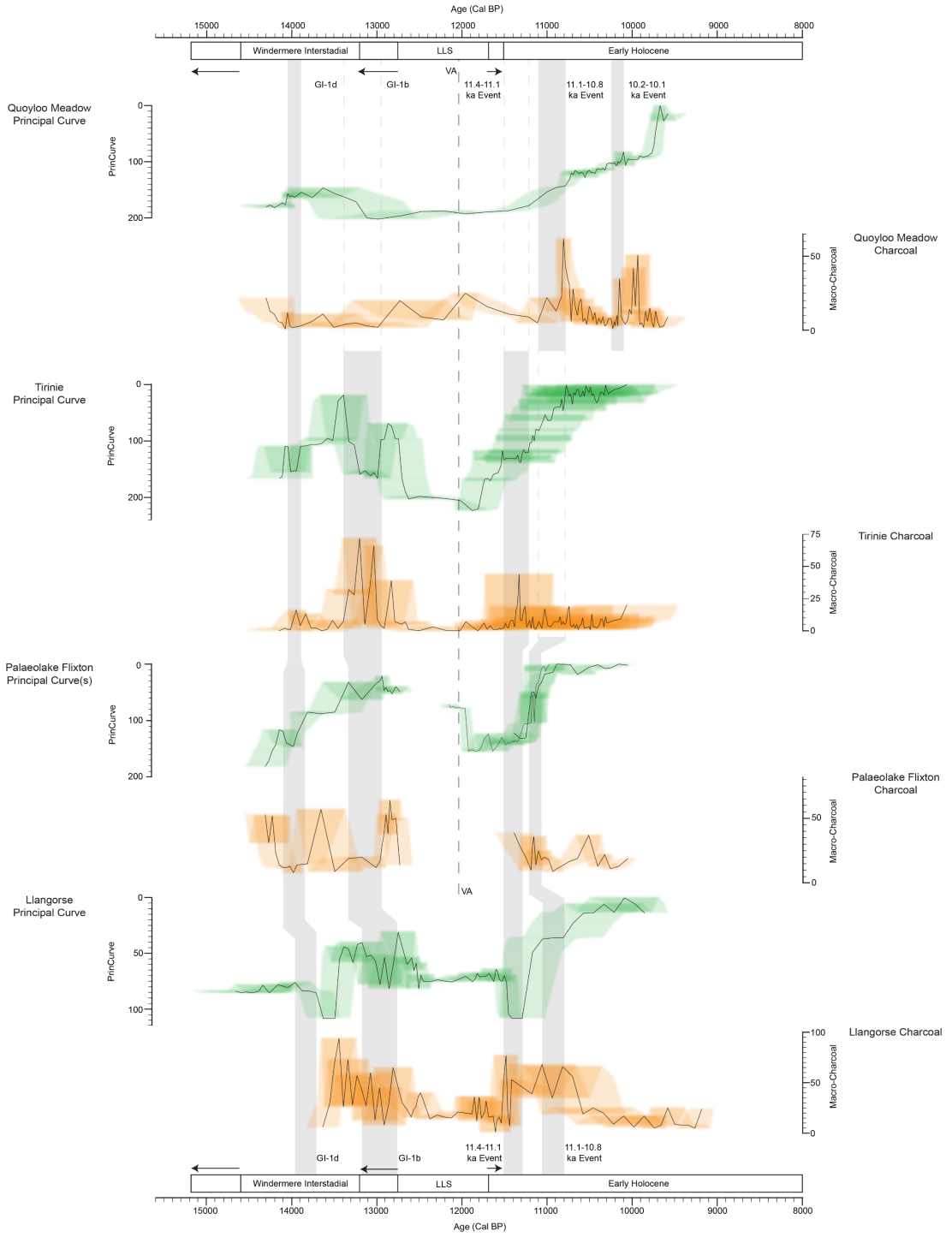

Figure 10.2 All pollen data within the principal curves (green) and charcoal data (orange) from each site studied as part of this thesis on a common age scale: Quoyloo Meadow, Tirinie, Palaeolake Flixton and Llangorse. Shading within each graph about the x-axis reveal 95 % chronological uncertainties. The Vedde Ash (12,023±43 Cal. BP; Bronk Ramsey et al., 2015) shows that Quoyloo Meadow, Tirinie and Palaeolake Flixton are tied records. Major millennial phases are shown on each record with arrows indicating their minimum/maximum extent. Grey shading on each of the figures highlight where centennial-scale vegetation reversions are identified (discussed in Section 10.2).

Table 10.1 Watts (1970) criteria updated by Edwards and Whittington (2010) for the elucidation of palynologically-based vegetation revertences. Specific criteria are outlined from which vegetation revertences are determined. If all criteria are met, a vegetative revertence can be demarked.

	Good modern standard of pollen flora				**Clear evidence of climatic reversion**				**More than one pollen spectra (and number)**			
Event age (Cal. ka BP)	**QM**	**Tir**	**PF**	**Lla**	**QM**	**Tir**	**PF**	**Lla**	**QM**	**Tir**	**PF**	**Lla**
14.1-13.7	Yes	Yes	Yes	Yes	Yes	Yes	Yes	Yes	Yes (4)	Yes (5)	Yes (4)	Yes (5)
13.6-13.5	Yes	Yes	Yes	Yes	**No**	**?**	**No**	**?**	**No**	Yes (2)	**No**	Yes (2)
13.5-12.8	Yes	Yes	Yes	Yes	**No**	Yes	Yes	Yes	**No**	Yes (5)	Yes (3)	Yes (3)
11.45-11.1	Yes	Yes	Yes	Yes	Yes	Yes	Yes	Yes	Yes (3)	Yes (5)	Yes (2)	Yes (3)
11.15-10.75	Yes	Yes	Yes	Yes	Yes	**N/A**	Yes	Yes	Yes (3)	**N/A**	Yes (3)	Yes (3)
10.2-10.1	Yes	Yes	Yes	Yes	Yes	**N/A**	**N/A**	**N/A**	Yes (4)	**N/A**	**N/A**	**N/A**

	Distinctive sedimentological changes				**Evidence for climatic deterioration**			
Event Age (Cal. ka BP)	**QM**	**Tir**	**PF**	**Lla**	**QM**	**Tir**	**PF**	**Lla**
14.1-13.7	Yes? (LOI)	Yes (Calc)	Yes	Yes (Calc)	Yes	Yes	Yes	Yes
13.6-13.5	**No**	Yes (Strat)	Yes (Calc/Strat)	Yes (Calc)	**No**	In part?	**No**	In part?
13.5-12.8	**No**	Yes (Calc/TOC/Strat)	Yes (Calc/Strat)	Yes (Calc)	**No**	Yes	Yes	Yes
11.45-11.1	Yes (LOI)	Yes (Calc/Strat)	Yes (Calc)	Yes (Calc)	Yes	Yes	Yes	Yes
11.15-10.75	Yes (LOI)	**N/A**	Yes (Calc/Strat)	Yes (TOC/Calc)	Yes	N/A	Yes	Yes
10.2-10.1	Yes (LOI/Calc)	**N/A**	**N/A**	**N/A**	Yes	N/A	N/A	N/A

Table 10.2 Event timing and the variable vegetation responses to abrupt climatic events depicted in Table 11.1 for A) the Windermere Interstadial and B) the early Holocene. Vegetation present are those that enter the landscape following a climatic deterioration. Dashes represent where no proxy data exist and N/O represents where vegetation responses remain unobserved.

A) Windermere Interstadial	**Age (Cal. ka BP)**		
Climatic Event	**14.14-13.73**	**13.6-13.50**	**13.45-12.80**
Site	**Revertence vegetation**	**Revertence vegetation**	**Revertence vegetation**
Quoyloo Meadow	*Pediastrum*, Poaceae, *Rumex*., *Artemisia*	**N/O**	**N/O**
Tirinie	Poaceae, *Rumex*, *Artemisia*	*Rumex*	Poaceae, *Rumex*, *Pediastrum*
Palaeolake Flixton	Poaceae, *Pediastrum*, Cyperaceae	**N/O**	*Juniperus*, Poaceae
Llangorse	Poaceae, *Rumex*, *Artemisia*	Poaceae	Poaceae, *Rumex*

B) Early Holocene	**Age (Cal. ka BP)**		
Climatic Event	**11.45-11.05**	**11.18-10.75**	**10.20-10.10**
Site	**Revertence vegetation**	**Revertence vegetation**	**Revertence vegetation**
Quoyloo Meadow	Poaceae, *Rumex*	*Pinus*, Cyperaceae	Poaceae, *Pinus*, *Rumex*
Tirinie	*Equisetum,* Poaceae*, Rumex*	**N/O**	**-**
Palaeolkae Flixton	*Salix*, Cyperaceae, *Pediastrum*	*Salix*, Poaceae	**-**
Llangorse	Poaceae	Poaceae	**-**

fuel source on the landscape, from which climatic conditions were favourable for greater fire incidence (Whitlock et al., 2003), notably greater aridity.

Percentage change along the gradient of the PC has been calculated to assist in revealing magnitudes of palynological change across the transect. At Quoyloo Meadow, the percentage change is 3 %; whilst at Tirinie, PF and Llangorse the percentage changes are 20, 15 and 8 %, respectively. Unfortunately, at Llangorse, during this phase of the record, the full potential of the PC is not realised, due to mono-specific taxon responses, in this instance *Juniperus*. At Llangorse, *Juniperus* proliferates at two points where little or no competition exists, giving the PC the appearance of decreased landscape stability. On the contrary, *Juniperus* reflects climatic amelioration (e.g. Walker et al., 1993a) following the climatic event associated with GI-1d. Therefore, whilst the low percentage changes in the PC may be real, they may also reflect minimum values.

The percentage differences between these sites clearly demonstrate that the greatest magnitudes of response are observed at Tirinie, with PF and Llangorse intermediary and Quoyloo Meadow revealing the weakest response. This may in part be a product of the magnitude of the climatic deterioration, which across Britain, is the most severe centennial-scale climatic event, although it is the least felt at Quoyloo Meadow and it is more pronounced at Tirinie and PF. However, it may also be related to local site factors. The underlying control is climate, a colder event in the northern latitudes will force greater vegetation change through increased abundances of Arctic/alpine vegetation (e.g. Birks and Ammann, 2000). However, altitudinal differences will exacerbate these changes. Clearly during this climatic event the nature of pollen response is different between sequences. This reveals differences in the magnitudes of vegetation change across Britain, the highest and lowest latitude sites do not reveal the greatest change whilst the relative mid-latitude sequences and Tirinie, which is at the greatest altitude, do. The duration of the revertences are variable, however, these are inherently tied to the duration of the climatic event where recovery is linked to climatic amelioration.

10.2.2 Mid-Windermere Interstadial vegetation revertence ca 13.60-13.50 Cal. ka BP (GI-1cii climatic event)

In contrast to the early WI revertence, under the criteria outlined in Table 10.1, a revertence is not suggested. At Quoyloo Meadow and PF, no criteria are met, whilst at Tirinie and Llangorse not all criteria are fully satisfied. Therefore, whilst increases in open ground taxa are noted, these are confined to single samples and could theoretically be a product of natural variability.

Reasons for the lack of response in pollen could be product of insensitivity of vegetation to lower magnitude climatic change; insensitivity to seasonal climatic change (Chapter 9) or; insufficient sample resolution. Whilst sample resolutions are lower at Llangorse the WI sequence is stratigraphically expanded, and at Tirinie, the samples are contiguously extracted, therefore, both approximate similar time-averaged per sample. It may be possible that resampling at higher resolutions may identify a phase of vegetation change. However, the climatic deterioration is of lower magnitude than the early and late WI climatic events, which suggests that climatic forcing is not sufficient to drive changes in vegetation. Across Ireland and Britain (e.g. Brooks and Birks, 2000a; Marshall et al., 2002; Bedford et al., 2004; Van Asch et al., 2012), mean annual and summer temperature variability has been recorded. Suggesting that sampling resolutions are insufficient to detect summer temperature change. Whilst, palynological and vegetation responses remain plausible, it is likely that the magnitudes of climatic change were insufficient at low-altitude sites (Quoyloo Meadow and PF), whilst insufficient sampling resolutions at high-altitude sites preclude formal attribution.

10.2.3 Late Windermere Interstadial vegetation revertence ca 13.45-12.80 Cal. ka BP (GI-1b climatic event)

In response to the GI-1b equivalent event in Britain, between 13.45-12.80 Cal. ka BP, clear palynologically-inferred vegetation revertences are depicted (Figure 10.2; Table 10.2). At Tirinie, the onset of the revertence is shown at 13.32 Cal. ka BP by a loss of tree birch alongside increases in open and disturbed ground herbaceous vegetation, displaying a community predominantly composed of Arctic/alpine taxa (*Rumex*, Poaceae, Caryophyllaceae, Compositae: Lactuceae, *Thalictrum*, Saxifragaceae). In contrast the lower latitude/lower altitude sites of PF (13.31 Cal. ka BP) and Llangorse (13.14 Cal. ka BP) exhibit a loss of tree birch with a proliferation of an open grassland; the dominant taxon is Poaceae, although minor increases in *Rumex* are noted at Llangorse. During the climatic event Llangorse demonstrates increases in *Filipendula*, which may reflect a latitudinal hydroclimatic gradient across Britain, with aridity in Scotland but not in south Wales. This may be unlikely given the aridity suggested at Hässeldala Port and Meerfelder Maar (Rach et al., 2014; Muschitiello et al., 2015) at this time, although as Llangorse is closer to the oceanic source this is unknown. Alternatively, the presence of *Filipendula* at Llangorse could demonstrate the greater temperature dependency of *Filipendula* than moisture at this time (Isarin and Bohncke, 1999). This climatic event or vegetation revertence is not observed at Quoyloo Meadow. Therefore, across Britain, the late Interstadial revertence is shown to exhibit variations in the nature of vegetation response and is broadly synchronous across Britain.

In contrast to the early WI event, the incidence of fire appears variable between Tirinie, PF and Llangorse. Specifically, at Llangorse fire occurs immediately prior to and after the greatest phase of vegetation change, which is closely aligned to the onset of the climatic deterioration. The opposite is true of Tirinie and PF where fire occurs after the greatest change in vegetation during the GI-1b climatic event. Fire may therefore be important at Llangorse as an additional parameter that further drives changes in vegetation (Whitlock et al., 2003). The disentanglement of this process is difficult however, and it may be that vegetation is more susceptible and a suitable fuel source on the landscape exists.

Nonetheless, the magnitudes of palynological change during the late WI revertence is highlighted by PC shifts of 66 %, 17 % and 38 % at Tirinie, PF and Llangorse respectively. At this point in the record the PC from Llangorse is not being driven by changes in *Juniperus*, thus these values are believed to be an accurate representation of the magnitudes of vegetation response to abrupt climatic change. The percentage differences between these sequences demonstrate that the greatest magnitudes of palynological change are at Tirinie, with magnitudes of change at Llangorse and PF much lower than the higher latitude site. Further, across all sequences the late WI vegetation revertence is greater in magnitude than the vegetation revertence associated with the early WI climatic event; which is notable considering the GI-1d-type climatic event is greater in magnitude than the GI-1b-type climatic event in Britain, with the exception of greater aridity observed at Tirinie. Therefore, whilst climatic change, and fire at Llangorse, drive shifts in vegetation across Britain, greater responses of vegetation cannot be solely attributed to the magnitude of the driving factor.

Two factors may explain this difference between sequences and highlight why magnitudes of change are larger for the GI-1b revertence in comparison to the GI-1d revertence. Firstly, the location of the site may explain the magnitude differences. At higher altitudes vegetation is closer to ecological thresholds, therefore following a climatic perturbation, the vegetation rapidly reorganises itself to a different ecological state (Candy et al., 2016); at Tirinie an Arctic/alpine tundra, whilst at Llangorse and PF an open grassland. The Arctic/alpine taxa clearly force the PC towards higher values. Secondly, antecedent vegetation prior to the climatic deterioration may explain magnitude differences with the presence of *Betula* woodland prior to the climatic event acting as a mediating factor. However, in comparing the three sites, *Betula* is present on the landscape at all sites prior to the climatic event. Although the woodland may be more developed at PF and Llangorse, it is unlikely be the overarching control in the magnitudes of change. It is therefore more likely that, in this instance, replacement

vegetation, which approximate that identified during the LLS at high latitudes exerts considerable influence over the PC shift. Therefore, a combination of these two factors may explain the differences in magnitudes observed. These two factors may help explain why the late WI revertence exhibits greater magnitudes than the former revertence, as *Betula* woodland is perceived to be absent on the landscape prior to the GI-1d climatic event, and the vegetation across Britain is pioneering, thus at an earlier stage of succession. Therefore, the late WI climatic event generates a different nature and magnitude of response across Britain, depending on latitudinal position; which is also greater in magnitude than the response to the early WI climatic event.

10.2.4 Loch Lomond Stadial vegetation variability ca 12.2-12.0 Cal. ka BP (GS-1)

Whilst millennial-scale vegetation change during the LLS is understood across Britain, subtle vegetation variability is shown. Vegetation variability appears to relate to climatic variability between 12.2-12.0 Cal. ka BP. At Quoyloo Meadow reduced percentages and concentrations of *Artemisia*, suggest a brief contraction of *Artemisia* on the landscape during the mid-Stadial. At Tirinie an inflection in the PC coincides with the suggestion of increased *Artemisia* during the second half of the LLS. *Artemisia* can survive relatively warm summers (Birks and Matthewes, 1978), however the suggestion for greater effective moisture on Orkney at this time may hinder growth of this xeric herb. Unfortunately, it is unknown whether δ*D* isotopic enrichment is related to climatic amelioration or rather reflects increased moisture availability (David Maas, pers. comm. 2018) but the reduction in *Artemisia* perhaps points to greater moisture availability. At Tirinie however, δ*D* has been interpreted as holding an evaporitic signal, masking moisture variability. Nonetheless greater *Artemisia* presence perhaps reflects a more arid latter half of the Stadial in Scotland, which may reflect growth of the LLS ice-cap over western Scotland, causing aridity in the lee of the ice-mass (MacLeod et al., 2011).

The clearest evidence of mid-Stadial change is observed from PF. Between 12.02-12.00 Cal. ka BP the PC shifts by 49 %. The taxa forcing this change include Cyperaceae and *Pediastrum*. The greater abundance of *Pediastrum* and the littoral Cyperaceae suggest a contraction of the lake body and a potential shift towards lower lake levels (Weckström et al., 2010), which is in line with the reduction in lake levels suggested at Wykeham Quarry (Lincoln, 2017) and across PF (Palmer et al., 2015). For PF lake levels to reduce, the latter half of the Stadial had to be more arid. The suggestion of greater aridity agrees with the observed changes at Tirinie, although not Quoyloo Meadow, which may be explained by the different ecotonal setting of the sites. These vegetation-based changes also align with the suggestion of a northerly migrating and ‘flickering’ westerly wind pattern after 12.2 Cal. ka BP following seasonal break-up of sea-ice (Bakke et al., 2009;

Lane et al., 2013) in the northern high latitudes. Model simulations covering GS-1 suggest that the latter half of the Stadial is more arid in continental Europe (Isarin et al., 1998) something clearly hinted at with increases in dry adapted vegetation and lacustrine change during the latter half of the LLS. Evidence from Scandinavia suggests that the latter half of the Stadial is more unstable (Bakke et al., 2009), perhaps reflecting increased moisture availability in the highest latitudes, which would include Quoyloo Meadow. British vegetation is therefore clearly sensitive to Stadial climatic variability identified across the European continent.

10.2.5 Early Holocene vegetation revertence ca 11.45-11.05 Cal. ka BP

Vegetation responses to Holocene climatic variability appear muted compared to the Interstadial; despite comparable forcing at least to the GI-1b-type event (Rasmussen et al., 2014). For the earliest Holocene climatic event, no vegetation response is noted at Quoyloo Meadow in the PC values. At PF (11.4 Cal. ka BP) high PC values are controlled by high abundances of *Salix*, Cyperaceae and *Pediastrum*, with the former perhaps indicating later snow lie in the Vale of Pickering (Wijk, 1986). This period at Llangorse is controlled predominantly by the loss of *Betula*, at the transition from *Betula cf*. *nana* and tree *Betula*, the loss of reworked pollen and variability in *Juniperus*. Like the GI-1b climatic event fire may have a further control on landscape conditions during the early Holocene. Principally, fire seems important in modulating the presence of *Juniperus*, with greater fire bounding abrupt increases and decreases in *Juniperus* (e.g. Thomas et al., 2007), suggesting that at Llangorse, fire is a response to climatic deterioration as opposed to the abundance of a fuel source. Nonetheless, Tirinie reveals a pause in the PC (7 % change), a product of reductions in *Betula* undiff., high Poaceae percentages and increases in *Equisetum*. Across Britain, palynological responses to unfavourable climatic conditions between 11.50-11.1 Cal. ka BP appear to reveal increases in open herbaceous taxa, with, on occasion greater disturbance indicators (Beerling, 1993) and pteridophyte taxa. Again, the greatest vegetation changes are observed at Tirinie (7 %). The expansion of *Equisetum* at Tirinie confirms suggestions from biomarker data that the climatic deterioration exhibited greater aridity, with vegetation tracking lacustrine contraction (Odland and del Moral, 2002).

Across all sequences, lower magnitudes of vegetation response are a consequence of the state of vegetation, with an open pioneering grassland following the LLS; which is relatively insensitive to change (Björk et al., 1997; Berglund et al., 2008). Further, Björk et al. (1997) suggested that individualistic plant responses are common to climatic events during the Holocene; a result of different site settings and the continued presence of cold-adapted taxa. Thus, whilst the Arctic tundra grassland of the LLS has been

replaced, pioneering taxa dominate and last vegetation shifts would not be expected (e.g. Björk et al., 1997). As with preceding events, the altitude of Tirinie may also exert additional control as specific plant physiological parameters may no longer be met, in this instance seasonal temperature and moisture requirements; postulated for contractions in *Betula* and *Empetrum nigrum*. Therefore, variability in vegetation responses are noted to abrupt climatic change across Britain to climatic events between 11.4-11.1 Cal. ka BP, however they appear muted compared to revertences during the WI.

10.2.6 Early Holocene vegetation revertence ca 11.15-10.75 Cal. ka BP

The second early Holocene climatic event across Britain produces similarities in vegetation response from 11.15 Cal. ka BP. The PC curves from Quoyloo Meadow and Llangorse reveal a pause during this interval, indicating a cessation in landscape vegetation development; whereas at PF a minor reversion towards greater PC values is observed (6 % shift), which occurred following an increase in fire in the PF catchment. Differences in timing are noted across these sequences, with the palynological changes occurring at 11.15 Cal. ka BP at PF, and at Llangorse and Quoyloo Meadow the onset of change occurs at 11.05 and 10.95 Cal. ka BP, coinciding with periods of climatic deterioration. Therefore, like the early Holocene revertence between 11.45-11.1 Cal. ka BP the revertence between 11.15-10.75 Cal. ka BP suggests that early Holocene revertences in Britain are characterised by increases in grassland abundance.

This revertence, as defined by the PC, exhibits greater magnitudes of change than changes in association with the first early Holocene climatic event. The greater magnitude shares similarities with the GI-1b revertence, in that the magnitudes of climatic change appear reduced compared to the GI-1d event, yet a greater vegetation response is observed. This trend is also observed in the Netherlands (Bohncke and Hoek, 2007). Originally, van Geel et al. (1981) associated secondary Holocene vegetation changes with greater winter temperature variability, which is possible here owing to the lack of change associated with summer temperature proxies. However, there is evidence that this interval is arid (Bohncke and Hoek, 2007). Aridity is shown at Quoyloo Meadow which appears to coincide with principal changes in taxa. Although as the greatest changes are identified at PF, which is the only sequence that displays summer temperature variability, it is probable that mean annual climatic change, with aridity, had a significant effect on vegetation at this time which is then modulated the influence of summer temperature. In effect summer temperature may force greater vegetation responses, this does however require further testing at this time.

10.2.7 Early Holocene vegetation revertence 10.20-10.10 Cal. ka BP

Evidence for later Holocene vegetation changes are identified at Quoyloo Meadow only. The highest magnitude centennial-scale climatic event recorded at Quoyloo Meadow is between 10.2-10.1 Cal ka BP. This climatic change, registered both in mean annual and summer temperature proxies (decline of -2.8°C), coincides with a pause and slight inversion in the PC, driven by increased Poaceae, *Rumex* and *Pinus* with losses of *Empetrum nigrum*. Despite the climatic expression of the 10.2 Cal. ka BP event being most strongly felt at Quoyoo Meadow, the vegetation response is not as substantial as changes in the WI (GI-1d). Grime et al. (2000) state that prior climatic extremes have no pre-conditioning effects on stable grassland communities. Further, from modelled and empirical evidence, the authors note that plant growth rate, life history and successional status influence the ability of an ecosystem to be resistant to climatic change. Therefore, the establishment of a stable grassland, rich in species composition at Quoyloo Meadow during the preceding ca 600-year period, outcompeted woodland taxa (Bunting, 1994) and likely offered greater resistance to climatic change. This is postulated as to why palynological changes are muted. The rapid recovery and increase in the PC following the climatic perturbation indicates that Quoyloo Meadow exhibits traits of resilience (e.g. Scheffer et al., 2009; Seddon et al., 2016). Therefore, climatic deteriorations drive vegetation changes during the Holocene, but the observed vegetation changes are of lower magnitude than the revertences during the WI likely due to the lack of stability in the WI system.

10.3 Magnitudes and nature of vegetation responses across Britain

As highlighted above, the magnitudes of vegetation responses to centennial-scale climatic events are variable at each site. Here the processes behind these magnitudes will be addressed.

10.3.1 Quoyloo Meadow

At Quoyloo Meadow, high-magnitude centennial-scale revertences are absent. Two scenarios may account for the lower magnitude vegetation change: 1) insufficient climatic forcing, hence weak vegetation responses; and 2) the location of the Orkney isles. Firstly, considering the discussion in Section 9.4.1 and 9.7, it may be that the Orkney archipelago experienced reduced magnitudes of climatic change owing to the buffering effects of the North Atlantic despite the latter being the source of centennial-scale events (Broecker et al., 1989; Clark et al., 2001). The influence of climate in driving vegetation change may therefore be reduced at Quoyloo Meadow. Secondly, the location of the sequence may be significant. A grassland community dominates throughout the LGIT at Quoyloo Meadow and woodland does not develop, likely due to migratory lags

to an island location (Birks, 1989); and/or specific ecological stressors preventing growth e.g. cool summer temperatures and high wind stress (Birks et al., 2012). Any climatic perturbation affecting this grassland would only influence an already open landscape, therefore greater resistance to climatic change is suggested (Grime et al., 2000). Therefore, knowledge of the ecotonal setting is vital in understanding the lack of large-scale vegetation responses to abrupt climatic change at Quoyloo Meadow. Due to the existence of a latitudinal vegetation gradient, specific ecological barriers and lower magnitudes of climatic change, Quoyloo Meadow is insensitive in recording centennial-scale vegetation change. It seems likely that this may have a bearing on similar sequences in Ireland (Walker et al., 2012).

10.3.2 Tirinie

In contrast with Quoyloo Meadow, the vegetation responses to abrupt climatic events at Tirinie are the largest observed across the whole transect suggesting that Tirinie is a key location within this thesis. This is demonstrated by the dominant disturbed ground taxa present during the GI-1d and GI-1b-type climatic events and the associated 20 % and 66 % shifts in PC values. It may be that at Tirinie: 1) climatic forcing is felt more than at other sequences, being a high latitude/upland site within Britain; 2) that the vegetation has enhanced sensitivity to climatic change; and/or 3) the persistence and location of residual Dimlington Stadial ice masses had a localised effect (Walker and Lowe, 2017). Firstly, as per Section 9.4.2, the climatic events appear more pronounced at Tirinie than across lower/higher latitude and lower altitude sites; which may represent the greater regional expression of climatic change at 56°N (e.g. Brooks and Birks, 2000a; Candy et al., 2016). Therefore, under greater climatic stressors the environmental response may be more pronounced. Secondly, greater magnitudes of multiple parameter climatic change signify the lack of inertia within the system to buffer against the effects of climatic deterioration, with the crossing of a threshold and vegetation driven to an alternative state (Scheffer et al., 2009). At Tirinie this is evidenced by the pronounced shift in vegetation indicating landscape stability (*Betula*) to vegetation suggesting landscape instability (*Rumex*) and associated changes in sediment input. Being at a relatively high altitude for Britain, it is plausible that, during a climatic event, the physiological parameters of thermophilic taxa may no longer be met (minimum summer/winter temperatures, moisture availability, edaphic state). Therefore, the change in the system may be rapid. For example, the contraction of *Betula*, within the GI-1b event, perhaps indicates the crossing of a threshold, with greater aridity and decreased mean annual and summer temperature driving this change (van Dinter and Birks, 1996). Finally, the proximity of ice during the LGIT (e.g. Hughes et al., 2016) and pre-conditioning of the landscape towards physiologically cooler or cold-adapted taxa may suggest that the

effects of a climatic perturbation would be more clearly expressed in the terrestrial system. Although ice does not encroach into the Tirinie catchment from minimal or maximal reconstructions (Hughes et al., 2016) the proximity of ice to Tirinie may act as an influence on the vegetation response through greater temperature suppression generating a greater response in vegetation.

Analysing the sequences presented within this thesis demonstrates that the area from Tirinie to Whitrig Bog, south-east Scotland (Brooks and Birks, 2000a) exhibit the greatest temperature shifts, indicating that the area between 55-56°N may be a hinge point in Britain. However, vegetation changes at Tirinie are likely not only driven by greater magnitudes of climatic change but also by altitudinal differences where thermophilous taxa are closer to their ecological thresholds generating the rapid and large-scale vegetation shifts (Birks and Birks, 2014).

10.3.3 Palaeolake Flixton

The mode and magnitude of vegetation response is different in north-east England than the higher latitude sites. Principally, revertences are dominated by Poaceae. Whilst other taxa, including *Rumex* and *Artemisia,* are recorded they do not feature as prominently. It is assumed that the different mode of response is a product of the lower magnitudes of climatic change or altitudinal/latitudinal setting, although geological differences (Chapter 3), between regions cannot be excluded. Thus, the vegetation assemblages during phases of climatic deterioration are reflective of a steppic community as Arctic/alpine communities are not recorded at PF. Reduced Arctic/alpine taxa during the LGIT at PF reveal that climatic conditions were not suitable to allow the proliferation of cold-adapted vegetation. The low relief landscape surrounding PF means that altitude would not be a moderating effect on vegetation at this site. The magnitudes of change, as devolved from the PC, are clearly not as great as those from Scotland.

10.3.4 Llangorse

Finally, at Llangorse, the PC reflects variable vegetation signals despite the clear shortcomings within the PC at this site (Chapter 8). For the GI-1d climatic event and the 11.4-11.1 ka climatic event, the PC is more complicated to interpret due to its response to many factors, in itself an interesting difference to the more northerly sites. Nevertheless, for the late WI revertence, Llangorse experiences greater magnitudes of change than PF. Whilst the full expression of the climatic events is unknown, the climatic events appear more muted at Llangorse (Table 10.1), which would affect vegetation response. During climatic deteriorations the vegetation is characterised by the predominance of open habitat grasslands. However, greater landscape instability is

suggested by increased disturbance indicators for the GI-1d-type event. Like PF, no ice is present during the LGIT barring small cirque glaciation at high-altitudes in the Brecon Beacons (Carr, 2001; Bickerdyke et al., 2018), therefore no ice-proximal effects, e.g. katabatic wind influence and temperature suppression (e.g. Muschitiello and Wohlfarth et al., 2015) would affect vegetation. It is therefore postulated that the greater altitude of the site in comparison to PF is a primary reason for more pronounced vegetation change at Llangorse than at PF (GI-1b) despite being at lower latitudes and experiencing more muted climatic variability. Like Tirinie, specific vegetation, e.g. *Betula*, may be closer to ecological boundaries as a result of the higher altitude, affecting the horizontal and vertical distribution of vegetation within the catchment. Following recovery from any climatic deterioration, the re-establishment of *Betula* woodland is rapid, indicating that migration distances are short and that populations of *Betula* persist in the catchment, signifying signs of resilience (Seddon et al., 2016). Therefore, the magnitudes of vegetation response at Llangorse in response to climatic change are largely greater than PF but not as great as Tirinie.

10.4 Regional comparisons to the vegetation proxy data

To highlight regional differences in vegetation, palynological data have been sought from sequences in Europe, from sites that display paired climatic and vegetation reconstructions (Table 10.2). This allows for an understanding of diachronous vegetation development across a wide spatial area. These comparative sequences include: Fiddaun, Ireland (van Asch et al., 2012); Whitrig Bog, south-east Scotland (Mayle et al., 1997); Hijkermeer, The Netherlands (Heiri et al., 2007); Hässeldala Port, southern Sweden (Wohlfarth et al., 2017) with Meerfelder Maar, west Germany (Litt and Stebich, 1999) presented as an auxiliary sequence despite no climatic data (Figure 10.3). While many other sites have been studied across north-west Europe they do not have readily available data from both pollen and climatic proxies and therefore comparisons with additional sequences are not possible. PCs have been applied to these sequences to delineate revertences and to highlight magnitudes of change. Equally, only Hässeldala Port and Fiddaun contain robust chronologies and their placement in relation to other sequences within Figure 10.4 is arbitrary. Therefore, whilst a discussion around the exact timing of the onset of various millennial/centennial-scale revertences is not possible, the patterns of variability can be discussed.

10.4.1 Millennial-scale vegetation comparisons

GI-1/Bølling-Allerød/Windermere/Woodgrange Interstadials

Across all comparative sequences, high *Pinus* percentages at the onset of the Interstadial demonstrate a far travelled component or re-worked pollen from old deposits

(Mayle et al., 1997; Litt and Stebich, 1999; Heiri et al., 2007; van Asch et al., 2012b; Wohlfarth et al., 2017). This compares favourably with observations of *Pinus* at Llangorse. Across all sequences barring, Meerfelder Maar, this *Pinus* phase appears with ameliorating climates (e.g. Mayle et al., 1997; Brooks and Birks, 2000a; Heiri et al., 2007; van Asch et al., 2012b; Wohlfarth et al., 2017) or warm summers (e.g. Heiri et al., 2007). As no quantified temperature data exists for Meerfelder Maar this is difficult to elucidate. However, Litt and Stebich (1999) in their original investigation, placed the *Pinus* zone in the Pleniglacial phase suggesting cool stadial climates.

Throughout the Interstadial, vegetation reconstructions diverge (Chapter 2). In Germany, The Netherlands, and Sweden the vegetation assemblages are dominated by *Betula* and *Betula*/*Pinus* woodland. Variations in woodland extent are noted, a product of regional variations in dominant climatic conditions, variable migration, soil conditions and taxon competition (Walker et al., 1994). The greatest extent of woodland appears in the central lowlands of the Netherlands (Heiri et al., 2007) reflective of earlier migration from refugial positions in central Europe (Willis et al., 2000). In contrast to vegetative development across Europe, the early Interstadial across Britain is defined by the development a steppe-like vegetation assemblage (Chapters 5 to 8) with *Betula cf. nana* at Quoyloo Meadow, Tirinie, Palaeolake Flixton, Llangose and Whitrig Bog (Mayle et al., 1997) with a co-development of *Juniperus* and *Empetrum* scrubland (Mayle et al., 1997; van Asch et al., 2012a). In contrast to sequences in Europe, *Betula* woodland is variable in time and space in Britain during the Interstadial, reflecting lags in vegetation development and migration across Europe (Pennington, 1986). In Ireland minimal *Betula* woodland is observed, which in the past has been suggested to relate to the influence of mega-fauna (Bradshaw and Mitchell, 1999). Furthermore, phases of greatest woodland development, as defined by the PCs, is variable across Europe (Figure 10.4). At Meerfelder Maar and Hijkermeer, peak PC values are defined by high *Betula* and *Pinus* percentages at the end of the Interstadial; reflective of the development of a mixed *Betula*/*Pinus* woodland (Litt and Stebich, 1999; Heiri et al., 2007; Wohlfarth et al., 2017). Equally, greatest woodland development at Whitrig Bog occurs during the mid-Interstadial but following a contraction, re-expands during the late Interstadial. This reflects an intermediary site between the high and low latitude sequences presented within this thesis, and arguably similar to the PC trends identified at Hässeldala Port and the *Betula* curve at Thomastown Bog (Turner et al., 2015).

The differential progression of the Interstadial across Europe has been noted by Moreno et al. (2014) who suggest different responses of variables related to climate and the biosphere. Moreno et al. (2014) note a difference in GI-1 records including a north-south

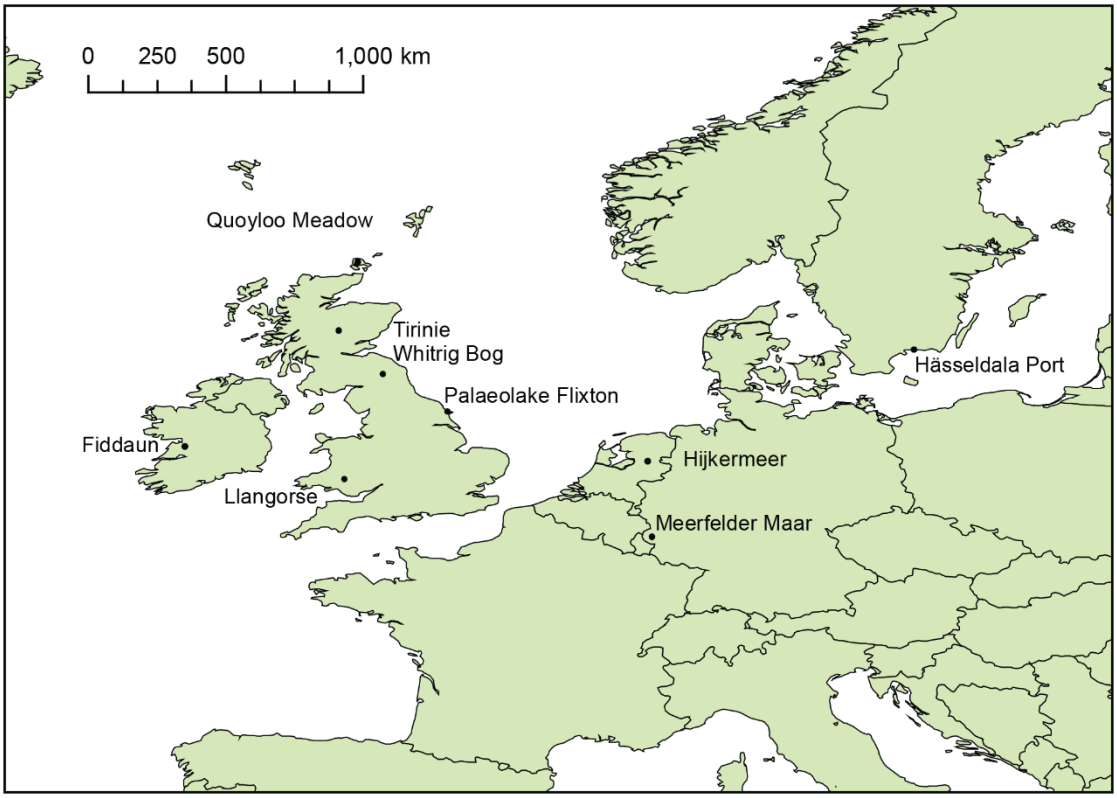

Figure 10.3 The series of sites across Britain and Europe used for comparison with sequences presented in this thesis. Sites presented in Chapters 5-8 are also shown.

difference between temperature variability but do not suggest latitudinal changes in relation to vegetation development. With the additional data presented in this thesis, it is possible to theorise latitudinal shifts, at least in vegetation development, and to use the evidence presented in Moreno et al. (2014) to support these inferences alongside other detailed data from Norway (Birks et al., 2014) (Figure 10.5). Locations south of Whitrig Bog and Hässeldala Port seem to display continuously increasing woodland development and landscape stability throughout the Interstadial (including $\delta^{13}C$ records of soil microbial activity in Chauvet and El Pindal cave systems (Genty et al., 2006; Moreno et al., 2010)). These developments have been shown in southern Europe to track summer insolation (Genty et al., 2006; Samartin et a., 2012b), although added complexity has been shown by Lotter et al. (2012). Whitrig Bog and Tirinie display an expansion of woodland (*Betula*) and a revertence towards the end of the Interstadial. Sites further north (Kråkenes and Lustvatnet) have negligible responses to Interstadial warming (Birks and Birks, 2014; Birks et al., 2014) and are seemingly insensitive to changes identified here. In this sense Quoyloo Meaodow appears transitional between mainland Scotland and Norway as it only has muted scrubland development. It should be noted that this apparent latitudinal gradient (Figure 10.5) applies differently to Ireland and although a two-part trend can be identified (similar to Tirinie) it seemingly occurs at an earlier stage (Figure 10.4).

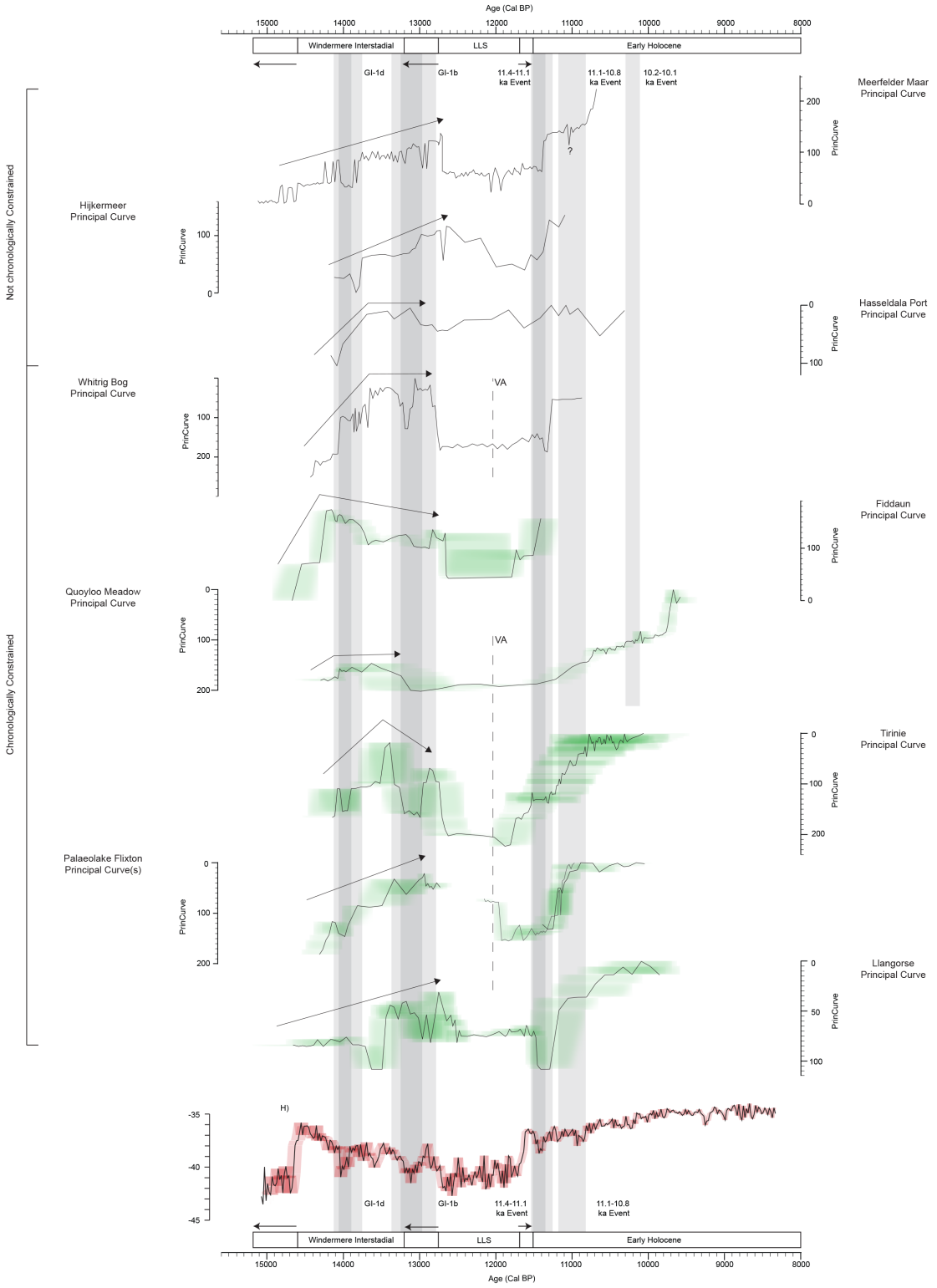

Figure 10.4 Comparisons of the Principal Curve (PC) applied to the pollen data from the British Isles and Europe for Meerfelder Maar (Litt and Stebich, 1999); Hijkermeer (Heiri et al., 2007); Whitrig Bog (Mayle et al., 1997); Fiddaun (van Asch et al., 2012a), Quoyloo Meadow, Tirinie, Palaeolake Flixton and Llangorse. Also shown is the NGRIP ^{18}O stratigraphy (Rasmussen et al., 2014) converted to a calendar timescale. The top three PCs contain no chronology and are placed against NGRIP arbitrarily. The timing and synchroneity of these records cannot therefore be directly compared to the other records and is compiled for illustrative purposes only. The arrows show directional vegetation development as defined by the PC. Shown in grey are the climatic events within Greenland with light grey shading applied to encapsulate the duration of vegetation response.

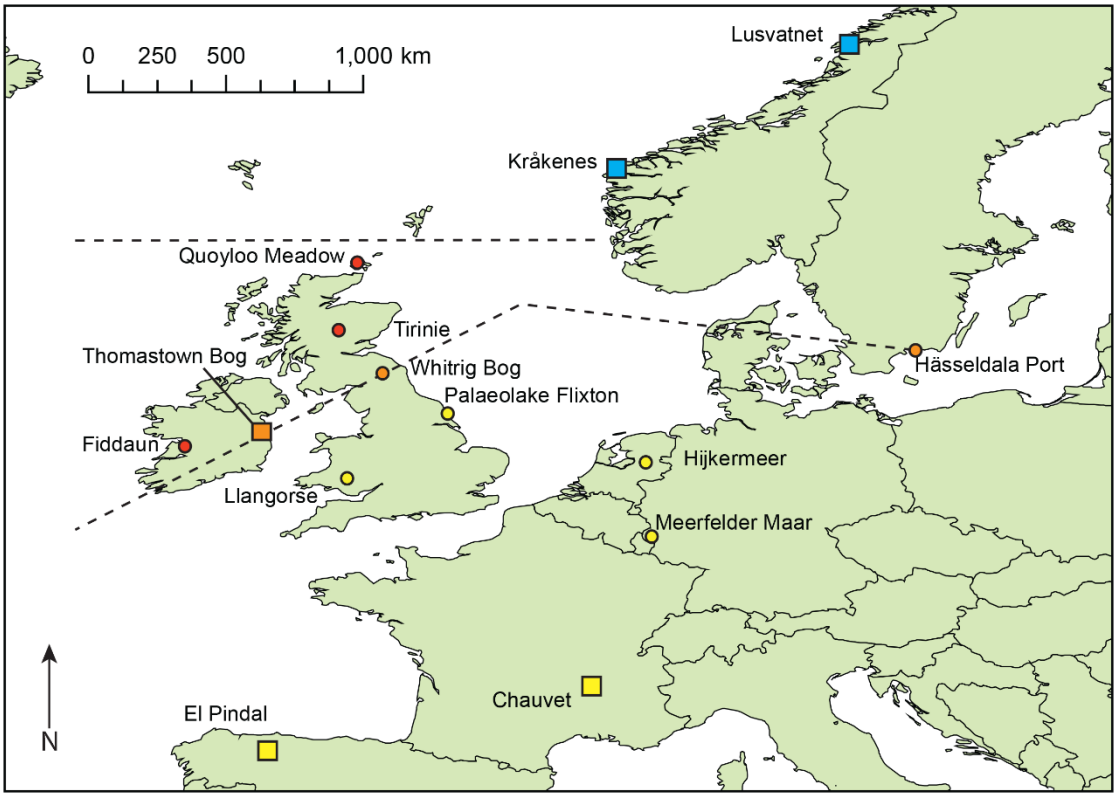

Figure 10.5 Shown here is a broad zonation of millennial-scale vegetation development during GI-1. Boxes highlight data from previously published studies (Birks et al., 2000; Birks et al., 2014; Moreno et al., 2014; Turner et al., 2015) whilst circles show data generated in this thesis or uses published data modelled along a principal curve. The dashed lines show the approximate divisions across Europe for GI-1 millennial-scale development. Southern latitudes in Britain and Europe (yellow) show woodland vegetation development during the Interstadial; sites sitting on this line (orange) show similar vegetation development between the mid-late Interstadial; above this line (red) shows woodland vegetation development during the mid-Interstadial; above the northern most line (blue) reveals negligible vegetation development during GI-1.

Nonetheless, it may be that westerly European locations became more sensitive to millennial-scale climatic change during the Interstadial when compared to continental settings. As the lower latitude changes are shown to track insolation (Genty et al., 2006), which would equally apply to the northern sites, this raises the intriguing issue of what might lead to these changes. Birks and Birks (2014) propose that Interstadial trends may reflect site internal factors alongside moisture availability rather than summer temperature variations. The data generated here would not support the moisture availability assertion suggested by Birks and Birks (2014) as this does not match with sites next to the moisture source being more preferentially affected, whilst the biomarker isotopic data presented at Tirinie and Quoyloo Meadow suggests a relatively humid end to the Interstadial. It is perhaps more likely that shifts in mean annual temperature are more important, filtered by antecedent conditions and the magnitude of identified climatic shifts. This is equally postulated as for what drives the increase in *Pinus* in Europe (Lotter et al., 2012). The magnitude and impact of the GI-1b-type event is also striking, as at

Tirinie, it coincides with a contraction of woodland which does not recover. The scale and impact of short-lived events are therefore also seen as important for millennial-scale variability.

GS-1/Younger Dryas/Loch Lomond/Nahanagan Stadial

The transition into the Stadial is shown in all vegetation reconstructions by a loss in woodland vegetation and an expansion of herbaceous taxa. At Meerfelder Maar, a contraction of *Betula*/*Pinus* woodland is noted with an increase in herbaceous species including Poaceae and Cyperaceae with heliophilous taxa including *Artemisia*, *Rumex* and *Helianthemum* reflecting the deterioration of climatic conditions. Within the PC this is manifest by a 35 % shift to lower values. A larger percentage shift is observed at Hijkermeer, 51 % (Figure 10.4; Figure 10.7). At Hässeldala however the PC does not adequately define the Stadial. It is possible that a 38 % change may define the Stadial at ca 13.1 Cal. ka BP. However due to insufficient sample resolutions this is difficult to ascertain. When compared to sequences in Britain differences are observed. Fiddaun is comparable to the shifts identified at Hijkermeer, 50 %, whilst Whitrig Bog experiences a 66 % shift.

Climatic deteriorations exhibit variable magnitudes across Europe, with the greatest climatic deteriorations observed in northern Europe and Britain (Chapter 9). It is plausible that vegetation responds in a linear manner to Stadial cooling, with a greater abundance of Arctic tundra vegetation observed in northern latitudes. Reduced magnitudes of climatic change can further explain the vegetation mosaic across Europe, as both high and low-altitude settings reveal tree birch (*Betula pubescens* macrofossils at Meerfelder Maar for example; Litt and Stebich, 1999) and *Pinus* during the Stadial (Heiri et al., 2007; Wohlfarth et al., 2017). Continued *Betula* populations suggest that ecological thresholds were not crossed during the Stadial at European sequences (e.g. Heiri et al., 2007). Indeed temperatures greater than 12°C, the thermal limit for tree birch (van Dinter and Birks, 1996), were maintained throughout. In contrast, the Stadial vegetation assemblage at Fiddaun and Whitrig Bog is dominated by *Artemisia*, *Thalictrum* and Caryophyllaceae (Mayle et al., 1997; van Asch et al., 2012a). The magnitudes of change at Fiddaun appear comparable to Hijkermeer, despite the lack of trees. This is perhaps due to greater abundances of Arctic tundra taxa. Thus, although the nature of vegetation change is different the magnitude is similar. Further, at Whitrig Bog, the vegetation shifts from a *Juniperus* scrub/open *Betula* woodland, to open herbaceous vegetation with *Betula nana* during the Stadial (Mayle et al., 1997). Hence a greater magnitude of vegetation response to Stadial cooling at Whitrig Bog considering antecedent vegetation.

The magnitudes of change across the European continent are agreeable with Tirinie (48 %); PF (41 %); Quoyloo Meadow (15 %) and Llangorse (48 %) (Figure 10.6). Whilst climate is a key control on the magnitude of vegetation change (stronger in high-latitudes) the greatest control is the status of antecedent vegetation prior to the vegetation revertence. It might be expected that PF and Llangorse would reveal the greatest magnitudes as a result of birch woodland during the late Windermere Interstadial. However, at both sequences there are local influences that influence the PC, including the hiatus in the PF record and the proposed presence of dwarf birch at Llangorse. The PC values are therefore not representative. Therefore, of all sequences analysed Whitrig Bog reveals the greatest magnitudes of change for the Stadial despite absolute temperatures being higher than further north (above 7.5°C). The latitudinal position of Whitrig Bog appears optimal in delimiting magnitudes of vegetation change at the transition between the Interstadial and the Stadial where the influence of local effects are negligible. This interpretation also supports the assertion by Walker and Lowe (2017) that Whitrig Bog may form a stratotype for the LGIT in Scotland as it is preferable to identify sites which delimit key changes in this period.

Early Holocene

The transition out of the Stadial into the early Holocene is revealed across Europe by a contraction of herbaceous populations and an expansion of scrub and woodland vegetation including *Juniperus*, *Betula* and *Pinus*. As aforementioned, in Britain and Ireland the vegetation dynamic is first shown by grassland which is successively replaced by *Juniperus*/*Empetrum*, *Betula* and *Corylus*, reflecting a succession from grassland to open *Corylus* woodland (e.g. Walker and Lowe, 2017). Locations that maintain elements of a birch/pine woodland during the Stadial appear to experience an earlier expansion of woodland taxa (chronological uncertainties notwithstanding). Unfortunately, many of the sequences presented here are curtailed during the early Holocene. A result of researcher aims and project goals signifying that the dynamics of early Holocene vegetation may be missed, either due to this cessation of study or because the sampling strategy is insufficient.

10.4.2 Centennial-scale vegetation revertences

GI-1/Bølling-Allerød/Windermere/Woodgrange Interstadials (GI-1d climatic event)

Similar to vegetation revertences identified across Britain, an early Interstadial revertence can be identified across many European sequences. Whilst the chronology is insufficient to define their precise onset/termination, this early Interstadial revertence is correlated with the GI-1d, Aegelsee, or Older Dryas phase (Chapter 2). At Meerfelder Maar, the most southerly site included in this comparison, the vegetation is dominated

by a species rich grassland, with Poaceae, *Artemisia* and *Thalictrum* (Litt and Stebich, 1999). At Hijkermeer, this phase is dominated by Cyperaceae, Poaceae, *Artemisia* and *Juniperus* (Heiri et al., 2007). Whilst it cannot be ascertained as to whether the lowest samples equate to GI-1d, at Hässeldala Port high percentages of *Artemisia* and Poaceae suggest a cold event. Whitrig Bog and Fiddaun display a similar style of vegetation revertence with losses of *Juniperus* and *Betula cf. nana* respectively with increases in Poaceae, Cyperaceae, *Rumex* and *Artemisia* (Mayle et al., 1997; van Asch et al., 2012a). Across Europe therefore this event is manifest by an opening of the landscape with a greater abundance of open vegetation types.

The magnitude of the palynological revertence is shown by a 38 %, 20 %, 13 % and 19 % shift in the PC from Meerfelder, Hijkermeer, Fiddaun and Whitrig Bog respectively (Figure 10.6). The strongest climatic deteriorations for this event are observed in Britain, (Figure 10.5; 10.6; 10.5), thus it might be expected that the greater magnitudes of palynological change would be largest in Britain, specifically eastern England and Scotland (Figure 10.6). However, this is not observed, and compared favourably to the 3 %, 20 %, 15 % and 8 % magnitudes of change identified at Quoyloo Meadow, Tirinie, PF and Llangorse respectively (Figure 10.6). As the climatic deteriorations are of lower magnitudes in mainland Europe, antecedent vegetation and sensitivity are perhaps more important in the vegetation response. At this time in Europe, owing to the pace of vegetation migration and following the establishment of mature soils (e.g. Pennington, 1986), vegetation is later successional with a shrub landscape and *Betula* (both prostrate and tree); which is contrasted with Britain, where vegetation is predominantly pioneering and has a wider ecological tolerance through its Arctic tundra associations (Lowe and Walker, 1986; Walker et al., 1994; Mayle et al., 1997; van Asch et al., 2012a). Therefore, the expression of this event is largely dependent on the successional stage. Whilst climate ultimately drives this change, it is apparent that location and ecological tolerances are more important when understanding the style of vegetation response.

GI-1/Bølling-Allerød/Windermere/Woodgrange Interstadials (GI-1b climatic event)

In contrast with the early Interstadial, the later Interstadial vegetation revertence is variably represented. Across mainland Europe, the vegetation is predominantly composed of a mixed *Betula*/*Pinus* woodland during the late Interstadial. To regress this woodland towards open environments, the magnitude of climatic forcing has to be large due to the wide ecological tolerances of *Pinus* (Hoek and Bohncke, 2001). As a result, generally, only slight increases in grassland taxa are noted. At Hijkermeer however, the GI-1b-type climatic deterioration occurs prior to the increase in *Pinus*, with its proliferation attributed to cooler winter temperatures and reduced drought stress (Tinner and Lotter,

2001; Heiri et al., 2007). Thus, vegetation gradients clearly exist across mainland Europe, with variable *Pinus* woodland and open grassland conspicuous with the late Interstadial climatic event. This revertence style is contrasted with Britain whereby losses in tree birch (predominantly dwarf birch in Ireland) and *Juniperus* are replaced with Poaceae and Cyperaceae (Mayle et al., 1997; van Asch et al., 2012a). Vegetation gradients are also present within Britain, whereby higher altitude sites display a greater presence of disturbed ground taxa (*Rumex* at Tirinie) whilst lower latitude sites are dominated by an open grassland. Fiddaun and Whitrig Bog (both lower altitudes) do not display an increase in *Rumex* during the late Interstadial event, suggesting that an altitudinal control exists with the nature of vegetation replacement.

The magnitudes of this revertence as recorded by the PC are 19 %, 18 %, 15 %, 35 % at Meerfelder Maar, Hijkermeer, Fiddaun and Whitrig Bog respectively compared with the percentage change at Tirinie, PF and Llangorse (66 %; 17 % and 38 %) (Figure 10.6). From this analysis, the magnitudes of the revertence in continental Europe are smaller when compared to the early Interstadial vegetation revertence (Figure 10.6). This highlights two key differences between British and European records; that vegetation revertences in response to the local expression of the GI-1b-type climatic event in Britain exhibit greater magnitudes than associated responses to the GI-1d-type climatic event whilst the opposite is true in continental Europe. This is surprising given the larger amplitudes of summer temperature change in association with the GI-1b-type climatic event across continental Europe than the GI-1d event (Heiri and Millet, 2005; Heiri et al., 2007; Figure 10.6). It is unknown whether this can be observed in oxygen isotopic profiles owing to the lack of records with sufficient sampling resolutions and sufficient chronologies. Nonetheless, much like phases associated with woodland development, the magnitude of climatic change cannot fully explain the magnitude of inferred vegetation revertence. Therefore, it may be possible that antecedent vegetation is the dominant control on magnitudes of the palynological response; or that a secondary climate parameter controls vegetation change which is diachronous between Britain and Europe.

The former scenario offers the simplest explanation as the establishment of a dense *Betula*/*Pinus* woodland; with *Pinus* containing wider ecological tolerances being a more continental taxon (Bohncke, 1993), will be more resistant to change in Europe during the GI-1b climatic event, as evidenced by the continued presence of *Pinus* in Europe during the Younger Dryas Stadial, a phase where temperatures were severely depressed and lower than climatic deteriorations during the Interstadial (Figure 10.8). This is best evidenced a Hijkermeer where Pinus was promoted during the climatic event (Tinner and

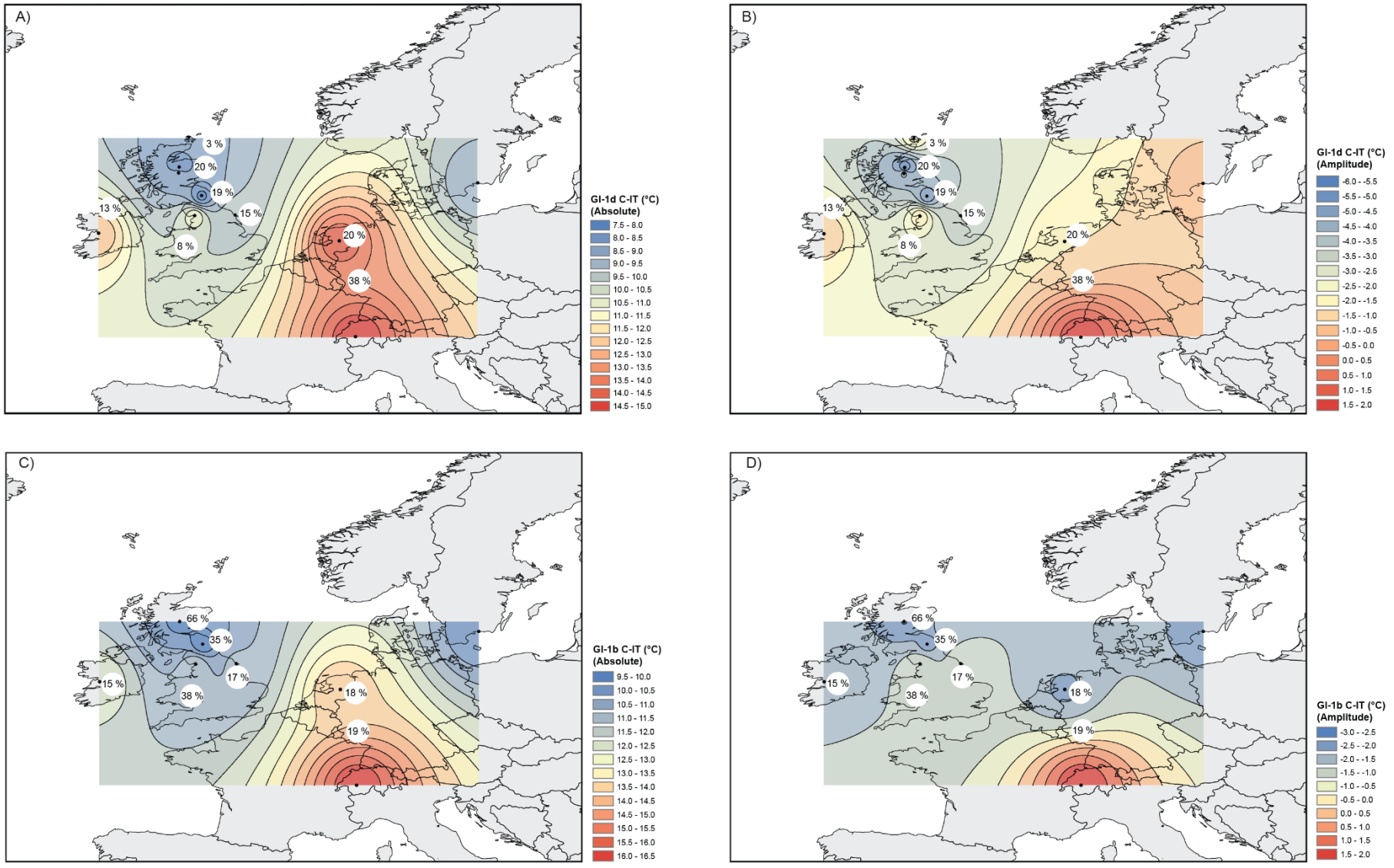
A)
3 %
20 %
19 %
13 %
15 %
20 %
8 %
38 %
GI-1d C-IT (°C)
(Absolute)
7.5 - 8.0
8.0 - 8.5
8.5 - 9.0
9.0 - 9.5
9.5 - 10.0
10.0 - 10.5
10.5 - 11.0
11.0 - 11.5
11.5 - 12.0
12.0 - 12.5
12.5 - 13.0
13.0 - 13.5
13.5 - 14.0
14.0 - 14.5
14.5 - 15.0
B)
3 %
20 %
19 %
13 %
15 %
20 %
8 %
38 %
GI-1d C-IT (°C)
(Amplitude)
-6.0 - -5.5
-5.5 - -5.0
-5.0 - -4.5
-4.5 - -4.0
-4.0 - -3.5
-3.5 - -3.0
-3.0 - -2.5
-2.5 - -2.0
-2.0 - -1.5
-1.5 - -1.0
-1.0 - -0.5
-0.5 - 0.0
0.0 - 0.5
0.5 - 1.0
1.0 - 1.5
1.5 - 2.0
C)
66 %
35 %
17 %
15 %
38 %
18 %
19 %
GI-1b C-IT (°C)
(Absolute)
9.5 - 10.0
10.0 - 10.5
10.5 - 11.0
11.0 - 11.5
11.5 - 12.0
12.0 - 12.5
12.5 - 13.0
13.0 - 13.5
13.5 - 14.0
14.0 - 14.5
14.5 - 15.0
15.0 - 15.5
15.5 - 16.0
16.0 - 16.5
D)
66 %
35 %
15 %
17 %
38 %
18 %
19 %
GI-1b C-IT (°C)
(Amplitude)
-3.0 - -2.5
-2.5 - -2.0
-2.0 - -1.5
-1.5 - -1.0
-1.0 - -0.5
-0.5 - 0.0
0.0 - 0.5
0.5 - 1.0
1.0 - 1.5
1.5 - 2.0

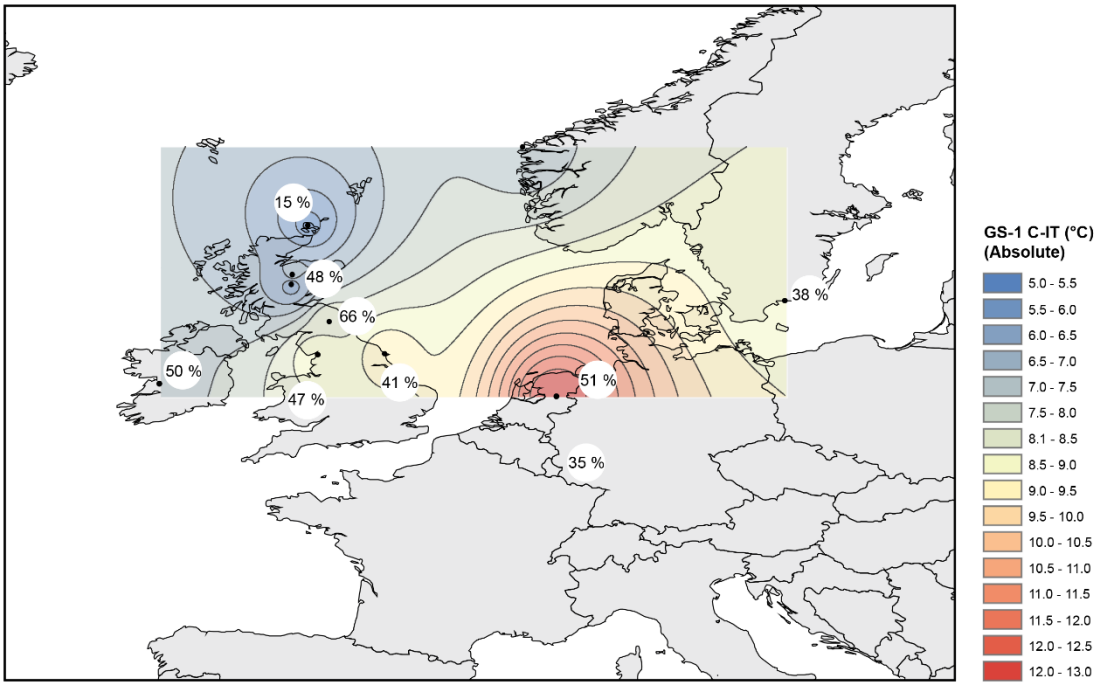

Figure 10.7 Inverse Distance weighted model of absolute C-IT values in close association with the Vedde Ash (12,023±43 Cal. BP; Bronk Ramsey et al., 2015) (As Figure 9.8). Superimposed on the model is the percentage change associated with the PC from preceding Interstadial values to vales reported during the Stadial.

Figure 10.6 (Page 368) Inverse Distance weighted models of absolute values and amplitudes of summer temperature change in Britain and Europe for the GI-1d and GI-1b climatic events (As Figure 9.6). Placed on this figure are percentage change associated with the PC curve for each of the climatic deterioration episodes. The graphs have been duplicated for absolute and amplitudes of summer temperature change.

Lotter, 2001), although the climatic deterioration was insufficient to generate a tundra community like the GI-1d and Stadial events. In Britain, although tree birch is evidenced during the mid-Interstadial, it is less resistant to climatic change. Furthermore, despite larger magnitudes for the GI-1b-type event in Europe, summer temperatures remained above 12°C, which is argued as the summer thermal limit for tree birch (van Dinter and Birks, 1996). Therefore, as the temperature threshold was not crossed, and due to local vegetation development (*Pinus*), vegetation appears more sensitive in Britain for the GI-1b event and possibly analogous to the vegetation assemblage in Europe during the early Interstadial.

Alternatively, additional climatic parameters may influence vegetation at each site. For example mean annual temperatures, seasonality and moisture availability may be more important (Birks and Birks, 2014). However, in continental Europe, a lack of suitably resolved paired isotopic and summer temperature records preclude an assessment of seasonality (e.g. Lotter et al., 1992; van Asch et al., 2013) and mean annual change. Equally, at Tirinie, a greater phase of aridity during the GI-1b event is postulated through

biomarker isotopic data, which suggests greater magnitudes of hydrological change in Britain. It is unknown whether this aridity phase is replicated across Europe owing to the paucity of biomarker studies. However, data from Meerfelder Maar and Hässeldala Port show evidence for a period of heightened aridity across Europe during the Gerzensee event (Rach et al., 2014; 2017; Muschitiello et al., 2015). Observations of aridity contradicts Birks and Birks (2014) assertion that moisture availability is the controlling factor for vegetation, as one might expect to observe similar vegetation responses in continental Europe and Britain. Therefore, it is more probable that successional stage and antecedent conditions result in the variable magnitudes of response across Europe, despite changes in the dominant climatic regime being the most likely control.

Stadial and early Holocene vegetation variability

Whilst climatic changes are well-recorded during the mid-Stadial (e.g. Bakke et al., 2009; Lane et al., 2013) vegetation responses are less well-understood. It has been shown that at PF, Tirinie and Quoyloo Meadow, potential vegetation responses occurred during the Stadial coinciding with lake level variability. However, with additional data from comparative sites, no vegetation variability is noted.

As stated previously many vegetation reconstructions do not continue into the Holocene and the direct impact of climate on vegetation remains largely unknown. As one of the aims of this thesis was to better understand variability between the Interstadial-Stadial-Holocene, this aim cannot be fully realised across the comparative sequences. Whilst poor chronologies exist, it is unlikely that the Whitrig Bog and Fiddaun records extend sufficiently into the Holocene, and the temporal resolution of Hässeldala Port is not sufficient to detect centennial-scale change. Therefore, Meerfelder Maar and Hijkermeer offer the only suitable records for comparison.

During the early Holocene at Meerfelder Maar, one revertence is identified, characterised by a decline in *Pinus* and an increase in *Betula*. Normally, chronological control during the early Holocene is difficult to achieve, however the deposition of the Ulmener Maar Tephra (UMT) (11 ka BP; Brauer et al., 1999) sits above this revertence, and it is likely that the event is comparable to either the 11.4 ka event in Greenland, or the 11.1 ka BP event identified across other European sequences (Figure 10.4; Blockley et al., 2018; Fiłoc et al., 2018) or the combined Pre-Boreal Oscillation (PBO) in Europe (e.g. Björk et al., 1997). A similar trend is observed at Hijkermeer where one single sample reversion of *Betula* may align with two depressions in summer temperature during the earliest Holocene (Heiri et al., 2007). Summer temperature declines are noted in Britain, albeit for PF only, however, *Betula* and PC variability appear to be comparable across Europe,

Figure 10.8 Demonstrating on a European map the percentage change in the PC for the 11.4-11.1 ka BP climatic deterioration during the earliest Holocene. No climatic data exists to show how climatic change across Europe. However, the greatest changes can be observed in Europe and the high latitudes of Britain. Only four data points exist for this revertence owing to the lack of complete coverage during the LGIT.

albeit higher in lower latitude sites (Figure 10.8). The Holocene is therefore a period that has not received adequate attention in previous studies, which needs addressing to better understand regional vegetation development.

10.5 Event phasing and lead/lag relationships

Through the collection of both high-resolution climatic and high-resolution vegetation data it is possible to look at the anatomy of individual climatic events and vegetation revertences. Unfortunately, this is not possible at Llangorse as due to the current sampling resolution it is unknown whether the onset of climatic change or vegetation revertences have been missed. It is also not possible to fully explore WI event phasing at Quoyloo Meadow due to the lack of oxygen isotopic data, the low-resolution summer temperature data, and the low magnitudes of vegetation shifts. Therefore, event phasing is presented for Tirinie and Palaeolake Flixton only. Greater value is gained from assessing the phase relationships at these sequences as all palaeodata has originated from the same stratigraphic sequence, which from available evidence is one of the few times this has been attempted in the LGIT in Britain. Whilst the chronological error of sample points is acknowledged, the drivers and responses are clearly disjunct as they

occur at different points in the stratigraphy. Thus, the decision to present data against age is valid, and although absolute chronological differences between samples may not be secure, greater meaningful value is gained from this approach.

Windermere Interstadial

Figure 10.9 and 10.10 detail the phasing of different climatic parameters and vegetation responses during the LGIT at Tirinie and PF. For the early Windermere Interstadial event associated with GI-1d in Greenland, depicted chronologically between 14.14-13.73 Cal. ka BP the onset of isotopic depletion at Tirinie, taken to reflect the onset of mean annual cooling occurs at 14.06 Cal. ka. BP (Figure 10.9). Whilst at PF this occurs at 14.14 Cal ka BP (details for this discrepancy in Chapter 9) (Figure 10.10). The onset of summer temperature change and aridity at Tirinie occurs at 14.03 Cal. ka BP, with the difference between mean annual and summer temperature change not too dissimilar at PF, ca 14.10 Cal. ka BP (Figure 10.9; 10.10). Therefore, in both sequences, annual or seasonal climatic deterioration occurs before summer temperature change and concurrent shifts in aridity. The bifurcation of the climate system is therefore clear which is only elucidated following multi-proxy climatic approach. In conjunction with changes in summer temperature and aridity, vegetation changes occur. Therefore, vegetation lags initial seasonal/mean annual temperature change, by ca 30 years at Tirinie and 40 years at PF (Figure 10.9; 10.10); but appear in phase with summer temperature and aridity fluctuations. The shorter lag at Tirinie, albeit marginal, may be the result of greater magnitudes of climatic change, but also the vegetation perhaps being more pioneering/early successional in nature. Further, the collection of multi-parameter climatic data indicates that centennial-scale vegetation changes, associated with GI-1d, are driven by a conflation of the climatic system once all climatic parameters are in accordance, with greater change following the crossing of a physiological threshold, or that vegetation is pre-conditioned to change following the onset of mean annual temperature declines. Only after the change in vegetative state does fire become locally important.

The late Windermere Interstadial event (GI-1b), between 13.45-12.8 Cal. ka BP, exhibits isotopic depletion at 13.45 Cal. ka BP at Tirinie, reflecting the onset of annual temperature change. Like the former climatic event, the onset of depletion in δD_{aq}, largely tracks $\delta^{18}O_{carb,}$ suggesting cooling and drying at 13.37 Cal ka BP. This is then succeeded by summer temperature change and a strengthening of $\delta^{18}O_{carb}$ and δD_{aq} depletion at 13.26 Cal. ka BP (Figure 10.9). Here vegetation revertences appear between the onset of mean annual temperature change and depletion in δD_{aq}. Vegetation changes appear, in this instance, to be driven by greater mean annual change (seasonality) which are

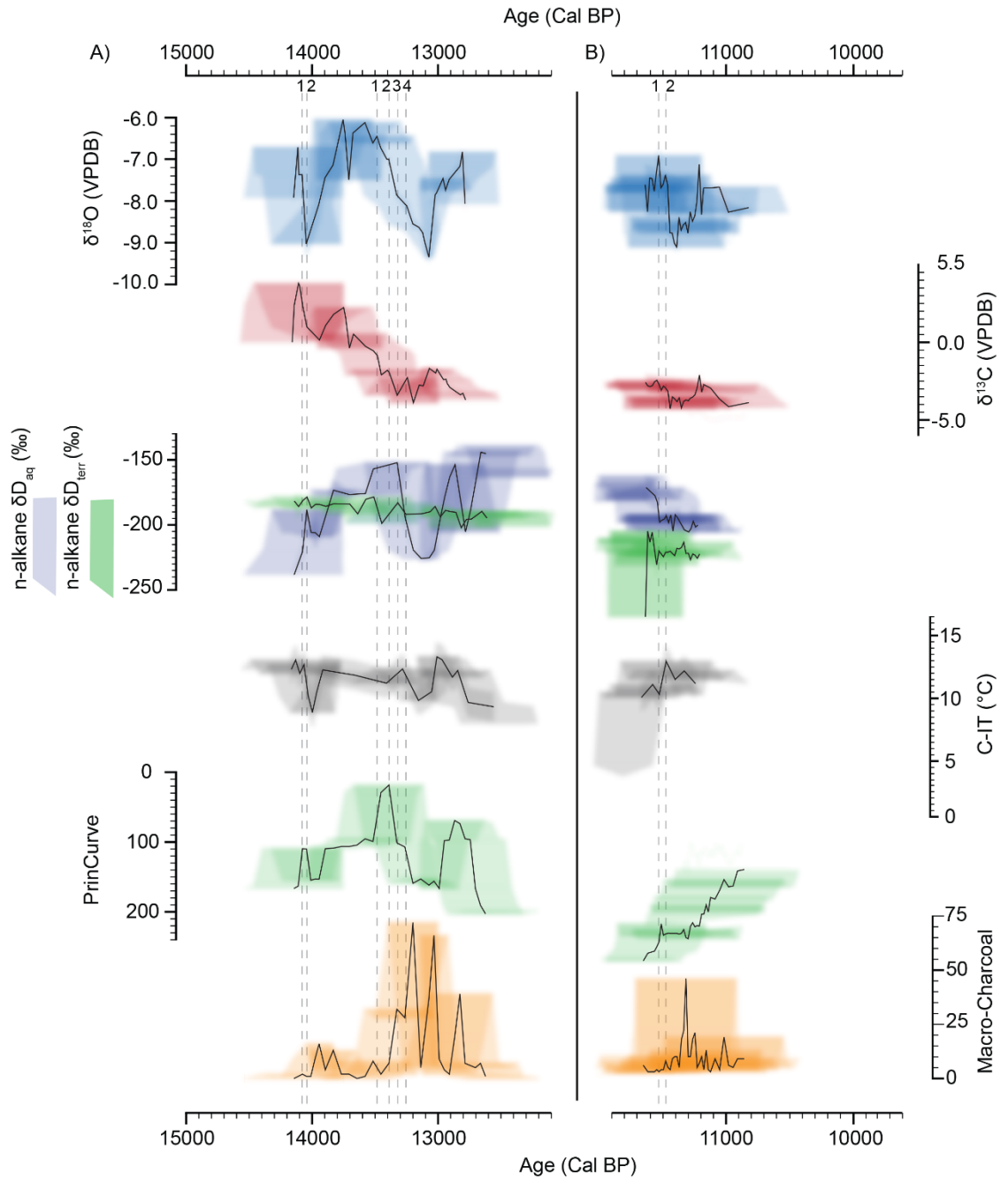

Figure 10.9 All climatic and vegetation data from Tirinie presented against age to highlight the phasing between climatic drivers and vegetation response. A) Event phasing during the Windermere Interstadial and B) event phasing during the Holocene. Numbering has been applied to represent changes in individual climatic parameters. 1) the onset of oxygen isotopic depletion; 2) the onset of the vegetation revertence; 3) the onset deuterium isotopic depletion; and 4) changes in summer temperatures. Where shifts are coeval multiple vertical lines have not been added.

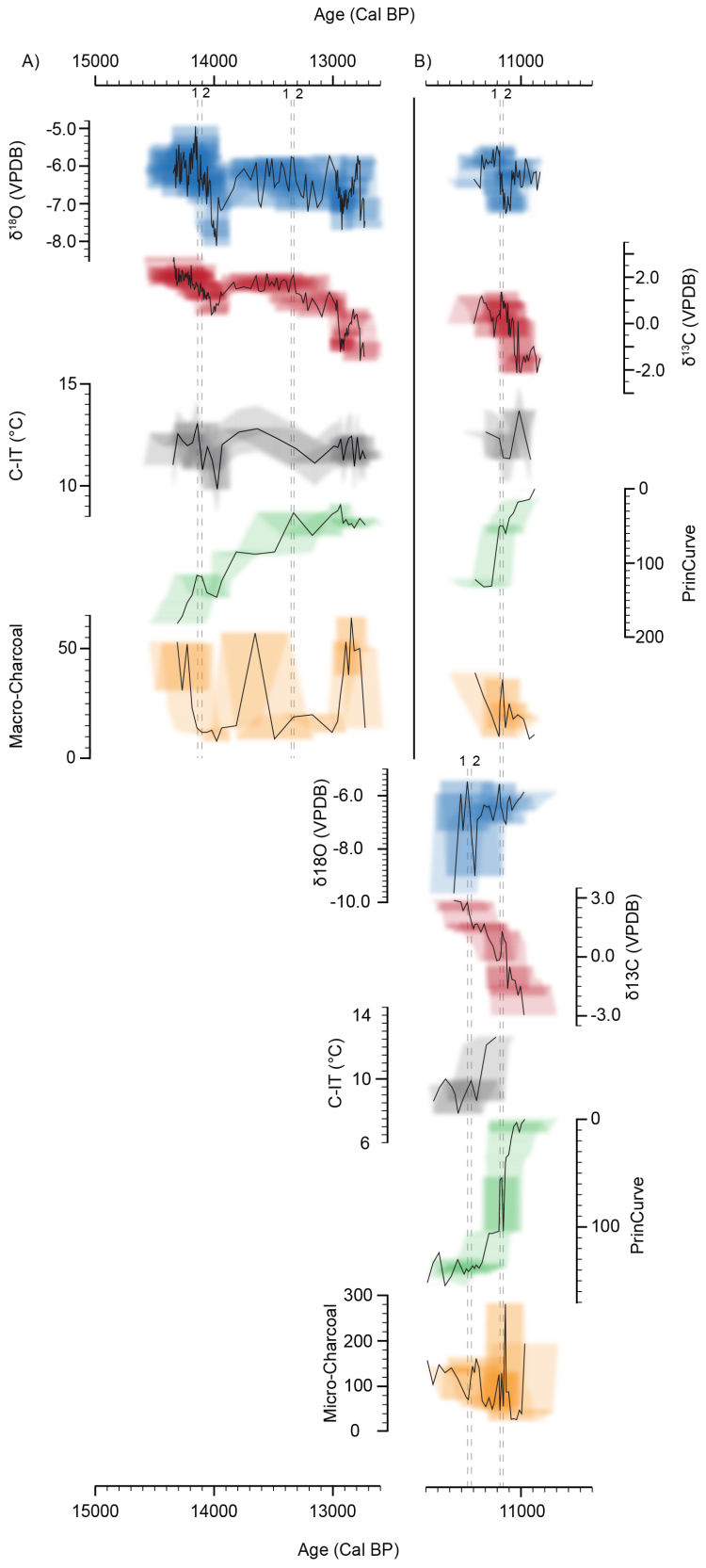

Figure 10.10 All climatic and environmental data from Palaeolake Flixton presented against age to highlight the phasing between climatic drivers and environmental response. A) Event phasing during the Windermere Interstadial and B) event phasing during the Holocene. As 10.8 numbering relates to shifts in different climatic parameters. 1) the onset of oxygen isotopic depletion; 2) the onset of vegetation revertences and other associated palaeocliamtic changes; where events occur at the same time, multiple vertical lines have not been added.

subsequently enhanced by shifts in aridity and summer temperature variability. This trend agrees with the assertion that annual temperature change is important for millennial-scale variability. Vegetation responses therefore lag the onset of climatic deterioration by ca 90 years, some 60 years longer than the GI-1d event. Whilst the magnitudes of climatic change are reduced for the GI-1b event, it is likely that *Betula* continued to persist on the landscape until the deterioration surpassed the physiological threshold for birch, only then was the change in *Betula* rapid. At PF the onset of climatic deterioration for the late Windermere Interstadial event occurs at 13.35 Cal. ka BP (Figure 10.10). Whilst the reduced resolution C-IT data cannot be used to infer the onset of summer temperature decline it is likely that the record closely resembles Tirinie. Equally, increased summer temperature decline occurs in association with the period of maximal isotopic depletion, between 13.21-13.15 Cal. ka BP. Vegetation change occurs at 13.31 Cal. ka BP (Figure 10.10). Thus, in contrast to Tirinie, the lag in vegetation response is similar to the GI-1d type event despite reduced climatic magnitudes which relates to the lower magnitudes of vegetation change and the nature of vegetation replacement (Section 10.2.3). Nonetheless, again changes are postulated to relate to the surpassing of ecological thresholds, with the transition in *Betula* occurring after a shift towards lower temperatures (van Dinter and Birks, 1996). It is therefore reasonable to assume that at Palaeolake Flixton mean annual and summer temperature change exert an element of control over the vegetation mosaic although the influence of hydrological parameters, cannot be attested for at this stage. Generating greater biomarker records from across Britain should be a research priority.

Early Holocene

During the Holocene, across both Tirinie and PF palynological lags are comparable to the early Windermere Interstadial event (Figure 10.9; 10.10). $\delta^{18}O_{carb}$ depletions occur at 11.49 Cal. ka BP at Tirinie, with δD_{aq} depletion occurring ca 50 years earlier. At PF (second Holocene event) $\delta^{18}O_{carb}$ depletion and summer temperature change occurs at ca 11.18 Cal. ka BP. The responses at Tirinie appear to closely parallel the depletion in δD_{aq} but also occur with enhanced $\delta^{18}O_{carb}$ depletion (Figure 10.9). Despite reduced magnitudes of climatic change, the shorter lag highlights both the reduced magnitudes of palynological change but also the state of vegetation prior to this shift, largely being dominated by open herbaceous taxa similar to that of the early Windermere Interstadial. At PF the vegetation appears to lag the onset of isotopic depletion by ca 35 years (Figure 10.10). This lag is comparable to the Interstadial events, which is surprising given low magnitudes of climatic change. Minimal summer temperature change during the early Holocene suggests that, at least during the early Holocene, vegetation responses may be a product of changes in aridity. The onset of the change in aridity, which is shown to

occur prior to any additional climatic parameter at Tirinie, may therefore exert strong control providing a viable reason for reduced vegetation lags to climatic change. Whilst hydrological data is not available for PF, aridity shifts may be key in understanding why, at PF, minimal lags are inferred between climatic deterioration and vegetation response.

10.6 Chapter summary

This chapter highlights variability in millennial-scale vegetation development and centennial-scale vegetation revertences across Britain. Principally, using the PC, the greatest phase of woodland development during the Interstadial is variable. In comparison with Europe it may be possible to zone phases of woodland development, with sites in southern Europe displaying continued woodland development during the Interstadial, and sites further north appearing to display a pause in development towards the end of the Interstadial, perhaps showing greater sensitivity to millennial-scale climatic change. Superimposed on these millennial trends are a series of high-magnitude revertence phases that are driven by the dominant climatic changes within Chapter 9. Vegetation therefore responds to climatic events akin to GI-1d and GI-1b events in Greenland and between potential correlatives across Europe between 12.2-12.0, 11.4-11.1, 11.1-10.8 and 10.3 ka BP. The PC reveals that across Britain these vegetation revertences are spatially heterogeneous and exhibit variable magnitudes depending on site location and magnitude of the specific climatic event. Of these events, vegetation responses during the Holocene appear muted.

Comparing data from this thesis to Europe reveals strong vegetation gradients across the European continent and diachronous vegetation responses to climatic change during the LGIT. The latter findings are only apparent when using Principal Curves. The palynological response to the GI-1d-type event displays the largest magnitudes of change in central Europe. This is in direct contrast with Britain where the GI-1b-type climatic event displays the greatest magnitudes of vegetation change. Both of these changes are coeval with lower magnitudes of climatic forcing. It is proposed that whilst climate drives these changes, antecedent vegetation and the position of thresholds are key in modulating the magnitude of response. Equally, it appears that with the expression of greater climatic forcing; between 55-56°N is a hinge point where large vegetation responses are observed, at least in Britain.

Finally, through the construction of multi-parameter climatic data, vegetation changes are shown to lag the onset of mean annual change and either respond when all climatic parameters are deteriorating or once an ecological threshold has been passed. This

assertion has only been possible through the analysis of multiple parameters at high-resolution with data originating from the same core sequence.

Chapter 11. Conclusions

Chapter 2 highlighted that whilst the terrestrial structure of millennial-scale (Windermere Interstadial, Loch Lomond Stadial, Early Holocene) climatic and environmental trends are well-known (e.g. Wohlfarth and Muschitiello, 2015), centennial- or decadal-scale climatic oscillations are less well understood. This includes the regional expression of climatic change, magnitudes of climatic events and parameterisation of climatic change. As climatic variability is not well constrained, environmental responses often go un-noticed. Where they are identified however, insufficient temporal resolutions preclude formal attribution. Through the application of multi-proxy and multi-parameter techniques, this study has improved the understanding of late Quaternary climatic and environmental change in Britain during the Last Glacial-Interglacial Transition (LGIT). During the course of this research this work has generated the first biomarker δ*D* record for moisture variability for the British Isles and the first across Europe for the early Lateglacial Interstadial. This thesis produces four of the five macro-charcoal records for the British Isles covering the LGIT, the other being Sluggan Bog (Walker et al., 2012). Five high-resolution pollen datasets have also been generated which are generally of a higher sample density than existing published records. Similarly, this thesis presents the first attempt to use Principal Curves (PCs) to address LGIT variability in Britain.

The major findings of this study can be split into two broad themes; palaeoclimatological and palaeoenvironmental. Principally, this study has highlighted, with greater certainty the ability to detect centennial-scale climatic variability throughout Britain during the LGIT. Secondly, this study clearly demonstrates palynological and vegetation responses to this climatic variability. The following sections present the major findings from this thesis.

11.1 Palaeoclimatic findings

1) The collection of multi-proxy climatic datasets from across Britain, allows an understanding of regional climatic development. Optimum mean annual and summer temperatures occur at different points during the Interstadial at the four sites. At Palaeolake Flixton peak summer temperatures occur at ca 14.14 Cal. ka BP. This is contrasted with Quoyloo Meadow, Llangorse and Tirinie where peak summer temperatures occurred at ca 13.37; 13.46; 12.99 Cal. ka BP respectively. At Tirinie peak annual temperatures occurred at 13.75 Cal. ka BP clearly demonstrating the difference in climatic evolution during the WI. The climatic transition into the Loch Lomond Stadial is shown to be time-transgressive across Britain with deteriorations occurring at Quoyloo Meadow (13.12 Cal. ka BP), followed by Tirinie (12.74 Cal. ka BP), Palaeolake Flixton

(12.74 Cal. ka BP), and Llangorse (12.51 Cal. ka BP), perhaps reflecting the southerly migration of the polar front.

2) Superimposed on these climatic trends are a series of centennial-scale climatic events. During the Windermere Interstadial across all sequences, with the exception of Quoyloo Meadow, two climatic events can be identified between ca 14.1-13.7 Cal. ka BP and 13.5-12.8 Cal. ka BP. Only the former is observed at Quoyloo Meadow owing to a compressed later Interstadial record. Within the early Holocene a series of events can be observed. A climatic deterioration between 11.45-11.1 Cal. ka BP is observed at Quoyloo Meadow, Tirinie, Palaeolake Flixton and Llangorse. Latter climatic deteriorations between 11.1-10.8 Cal. ka BP can be observed at Palaeolake Flixton, Llangorse and Quoyloo Meadow. An event is also clearly shown at Quoyloo Meadow between 10.2-10.1 Cal. ka BP.

3) These climatic deteriorations, within chronological uncertainties, align with the GI-1d (14.1-13.7 Ca. ka BP) and GI-1b (13.5-12.8 Cal. ka BP) and possibly the 11.4 ka BP events within the NGRIP GICC05 isotopic record (Rasmussen et al., 2014). However, the climatic deteriorations between 11.4-11.1, 11.1-10.8 and 10.2-10.1 Cal. ka BP appear to have no formal correlatives in Greenland. The identification of the 10.2-10.1 Cal. ka BP event at Quoyloo Meadow, represents the first occurrence of this phase in Britain across multiple climatic parameters.

4) These centennial-scale oscillations are clearly visible across multiple climatic parameters. Stable isotopic depletions for each of the events depicted above reveal changes in mean annual temperature, which occur alongside summer temperature change inferred from chironomids. A final component of this research has been to produce compound specific deuterium isotopic biomarker analyses, the first of its kind in Britain, covering this time-period. Aligned to mean annual and summer temperature change for the events above, hydroclimatic variability is noted in Scotland.

.

5) The magnitudes of climatic deteriorations are variable across Britain. The GI-1d-type event, with the exception of the isotopic profile at Tirinie, is the strongest centennial-scale climatic deterioration detected, recorded across both summer and annual temperature proxies. The GI-1b-type event exhibits reduced magnitudes of mean annual and summer temperature change. The magnitudes of the early Holocene events exhibit reduced amplitudes but in some instances are comparable to the GI-1b event.

6) Across the latitudinal transect climatic gradients are observed. The magnitudes of climatic events are generally stronger in the high-latitude (Tirinie and Palaeolake Flixton) and high-altitude sequences (Tirinie). The amplitudes of mean annual and summer temperature change are lower at Llangorse and are lowest at Quoyloo Meadow. Distance from the ocean appears key, with muted climatic deteriorations with increased proximity. The greatest amplitudes of climatic variability are recorded at Tirinie, demonstrating that climatic change is more pronounced between 55-56°N.

7) Comparison of climatic data from Britain with highly resolved climatic datasets from Europe reveal differences in climatic evolution during the LGIT. The creation of isopleth maps demonstrat that, in contrast to Britain, the strongest Interstadial climatic deterioration in continental Europe is the GI-1b-type event, at least in terms of summer temperature. It is postulated that regional differences may relate to a different forcing mechanism between the two Interstadial events, with the GI-1b-type event potentially also affected by solar variability.

8) Contrary to a recent publication, reductions in summer and annual temperatures, and suggested shorter growing seasons can be observed across multiple lines of proxy evidence in NW Europe, not only for the Lateglacial Stadial but also for shorter centennial-scale events (Schenk et al., 2018). This data therefore, refutes the suggestion of warmer summers during the Younger Dryas as proposed by Schenk et al. (2018)

11.2 Palaeoenvironmental findings

1) The high-resolution palynological reconstruction has facilitated an understanding of differential vegetation development in Britain. Woodland development as defined by the PCs appears out of phase with optimal climatic conditions, largely due to lags in vegetation adjustments (Pennington, 1986). During the Interstadial woodland vegetation appears to be a product of distance from migratory paths across Europe and displacement positions of outwardly-migrating taxa following the GI-1b-type event in Britain. Thus, greatest vegetation development is observed at 13.39 and 13.63 Cal. ka BP at Tirinie and Quoyloo Meadow; but is associated with climatic amelioration towards the end of the Interstadial at Palaeolake Flixton and Llangorse, 12.91 and 12.75 Cal. ka BP. The vegetation response to Loch Lomond Stadial cooling follows the same trend as the climatic data where biostratigraphic changes are first observed at Quoyloo Meadow, then Tirinie, Palaeolake Flixton and Llangorse. The point at which Holocene vegetation succession surpasses that of the Interstadial occurs between 10.8-11.0 Cal. ka BP across all sequences as defined by the PC.

2) Analysing sequences at high-resolution enabled the detection of centennial-scale vegetation revertences. This has been aided by the construction of PCs. Inflections in the PC suggest vegetation changes in association with the abrupt climatic events defined in each record. In contrast to woodland development, vegetation changes appear to be driven by climatic deteriorations depicted above.

3) Even within the relatively restricted latitudinal range of Britain, this research has demonstrated variability in vegetation responses to abrupt climatic events. At higher latitudes and higher altitudes vegetation changes are expressed as a regression in woody taxa, with expansions in Arctic/alpine and disturbed-ground assemblages. In contrast, the lower latitude sequences of Palaeolake Flixton and Llangorse reveal a landscape opening with increased open grassland communities.

4) The construction of PCs further allow for an understanding of the magnitudes of vegetation change across Britain. In association with the GI-1d-type event, the magnitudes of vegetation change are small, albeit with the largest vegetation changes inferred from the high-altitude sequence of Tirinie. The GI-1b-type revertence is defined by greater amplitudes of change with the largest inferred from Tirinie, Llangorse then Palaeolake Flixton. It is postulated that the high-altitude sequences contain vegetation that is closer to ecological boundaries, thus any perturbation would generate a larger response. Equally, however, the climatic deteriorations are most pronounced at Tirinie. The discrepancy between the two revertences relates to antecedent vegetation, with vegetation surrounding the GI-1d-type event largely pioneering. The GI-1b revertence however, occurred following the establishment of greater abundances of woodland. The same scenario is true for early Holocene revertences, where vegetation is much more pioneering. The lack of high-magnitude change at Quoyloo Meadow, relates to the different ecotonal setting of the sequence, which is dominated by a grassland throughout the LGIT.

5) The comparison of vegetation data with additional sites in Europe and Britain highlights two key differences. The early Interstadial vegetation revertence is greater in magnitude than the latter in continental Europe. Which is a direct contrast with the results from Britain. This highlights the role of antecedent vegetation in delineating magnitudes of vegetation change. The vegetation mosaic in Europe is more developed during the late Interstadial (closed *Betula*/*Pinus* woodland) than Britain (scrub or open *Betula* woodland). Thus, despite greater forcing than the earlier climatic event, late Interstadial vegetation is more resistant to change owing to wider ecological tolerances of *Pinus*.

6) The analysis of the magnitudes of climatic change, reveals that in Britain the latitudes between 54-57°N may reveal a hinge point where both the greatest magnitudes of climatic and environmental change can be observed. This is evidenced from large scale millennial- and centennial-scale shifts in vegetation occurring at this point which appears to be different from southern Europe and the northern high latitudes. Therefore, vegetation development can be zoned across much of Europe.

7) The first known occurrence in Britain, the palynological data suggests mid-Stadial variability between 12.2-12.0 Cal. ka BP. At Palaeolake Flixton a change in the PC driven by increases in Cyperaceae and *Pediastrum* suggests a phase of lowered lake levels and aridity following the deposition of the Vedde Ash. This is also reflected at Tirinie whereby greater abundances of the xeric *Artemisia* are observed following 12.0 Cal. ka BP. Variability in *Artemisia* is shown over the same period at Quoyloo Meadow although reduced *Artemisia* and increased moisture availability postulated from biomarker δ*D* suggests the opposite pattern at Quoyloo. These variations highlight vegetation changes aligned with the mid-Stadial transition identified across Europe (e.g. Lane et al., 2013). Interestingly, more aridity in continental Europe and southern Britain during this time and the suggestion of enhanced moisture availability in Orkney, supports the model that the Fennoscandian ice-sheet had a role in determining atmospheric wind patterns during this period, with a diverging airflow across northern Britain (Schenk et al., 2018).

8) In response to these centennial-scale events, and contrary to popular belief, fire is an important agent of change in the British landscape. At Tirinie, Quoyloo Meadow and Palaeolake Flixton fire appears to lag change in vegetation conditions. At Llangorse however, fire appears to align more so with the onset of climatic deterioration which may drive additional change.

11.3 Combined palaeoclimatic and palaeoenvironmental findings

1) The multi-proxy, multi-parameter approach with palaeodata originating from the same stratigraphic core sequence allowed for the reduction of homotaxial error and greater confidence in elucidating phase relationships between driver and response variables.

2) Phase relationships are best understood from Palaeolake Flixton and Tirinie, as these sites display the greatest densities of proxy data. For each centennial-scale deterioration episodes, climatic change precedes vegetation shifts.

3) Across both sequences, for the GI-1d-type event, mean annual temperature change occurs first, with later shifts in summer temperature, hydroclimate and vegetation occurring synchronously. Whilst clearly expressed in the stratigraphy, the age model allows for an approximate lag of 30 and 40 years at Tirinie and Palaeolake Flixton.

4) The GI-1b-type event is more complex. At Tirinie, mean annual temperature shifts occur first, with later successive shifts in hydroclimate then summer temperature. Vegetation responses occur before heightened aridity and summer temperature change suggesting a seasonality control on vegetation. Nonetheless, the changes in vegetation occur 90 years following the onset of isotopic depletion. At Palaeolake Flixton mean annual temperature change precedes changes in vegetation, however the lag is reduced to 40 years. This is postulated to reflect the different style of vegetation response to the latter Interstadial event at PF than Tirinie.

6) The phasing of Holocene events is similar to the early Interstadial event with reduced lag. However, it appears that hydroclimatic controls are more important than temperature during the Holocene.

11.4 Wider significance

This study demonstrates the importance of reconstructing climatic and environmental variability in Britain during the LGIT and demonstrates climatic and environmental gradients (Brooks and Langdon, 2014; Moreno et al., 2014).

Against this backdrop an assessment of the climatic background for ice-sheet growth may be gained. Variability in peak warmth and aridity for example, may lend weight to current theories on Interstadial rise vs. Stadial rise of the Loch Lomond Stadial glaciers (MacLeod et al., 2011; Bromley et al., 2018). Bromley et al. (2018) argue for an Interstadial rise of glaciers. The authors note that glacier mass balance is controlled by cool summer conditions which initiate ice-sheet growth during the Interstadial. However, this is incongruent with observations of peak summer warmth between 13.37-12.99 Cal. ka BP, late in the Interstadial at Quoyloo Meadow and Tirinie; two relatively ice proximal sites. Further, in contrast to the Greenland records, no declining temperature trends are observed during the Interstadial. The suggestion of aridity during the GI-1b climatic event at Tirinie, would also not be favourable with glacial growth; the starvation of precipitation is more likely to cause glacial retreat (Golledge et al., 2008). It was hoped that hydroclimatic reconstructions from within Loch Lomond Stadial sediments would help elucidate different glacial advance/retreat patterns. Unfortunately, this is not possible, due to the complex signal within δD at Tirinie but the suggestion of a mid-Stadial

transition in Britain, falling lake levels at Palaeolake Flixton and greater *Artemisia* at Tirinie post Vedde Ash deposition, highlights greater aridity. This finding corroborates model simulations (Isarin et al., 1998) and evidence from central and northern Europe (Bakke et al., 2009; Lane et al., 2013) suggesting an arid Stadial post 12.2-12.0 Cal. ka BP. Nonetheless, the cold summer temperatures post Vedde Ash deposition at Tirinie, may suggest a similar scenario to Loch Ashik, Isle of Skye (Brooks et al., 2012). Here enhanced winter precipitation has been suggested to form late-lying snow packs, which following spring melt, affect lake water conditions (Brooks et al., 2012). In the lee of the West Highland ice-field this is postulated as the same mechanism, perhaps providing further evidence towards late-Stadial glacier growth in specific catchments (MacLeod et al., 2011). The data collected here therefore adds to a growing body of evidence to help constrain cryospheric landscape change.

Whilst not explicitly assessed, highly resolved chronologically constrained climatic and environmental data within this thesis allows for a better understanding of upper Palaeolithic and Mesolithic occupation patterns in Britain. It is debated whether human populations are resilient or suffer population crashes associated with climatic variability (e.g. Wicks and Mithen, 2014; Griffiths and Robinson, 2018), specifically in relation to the 8.2 ka BP event. The recent publication of research from the Star Carr archaeological sequence, which includes data from this thesis, suggests that human populations were able to survive through the climatically complex early Holocene period and that background environmental variability had little impact on Mesolithic populations (Blockley et al., 2018). Evidence for upper Palaeolithic occupation change in reference to climatic and environmental variability is less well known. However, it is proposed that Britain was occupied during the upper Palaeolithic (Windermere Interstadial) at Seamer Carr and Flixton, both on the shores of Palaeolake Flixton (e.g. Conneller, 2007). Should occupation histories be established, the data produced as part of this thesis are directly relatable, with larger scale climatic and environmental change during the Interstadial likely having a greater impact on human populations. Thus, these data can be used as a baseline from which to understand human occupation patterns in Britain.

11.5 Future research and recommendations

This study has demonstrated the power of multi-proxy, multi-parameter, high-resolution climatic and environmental research. This has greatly advanced knowledge of the evolution of climate, and specific climatic parameters, and provided evidence of diachronous environmental development across Britain during the LGIT. However, this study also highlights that greater research is needed to better define the regional expression of climatic and environmental change. Whilst this study goes someway to

producing the basis of a spatial lattice across Britain, gaps still exist. Thus, as in Chapters 9 and 10 climatic evolution is defined through interpolation. Therefore, increasing the quantity of sequences across Britain from which to test whether regional climatic gradients exist is of paramount importance. Highlighted by this study are the lack of sequences across large swathes of England, specifically south-east England, where better understanding is required to test climatic teleconnections between Britain and continental Europe. The same may be true of north Wales, where better connections may be made to Ireland.

This thesis represents one of few studies that seeks to reconstruct different climatic parameters. Often research is aligned to one climatic proxy, for example stable isotopic or summer temperature reconstructions (e.g. Brooks et al., 2012; Whittington et al., 2015) and whilst these approaches are powerful; individually they fail to adequately define the climate system. This thesis has clearly shown that one singular proxy source does not define the total amount of climatic change during specific phases of deterioration. The magnitude of isotopic change, for the GI-1d and GI-1b events at Tirinie for example, cannot be explained by the same magnitude of summer temperature shifts. Whilst in part this may relate to complex isotopic controls, greater isotopic change is likely to be a result of greater mean annual change, hinting at greater seasonality. Therefore, a greater number of combined isotopic and chironomid studies are required across Britain to highlight inter-proxy variabilities or proxy discrepancies. Equally, a better method of constraining winter temperature change is required, where or what proxy source this may originate from however is not clear.

The addition of compound specific deuterium isotopic biomarker reconstructions to the proxy arsenal has allowed, for the first time in Britain, the realisation of hydroclimatic variability during the LGIT. The focus of biomarker research on the continent has largely been directed towards millennial-scale changes, specifically the GS-1/Younger Dryas period. This study has highlighted the need for evidence of hydroclimatic variability at the centennial-scale because only Tirinie reveals hydroclimatic change within abrupt climatic events. Whether these aridity changes can be seen elsewhere in Britain and Europe during the LGIT remains to be seen.

Despite the number of vegetation reconstructions applicable to the LGIT across Britain, a dearth of studies exist that reconstruct vegetation considering inherent climatic complexity. Much like the discussion centred around climate, this study offers one of the best attempts to produce a regional vegetational synthesis related to abrupt climatic change. Whilst it is suggested that between 54-57°N a hinge point exists for vegetative

expression; more studies are required across Britain that tests this theory. The recommendations arising from the environmental reconstructions should be that vegetation analyses are routinely performed at high-resolution, maximising the potential for the understanding of vegetation dynamics and local influences on landscape conditions.

Finally, where possible, it should be commonplace to extract all proxy materials from the same stratigraphic core sequence at comparable depths and develop a robust chronology. This has been applied where possible within this thesis which circumvents issues of homotaxial error (e.g. Whittington et al., 2015). It is only through this approach that the phasing of driver and response variables can be defined and placed against age. Across Britain this is not routinely performed and is a necessity to advance Quaternary thinking during the LGIT. Whilst the practicalities of this approach are acknowledged and may not be completely possible with conventional narrow-gauge sampling equipment, wider-gauge sampling equipment exists, which further increases possibilities for successful dating. At the very least this approach should be attempted. Once applied a better understanding of time-transgressive climatic and environmental change will be gained across Britain.

Bibliography

Adolphi, F., Muscheler, R., Svensson, A., Aldahan, A., Possnert, G., Beer, J., Sjolte, J., Björck, S., Matthes, K., and Thiéblemont, R. (2014). 'Persistent link between solar activity and Greenland climate during the Last Glacial Maximum.' *Nature Geoscience*, 7(9), pp. 662-666.

Aichner, B., Herzschuh, U., Wilkes, H., Vieth, A., and Böhner, J. (2010). 'δD values of *n*-alkanes in Tibetan lake sediments and aquatic macrophytes–A surface sediment study and application to a 16 ka record from Lake Koucha.' *Organic Geochemistry*, 41(8), pp.779-790.

Aichner, B., Ott, F., Słowiński, M., Noryśkiewicz, A.M., Brauer, A., and Sachse, D. (2018). 'Leaf wax n-alkane distributions record ecological changes during the Younger Dryas at Trzechowskie paleolake (Northern Poland) without temporal delay.' *Climate of the Past discussions.*

Aitchison, J. (1986). *The Statistical Analysis of Compositional Data*. London: Chapman and Hall, 416pp.

Albert, B., Innes, J., Blackford, J., Taylor, B., Conneller, C., and Milner, N. (2016). 'Degradation of the wetland sediment archive at Star Carr: An assessment of current palynological preservation,' *Journal of Archaeological Science: Reports*, 6, pp. 488–495.

Alley, R. B., and Ágústsdóttir, A. M. (2005). 'The 8k event: cause and consequences of a major Holocene abrupt climate change.' *Quaternary Science Reviews*, 24(10), pp. 1123-1149.

Alley, R.B., and Cuffey, K.M. (2001). 'Oxygen-and hydrogen-isotopic ratios of water in precipitation: beyond paleothermometry.' *Reviews in Mineralogy and Geochemistry*, 43(1), pp. 527-553.

Ammann, B., and Lotter, A.F. (1989). 'Late-Glacial radiocarbon-and palynostratigraphy on the Swiss Plateau.' *Boreas*, 18(2), pp. 109-126.

Ammann, B., Birks, H.J.B., Brooks, S.J., Eicher, U., von Grafenstein, U., Hofmann, W., Lemdahl, G., Schwander, J., Tobolski, K., and Wick, L. (2000). 'Quantification of biotic responses to rapid climatic changes around the Younger Dryas—a synthesis.' *Palaeogeography, Palaeoclimatology, Palaeoecology*, 159(3-4), pp. 313-347.

Ammann, B., Lotter, A.F., Eicher, U., Gaillard, M.J., Wohlfarth, B., Haeberli, W., Lister, G., Maisch, M., Niessen, F., and Schlüchter, C. (1994). 'The Würmian Late-glacial in lowland Switzerland.' *Journal of Quaternary Science*, 9(2), pp. 119-125.

Ammann, B., van Leeuwen, J.F., van der Knaap, W.O., Lischke, H., Heiri, O., and Tinner, W. (2013). 'Vegetation responses to rapid warming and to minor climatic fluctuations during the Late-Glacial Interstadial (GI-1) at Gerzensee (Switzerland).' *Palaeogeography, Palaeoclimatology, Palaeoecology*, 391, pp. 40-59.

Andersen, S.T. (1967). 'Tree-pollen rain in a mixed deciduous forest in south Jutland (Denmark).' *Review of Palaeobotany and Palynology*, 3(1), pp. 267-275.

Andresen, C.S., Björck, S., Jessen, C., and Rundgren, M. (2007). 'Early Holocene terrestrial climatic variability along a North Atlantic Island transect: palaeoceanographic implications.' *Quaternary Science Reviews*, 26(15-16), pp. 1989-1998.

Andrews, J.E. (2006). ‘Palaeoclimatic records from stable isotopes in riverine tufas: synthesis and review.’ *Earth Science Reviews*, 75(1-4), pp. 85-104.

Assarson, G. and Granlund, E. (1924). ‘En metod for pollenanalys av minerogena jordarter.’ Geologiska Föreningens I Stockholm Förhandlingar, 46, pp. 76-82.

Atkinson, T.C., Briffa, K.R., and Coope, G.R. (1987). ‘Seasonal temperatures in Britain during the past 22,000 years, reconstructed using beetle remains.’ *Nature*, 325(6105), pp. 587-592.

Bakke, J., Lie, Ø., Heegaard, E., Dokken, T., Haug, G.H., Birks, H.H., Dulski, P., and Nilsen, T. (2009). ‘Rapid oceanic and atmospheric changes during the Younger Dryas cold period.’ *Nature Geoscience*, 2(3), pp. 202-205.

Ballantyne, C.K. (1989). ‘The Loch Lomond Stadial on the Isle of Skye, Scotland: glacial reconstruction and palaeoclimatic implications.’ *Journal of Quaternary Science*, 4(2), pp. 95–108.

Ballantyne, C.K. (2010). ‘Extent and deglacial chronology of the last British-Irish Ice Sheet: Implications of exposure dating using cosmogenic isotopes.’ *Journal of Quaternary Science*, 25(4), pp.515–534.

Ballantyne, C.K., Hall, A.M., Phillips, W., Binnie, S., and Kubik, P.W. (2007). ‘Age and significance of former low-altitude corrie glaciers on Hoy, Orkney Islands.’ *Scottish Journal of Geology*, 43(2), pp. 107–114.

Ballantyne, C.K., and Stone, J.O. (2012). ‘Did large ice caps persist on low ground in north-west Scotland during the Lateglacial Interstade?’ *Journal of Quaternary Science*, 27(3), pp. 297–306.

Ballantyne, C.K., Stone, J.O., and McCarroll, D. (2008). ‘Dimensions and chronology of the last ice sheet in Western Ireland,’ *Quaternary Science Reviews*, 27, pp. 185–200.

Bartley, D.D. (1962). ‘The stratigraphy and pollen analysis of lake deposits near Tadcaster, Yorkshire.’ *New Phytologist*, 61(3), pp. 277-287.

Bartley, D.D., Chambers, C., and Hart-Jones, B. (1976). ‘The vegetational history of parts of south and east Durham.’ *New Phytologist*, 77(2), pp. 437-468.

Bateman, M.D., Buckland, P.C., Chase, B., Frederick, C.D., and Gaunt, G.D. (2008). ‘The Late-Devensian proglacial Lake Humber: New evidence from littoral deposits at Ferrybridge, Yorkshire, England.’ *Boreas*, 37(2), pp. 195–210.

Bateman, M.D., Evans, D.J.A., Buckland, P.C., Connell, E.R., Friend, R.J., Hartmann, D., Moxon, H., Fairburn, W.A., Panagiotakopulu, E., and Ashurst, R.A. (2015). ‘Last glacial dynamics of the Vale of York and North Sea lobes of the British and Irish ice sheet,’ *Proceedings of the Geologists’ Association*, 126(6), pp. 712–730.

Bedford, A., Jones, R., Lang, B., Brooks, S., and Marshall, J. D. (2004). 'A Late-glacial chironomid record from Hawes Water, north west England.' *Journal of Quaternary Science*, 19(3), pp. 281-290.

Beerling, D.J., Chaloner, W.G., Huntley, B., Pearson, J.R.A., and Tooley, M.J. (1993). ‘Stomatal density responds to the glacial cycle of environmental change.’ *Proceedings of the Royal Society series B: Biological Sciences,* 251(1331), pp. 133-138.

Bell, J.N.B., and Tallis, J.H. (1973). '*Empetrum nigrum L.*' *Journal of Ecology*, 61(1), pp. 289-305.

Bengtsson, L., and Enell, M. (1986). 'Chemical Analysis.' In: Berglung, B.E. (Ed.). *Handbook of Holocene Palaeoecology and Palaeohydrology*. Chichester: John Wiley and Sons Ltd, pp. 423-451.

Benn, D.I., and Evans, D.J.A. (2008). 'A Younger Dryas ice cap to the north of Glen Roy: a new perspective of the origin of the Turret Fan.' In: Palmer, A.P., Lowe, J.J., and Rose, J. (Eds.). *The Quaternary of Glen Roy and Vicinity: Field Guide*, London: Quaternary Research Association, pp. 158–161.

Benn, D.I., and Lukas, S. (2006). 'Younger Dryas glacial landsystems in North West Scotland: an assessment of modern analogues and palaeoclimatic implications.' *Quaternary Science Reviews*, 25, pp. 2390–2408.

Bennet, K.D., and Willis, K.J. (2001). 'Pollen.' In: Smol, J.P., Birks, H.J.B., and Last, W.M. (Eds.). *Tracking Environmental Change Using Lake Sediments. Volume 3: Terrestrial, Algal and Siliceous Indicators.* Dordrecht, The Netherlands: Kluwer Academic Publishers, pp. 5-32.

Bennett, K.D. (1983). 'Devensian Late-Glacial and Flandrian vegetation history at Hockham Mere, Norfolk, England.' *New Phytologist*, 95(3), pp. 457-487.

Bennett, K.D., Boreham, S., Sharp, M.J., and Switsur, V.R. (1992) 'Holocene History of Environment, Vegetation and Human Settlement on Catta Ness, Lunnasting, Shetland.' *Journal of Ecology*, 80(2), pp. 241–273.

Bennett, M.R., and Boulton, G.S. (1993). 'Deglaciation of the Younger Dryas or Loch Lomond Stadial ice-field in the northern Highlands, Scotland.' *Journal of Quaternary Science*, 8(2), pp. 133–145.

Bennion, H., and Appleby, P. (1999). 'An assessment of recent environmental change in Llangorse Lake using palaeolimnology.' *Aquatic Conservation: Marine and Freshwater Ecosystems*, 9(4), pp. 361–375.

Benson-Evans, K., Antoine, R., and Antoine, S. (1999). 'Studies of the water quality and algae of Llangorse Lake.' *Aquatic Conservation: Marine and Freshwater Ecosystems*, 9(5), pp. 425–439.

Berger, A. (1978). 'Long-term variations of daily insolation and Quaternary climatic changes.' *Journal of the Atmospheric Sciences*, 35(12), pp. 2362-2367.

Berger, A., and Loutre, M.F. (1991). 'Insolation values for the climate of the last 10 million years.' *Quaternary Science Reviews*, 10(4), pp. 297-317.

Berglund, B.E., Gaillard, M.J., Björkman, L., and Persson, T. (2008). 'Long-term changes in floristic diversity in southern Sweden: palynological richness, vegetation dynamics and land-use.' *Vegetation history and Archaeobotany*, 17(5), pp. 573-583.

Bickerdike, H.L., Evans, D.J.A., Stokes, C.R., and Ó Cofaigh, C. (2018). 'The glacial geomorphology of the Loch Lomond (Younger Dryas) Stadial in Britain: a review.' *Journal of Quaternary Science*, 33(1), pp. 1–54.

Birks, H.H., Aarnes, I., Bjune, A.E., Brooks, S.J., Bakke, J., Kühl, N., and Birks, H.J.B. (2014). 'Lateglacial and early-Holocene climate variability reconstructed from multi-

proxy records on Andøya, northern Norway.' *Quaternary Science Reviews*, 89, pp. 108-122.

Birks, H.H., and Ammann, B. (2000). 'Two terrestrial records of rapid climatic change during the glacial–Holocene transition (14,000–9,000 calendar years BP) from Europe.' *Proceedings of the National Academy of Sciences*, 97(4), pp. 1390-1394.

Birks, H.H., and Birks, H.J.B. (2000). 'Future uses of pollen analysis must include plant macrofossils.' *Journal of biogeography*, 27(1), pp. 31-35.

Birks, H.H., and Birks, H.J.B. (2014). 'To what extent did changes in July temperature influence Lateglacial vegetation patterns in NW Europe?' *Quaternary Science Reviews*, 106, pp. 262-277.

Birks, H.H. (1970). 'Studies in the Vegetational History of Scotland: I. A Pollen Diagram from Abernethy Forest, Inverness-Shire.' *The Journal of Ecology*, pp. 827-846.

Birks, H.H. (1994). 'Late-glacial vegetational ecotones and climatic patterns in Western Norway.' *Vegetation History and Archaeobotany*, 3(2), pp. 107-119.

Birks, H.H. (2015). 'South to north: Contrasting late-glacial and early-Holocene climate changes and vegetation responses between south and north Norway.' *The Holocene*, 25(1), pp. 37-52.

Birks, H.H., and Matthewes, R.W. (1978). 'Studies in the vegetational history of Scotland.' *New Phytologist*, 80(2), pp. 455-484.

Birks, H.H., Battarbee, R.W., and Birks, H.J.B. (2000). 'The development of the aquatic ecosystem at Kråkenes Lake, western Norway, during the late glacial and early Holocene-a synthesis.' *Journal of Paleolimnology*, 23(1), pp. 91-114.

Birks, H.H., Jones, V.J., Brooks, S.J., Birks, H.J.B., Telford, R.J., Juggins, S., and Peglar, S.M. (2012). 'From cold to cool in northernmost Norway: Lateglacial and early Holocene multi-proxy environmental and climate reconstructions from Jansvatnet, Hammerfest.' *Quaternary Science Reviews*, 33, pp. 100-120.

Birks, H.H., Larsen, E., and Birks, H.J.B. (2005). 'Did tree-*Betula*, *Pinus* and *Picea* survive the last glaciation along the west coast of Norway? A review of the evidence, in light of Kullman (2002).' *Journal of Biogeography*, 32(8), pp. 1461-1471.

Birks, H.J.B. (1970). 'Inwashed pollen spectra at Loch Fada, Isle of Skye.' *New Phytologist*, 69(3), pp. 807-820.

Birks, H.J.B. (1973). *Past and Present Vegetation of the Isle of Skye– a Palaeoecological Study.* Cambridge: Cambridge University Press, 415pp.

Birks, H.J.B. (1989). 'Holocene isochrone maps and patterns of tree-spreading in the British Isles.' *Journal of Biogeography*, pp. 503-540.

Bishop, W.W., and Coope, G.R. (1977). 'Stratigraphical and faunal evidence for Late-Glacial and early Flandrian environments in south west Scotland.' In: Gray, J.M., and Lowe, J.J. (Eds.). *Studies in the Scottish Late-Glacial Environment,* Oxford: Pergammon Press, pp. 61-88.

Björck, S., Kromer, B., Johnsen, S., Bennike, O., Hammarlund, D., Lemdahl, G., Possnert, G., Rasmussen, T.L., Wohlfarth, B., Hammer, C.U., and Spurk, M. (1996).

‘Synchronized terrestrial-atmospheric deglacial records around the North Atlantic.’ *Science*, 274(5290), pp. 1155-1160.

Björck, S., Muscheler, R., Kromer, B., Andresen, C.S., Heinemeier, J., Johnsen, S.J., Conley, D., Koç, N., Spurk, M., and Veski, S. (2001). ‘High-resolution analyses of an early Holocene climate event may imply decreased solar forcing as an important climate trigger.’ *Geology*, 29(12), pp. 1107-1110.

Björck, S., Rundgren, M., Ingólfsson, Ó., and Funder. S. (1997). ‘The Preboreal oscillation around the Nordic Seas: terrestrial and lacustrine responses.’ *Journal of Quaternary Science,* 12(6), pp. 455-465.

Björck, S., Walker, M.J., Cwynar, L.C., Johnsen, S., Knudsen, K.L., Lowe, J.J., and Wohlfarth, B. (1998). ‘An 'event' stratigraphy for the Last Termination in the north Atlantic region based on the Greenland ice-core record: a proposal by the INTIMATE group.’ *Journal of Quaternary Science*, 13(4), pp. 283-292.

Blockley, S.P.E., Candy, I., Matthews, I.P., Langdon, P., Langdon, C., Palmer, A.P., Lincoln, P., Abrook, A., Taylor, B., Conneller, C., Bayliss, A., MacLeod, A., Deeprose, L., Darvill, C., Kearney, R., Beavan, N., Staff, R., Bamforth, M., Taylor, M., and Milner, N. (2018). ‘The resilience of postglacial hunter-gatherers to abrupt climate change.’ *Nature ecology and evolution*, 2, pp. 810-818.

Blokker, P., Schouten, S., van den Ende, H., de Leeuw, J.W., Hatcher, P.G., and Damsté, J.S.S. (1998). ‘Chemical structure of algaenans from the fresh water algae *Tetraedron minimum*, *Scenedesmus communis* and *Pediastrum boryanum*.’ *Organic Geochemistry*, 29(5-7), pp. 1453-1468.

Blunier, T., Chappellaz, J., Schwander, J., Dällenbach, A., Stauffer, B., Stocker, T.F., Raynaud, D., Jouzel, J., Clausen, H.B., Hammer, C.U., and Johnsen, S.J. (1998). 'Asynchrony of Antarctic and Greenland climate change during the last glacial period.' *Nature*, 394(6695), pp. 739-743.

Bohncke, S.J.P. (1993). ‘Lateglacial environmental changes in the Netherlands: Spatial and temporal patterns: A contribution to the ‘North Atlantic seaboard programme’of IGCP-253, Termination of the Pleistocene.’ *Quaternary Science Reviews*, 12(8), pp. 707-717.

Bohncke, S.J.P., and Hoek, W.Z. (2007). ‘Multiple oscillations during the Preboreal as recorded in a calcareous gyttja, Kingbeekdal, The Netherlands.’ *Quaternary Science Reviews*, 26(15-16), pp. 1965-1974.

Bond, G., Broecker, W., Johnsen, S., McManus, J., Labeyrie, L., Jouzel, J., and Bonani, G. (1993). 'Correlations between climate records from north Atlantic sediments and Greenland ice.' *Nature*, 365, pp. 143-147.

Bond, G., Kromer, B., Beer, J., Muscheler, R., Evans, M.N., Showers, W., Hoffmann, S., Lotti-Bond, R., Hajdas, I., and Bonani, G. (2001). ‘Persistent solar influence on North Atlantic climate during the Holocene.’ *Science*, 294(5549), pp. 2130-2136.

Bond, G., Showers, W., Cheseby, M., Lotti, R., Almasi, P., de Menocal, P., Priore, P., Cullen., H., Hajdas, I., and Bonani, G. (1997). 'A pervasive millennial-scale cycle in north Atlantic Holocene and glacial climates.' S*cience*, 278(5341), pp. 1257-1266.

Bond, G.C., Showers, W., Elliot, M., Evans, M., Lotti, R., Hajdas, I., Bonani, G., and Johnson, S.J. (1999). ‘The North Atlantic's 1-2 kyr climate rhythm: relation to Heinrich

events, Dansgaard/Oeschger cycles and the Little Ice Age.' *Mechanisms of Global Climate Change at Millennial Time Scales*, 112, pp. 35-58.

Bos, J.A., Bohncke, S.J., and Janssen, C.R. (2006). 'Lake-level fluctuations and small-scale vegetation patterns during the late glacial in The Netherlands.' *Journal of Paleolimnology*, 35(2), pp. 211-238.

Bos, J.A., Bohncke, S.J., Kasse, C., and Vandenberghe, J. (2001). 'Vegetation and climate during the Weichselian Early Glacial and Pleniglacial in the Niederlausitz, eastern Germany—macrofossil and pollen evidence.' *Journal of Quaternary Science,* 16(3), pp. 269-289.

Bos, J.A., De Smedt, P., Demiddele, H., Hoek, W.Z., Langohr, R., Marcelino, V., van Asch, N., van Damme, D., van der Meeren, T., Verniers, J., Boeckx, P., Boudin, M., Court-Picon, M., Finke, P., Gelorini, V., Gobert, S., Heiri, O., Martens, K., Mostaert, F., Serbruyns, L.S., van Strydonck, M., and Crombe, P. (2017). 'Multiple oscillations during the Lateglacial as recorded in a multi-proxy, high-resolution record of the Moervaart palaeolake (NW Belgium).' *Quaternary Science Reviews*, 162, pp. 26-41.

Bos, J.A., van Geel, B., van der Plicht, J., and Bohncke, S.J. (2007). 'Preboreal climate oscillations in Europe: wiggle-match dating and synthesis of Dutch high-resolution multi-proxy records.' *Quaternary Science Reviews*, 26(15-16), pp. 1927-1950.

Bos, J.A., Verbruggen, F., Engels, S., and Crombé, P. (2013). 'The influence of environmental changes on local and regional vegetation patterns at Rieme (NW Belgium): implications for Final Palaeolithic habitation.' *Vegetation history and archaeobotany*, 22(1), pp. 17-38.

Bowen, D.Q. (1973). 'The Pleistocene history of Wales and the borderland.' *Geological Journal*, 8(2), pp. 207–224.

Bowen, D.Q., Phillips, F.M., McCabe, A.M., Knutz, P.C., and Sykes, G. (2002). 'New data for the Last Glacial Maximum in Great Britain and Ireland.' *Quaternary Science Reviews*, 21(1–3), pp. 89–101.

Boyd, W.E., and Dickson, J.H. (1986). 'Patterns in the geographical distribution of the early Flandrian *Corylus* rise in southwest Scotland.' *New Phytologist*, 102(4), pp. 615-623.

Boyle, J.F. (2001). 'Inorganic Geochemical Methods in Palaeolimnology.' In: Last, W.M., and Smol, J.P. (Eds.). *Tracking Environmental Change Using Lake Sediments. Volume 2: Physical and Geochemical Methods,* Dordrecht, The Netherlands: Kluwer Academic Publishers, pp. 83-141.

Bradshaw, R., and Mitchell, F. J. (1999). 'The palaeoecological approach to reconstructing former grazing–vegetation interactions.' *Forest Ecology and management*, 120(1), pp. 3-12.

Bradwell, T. (2006). 'The Loch Lomond Stadial glaciation in Assynt: A reappraisal.' *Scottish Geographical Journal*, 122(4), pp. 274–292.

Bradwell, T., Stoker, M.S., Golledge, N.R., Wilson, C.K., Merritt, J.W., Long, D., Everest, J.D., Hestvik, O.B., Stevenson, A.G., Hubbard, A.L., Finlayson, A.G., and Mathers, H.E. (2008). 'The northern sector of the last British Ice Sheet: Maximum extent and demise.' *Earth-Science Reviews*, 88(3–4), pp. 207–226.

Branch, N. (1999). *Vegetation history and human activity in the Ligurian Apennines and Alps, Italy, during the last 14,000 years*. Unpublished PhD thesis, Royal Holloway, University of London.

Brasier, A.T., Morris, J.L., and Hillier, R.D. (2014). 'Carbon isotopic evidence for organic matter oxidation in soils of the Old Red Sandstone (Silurian to Devonian, South Wales, UK).' *Journal of the Geological Society*, 171, pp. 621-634.

Brauer, A., Endres, C., Günter, C., Litt, T., Stebich, M., and Negendank, J.F. (1999). 'High resolution sediment and vegetation responses to Younger Dryas climate change in varved lake sediments from Meerfelder Maar, Germany.' *Quaternary Science Reviews*, 18(3), pp. 321-329.

Brauer, A., Haug, G.H., Dulski, P., Sigman, D.M., and Negendank, J.F. (2008). 'An abrupt wind shift in western Europe at the onset of the Younger Dryas cold period.' *Nature Geoscience*, 1(8), pp. 520-523.

Brauer, A., Litt, T., Negendank, J.F., and Zolitschka, B. (2001). 'Lateglacial varve chronology and biostratigraphy of lakes Holzmaar and Meerfelder Maar, Germany.' *Boreas*, 30(1), pp. 83-88.

Broecker, W. S. (1998). 'Paleocean circulation during the last de-glaciation: a bipolar seesaw?' *Paleoceanography*, 13(2), pp. 119-121.

Broecker, W.S. (2006). 'Abrupt climate change revisited.' *Global and Planetary Change*, 54(3-4), pp. 211-215.

Broecker, W.S., and Denton, G.H. (1989). 'The role of ocean-atmosphere reorganizations in glacial cycles.' *Geochimica et Cosmochimica Acta*, 53(10), pp. 2465-2501.

Broecker, W.S., Kennett, J.P., Flower, B.P., Teller, J.T., Trumbore, S., Bonani, G., and Wolfli, W. (1989). 'Routing of meltwater from the Laurentide Ice Sheet during the Younger Dryas cold episode.' *Nature*, 341(6240), pp. 318-321

Broecker, W.S., Peteet, D.M., and Rind, D. (1985). 'Does the ocean–atmosphere system have more than one stable mode of operation?' *Nature*, 315(6014), pp. 21-26.

Bromley, G.R.M., Putnam, A.E., Borns, H., Lowell, T., Sandford, T., and Barrell, D. (2018). 'Interstadial rise and Younger Dryas demise of Scotland's last ice fields.' *Paleoceanography and Paleoclimatology*, 33(4), pp. 412-429.

Bromley, G.R.M., Putnam, A.E., Rademaker, K.M., Lowell, T. V., Schaefer, J.M., Hall, B., Winckler, G., Birkel, S.D., and Borns, H.W. (2014). 'Younger Dryas deglaciation of Scotland driven by warming summers.' *Proceedings of the National Academy of Sciences*, 111(17), pp. 6215–6219.

Bronk Ramsey, C. (2008). 'Deposition models for chronological records.' *Quaternary Science Reviews*, 27(1), pp. 42-60.

Bronk Ramsey, C. (2009). 'Bayesian analysis of radiocarbon dates.' *Radiocarbon*, 51(1), pp. 337-360.

Bronk Ramsey, C., Albert, P.G., Blockley, S.P.E., Hardiman, M., Housley, R.A., Lane, C.S., Lee, S., Matthews, I.P., Smith, V.C., and Lowe, J.J. (2015). 'Improved age estimates for key Late Quaternary European tephra horizons in the RESET lattice.' *Quaternary Science Reviews*, 118, pp. 18-32.

Bronk Ramsey, C., and Lee, S. (2013). 'Recent and planned developments of the program OxCal.' *Radiocarbon*, 55(2-3), pp. 720-730.

Brooks, S.J., and Birks, H.J.B. (2000a). 'Chironomid-inferred Late-Glacial air temperatures at Whitrig Bog, south east Scotland.' *Journal of Quaternary Science*, 15(8), pp. 759-764.

Brooks, S.J., and Birks, H.J.B. (2000b). 'Chironomid-inferred Late-Glacial and early Holocene mean July air temperatures for Kråkenes Lake, western Norway.' *Journal of Paleolimnology*, 23(1), pp. 77-89.

Brooks, S.J., and Birks, H.J.B. (2001). 'Chironomid-inferred air temperatures from Lateglacial and Holocene sites in north-west Europe: progress and problems.' *Quaternary Science Reviews*, 20(16), pp. 1723-1741.

Brooks, S.J., Davies, K.L., Mather, K.A., Matthews, I.P., and Lowe, J.J. (2016). 'Chironomid-inferred summer temperatures for the Last Glacial–Interglacial Transition from a lake sediment sequence in Muir Park Reservoir, west-central Scotland.' *Journal of Quaternary Science*, 31(3), pp. 214-224.

Brooks, S.J., Matthews, I.P., Birks, H.H., and Birks, H.J.B. (2012). 'High resolution Lateglacial and early-Holocene summer air temperature records from Scotland inferred from chironomid assemblages.' *Quaternary Science Reviews*, 41, pp. 67-82.

Brooks, S.J., and Langdon, P.G. (2014). 'Summer temperature gradients in northwest Europe during the Lateglacial to early Holocene transition (15–8 ka BP) inferred from chironomid assemblages.' *Quaternary International*, 341, pp. 80-90.

Broström, A., Nielsen, A.B., Gaillard, M.J., Hjelle, K., Mazier, F., Binney, H., Bunting, J., Fyfe, R., Meltsov, V., Poska, A., and Räsänen, S. (2008). 'Pollen productivity estimates of key European plant taxa for quantitative reconstruction of past vegetation: a review.' *Vegetation History and Archaeobotany*, 17(5), pp. 461-478.

Brown, A.P. (1971). 'The *Empetrum* pollen record as a climatic indicator in the Late Weichselian and Early Flandrian of the British Isles.' *New Phytologist*, 70(5), pp. 841-849.

Brysting, A.K., Gabrielsen, T.M., Sørlibråten, O., Ytrehorn, O., and Brochmann, C. (1996). 'The Purple Saxifrage, *Saxifraga oppositifolia*, in Svalbard: two taxa or one?' *Polar Research*, 15(2), pp. 93-105.

Buckley, M.W., and Marshall, J. (2016). 'Observations, inferences, and mechanisms of the Atlantic Meridional Overturning Circulation: A review.' *Reviews of Geophysics*, 54(1), pp. 5-63.

Bunce, R.G.H. (1968). 'An ecological study of Ysgolion Duon, a mountain cliff in Snowdonia.' *The Journal of Ecology*, 56(1), pp. 59-75.

Bunting, M.J. (1994). 'Vegetation history of Orkney, Scotland; pollen records from two small basins in west Mainland.' *New Phytologist*, 128(4), pp. 771-792.

Bunting, M.J. (1996) 'Holocene vegetation and environment of Orkney.' In: Hall, A.M. (Ed.). *The Quaternary of Orkney: Field Guide*, Cambridge: Quaternary Research Association, pp. 20–29.

Busfield, M.E., Lee, J.R., Riding, J.B., Zalasiewicz, J., and Lee, S.V. (2015). 'Pleistocene till provenance in east Yorkshire: reconstructing ice flow of the British North Sea Lobe.' *Proceedings of the Geologists' Association*, 126(1), pp. 86-99.

Cabedo-Sanz, P., Belt, S.T., Knies, J., and Husum, K. (2013). 'Identification of contrasting seasonal sea ice conditions during the Younger Dryas.' *Quaternary Science Reviews*, 79, pp. 74-86.

Campbell, E., and Lane, A. (1989). 'Llangorse: a 10th-century royal crannog in Wales', *Antiquity*, 63(241), pp. 675–681.

Candy, I., Abrook, A., Elliot, F., Lincoln, P., Matthews, I.P., and Palmer, A.P. (2016). 'Oxygen isotopic evidence for high-magnitude, abrupt climatic events during the Lateglacial Interstadial in north-west Europe: analysis of a lacustrine sequence from the site of Tirinie, Scottish Highlands.' *Journal of Quaternary Science*, 31(6), pp. 607-621.

Candy, I., Farry, A., Darvill, C. M., Palmer, A. P., Blockley, S. P. E., Matthews, I. P., MacLeod, A., Deeprose, L., Farley, N., Kearney, R., Conneller, C., Taylor, B., and Milner, N. (2015) 'The evolution of Palaeolake Flixton and the environmental context of Star Carr: An oxygen and carbon isotopic record of environmental change for the early Holocene', *Proceedings of the Geologists' Association*, 126(1), pp. 60–71.

Candy, I., Palmer, A.P., Blockley, S.P.E., Matthews, I.P., MacLeod, A., Farley, N., Farry, A., Kearney, R., Abrook, A., and Darvill, C.M. (2017). '^{13}C and ^{18}O analysis of lacustrine marls from Palaeolake Flixton.' In: Eddey, L., Lincoln, P., Matthews, I.P., Palmer, A.P., and Bateman, M.D. (Eds.). *The Quaternary of the Vale of Pickering: Field Guide*, London: Quaternary Research Association, pp.124–127.

Candy, I., Stephens, M., Hancock, J.D.R., and Waghorne, R.S. (2011). 'Palaeoenvironments of ancient human occupation: the application of oxygen and carbon isotopes to the reconstruction of Pleistocene environments.' In: Ashton, N., Lewis, S.G., Stringer, C. (Eds.), *The Ancient Human Occupation of Britain Project. Developments in Quaternary Science, Volume 14*, London: Elsevier, pp. 23-37.

Carcaillet, C., Bouvier, M., Fréchette, B., Larouche, A.C., and Richard, P.J. (2001). 'Comparison of pollen-slide and sieving methods in lacustrine charcoal analyses for local and regional fire history.' *The Holocene*, 11(4), pp. 467-476.

Carcaillet, C., Perroux, A.S., Genries, A., and Perrette, Y. (2007). 'Sedimentary charcoal pattern in a karstic underground lake, Vercors massif, French Alps: implications for palaeo-fire history.' *The Holocene*, 17(6), pp. 845-850.

Carr, S.J. (2001). 'A glaciological approach for the discrimination of Loch Lomond Stadial glacial landforms in the Brecon Beacons, South Wales.' *Proceedings of the Geologists' Association*, 112(3), pp. 253–262.

Carr, S.J., Coleman, C.G., Humpage, A.J., and Shakesby, R.A. (2007). 'Preface.' In: Carr, S.J., Coleman, C.G., Humpage, A.J., and Shakesby, R.A. (Eds.). *The Quaternary of the Brecon Beacons: Field Guide*, London: Quaternary Research Association, pp. v–vi.

Cerling, T.E., and Quade, J. (1993). 'Stable Carbon and Oxygen Isotopes in Soil Carbonate.' In: Swart, P.K., Lohmann, K.C., McKenzie, J., and Savin, S. (Eds.). *Climate Change in Continental Isotopic Records*, Washington DC: American Geophysical Union, pp. 217-231.

Chambers, F.M. (1985). ‘Flandrian environmental history of the Llynfi catchment, South Wales.’ *Ecologia Mediterranea*, 11, pp. 73–80.

Chambers, F.M. (1999). ‘The Quaternary history of Llangorse Lake: implications for conservation.’ *Aquatic Conservation: Marine and Freshwater Ecosystems*, 9(4), pp 343–359.

Chambers, F.M. (2007). ‘Llangorse Lake.’ In: Carr, S.J., Coleman, C.G., Humpage, A.J., and Shakesby, R.A. (Eds.). *The Quaternary of the Brecon Beacons: Field Guide*, London: Quaternary Research Association, pp. 230–234.

Chambers, F.M., and Blackford, J.J. (2001). ‘Mid-and late-Holocene climatic changes: a test of periodicity and solar forcing in proxy-climate data from blanket peat bogs.’ *Journal of Quaternary Science*, 16(4), pp. 329-338.

Charlesworth, J.K. (1929). ‘The South Wales end-moraine.’ *Quarterly Journal of the Geological Society*, 339, pp. 335–358.

Cheng, H., Edwards, R.L., Broecker, W.S., Denton, G.H., Kong, X., Wang, Y., Zhang, R., and Wang, X. (2009). ‘Ice age terminations.’ *Science*, 326(5950), pp. 248-252.

Clark, C.D., Evans, D.J.A., Khatwa, A., Bradwell, T.O.M., Jordan, C.J., and Marsh, S.H. (2004). ‘Map and GIS database of glacial landforms and features related to the last British Ice Sheet.’ *Boreas*, 33, pp. 359–375.

Clark, C.D., Hughes, A.L.C., Greenwood, S.L., Jordan, C., and Sejrup, H.P. (2012). ‘Pattern and timing of retreat of the last British-Irish Ice Sheet.’ *Quaternary Science Reviews*, 44, pp. 112–146.

Clark, J.G.D. (1954). *Excavations at Star Carr*. Cambridge: Cambridge University Press. 256pp.

Clark, P.U., Alley, R.B., Keigwin, L.D., Licciardi, J.M., Johnsen, S.J., and Wang, H. (1996). ‘Origin of the first global meltwater pulse following the last glacial maximum.’ *Paleoceanography*, 11(5), pp. 563–577.

Clark, P.U., Marshall, S.J., Clarke, G.K., Hostetler, S.W., Licciardi, J.M., and Teller, J.T. (2001). ‘Freshwater forcing of abrupt climate change during the last glaciation.’ *Science*, 293(5528), pp. 283-287.

Clark, P.U., Pisias, N.G., Stocker, T.F., and Weaver, A.J. (2002). ‘The role of the thermohaline circulation in abrupt climate change.’ *Nature*, 415(6874), pp. 863-869.

Clark, C.D., Hughes, A.L., Greenwood, S.L., Jordan, C., and Sejrup, H.P. (2012a). ‘Pattern and timing of retreat of the last British-Irish Ice Sheet.’ *Quaternary Science Reviews*, 44, pp.112-146.

Clark, P.U., Shakun, J.D., Baker, P.A., Bartlein, P.J., Brewer, S., Brook, E., Carlson, A.E., Cheng, H., Kaufman, D.S., Liu, Z., Marchitto, T.M., Mix, A.C., Morrill, C., Otto-Bliesner, B.L., Pahnke, K., Russell, J.M., Whitlock, C., Adkins, J.F., Blois, J.L., Clark, J., Colman, S.M., Curry, W.B., Flower, B.P., He, F., Johnson, T.C., Lynch-Stieglitz, J., Markgraf, V., McManus, J., Mitrovica, J.X., Moreno, P.I., and Williams, J.W. (2012b). ‘Global climate evolution during the last deglaciation.’ *Proceedings of the National Academy of Sciences*, 109(19), pp. E1134-E1142.

Cloutman, E.W. (1988). ‘Palaeoenvironments in the Vale of Pickering. Part 1: Stratigraphy and Palaeogeography of Seamer Carr, Star Carr and Flixton Carr.’ *Proceedings of the Prehistoric Society*, 54, pp. 1–19.

Cloutman, E.W., and Smith, A.G. (1988). ‘Palaeoenvironments in the Vale of Pickering. Part 3: Environmental History at Star Carr.’ *Proceedings of the Prehistoric Society*, 54, pp. 37–58.

Coleman, C.G., and Parker, A.G. (2007). ‘Waen Ddu Bog.’ In: Carr, S.J., Coleman, C.G., Humpage, A.J., and Shakesby, R.A. (Eds.). *The Quaternary of the Brecon Beacons: Field Guide*, London: Quaternary Research Association, pp.197–200.

Condron, A., and Winsor, P. (2012). ‘Meltwater routing and the Younger Dryas.’ *Proceedings of the National Academy of Sciences*, 109(49), pp.19928-19933.

Conneller, C. (2007) ‘Inhabiting new landscapes: Settlement and mobility in britain after the last glacial maximum.’ *Oxford Journal of Archaeology*, 26(3), pp. 215–237.

Cook, C.D.K. (1962). ‘*Sparganium erectum* L. (*S. ramosum* Hudson, nom. illeg.).’ *Journal of Ecology*, pp. 247-255.

Coope, G.R., and Lemdahl, G. (1995). 'Regional differences in the Late-Glacial climate of northern Europe based on coleopteran analysis.' *Journal of Quaternary Science*, 10(4), pp. 391-395.

Coope, G.R., Lemdahl, G., Lowe, J.J., and Walkling, A. (1998). ‘Temperature gradients in northern Europe during the last glacial–Holocene transition (14-9 ^{14}C kyr BP) interpreted from coleopteran assemblages.’ *Journal of Quaternary Science*, 13(5), pp. 419-433.

Cope, J.C.W. (1974). ‘New information on the Kimmeridge Clay of Yorkshire.’ *Proceedings of the Geologists’ Association*, 85(2), pp. 211–221.

Cranwell, P.A. (1984). ‘Lipid geochemistry of sediments from Upton Broad, a small productive lake.’ *Organic Geochemistry*, 7(1), pp. 25-37.

Craig, H. (1961). ‘Isotopic variations in meteoric waters.’ *Science*, 133(3465), pp. 1702-1703.

Holden, J., and Rose, R. (2011). ‘Temperature and surface lapse rate change: a study of the UK's longest upland instrumental record.’ *International Journal of Climatology*, 31(6), pp. 907-919.

Curtis, T.G.F., Bassett, J.A., and McGough, H.N. (1985). ‘The present status and ecology of *Helianthemum nummularium* (L.) Miller in Ireland.’ *The Irish Naturalists' Journal*, 21(12), pp. 515-517.

Cushing, E.J. (1964). ‘Redeposited pollen in Late Wisconsin pollen spectra from east-central Minnesota.’ *American Journal of Science*, 262(9), pp. 1075-1088.

Cushing, E.J. (1967). ‘Evidence for differential pollen preservation in late Quaternary sediments in Minnesota.’ *Review of Palaeobotany and Palynology*, 4(1), pp. 87-101.

Dahl, S.O., Nesje, A., Lie, Ø., Fjordheim, K., and Matthews, J.A. (2002). ‘Timing, equilibrium-line altitudes and climatic implications of two early-Holocene glacier readvances during the Erdalen Event at Jostedalsbreen, western Norway.’ *The Holocene*, 12(1), pp. 17-25.

Dansgaard, W. (1964). 'Stable isotopes in precipitation.' *Tellus*, 16(4), pp. 436-468.

Dansgaard, W., Johnsen, S.J., Clausen, H.B., Dahl-Jensen, D., Gundestrup, N.S., Hammer, C.U., Hvidberg, C.S., Steffensen, J.P., Sveinbjörnsdóttir, A.E., Jouzel, J., and Bond, G. (1993). 'Evidence for general instability of past climate from a 250-kyr ice-core record.' *Nature*, 364(6434), pp. 218-220.

Dark, P. (1998a). 'Lake-edge Sequences: Results.' In: Mellars, P., and Dark, P. (Eds.). *Star Carr in Context*, Cambridge: McDonald Institute for Archaeological Research, pp. 125–146.

Dark, P. (1998b). 'Radiocarbon Dating of the Lake-edge Deposits.' In: Mellars, P., and Dark, P. (Eds.). *Star Carr in Context*, Cambridge: McDonald Institute for Archaeological Research, pp. 119–124.

Dark, P. (1998c). 'The Lake-centre Sequence: Results.' In: Mellars, P., and Dark, P. (Eds.). *Star Carr in Context*, Cambridge: McDonald Institute for Archaeological Research, pp. 163–178.

Dark, P. (1998d). 'Introduction and Methods.' In: Mellars, P., and Dark, P. (Eds.). *Star Carr in Context*, Cambridge: McDonald Institute for Archaeological Research, pp. 111–118.

Dark, P. (2017). 'Monitoring recent pollen preservation changes at Star Carr: a comment on Albert et al. (2016).' *Journal of Archaeological Science: Reports*, 12, pp. 28–31.

Darling, W.G. (2004). 'Hydrological factors in the interpretation of stable isotopic proxy data present and past: a European perspective.' *Quaternary Science Reviews*, 23(7-8), pp. 743-770.

Darvill, C. (2011). *The Lateglacial at Star Carr: A sedimentological and stable isotopic investigation of palaeoenvironmental change in northeast England.* Unpublished MSc thesis, Royal Holloway, University of London.

Davies, B.J., Roberts, D.H., Bridgland, D.R., Cofaigh, C.Ó., and Riding, J.B. (2011). 'Provenance and depositional environments of Quaternary sediments from the western North Sea Basin.' *Journal of Quaternary Science*, 26(1), pp. 59–75.

Davis, M.B. (1983). 'Quaternary history of deciduous forests of eastern North America and Europe.' *Annals of the Missouri Botanical Garden*, 70(3), pp. 550-563.

Davis, M.B., and Shaw, R.G. (2001). 'Range shifts and adaptive responses to Quaternary climate change.' *Science*, 292(5517), pp. 673-679.

Day, P. (1996). 'Devensian Late-glacial and early Flandrian environmental history of the Vale of Pickering, Yorkshire, England.' *Journal of Quaternary Science*, 11(1), pp. 9-24.

de Klerk, P. (2008). 'Patterns in vegetation and sedimentation during the Weichselian Late-glacial in north-eastern Germany.' *Journal of Biogeography*, 35(7), pp. 1308-1322.

Dean, W.E. (1974). 'Determination of carbonate and organic matter in calcareous sediments and sedimentary rocks by loss on ignition: comparison with other methods.' *Journal of Sedimentary Petrology,* 44(1), pp. 242-248.

Dearing, J. A. (1999). *Environmental Magnetic Susceptibility: using the Bartington MS2 System, Second Edition.* England: Chi Publishing, 54pp.

Denton, G.H., Anderson, R.F., Toggweiler, J.R., Edwards, R.L., Schaefer, J.M., and Putnam, A.E. (2010). 'The last glacial termination.' *Science*, 328(5986), pp. 1652-1656.

Deschamps, P., Durand, N., Bard, E., Hamelin, B., Camoin, G., Thomas, A.L., Henderson, G.M., Okuno, J., and Yokoyama, Y. (2012). 'Ice-sheet collapse and sea-level rise at the Bølling warming 14,600 years ago.' *Nature*, 483(7391), pp. 559-564.

Diefendorf, A.F., Freeman, K.H., Wing, S.L., and Graham, H.V. (2011). 'Production of n-alkyl lipids in living plants and implications for the geologic past.' *Geochimica et Cosmochimica Acta*, 75(23), pp. 7472-7485.

Diefendorf, A.F., Patterson, W.P., Holmden, C., and Mullins, H.T. (2008). 'Carbon isotopes of marl and lake sediment organic matter reflect terrestrial landscape change during the late Glacial and early Holocene (16,800 to 5,540 cal yr BP): a multiproxy study of lacustrine sediments at Lough Inchiquin, western Ireland.' *Journal of Paleolimnology*, 39(1), pp. 101-115.

Diefendorf, A.F., Patterson, W.P., Mullins, H.T., Tibert, N., and Martini, A. (2006). 'Evidence for high-frequency late Glacial to mid-Holocene (16,800 to 5500 cal yr BP) climate variability from oxygen isotope values of Lough Inchiquin, Ireland.' *Quaternary Research*, 65(1), pp. 78-86.

Duncan A.D., and Hamilton, R.F.M. (1988). 'Palaeolimnology and organic geochemistry of the Middle Devonian in the Orcadian Basin.' In: Fleet, A.J., Kelts, K., and Talbot, M.R. (Eds.). *Lacustrine Petroleum Source Rocks (Geological Society Special Publication No. 40)*, Oxford: Blackwell Scientific Publications, pp. 173-201.

Eddey, L., and Lincoln, P. (2017). 'Kirkham Gorge.' In: Eddey, L., Lincoln, P., Matthews, I.P., Palmer, A.P., and Bateman, M.D. (Eds.). *The Quaternary of the Vale of Pickering: Field Guide*, London: Quaternary Research Association, pp. 47–56.

Eddey, L., Lincoln, P., and Palmer, A.P. (2017). 'The Late Quaternary Glaciation of the Vale of Pickering.' In: Eddey, L., Lincoln, P., Matthews, I.P., Palmer, A.P., and Bateman, M.D. (Eds.). *The Quaternary of the Vale of Pickering: Field Guide*, London: Quaternary Research Association, pp. 11–20.

Edwards, K.J., and Whittington, G. (2010). 'Lateglacial palaeoenvironmental investigations at Wester Cartmore Farm, Fife and their significance for patterns of vegetation and climate change in east-central Scotland.' *Review of Palaeobotany and Palynology*, 159(1-2), pp. 14-34.

Edwards, K.J., Bennett, K.D., and Davies, A.L. (2018). 'Palaeoecological perspectives on Holocene environmental change in Scotland.' *Earth and Environmental Science Transactions of The Royal Society of Edinburgh*, pp.1-19.

Eglinton, T.I., and Eglinton, G. (2008). 'Molecular proxies for paleoclimatology.' *Earth and Planetary Science Letters*, 275(1-2), pp. 1-16.

Elias, S.A., and Matthews, I.P. (2014). 'A comparison of reconstructions based on aquatic and terrestrial beetle assemblages: Late glacial–Early Holocene temperature reconstructions for the British Isles.' *Quaternary International*, 341, pp. 69-79.

Ellis-Gruffydd, I.D. (1977). 'Late Devensian glaciation in the upper Usk basin.' *Cambria*, 4(1), pp. 46–55.

Engels, S., and van Geel, B. (2012). 'The effects of changing solar activity on climate: contributions from palaeoclimatological studies.' *Journal of Space Weather and Space Climate*, 2, pp. A09.

Engels, S., Brauer, A., Buddelmeijer, N., Martín-Puertas, C., Rach, O., Sachse, D., and van Geel, B. (2016). 'Subdecadal-scale vegetation responses to a previously unknown late-Allerød climate fluctuation and Younger Dryas cooling at Lake Meerfelder Maar (Germany).' *Journal of Quaternary Science*, 31(7), pp. 741-752.

Engels, S., Self, A.E., Luoto, T.P., Brooks, S.J., and Helmens, K.F. (2014). 'A compmarison of three Eurasian chironomid-climate calibration datasets on a W-E continentality gradient and the implications for quantitative temperature reconstructions.' *Journal of Palaeolimnology*, 51(4), pp. 529-547.

Erdtman, G. (1934). 'Über die verwendung von essigsäureanhydrid bei pollenuntersunchungen.' *Svensk Botanisk Tidskrift*, 28, pp. 354-358.

Evans, D.J.A., Bateman, M.D., Roberts, D.H., Medialdea, A., Hayes, L., Duller, G.A.T., Fabel, D., and Clark, C.D. (2017). 'Glacial Lake Pickering: stratigraphy and chronology of a proglacial lake dammed by the North Sea Lobe of the British–Irish Ice Sheet.' *Journal of Quaternary Science*, 32(2), pp. 295–310.

Evans, D.J.A., Clark, C.D., and Mitchell, W.A. (2005). 'The last British Ice Sheet: A review of the evdence utilised in the compilation of the Glacial Map of Britain.' *Earth-Science Reviews*, 70(3–4), pp. 253–312.

Evans, D.J.A., and Thomson, S.A. (2010). 'Glacial sediments and landforms of Holderness, eastern England: A glacial depositional model for the North Sea Lobe of the British-Irish Ice Sheet.' *Earth-Science Reviews*, 101, pp. 147–189.

Faegri, K., and Iversen, J. (1989). *Textbook of Pollen Analysis, 4th Edition*. Chichester: John Wiley and Sons, 340pp.

Fairburn, W.A., and Bateman, M.D. (2016). 'A new multi-stage recession model for Proglacial Lake Humber during the retreat of the last British-Irish Ice Sheet.' *Boreas*, 45(1), pp. 133–151.

Ficken, K.J., Li, B., Swain, D.L., and Eglinton, G. (2000). 'An n-alkane proxy for the sedimentary input of submerged/floating freshwater aquatic macrophytes.' *Organic geochemistry*, 31(7-8), pp. 745-749.

Fiłoc, M., Kupryjanowicz, M., Rzodkiewicz, M., and Suchora, M. (2018). 'Response of terrestrial and lake environments in NE Poland to Preboreal cold oscillations (PBO).' *Quaternary International*, pp. 101-117.

Finlayson, A., and Bradwell, T. (2007). 'Evidence for Loch Lomond Stadial ice cap glaciation of the Beinn Dearg massif, northern Scotland.' *Quaternary Newsletter*, 113, pp. 10–17.

Finlayson, A.G. (2006). 'Glacial geomorphology of the Creag Meagaidh Massif, Western Grampian Highlands: Implications for local glaciation and palaeoclimate during the Loch Lomond Stadial.' *Scottish Geographical Journal*, 122(4), pp. 293–307.

Firestone, R.B., West, A., Kennett, J.P., Becker, L., Bunch, T.E., Revay, Z.S., Schultz, P.H., Belgya, T., Kennett, D.J., Erlandson, J.M., Dickenson, O.J., Goodyear, A.C., Harris, R.S., Howard, G.A., Kloosterman, J.B., Lechler, P., Mayewski, P.A.,

Montgomery, J., Poreda, R., Darrah, T., Que Hee, S.S., Smith, A.R., Stich, A., Topping, W., Wittke, J.H., and Wolbach, W.S. (2007). 'Evidence for an extraterrestrial impact 12,900 years ago that contributed to the megafaunal extinctions and the Younger Dryas cooling.' *Proceedings of the National Academy of Sciences*, 104(41), pp. 16016-16021.

Fisher, T.G., Smith, D.G., and Andrews, J.T. (2002). 'Preboreal oscillation caused by a glacial Lake Agassiz flood.' *Quaternary Science Reviews*, 21(8-9), pp. 873-878.

Fleitmann, D., Cheng, H., Badertscher, S., Edwards, R.L., Mudelsee, M., Göktürk, O.M., Fankhauser, A., Pickering, R., Raible, C.C., Matter, A., Kramers, J., and Tüysüz. O. (2009). 'Timing and climatic impact of Greenland interstadials recorded in stalagmites from northern Turkey.' *Geophysical Research Letters*, 36(19).

Fletcher, W.J., Goni, M.F.S., Allen, J.R., Cheddadi, R., Combourieu-Nebout, N., Huntley, B., Lawson, I., Londeix, L., Magri, D., Margari, V., Müller, U.C., Naughton, F., Novenko, E., Roucoux, K., and Tzedakis, P.C. (2010). 'Millennial-scale variability during the last glacial in vegetation records from Europe.' *Quaternary Science Reviews*, 29(21-22), pp. 2839-2864.

Forster, M., and Flenley, J.R. (1993). 'Pollen purification and fractionation by equilibrium density gradient centrifugation.' *Palynology*, 17(1), pp. 137-155.

Gale, S., and Hoare, P. (1991). *Quaternary Sediments: Petrographic methods for the study of unlithified rocks*. New York: Belhaven and Halsted Press, 327pp.

Garcin, Y., Schwab, V. F., Gleixner, G., Kahmen, A., Todou, G., Séné, O., Onana, J-M., Achoundong, G., and Sachse, D. (2012). 'Hydrogen isotope ratios of lacustrine sedimentary n-alkanes as proxies of tropical African hydrology: insights from a calibration transect across Cameroon.' *Geochimica et Cosmochimica Acta*, 79, pp. 106-126.

Garnett, E.R., Andrews, J.E., Preece, R.C., and Dennis, P.F. (2004). 'Climatic change recorded by stable isotopes and trace elements in a British Holocene tufa.' *Journal of Quaternary Science*, 19(3), pp. 251-262.

Gat, J.R. (1980). 'The isotopes of oxygen and hydrogen in precipitation.' In: Fritz, P., and Fontes, J.C. (Eds.). *Handbook of environmental isotope geochemistry, Volume 1*, Amsterdam: Elsevier, pp. 21-47.

Gauch, H.G. (1982). '*Multivariate Analysis in Community Ecology*.' Cambridge: Cambridge University Press, 312pp.

Geikie, A. (1877). 'The Glacial Geology of Orkney and Shetland.' *Nature*, 16, pp. 414–416.

Genty, D., Blamart, D., Ghaleb, B., Plagnes, V., Causse, C., Bakalowicz, M., Zouari, K., Chkir, N., Hellstrom, J., Wainer, K., and Bourges, F. (2006). 'Timing and dynamics of the last deglaciation from European and North African δ13C stalagmite profiles—comparison with Chinese and South Hemisphere stalagmites.' *Quaternary Science Reviews*, 25(17-18), pp. 2118-2142.

George, T.N. (1970). *British Regional Geology: South Wales*, London: HMSO, Institute of Geological Sciences, 168pp.

Godwin, H. (1956). *The History of the British Flora: A Factual Basis for Phytogeography*. Cambridge: Cambridge University Press, 384pp.

Godwin, H. (1975). *The History of the British Flora: A Factual Basis for Phytogeography (2nd Edition).* Cambridge: Cambridge University Press, 580pp.

Golledge, N.R., Hubbard, A., and Sugden, D.E. (2008). 'High-resolution numerical simulation of Younger Dryas glaciation in Scotland.' *Quaternary Science Reviews*, 27(9), pp. 888-904.

Golledge, N.R. (2010). 'Glaciation of Scotland during the Younger Dryas Stadial: a review', 25(4), pp. 550–566.

Golledge, N.R., Menviel, L., Carter, L., Fogwill, C.J., England, M.H., Cortese, G., and Levy, R.H. (2014). 'Antarctic contribution to meltwater pulse 1A from reduced Southern Ocean overturning.' *Nature communications*, 5, 5107.

Gonfiantini, R., Roche, M.A., Olivry, J.C., Fontes, J.C., and Zuppi, G.M. (2001.) 'The altitude effect on the isotopic composition of tropical rains.' *Chemical Geology*, 181(1-4), pp. 147-167.

Gray, J.M., and Lowe, J.J. (1977). 'The Scottish Lateglacial Environment: a synthesis.' In: Gray, J.M., and Lowe, J.J. (Eds.). *Studies in the Scottish Late-Glacial Environment*, Oxford: Pergammon Press, pp. 163-181.

Griffiths, S., and Robinson, E. (2018). 'The 8.2 ka BP Holocene climate change event and human population resilience in northwest Atlantic Europe.' *Quaternary International*, 465, pp. 251-257.

Grime, J.P., Brown, V.K., Thompson, K., Masters, G.J., Hillier, S.H., Clarke, I.P., Askew, A.P., Corker, D., and Kielty, J.P. (2000). 'The response of two contrasting limestone grasslands to simulated climate change.' *Science*, 289(5480), pp. 762-765.

Grimm, E.C. (1987). 'CONISS: a FORTRAN 77 program for stratigraphically constrained cluster analysis by the method of incremental sum of squares.' *Computers & Geosciences*, 13(1), pp. 13-35.

Håkansson, S. (1985). 'A review of various factors influencing the stable carbon isotope ratio of organic lake sediments by the change from glacial to post-glacial environmental conditions.' *Quaternary Science Reviews*, 4(2), pp. 135-146.

Hall, A.M., Riding, J.B., and Brown, J.F. (2016a). 'The last glaciation in Orkney, Scotland: glacial stratigraphy, event sequence and flow paths.' *Scottish Journal of Geology*, 52(2), pp. 90–101.

Hall, A.M., Binnie, S.A., Sugden, D., Dunai, T.J., and Wood, C. (2016b). 'Late readvance and rapid final deglaciation of the last ice sheet in the Grampian Mountains, Scotland.' *Journal of Quaternary Scence*, 31(8), pp. 869–878.

Hall, A.M., and Whittington, G. (1989). 'Late Devensian glaciation of southern Caithness.' *Scottish Journal of Geology*, 25(3), pp. 307–324.

Hammarlund, D. (1993). 'A distinct δ13C decline in organic lake sediments at the Pleistocene-Holocene transition in southern Sweden.' *Boreas*, 22(3), pp. 236-243.

Hammarlund, D., Aravena, R., Barnekow, L., Buchardt, B., and Possnert, G. (1997). 'Multi-component carbon isotope evidence of early Holocene environmental change and carbon-flow pathways from a hard-water lake in northern Sweden.' *Journal of Paleolimnology*, 18(3), pp. 219-233.

Hammarlund, D., Björck, S., Buchardt, B., Israelson, C., and Thomsen, C.T. (2003). 'Rapid hydrological changes during the Holocene revealed by stable isotope records of lacustrine carbonates from Lake Igelsjön, southern Sweden.' *Quaternary Science Reviews*, 22(2-4), pp. 353-370.

Hays, J.D., Imbrie, J., and Shackleton, N.J. (1976). 'Variations in the Earth's orbit: pacemaker of the ice ages.' *Science*, 194(4270), pp. 1121-1132.

Heiri, O., and Millet, L. (2005). 'Reconstruction of Late Glacial summer temperatures from chironomid assemblages in Lac Lautrey (Jura, France).' *Journal of Quaternary Science*, 20(1), pp.33-44.

Heiri, O., Cremer, H., Engels, S., Hoek, W.Z., Peeters, W., and Lotter, A.F. (2007). 'Lateglacial summer temperatures in the Northwest European lowlands: a chironomid record from Hijkermeer, The Netherlands.' *Quaternary Science Reviews*, 26(19-21), pp. 2420-2437.

Heiri, O., Lotter, A.F., and Lemcke, G., (2001). 'Loss on ignition as a method for estimating organic and carbonate content in sediments: reproducibility and comparability of results.' *Journal of paleolimnology*, 25(1), pp. 101-110.

Heusser, C.J., and Igarashi, Y. (1994). 'Quaternary migration pattern of *Selaginella selaginoides* in the North Pacific.' *Arctic and Alpine Research*, 26(2), pp. 187-192.

Hoek, W.Z. (1997). 'Late-glacial and early Holocene climatic events and chronology of vegetation development in the Netherlands.' *Vegetation History and Archaeobotany*, 6(4), pp. 197-213.

Hoek, W.Z. (2001). 'Vegetation response to the ~14.7 and ~11.5 ka cal. BP climate transitions: is vegetation lagging climate?' *Global and Planetary Change*, 30(1-2), pp. 103-115.

Hoek, W.Z., and Bohncke, S.J.P. (2001). 'Oxygen-isotope wiggle matching as a tool for synchronising ice-core and terrestrial records over Termination 1.' *Quaternary Science Reviews*, 20(11), pp. 1251-1264.

Hoek, W.Z., and Bohncke, S.J.P. (2002). 'Climatic and environmental events over the Last Termination, as recorded in The Netherlands: a review.' *Netherlands Journal of Geosciences*, 81(1), pp. 123-137.

Hogg, A., Southon, J., Turney, C., Palmer, J., Ramsey, C.B., Fenwick, P., Boswijk, G., Friedrich, M., Helle, G., Hughen, K., and Jones, R. (2016). 'Punctuated shutdown of Atlantic meridional overturning circulation during Greenland Stadial 1.' *Scientific reports*, 6, p.25902.

Howells, M.F. (2007) *British Regional Geology: Wales*. Nottingham: British Geological, 230 pp.

Hu, F.S., Kaufman, D., Yoneji, S., Nelson, D., Shemesh, A., Huang, Y., Tian, J., Bond, G., Clegg, B., and Brown, T. (2003). 'Cyclic variation and solar forcing of Holocene climate in the Alaskan subarctic.' *Science*, 301(5641), pp. 1890-1893.

Hubbard, A., Bradwell, T., Golledge, N., Hall, A.M., Patton, H., Sugden, D., Cooper, R., and Stoker, M. (2009). 'Dynamic cycles, ice streams and their impact on the extent, chronology and deglaciation of the British–Irish ice sheet.' *Quaternary Science Reviews*, 28, pp. 758–776.

Hughen, K.A., Overpeck, J.T., Peterson, L.C., and Trumbore, S. (1996). 'Rapid climate changes in the tropical Atlantic region during the last deglaciation.' *Nature*, 380(6569), pp. 51-54.

Hughes, A.L., Gyllencreutz, R., Lohne, Ø.S., Mangerud, J., and Svendsen, J.I. (2016). 'The last Eurasian ice sheets–a chronological database and time-slice reconstruction, DATED-1.' *Boreas*, 45(1), pp.1-45.

Hulme, P.D., and Shirriffs, J. (1994). 'The Late-Glacial and Holocene Vegetation of the Lang Lochs Mire Area, Gulberwick, Shetland: A Pollen and Macrofossil Investigation.' *New Phytologist*, 128(4), pp. 793–806.

Humpage, A.J. (2007). 'Llangorse lake and the Llynfi basin: geomorphological setting and glacial history.' In: Carr, S.J., Coleman, C.G., Humpage, A.J., and Shakesby, R.A. (Eds.). *The Quaternary of the Brecon Beacons: Field Guide*, London: Quaternary Research Association, pp. 216–219.

Hunt, T.G., and Birks, H.J.B. (1982). 'Devensian late-glacial vegetational history at Sea Mere, Norfolk.' *Journal of Biogeography*, 9(6), pp.517-538.

Huntley, B. (1991). 'How plants respond to climate change: migration rates, individualism and the consequences for plant communities.' *Annals of Botany*, 67, pp. 15-22.

Huntley, B., and Birks, H.J.B. (1983). *An atlas of past and present pollen maps for Europe: 0-13,000 years ago*, Cambridge: Cambridge University Press, 688 pp.

Hurrell, J.W., and Deser, C. (2010). 'North Atlantic climate variability: the role of the North Atlantic Oscillation.' *Journal of Marine Systems*, 79(3-4), pp. 231-244.

IAEA/WMO, (2018). 'Global network of isotopes in precipitation.' The *GNIP database.*

Imbrie, J., Berger, A., Boyle, E.A., Clemens, S.C., Duffy, A., Howard, W.R., Kukla, G., Kutzbach, J., Martinson, D.G., McIntyre, A., Mix, A.C., Molfino, B., Morley, J.J., Peterson, L.C., Pisias, N.G., Prell, W.L., Raymo, M.E., Shackleton, N.J., and Toggweiler, J.R. (1993). 'On the structure and origin of major glaciation cycles 2. The 100,000-year cycle.' *Paleoceanography*, 8(6), pp. 699-735.

Imbrie, J., Boyle, E.A., Clemens, S.C., Duffy, A., Howard, W.R., Kukla, G., Kutzbach, J., Martinson, D.G., McIntyre, A., Mix, A.C., Molfino, B., Morley, J.J., Peterson, L.C., Pisias, N.G., Prell, W.L., Raymo, M.E., Shackleton, N.J., and Toggweiler, J.R. (1992). 'On the structure and origin of major glaciation cycles 1. Linear responses to Milankovitch forcing.' *Paleoceanography*, 7(6), pp. 701-738.

IPCC. (2007). *Climate Change 2007: The Physical Science Basis. Contribution of Working Group I to the Fourth Assessment Report of the Intergovernmental Panel on Climate change*. In: Solomon, S., Qin, D., Manning, M., Chen, Z., Marquis, M., Averyt, K.B., Tignor, M., and Miller, H.L. (Eds.). Cambridge: Cambridge University Press, 966 pp.

Isarin, R.F., and Bohncke, S.J. (1999). 'Mean July temperatures during the Younger Dryas in northwestern and central Europe as inferred from climate indicator plant species.' *Quaternary Research*, 51(2), pp. 158-173.

Isarin, R.F., Renssen, H., and Koster, E.A. (1997). 'Surface wind climate during the Younger Dryas in Europe as inferred from aeolian records and model

simulations.' *Palaeogeography, Palaeoclimatology, Palaeoecology*, 134(1-4), pp. 127-148.

Isarin, R.F., Renssen, H., and Vandenberghe, J. (1998). 'The impact of the North Atlantic Ocean on the Younger Dryas climate in northwestern and central Europe.' *Journal of Quaternary Science*, 13(5), pp. 447-453.

Jansson, K.N., and Glasser, N.F. (2008). 'Modification of peripheral mountain ranges by former ice sheets: The Brecon Beacons, Southern UK.' *Geomorphology*, 97(1–2), pp. 178–189.

Jeffers, E.S., Bonsall, M.B., Brooks, S.J., and Willis, K. J. (2011). 'Abrupt environmental changes drive shifts in tree–grass interaction outcomes.' *Journal of Ecology*, 99(4), pp. 1063-1070.

Jessen, K. (1935). 'Archaeological dating in the history of north Jutland's vegetation.' *Acta Archaeologica*, 5(3), pp. 185-214.

Johnsen, S. J., Clausen, H.B., Dansgaard, W., Fuhrer, K., Gundestrup, N., Hammer, C. U., Iversen, P., Jouzel, J., Stauffer, B., and Steffensen, J.P. (1992). 'Irregular glacial interstadials recorded in a new Greenland ice core.' *Nature*, 359(6393), pp. 311-313.

Johnsen, S.J., Dahl-Jensen, D., Gundestrup, N., Steffensen, J.P., Clausen, H.B., Miller, H., Masson-Delmotte, V., Sveinbjörnsdottir, A.E., and White, J.W. (2001). 'Oxygen isotope and palaeotemperature records from six Greenland ice-core stations: Camp Century, Dye-3, GRIP, GISP2, Renland and NorthGRIP.' *Journal of Quaternary Science*, 16(4), pp. 299-307.

Jones, G., Lane, C.S., Brauer, A., Davies, S.M., De Bruijn, R., Engels, S., Haliuc, A., Hoek, W.Z., Merkt, J., Sachse, D., Turner, F., and Wagner-Cremer, F. (2018). 'The Lateglacial to early Holocene tephrochronological record from Lake Hämelsee, Germany: a key site within the European tephra framework.' *Boreas*, 47(1), pp. 28-40.

Jones, R., Benson-Evans, K., and Chambers, F.M. (1985). 'Human influence upon sedimentation in Llangorse Lake, Wales.' *Earth Surface Processes and Landforms*, 10(3), pp. 227–235.

Jones, R., Chambers, F.M., and Benson-Evans, K. (1991). 'Heavy metals (Cu and Zn) in recent sediments of Llangorse Lake, Wales: non-ferrous smelting, Napoleon and the price of wheat - a palaeoecological study.' *Hydrobiologia*, 214(1), pp. 149–154.

Jones, R.T., Marshall, J.D., Crowley, S.F., Bedford, A., Richardson, N., Bloemendal, J., and Oldfield, F. (2002). 'A high resolution, multiproxy Late-glacial record of climate change and intrasystem responses in northwest England.' *Journal of Quaternary Science*, 17(4), pp. 329-340.

Jouzel, J., Lorius, C., Petit, J.R., Genthon, C., Barkov, N.I., Kotlyakov, V.M., and Petrov, V.M. (1987). 'Vostok ice core: a continuous isotope temperature record over the last climatic cycle (160,000 years).' *Nature*, 329(6138), pp. 403-408.

Jowsey, P. C. (1966). 'An improved peat sampler.' *New Phytologist,* 65, pp. 245-248.

Juggins, S. (2016). C2 Version 1.7.7. *Software for ecological and palaeoecological data analysis and visualisation*. Newcastle upon Tyne: Newcastle University. [Software].

Juggins, S. (2017). Rioja: Analysis of Quaternary Science Data, R package Version 0.9-15.1. [Software] (http://cran.r-project.org/package=rioja).

Kahmen, A., Hoffmann, B., Schefuß, E., Arndt, S.K., Cernusak, L.A., West, J.B., and Sachse, D. (2013). 'Leaf water deuterium enrichment shapes leaf wax n-alkane δD values of angiosperm plants II: Observational evidence and global implications.' *Geochimica et Cosmochimica Acta*, 111, pp. 50-63.

Kearney, R., Albert, P.G., Staff, R.A., Pál, I., Veres, D., Magyari, E., and Ramsey, C.B. (2018). 'Ultra-distal fine ash occurrences of the Icelandic Askja-S Plinian eruption deposits in Southern Carpathian lakes: New age constraints on a continental scale tephrostratigraphic marker.' *Quaternary Science Reviews*, 188, pp.174-182.

Kelly, T.J., Hardiman, M., Lovelady, M., Lowe, J.J., Matthews, I.P., and Blockley, S.P.E (2017). 'Scottish early Holocene vegetation dynamics based on pollen and tephra records from Inverlair and Loch Etteridge, Inverness-shire.' *Proceedings of the Geologists' Association*, 128(1), pp. 125-135.

Kelts, K., and Hsü, K.J. (1978). 'Freshwater carbonate sedimentation.' In: Lerman, A. (Ed). *Lakes: Chemistry, Geology, Physics,* New York: Springer, pp. 295-323.

Kendall, P.F. (1902). 'A system of glacier-lakes n the Cleveland Hills.' *Quarterly Journal of the Geological Society*, 58, pp. 471–571.

Kent, P. (1980). *British Regional Geology: From the Tees to the Wash, Second Edition*. London: HMSO, Institute of Geological Sciences, 160pp.

Klitgaard-Kristensen, D., Sejrup, H.P., and Haflidason, H. (2001). 'The last 18 kyr fluctuations in Norwegian Sea surface conditions and implications for the magnitude of climatic change: evidence from the North Sea.' *Paleoceanography*, 16(5), pp. 455-467.

Kruckeberg, A.R. (2004). *Geology and Plant Life: The Effects of Landforms and Rock Types on Plants*, Seattle: University of Washington Press, 304pp.

Krüger, S., Dörfler, W., Bennike, O., and Wolters, S. (2017). Life in Doggerland–palynological investigations of the environment of prehistoric hunter-gatherer societies in the North Sea Basin. *E&G Quaternary Science Journal*, 66(1), pp. 3–13.

Kuhlbrodt, T., Griesel, A., Montoya, M., Levermann, A., Hofmann, M., and Rahmstorf, S. (2007). 'On the driving processes of the Atlantic meridional overturning circulation.' *Reviews of Geophysics*, 45(2).

Kulesza, P., Suchora, M., Pidek, I.A., and Alexandrowicz, W.P. (2011). 'Chronology and directions of Late Glacial paleoenvironmental changes: A multi-proxy study on sediments of Lake Słone (SE Poland).' *Quaternary International*, 238(1-2), pp. 89-106.

Lane, C.S., Blockley, S.P.E., Bronk Ramsey, C., and Lotter, A.F. (2011). 'Tephrochronology and absolute centennial scale synchronisation of European and Greenland records for the last glacial to interglacial transition: a case study of Soppensee and NGRIP.' *Quaternary International*, 246(1-2), pp. 145-156.

Lane, C.S., Brauer, A., Blockley, S.P.E., and Dulski, P. (2013). 'Volcanic ash reveals time-transgressive abrupt climate change during the Younger Dryas.' *Geology*, 41(12), pp. 1251-1254.

Lang, B., Brooks, S.J., Bedford, A., Jones, R.T., Birks, H.J.B., and Marshall, J.D. (2010). 'Regional consistency in Late-Glacial chironomid-inferred temperatures from five sites in north-west England.' *Quaternary Science Reviews*, 29(13), pp. 1528-1538.

Larocque-Tobler, I., Heiri, O., and Wehrli, M. (2010). 'Late Glacial and Holocene temperature changes at Egelsee, Switzerland, reconstructed using subfossil chironomids.' *Journal of Paleolimnology*, 43(4), pp. 649-666.

Larsen, J.J., and Nygaard, N.N. (2014). 'Lateglacial and early Holocene tephrostratigraphy and sedimentology of the Store Slotseng basin, SW Denmark: a multi-proxy study. *Boreas*, 43(2), pp. 349-361.

Lehman, S.J., and Keigwin, L.D. (1992). 'Sudden changes in North Atlantic circulation during the last deglaciation.' *Nature*, 356(6372), pp. 757-762.

Lemdahl, G. (1991). 'A rapid climatic change at the end of the Younger Dryas in south Sweden: palaeoclimatic and palaeoenvironmental reconstructions based on fossil insect assemblages.' *Palaeogeography, Palaeoclimatology, Palaeoecology*, 83(4), pp. 313-331.

Leng, M.J., and Marshall, J.D. (2004). 'Palaeoclimate interpretation of stable isotope data from lake sediment archives.' *Quaternary Science Reviews*, 23(7-8), pp. 811-831.

Leng, M.J., Jones, M.D., Frogley, M.R., Eastwood, W.J., Kendrick, C.P., and Roberts, C.N. (2010). 'Detrital carbonate influences on bulk oxygen and carbon isotope composition of lacustrine sediments from the Mediterranean.' *Global and Planetary Change*, 71(3-4), pp. 175-182.

Leslie, A.B., Tucker, M.E., and Spiro, B. (1992). 'A sedimentological and stable isotopic study of travertines and associated sediments within Upper Triassic lacustrine limestones, South Wales, UK.' *Sedimentology*, 39(4), pp. 613-629.

Lewis, C.A. (1970). 'The Upper Wye and Usk Regions.' In: Lewis, C.A. (Ed.). *The Glaciations of Wales and Adjoining Regions*, London: Longman, pp. 147–173.

Lewis, S.C., LeGrande, A.N., Kelley, M., and Schmidt, G.A. (2010). 'Water vapour source impacts on oxygen isotope variability in tropical precipitation during Heinrich events.' *Climate of the Past*, 6(3), pp. 325-343.

Licciardi, J.M., Teller, J.T., and Clark, P.U. (1999). 'Freshwater routing by the Laurentide Ice Sheet during the last deglaciation.' Geophysical Monograph -American Geophysical Union, 112, pp. 177-202.

Lincoln, P. (2017) *Environmental and Landscape Responses to Abrupt Climatic Change during the Last Termination (Ca. 21-11 Cal Ka BP) in the Vale of Pickering, NE England*. Unpublished PhD thesis, Royal Holloway, University of London.

Lisiecki, L.E., and Raymo, M.E. (2005). 'A Pliocene-Pleistocene stack of 57 globally distributed benthic δ18O records.' *Paleoceanography*, 20, PA1003,

Lind, E.M., and Wastegård, S. (2011). 'Tephra horizons contemporary with short early Holocene climate fluctuations: new results from the Faroe Islands.' *Quaternary International*, 246(1-2), pp. 157-167.

Litt, T., and Stebich, M. (1999). 'Bio-and chronostratigraphy of the lateglacial in the Eifel region, Germany.' *Quaternary International*, 61(1), pp. 5-16.

Litt, T., Brauer, A., Goslar, T., Merkt, J., Bałaga, K., Müller, H., Ralska-Jasiewiczowa, M., Stebich, M., and Negendank, J.F. (2001). 'Correlation and synchronisation of Lateglacial continental sequences in northern central Europe based on annually laminated lacustrine sediments.' *Quaternary Science Reviews*, 20(11), pp. 1233-1249.

Liu, H., and Liu, W. (2016). 'n-Alkane distributions and concentrations in algae, submerged plants and terrestrial plants from the Qinghai-Tibetan Plateau.' *Organic Geochemistry*, 99, pp. 10-22.

Liu, H., Yang, H., Cao, Y., and Liu, W. (2018). 'Compound-specific δD and its hydrological and environmental implication in the lakes on the Tibetan Plateau.' *Science China Earth Sciences*, 61(6), pp. 765-777.

Liu, W., Yang, H., and Li, L. (2006). 'Hydrogen isotopic compositions of *n*-alkanes from terrestrial plants correlate with their ecological life forms.' *Oecologia*, 150(2), pp. 330-338.

Lohne, Ø.S., Mangerud, J., and Birks, H.H. (2014). 'IntCal13 calibrated ages of the Vedde and Saksunarvatn ashes and the Younger Dryas boundaries from Kråkenes, western Norway.' *Journal of Quaternary Science*, 29(5), pp. 506-507.

Lotter, A.F., Eicher, U., Siegenthaler, U., and Birks, H.J.B. (1992). 'Late-Glacial climatic oscillations as recorded in Swiss lake sediments.' *Journal of Quaternary Science*, 7(3), pp. 187-204.

Lotter, A.F. (1999). 'Late-glacial and Holocene vegetation history and dynamics as shown by pollen and plant macrofossil analyses in annually laminated sediments from Soppensee, central Switzerland.' *Vegetation History and Archaeobotany*, 8(3), pp. 165-184.

Lotter, A.F., Heiri, O., Brooks, S.J., van Leeuwen, J.F., Eicher, U., and Ammann, B. (2012). 'Rapid summer temperature changes during Termination 1a: high-resolution multi-proxy climate reconstructions from Gerzensee (Switzerland).' *Quaternary Science Reviews*, 36, pp. 103-113.

Lowe, J.J. (2001). 'Abrupt climatic changes in Europe during the last glacial–interglacial transition: the potential for testing hypotheses on the synchroneity of climatic events using tephrochronology.' *Global and Planetary Change*, 30(1), pp. 73-84.

Lowe, J. J., and Lowe, S. (1989). 'Interpretation of the pollen stratigraphy of Late Devensian lateglacial and early Flandrian sediments at Llyn Gwernan, near Cader Idris, North Wales.' *New Phytologist*, 113(3), pp. 391-408.

Lowe, J.J., and Walker, M.J.C. (1986). 'Late-Glacial and early Flandrian environmental history of the Isle of Mull, Inner Hebrides, Scotland.' *Transactions of the Royal Society of Edinburgh: Earth Sciences*, 77(1), pp. 1-20

Lowe, J.J., and Walker, M.J.C. (2000). 'Radiocarbon dating the Last Glacial-Interglacial Transition (Ca. 14–9 ^{14}C Ka Bp) in terrestrial and marine records: the need for new quality assurance protocols.' *Radiocarbon*, 42(1), pp. 53-68.

Lowe, J.J. (1982). 'Three Flandrian pollen profiles from the Teith Valley, Perthshire, Scotland.' *New Phytologist*, 90(2), pp. 355-370.

Lowe, J.J., and NASP Members. (1995). 'Palaeoclimate of the North Atlantic seaboards during the last glacial/interglacial transition.' *Quaternary International*, 28, pp. 51-61.

Lowe, J.J., and Walker, M.J.C. (1977) ‘The reconstruction of the Late-Glacial environment in the southern and eastern Grampian Highlands.’ In: Gray, J.M., and Lowe, J.J. (Eds.). *Studies in the Scottish Late-Glacial Environment*, Oxford: Pergammon Press, pp. 101–118.

Lowe, J.J., and Walker, M.J.C. (2014). *Reconstructing Quaternary Environments, Third Edition.* Abingdon: Routledge, 538 pp.

Lowe, J.J., Birks, H.H., Brooks, S.J., Coope, G.R., Harkness, D.D., Mayle, F.E., Sheldrick, C., Turney, C.S.M., and Walker, M.J.C. (1999). ‘The chronology of palaeoenvironmental changes during the Last Glacial-Holocene transition: towards an event stratigraphy for the British Isles.’ *Journal of the Geological Society*, 156(2), pp. 397-410.

Lowe, J.J., Rasmussen, S.O., Björck, S., Hoek, W.Z., Steffensen, J.P., Walker, M.J.C., Yu, Z.C., and INTIMATE Members. (2008). 'Synchronisation of palaeoenvironmental events in the north Atlantic region during the Last Termination: a revised protocol recommended by the INTIMATE group.' *Quaternary Science Reviews*, 27(1), pp. 6-17.

Lowry, D., and Grassineau, N. (2009). ‘Are there four cycles of extreme climate change in the Neoproterozoic Dalradian Supergroup of Scotland and Ireland?’ *Geochimica et Cosmochimica Acta*, 73(13), pp. A794-A794.

MacLeod, A., Palmer, A.P., Lowe, J.J, Rose, J., Bryant, C., and Merritt, J. (2011). ‘Timing of glacier response to Younger Dryas climatic cooling in Scotland.’ *Global and Planetary Change*, 79(3-4), pp. 264-274.

Magny, M., Aalbersberg, G., Bégeot, C., Benoit-Ruffaldi, P., Bossuet, G., Disnar, J.R., Heiri, O., Laggoun-Defarge, F., Mazier, F., Millet, L., Peyron, O., Vannière, B., and Walter-Simonnet, A.V. (2006). ‘Environmental and climatic changes in the Jura mountains (eastern France) during the Lateglacial–Holocene transition: a multi-proxy record from Lake Lautrey.’ *Quaternary Science Reviews*, 25(5-6), pp.414-445.

Magny, M., Vannière, B., De Beaulieu, J.L., Bégeot, C., Heiri, O., Millet, L., Peyron, O., and Walter-Simonnet, A.V. (2007). ‘Early-Holocene climatic oscillations recorded by lake-level fluctuations in west-central Europe and in central Italy.’ *Quaternary Science Reviews*, 26(15-16), pp. 1951-1964.

Mangerud, J., Andersen, S. T., Berglund, B. E., and Donner, J. J. (1974). ‘Quaternary stratigraphy of Norden, a proposal for terminology and classification.’ *Boreas*, 3(3), pp. 109-126.

Mangili, C., Brauer, A., Plessen, B., Dulski, P., Moscariello, A., and Naumann, R. (2010). ‘Effects of detrital carbonate on stable oxygen and carbon isotope data from varved sediments of the interglacial Piànico palaeolake (Southern Alps, Italy).’ *Journal of Quaternary Science*, 25(2), pp. 135-145.

Marshall, J.D., Jones, R.T., Crowley, S.F., Oldfield, F., Nash, S., and Bedford, A. (2002). ‘A high resolution Late-Glacial isotopic record from Hawes Water, north-west England: climatic oscillations: calibration and comparison of palaeotemperature proxies.’ *Palaeogeography, Palaeoclimatology, Palaeoecology*, 185(1), pp. 25-40.

Martin-Puertas, C., Matthes, K., Brauer, A., Muscheler, R., Hansen, F., Petrick, C., Aldahan, A., Possnert, G., and van Geel, B. (2012). ‘Regional atmospheric circulation shifts induced by a grand solar minimum.’ *Nature Geoscience*, 5(6), pp. 397-401

Martinson, D.G., Pisias, N.G., Hays, J.D., Imbrie, J., Moore, T.C., and Shackleton, N.J. (1987). 'Age dating and the orbital theory of the ice ages: development of a high-resolution 0 to 300,000-year chronostratigraphy.' *Quaternary Research*, 27(1), pp. 1-29.

Masson-Delmotte, V., Jouzel, J., Landais, A., Stievenard, M., Johnsen, S.J., White, J.W., Werner, M., Sveinbjörnsdottir, A.E., and Fuhrer, K. (2005). 'GRIP deuterium excess reveals rapid and orbital-scale changes in Greenland moisture origin.' *Science*, 309(5731), pp.118-121.

Matthews, I.P., Birks, H.H., Bourne, A.J., Brooks, S.J., Lowe, J.J., Macleod, A., and Pyne-O'Donnell, S.D.F. (2011). 'New age estimates and climatostratigraphic correlations for the Borrobol and Penifiler Tephras: evidence from Abernethy Forest, Scotland', *Journal of Quaternary Science*, 26(3), pp. 247–252.

Mauquoy, D., van Geel, B., Blaauw, M., and van der Plicht, J. (2002). 'Evidence from northwest European bogs shows 'Little Ice Age' climatic changes driven by variations in solar activity.' *The Holocene*, 12(1), pp. 1-6.

Mayle, F.E., Bell, M., Birks, H.H., Brooks, S.J., Coope, G.R., Lowe, J.J., Sheldrick, C., Shijie, L., Turney, C.S.M., and Walker, M.J.C. (1999). 'Climate variations in Britain during the Last Glacial–Holocene transition (15.0–11.5 Cal. ka BP): comparison with the GRIP ice-core record.' *Journal of the Geological Society*, 156(2), pp. 411-423.

Mayle, F.E., Lowe, J.J., and Sheldrick, C. (1997). 'The Late Devensian Late-Glacial palaeoenvironmental record from Whitrig Bog, SE Scotland. 1: Lithostratigraphy, geochemistry and palaeobotany.' *Boreas*, 26(4), pp. 279-295.

Mellars, P., and Dark, P. (1998). *Star Carr in Context*: *new archaeological and palaeoecological investigations at the early Mesolithic site of Star Carr, north Yorkshire*. Cambridge: McDonald Institute for Archaeological Research, 250pp.

Merkt, J., and Müller, H. (1999). 'Varve chronology and palynology of the Lateglacial in Northwest Germany from lacustrine sediments of Hämelsee in Lower Saxony.' *Quaternary International*, 61(1), pp. 41-59.

Meyers, P.A., and Lallier-Vergès, E. (1999). 'Lacustrine sedimentary organic matter records of late Quaternary paleoclimates.' *Journal of Paleolimnology*, 21(3), pp. 345-372.

Millspaugh, S.H., and Whitlock, C. (1995). 'A 750-year fire history based on lake sediment records in central Yellowstone National Park, USA.' *The Holocene*, 5(3), pp. 283-292.

Milner, N., Bamforth, M., Beale, G., Carty, J.C., Konstantinos, C., Croft, S., Conneller, C., Elliott, B., Fitton, L.C., Knight, B., Kroger, R., Little, A., Needham, A., Robson, H.K., Rowley, C.C.A., and Taylor, B. (2016). 'A Unique Engraved Shale Pendant from the Site of Star Carr: the oldest Mesolithic art in Britain.' *Internet Archaeology*, 40.

Milner, N., Conneller, C., Elliott, B., Koon, H., Panter, I., Penkman, K., Taylor, B., and Taylor, M. (2011a). 'From riches to rags: Organic deterioration at Star Carr.' *Journal of Archaeological Science*, 38(10), pp. 2818–2832.

Milner, N., Lane, P., Taylor, B., Conneller, C., and Schadla-Hall, T. (2011b). 'Star Carr in a Postglacial Lakescape: 60 Years of Research,' *Journal of Wetland Archaeology*, 11(1), pp. 1–19.

Mix, A.C., Bard, E., and Schneider, R. (2001). 'Environmental processes of the ice age: land, oceans, glaciers (EPILOG).' *Quaternary Science Reviews*, 20(4), pp. 627-657.

Moar, N.T. (1969). 'Two Pollen Diagrams from the Mainland, Orkney Islands.' *New Phytologist*, 68(1), pp. 201–208.

Moles, N.R., Boyce, A.J., and Fallick, A.E. (2015). 'Abundant sulphate in the Neoproterozoic ocean: implications of constant $\delta^{34}S$ of barite in the Aberfeldy SEDEX deposits, Scottish Dalradian.' In: Jenkin, J.R.T., Lusty, P.A.J., McDonald, I., Smith, M.P., Boyce, A.J., and Wilkinson, J.J. (Eds.). *Ore Deposits in an Evolving Earth*, London: Geological Society Special Publications, pp. 189-212

Moore, P.D., Webb, J.A., and Collinson, M.E. (1991). *Pollen Analsyis.* Oxford: Blackwell Scientific Publications, 216pp.

Moreno, A., Stoll, H.M., Jiménez-Sánchez, M., Cacho, I., Valero-Garcés, B., Ito, E., and Edwards, L.R. (2010). 'A speleothem record of rapid climatic shifts during last glacial period from Northern Iberian Peninsula.' *Global and Planetary Change*, 71(218), pp. e231.

Moreno, A., Svensson, A., Brooks, S.J., Connor, S., Engels, S., Fletcher, W., Genty, D., Heiri, O., Labuhn, I., Perşoiu, A., Peyron, O., Sedori, L., Valero-Garcés, B., Wulf, S., and Zanchetta, G. (2014). 'A compilation of Western European terrestrial records 60–8 ka BP: towards an understanding of latitudinal climatic gradients.' *Quaternary Science Reviews*, 106, pp.167-185.

Mortensen, M.F., Birks, H.H., Christensen, C., Holm, J., Noe-Nygaard, N., Odgaard, B.V., Olsen, J., and Rasmussen, K.L. (2011). 'Lateglacial vegetation development in Denmark–new evidence based on macrofossils and pollen from Slotseng, a small-scale site in southern Jutland.' *Quaternary Science Reviews*, 30(19-20), pp. 2534-2550.

Muschitiello, F., and Wohlfarth, B. (2015). 'Time-transgressive environmental shifts across Northern Europe at the onset of the Younger Dryas.' *Quaternary Science Reviews*, 109, pp.49-56.

Muschitiello, F., Pausata, F.S., Watson, J.E., Smittenberg, R.H., Salih, A.A., Brooks, S.J., Whitehouse, N.J., Karlatou-Charalampopoulou, A., and Wohlfarth, B. (2015). 'Fennoscandian freshwater control on Greenland hydroclimate shifts at the onset of the Younger Dryas.' *Nature communications*, 6, 8939.

Mykura, M. (1976). *British Regional Geology: Orkney and Shetland*. Edinburgh: Institute of Geological Sciences, HMSO, NERC, 159pp.

Nakagawa, T., Brugiapaglia, E., Digerfeldt, G., Reille, M., Beaulieu, J.L.D., and Yasuda, Y. (1998). 'Dense-media separation as a more efficient pollen extraction method for use with organic sediment/deposit samples: comparison with the conventional method.' *Boreas*, 27(1), pp. 15-24.

Nesje, A., Dahl, S.O., and Bakke, J. (2004). 'Were abrupt Lateglacial and early-Holocene climatic changes in northwest Europe linked to freshwater outbursts to the North Atlantic and Arctic Oceans?' *The Holocene*, 14(2), pp. 299-310.

Ó Cofaigh, C., and Evans, D.J.A. (2001). 'Deforming bed conditions associated with a major ice stream of the last British ice sheet.' *Geology*, 29(9), pp. 795–798.

O'Connor, T., and Bunting, M.J. (2009). 'Environmental change in an Orkney wetland: plant and molluscan evidence from Quoyloo Meadow.' In: Allen, M.J., Sharples, N., and O'Conner, T.P. (Eds.). *Land and People: Papers in Memory of John G. Evans. Allen*, The Prehistoric Society, Prehistoric Society Research Paper; Number 2: London, pp. 162–168.

O'Connell, M., Huang, C.C., and Eicher, U. (1999). 'Multidisciplinary investigations, including stable-isotope studies, of thick Late-glacial sediments from Tory Hill, Co. Limerick, western Ireland.' *Palaeogeography, Palaeoclimatology, Palaeoecology*, 147(3-4), pp. 169-208.

Odland, A., and del Moral, R. (2002). 'Thirteen years of wetland vegetation succession following a permanent drawdown, Myrkdalen Lake, Norway.' *Plant Ecology*, 162(2), pp. 185-198.

Oksanen, J., Blanchet, F.G., Kindt, R., Legendre, P., Minchin, P.R., O'hara, R.B., Simpson, G.L., Solymos, P., Stevens, M.H.H., Wagner, H., and Oksanen, M.J. (2018). Package 'vegan' Community ecology package, R package version 2.5-2 [Software] https://cran.ism.ac.jp/web/packages/vegan/vegan.pdf

Palmer, A.P., Matthews, I.P., Candy, I., Blockley, S.P.E., Maceod, A., Darvill, C., Milner, N., Conneller, C., and Taylor, B. (2017). 'The bathymetry and lithostratigraphy of sediments in Palaeolake Flixton, north Yorkshire.' In: Eddey, L., Lincoln, P., Matthews, I.P., Palmer, A.P., and Bateman, M.D. (Eds.). *The Quaternary of the Vale of Pickering: Field Guide*, London: Quaternary Research Association, pp. 124-128.

Palmer, A.P., Matthews, I.P., Candy, I., Blockley, S.P.E., MacLeod, A., Darvill, C.M., Milner, N., Conneller, C., and Taylor, B. (2015). 'The evolution of Palaeolake Flixton and the environmental context of Star Carr, NE. Yorkshire: Stratigraphy and sedimentology of the Last Glacial-Interglacial Transition (LGIT) lacustrine sequences.' *Proceedings of the Geologists' Association*, 126(1), pp. 50–59.

Palmer, A.P., Rose, J., Lowe, J.J., and MacLeod, A. (2010). 'Annually resolved events of Younger Dryas glaciation in Lochaber (Glen Roy and Glen Spean), Western Scottish Highlands,' *Journal of Quaternary Science*, 25(4), pp. 581–586.

Palmer, A.P., Rose, J., Lowe, J.J., and Walker, M.J.C. (2007). 'The pre-Holocene succession of glaciolacustrine sediments within Llangorse basin.' In: Carr, S.J., Coleman, C.G., Humpage, A.J., and Shakesby, R.A. (Eds.). *The Quaternary of the Brecon Beacons: Field Guide*, London: Quaternary Research Association, pp. 220-229.

Palmer, A.P., Rose, J., Lowe, J.J., and Walker, M.J.C. (2008). 'Annually laminated Late Pleistocene sediments from Llangorse Lake, South Wales, UK: a chronology for the pattern of ice wastage.' *Proceedings of the Geologists' Association*, 119, pp. 245–258.

Paus, A. (2010). 'Vegetation and environment of the Rødalen alpine area, Central Norway, with emphasis on the early Holocene.' *Vegetation History and Archaeobotany*, 19(1), pp. 29-51.

Peach, B.N., and Horne, J. (1880). 'The glaciation of the Orkney Islands.' *Quarterly Journal of the Geological Society*, 36(1–4), pp. 648–663.

Pennington, W. (1977). 'The Late Devensian flora and vegetation of Britain.' Philosophical *Transactions of the Royal Society Series B Biological Sciences*, 280(972), pp. 247-271.

Pennington, W. (1986). ‘Lags in adjustment of vegetation to climate caused by the pace of soil development. Evidence from Britain.’ *Plant Ecology*, 67(2), pp. 105-118.

Pennington, W., Haworth, E.Y., Bonny, A.P., and Lishman, J.P. (1972). ‘Lake Sediments in Northern Scotland.’ *Philosophical Transactions of the Royal Society of London, Series B, Biological Sciences*, 264(861), pp. 191–294.

Phillips, F.M., Bowen, D.Q., and Elmore, D. (1994). ‘Surface Exposure Dating of Glacial Features in Great Britain Using Cosmogenic Chlorine-36: Preliminary Results.’ *Mineralogical Magazine*, 58A(2), pp. 722–723.

Phillips, W.M., Hall, A.M., Ballantyne, C.K., Binnie, S., Kubric, P.W., and Freeman, S. (2008). ‘Extent of the last ice sheet in northern Scotland tested with cosmogenic 10Be exposure ages.’ *Journal of Quaternary Science*, 23(2), pp. 101–107.

Piasentier, E., Bovolenta, S., and Malossini, F. (2000). ‘The n-alkane concentrations in buds and leaves of browsed broadleaf trees.’ *The Journal of Agricultural Science*, 135(3), pp. 311-320.

Pollard, A.M., Blockley, S.P.E., and Lane, C.S. (2006). ‘Some numerical considerations in the geochemical analysis of distal microtephra.’ *Applied Geochemistry*, 21(10), pp. 1692-1714.

Power, M.J., Marlon, J., Ortiz, N., Bartlein, P.J., Harrison, S.P., Mayle, F.E., Ballouche, A., Bradshaw, R.H.W., Carcaillet, C., Cordova, C., Mooney, S., Moreno, P.I., Prentice, I.C., Thonicke, K., Tinner, W., Whitlock, C., Zhang, Y., Zhao, Y., Ali, A.A., Anderson, R.S., Beer, R., Behling, H., Briles, C., Brown, K.J., Brunelle, A., Bush, M., Camill, P., Chu, G.Q., Clark, J., Colombaroli, D., Connor, S., Daniau, A.L., Daniels, M., Dodson, J., Doughty, E., Edwards, M.E., Fisinger, W., Foster, D., Frechette, J., Gaillard, M.-J., Gavin, D.G., Gobet, E., Haberle, S., Hallett, D.J., Higuera, P., Hope, G., Horn, S., Inoue, J., Kaltenreider, P., Kennedy, L., Kong, Z.C., Larsen, C., Long, C.J., Lynch, J., Lynch, E.A., McGlone, M., Meeks, S., Mensing, S., Meyer, G., Minckley T., Mohr, J., Nelson, D.M., New, J., Newnham, R., Noti, R., Oswald, W., Pierce, J., Richard, P.J.H., Rowe, C., Sanchez Goñi, M.F., Shuman, B.N., Takahara, H., Toney, J., Turney, C., Urrego-Sanchez, D.H., Umbanhowar, C., Vandergoes, M., Vanniere, B., Vescovi, E., Walsh, M., Wang, X., Williams, N., Wilmshurst, J., and Zhang, J.H. (2008). 'Changes in fire regimes since the Last Glacial Maximum: an assessment based on a global synthesis and analysis of charcoal data.' *Climate Dynamics*, 30(7-8), pp. 887-907.

Prave, A.R., Fallick, A.E., Thomas, C.W., and Graham, C.M. (2009). ‘A composite C-isotope profile for the Neoproterozoic Dalradian Supergroup of Scotland and Ireland.’ *Journal of the Geological Society*, 166(5), pp. 845-857.

Prentice, I.C. (1985). 'Pollen representation, source area, and basin size: toward a unified theory of pollen analysis.' *Quaternary Research*, 23(1), pp. 76-86.

Prentice, I.C., Bartlein, P.J., and Webb, T. (1991). 'Vegetation and climate change in eastern North America since the last glacial maximum.' *Ecology*, 72(6), pp. 2038-2056.

Preston, C.D., Pearman, D.A., and Dines, T. D. (2002) *New Atlas of the British and Irish Flora,* Oxford: Oxford University Press, 922 pp.

Punt, W., Hoen, P. P., Blackmore, S., Nilsson, S., and Le Thomas, A. (2007). ‘Glossary of pollen and spore terminology.’ *Review of Palaeobotany and Palynology*, 143(1), pp. 1-81.

Pyne-O'Donnell, S.D.F., Blockley, S.P.E., Turney, C.S.M., and Lowe, J.J. (2008) 'Distal volcanic ash layers in the Lateglacial Interstadial (GI-1): problems of stratigraphic discrimination.' *Quaternary Science Reviews*, 27(1–2), pp. 72–84.

Pyne-O'Donnell, S.D.F (2007). 'Three new distal tephras in sediments spanning the Last Glacial–Interglacial Transition in Scotland.' *Journal of Quaternary Science*, 22(6), pp. 559-570.

Quevedo, L., Rodrigo, A., and Espelta, J.M. (2007). 'Post-fire resprouting ability of 15 non-dominant shrub and tree species in Mediterranean areas of NE Spain.' *Annals of Forest Science*, 64(8), pp. 883-890.

Quinn, P.J., and Williams, W.P. (1978). 'Plant lipids and their role in membrane function.' *Progress in Biophysics and Molecular Biology*, 34, pp. 109-173.

Rach, O., Brauer, A., Wilkes, H., and Sachse, D. (2014). 'Delayed hydrological response to Greenland cooling at the onset of the Younger Dryas in western Europe.' *Nature Geoscience*, 7(2), pp. 109-112.

Rach, O., Kahmen, A., Brauer, A., and Sachse, D. (2017). 'A dual-biomarker approach for quantification of changes in relative humidity from sedimentary lipid D⁄H ratios.' *Climate of the Past*, 13(7), pp. 741-757.

Rae, D.E (1976). *Apspects of Glaciation in Orkney*. Unpublished PhD thesis, University of Liverpool, 469pp.

Rahmstorf, S. (2002). 'Ocean circulation and climate during the past 120,000 years.' *Nature*, 419(6903), pp. 207-214.

Ranner, P.H. (2005). *Lateglacial and early Holocene environmental changes along the northwest European continental margin.* Unpublished PhD thesis, Durham University.

Ranner, P.H., Allen, J.R., and Huntley, B. (2005). 'A new early Holocene cryptotephra from northwest Scotland.' *Journal of Quaternary Science*, 20(3), pp. 201-208.

Rasmussen, S.O., Andersen, K.K., Svensson, A.M., Steffensen, J.P., Vinther, B.M., Clausen, H.B., Siggaard-Andersen, M.L., Johnsen, S.J., Larsen, L.B., Dahl-Jensen, D., Bigler, M., Rothlisberger, R., Fischer, H., Gotto-Azuma, K., Hansson, M.E., and Ruth, U. (2006). 'A new Greenland ice core chronology for the last glacial termination.' *Journal of Geophysical Research: Atmospheres*, 111(D6).

Rasmussen, S.O., Bigler, M., Blockley, S.P., Blunier, T., Buchardt, S.L., Clausen, H.B., Cvijanovic, I., Dahl-Jensen, D., Johnsen, S.J., Fischer, H., Gkinis, V., Guillevic, M., Hoek, W.Z., Lowe, J.J., Pedro, J.B., Popp, T., Seierstad. I.K., Steffensen, J.P., Svensson, A.M., Vallelonga, P., Vinther, B.M., Walker, M.J.C., Wheatley,J.J., and Winstrup, M. (2014). 'A stratigraphic framework for abrupt climatic changes during the Last Glacial period based on three synchronized Greenland ice-core records: refining and extending the INTIMATE event stratigraphy.' *Quaternary Science Reviews*, 106, pp. 14-28.

Rasmussen, S.O., Vinther, B.M., Clausen, H.B., and Andersen, K.K. (2007). 'Early Holocene climate oscillations recorded in three Greenland ice cores', *Quaternary Science Reviews*, 26(15–16), 1907–1914.

Reille, M. (1992). *Pollen et Spores D'Europe et D'Afrique du Nord.* Marseille: Laboratoire de Botanique Historique et Palynologie, 520pp.

Reimer, P.J., Bard, E., Bayliss, A., Beck, J.W., Blackwell, P.G., Bronk Ramsey, C., Buck, C.E., Cheng, H., Edwards, R.L., Friedrich, M. and Grootes, P.M., Guilderson, T. P., Haflidason, H., Hajdas, I., Hatté, C., Heaton, T.J., Hoffman, D.L., Hogg, A.G., Hughen, K.A., Kaiser, K.F., Kromer, B., Manning, S.W., Niu, M., Reimer, R.W., Richards, D.A., Scott, E.M., Southon, J.R., Staff, R.A., Turney, C.S.M., and van der Plicht, J. (2013). 'IntCal13 and Marine13 radiocarbon age calibration curves 0–50,000 years Cal. BP.' *Radiocarbon*, 55(4), pp. 1869-1887.

Renssen, H., and Isarin, R.F.B. (1997). 'Surface temperature in NW Europe during the Younger Dryas: AGCM simulation compared with temperature reconstructions.' *Climate Dynamics*, 14(1), pp. 33-44.

Renssen, H., Mairesse, A., Goosse, H., Mathiot, P., Heiri, O., Roche, D.M., Nisancioglu, K.H., and Valdes, P.J. (2015). 'Multiple causes of the Younger Dryas cold period.' *Nature Geoscience*, 8(12), pp .946-949.

Rey, F., Gobet, E., van Leeuwen, J.F., Gilli, A., van Raden, U.J., Hafner, A., Wey, O., Rhiner, J., Schmocker, D., Zünd, J., and Tinner, W. (2017). 'Vegetational and agricultural dynamics at Burgäschisee (Swiss Plateau) recorded for 18,700 years by multi-proxy evidence from partly varved sediments.' *Vegetation History and Archaeobotany*, 26(6), pp. 571-586.

Riviere, G., Laine, A., Lapeyre, G., Salas-Mélia, D., and Kageyama, M. (2010). 'Links between Rossby wave breaking and the North Atlantic Oscillation–Arctic Oscillation in present-day and Last Glacial Maximum climate simulations.' *Journal of Climate*, 23(11), pp. 2987-3008.

Rohling, E.J., and Pälike, H. (2005). 'Centennial-scale climate cooling with a sudden cold event around 8,200 years ago.' *Nature*, 434(7036), pp. 975-979.

Romanek, C.S., Grossman, E.L., and Morse, J.W. (1992). 'Carbon isotopic fractionation in synthetic aragonite and calcite: effects of temperature and precipitation rate.' *Geochimica et cosmochimica acta*, 56(1), pp. 419-430.

Rose, J. (1985). 'The Dimlington Stadial/Dimlington Chronozone: a proposal for naming the main glacial episode of the Late Devensian in Britain.' *Boreas*, 14(3), pp. 225-230.

Rozanski, K., Araguás-Araguás, L., and Gonfiantini, R. (1992). 'Relation between long-term trends of oxygen-18 isotope composition of precipitation and climate.' *Science*, 258(5084), pp. 981-985.

Rozanski, K., Araguás-Araguás, L., and Gonfiantini, R. (1993). 'Isotopic patterns in modern global precipitation' In: Swart, P.K., Lohmann, K.C., McKenzie. J., and Savin. S. (Eds.). *Climate Change in Continental Isotopic Records*, Washington DC: American Geophysical Union, pp. 1-36.

Ruddiman, W.F. (2006). 'Orbital changes and climate.' *Quaternary Science Reviews*, 25(23), pp. 3092-3112.

Ruddiman, W.F., and McIntyre, A. (1981). 'Oceanic mechanisms for amplification of the 23,000-year ice-volume cycle.' *Science*, 212(4495), pp. 617-627.

Sachse, D., Billault, I., Bowen, G.J., Chikaraishi, Y., Dawson, T.E., Feakins, S.J., Freeman, K.H., Magill, C.R., McInerney, F.A., van der Meer, M.T.J., Polisar, P., Robins, R.J., Sachs, J.P., Schmidt, H-L., Sessions, A.L., White, J.W.C., West, J.B., and Kahmen, A. (2012). 'Molecular paleohydrology: interpreting the hydrogen-isotopic

composition of lipid biomarkers from photosynthesizing organisms.' *Annual Review of Earth and Planetary Sciences*, 40, pp. 221-249.

Sachse, D., Kahmen, A., and Gleixner, G. (2009). 'Significant seasonal variation in the hydrogen isotopic composition of leaf-wax lipids for two deciduous tree ecosystems (*Fagus sylvativa* and *Acerpseudoplatanus*).' *Organic Geochemistry*, 40(6), pp. 732-742.

Sachse, D., Radke, J., and Gleixner, G. (2004). 'Hydrogen isotope ratios of recent lacustrine sedimentary *n*-alkanes record modern climate variability.' *Geochimica et Cosmochimica Acta*, 68(23), pp. 4877-4889.

Sachse, D., Radke, J., and Gleixner, G. (2006). 'δD values of individual *n*-alkanes from terrestrial plants along a climatic gradient–Implications for the sedimentary biomarker record.' *Organic Geochemistry*, 37(4), pp. 469-483.

Sæther, O.A. (1979). 'Chironomid communities as water quality indicators.' *Ecography*, 2(2), pp. 65-74.

Samartin, S., Heiri, O., Vescovi, E., Brooks, S.J., and Tinner, W. (2012). 'Lateglacial and early Holocene summer temperatures in the southern Swiss Alps reconstructed using fossil chironomids.' *Journal of Quaternary Science*, 27(3), pp. 279-289.

Samartin, S., Heiri, O., Lotter, A.F., and Tinner, W. (2012). 'Climate warming and vegetation response after Heinrich event 1 (16 700–16 000 Cal. yr BP) in Europe south of the Alps.' *Climate of the Past*, 8(6), pp. 1913-1927.

Sarmaja-Korjonen, K., Seppänen, A., and Bennike, O. (2006). 'Pediastrum algae from the classic late glacial Bølling Sø site, Denmark: response of aquatic biota to climate change.' *Review of Palaeobotany and Palynology*, 138(2), pp. 95-107.

Scheffer, M., Bascompte, J., Brock, W.A., Brovkin, V., Carpenter, S.R., Dakos, V., Held, H., Van Nes, E.H., Rietkerk, M., and Sugihara, G. (2009). 'Early-warning signals for critical transitions.' *Nature*, 461(7260), p.53-59

Schenk, F., Väliranta, M., Muschitiello, F., Tarasov, L., Heikkilä, M., Björck, S., Brandefelt, J., Johansson, A.V., Näslund, J.O., and Wohlfarth, B. (2018). 'Warm summers during the Younger Dryas cold reversal.' *Nature communications*, 9, 1634.

Schwander, J., Eicher, U., and Ammann, B. (2000). 'Oxygen isotopes of lake marl at Gerzensee and Leysin (Switzerland), covering the Younger Dryas and two minor oscillations, and their correlation to the GRIP ice core.' *Palaeogeography, Palaeoclimatology, Palaeoecology*, 159(3-4), pp. 203-214.

Searl, A. (1989). 'Diagenesis of the Gully Oolite (Lower Carboniferous) South Wales.' *Geological Journal*, 24(4), pp. 275-293.

Seddon, A.W., Macias-Fauria, M., and Willis, K.J. (2015). 'Climate and abrupt vegetation change in northern Europe since the last de-glaciation.' *The Holocene*, 25(1), pp. 25-36.

Seddon, A.W., Macias-Fauria, M., Long, P.R., Benz, D., and Willis, K.J. (2016). 'Sensitivity of global terrestrial ecosystems to climate variability.' *Nature*, 531(7593), pp. 229-232.

Sejrup, H.P., Clark, C.D., and Hjelstuen, B.O. (2016). 'Rapid ice sheet retreat triggered by ice stream debuttressing: Evidence from the North Sea.' *Geology*, 44(5), pp. 355–358.

Sejrup, H.P., Hjelstuen, B.O., Dahlgren, K.I.T., Haflidason, H., Kuijpers, A., Nygård, A., Praeg, D., Stoker, M.S., Vorren, T.O., and Kuijpers, A. (2005). 'Pleistocene glacial history of the NW European continental margin.' *Marine and Petroleum Geology*, 22, pp. 1111–1129.

Sejrup, H.P., Hjelstuen, B.O., Nygård, A., Haflidason, H., and Mardal, I. (2015). 'Late Devensian ice-marginal features in the central North Sea - processes and chronology.' *Boreas*, 44(1), pp. 1–13.

Self, A. (2010). *The relationship between chironomids and climate in high latitude Eurasian lakes: implications for reconstructing Late Quaternary climate variability from subfossil chironomid assemblages in lake sediments from northern Russia.* Unpublished PhD Thesis, University College London, 454 pp.

Seppä, H. (2013). 'Pollen Analysis, Principles.' In: Elias, S.A., and Mock, C.J. (Eds.). *Encyclopedia of Quaternary Science, Second Edition*, Amsterdam: Elsevier, pp. 794-804.

Severinghaus, J.P., Sowers, T., Brook, E.J., Alley, R.B., and Bender, M.L. (1998). 'Timing of abrupt climate change at the end of the Younger Dryas interval from thermally fractionated gases in polar ice.' *Nature*, 391(6663), p.141-146.

Shackleton, N.J. (2000). 'The 100,000-year ice-age cycle identified and found to lag temperature, carbon dioxide, and orbital eccentricity.' *Science*, 289(5486), pp. 1897-1902.

Shakesby, R.A., and Matthews, J.A. (1993). 'Loch Lomond-Stadial Glacier at Fan-Hir, Mynydd-Du (Brecon Beacons), South Wales: Critical Evidence and Paleoclimatic Implications.' *Geological Journal*, 28, pp. 69–79.

Shindell, D.T., Schmidt, G.A., Mann, M.E., Rind, D., and Waple, A. (2001). 'Solar forcing of regional climate change during the Maunder Minimum.' *Science*, 294(5549), pp. 2149-2152.

Simpson, G.L., and Birks, H.J.B. (2012). 'Statistical learning in Palaeolimnology.' In: Birks, H.J.B., Lotter, A.F., Juggins, S., and Smol, J.P (Eds.). *Tracking Environmental Change Using Lake Sediments. Volume 5: Data Handling and Numerical Techniques.* Dordrecht, The Netherlands: Kluwer Academic Publishers, pp. 249-327.

Simpson, G., and Oksanen, J. (2016). Analogue and Weighted Averaging Methods for Palaeoecology, R package Version 0.17-0. [Software] (https://cran.r-project.org/web/packages/analogue/analogue.pdf)

Sissons, J.B. (1978). 'The parallel roads of Glen Roy and adjecent glens Scotland.' *Boreas*, 7, pp. 229–244.

Sissons, J.B. (1979a). 'The limit of the Loch Lomond Advance in Glen Roy and vicinity.' *Scottish Journal of Geology*, 15, pp. 31–42.

Sissons, J.B. (1979b). 'The Loch Lomond Stadial in the British Isles.' *Nature*, 280, pp. 199–203.

Sissons, J.B. (1979c). ‘The Loch Lomond advance in the Cairngorm mountains,’ *Scottish Geographical Magazine*, 95(2), pp. 66–82.

Sissons, J.B. (1980). ‘Palaeoclimatic inferences from Loch Lomond Advance glaciers.’ In: Lowe, J.J., Gray, J.M., and Robinson, J.E. (Eds.). *Studies in the Lateglacial of North-West Europe*, Oxford: Pergammon Press, pp. 31–43.

Sissons, J.B., and Sutherland, D.G. (1976). ‘Climatic Inferences from former Glaciers in the South-East Grampian Highlands, Scotland.’ *Journal of Glaciology*, 17(76), pp. 325–346.

Słowiński, M., Zawiska, I., Ott, F., Noryśkiewicz, A.M., Plessen, B., Apolinarska, K., Rzodkiewicz, M., Michczyńska, D.J., Wulf, S., Skubała, P., Kordowski, J., Błaszkiewicz, M., and Brauer, A. (2017). ‘Differential proxy responses to late Allerød and early Younger Dryas climatic change recorded in varved sediments of the Trzechowskie palaeolake in Northern Poland.’ *Quaternary Science Reviews*, 158, pp. 94-106.

Small, D., and Fabel, D. (2016). ‘Was Scotland deglaciated during the Younger Dryas?’ *Quaternary Science Reviews*, 145, pp. 259–263.

Small, D., Rinterknecht, V., Austin, W.E.N., Bates, R., Benn, D.I., Scourse, J.D., Bourles, D., Aster, T., and Hibbert, F.D. (2016). ‘Implications of 36Cl exposure ages from Skye, northwest Scotland for the timing of ice stream deglaciation and deglacial ice dynamics.’ *Quaternary Science Reviews*, 150, pp. 130–145.

Stace, C. (2010). *New Flora of the British Isles, 3rd Edition*. Cambridge: Cambridge University Press, 1266pp.

Stanford, J.D., Rohling, E.J., Bacon, S., Roberts, A.P., Grousset, F.E., and Bolshaw, M. (2011). ‘A new concept for the paleoceanographic evolution of Heinrich event 1 in the North Atlantic.’ *Quaternary Science Reviews*, 30(9-10), pp. 1047-1066.

Steffensen, J.P., Andersen, K.K., Bigler, M., Clausen, H.B., Dahl-Jensen, D., Fischer, H., Goto-Azuma, K., Hansson, M., Johnsen, S.J., Jouzel, J., Masson-Delmotte, V., Popp, T., Rasmussen, S.O., Rothlisberger, R., Ruth, R., Stauffer, B., Siggaard-Andersen, M.L., Sveinbjörnsdottir, A.E., Svensson, A., and White, J.W. (2008). 'High-resolution Greenland ice-core data show abrupt climate change happens in few years.' *Science*, 321(5889), pp. 680-684.

Steinhilber, F., Abreu, J.A., Beer, J., Brunner, I., Christl, M., Fischer, H., Heikkilä, U., Kubik, P.W., Mann, M., McCracken, K.G., Miller, H., Mayahara, H., Oerter, H., and Wilhelm, F. (2012). ‘9,400 years of cosmic radiation and solar activity from ice cores and tree rings.’ *Proceedings of the National Academy of Sciences*, 109(16), pp. 5967-5971.

Steinhilber, F., Beer, J., and Fröhlich, C. (2009). ‘Total solar irradiance during the Holocene.’ *Geophysical Research Letters*, 36(19).

Stephenson, D., and Gould, D. (1995) *British Regional Geology: Grampian Highlands*, Fourth edition, Nottingham: British Geological Survey, 281pp.

Stocker, T.F. (1999). 'Abrupt climate changes: from the past to the future– a review.' *International Journal of Earth Sciences*, 88(2), pp. 365-374.

Sugita, S. (1994). ‘Pollen representation of vegetation in Quaternary sediments: theory and method in patchy vegetation.’ *Journal of Ecology*, 82(4), pp. 881-897.

Sutherland, D.G. (1991). ‘The glaciation of the Shetland and Orkney Islands.’ In: Ehlers, J., Gibbard, P.L., and Rose, J. (Eds.). *Glacial Deposits in Great Britain and Ireland*, Rotterdam: Balkema, pp. 121–127.

Sutherland, D.G. (1993). ‘Ward Hill, Enegars Corrie and Dwarfie Hamars.’ In: Gordon, J.E., and Sutherland, D.G. (Eds.). *Quaternary of Scotland*, London: Chapman and Hall, pp. 80–82.

Talbot, M.R. (1990). ‘A review of the palaeohydrological interpretation of carbon and oxygen isotopic ratios in primary lacustrine carbonates.’ *Chemical Geology: Isotope Geoscience Section*, 80(4), pp. 261-279.

Tallantire, P.A. (2002). ‘The early-Holocene spread of hazel (*Corylus avellana L.*) in Europe north and west of the Alps: an ecological hypothesis.’ *The Holocene*, 12(1), pp. 81-96.

Tarasov, L., and Peltier, W.R. (2005). ‘Arctic freshwater forcing of the Younger Dryas cold reversal.’ *Nature*, 435(7042), pp. 662-665

Taylor, B., Elliott, B., Conneller, C., Milner, N., Bayliss, A., Knight, B., and Bamforth, M. (2017). ‘Resolving the Issue of Artefact Deposition at Star Carr.’ *Proceedings of the Prehistoric Society*, 83, pp. 23–42.

ter Braak, C.J., and Prentice, I.C. (1988). ‘A theory of gradient analysis.’ *Advances in Ecological Research*, 18, pp. 271-317.

Thomas, P.A., El-Barghathi, M., and Polwart, A. (2007). ‘Biological flora of the British Isles: Juniperus communis L.’ *Journal of Ecology*, 95(6), pp. 1404-1440.

Thornalley, D.J., McCave, I.N., and Elderfield, H. (2010). ‘Freshwater input and abrupt deglacial climate change in the North Atlantic.’ *Paleoceanography*, 25(1).

Timms, R.G.O. (2016). *Developing a refined tephrostratigraphy for Scotland, and constraining abrupt climatic oscillations of the Last Glacial-Interglacial Transition (Ca. 16-8 ka BP) using high resolution tephrochronologies*. Unpublished PhD thesis, Royal Holloway, University of London.

Timms, R.G.O., Matthews, I.P., Palmer, A.P., Candy, I., and Abel, L. (2017). ‘A high-resolution tephrostratigraphy from Quoyloo Meadow, Orkney, Scotland: Implications for the tephrostratigraphy of NW Europe during the Last Glacial-Interglacial Transition.’ *Quaternary Geochronology*, 40, pp. 67–81.

Tinner, W., and Lotter, A.F. (2001). ‘Central European vegetation response to abrupt climate change at 8.2 ka.’ *Geology*, 29(6), pp. 551-554.

Tipping, R. M. (1991a). ‘Climatic change in Scotland during the Devensian Late-Glacial: the palynological record.’ In: Barton, N., Roberts, A.J., and Roe, D.A. (Eds.). *The Late Glacial in North-west Europe*, Council for British Archaeology Research Report 77, pp. 7-21.

Tipping, R.M. (1991b). 'The climatostratigraphic subdivision of the Devensian Late-Glacial: evidence from a pollen site near Oban, western Scotland.' *Journal of Biogeography*, 18(1), pp. 89-10.

Tipping, R.M. (1989). ‘Devensian Lateglacial Vegetation History at Loch Barnluasgan, Argyllshire, Western Scotland.’ *Journal of Biogeography*, 16(5), pp. 435–447.

Troels-Smith, J. (1955). 'Characterisation of unconsolidated sediments.' *Geological Survey of Denmark: Series 5*, 5(10), pp. 1-73.

Turner, J.N., Holmes, N., Davis, S.R., Leng, M.J., Langdon, C., and Scaife, R.G. (2015). 'A multiproxy (micro-XRF, pollen, chironomid and stable isotope) lake sediment record for the Lateglacial to Holocene transition from Thomastown Bog, Ireland.' *Journal of Quaternary Science*, 30(6), pp.514-528.

Turney, C.S.M., Harkness, D.D., and Lowe, J.J. (1997). 'The use of microtephra horizons to correlate Late-glacial lake sediment successions in Scotland,' *Journal of Quaternary Science*, 12(6), pp. 525–531.

Urrutia, R., Araneda, A., Cruces, F., Torres, L., Chirinos, L., Treutler, H.C., Fagel, N., Bertrand, S., Alvial, I., Barra, R., and Chapron, E. (2007). 'Changes in diatom, pollen, and chironomid assemblages in response to a recent volcanic event in Lake Galletué (Chilean Andes).' *Limnologica-Ecology and Management of Inland Waters*, 37(1), pp. 49-62.

van Asch, N., and Hoek, W.Z. (2012). 'The impact of summer temperature changes on vegetation development in Ireland during the Weichselian Lateglacial Interstadial.' *Journal of Quaternary Science*, 27(5), pp. 441-450.

van Asch, N., Heiri, O., Bohncke, S.J., and Hoek, W.Z. (2013). 'Climatic and environmental changes during the Weichselian Lateglacial Interstadial in the Weerterbos region, the Netherlands.' *Boreas*, 42(1), pp. 123-139.

van Asch, N., Lutz, A.F., Duijkers, M.C., Heiri, O., Brooks, S.J., and Hoek, W.Z. (2012a). 'Rapid climate change during the Weichselian Late-Glacial in Ireland: chironomid-inferred summer temperatures from Fiddaun, Co. Galway.' *Palaeogeography, Palaeoclimatology, Palaeoecology*, 315-316, pp. 1-11.

van Asch, N., Kloos, M.E., Heiri, O., de Klerk, P., and Hoek, W.Z., (2012b). 'The younger dryas cooling in northeast Germany: summer temperature and environmental changes in the Friedländer Groβe Wiese region.' *Journal of Quaternary Science*, 27(5), pp. 531-543.

van den Bogaard, P. (1995). '40Ar/39Ar ages of sanidine phenocrysts from Laacher See Tephra (12,900 yr BP): Chronostratigraphic and petrological significance.' *Earth and Planetary Science Letters*, 133(1-2), pp. 163-174.

van den Bos, V., Engels, S., Bohncke, S.J.P., Cerli, C., Jansen, B., Kalbitz, K., Peterse, F., Renssen, H., and Sachse, D. (2018). 'Late Holocene changes in vegetation and atmospheric circulation at Lake Uddelermeer (The Netherlands) reconstructed using lipid biomarkers and compound-specific δD analysis.' *Journal of Quaternary Science*, 33(1), pp. 100-111.

van der Plicht, J., Van Geel, B., Bohncke, S.J.P., Bos, J.A.A., Blaauw, M., Speranza, A.O.M., Muscheler, R., and Björck, S. (2004). 'The Preboreal climate reversal and a subsequent solar-forced climate shift.' *Journal of Quaternary Science*, 19(3), pp. 263-269.

van der Plicht. J. (2007). 'Radiocarbon Dating. Variations inatmospheric ^{14}C.' In: Elias, S.A. (Ed.). *Encyclopedia of Quaternary Science*, Amsterdam: Elsevier, pp. 2923-2931.

van Dinter, M., and Birks, H.H. (1996). 'Distinguishing fossil Betula nana and *B. pubescens* using their wingless fruits: implications for the late-glacial vegetational history of western Norway.' *Vegetation History and Archaeobotany*, 5(3), pp. 229-240.

van Geel, B., Bohncke, S.J.P., and Dee, H. (1980). ‘A palaeoecological study of an upper Late Glacial and Holocene sequence from “De Borchert”, The Netherlands.’ *Review of Palaeobotany and Palynology*, 31, pp. 367-448.

van Geel, B., Coope, G.R., and van der Hammen, T. (1989). ‘Palaeoecology and stratigraphy of the Lateglacial type section at Usselo (The Netherlands).’ *Review of Palaeobotany and Palynology*, 60(1-2), pp. 25-129.

van Raden, U.J., Colombaroli, D., Gilli, A., Schwander, J., Bernasconi, S.M., van Leeuwen, J., Leuenberger, M., and Eicher, U. (2013). 'High-resolution Late-Glacial chronology for the Gerzensee lake record (Switzerland): $\delta^{18}O$ correlation between a Gerzensee-stack and NGRIP.' *Palaeogeography, Palaeoclimatology, Palaeoecology*, 391, pp. 13-24.

Vasari, Y. (1977). ‘Radiocarbon dating of the Late-Glacial and Early-Flandrian vegetational succession in the Scottish Highlands and the Isle of Skye.’ In: Gray, J.M., and Lowe, J.J. (Eds.). *Studies in the Scottish Late-Glacial Environment*, Oxford: Pergammon Press, pp. 143-162.

von Grafenstein, U., Belmecheri, S., Eicher, U., van Raden, U.J., Erlenkeuser, H., Andersen, N., and Ammann, B. (2013). ‘The oxygen and carbon isotopic signatures of biogenic carbonates in Gerzensee, Switzerland, during the rapid warming around 14,685 years BP and the following interstadial.’ *Palaeogeography, palaeoclimatology, palaeoecology*, 391, pp. 25-32.

von Grafenstein, U., Eicher, U., Erlenkeuser, H., Ruch, P., Schwander, J., and Ammann, B. (2000). ‘Isotope signature of the Younger Dryas and two minor oscillations at Gerzensee (Switzerland): palaeoclimatic and palaeolimnologic interpretation based on bulk and biogenic carbonates.’ *Palaeogeography, Palaeoclimatology, Palaeoecology*, 159(3-4), pp. 215-229.

von Grafenstein, U., Erlenkeuser, H., Brauer, A., Jouzel, J., and Johnsen, S.J, (1999). ‘A mid-European decadal isotope-climate record from 15,500 to 5000 years BP.’ *Science*, 284(5420), pp. 1654-1657.

Walker, D., Godwin, H. (1954). ‘Lake-stratigraphy, pollen analysis and vegetational history.’ In: Clark, J.G.D. (Ed.). *Excavations at Starr Carr*, Cambridge: Cambridge University Press, pp. 25–69.

Walker, I.R. (1987). ‘Chironomidae (Diptera) in paleoecology.’ *Quaternary Science Reviews*, 6(1), pp. 29-40.

Walker, I.R., and Mathewes, R.W., (1987). ‘Chironomidae (Diptera) and postglacial climate at Marion Lake, British Columbia, Canada.’ *Quaternary Research*, 27(1), pp. 89-102.

Walker, I.R., Smol, J.P., Engstrom, D.R., and Birks, H.J.B. (1991). ‘An assessment of Chironomidae as quantitative indicators of past climatic change.’ *Canadian Journal of Fisheries and Aquatic Sciences*, 48(6), pp. 975-987.

Walker, M.J.C., and Lowe, J.J. (2017). ‘Lateglacial environmental change in Scotland.’ *Earth and Environmental Science Transactions of The Royal Society of Edinburgh*, pp. 1-26.

Walker, M.J.C., Coope, G.R., and Lowe, J.J. (1993a). ‘The Devensian (Weichselian) Lateglacial palaeoenvironmental record from Gransmoor, East Yorkshire, England: A

contribution to the ‘North Atlantic seaboard programme’ of IGCP-253, ‘Termination of the Pleistocene.’’ *Quaternary Science Reviews*, 12(8), pp. 659-680.

Walker, M.J.C., Griffiths, H.I., Ringwood, V., and Evans, J.G. (1993b). ‘An early-Holocene pollen, mollusc and ostracod sequence from lake marl at Llangorse Lake, South Wales, UK.’ *The Holocene*, 3(2), pp. 138-149.

Walker, M.J.C., Lowe, J.J., Blockley, S.P.E., Bryant, C., Coombes, P., Davies, S., Hardiman, M., Turney, C.S.M., and Watson, J. (2012). ‘Lateglacial and early Holocene palaeoenvironmental ‘events’ in Sluggan Bog, Northern Ireland: comparisons with the Greenland NGRIP GICC05 event stratigraphy.’ *Quaternary Science Reviews*, 36, pp. 124-138.

Walker, M.J.C., Johnsen, S., Rasmussen, S.O., Popp, T., Steffensen, J.P., Gibbard, P., Hoek, W., Lowe, J.J., Andrews, J., Björck, S., Cwynar, L.C., Hughen, K., Kershaw, P., Kromer, B., Litt, T., Lowe, D., Nakagawa, T., Newnham, R., and Schwander, J. (2009). ‘Formal definition and dating of the GSSP (Global Stratotype Section and Point) for the base of the Holocene using the Greenland NGRIP ice core and selected auxiliary records.’ *Journal of Quaternary Science*, 24(1), pp. 3-17.

Walker, M.J.C. (1975). 'Late-Glacial and early Post-Glacial environmental history of the central Grampian Highlands, Scotland.' *Journal of Biogeography*, 2(4), pp. 265-284.

Walker, M.J.C. (1982). ‘The Late-Glacial and Early Flandrian Deposits at Traeth Mawr, Brecon Beacons, South Wales,’ *New Phytologist*, 90(1), pp. 177–194.

Walker, M.J.C. (2007a). ‘Craig-y-Fro: pollen stratigraphy and dating.’ In: Carr, S.J., Coleman, C.G., Humpage, A.J., and Shakesby, R.A. (Eds.). *The Quaternary of the Brecon Beacons: Field Guide*, London: Quaternary Research Association, pp. 128–129.

Walker, M.J.C. (2007b). ‘Craig Cerrig-gleisiad: pollen stratigraphy and dating.’ In: Carr, S.J., Coleman, C.G., Humpage, A.J., and Shakesby, R.A. (Eds.). *The Quaternary of the Brecon Beacons: Field Guide*, London: Quaternary Research Association, pp. 142–144.

Walker, M.J.C., and Harkness, D.D. (1990). ‘Radiocarbon dating the Devensian Lateglacial in Britain: new evidence from Llanilid, South Wales.’ *Journal of Quaternary Science*, 5(2), pp. 135-144.

Walker, M.J.C., and Lowe, J.J. (1990). 'Reconstructing the environmental history of the Last Glacial-Interglacial Transition: evidence from the Isle of Skye, Inner Hebrides, Scotland.' *Quaternary Science Reviews*, 9(1), pp. 15-49.

Walker, M.J.C., Bohncke, S.J.P., Coope, G.R., O' Connell, M., Usinger, H., and Verbruggen, C. (1994). ‘The Devensian/Weichselian Late-glacial in northwest Europe (Ireland, Britain, north Belgium, The Netherlands, northwest Germany).’ *Journal of Quaternary Science*, 9(2), pp. 109-118.

Walker, M.J.C., Bryant, C., Coope, G.R., Harkness, D.D., Lowe, J.J., and Scott, E.M. (2001). ‘Towards a radiocarbon chronology of the Late-Glacial: sample selection strategies.’ *Radiocarbon*, 43(2B), pp. 1007-1019.

Walker, M.J.C., Coope, G.R., Sheldrick, C., Turney, C.S.M., Lowe, J.J., Blockley, S.P.E., and Harkness, D.D. (2003). ‘Devensian Lateglacial environmental changes in Britain: a multi-proxy environmental record from Llanilid, South Wales, UK.’ *Quaternary Science Reviews*, 22(5-7), pp. 475-520.

Walker, M.J.C., and Lowe, J.J. (1977). 'Postglacial environmental history of Rannoch Moor, Scotland. 1. Three pollen diagrams from the Kingshouse area.' *Journal of Biogeography*, 4(4), pp. 333–351.

Walkley, A., and Black, I.A. (1934). 'An examination of the Degtjareff method for determining soil organic matter, and a proposed modification of the chromic acid titration method.' *Soil Science,* 37, pp. 29-38.

Watson, J. (2008). *Quantifying Late Glacial climate change in Northwestern Europe using two insect proxies*. Unpublished PhD Thesis, The Queen's University of Belfast, 365 pp.

Watson, J.E., Brooks, S.J., Whitehouse, N.J., Reimer, P.J., Birks, H.J.B., and Turney, C.S.M. (2010). 'Chironomid-inferred late-glacial summer air temperatures from Lough Nadourcan, Co. Donegal, Ireland.' *Journal of Quaternary Science*, 25(8), pp. 1200-1210.

Watts, W.A. (1970). 'Criteria for identification of Late-glacial climatic oscillations, with special reference to the Bölling Oscillation.' *American Quaternary Association, 1st Meeting Abstracts (1970),* pp. 144-145*.*

Watts, W.A. (1977). 'The late Devensian vegetation of Ireland.' *Philosophical Transactions of the Royal Society of London. Series B, Biological Sciences*, 280(972), pp. 273-293.

Webb, T. (1986). 'Is vegetation in equilibrium with climate? How to interpret late-Quaternary pollen data.' *Vegetatio*, 67(2), pp. 75-91.

Weckström, K., Weckström, J., Yliniemi, L.M., and Korhola, A. (2010). 'The ecology of Pediastrum (Chlorophyceae) in subarctic lakes and their potential as paleobioindicators.' *Journal of Paleolimnology*, 43(1), pp. 61-73.

Wehrli, M., Tinner, W., and Ammann, B. (2007). '16 000 years of vegetation and settlement history from Egelsee (Menzingen, central Switzerland).' *The Holocene*, 17(6), pp. 747-761.

West, R.G. (1970). 'Pollen zones in the Pleistocene of Great Britain and their correlation.' *New Phytologist*, 69(4), pp. 1179-1183.

Whitlock, C., and Larsen, C. (2001). 'Charcoal as a Fire Proxy.' In: Smol, J.P., Birks, H.J.B., and Last, W.M. (Eds.). *Tracking Environmental Change Using Lake Sediments. Volume 3: Terrestrial, Algal and Siliceous Indicators.* Dordrecht, The Netherlands: Kluwer Academic Publishers, pp. 75-97.

Whitlock, C., Shafer, S.L., and Marlon, J. (2003). 'The role of climate and vegetation change in shaping past and future fire regimes in the northwestern US and the implications for ecosystem management.' *Forest ecology and management*, 178(1-2), pp. 5-21.

Whittington, G., Buckland, P., Edwards, K.J., Greenwood, M., Hall, A.M., and Robinson, M. (2003). 'Multiproxy Devensian Late-glacial and Holocene environmental records at an Atlantic coastal site in Shetland.' *Journal of Quaternary Science*, 18(2), pp. 151–168.

Whittington, G., Edwards, K.J., Zanchetta, G., Keen, D.H., Bunting, M.J., Fallick, A.E., and Bryant, C. L. (2015). 'Lateglacial and early Holocene climates of the Atlantic

margins of Europe: Stable isotope, mollusc and pollen records from Orkney, Scotland.' *Quaternary Science Reviews*, 122, pp. 112-130.

Whittington, G., Fallick, A.E., and Edwards, K.J. (1996). 'Stable oxygen isotope and pollen records from eastern Scotland and a consideration of Late-Glacial and early Holocene climate change for Europe.' *Journal of Quaternary Science*, 11(4), pp. 327-340.

Wick, L. (2000). 'Vegetational response to climatic changes recorded in Swiss Late Glacial lake sediments.' *Palaeogeography, Palaeoclimatology, Palaeoecology*, 159(3-4), pp. 231-250.

Wick, L., and Tinner, W. (1997). 'Vegetation changes and umbertine fluctuations in the Central Alps as indicators of Holocene climatic oscillations.' *Arctic and Alpine Research*, 29(4), pp. 445-458.

Wicks, K., and Mithen, S. (2014). 'The impact of the abrupt 8.2 ka cold event on the Mesolithic population of western Scotland: a Bayesian chronological analysis using 'activity events' as a population proxy.' *Journal of Archaeological Science*, 45, pp. 240-269.

Wijk, S. (1986). 'Performance of *Salix herbacea* in an alpine snow-bed gradient.' *Journal of Ecology*, pp. 675-684.

Williams, J.W., Blois, J.L., and Shuman, B.N. (2011). 'Extrinsic and intrinsic forcing of abrupt ecological change: case studies from the late Quaternary.' *Journal of Ecology*, 99(3), pp. 664-677.

Willis, K.J., Rudner, E., and Sümegi, P. (2000). 'The full-glacial forests of central and southeast Europe.' *Quaternary Research*, 53(2), pp. 203-213.

Wohlfarth, B. (1996). 'The chronology of the last termination: a review of radiocarbon-dated, high-resolution terrestrial stratigraphies.' *Quaternary Science Reviews*, 15(4), pp. 267-284.

Wohlfarth, B., Blaauw, M., Davies, S.M., Andersson, M., Wastegård, S., Hormes, A., and Possnert, G. (2006). 'Constraining the age of Lateglacial and early Holocene pollen zones and tephra horizons in southern Sweden with Bayesian probability methods.' *Journal of Quaternary Science*, 21(4), pp. 321–334.

Wohlfarth, B., Muschitiello, F., Greenwood, S.L., Andersson, A., Kylander, M., Smittenberg, R.H., Steinthorsdottir, M., Watson, J., and Whitehouse, N.J. (2017). 'Hässeldala–a key site for Last Termination climate events in northern Europe.' *Boreas*, 46(2), pp.143-161.

Wulf, S., Ott, F., Słowiński, M., Noryśkiewicz, A.M., Dräger, N., Martin-Puertas, C., Czymzik, M., Neugebauer, I., Dulski, P., Bourne, A.J., Błaszkiewicz, M., and Brauer, A. (2013). 'Tracing the Laacher See Tephra in the varved sediment record of the Trzechowskie palaeolake in central Northern Poland.' *Quaternary Science Reviews*, 76, pp. 129-139.

Zhang, Z., and Sachs, J.P. (2007). 'Hydrogen isotope fractionation in freshwater algae: I. Variations among lipids and species.' *Organic Geochemistry*, 38(4), pp. 582-608.